Hoefs

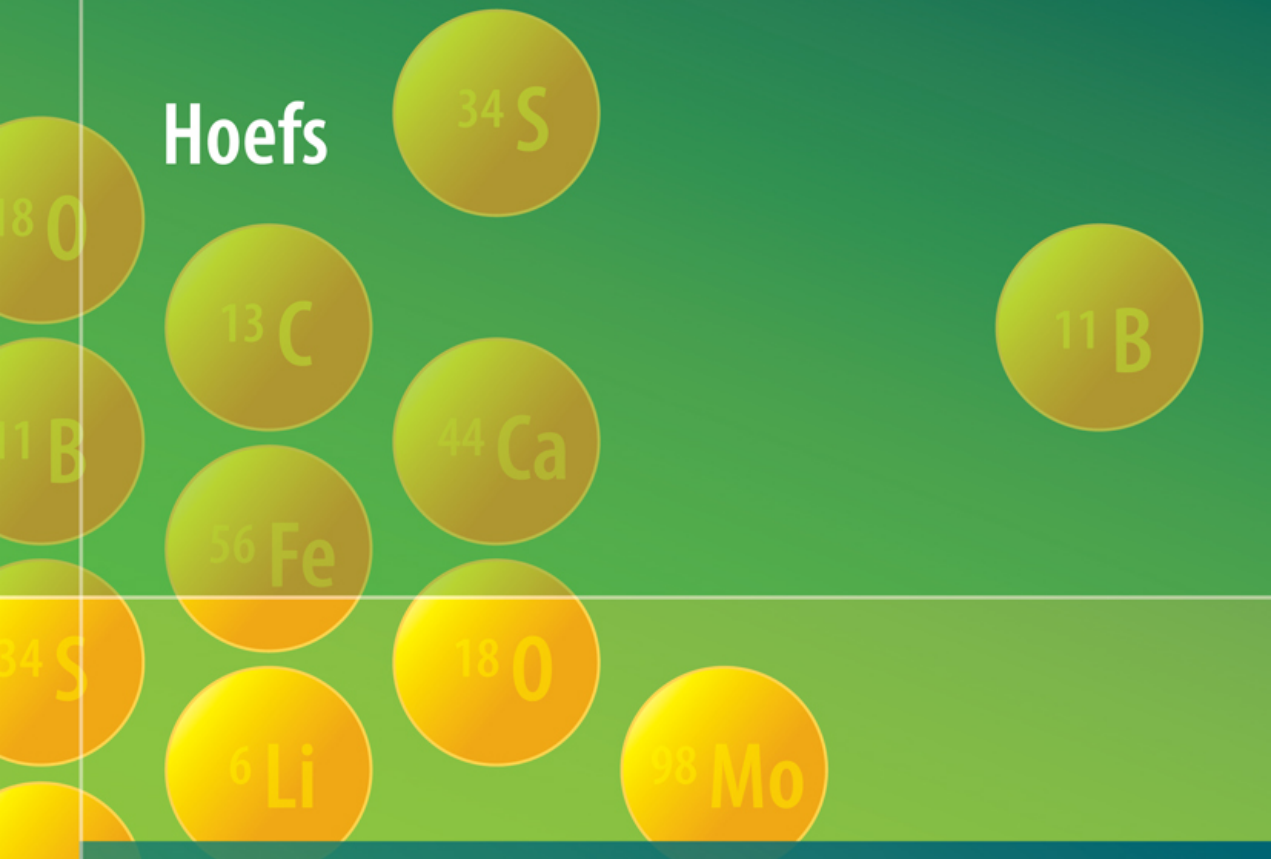

Stable Isotope Geochemistry

6th Edition

Springer

Stable Isotope Geochemistry

Jochen Hoefs

Stable Isotope Geochemistry

Sixth Edition

Springer

Jochen Hoefs

University of Göttingen
Goldschmidtstr. 1
37077 Göttingen
Germany

ISBN: 978-3-540-70703-5 e-ISBN: 978-3-540-70708-0

Library of Congress Control Number: 2008933507

Cover design: deblik, Berlin

Printed on acid-free paper

springer.com

Preface

Stable isotope investigations in the earth sciences continue to grow, maybe faster than ever before. After publication of the 5th edition, tremendous progress has been achieved in many subfields of stable isotope geochemistry. To name a few:

- Applications of Multicollector - ICP-MS has grown rapidly and now enable investigations on natural isotope variations of a wide range of transition and heavy elements that could not previously be measured with adequate precision.
- Precise ion probe measurements on the micrometer scale allow the detection of the growth and dissolution history of minerals.
- Evidence for mass-independent fractionation in a variety of compounds and elements has increased considerably.
- High precision analysis of the multiple rare isotopes of a specific element permit the distinction of different mass-dependent fractionation mechanisms.
- Precise measurements of molecules containing more than one rare isotope indicate non-random distributions of the rare isotopes, which potentially may be utilized as one-mineral thermometers.

These recent advances made a further revision necessary. Again I have tried to provide a contemporary overview of the entire field of stable isotope geochemistry enabling a quick access to the most recent literature, although many references date back to the 1960 and 1970s when seminal papers were published. I am fully aware of omissions and shortcomings, but I hope the new edition gives a well balanced discussion of the whole field including the new isotope systems introduced mainly by MC-ICP-MS techniques.

My colleagues Michael Böttcher, Max Coleman, Alan Matthews and Harald Strauß have reviewed an early draft, which is gratefully acknowledged. Yongsheng He was of great help during the preparation of some figures. I take, however, full responsibility for any shortcomings that remain.

Contents

Chapter 1
Theoretical and Experimental Principles

1.1 General Characteristics of Isotopes

Isotopes are atoms whose nuclei contain the same number of protons but a different number of neutrons. The term *isotopes* is derived from Greek (meaning equal places) and indicates that isotopes occupy the same position in the periodic table.

It is convenient to denote isotopes in the form ${}^{m}_{n}\mathrm{E}$, where the superscript m denotes the mass number (i.e., sum of the number of protons and neutrons in the nucleus) and the subscript n denotes the atomic number of an element, E. For example, ${}^{12}_{6}\mathrm{C}$ is the isotope of carbon which has six protons and six neutrons in its nucleus. The atomic weight of each naturally occurring element is the average of the weights contributed by its various isotopes.

Isotopes can be divided into two fundamental kinds, stable and unstable (radioactive) species. The number of stable isotopes is about 300; whilst over 1,200 unstable ones have been discovered so far. The term *stable* is relative, depending on the detection limits of radioactive decay times. In the range of atomic numbers from 1 (H) to 83 (Bi), stable nuclides of all masses except 5 and 8 are known. Only 21 elements are pure elements, in the sense that they have only one stable isotope. All other elements are mixtures of at least two isotopes. The relative abundance of different isotopes of an element may vary substantially. In copper, for example, ${}^{63}\mathrm{Cu}$ accounts for 69% and ${}^{65}\mathrm{Cu}$ for 31% of all copper nuclei. For the light elements, however, one isotope is predominant, the others being present only in trace amounts.

The stability of nuclides is characterized by several important rules, two of which are briefly discussed here. The first is the so-called symmetry rule, which states that in a stable nuclide with low atomic number, the number of protons is approximately equal to the number of neutrons, or the neutron-to-proton ratio, N/Z, is approximately equal to unity. In stable nuclei with more than 20 protons or neutrons, the N/Z ratio is always greater than unity, with a maximum value of about 1.5 for the heaviest stable nuclei. The electrostatic Coulomb repulsion of the positively charged protons grows rapidly with increasing Z. To maintain the stability in the nuclei, more

J. Hoefs, *Stable Isotope Geochemistry,*

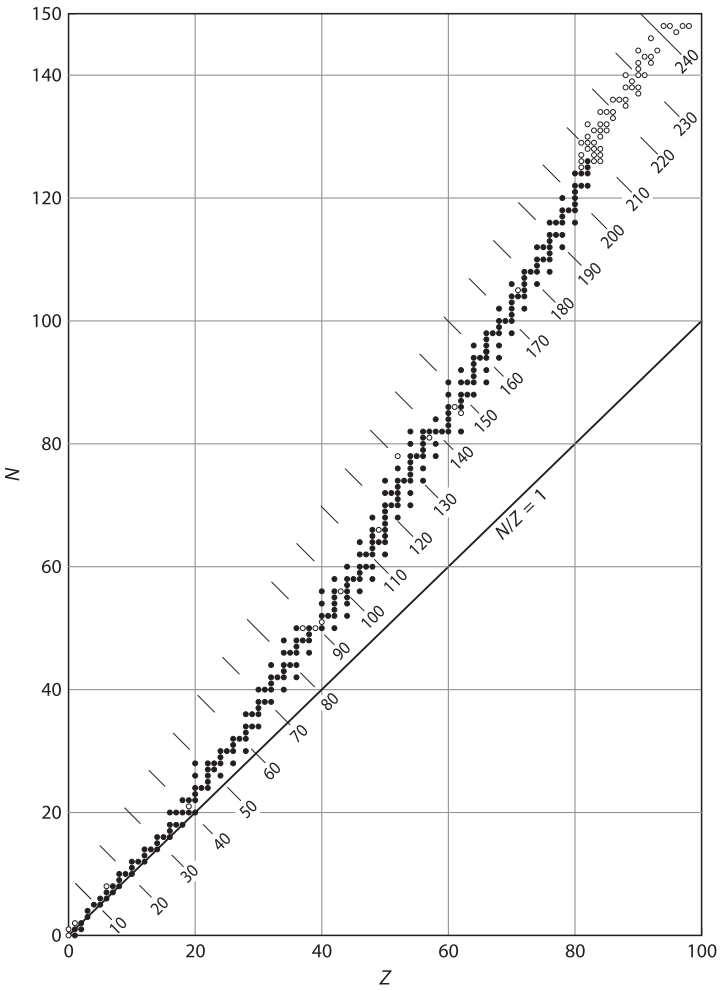

Fig. 1.1 Plot of number of protons (Z) and number of neutrons (N) in stable (*filled circles*) and unstable (*open circles*) nuclides

neutrons (which are electrically neutral) than protons are incorporated into the nucleus (see Fig. 1.1).

The second rule is the so-called *Oddo–Harkins* rule, which states that nuclides of even atomic numbers are more abundant than those with odd numbers. As shown in Table 1.1, the most common of the four possible combinations is even–even and the least common is odd–odd.

The same relationship is demonstrated in Fig. 1.2, which shows that there are more stable isotopes with even, than with odd, proton numbers.

Radioactive isotopes can be classified as being either artificial or natural. Only the latter are of interest in geology, because they are the basis for radiometric dating

Table 1.1 Types of atomic nuclei and their frequency of occurrence

Z–*N* combination	Number of stable nuclides
Even–even	160
Even–odd	56
Odd–even 50	50
Odd–odd	5

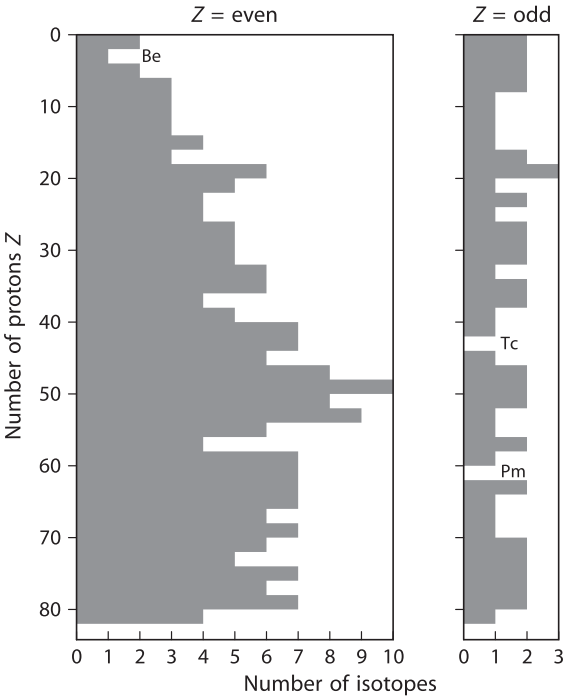

Fig. 1.2 Number of stable isotopes of elements with even and odd number of protons (radioactive isotopes with half-lives greater than 10^9 years are included)

methods. Radioactive decay processes are spontaneous nuclear reactions and may be characterized by the radiation emitted, i.e., α-, β-, and/or γ-emission. Decay processes may also involve electron capture.

Radioactive decay is one process that produces variations in isotope abundance. The second cause for differences in isotope abundance is isotope fractionation, caused by small chemical and physical differences between the isotopes of an element. It is exclusively this important process that will be discussed in the following chapters.

1.2 Isotope Effects

Differences in chemical and physical properties arising from variations in atomic mass of an element are called *isotope effects*. It is well known that the electronic structure of an element essentially determines its chemical behaviour, whereas the nucleus is more or less responsible for its physical properties. Since, all isotopes of a given element contain the same number and arrangement of electrons, a far-reaching similarity in chemical behaviour is the logical consequence. But this similarity is not unlimited; certain differences exist in physicochemical properties due to mass differences. The replacement of any atom in a molecule by one of its isotopes produces a very small change in chemical behaviour. The addition of one neutron can, for instance, considerably depress the rate of chemical reaction. Furthermore, it leads, for example, to a shift of the lines in the Raman- and IR-spectra. Such mass differences are most pronounced among the lightest elements. For example, some differences in physicochemical properties of $H_2{}^{16}O$, $D_2{}^{16}O$, $H_2{}^{18}O$ are listed in Table 1.2. To summarize, the properties of molecules differing only in isotopic substitution are qualitatively the same, but quantitatively different.

Differences in the chemical properties of the isotopes of H, C, N, O, S, and other elements have been calculated by the methods of statistical mechanics and also determined experimentally. These differences in the chemical properties can lead to considerable separation of the isotopes during chemical reactions.

The theory of isotope effects and a related isotope fractionation mechanism will be discussed very briefly. For a more detailed introduction to the theoretical background, see Bigeleisen and Mayer (1947), Urey (1947), Melander (1960), Bigeleisen (1965), Richet et al. (1977), O'Neil (1986), Criss (1999), Chacko et al. (2001), Schauble (2004), and others.

Differences in the physicochemical properties of isotopes arise as a result of quantum mechanical effects. Figure 1.3 shows schematically the energy of a diatomic molecule, as a function of the distance between the two atoms. According to the quantum theory, the energy of a molecule is restricted to certain discrete energy levels. The lowest level is not at the minimum of the energy curve, but above it by an amount $1/2h\nu$ where h is Planck's constant and ν is the frequency with

Table 1.2 Characteristic physical properties of $H_2{}^{16}O$, $D_2{}^{16}O$, and $H_2{}^{18}O$

Property	$H_2{}^{16}O$	$D_2{}^{16}O$	$H_2{}^{18}O$
Density (20°C, in g cm^{-3})	0.997	1.1051	1.1106
Temperature of greatest density (°C)	3.98	11.24	4.30
Melting point (760 Torr, in °C)	0.00	3.81	0.28
Boiling point (760 Torr, in °C)	100.00	101.42	100.14
Vapour pressure (at 100°C, in Torr)	760.00	721.60	
Viscosity (at 20°C, in centipoise)	1.002	1.247	1.056

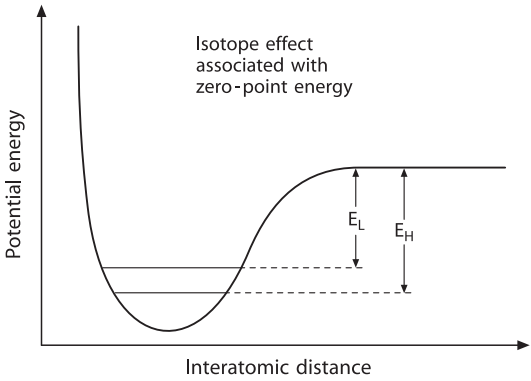

Fig. 1.3 Schematic potential energy curve for the interaction of two atoms in a stable molecule or between two molecules in a liquid or solid (after Bigeleisen 1965)

which the atoms in the molecule vibrate with respect to one another. Thus, even in the ground state at a temperature of absolute zero, the vibrating molecule would possess certain zero-point energy above the minimum of the potential energy curve of the molecule. It vibrates with its fundamental frequency, which depends on the mass of the isotopes. In this context, it is important to note that vibrational motions dominate chemical isotope effects; rotational and translational motions either have no effect on isotope separations or are subordinate. Therefore, molecules of the same chemical formula that have different isotopic species will have different zero-point energies: the molecule of the heavy isotope will have a lower zero-point energy than the molecule of the light isotope, as it has a lower vibrational frequency. This is shown schematically in Fig. 1.3, where the upper horizontal line (E_L) represents the dissociation energy of the light molecule and the lower line (E_H), that of the heavy one. E_L is actually not a line, but an energy interval between the zero-point energy level and the *continuou*s level. This means that the bonds formed by the light isotope are weaker than bonds involving the heavy isotope. Thus, during a chemical reaction, molecules bearing the light isotope will, in general, react slightly more readily than those with the heavy isotope.

1.3 Isotope Fractionation Processes

The partitioning of isotopes between two substances or two phases of the same substance with different isotope ratios is called *isotope fractionation*. The main phenomena producing isotope fractionations are

1. Isotope exchange reactions (equilibrium isotope distribution)
2. Kinetic processes that depend primarily on differences in reaction rates of isotopic molecules

1.3.1 Isotope Exchange

Isotope exchange includes processes with very different physicochemical mechanisms. Here, the term *isotope exchange* is used for all situations, in which there is no net reaction, but in which the isotope distribution changes between different chemical substances, between different phases, or between individual molecules.

Isotope exchange reactions are a special case of general chemical equilibrium and can be written

$$\mathrm{a}A_1 + \mathrm{b}B_2 = \mathrm{a}A_2 + \mathrm{b}B_1, \tag{1.1}$$

where the subscripts indicate that species A and B contain either the light or heavy isotope 1 or 2, respectively. For this reaction, the equilibrium constant is expressed by

$$K = \frac{\left(\frac{A_2}{A_1}\right)^{\mathrm{a}}}{\left(\frac{B_2}{B_1}\right)^{\mathrm{b}}}, \tag{1.2}$$

where the terms in parentheses may be, for example, the molar ratios of any species. Using the methods of statistical mechanics, the isotopic equilibrium constant may be expressed in terms of the partition functions Q of the various species

$$k = \frac{\left(\frac{Q_{A2}}{Q_{A1}}\right)}{\left(\frac{Q_{B2}}{Q_{B1}}\right)}. \tag{1.3}$$

Thus, the equilibrium constant then is simply the quotient of two partition function ratios, one for the two isotopic species of A, the other for B.

The partition function is defined by

$$Q = \sum\nolimits_i (g_i \exp(-E_i/kT)), \tag{1.4}$$

where the summation is over all the allowed energy levels, E_i, of the molecules and g_i is the degeneracy or statistical weight of the ith level [of E_i], k is the Boltzmann constant and T is the temperature. Urey (1947) has shown that for the purpose of calculating partition function ratios of isotopic molecules, it is very convenient to introduce, for any chemical species, the ratio of its partition function to that of the corresponding isolated atom, which is called the reduced partition function. This reduced partition function ratio can be manipulated exactly in the same way as the normal partition function ratio. The partition function of a molecule can be separated into factors corresponding to each type of energy: translation, rotation, and vibration

$$Q_2/Q_1 = (Q_2/Q_1)_{\mathrm{trans}}\,(Q_2/Q_1)_{\mathrm{rot}}\,(Q_2/Q_1)_{\mathrm{vib}}\,. \tag{1.5}$$

The difference of the translation and rotation energy is more or less the same among the compounds appearing at the left- and right-hand side of the exchange reaction equation, except for hydrogen, where rotation must be taken into account. This

leaves differences in vibrational energy as the predominant source of isotope effects. The term, vibrational energy can be separated into two components. The first is related to the zero-point energy difference and accounts for most of the variation with temperature. The second term represents the contributions of all the other bound states and is not very different from unity. The complications which may occur relative to this simple model are mainly that the oscillator is not perfectly harmonic, so an *inharmonic* correction has to be added.

For geologic purposes, the dependence of the equilibrium constant K on temperature is the most important property (4). In principle, isotope fractionation factors for isotope exchange reactions are also slightly pressure-dependent because isotopic substitution makes a minute change in the molar volume of solids and liquids. Experimental studies up to 20 kbar by Clayton et al. (1975) have shown that the pressure dependence for oxygen is, however, less than the limit of analytical detection. Thus, as far as it is known today, the pressure dependence seems with the exception of hydrogen to be of no importance for crustal and upper mantle environments (but see Polyakov and Kharlashina 1994).

Isotope fractionations tend to become zero at very high temperatures. However, they do not decrease to zero monotonically with increasing temperatures. At higher temperatures, fractionations may change sign (called crossover) and may increase in magnitude, but they must approach zero at very high temperatures. Such crossover phenomena are due to the complex manner by which thermal excitation of the vibration of atoms contributes to an isotope effect (Stern et al. 1968).

For ideal gas reactions, there are two temperature regions where the behaviour of the equilibrium constant is simple: at low temperatures (generally much below room temperature), the natural logarithm of K ($\ln\ K$) follows $\sim 1/T$ where T is the absolute temperature and at high temperatures, the approximation becomes $\ln\ K\ \sim\ 1/T^2$.

The temperature ranges in which these simple behaviours are approximated depend on the vibrational frequencies of the molecules involved in the reaction. For the calculation of a partition function ratio for a pair of isotopic molecules, the vibrational frequencies of each molecule must be known. When solid materials are considered, the evaluation of partition function ratios becomes even more complicated, because it is necessary to consider not only the independent internal vibrations of each molecule, but also the lattice vibrations.

1.3.1.1 Fractionation Factor (α)

For isotope exchange reactions in geochemistry, the equilibrium constant K is often replaced by the fractionation factor $\tilde{\alpha}$. The fractionation factor is defined as the ratio of the numbers of any two isotopes in one chemical compound A divided by the corresponding ratio for another chemical compound B:

$$\alpha_{\mathrm{A-B}} = \frac{R_{\mathrm{A}}}{R_{\mathrm{B}}}. \tag{1.6}$$

If the isotopes are randomly distributed over all possible positions in the compounds A and B, then α is related to the equilibrium constant K by

$$\alpha = \mathrm{K}^{1/\mathrm{n}} \tag{1.7}$$

where n is the number of atoms exchanged. For simplicity, isotope exchange reactions are written such that only one atom is exchanged. In these cases, the equilibrium constant is identical to the fractionation factor. For example, the fractionation factor for the exchange of ^{18}O and ^{16}O between water and $CaCO_3$ is expressed as follows:

$$\mathrm{H_2{}^{18}O} + \frac{1}{3}\mathrm{CaC^{16}O_3} \Leftrightarrow \mathrm{H_2{}^{16}O} + \frac{1}{3}\mathrm{CaC^{18}O_3} \tag{1.8}$$

with the fractionation factor $\alpha CaCO_3$–H_2O defined as:

$$\alpha\mathrm{CaCO_3} - \mathrm{H_2O} = \frac{\left(\frac{^{18}\mathrm{O}}{^{16}\mathrm{O}}\right)_{\mathrm{CaCO_3}}}{\left(\frac{^{18}\mathrm{O}}{^{16}\mathrm{O}}\right)_{\mathrm{H_2O}}} = 1.031\,\mathrm{at}\,25^{\circ}\mathrm{C}. \tag{1.9a}$$

It has become common practice in recent years to replace the fractionation factor α by the ε-value (or separation factor), which is defined as

$$\varepsilon = \alpha - 1. \tag{1.9b}$$

because $\varepsilon \times 1{,}000$ approximates the fractionation in parts per thousand, similar to the $\tilde{\delta}$ value (see below).

1.3.1.2 The Delta Value (δ)

In isotope geochemistry, it is a common practice to express isotopic composition in terms of *delta*-(δ) values. For two compounds, A and B, whose isotopic compositions have been measured in the laboratory by conventional mass spectrometry:

$$\delta_{\mathrm{A}} = \left(\frac{R_{\mathrm{A}}}{R_{\mathrm{st}}} - 1\right) 10^3\ (\%) \tag{1.10}$$

and

$$\delta_{\mathrm{B}} = \left(\frac{R_{\mathrm{B}}}{R_{\mathrm{st}}} - 1\right) 10^3\ (\%), \tag{1.11}$$

where R_{A} and R_{B} are the respective isotope ratio measurements for the two compounds and R_{St} is the defined isotope ratio of a standard sample.

For the two compounds A and B, the δ-values and fractionation factor α are related by:

$$\delta_{\mathrm{A}} - \delta_{\mathrm{B}} = \Delta_{\mathrm{A-B}} \approx 10^3 \ln \alpha_{\mathrm{A-B}}. \tag{1.12}$$

Table 1.3 Comparison between δ, α, and $10^3 \ln \alpha_{A-B}$

δ_A	δ_B	Δ_{A-B}	α_{A-B}	$10^3 \ln \alpha_{A-B}$
1.00	0	1.00	1.001	1.00
5.00	0	5.00	1.005	4.99
10.00	0	10.00	1.01	9.95
15.00	0	15.00	1.015	14.98
20.00	0	20.00	1.02	19.80
10.00	5.00	5.00	1.00498	4.96
20.00	15.00	5.00	1.00493	4.91
30.00	15.00	15.00	1.01478	14.67
30.00	20.00	10.00	1.00980	9.76
30.00	10.00	20.00	1.01980	19.61

Table 1.3 illustrates the closeness of the approximation. Considering experimental uncertainties in isotope ratio determinations (typically $\geq 0.1‰$), these approximations are excellent for differences in δ-values less than about 10 and for δ-values that are relatively small in magnitude.

1.3.1.3 Evaporation–Condensation Processes

Of special interest in stable isotope geochemistry are evaporation–condensation processes, because differences in the vapour pressures of isotopic compounds lead to significant isotope fractionations. For example, from the vapour pressure data for water given in Table 1.2, it is evident that the lighter molecular species are preferentially enriched in the vapour phase, the extent depending upon the temperature. Such an isotopic separation process can be treated theoretically in terms of fractional distillation or condensation under equilibrium conditions as is expressed by the Rayleigh (1896) equation. For a condensation process, this equation is

$$\frac{R_V}{R_{V_0}} = f^{\alpha-1}, \tag{1.13}$$

where R_{vo} is the isotope ratio of the initial bulk composition and R_v is the instantaneous ratio of the remaining vapour (v); f is the fraction of the residual vapour, and the fractionation factor α is given by R_l/R_V (l = liquid). Similarly, the instantaneous isotope ratio of the condensate (R_l) leaving the vapour is given by

$$\frac{R_l}{R_{V_0}} = \alpha f^{\alpha-1} \tag{1.14}$$

and the average isotope ratio of the separated and accumulated condensate (R_l) at any time of condensation is expressed by

$$\frac{\overline{R}_l}{R_{v_0}} = \frac{1-f^{\alpha}}{1-f}. \tag{1.15}$$

For a distillation process, the instantaneous isotope ratios of the remaining liquid and the vapour leaving the liquid are given by

$$\frac{R_l}{R_{l_0}} = f^{\left(\frac{1}{\alpha}-1\right)} \tag{1.16}$$

and

$$\frac{\overline{R}_v}{R_{l_0}} = \frac{1}{\alpha} f^{\left(\frac{1}{\alpha}-1\right)}. \tag{1.17}$$

The average isotope ratio of the separated and accumulated vapour is expressed by

$$\frac{\overline{R}_v}{R_{l_0}} = \frac{1-f^{1/\alpha}}{1-f} (f = \text{fraction of residual liquid}) \tag{1.18}$$

Any isotope fractionation occurring in such a way that the products are isolated from the reactants immediately after formation will show a characteristic trend in isotopic composition. As condensation or distillation proceeds, the residual vapour or liquid will become progressively depleted or enriched with respect to the heavy isotope. A natural example is the fractionation between oxygen isotopes in the water vapour of a cloud and the raindrops released from the cloud. The resulting decrease of the $^{18}O/^{16}O$ ratio in the residual vapour and the instantaneous isotopic composition of the raindrops released from the cloud are shown in Fig. 1.4 as a function of the fraction of vapour remaining in the cloud.

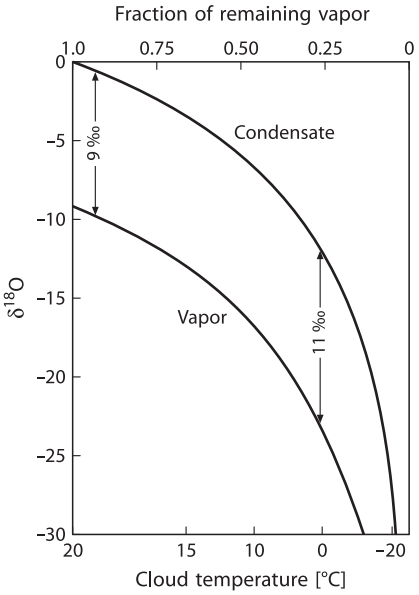

Fig. 1.4 $\delta^{18}O$ in a cloud vapour and condensate plotted as a function of a fraction of remaining vapour in a cloud for a Rayleigh process. The temperature of the cloud is shown on the lower axis. The increase in fractionation with decreasing temperature is taken into account (after Dansgaard 1964)

1.3.2 Kinetic Effects

The second main phenomena producing fractionations are kinetic isotope effects, which are associated with incomplete and unidirectional processes like evaporation, dissociation reactions, biologically mediated reactions, and diffusion. The latter process is of special significance for geological purposes, which warrants separate treatment (Sect. 1.3.3). A kinetic isotope effect also occurs, when the rate of a chemical reaction is sensitive to atomic mass at a particular position in one of the reacting species.

The theory of kinetic isotope fractionations has been discussed by Bigeleisen and Wolfsberg (1958), Melander (1960), and Melander and Saunders (1980). Knowledge of kinetic isotope effects is very important, because it can provide information about details of reaction pathways.

Quantitatively, many observed deviations from simple equilibrium processes can be interpreted as consequences of the various isotopic components having different rates of reaction. Isotope measurements taken during unidirectional chemical reactions always show a preferential enrichment of the lighter isotope in the reaction products. The isotope fractionation introduced during the course of an unidirectional reaction may be considered in terms of the ratio of rate constants for the isotopic substances. Thus, for two competing isotopic reactions

$$k_1 \rightarrow k_2, \tag{1.19a}$$

$$A_1 \rightarrow B_1, \text{ and } A_2 \rightarrow B_2, \tag{1.19b}$$

the ratio of rate constants for the reaction of light and heavy isotope species k_1/k_2, as in the case of equilibrium constants, is expressed in terms of two partition function ratios, one for the two reactant isotopic species, and one for the two isotopic species of the activated complex or transition state, A^X:

$$\frac{k_1}{k_2} = \left[\frac{Q^*_{(A_2)}}{Q^*_{(A_1)}} \Big/ \frac{Q^*_{(A_2^X)}}{Q^*_{(A_1^X)}}\right] \frac{\nu_1}{\nu_2}. \tag{1.20}$$

The factor ν_1/ν_2 in the expression is a mass term ratio for the two isotopic species. The determination of the ratio of rate constants is, therefore, principally the same as the determination of an equilibrium constant, although the calculations are not so precise because of the need for detailed knowledge of the transition state. The term *transition state* refers to the molecular configuration that is most difficult to attain along the path between the reactants and the products. This theory follows the concept that a chemical reaction proceeds from some initial state to a final configuration by a continuous change, and that there is some critical intermediate configuration called the activated species or transition state. There are a small number of activated molecules in equilibrium with the reacting species and the rate of reaction is controlled by the rate of decomposition of these activated species.

1.3.3 Mass Dependent and Mass Independent Isotope Effects

1.3.3.1 Mass Dependent Effects

At thermodynamic equilibrium, isotope distributions are strictly governed by relative mass differences among different isotopes of an element. Mass dependent relationships hold for many kinetic processes as well. Thus, it has been a common belief that for most natural reactions, isotope effects arise solely because of isotopic mass differences. This means that for an element with more than two isotopes, such as oxygen or sulfur, the enrichment of ^{18}O relative to ^{16}O or ^{34}S relative to ^{32}S is expected to be approximately twice as large as the enrichment of ^{17}O relative to ^{16}O or as the enrichment of ^{33}S relative to ^{32}S. Therefore, for many years, interest in measuring more than one isotope ratio of a specific element was limited. Recent improvements of multiple-stable isotope analysis have demonstrated, however, that different mass dependent processes (e.g., diffusion, metabolism, high temperature equilibrium processes) can deviate by a few per cent and follow slightly different mass dependent fractionation laws (Young et al. 2002; Miller 2002; Farquhar et al. 2003). These very small differences are measurable and have been documented for oxygen (Luz et al. 1999), magnesium (Young et al. 2002), and sulfur (Farquhar et al. 2003).

It is a common practice to describe mass dependent isotope fractionation processes by a single linear curve on a three-isotope-plot (Matsuhisa et al. 1978). The resulting straight lines are referred to as terrestrial mass fractionation lines and deviations from it are used as indicating nonmass-dependent isotope effects. The three-isotope-plot is based on the approximation of a power law function to linear format. To describe how far a sample plots off the mass-dependent fractionation line, a new term has been introduced: $\Delta^{17}O$, $\Delta^{25}Mg$, $\Delta^{33}S$, etc. Several definitions of Δ have been introduced in the literature, which have been discussed by Assonov and Brenninkmeijer (2005). The simplest definition is given by:

$$\Delta^{17}O = \delta^{17}O - \lambda\delta^{18}O$$
$$\Delta^{25}Mg = \delta^{25}Mg - \lambda\delta^{26}Mg$$
$$\Delta^{33}S = \delta^{33}S - \lambda\delta^{34}S,$$

where λ is the main parameter that characterizes the mass dependent fractionation. The value of the coefficient λ depends on molecular mass, which for oxygen may range from 0.53 for atomic oxygen to 0.500 for species with high molecular weight. Recent progress in high precision measurement of isotope ratios allows to distinguish λ-values in the third decimal, which has obscured the difference between mass dependent and mass-independent fractionations at small Δ-values (Farquhar and Wing 2003).

1.3.3.2 Mass-Independent Effects

A few processes in nature do not follow the above mass-dependent fractionations. Deviations from mass-dependent fractionations were first observed in meteorites (Clayton et al. 1973) and in ozone (Thiemens and Heidenreich 1983). These mass-independent fractionations (MIF) describe relationships that violate the mass-dependent rules $\delta^{17}O \approx 0.5\delta^{18}O$ or $\delta^{33}S \approx 0.5\delta^{34}S$ and produce isotopic compositions with nonzero $\Delta^{17}O$ and $\Delta^{33}S$.

A number of experimental and theoretical studies have focused on the causes of mass-independent fractionation effects, but as summarized by Thiemens (1999), the mechanism for mass-independent fractionations remains uncertain. The best studied reaction is the formation of ozone in the stratosphere. Mauersberger et al. (1999) demonstrated experimentally that it is not the symmetry of a molecule that determines the magnitude of ^{17}O enrichment, but it is the difference in the geometry of the molecule. Gao and Marcus (2001) presented an advanced model, which has led to a better understanding of nonmass-dependent isotope effects.

Mass-independent isotopic fractionations are widespread in the earth's atmosphere and have been observed in O_3, CO_2, N_2O, and CO, which are all linked to reactions involving stratospheric ozone (Thiemens 1999). For oxygen, this is a characteristic marker in the atmosphere (see Sect. 3.9). These processes probably also play a role in the atmosphere of Mars and in the pre-solar nebula (Thiemens 1999). Oxygen isotope measurements in meteorites demonstrate that the effect is of significant importance in the formation of the solar system (Clayton et al. 1973a) (Sect. 3.1).

There are numerous terrestrial solid reservoirs, where mass-independent isotope variations have been observed. Farquhar et al. (2000c) and Bao et al. (2000) reported mass-independent oxygen isotope fractionations in terrestrial sulfates. A positive ^{17}O excess in sulfate has been found to be almost ubiquitous in desert environments (Bao et al. 2001). Significant mass-independent sulfur isotope fractionations have been reported by Farquhar et al. (2000c) in sulfides older than 2.4 Ga, whereas these fractionations do not occur in measurable amounts in sulfides younger than 2.4 Ga (see Fig. 3.29). Smaller, but clearly resolvable, MIFs have been measured in volcanic aerosol sulfates in polar ice (Baroni et al. 2007). Photolysis of SO_2 to sulfuric acid is thought to be the source reaction for these sulfur MIFs (Farquhar et al. 2001). These recent findings indicate that nonmass-dependent isotope fractionations are more abundant than originally thought and constitute a novel form of isotopic fingerprint.

1.3.4 Multiply Substituted Isotopologues

In stable isotope geochemistry, generally bulk isotopic compositions of natural samples are given (e.g., $\delta^{13}C$, $\delta^{18}O$, etc.). In the measured gases, bulk compositions depend only on abundances of molecules containing one rare isotope (e.g., $^{13}C^{16}O^{16}O$

Table 1.4 Stochastic abundances of CO_2 isotopologues (Eiler 2007)

Mass	Isotopologue	Relative abundance
44	$^{12}C^{16}O_2$	98.40%
45	$^{13}C^{16}O_2$	1.11%
	$^{12}C^{17}O^{16}O$	748 ppm
46	$^{12}C^{18}O^{16}O$	0.40%
	$^{13}C^{17}O^{16}O$	8.4 ppm
	$^{12}C^{17}O_2$	0.142 ppm
47	$^{13}C^{18}O^{16}O$	44.4 ppm
	$^{12}C^{17}O^{18}O$	1.50 ppm
	$^{13}C^{17}O_2$	1.60 ppb
48	$^{12}C^{18}O_2$	3.96 ppm
	$^{13}C^{17}O^{18}O$	16.8 ppb
49	$^{13}C^{18}O_2$	44.5 ppb

or $^{12}C^{18}O^{16}O$). However, there also exist in very low concentration, molecules having more than one rare isotope such as $^{13}C^{18}O^{16}O$ or $^{12}C^{18}O^{17}O$. These so-called isotopologues are molecules that differ from one another only in isotopic composition. Table 1.4 gives the stochastic abundances of isotopologues of CO_2.

Already Urey (1947) and Bigeleisen and Mayer (1947) recognized that multiply substituted isotoplogues have unique thermodynamic properties different from singly substituted isotopologues of the same molecule. Natural distributions of multiply substituted isotopologues can thus provide unique constraints on geological, geochemical, and cosmochemical processes (Wang et al. 2004).

Normal gas-source mass spectrometers do not allow meaningful abundance measurements of these very rare species. However, if some demands on high abundance sensitivity, high precision, and high mass resolving power are met, John Eiler and his group (e.g., Eiler and Schauble 2004; Affek and Eiler 2006; Eiler 2007) have reported precise ($<0.1‰$) measurements of CO_2 with mass 47 (Δ_{47}-values) with an especially modified, but normal gas-source mass spectrometer. Δ_{47}-values are defined as $‰$ difference between the measured abundance of all molecules with mass 47 relative to the abundance of 47, expected for the stochastic distribution.

This new technique is also termed *clumped isotope geochemistry* (Eiler 2007) because the respective species are produced by clumping two rare isotopes together. Deviations from stochastic distributions may result from all processes of isotope fractionation observed in nature. Thus, processes that lead to isotope fractionations of bulk compositions also lead to fractionations of multiply substituted isotopologues, implying that clumped isotope geochemistry is potentially applicable to many geochemical problems (Eiler 2007). So far, the most used application is a carbonate thermometer based on the formation of the CO_3^- group containing both ^{13}C and ^{18}O. Schauble et al. (2006) calculated an $\sim 0.4‰$ excess of $^{13}C^{18}O^{16}O$ groups in carbonate groups at room temperature relative to what would be expected in a stochastic mixture of carbonate isotopologues with the same bulk $^{13}C/^{12}C$,

$^{18}O/^{16}O$, and $^{17}O/^{16}O$ ratios. The excess amount of $^{13}C^{18}O^{16}O$ decreases with increasing temperature and thus may serve as a thermometer (Ghosh et al. 2006).

Potentially, the advantage of this thermometer will be that it allows the determination of temperatures of carbonate formation without knowing the isotope composition of the fluid. Came et al. (2007), for example, presented temperature estimates for early Silurian and late Carboniferous seawater, which are consistent with varying CO_2 concentrations.

1.3.5 Diffusion

Ordinary diffusion can cause significant isotope fractionations. In general, light isotopes are more mobile and hence diffusion can lead to a separation of light from heavy isotopes. For gases, the ratio of diffusion coefficients is equivalent to the inverse square root of their masses. Consider the isotopic molecules of carbon in CO_2 with masses $^{12}C^{16}O^{16}O$ and $^{13}C^{16}O^{16}O$ having molecular weights of 44 and 45. Solving the expression, equating the kinetic energies ($1/2\,m\,v^2$) of both species, the ratio of velocities is equivalent to the square root of 45/44 or 1.01. That is regardless of temperature, the average velocity of $^{12}C^{16}O^{16}O$ molecules is about 1% greater than the average velocity of $^{13}C^{16}O^{16}O$ molecules in the same system. This isotope effect, however, is more or less limited to ideal gases, where collisions between molecules are infrequent and intermolecular forces are negligible. The carbon isotope fractionation of soil–CO_2 due to diffusional movement has been estimated to be around 4‰ for instance (Cerling 1984; Hesterberg and Siegenthaler 1991).

Distinctly different from ordinary diffusion is the process of thermal diffusion in that a temperature gradient results in a mass transport. The greater the mass difference, the greater is the tendency of the two species to separate by thermal diffusion. A natural example of thermal diffusion has been presented by Severinghaus et al. (1996), who observed a small isotope depletion of ^{15}N and ^{18}O in air from a sand dune relative to the free atmosphere. This observation is contrary to the expectation that heavier isotopes in unsaturated zones of soils would be enriched by gravitational settling. Such thermally driven diffusional isotope effects have also been described in air bubbles from ice cores (Severinghaus et al. 1998; Severinghaus and Brook 1999; Grachiev and Severinghaus 2003). Surprisingly large fractionations by thermal diffusion at very high temperatures have been reported by Richter (2007), who observed 8‰ fractionation for $^{26}Mg/^{24}Mg$ associated with a change of only 150°C across molten basalt. Earlier diffusion experiments by Richter et al. (1999, 2003) between molten basalt and rhyolite also demonstrated considerable isotope fractionations of Li, Ca, and Ge (the latter used as a Si analogue). Especially for Li, diffusion processes occurring at high temperatures seem to be of first order importance (see p. 44). Thus the notion that isotope fractionations above 1,000°C appear to be negligible has to be reconsidered.

In solutions and solids, the relationships are much more complicated than in gases. The term *solid state diffusion* generally includes volume diffusion and diffusion mechanisms where the atoms move along paths of easy diffusion such as grain boundaries and surfaces. Diffusive-penetration experiments indicate a marked enhancement of diffusion rates along grain boundaries, which are orders of magnitude faster than for volume diffusion. Thus, grain boundaries can act as pathways of rapid exchange. Volume diffusion is driven by the random temperature-dependent motion of an element or isotope within a crystal lattice and it depends on the presence of point defects, such as vacancies or interstitial atoms within the lattice.

The flux F of elements or isotopes diffusing through a medium is proportional to the concentration gradient $(\mathrm{d}c/\mathrm{d}x)$ such that:

$$F = -D(\mathrm{d}c/\mathrm{d}x) \quad (\text{Fick's first law}), \tag{1.21}$$

where D represents the diffusion coefficient, and the minus sign denotes that the concentration gradient has a negative slope, i.e., elements or isotopes move from points of high concentration towards points of low concentration. The diffusion coefficient D varies with temperature according to the Arrhenius relation

$$D = D_{\mathrm{o}}\, e^{(-Ea/RT)}, \tag{1.22}$$

where D_{o} is a temperature-independent factor, Ea is the activation energy, R is the gas constant and T is in Kelvin.

In recent years, there have been several attempts to determine diffusion coefficients, mostly utilizing secondary ion mass spectrometry (SIMS), where isotope compositions have been measured as a function of depth below a crystal surface after exposing the crystal to solutions or gases greatly enriched with the heavy isotopic species.

A plot of the logarithm of the diffusion coefficient versus reciprocal temperature yields a linear relationship over a significant range of temperature for most minerals. Such an Arrhenius plot for various minerals is shown in Fig. 1.5, which illustrates the variability in diffusion coefficients for different minerals. The practical application of this fact is that the different minerals in a rock will exchange oxygen at different rates and become closed systems to isotopic exchange at different temperatures. As a rock cools from the peak of a thermal event, the magnitude of isotope fractionations between exchanging minerals will increase. The rate at which the coexisting minerals can approach equilibrium at the lower temperature is limited by the volume diffusion rates of the respective minerals.

Several models for diffusive transport in and among minerals have been discussed in the literature one is the fast grain boundary (FGB) model of Eiler et al. (1992, 1993). The FGB model considers the effects of diffusion between non-adjacent grains and shows that, when mass balance terms are included, closure temperatures become a strong function of both the modal abundances of constituent minerals and the differences in diffusion coefficients among all coexisting minerals.

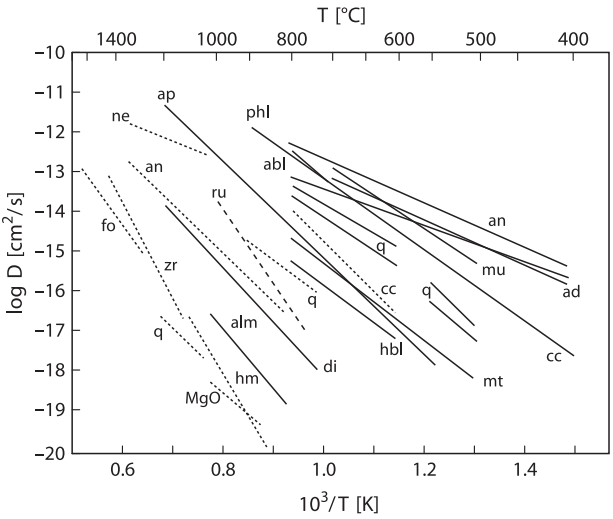

Fig. 1.5 Arrhenius plot of diffusion coefficients versus reciprocal temperatures for various minerals. Data from phases reacted under *wet* conditions are given as *solid lines*, whereas *dry* conditions are represented by *dashed lines*. Note that the rates for dry systems are generally lower and have higher activation energies (*steeper slope*s). (Modified after Cole and Chakraborty 2001)

1.3.6 Other Factors Influencing Isotopic Fractionations

1.3.6.1 Pressure

It is commonly assumed that temperature is the main variable determining the isotopic fractionation and that the effect of pressure is negligible, because molar volumes do not change with isotopic substitution. This assumption is generally fulfilled, except for hydrogen. Driesner (1997), Horita and Berndt (1999, 2002), and Polyakov et al. (2006) have shown, however, that for isotope exchange reactions involving water, changes of pressure can influence isotope fractionations. Driesner (1997) calculated hydrogen isotope fractionations between epidote and water and observed a change from $-90‰$ at 1 bar to $-30‰$ at 4,000 bars at 400°C. Horita and Berndt (1999, 2002) presented experimental evidence for a pressure effect in the system brucite $Mg(OH)_2$– water. Theoretical calculations indicate that pressure effects largely result on water rather than brucite. Thus, it is likely that D/H fractionations of any hydrous mineral are subject to similar pressure effects (Horita et al. 2002). These pressure effects have to be taken into account when calculating the hydrogen isotope composition of the fluid from the mineral composition.

1.3.6.2 Chemical Composition

Qualitatively, the isotopic composition of a mineral depends to a very high degree upon the nature of the chemical bonds within the mineral and to a smaller degree upon the atomic mass of the respective elements. In general, bonds to ions with a high ionic potential and small size are associated with high vibrational frequencies and have a tendency to incorporate preferentially the heavy isotope. This relationship can be demonstrated by considering the bonding of oxygen to the small highly charged Si^{4+} ion, compared to the relatively large Fe^{2+} ion of the common rock-forming minerals. In natural mineral assemblages, quartz is the most ^{18}O-rich mineral and magnetite is the most ^{18}O-deficient given equilibration in the system. Furthermore, carbonates are always enriched in ^{18}O relative to most other mineral groups because oxygen is bonded to the small, highly charged C^{4+} ion. The mass of the divalent cation is of secondary importance to the C–O bonding. However, the mass effects are apparent in ^{34}S distributions among sulfides, where, for example, ZnS always concentrates ^{34}S relative to coexisting PbS.

Compositional effects in silicates are complex and difficult to deduce, because of the very diverse substitution mechanisms in silicate minerals (Kohn and Valley 1998c). The largest fractionation effect is clearly related to the NaSi = CaAl substitution in plagioclases, which is due to the higher Si to Al ratio of albite and the greater bond strength of the Si–O bond relative to the Al–O bond. In pyroxenes, the jadeite ($NaAlSi_2O_6$)–diopside ($CaMgSi_2O_6$) substitution also involves Al, but Al in this case replaces an octahedral rather than tetrahedral site. Chacko et al. (2001) estimate that at high temperatures the Al-substitution in pyroxenes is about $0.4‰$ per mole Al-substitution in the tetrahedral site. The other very common substitutions, the Fe–Mg and the Ca–Mg substitution, do not generate any significant difference in fractionation (Chacko et al. 2001).

1.3.6.3 Crystal Structure

Structural effects are secondary in importance to those arising from the primary chemical bonding; the heavy isotope being concentrated in the more closely packed or well-ordered structures. The ^{18}O and D fractionations between ice and liquid water arise mainly from differences in the degree of hydrogen bonding (order). A relatively large isotope effect associated with structure is observed between graphite and diamond (Bottinga 1969b). With a modified increment method, Zheng (1993a) has calculated this structural effect for the SiO_2 and Al_2SiO_5 polymorphs and demonstrated that ^{18}O will be enriched in the high pressure forms. In this connection, it should be mentioned, however, that Sharp (1995) by analyzing natural Al_2SiO_5 minerals observed no differences for kyanite versus sillimanite.

1.3.7 Isotope Geothermometers

Isotope thermometry has become well established since the classic paper of Harold Urey (1947) on the thermodynamic properties of isotopic substances. The partitioning of two stable isotopes of an element between two mineral phases can be viewed as a special case of element partitioning between two minerals. The most important difference between the two exchange reactions is the pressure-insensitivity of isotope partitioning due to the negligible ΔV of reaction for isotope exchange. This represents a considerable advantage relative to the numerous types of other geothermometers, all of which exhibit a pressure dependence.

The necessary condition to apply an isotope geothermometer is isotope equilibrium. Isotope exchange equilibrium should be established during reactions whose products are in *chemical* and *mineralogical* equilibrium. Demonstration that the minerals in a rock are in oxygen isotope equilibrium is a strong evidence that the rock is in chemical equilibrium. To break Al–O and Si–O bonds and allow rearrangement towards oxygen isotope equilibrium needs sufficient energy to effect chemical equilibrium as well.

Theoretical studies show that the fractionation factor α for isotope exchange between minerals is a linear function of $1/T^2$, where T is temperature in degrees Kelvin. Bottinga and Javoy (1973) demonstrated that O-isotopic fractionation between anhydrous mineral pairs at temperatures $>500^\circ$C can be expressed in terms of a relationship of the form:

$$1{,}000 \ln \alpha = A/T^2, \tag{1.23}$$

which means that the factor A has to be known in order to calculate a temperature of equilibration. By contrast, fractionations at temperatures $<500^\circ$C can be expressed by an equation of the form

$$1{,}000 \ln \alpha = A/T^2 + B. \tag{1.24}$$

Although in many instances, B is approximately zero simplifying the expression.

One drawback to isotope thermometry in slowly cooled metamorphic and magmatic rocks is that, temperature estimates are often significantly lower than those from other geothermometers. This results from isotopic resetting associated with retrograde isotope exchange between coexisting phases or with transient fluids. During cooling in closed systems, volume diffusion may be the principal mechanism by which isotope exchange occurs between coexisting minerals.

Giletti (1986) proposed a model in which experimentally-derived diffusion data can be used in conjunction with measured isotope ratios to explain disequilibrium isotope fractionations in slowly cooled, closed-system mineral assemblages. This approach describes diffusional exchange between a mineral and an infinite reservoir, whose bulk isotopic composition is constant during exchange. However, mass balance requires that loss or gain of an isotope from one mineral must be balanced by a change in the other minerals still subject to isotopic exchange. Numerical modeling

by Eiler et al. (1992) has shown that closed-system exchange depends not only on modal proportions of all of the minerals in a rock, but also on oxygen diffusivity in minerals, grain size, grain shape, and cooling rate. As shown by Kohn and Valley (1998c), there is an important water fugacity dependence as well. In the presence of fluids, further complications may arise because isotope exchange may also occur by solution-reprecipitation or chemical reaction rather than solely by diffusion.

Three different methods have been used to determine the equilibrium fractionations for isotope exchange reactions:

(a) Theoretical calculations
(b) Experimental determinations in the laboratory
(c) Empirical or semiempirical calibrations

Method (c) is based on the idea that the calculated *formation temperature* of a rock (calculated from other geothermometers) serves as a calibration to the measured isotopic fractionations, assuming that all minerals were at equilibrium. However, because there is evidence that equilibrium is not always attained or retained in nature, such empirical calibrations should be regarded with caution.

Nevertheless, rigorous applications of equilibrium criteria to rock-type and the minerals investigated can provide important information on mineral fractionations (Kohn and Valley 1998c; Sharp 1995; Kitchen and Valley 1995).

1.3.7.1 Theoretical Calculations

Calculations of equilibrium isotope fractionation factors have been particularly successful for gases. Richet et al. (1977) calculated the partition function ratios for a large number of gaseous molecules. They demonstrated that the main source of error in the calculation is the uncertainty in the vibrational molecular constants.

The theory developed for perfect gases could be extended to solids, if the partition functions of crystals could be expressed in terms of a set of vibrational frequencies that correspond to its various fundamental modes of vibration (O'Neil 1986). By estimating thermodynamic properties from elastic, structural, and spectroscopic data, Kieffer (1982) and subsequently Clayton and Kieffer (1991) calculated oxygen isotope partition function ratios and from these calculations derived a set of fractionation factors for silicate minerals. The calculations have no inherent temperature limitations and can be applied to any phase for which adequate spectroscopic and mechanical data are available. They are, however, limited in accuracy as a consequence of the approximations needed to carry out the calculations and the limited accuracy of the spectroscopic data.

Isotope fractionations in solids depend on the nature of the bonds between atoms of an element and the nearest atoms in the crystal structure (O'Neil 1986). The correlation between bond strength and oxygen isotope fractionation was investigated by Schütze (1980), who developed an *increment* method for predicting oxygen isotope fractionations in silicate minerals. Richter and Hoernes (1988) applied this method to the calculation of oxygen isotope fractionations between silicate minerals and

water. More recently, Zheng (1991, 1993b, c) extended the increment method by using parameters of crystal chemistry with no empirical factor. The fractionation factors calculated using these methods over the temperature range 0–1,200°C are in relatively good agreement with experimental calibrations.

1.3.7.2 Experimental Calibrations

In general, experimental calibrations of isotope geothermometers have been performed between 250 and 800°C. The upper temperature limit is usually determined by the stability of the mineral being studied or by limitations of the experimental apparatus, whereas the lower temperature limit is determined by the decreasing rate of exchange.

Various experimental approaches have been used to determine fractionation factors. The three most common techniques are described below:

Two-Direction Approach
This method is analogous to reversing reactions in experimental petrology and is the only method by which the attainment of equilibrium can be convincingly demonstrated. Equilibrium fractionations are achieved by starting on opposite sides of the equilibrium distribution.

Partial-Exchange Technique
The partial-exchange technique is used when rates of isotopic exchange are relatively low and is based on the assumption that the rates of isotope exchange for companion exchange experiments are identical. Experimental runs have to be the same in every respect, except in the isotopic compositions of the starting materials. Rates of isotope exchange reactions in heterogeneous systems are relatively high at first (surface control) and then become progressively lower with time (diffusion control). Four sets of experiments are shown in Fig. 1.6 for the CO_2 – graphite system (after Scheele and Hoefs 1992). Northrop and Clayton (1966) presented a set of equations to describe the kinetics of isotope exchange reactions and developed a general equation for the partial-exchange technique. At low degrees of exchange, the fractionations determined by the partial-exchange technique are often larger than the equilibrium fractionations (O'Neil 1986).

Three-Isotope Method
This method, introduced by Matsuhisa et al. (1978) and later modified by Matthews et al. (1983a), uses the measurement of both $^{17}O/^{16}O$ and $^{18}O/^{16}O$ fractionations in a single experiment that has gone to equilibrium. The initial $^{18}O/^{16}O$ fractionation for the mineral–fluid system is selected to be close to the assumed equilibrium, while the initial $^{17}O/^{16}O$ fractionation is chosen to be very different from the

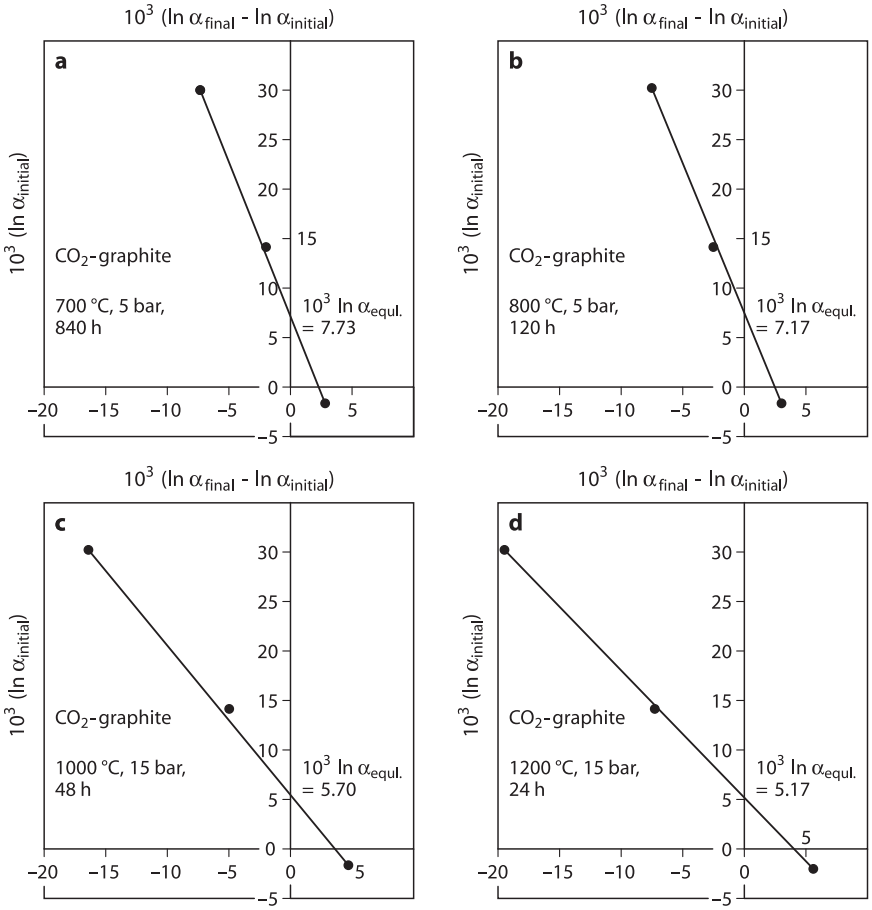

Fig. 1.6 CO_2-graphite partial-exchange experiments in a Northrop and Clayton plot at 700, 800, 1,000 and 1,200°C. The connecting line in experiment at 1,200°C has a plane slope and defines the intercept more precisely than the experiment at 700°C (after Scheele and Hoefs 1992)

equilibrium value. In this way, the change in the $^{17}O/^{16}O$ fractionations monitor the extent of isotopic exchange and the $^{18}O/^{16}O$ fractionations reflect the equilibrium value. Figure 1.7 gives a schematic diagram of the three-isotope-exchange method.

Most of the published data on mineral fractionations have been determined by exchange of single minerals with water. This approach is limited by two factors: (1) many minerals are unstable, melt, or dissolve in the presence of water and (2) the temperature dependence of the fractionation factor for aqueous systems is complicated as a consequence of the high vibrational frequencies of the water molecule. An alternative approach to the experimental determination of isotope fractionation between minerals was first employed by Clayton et al. (1989) and Chiba et al. (1989), who demonstrated that both limitations can be avoided by using $CaCO_3$, instead of H_2O, as the common exchange medium. These studies showed

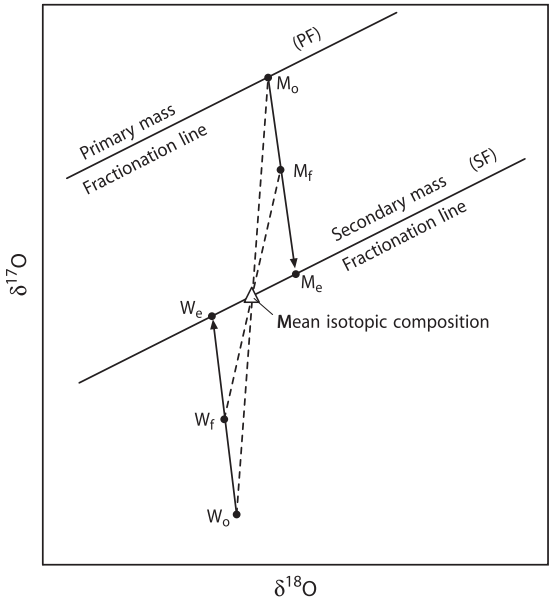

Fig. 1.7 Schematic representation of the three-isotope exchange method. Natural samples plotted on the primary mass fractionation line (PF). Initial isotopic composition are mineral (M_o) and water (W_o) which is well removed from equilibrium with M_o in $\delta^{17}O$, but very close to equilibrium with M_o in $\delta^{18}O$. Complete isotopic equilibrium is defined by a secondary mass fractionation line (SF) parallel to PF and passing through the bulk isotopic composition of the mineral plus water system. Isotopic compositions of partially equilibrated samples are M_f and W_f and completely equilibrated samples are M_e and W_e. Values for M_e and W_e can be determined by extrapolation from the measured values of M_o, M_f, W_o, and W_f (after Matthews et al. 1983a

that most common silicates undergo rapid oxygen isotope exchange with $CaCO_3$ at temperatures above 600°C and pressures of 15 kbar.

Advantages of the carbonate-exchange technique are: (1) experiments up to 1,400°C, (2) no problems associated with mineral solubility and (3) ease of mineral separation (reaction of carbonate with acid). Mineral fractionations derived from hydrothermal and carbonate exchange techniques are generally in good agreement except for fractionations involving quartz and calcite. A possible explanation is a salt effect in the quartz–water system, but no salt effect has been observed in the calcite–water system (Hu and Clayton 2003).

1.4 Basic Principles of Mass Spectrometry

Mass spectrometric methods are, by far, the most effective means of measuring isotope abundances. A mass spectrometer separates charged atoms and molecules on the basis of their masses and motions in magnetic and/or electrical fields. The design

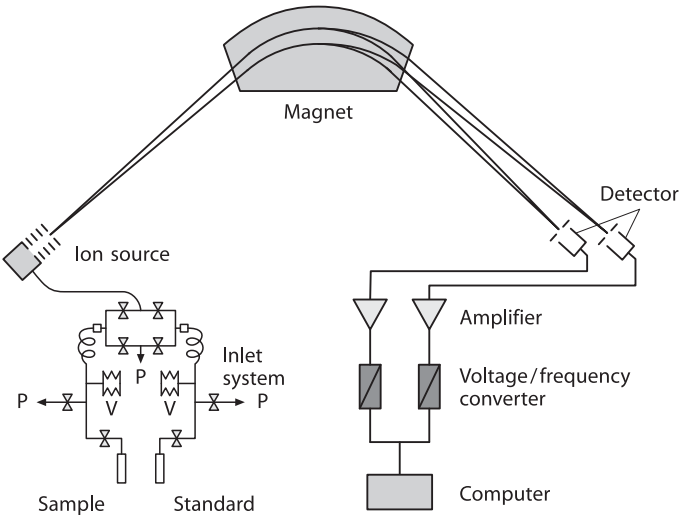

Fig. 1.8 Schematic representation of a gas-source mass spectrometer for stable isotope measurements. P denotes pumping system, *V* denotes a variable volume

and applications of the many types of mass spectrometers are too broad to cover here. Therefore, only the principles of mass analysis will be discussed briefly (for a more detailed review see Brand (2002)).

In principle, a mass spectrometer may be divided into four different central constituent parts: (1) the inlet system, (2) the ion source, (3) the mass analyzer, and (4) the ion detector (see Fig. 1.8).

1. Special arrangements for the *inlet system* include a changeover valve. This allows rapid, consecutive analysis between two gas samples (sample and standard gas) within a couple of seconds. The two gases are fed from reservoirs by capillaries of around 0.1 mm in diameter and about 1 m in length. While one gas flows to the ion source, the other flows to a waste pump so that flow through the capillaries remains uninterrupted. To avoid a mass discrimination, isotope abundance measurements of gaseous substances are carried out utilizing viscous gas flow. During viscous gas flow, the free path length of molecules is small, molecule collisions are frequent (causing the gas to be well mixed), and no mass separation takes place. At the end of the viscous-flow inlet system, there is a *leak*, a constriction in the flow line. The smallest amount of sample that can be analyzed with high precision using the dual inlet system is limited by the maintenance of viscous-flow conditions. This is generally in the order of 15–20 mbar (Brand 2002). When trying to reduce sample size, it is necessary to concentrate the gas into a small volume in front of the capillary.
2. The *ion source* is that part of the mass spectrometer, where ions are formed, accelerated, and focused into a narrow beam. In the ion source, the gas flow is always molecular. Ions of gaseous samples are most reliably produced by electron

bombardment. A beam of electrons is emitted by a heated filament, usually tungsten or rhenium and is accelerated by electrostatic potentials to an energy between 50 and 150 eV before entering the ionization chamber, which maximizes the efficiency of single ionization. Following ionization, any charged molecule can be further fragmented into several pieces depending on the energy the ion has acquired, producing a mass spectrum of a specific compound.

To increase the ionization probability, a homogeneous weak magnetic field is used to keep the electrons on a spiral path. At the end of the ionization chamber, electrons are collected in a positively charged trap, where the electron current is measured and kept constant by the emission regulator circuitry.

The ionized molecules are drawn out of the electron beam by action of an electric field, subsequently accelerated by up to several kV and their path shaped into a beam, which passes through an exit slit into the analyzer. Thus, the positive ions entering the magnetic field are essentially monoenergetic, i.e., they will possess the same kinetic energy, given by the equation:

$$1/2Mv^2 = eV. \tag{1.25}$$

The efficiency of the ionization process determines the sensitivity of the mass spectrometer, which generally is on the order of 1,000–2,000 molecules per ion (Brand 2002).

3. The *mass analyzer* separates the ion beams emerging from the ion source according to their m/e (mass/charge) ratios. As the ion beam passes through the magnetic field, the ions are deflected into circular paths, the radii of which are proportional to the square root of m/e. Thus, the ions are separated into beams, each characterized by a particular value of m/e.

In 1940, Nier introduced the sector magnetic analyzer. In this type of analyzer, deflection takes place in a wedge-shaped magnetic field. The ion beam enters and leaves the field at right angles to the boundary, so the deflection angle is equal to the wedge angle, for instance, 60°. The sector instrument has the advantage of its source and detector being comparatively free from the mass-discriminating influence of the analyzer field.

4. After passing through the magnetic field, the separated ions are collected in *ion detectors*, where the input is converted into an electrical impulse, which is then fed into an amplifier. The use of multiple detectors to simultaneously integrate the ion currents was introduced by Nier et al. (1947). The advantage of the simultaneous measurement with two separate amplifiers is that relative fluctuations of the ion currents as a function of time are the same for all m/e beams. Each detector channel is fitted with a high ohmic resistor appropriate for the mean natural abundance of the ion current of interest.

Modern isotope ratio mass spectrometers have at least three Faraday collectors, which are positioned along the focal plane of the mass spectrometer. Because the spacing between adjacent peaks changes with mass and because the scale is not linear, each set of isotopes often requires its own set of Faraday cups.

1.4.1 Continuous Flow: Isotope Ratio Monitoring Mass Spectrometers

Between the early 1950s, when the dual viscous-flow mass spectrometer was introduced by Nier and the mid 1980s only minor modifications have been made on the hardware of commercial mass spectrometers. Special efforts have been undertaken in the past years to reduce the sample size for isotope measurements. This has led to a modification of the classic dual inlet technique to the continuous-flow isotope ratio monitoring mass spectrometer in which the gas to be analyzed is a trace gas in a stream of carrier gas, which achieves viscous-flow conditions. Today, the majority of gas mass spectrometers are sold with the continuous flow system, instead of the dual inlet system.

The classical off-line procedures for sample preparations are time consuming and analytical precision depends on the skill of the investigator. With on-line techniques, using a combination of an elemental analyzer directly coupled to the mass spectrometer many problems of the off-line preparation can be overcome and minimized. Differences in both techniques are summarized in Table 1.5.

This new generation of mass spectrometers is often combined with chromatographic techniques. The sample size required for an isotope measurement has been drastically reduced to the nano- or even pico-molar range (Merritt and Hayes 1994). Important features of the GC–IRMS technique are (Brand 2002):

1. Ion currents are measured in the order in which molecules emerge from a GC column, without significant capability of modifying their intensity relative to the reference gas. Chromotagraphy separates not only different chemical species, but also the different isotope species, which means that the isotope composition of a compound varies across the peak of the chemical species after elution. Therefore, each peak must be integrated over its entire width to obtain the true isotope ratio.
2. The time for measurement of the isotope signals is restricted by the width of the chromatographic peak. For sharply defined peaks, this can mean less than 5 s.

Table 1.5 Differences between the offline and online techniques

Offline method (dual inlet)	Online method (continuous flow)
Offline sample preparation	Online sample preparation
Offline purification of gases	Purification of gases by GC column
Large sample size (mg)	Small sample size (micrograms)
Direct inlet of sample gas	Sample gas inlet via carrier gas
Pressure adjust of both gases	No pressure adjust, linearity, and stability of the system are necessary conditions
Sample/standard changes (>6 times)	One peak per sample
δ-value calculated from statistical mean	δ-value calculated by peak integration and reference gas
System calibration on a monthly basis	System calibration on a daily basis and during the run
Little problems with homogeneity of sample	Problems with homogeneity of sample

3. Absolute sensitivity is much more important than with the dual inlet system. Since sample sizes required for chromatography are significantly smaller, it is often important to use a significantly large set of samples in order to obtain a statistically sound data base.

Standardization has to be accomplished through the use of an added internal standard, whose isotopic composition has been determined using conventional techniques.

The development of this technique has proceeded along several independent paths with two principal lines being elemental analyzer–IRMS and capillary gas chromatography–IRMS. In elemental analyzers, samples are combusted to CO_2, N_2, SO_2, and H_2O, which are either chemically trapped or separated on GC columns. The advantages of these techniques are an automated preparation with low costs per sample and a large sample through-put.

1.5 Standards

The accuracy with which *absolute* isotope abundances can be measured is substantially poorer than the precision with which *relative* differences in isotope abundances between two samples can be determined. Nevertheless, the determination of absolute isotope ratios is very important, because these numbers form the basis for the calculation of the relative differences, the δ-values. Table 1.6 summarizes absolute isotope ratios of primary standards used by the international stable isotope community.

To compare isotope data from different laboratories, an internationally accepted set of standards is necessary. Irregularities and problems concerning standards have been evaluated by Friedman and O'Neil (1977), Gonfiantini (1978, 1984), Coplen

Table 1.6 Absolute isotope ratios of international standards. (After Hayes 1983)

Standard	Ratio	Accepted value ($\times 10^6$) (with 95% confidence interval)	Source
SMOW	D/H	155.76 ± 0.10	Hagemann et al. (1970)
	$^{18}O/^{16}O$	$2,005.20 \pm 0.43$	Baertschi (1976)
	$^{17}O/^{16}O$	373 ± 15	Nier (1950), corrected by Hayes (1983)
PDB	$^{13}C/^{12}C$	$11,237.2 \pm 2.9$	Craig (1957)
	$^{18}O/^{16}O$	2067.1 ± 2.1	
	$^{17}O/^{16}O$	379 ± 15	
Air nitrogen	$^{15}N/^{14}N$	$3,676.5 \pm 8.1$	Junk and Svec (1958)
Canyon Diablo Troilite (CDT)	$^{34}S/^{32}S$	$45,004.5 \pm 9.3$	Jensen and Nakai (1962)

et al. (1983), Coplen (1996), and Coplen et al. (2006). The accepted unit of isotope ratio measurements is the delta value (δ given in per mill (‰). The $\tilde{\delta}$ value is defined as

$$\delta \text{ in } \% = \frac{R_{(\text{Sample})} - R_{(\text{Standard})}}{R_{(\text{Standard})}} 1{,}000, \tag{1.26}$$

where R represents the measured isotope ratio. If $\delta_A > \delta_B$, it is convenient to speak of A being enriched in the rare or *heavy* isotope, compared to B. Unfortunately, not all of the δ-values cited in the literature are given relative to a single universal standard, so that often several standards of one element are in use. To convert δ-values from one standard to another, the following equation may be used

$$\delta_{X-A} = \left[\left(\frac{\delta_{B-A}}{10^3} + 1 \right) \left(\frac{\delta_{X-B}}{10^3} + 1 \right) - 1 \right] 10^3, \tag{1.27}$$

where X represents the sample, A and B different standards.

For different elements, a convenient *working standard* is used in each laboratory. However, all values measured relative to the respective *working standard* are reported in the literature relative to a universal standard.

As an example, for the relationship between the content of an isotope in % and the δ-value in ‰, Fig. 1.9 demonstrates that large changes in the δ-value only involve very small changes in the heavy isotope content (in this case the ^{18}O content). An ideal standard used worldwide as the *zero-point* on a δ-scale should satisfy the following requirements:

1. Be homogeneous in composition
2. Be available in relatively large amounts
3. Be easy to handle for chemical preparation and isotopic measurement, and
4. Have an isotope ratio near the middle of the natural range of variation

Among the reference samples now used, relatively few meet all of these requirements. For instance, the situation for the SMOW standard is rather confusing. The

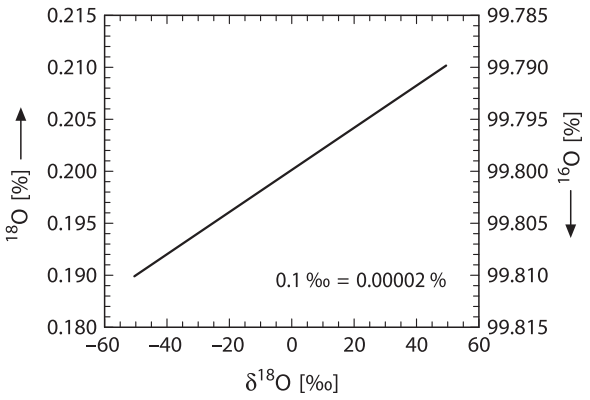

Fig. 1.9 Relationship between ^{18}O (^{16}O) content in per cent and δ^{18}O in per mill

Table 1.7 Worldwide standards in use for the isotopic composition of hydrogen, boron, carbon, nitrogen, oxygen, silicium, sulfur, and chlorine

Element	Standard	Standard
H	Standard Mean Ocean Water	V-SMOW
B	Boric acid (NBS)	SRM 951
C	Belemnitella americana from the Cretaceous Peedee formation, South Carolina	V-PDB
N	Air nitrogen	N2 (atm.)
O	Standard Mean Ocean Water	V-SMOW
Si	Quartz sand	NBS-28
S	Troilite (FeS) from the Canyon Diablo iron meteorite	V-CDT
Cl	Seawater chloride	SMOC

SMOW standard was originally a hypothetical water sample with an isotopic composition very similar to average untreated ocean water (Craig 1961b), but being defined in terms of a water sample distributed by the National Bureau of Standards (NBS-1). Later, the IAEA distributed a distilled water sample named V-SMOW (Vienna-SMOW), which is very close to, but not identical in isotope composition to, the original SMOW standard. The worldwide standards now in general use are given in Table 1.7.

The problems related to standards are discussed by an IAEA advisory group, which meet from time to time. As a result of these meetings, the quality and availability of the existing standards and the need of new standards have been discussed and agreed.

A further advancement comes from inter-laboratory comparison of two standards having different isotopic composition that can be used for a normalization procedure correcting for all proportional errors due to mass spectrometry and to sample preparation. Ideally, the two standard samples should have isotope ratios as different as possible, but still within the range of natural variations. There are, however, some problems connected with data normalization, which are still under debate. For example, the CO_2 equilibration of waters and the acid extraction of CO_2 from carbonates are indirect analytical procedures, involving temperature-dependent fractionation factors (whose values are not beyond experimental uncertainties) with respect to the original samples and which might be re-evaluated on the normalized scale.

Table 1.8 summarizes gases, which are used for mass spectrometric analysis of the various elements.

1.6 General Remarks on Sample Preparation Methods for Gases

Isotopic differences between samples to be measured are often extremely small. Therefore, great care has to be taken to avoid any isotope fractionation during chemical or physical treatment of the sample. The quality of a stable isotope analysis is

Table 1.8 Gases most commonly used in isotope ratio in mass spectrometry

Element	Gas
H	H_2
C	CO_2, CO
N	N_2
O	CO_2, CO, O_2
S	SO_2, SF_6
Si	SiF_4

determined by the purity of the gas prepared from the sample, quantitative yield, blank, and memory effects.

To convert geologic samples to a suitable form for analysis, many different chemical preparation techniques must be used. These diverse techniques all have one general feature in common: any preparation procedure providing a yield of less than 100% may produce a reaction product that is isotopically different from the original specimen because the different isotopic species have different reaction rates.

A quantitative yield of a pure gas is usually necessary for the mass spectrometric measurement in order to prevent not only isotope fractionation during sample preparation, but also interference in the mass spectrometer. Contamination with gases having the same molecular masses and similar physical properties may be a serious problem. This is especially critical with CO_2 and N_2O, (Craig and Keeling 1963), and N_2 and CO. When CO_2 is used, interference by hydrocarbons and a CS^+ ion may also pose a problem.

Contamination may result from incomplete evacuation of the vacuum system and/or from degassing of the sample. The system blank should be normally less than 1% of the amount of gas prepared from a sample for analysis. For very small sample sizes, the blank may ultimately limit the analysis. Memory effects result from samples that have previously been analyzed. They will become noticeable, when samples having widely different isotopic compositions are analyzed consecutively.

How gases are transferred, distilled, or otherwise processed in vacuum lines is briefly discussed under the different elements. A more detailed description can be found in the recently published *Handbook of Stable Isotope Analytical Techniques*, edited by de Groot (2004).

All errors due to chemical preparation limit the overall precision of an isotope ratio measurement to usually 0.1–0.2‰, while modern mass spectrometer instrumentation enables a precision better than 0.02‰ for light elements other than hydrogen. Larger uncertainties are expected, when elements present in a sample at very low concentration are extracted by chemical methods (e.g., carbon and sulfur from igneous rocks).

Commercial combustion elemental analyzers perform a flash combustion, converting samples to CO_2, H_2O, N_2, and SO_2 simultaneously. These different gases are then chemically trapped, converted, or separated on GC columns and measured in a continuous flow mass spectrometer. This technique allows the determination

of several isotope ratios from the same component, increasing the possibilities of isotope fingerprinting of organic and inorganic compounds containing isotopes of more than one element of interest. Because of very high combustion temperatures, the quantitative conversion of the sample material is guaranteed.

1.7 Microanalytical Techniques

In recent years, microanalytical techniques, which permit relatively precise isotopic determinations on a variety of samples that are orders of magnitude smaller than those used in conventional techniques, have become increasingly important. Different approaches have been used in this connection, which generally reveal greater isotope heterogeneity than conventional analytical approaches. As a rule of thumb: the smaller the scale of measurement, the larger the sample heterogeneity.

1.7.1 Laser Microprobe

Laser assisted extraction is based on the fact that the energy of the laser beam is absorbed efficiently by a number of natural substances of interest. The absorption characteristics depend on the structure, composition, and crystallinity of the sample. High energy, finely-focussed laser beams have been used for some years for Ar isotope analysis. The first well-documented preparation techniques with CO_2 and Nd–YAG laser systems for stable isotope determinations have been described by Crowe et al. (1990), Kelley and Fallick (1990) and Sharp (1990). Their results show that sub-milligram quantities of mineral can be analyzed for oxygen, sulfur, and carbon. In order to achieve precise and accurate measurements, the samples have to be evaporated completely because steep thermal gradients during laser heating induce isotopic fractionations (Elsenheimer and Valley 1992). The thermal effects of CO_2 and Nd–YAG laser assisted preparation techniques require that sample sections be cut into small pieces before total evaporation. The spatial resolution of this technique is limited to about 500 µm.

Thermal effects can be overcome by vapourizing samples with ultraviolet (UV) KrF and ArF lasers, thus making possible in situ oxygen isotope analysis of silicates (Wiechert and Hoefs 1995; Fiebig et al. 1999; Wiechert et al. 2002).

1.7.2 Secondary Ion Mass Spectrometry

Two different types of SIMS are generally used: the Cameca f-series and the SHRIMP (Sensitive High mass Resolution Ion MicroProbe) series (Valley and Graham 1993; Valley et al. 1998; McKibben and Riciputi 1998). Analysis in the

ion-microprobe is accomplished by sputtering a sample surface using a finely focused primary ion beam producing secondary ions, which are extracted and analyzed in the secondary mass spectrometer. The main advantages of this technique are its high sensitivity, high spatial resolution, and its small sample size. Sputter pits for a typical 30 min SIMS analyses have a diameter of 10–30 μm and a depth of 1–6 μm, a spatial resolution that is an order of magnitude better than laser techniques. Disadvantages are that the sputtering process produces a large variety of molecular secondary ions along with atomic ions, which interfere with the atomic ions of interest and that the ionization efficiencies of different elements vary by many orders of magnitude and strongly depend on the chemical composition of the sample. This *matrix* effect is one of the major problems of quantitative analysis. The two instruments (Cameca and SHRIMP) have technical features, such as high resolving power and energy filtering, which help to overcome the problems of the presence of molecular isobaric interferences and the matrix dependence of secondary ion yields.

Fitzsimons et al. (2000) have reviewed the factors that influence the precision of SIMS stable isotope data. All sample analyses must be calibrated for instrumental mass fractionation using SIMS analyses of a standard material. Under favorable circumstances, precision can reach a few tenths of a per mill. The latest version of ion-microprobe is the Cameca-IMS-1280 type, allowing further reduction in sample and spot size and achieving precise analysis of isotope ratios at the 0.1‰ level (Page et al. 2007).

1.8 Stable Isotope Variations of Heavy Elements

Advances in TIMS-techniques and the introduction of multiple collector–ICP–MS (MC–ICP–MS) techniques have enabled the research on natural variations of a wide range of transition and heavy metal systems for the first time, which so far could not have been measured with the necessary precision. The advent of MC–ICP–MS has improved the precision on isotope measurements to about 40 ppm on elements such as Zn, Cu, Fe, Cr, Mo, and Tl. The technique combines the strength of the ICP technique (high ionization efficiency for nearly all elements) with the high precision of thermal ion source mass spectrometry equipped with an array of Faraday collectors. The uptake of elements from solution and ionization in a plasma allows correction for instrument-dependent mass fractionations by addition of external spikes or the comparison of standards with samples under identical operating conditions. All MC–ICP–MS instruments need Ar as the plasma support gas, in a similar manner to that commonly used in conventional ICP–MS. Mass interferences are thus an inherent feature of this technique, which may be circumvented by using desolvating nebulisers.

Maréchal et al. (1999) and Zhu et al. (2000a) first described techniques for the determination of Cu- and Zn-isotope ratios. Observed variations at low temperatures are on the order of several ‰, much more than originally expected on the basis

of the relatively small mass differences among isotopes of heavier elements. The magnitude of fractionations depends on several factors such as the participation of redox reactions and biologically mediated reactions. Fractionation mechanisms responsible for the observed variations are so far unknown in most cases but should be the same as for light elements. Of special importance seem speciation and absorption phenomena. Since most metals can coordinate with a number of ligands, isotope effects between dissolved aqueous species particularly at different redox states are therefore of special importance (Anbar and Rouxel 2007). Furthermore, absorption of dissolved species on particle surfaces represents another important fractionation mechanism. A small number of studies have demonstrated small fractionations $<1‰$ as metal ions are removed from solution onto oxide surfaces. Generally, the heavier isotope preferentially absorbs on metal oxide surfaces, which is consistent with shorter metal–oxygen bonds and lower coordination number for the absorbed relative to the aqueous species (Balistrieri et al. 2008). The largest fractionation (1.8‰) so far observed occurs between dissolved and absorbed Mo (Barling and Anbar 2004).

Schauble (2004) applied the theory of stable isotope fractionation to nontraditional isotope systems. He pointed out that, differences in coordination numbers among coexisting phases control isotope fractionation of cations. The lighter isotope preferentially occupies the higher coordinated site. Thus, differences in isotope composition of lithophile elements such as Mg, Ca, and Li are likely to reflect changes in coordination numbers

Although equilibrium fractionations have been documented for some transition metal (i.e., Fe), they should be small and may be overwhelmed by kinetic fractionations in low-temperature and biological systems (Schauble 2004). For any transition metal, it remains to be demonstrated that biological effects dominate the natural isotope variability.

Table 1.9 gives a summary of the respective heavy elements and the isotope variations observed so far.

Table 1.9 Natural variation ranges of heavy elements and some important geochemical properties probably causing the variations

Element	Isotopes	Variations in ‰	Geochemistry
$_{24}$Cr	4 isotopes (50, 52, 53, 54)	5 (?) (53/52)	Cr^{3+}, Cr^{6+}; (contaminant)
$_{26}$Fe	4 isotopes (54, 56, 57, 58)	5 (56/54)	Fe^{2+}, Fe^{3+}, Fe^{0} iron bacteria
$_{29}$Cu	^{63}Cu, ^{65}Cu	>7	Cu^{+}, Cu^{2+}, Cu^{0}
$_{30}$Zn	4 isotopes (64, 66, 67, 68)	1 (66/64)	No redox reactions
$_{34}$Se	6 isotopes (from 74 to 82)	~10(82/76)	Similarity with S
$_{42}$Mo	7 isotopes (from 92 to 100)	3 (97/95)	Mo^{6+}, Mo^{2+}
$_{80}$Hg	7 isotopes (from 196 to 204	5	highly volatile Hg^{+}, Hg^{2+}, Hg^{0}
$_{81}$Tl	^{203}Tl, ^{205}Tl	2	Tl^{+}, Tl^{3+} highly volatile

Chapter 2
Isotope Fractionation Processes of Selected Elements

The foundations of stable isotope geochemistry were laid in 1947 by Urey's classic paper on the thermodynamic properties of isotopic substances and by Nier's development of the ratio mass spectrometer. Before discussing details of the naturally occurring variations in stable isotope ratios, it is useful to describe some generalities that are pertinent to the field of non-radiogenic isotope geochemistry as a whole.

1. Isotope fractionation is pronounced when the mass differences between the isotopes of a specific element are large relative to the mass of the element. Therefore, isotope fractionations are especially large for the light elements (up to a mass number of about 40). Recent developments in analytical techniques have opened the possibility to detect small variations in elements with much higher mass numbers. The heaviest element for which natural variations have been reported is thallium with isotopes of masses 203 and 205 (Rehkämper and Halliday 1999).
2. All elements that form solid, liquid, and gaseous compounds stable over a wide temperature range are likely to have variations in isotopic composition. Generally, the heavy isotope is concentrated in the solid phase in which it is more tightly bound. Heavier isotopes tend to concentrate in molecules in which they are present in the highest oxidation state.
3. Mass balance effects can cause isotope fractionations because modal proportions of substances can change during a chemical reaction. They are especially important for elements in situations where these coexist in molecules of reduced and oxidized compounds. Conservation of mass in an n component system can be described by

$$\delta_{(\text{system})} = \sum x_i \, \delta_i \tag{2.1}$$

   where "x_i" is the mole fraction of the element in question for each of n phases within the system.
4. Isotopic variations in most biological systems are mostly caused by kinetic effects. During biological reactions (e.g. photosynthesis, bacterial processes) the lighter isotope is very often enriched in the reaction product relative to the substrate. Most of the fractionations in biological reactions generally take place

J. Hoefs, *Stable Isotope Geochemistry,*

during the so-called rate determining step, which is the slowest step. It commonly involves a large reservoir, where the material actually used is small compared to the size of the reservoir.

2.1 Hydrogen

Until 1931 it was assumed that hydrogen consisted of only one isotope. Urey et al. (1932) detected the presence of a second stable isotope, which was called deuterium. (In addition to these two stable isotopes there is a third naturally occuring but radioactive isotope, ^{3}H, tritium, with a half-life of approximately 12.5 years). Rosman and Taylor (1998) gave the following average abundances of the stable hydrogen isotopes:

$$^{1}H : 99.9885\%$$

$$^{2}D : 0.0115\%$$

The isotope geochemistry of hydrogen is particularly interesting, for two reasons:

1. Hydrogen is omnipresent in terrestrial environments occurring in different oxidation states in the forms of H_2O, H_3O^+, OH^-, H_2 and CH_4, even at great depths within the Earth. Therefore, hydrogen is envisaged to play a major role, directly or indirectly, in a wide variety of naturally occurring geological processes.
2. Hydrogen has by far the largest mass difference relative to the mass of the element between its two stable isotopes. Consequently hydrogen exhibits the largest variations in stable isotope ratios of all elements.

The ranges of hydrogen isotope compositions of some geologically important reservoirs are given in Fig. 2.1. It is noteworthy that all rocks on Earth have somewhat similar hydrogen isotope compositions, which is a characteristic feature of hydrogen, but not of the other elements. The reason for this overlap in isotope composition for rocks is likely due to the enormous amounts of water that have been cycled through the outer shell of the Earth.

2.1.1 Preparation Techniques and Mass Spectrometric Measurements

Determination of the D/H ratio of water is performed on H_2-gas. There are two different preparation techniques: (1) equilibration of milliliter-sized samples with gaseous hydrogen gas, followed by mass-spectrometric measurement and back calculation of the D/H of the equilibrated H_2 (Horita 1988). Due to the very large fractionation factor (0.2625 at 25°C) the measured H_2 is very much depleted in D, which complicates the mass-spectrometric measurement. (2) water is converted to hydrogen by passage over hot metals (uranium: Bigeleisen et al. 1952; Friedman 1953;

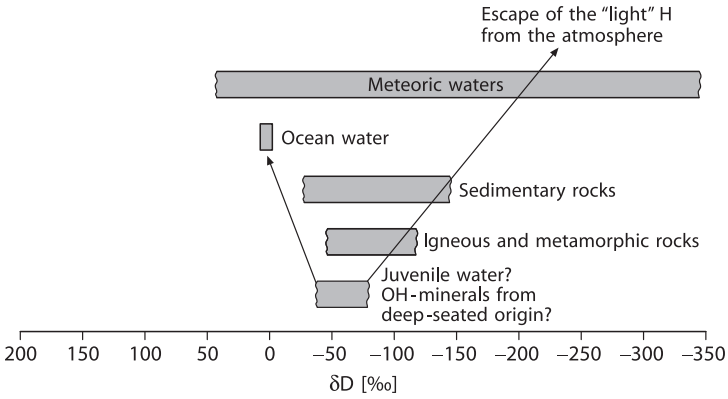

Fig. 2.1 δD ranges of some geologically important reservoirs

Godfrey 1962, zinc: Coleman et al. 1982, chromium: Gehre et al. 1996). This is still the classic method and commonly used.

A difficulty in measuring D/H isotope ratios is that, along with the H_2^+ and HD^+ formation in the ion source, H_3^+ is produced as a by-product of ion-molecule collisions. Therefore, a H_3^+ correction has to be made. The amount of H_3^+ formed is directly proportional to the number of H_2 molecules and H^+ ions. Generally the H_3^+ current measured for hydrogen from ocean water is on the order of 16% of the total mass 3. The relevant procedures for correction have been evaluated by Brand (2002).

Analytical uncertainty for hydrogen isotope measurements is usually in the range ±0.5 to ±5‰ depending on different sample materials, preparation techniques and laboratories.

Burgoyne and Hayes (1998) and Sessions et al. (1999) introduced the continuously flow technique for the D/H measurement of individual organic compounds. The precise measurement of D/H ratios in a He carrier poses a number of analytical problems, related to the tailing from the abundant $^4He^+$ onto the minor HD^+ peak as well as on reactions occurring in the ion source that produce H_3^+. However, these problems have been overcome and precise hydrogen isotope measurements of individual organic compounds are possible.

2.1.2 Standards

There is a range of standards for hydrogen isotopes. The primary reference standard, the zero point of the δ-scale, is V-SMOW, which is virtually identical in isotopic composition with the earlier defined SMOW, being a hypothetical water sample orginally defined by Craig (1961b).

Table 2.1 Hydrogen isotope standards

Standards	Description	δ-value
V-SMOW	Vienna Standard Mean Ocean Water	0
GISP	Greenland Ice Sheet Precipitation	−189.9
V-SLAP	Vienna Standard Light Antarctic Precipitation	−428
NBS-30	Biotite	−65

V-SMOW has a D/H ratio that is higher than most natural samples on Earth, thus δD-values in the literature are generally negative. The other standards, listed in Table 2.1, are generally used to verify the accuracy of sample preparation and mass spectrometry.

2.1.3 Fractionation Processes

The most effective processes in the generation of hydrogen isotope variations in the terrestrial environment are phase transitions of water between vapor, liquid, and ice through evaporation/precipitation and/or boiling/condensation in the atmosphere, at the Earth's surface, and in the upper part of the crust. Differences in H-isotopic composition arise due to vapor pressure differences of water and, to a smaller degree, to differences in freezing points. Because the vapor pressure of HDO is slightly lower than that of H_2O, the concentration of D is lower in the vapor than in the liquid phase. In a simple, but elegant experiment Ingraham and Criss (1998) have monitored the effect of vapor pressure on the rate of isotope exchange between water and vapor, which is shown in Fig. 2.2. Two beakers with isotopically differing waters were juxtaposed in a sealed box to monitor the exchange process at different temperatures (in this case 21 and 52°C). As shown in Fig. 2.12 in the 52°C experiment the isotopic composition of the water changes rapidly and nearly reaches equilibrium in only 27 days.

Horita and Wesolowski (1994) have summarized experimental results for the hydrogen isotope fractionation between liquid water and water vapor in the temperature range 0–350°C (see Fig. 2.3). Hydrogen isotope fractionations decrease rapidly with increasing temperatures and become zero at 220–230°C. Above the crossover temperature, water vapor is more enriched in deuterium than liquid water. Fractionations again approach zero at the critical temperature of water (Fig. 2.3).

From experiments, Lehmann and Siegenthaler (1991) determined the equilibrium H-isotope fractionation between ice and water to be +21.2‰. Under natural conditions, however, ice will not necessarily be formed in isotopic equilibrium with the bulk water, depending mainly on the freezing rate.

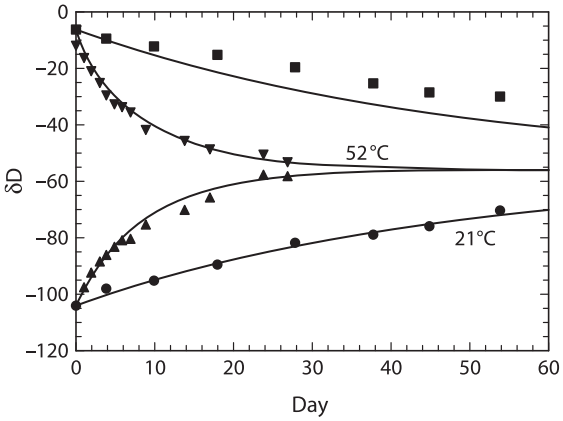

Fig. 2.2 δD values versus time for two beakers that have equal surface areas and equal volumes undergoing isotopic exchange in sealed systems. In both experiments at 21 and 52°C isotope ratios progress toward an average value of −56‰ via exchange with ambient vapour. *Solid curves* are calculated, *points* are experimental data (after Criss, 1999)

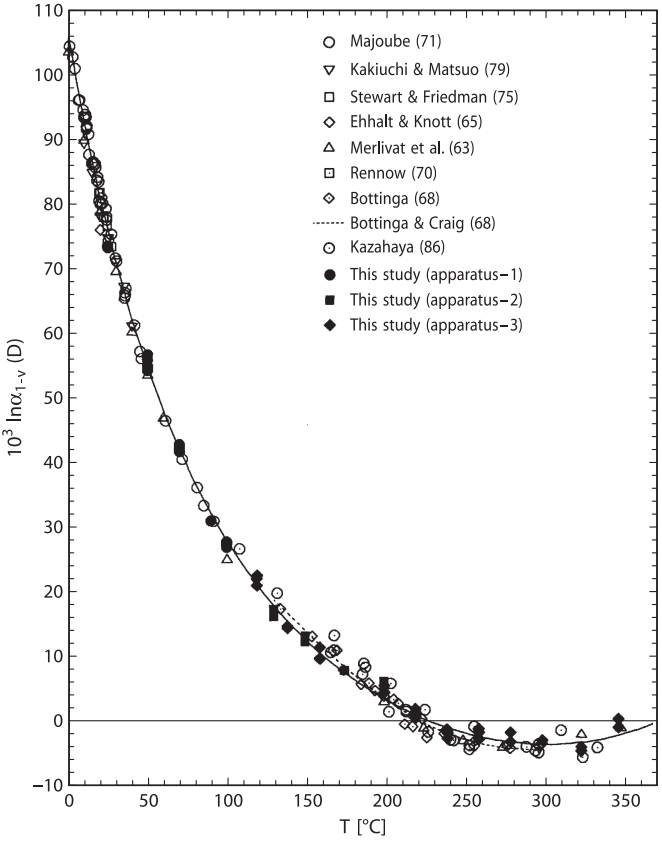

Fig. 2.3 Experimentally determined fractionation factors between liquid water and water vapour from 1 to 350°C (after Horita and Wesolowski, 1994)

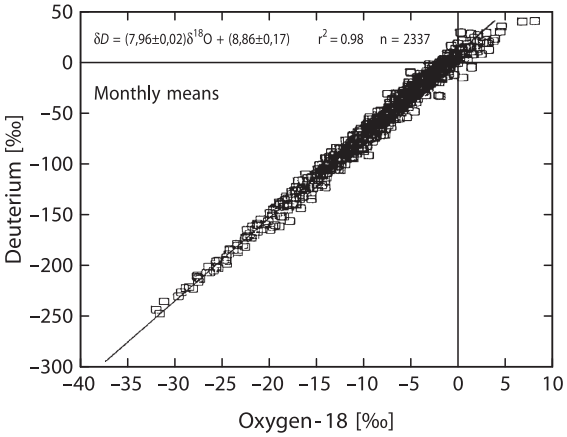

Fig. 2.4 Global relationship between monthly means of δD and $\delta^{18}O$ in precipitation, derived for all stations of the IAEA global network. *Line* indicates the global meteoric water line (MWL) (after Rozanski et al. 1993)

In all processes concerning the evaporation and condensation of water, hydrogen isotopes are fractionated in a similar fashion to those of oxygen isotopes, albeit with a different magnitude, because a corresponding difference in vapor pressures exists between H_2O and HDO in one case and $H_2^{16}O$ and $H_2^{18}O$ in the other.

Therefore, the hydrogen and oxygen isotope distributions are correlated for meteoric waters. Craig (1961a) first defined the generalized relationship:

$$\delta D = 8\delta^{18}O + 10,$$

which describes the interdependence of H- and O-isotope ratios in meteoric waters on a global scale.

This relationship, shown in Fig. 2.4, is described in the literature as the "Global Meteoric Water Line (GMWL)".

Neither the numerical coefficient 8 nor the constant 10, also called the deuterium excess d, are constant in nature. Both may vary depending on the conditions of evaporation, vapor transport and precipitation and, as a result, offer insight into climatic processes. The deuterium excess d is a valuable tool to derive information on relative humidities.

2.1.3.1 Equilibrium Exchange Reactions

D/H fractionations among gases are extraordinarily large, as calculated by Bottinga (1969a) and Richet et al. (1977) and plotted in Fig. 2.5. Even in magmatic systems, fractionation factors are sufficiently large to affect the δD-value of dissolved water in melts during degassing of H_2, H_2S or CH_4. The oxidation of H_2 or CH_4 to H_2O

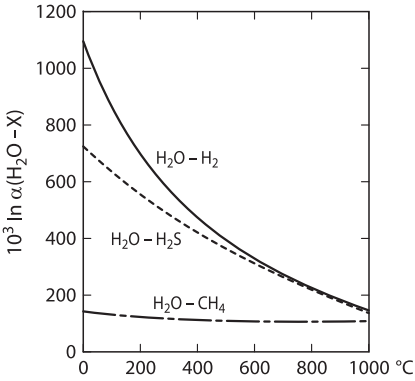

Fig. 2.5 D/H fractionations between H_2O – H_2, H_2O – H_2S and H_2O – CH_4 (from calculated data of Richet et al. 1977)

and CO_2 may also have an effect on the isotopic composition of water dissolved in melts due to the large fractionation factors.

With respect to mineral-water systems, different experimental studies obtained widely different results for the common hydrous minerals with respect to the absolute magnitude and the temperature dependence of D/H fractionations (Suzuoki and Epstein 1976; Graham et al. 1980; Vennemann et al. 1996). Suzuoki and Epstein (1976) first demonstrated the importance of the chemical composition of the octahedral sites in crystal lattices to the mineral H-isotope composition. Subsequently, isotope exchange experiments by Graham et al. (1980, 1984) suggested that the chemical composition of sites other than the octahedral sites can also affect hydrogen isotope compositions. These authors postulate a qualitative relationship between hydrogen-bond distances and hydrogen isotope fractionations: the shorter the hydrogen bond, the more depleted the mineral is in deuterium.

On the basis of theoretical calculations, Driesner (1997) proposed that many of the discrepancies between the experimental studies were due to pressure differences at which the experiments were carried out. Thus for hydrogen, pressure is a variable that must be taken into account in fluid-bearing systems. Later, Horita et al. (1999) presented experimental evidence for a pressure effect between brucite and water.

Chacko et al. (1999) developed an alternative method for the experimental determination of hydrogen isotope fractionation factors. Instead of using powdered minerals as starting materials these authors carried out exchange experiments with large single crystals and then analyzed the exchanged rims with the ion probe. Although the precision of the analytical data is less than that for conventional bulk techniques, the advantage of this technique is that it allows the determination of fractionation factors in experiments in which isotopic exchange occurs by a diffusional process rather than by a combination of diffusion and recrystallization.

In summary, as discussed by Vennemann and O'Neil (1996), discrepancies between published experimental calibrations in individual mineral–water systems are difficult to resolve, which limits the application of D/H fractionations in mineral–water systems to estimate δD-values of coexisting fluids.

2.1.3.2 Kinetic Isotope Effects

Large hydrogen isotope fractionations occur during the conversion of hydrogen from water to organic matter. The magnitude of H isotope fractionations is generally controlled by the biochemical pathways used. Although details of this complex process are still unknown, there is discussion about the quantitative role of kinetic and equilibrium isotope fractionations. Tremendous progress has been achieved through the introduction of the compound specific hydrogen isotope analysis (Sessions et al. 1999; Sauer et al. 2001; Schimmelmann et al. 2006), which allows the δD analysis of individual biochemical compound. Further details are discussed in Sect. 3.10.1.2.

2.1.3.3 Other Fractionation Effects

In salt solutions, isotopic fractionations can occur between water in the "hydration sphere" and free water (Truesdell 1974). The effects of dissolved salts on hydrogen isotope activity ratios in salt solutions can be qualitatively interpreted in terms of interactions between ions and water molecules, which appear to be primarily related to their charge and radius. Hydrogen isotope activity ratios of all salt solutions studied so far are appreciably higher than H-isotope composition ratios. As shown by Horita et al. (1993), the D/H ratio of water vapor in isotope equilibrium with a solution increases as salt is added to the solution. Magnitudes of the hydrogen isotope effects are in the order $CaCl_2 > MgCl_2 > MgSO_4 > KCl \sim NaCl > NaSO_4$ at the same molality.

Isotope effects of this kind are relevant for an understanding of the isotope composition of clay minerals and absorption of water on mineral surfaces. The tendency for clays and shales to act as semipermeable membranes is well known. This effect is also known as "ultrafiltration". Coplen and Hanshaw (1973) postulated that hydrogen isotope fractionations may occur during ultrafiltration in such a way that the residual water is enriched in deuterium due to its preferential adsorption on the clay minerals and its lower diffusivity.

2.2 Lithium

Lithium has two stable isotopes with the following abundances (Rosman and Taylor 1998):

^{6}Li 7.59%
^{7}Li 92.41%

Lithium is one of the rare elements where the lighter isotope is less abundant than the heavier one. In order to be consistent with the other isotope systems lithium isotope ratios are reported as δ^{7}Li-values.

The large mass difference relative to the mass of the element between ^{6}Li and ^{7}Li of about 16% is a favorable condition for their fractionation in nature. Taylor and Urey (1938) found a change of 25% in the Li-isotope ratio when Li-solutions percolate through a zeolite column. Thus, fractionation of Li-isotopes might be expected in geochemical settings in which cation exchange processes are involved.

Early workers had to struggle with serious lithium fractionation effects during mass spectrometric analysis. Today most workers use the multicollector sector ICP-MS technique first described by Tomascak et al. (1999). Improvements of the analytical techniques in recent years have lead to an accuracy better than 0.3‰. Unfortunately, there are no internationally accepted Li isotope values for rocks or waters. James and Palmer (2000) have determined nine international rock standards ranging from basalt to shale relative to the so-called NIST L-SVEC standard.

i) Characteristic features of Li isotope geochemistry

Lithium isotope geochemistry is characterized by a difference close to 30‰ between ocean water ($\delta^{7}Li + 31‰$) and bulk silicate earth with a δ^{7} Li-value of 3.2‰ (Seitz et al. 2007). In this respect lithium isotope geochemistry is very similar to that of boron (see p. 45). The isotopic difference between the mantle and the ocean can be used as a powerful tracer to constrain water/ rock interactions (Tomaszak 2004). Figure 2.6 gives an overview of Li-isotope variations in major geological reservoirs.

During weathering ^{7}Li is preferentially mobilized, whereas ^{6}Li is enriched in the weathering residue. Rudnick et al. (2004) have demonstrated that Li isotope fractionation correlates directly with the degree of weathering and that very light $\delta^{7}Li$ of $-20‰$ can be produced in soils. Thus, very effective Li-isotope fractionation processes are operative in the sedimentary environment. By analyzing major rivers, Huh et al. (1998) observed a large variation in $\delta^{7}Li$ in river waters with the suspended load being systematically lighter than the dissolved load.

Mantle-derived basalts, on the other hand, have a relatively uniform composition with $\delta^{7}Li$ values of $4 \pm 2‰$ (Tomaszak 2004; Elliott et al. 2004). The continental crust generally has a lighter Li isotope composition than the upper mantle from which it was derived (Teng et al. 2004). Considering the small Li isotope fractionation at high temperature igneous differentiation processes (Tomaszak 2004), pristine

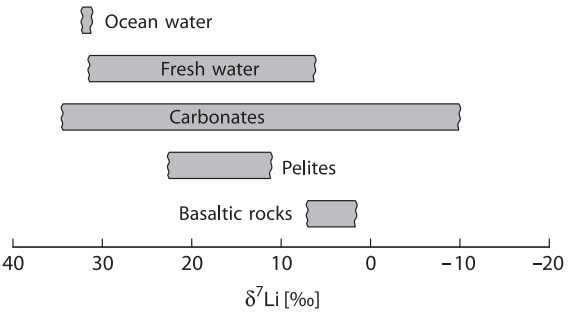

Fig. 2.6 Lithium isotope variations in major geological reservoirs

continental crust should not be too different in Li isotope composition from the mantle. Because this is not the case, the isotopically light crust must have been modified by secondary processes, such as weathering, hydrothermal alteration and prograde metamorphism (Teng et al. 2007).

Given the homogeneity of basaltic rocks, it is surprising that peridotites have a wide range in δ^7Li values from values as low as $-17‰$ (Nishio et al. 2004) to values as high as $+10‰$ (Brooker et al. 2004). This unexpected finding can be explained by diffusion processes that affect mantle minerals during melt migration (Parkinson et al. 2007). The latter authors have demonstrated that ^{6}Li diffuses 3% faster than ^{7}Li in silicate minerals consistent with diffusion experiments by Richter et al. (2003). Thus diffusion at magmatic temperatures is a very effective mechanism for generating large variations in ^{7}Li/^{6}Li ratios (Lundstrom et al. 2005; Teng et al. 2006; Rudnick and Ionov 2007). Although diffusion profiles will relax with time the existence of sharp δ^7 Li-profiles suggest diffusional Li isotope fractionation over short timescales (days to a few months) and therefore diffusion profiles in mantle minerals may be used as geospeedometers (Parkinson et al. 2007). At the same time diffusion may obliterate primary mantle signatures.

During fluid–rock interaction, Li as a fluid-mobile element will enrich in aqueous fluids. It might therefore be expected that δ^7Li enriched seawater incorporated into altered oceanic crust should be removed during subduction zone metamorphism. Continuous dehydration of pelagic sediments and altered oceanic crust results in ^{7}Li-depleted rocks and in ^{7}Li enriched fluids. A subducting slab therefore should introduce large amounts of ^{7}Li into the mantle wedge. To quantitatively understand this process Li isotope fractionation factors between minerals and coexisting fluids must be known. First attempts have been undertaken by Wunder et al. (2006, 2007) by determining experimentally the Li isotope fractionations between pyroxene, mica, staurolite and Cl^- and OH^- bearing fluids. These authors showed that ^{7}Li is preferentially partitioned into the fluid.

Because Li isotopes may be used as a tracer to identify the existence of recycled material in the mantle, systematic studies of arc lavas have been undertaken (Moriguti and Nakamura 1998; Tomascak et al. 2000; Leeman et al. 2004 and others). However, most arc lavas have δ^7Li values that are indistinguishable from those of MORB. Thus Li seems to be decoupled from other fluid mobile elements, because Li can partition into Mg-silicates (pyroxene, olivine) in the mantle (Tomascak et al. 2002).

Lithium is a conservative element in the ocean with a residence time of about one million year. Its isotope composition is maintained by inputs of dissolved Li from rivers (average $\delta^7\text{Li} + 23‰$, Huh et al. 1998) and high-temperature hydrothermal fluids at ocean ridges at one hand and low temperature removal of Li into oceanic basalts and marine sediments at the other. Any variance in these sources and sinks thus should cause secular variations in the isotope composition of oceanic Li. And indeed in a first attempt Hoefs and Sywall (1997) interpreted Li isotope variations in well preserved carbonate shells as indicating secular variations of the oceanic Li-cycle.

2.3 Boron

Boron has two stable isotopes with the following abundances (Rosman and Taylor 1998).

^{10}B 19.9%
^{11}B 80.1%

The large mass difference between ^{10}B and ^{11}B and large chemical isotope effects between different species (Bigeleisen 1965) make boron a very promising element to study for isotope variations. The utility of boron isotopes as a geochemical tracer stems from the high mobility of boron during high- and low-temperature fluid-related processes, showing a strong affinity for any vapor phases present.

The lowest observed δ^{11}B-values of around $-30‰$ are for certain tourmalines (Chaussidon and Albarede 1992) and some non-marine evaporite sequences (Swihart et al. 1986), whereas the most enriched ^{11}B-reservoir is given by brines from Australia and Israel (Dead Sea) which have δ^{11}B-values of up to 60‰ (Vengosh et al. 1991a, b). A very characteristic feature of boron geochemistry is the isotopic composition of ocean water with a constant δ^{11}B-value of 39.5‰ (Spivack and Edmond 1987), which is about 50‰ heavier than average continental crust value of $-10 \pm 2‰$ (Chaussidon and Albarede 1992). Isotope variations of boron in some geological reservoirs are shown in Fig. 2.7.

Methods
In recent years solid source mass-spectrometry has provided an effective means for B-isotope analysis. Two different methods have been developed, which have been summarized by Swihart (1996). The first was a positive thermal ionization technique using $Na_2BO_2^+$ ions initially developed by McMullen et al. (1961). Subsequently, Spivack and Edmond (1986) modified this technique by using $Cs_2BO_2^+$

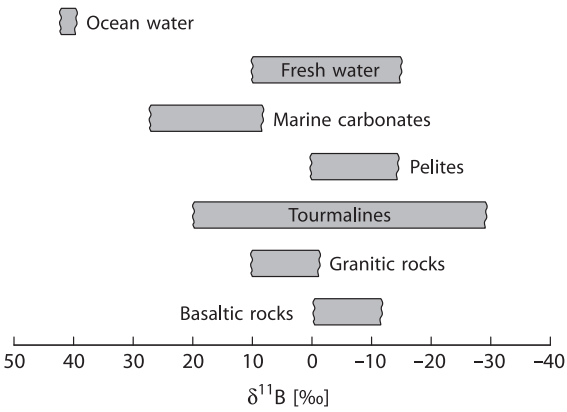

Fig. 2.7 Boron isotope variations in some geologically important reservoirs

ions (measurement of the masses 308 and 309). The substitution of ^{133}Cs for ^{23}Na increases the molecular mass and reduces the relative mass difference of its isotopic species, which limits the thermally induced mass dependent isotopic fractionation. This latter method has a precision of about ±0.25‰, which is better by a factor of 10 than the $Na_2BO_2^+$ method. Another method has been used by Chaussidon and Albarede (1992), who performed boron isotope determinations with an ion-microprobe having an analytical uncertainty of about ±2‰. Recently, Leceyer et al. (2002) described the use of MC–ICP–MS for B isotopic measurements of waters, carbonates, phosphates and silicates with an external reproducibilty of ±0.3‰.

As analytical techniques have been consistently improved in recent years, the number of boron isotope studies has increased rapidly. Reviews have been given by Barth (1993) and by Palmer and Swihart (1996). The total boron isotope variation documented to date is about 90‰. $\delta^{11}B$-values are generally given relative NBS boric acid SRM 951, which is prepared from a Searles Lake borax. This standard has a $^{11}B/^{10}B$ ratio of 4.04558 (Palmer and Slack 1989).

pH dependence of isotope fractionations

Boron is generally bound to oxygen or hydroxyl groups in either triangular (e.g., BO_3) or tetrahedral (e.g., $B(OH)_4^-$) coordination. The dominant isotope fractionation process occurs in aqueous systems via an equilibrium exchange process between boric acid ($B(OH)_3$) and coexisting borate anion ($B(OH)_4^-$). At low pH-values trigonal $B(OH)_3$ predominates, at high pH-values tetrahedral $B(OH)_4^-$ is the primary anion. The pH-dependence of the two boron species and their related isotope fractionation is shown in Fig. 2.8 (after Hemming and Hanson 1992). The pH dependence has been used reconstructing past ocean pH-values by measuring the boron isotope composition of carbonates e.g. foraminifera. This relies on the fact that mainly the charged species $B(OH)_4^-$ is incorporated into carbonate minerals with small to insignificant fractionations (Hemming and Hanson 1992; Sanyal et al. 2000).

Because of the inability to quantitatively separate the two species in solution, a theoretically calculated fractionation factor of about 1.0194 at 25°C has been widely used for p_H estimates (Kakihana et al. 1977). As recently shown by Zeebe (2005) and Klochko et al. (2006) the equilibrium fractionation factor appears to be significantly larger than the theoretical value of Kakihana et al. (1977) used in paleo-pH studies. Klochko et al. (2006), for instance, reported a fractionation factor of 1.0272.

This approach has been not only used to directly estimate the ocean pH from $\delta^{11}B$ of foraminifera but to estimate from the p_H the past atmospheric CO_2 concentrations (i.e. Pearson and Palmer 1999, 2000; Pagani et al. 2005). An increase in atmospheric CO_2 results in increased dissolved CO_2 in ocean water, which in turn causes a reduction in oceanic p_H. A note of caution was presented by Lemarchand et al. (2000) who suggested that boron isotope variations in foraminifera depend at least in part on variations in the supply of riverine boron to the ocean during the geologic past. And indeed the boron isotope composition of rivers can be extremely variable (Rose et al. 2000; Lemarchand et al. 2002). Joachimski et al. (2005) presented evidence

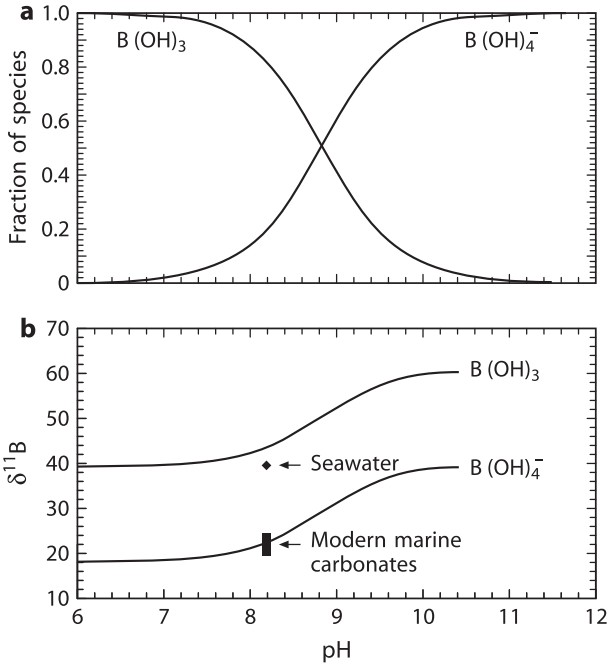

Fig. 2.8 (**a**) Distribution of aqueous boron species versus ph; (**b**) $\delta^{11}B$ of the two dominant species $B(OH)_3$ and $B(OH)_4^-$ versus ph (after Hemming and Hanson, 1992)

that Paleozoic oceans were lower in $\delta^{11}B$ by up to 10‰, which supports conclusions that boron isotope ratios cannot be used as a reliable paleo-pH indicator.

Fluid-rock interactions

Boron and – as already demonstrated – lithium are useful tracers for mass transfer estimates in subduction zones. Both elements are mobilized by fluids and melts and display considerable isotope fractionation during dehydration reactions. Concentrations of B and Li are low in mantle derived materials, whereas they are high in sediments, altered oceanic crust and continental crust. Any input of fluid and melt from the subducting slab into the overlying mantle has a strong impact on the isotope composition of the mantle wedge and on magmas generated there. Experimental studies of boron isotope fractionation between hydrous fluids, melts and minerals have shown that ^{11}B preferentially partitions into the fluid relative to minerals or melts (Palmer et al. 1987; Williams et al. 2001; Wunder et al. 2005; Liebscher et al. 2005), ranging from about 33‰ for fluid–clay (Palmer et al. 1987) to about 6‰ for fluid–muscovite at 700°C (Wunder et al. 2005) and to a few ‰ for fluid-melt above $1,000$°C (Hervig et al. 2002). The main fractionation effect seems to be due to the change from trigonal boron in neutral pH hydrous fluid to tetrahedrally coordinated boron in most rock forming minerals.

Tourmaline

Tourmaline is the most abundant reservoir of boron in metamorphic and magmatic rocks. It is stable over a very large p–T range. Since volume diffusion of B isotopes is insignificant in tourmalines (Nakano and Nakamura 2001), isotopic heterogeneities of zoned tourmalines should be preserved up to at least 600°C. Swihart and Moore (1989), Palmer and Slack (1989), Slack et al. (1993), Smith and Yardley (1996) and Jiang and Palmer (1998) analyzed tourmaline from various geological settings and observed a large range in δ^{11}B-values which reflects the different origins of boron and its high mobility during fluid related processes. By using the SIMS method, Marschall et al. (2008) demonstrated that boron isotopes in zoned tourmalines indeed may reflect different stages of tourmaline growth.

Because tourmaline is usually the only boron-bearing mineral of significance, recrystallization of tourmaline will not produce any change in its ^{11}B-content, unless boron is lost or gained by the system. If boron is lost from the rock, the δ^{11}B-value of the recrystallized tourmaline will be lower than the original value because ^{11}B is preferentially partitioned into the fluid phase. Meyer et al. (2008) experimentally determined the boron partitioning between tourmaline and fluid. In the temperature range from 400 to 700°C ^{11}B preferentially fractionates into the fluid, but to a smaller degree than determined by Palmer et al. (1992).

2.4 Carbon

Carbon occurs in a wide variety of compounds on Earth, from reduced organic compounds in the biosphere to oxidized inorganic compounds like CO_2 and carbonates. The broad spectrum of carbon-bearing compounds involved in low- and high-temperature geological settings can be assessed on the basis of carbon isotope fractionations.

Carbon has two stable isotopes (Rosman and Taylor 1998)

$^{12}\text{C} = 98.93\%$ (reference mass for atomic weight scale)
$^{13}\text{C} = 1.07\%$

The naturally occurring variations in carbon isotope composition are greater than 120‰, neglecting extraterrestrial materials. Heavy carbonates with δ^{13}C-values $> +20$‰ and light methane of < -100‰ have been reported in the literature.

2.4.1 Preparation Techniques

The gases used in $^{13}\text{C}/^{12}\text{C}$ measurements are CO_2 and recently CO during pyrolysis applications. For CO_2 the following preparation methods exist:

1. Carbonates are reacted with 100% phosphoric acid at temperatures between 20 and 90°C (depending on the type of carbonate) to liberate CO_2 (see also "oxygen").

2. Organic compounds are generally oxidized at high temperatures (850–1,000°C) in a stream of oxygen or by an oxidizing agent like CuO. In the last few years, a new methodology to measure ^{13}C-contents of individual compounds in complex organic mixtures has been developed. This so-called GC–C–MS technique employs a capillary column gas chromatograph, a combusion interface to produce CO_2 and a modified conventional gas mass–spectrometer and can measure individual carbon compounds in mixtures of sub-nanogram samples with a precision of better than $\pm 0.5‰$.

2.4.2 Standards

As the commonly used international reference standard PDB has been exhausted for several decades, there is a need for introducing new standards. Even though several different standards are in use today, the international standard the δ-values are referred to remains to be the PDB-standard (Table 2.2).

2.4.3 Fractionation Processes

The two main terrestrial carbon reservoirs, organic matter and sedimentary carbonates, have distinctly different isotopic characteristics because of the operation of two different reaction mechanisms:

1. Isotope equilibrium exchange reactions within the inorganic carbon system "atmospheric CO_2 – dissolved bicarbonate – solid carbonate" lead to an enrichment of 13C in carbonates.
2. Kinetic isotope effects during photosynthesis concentrate the light isotope 12C in the synthesized organic material.

1. The inorganic carbonate system is comprised of multiple chemical species linked by a series of equilibria:

$$CO_{2(aq)} + H_2O = H_2CO_3 \tag{2.2}$$

$$H_2CO_3 = H^+ + HCO_3^- \tag{2.3}$$

$$HCO_3^- = H^+ + CO_3^{2-} \tag{2.4}$$

Table 2.2 δ^{13}C-values of NBS-reference samples relative to PDB

NBS-18	Carbonatite	−5.00
NBS-19	Marble	+1.95
NBS-20	limestone	−1.06
NBS-21	Graphite	−28.10

The carbonate (CO_3^{2-}) ion can combine with divalent cations to form solid minerals, calcite and aragonite being the most common

$$Ca^{2+} + CO_3^{2-} = CaCO_3 \tag{2.5}$$

An isotope fractionation is associated with each of these equilibria, the ^{13}C-differences between the species depend only on temperature, although the relative abundances of the species are strongly dependent on pH. Several authors have reported isotope fractionation factors for the system dissolved inorganic carbon (DIC) – gaseous CO_2) (Vogel et al. 1970; Mook et al. 1974; Zhang et al. 1995). The major problem in the experimental determination of the fractionation factor is the separation of the dissolved carbon phases (CO_{2aq}, HCO^{3-}, CO^{3-}) because isotope equilibrium among these phases is reached within seconds. Figure 2.9 summarizes carbon isotope fractionations between various geologic materials and gaseous CO_2 (after Chacko et al. 2001).

The generally accepted carbon isotope equilibrium values between calcium carbonate and dissolved bicarbonate are derived from inorganic precipitate data of Rubinson and Clayton (1969), Emrich et al. (1970), and Turner (1982). What is often not adequately recognized is the fact that systematic C-isotope differences exist between calcite and aragonite. Rubinson and Clayton (1969) and Romanek et al. (1992) found calcite and aragonite to be 0.9 and 2.7‰ enriched in ^{13}C relative to bicarbonate at 25°C. Another complicating factor is that shell carbonate – precipitated by marine organisms – is frequently not in isotopic equilibrium with the ambient dissolved bicarbonate. Such so-called "vital" effects can be as large as a few permil (see discussion on p. 198).

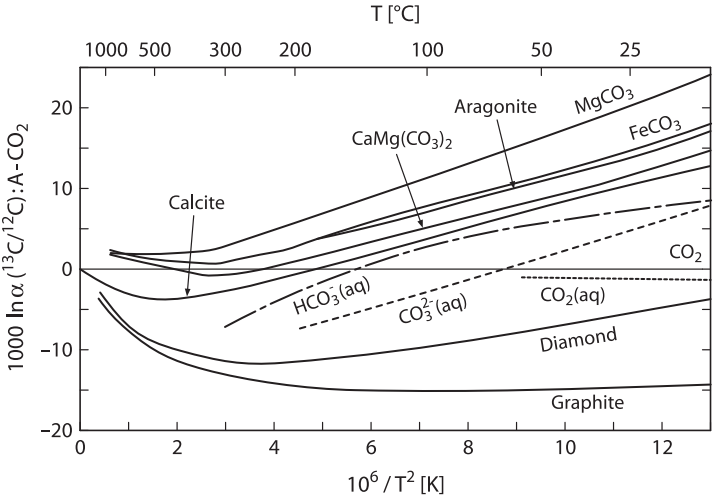

Fig. 2.9 Carbon isotope fractionations between various geologic materials and CO_2 (after Chacko et al. 2001)

Carbon isotope fractionations under equilibrium conditions are important not only at low-temperature, but also at high temperatures within the system carbonate, CO_2, graphite, and CH_4. Of these, the calcite–graphite fractionation has become a useful geothermometer (e.g., Valley and O'Neil 1981; Scheele and Hoefs 1992; Kitchen and Valley 1995) (see discussion on p. 227).

2. Early reviews by O'Leary (1981) and Farquhar et al. (1989) have provided the biochemical background of carbon isotope fractionations during photosynthesis, with more recent accounts by Hayes (2001) and Freeman (2001).

The main isotope-discriminating steps during biological carbon fixation are (1) the uptake and intracellular diffusion of CO_2 and (2) the biosynthesis of cellular components. Such a two-step model was first proposed by Park and Epstein (1960):

$$CO_{2(\text{external})} \leftrightarrow CO_{2(\text{internal})} \rightarrow \text{organic molecule}$$

From this simplified scheme, it follows that the diffusional process is reversible, whereas the enzymatic carbon fixation is irreversible. The two-step model of carbon fixation clearly suggests that isotope fractionation is dependent on the partial pressure of CO_2, i.e. pCO_2 of the system. With an unlimited amount of CO_2 available to a plant, the enzymatic fractionation will determine the isotopic difference between the inorganic carbon source and the final bioproduct. Under these conditions, ^{13}C fractionations may vary from -17 to $-40‰$ (O'Leary 1981). When the concentration of CO_2 is the limiting factor, the diffusion of CO_2 into the plant is the slow step in the reaction and carbon isotope fractionation of the plant decreases.

Atmospheric CO_2 first moves through the stomata, dissolves into leaf water and enters the outer layer of photosynthetic cells, the mesophyll cell. Mesophyll CO_2 is directly converted by the enzyme ribulose biphosphate carboxylase/oxygenase ("Rubisco") to a six carbon molecule that is then cleaved into two molecules of phosphoglycerate (PGA), each with three carbon atoms (plants using this photosynthetic pathway are therefore called C_3 plants). Most PGA is recycled to make ribulose biphosphate, but some is used to make carbohydrates. Free exchange between external and mesophyll CO_2 makes the carbon fixation process less efficient, which causes the observed large ^{13}C-depletions of C3 plants.

C4 plants incorporate CO_2 by the carboxylation of phosphoenolpyruvate (PEP) via the enzyme PEP carboxylase to make the molecule oxaloacetate which has 4 carbon atoms (hence C4). The carboxylation product is transported from the outer layer of mesophyll cells to the inner layer of bundle sheath cells, which are able to concentrate CO_2, so that most of the CO_2 is fixed with relatively little carbon fractionation.

In conclusion, the main controls on carbon fractionation in plants are the action of a particular enzyme and the "leakiness" of cells. Because mesophyll cells are permeable and bundle sheath cells are less permeable, C_3 vs C_4 plants have ^{13}C-depletions of $-18‰$ versus $-4‰$ relative to atmospheric CO_2 (see Fig. 2.10).

Work summarized by Hayes (1993) and Hayes (2001) has demonstrated that the final carbon isotope composition of naturally synthesized organic matter depends on a complex set of parameters. (1) the ^{13}C-content of the carbon source, (2) isotope

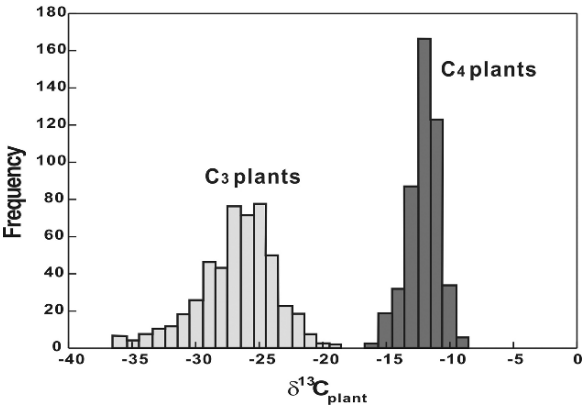

Fig. 2.10 Histogram of $\delta^{13}C$-values of C_3 and C_4 plants (after Cerling and Harris, 1999)

effects associated with the assimilation of carbon, (3) isotope effects associated with metabolism and biosynthesis and (4) cellular carbon budgets.

Even more complex is C-isotope fractionation in aquatic plants. Factors that control the $\delta^{13}C$ of phytoplankton include temperature, availability of $CO_2(aq)$, light intensity, nutrient availability, pH and physiological factors such as cell size and growth rate (Laws et al. 1995, 1997; Bidigare et al. 1997; Popp et al. 1998 and others). In particular the relationship between C-isotope composition of phytoplankton and concentration of oceanic dissolved CO_2 has been subject of considerable debate because of its potential as a palaeo-CO_2 barometer (see discussion).

Since the pioneering work of Park and Epstein (1960) and Abelson and Hoering (1961) it is well known that ^{13}C is not uniformly distributed among the total organic matter of plant material, but varies between carbohydrates, proteins and lipids. The latter class of compounds is considerably depleted in ^{13}C relative to the other products of biosynthesis. Although the causes of these ^{13}C-differences are not entirely clear, kinetic isotope effects seem to be more plausible (De Niro and Epstein 1977; Monson and Hayes 1982) than thermodynamic equilibrium effects (Galimov 1985a, 2006). The latter author argued that ^{13}C-concentrations at individual carbon positions within organic molecules are principally controlled by structural factors. Approximate calculations suggested that reduced C – H bonded positions are systematically depleted in ^{13}C, while oxidized C – O bonded positions are enriched in ^{13}C. Many of the observed relationships are qualitatively consistent with that concept. However, it is difficult to identify any general mechanism by which thermodynamic factors should be able to control chemical equilibrium within a complex organic structure. Experimental evidence presented by Monson and Hayes (1982) suggests that kinetic effects will be dominant in most biological systems.

2.4.4 Interactions between the Carbonate-Carbon Reservoir and Organic Carbon Reservoir

Variations in ^{13}C content of some important carbon compounds are schematically demonstrated in Fig. 2.11: The two most important carbon reservoirs on Earth, marine carbonates and the biogenic organic matter, are characterized by very different isotopic compositions: the carbonates being isotopically heavy with a mean $\delta^{13}C$-value around 0‰ and organic matter being isotopically light with a mean $\delta^{13}C$-value around −25‰. For these two sedimentary carbon reservoirs an isotope mass balance must exist such that:

$$\delta^{13}C_{input} = f_{org}\delta^{13}C_{org} + \left(1 - f_{org}\right)\delta^{13}C_{carb} \tag{2.6}$$

If δ input, δ_{org}, δ_{carb} can be determined for a specific geologic time, f_{org} can be calculated, where f_{org} is the fraction of organic carbon entering the sediments. It should be noted that f_{org} is defined in terms of the global mass balance and is independent of biological productivity referring to the burial rather than the synthesis of organic material. That means that large f_{org} values might be a result of high productivity and average levels of preservation of organic material or of low levels of productivity and high levels of preservation.

The $\delta^{13}C$-value for the input carbon cannot be measured precisely but can be estimated with a high degree of certainty. As will be shown later, mantle carbon has an isotopic composition around −5‰ and estimates of the global average isotope composition for crustal carbon also fall in that range. Assigning −5‰ to $\delta^{13}C$-input, a modern value for f_{org} is calculated as 0.2 or expressed as the ratio of $C_{org}/C_{carb} = 20/80$. As will be shown later (Chapter) f_{org} has obviously changed during specific periods of the Earth's history (e.g. Hayes et al. 1999). With each molecule of organic carbon being buried, a mole of oxygen is released to the atmo-

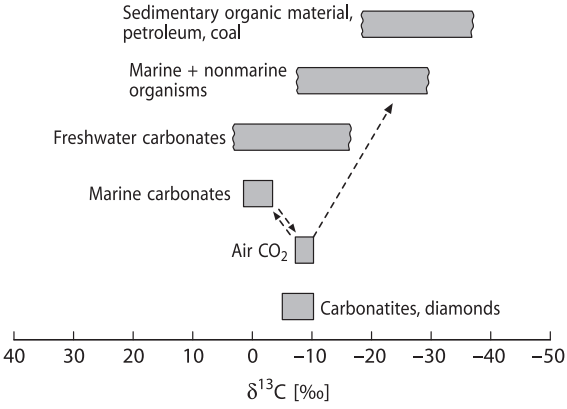

Fig. 2.11 $\delta^{13}C$-values of some important carbon reservoirs

sphere. Hence, knowledge of f_{org} is of great value in reconstructing the crustal redox budget.

2.5 Nitrogen

More than 99% of the known nitrogen on or near the Earth's surface is present as atmospheric N_2 or as dissolved N_2 in the ocean. Only a minor amount is combined with other elements, mainly C, O, and H. Nevertheless, this small part plays a decisive role in the biological realm. Since nitrogen occurs in various oxidation states and in gaseous, dissolved, and solid forms (N_2, NO_3^-, NO_2^-, NH_3, NH_4^+), it is a highly suitable element for the search of natural variations in its isotopic composition. Schoenheimer and Rittenberg (1939) were the first to report nitrogen isotopic variations in biological materials. Today, the range of reported $\delta^{15}N$-values covers 100‰, from about −50 to +50‰. However, most δ-values fall within the much narrower spread from −10 to +20‰, as described in more recent reviews of the exogenic nitrogen cycle by Heaton (1986), Owens (1987), Peterson and Fry (1987) and Kendall (1998).

Nitrogen consists of two stable isotopes, ^{14}N and ^{15}N. Atmospheric nitrogen, given by Rosman and Taylor (1998) has the following composition:

$^{14}N : 99.63\%$
$^{15}N : 0.37\%$.

N_2 is used for $^{15}N/^{14}N$ isotope ratio measurements, the standard is atmospheric N_2. Various preparation procedures have been described for the different nitrogen compounds (Bremner and Keeney 1966; Owens 1987; **? ?**; Kendall and Grim 1990; Scholten 1991 and others). In the early days of nitrogen isotope investigations the extraction and combustion techniques potentially involved chemical treatments that could have introduced isotopic fractionations. In recent years, simplified techniques for combustion have come into routine use, so that a precision of 0.1–0.2‰ for $\delta^{15}N$ determinations can be achieved. Organic nitrogen-compounds are combusted to CO_2, H_2O and N_2, the product gases are separated from each other cryogenically and the purified N_2 is trapped on molecular sieves for mass-spectrometric analysis.

To understand the processes leading to the nitrogen isotope distribution in the geological environment, a short discussion of the biological nitrogen cycle is required. Atmospheric nitrogen, the most abundant form of nitrogen, is the least reactive species of nitrogen. It can, however, be converted to "fixed" nitrogen by bacteria and algae, which, in turn, can be used by biota for degradation to simple nitrogen compounds such as ammonium and nitrate. Thus, microorganisms are responsible for all major conversions in the biological nitrogen cycle, which generally is divided into fixation, nitrification, and denitrification. Other bacteria return nitrogen to the atmosphere as N_2.

The term *fixation* is used for processes that convert unreactive atmospheric N_2 into reactive nitrogen such as ammonium, usually involving bacteria. Fixation commonly produces organic materials with δ^{15}N-values slightly less than 0‰ ranging from −3 to +1 (Fogel and Cifuentes 1993) and occurs in the roots of plants by many bacteria. The large amount of energy needed to break the molecular nitrogen bond makes nitrogen fixation a very inefficient process with little associated N-isotope fractionation.

Nitrification is a multi-step oxidation process mediated by several different autotrophic organisms. Nitrate is not the only product of nitrification, different reactions produce various nitrogen oxides as intermediate species. Nitrification can be described as two partial oxidation reactions, each of which proceeds separately.

Oxidation by Nitrosomas ($NH_4 \rightarrow NO_{2-}$) followed by oxidation by Nitrobacter (NO_2fiNO_3). Because the oxidation of nitrite to nitrate is generally rapid, most of the N-isotope fractionations is caused by the slow oxidation of ammonium by Nitrosomas. In N-limited systems fractionations are minimal.

Denitrification (reduction of more oxidized forms to more reduced forms of nitrogen) is a multi-step process with various nitrogen oxides as intermediate compounds resulting from biologically mediated reduction of nitrate. Denitrification takes place in poorly aerated soil and in stratified anaerobic water bodies. Denitrification supposedly balances the natural fixation of nitrogen, if it did not occur, then atmospheric nitrogen would be exhausted in less than 100 million years. Denitrification causes the δ^{15}N-values of the residual nitrate to increase exponentially as nitrate concentrations decrease. Experimental investigations have demonstrated that fractionation factors may change from 10 to 30‰, with the largest values obtained under lowest reduction rates. Generally, the same factors that influence isotope fractionation during bacterial sulfate reduction are also operative during bacterial denitrification. Table 2.3, which gives a summary of observed N-isotope fractionations, clearly indicates the dependence of fractionations on nitrogen concentrations and

Table 2.3 Naturally observed isotope fractionation for nitrogen assimilation (after Fogel and Cifuentes Fogel and Cifuentes 1993)

N_2 fixation	−3 to +1‰
NH_4^+ assimilation	
Cultures	
Millimolar concentrations	0 to −15‰
Micromolar concentrations	−3 to −27‰
Field observations	
Micromolar concentrations	−10‰
NO_3^- assimilation	
Cultures	
Millimolar concentrations	0 to −24‰
Micromolar concentrations	−10‰
Field observations	
Micromolar concentrations	−4 to −5‰

demonstrates, that at low nitrogen concentrations fractionations are nearly zero because virtually all the nitrogen is used.

So far, only kinetic isotope effects have been considered, but isotopic fractionations associated with equilibrium exchange reactions have been demonstrated for the common inorganic nitrogen compounds (Letolle 1980). Of special importance in this respect is the ammonia volatilization reaction:

$$NH_{3gas} \leftrightarrow NH^{+}_{4aq}$$

for which isotope fractionation factors of 1.025–1.035 have been determined (Kirshenbaum et al. 1947; Mariotti et al. 1981). Experimental data by Nitzsche and Stiehl (1984) indicate fractionation factors of 1.0143 at 250°C and of 1.0126 at 350°C very small ^{15}N-enrichment of about 0.1‰ occurs during the solution of atmospheric N_2 in ocean water (Benson and Parker 1961).

Nitrogen isotope studies are extremely important for evaluating the source and fate of nitrogen in the marine and terrestrial environment. $\delta^{15}N$-values measured in the water column of the ocean and in sediments depend on the many nitrogen isotope fractionation reactions in the biological cycle. Nitrogen isotopes have been used as a paleoceanographic proxy, because they record changes of nutrient dynamics and ventilation that affects denitrification in the water column (e.g. Farrell et al. 1995). This approach is based on the fact that particulate organic nitrogen depends on (1) the isotopic composition of dissolved nitrate, which in oxygenated waters has a $\delta^{15}N$-value of about -6‰ (in anoxic waters where denitrification occurs the $\delta^{15}N$-value is significantly higher, up to 18.8‰ in the tropical North Pacific; Cline and Kaplan 1975) and on (2) isotope fractionation that occurs during nitrogen uptake by phytoplankton. In the photic zone phytoplankton preferentially incorporates ^{14}N, which results in a corresponding ^{15}N-enrichment in the residual nitrate. The N-isotope composition of settling organic detritus thus varies depending on the extent of nitrogen utilization: low ^{15}N contents indicate low relative utilisation, high ^{15}N contents indicate a high utilization.

Much of the initial organic nitrogen reaching the sediment/water interface is lost during early diagenesis. Nevertheless the nitrogen isotope composition of sediments is primarely determined by the source organic matter. Source studies have been undertaken to trace the contribution of terrestrial organic matter to ocean water and to sediments (i.e. Sweeney et al. 1978; Sweeney and Kaplan 1980). Such studies are based, however, on the assumption that the ^{15}N content remains unchanged in the water column. Investigations by Cifuentes et al. (1989), Altabet et al. (1991), and Montoya et al. (1991) have demonstrated that there may be rapid temporal (even on a time scale of days) and spatial changes in the nitrogen isotope composition of the water column due to biogeochemical processes. This complicates a clear distinction between terrestrial and marine organic matter, although marine organic matter generally has a higher $^{15}N/^{14}N$ ratio than terrestrial organic matter.

The organic matter in sediments has a mean $\delta^{15}N$-value of around $+7$‰ (Sweeney et al. 1978). During diagenesis biological and thermal degradation of

the organic matter results in the formation of ammonium (NH_4) which can be incorporated for potassium in clay minerals. This nitrogen in the crystal lattice of clay minerals and micas is mainly derived from decomposing organic matter and thus has a very similar isotopic composition as the organic matter (Scholten 1991; Williams et al. 1995).

During metamorphism of sediments, there is a significant loss of ammonium during devolatilisation, which is associated with a nitrogen fractionation, leaving behind ^{15}N residues (Haendel et al. 1986; Bebout and Fogel 1992; Jia 2006). Thus high-grade metamorphic rocks and granites are relatively enriched in ^{15}N and typically have $\delta^{15}N$-values between 8 and 10‰. Sadofsky and Bebout (2000) have examined the nitrogen isotope fractionation among coexisting micas, but could not find any characteristic difference between biotite and white mica.

In summary, nitrogen in sediments and crustal rocks exhibits positive $\delta^{15}N$-values around 6‰. In contrast, mantle nitrogen extracted from MORB glasses (Marty and Humbert 1997; Marty and Zimmermann 1999) and from diamonds (Javoy et al. 1986; Cartigny et al. 1997) have average $\delta^{15}N$-values of around -5‰. These similar values for subcontinental and MORB mantle suggests a homogeneous distribution of nitrogen isotopes in the mantle. $\delta^{15}Nt$-values thus are an important tracer to distinguish mantle-derived from crustal derived nitrogen.

Many studies have shown that nitrogen isotopes can be used in environmental studies. Fertilizer, animal wastes or sewage are the main sources of nitrate pollution in the hydrosphere. Under favorable conditions, these N-bearing compounds can be isotopically distinguished from each other (Heaton 1986). Anthropogenic fertilizers have $\delta^{15}N$-values in the range -4 to $+4$‰ reflecting their atmospheric source, whereas animal waste typically has $\delta^{15}N$-values > 5‰. Soil-derived nitrate and fertilizer nitrate commonly have overlapping $\delta^{15}N$-values. $\delta^{15}N$ can potentially also be used as trophic level indicator.

Figure 2.12 gives an overview about the nitrogen isotope variations in some important reservoirs.

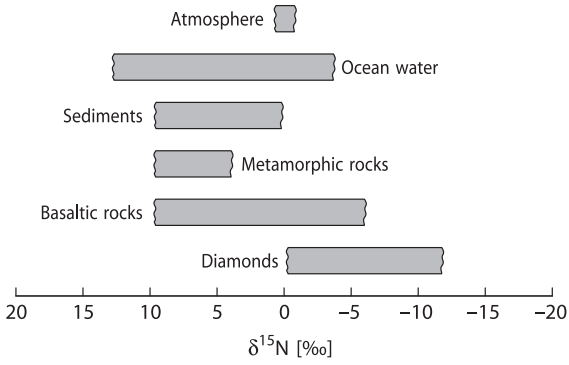

Fig. 2.12 $\delta^{15}N$-values of geologically important reservoirs

2.6 Oxygen

Oxygen is the most abundant element on Earth. It occurs in gaseous, liquid and solid compounds, most of which are thermally stable over large temperature ranges. These facts make oxygen one of the most interesting elements in isotope geochemistry.

Oxygen has three stable isotopes with the following abundances (Rosman and Taylor 1998)

$^{16}O : 99.757\%$
$^{17}O : 0.038\%$
$^{18}O : 0.205\%$

Because of the higher abundance and the greater mass difference, the $^{18}O/^{16}O$ ratio is normally determined, which may vary in natural samples by about 10% or in absolute numbers from about 1:475 to 1:525.

2.6.1 Preparation Techniques

CO_2 is the gas generally used for mass-spectrometric analysis. More recently CO and O_2 have also been used in high temperature conversion of organic material and in laser probe preparation techniques. A wide variety of methods have been described to liberate oxygen from the various oxygen-containing compounds.

Oxygen in silicates and oxides is usually liberated through fluorination with F_2, BrF_5 or ClF_3 in nickel-tubes at 500 to 650°C (Taylor and Epstein 1962; Clayton and Mayeda 1963; Borthwick and Harmon 1982) or by heating with a laser (Sharp 1990). Decomposition by carbon reduction at 1,000 to 2,000°C may be suitable for quartz and iron oxides but not for all silicates (Clayton and Epstein 1958). The oxygen is converted to CO_2 over heated graphite or diamond. Care must be taken to ensure quantitative oxygen yields, which can be a problem in the case of highly refractive minerals like olivine and garnet. Low yields may result in anomalous $^{18}O/^{16}O$ ratios, high yields are often due to excess moisture in the vacuum extraction line.

Conventional fluorination is usually done on 10–20 mg of whole-rock powder or minerals separated from much larger samples; the inability to analyze small quantities means that natural heterogeneity cannot be detected by such bulk techniques. Recent advances in the development of laser microprobes, first described by Sharp (1990), have revolutionized mineral analyses. Laser techniques have both the resolution and precision to investigate isotopic zoning within single mineral grains and mineral inter- and overgrowths.

The standard procedure for the isotope analysis of carbonates is the reaction with 100% phosphoric acid at 25°C first described by McCrea (1950). The following reaction equation:

$$MeCO_3 + H_3PO_4 \rightarrow MeHPO_4 + CO_2 + H_2O \qquad (2.7)$$

where Me is a divalent cation, shows that only two-thirds of the carbonate oxygen present in the product CO_2 is liberated, and thus a significant isotope effect is observed, which is on the order of 10‰, but varies up to a few ‰ depending on the cation, the reaction temperature and the preparation procedure. The so-called acid fractionation factor must be precisely known to obtain the oxygen isotope ratio of the carbonate. This can be done by measuring the $\delta^{18}O$-value of the carbonate by fluorination with BrF_5, first described by Sharma and Clayton (1965).

Experimental details of the phosphoric acid method vary significantly among different laboratories. The two most common varieties are the "sealed vessel" and the "acid bath" methods. In the latter method the CO_2 generated is continuously removed, while in the former it is not. Swart et al. (1991) demonstrated that the two methods exhibit a systematic ^{18}O difference between 0.2 and 0.4‰ over the temperature range 25 to 90°C. Of these the acid-bath method probably provides the more accurate results. A further modification of this technique is referred to as the "individual acid bath", in which contaminations from the acid delivery system are minimized. Wachter and Hayes (1985) demonstrated that careful attention must be given to the phosphoric acid. In their experiments best results were obtained by using a 105% phosphoric acid and a reaction temperature of 75°C. This high reaction temperature should not be used when attempting to discriminate between mineralogically distinct carbonates by means of differential carbonate reaction rates.

Because some carbonates like magnesite or siderite react very sluggishly at 25°C, higher reaction temperatures are necessary to extract CO_2 from these minerals. Reaction temperatures have varied up to 90 or even 150°C (Rosenbaum and Sheppard 1986; Böttcher 1996), but there still exist considerable differences in the fractionation factors determined by various workers. For example fractionations between aragonite and calcite remain controversial and different workers have reported fractionations from negative to positive. Nevertheless there seems to be a general agreement that the fractionation factor for aragonite is about 0.6‰ higher than for calcite (Tarutani et al. 1969; Kim and O'Neil 1997), although Grossman and Ku (1986) have reported a value of up to 1.2‰. The dolomite-calcite fractionation may vary depending on specific composition (Land 1980). Table 2.4 reports acid fractionation factors for various carbonates.

Phosphates are first dissolved, then precipitated as silver phosphate (Crowson et al. 1991). Ag_3PO_4 is preferred because it is non-hydroscopic and can be precipitated rapidly without numerous chemical purification steps (O'Neil et al. 1994). This Ag_3PO_4 is then fluorinated (Crowson et al. 1991), reduced with C either in a furnace (O'Neil et al. 1994) or with a laser (Wenzel et al. 2000) or pyrolyzed (Vennemann et al. 2002). Because PO_4 does not exchange oxygen with water at room temperature (Kolodny et al. 1983), the isotopic composition of the Ag_3PO_4 is that of the PO_4 component of the natural phosphate. As summarized by Vennemann et al. (2002) conventional fluorination remains the most precise and accurate analytical technique for Ag_3PO_4. Laser techniques on bulk materials have also been attempted (Cerling and Sharp 1996; Kohn et al. 1996; Wenzel et al. 2000), but because fossil phosphates invariably contain diagenetic contaminants, chemical processing and analysis of a specific component (CO_3 or PO_4) is ordinarily performed.

Table 2.4 Acid fractionation factors for various carbonates determined at 25°C (modified after Kim et al. 2007)

Mineral	α	Reference
Calcite	10.30	Kim et al. (2007)
Aragonite	10.63	Kim et al. (2007)
	11.14	Gilg (2007)
Dolomite	11.75	Rosenbaum and Sheppard (1986)
Magnesite	10.79 (50°C)	Das Sharma et al. (2002)
Siderite	11.63	Carothers et al. (1988)
Witherite	10.57	Kim and O·Neil (1997)

Sulfates are precipitated as $BaSO_4$, and then reduced with carbon at 1,000°C to produce CO_2 and CO. The CO is either measured directly or converted to CO_2 by electrical discharge between platinum electrodes (Longinelli and Craig 1967). Total pyrolysis by continuous flow methods has made the analysis of sulfate oxygen more precise and less time-consuming than the off-line methods. Bao and Thiemens (2000) have used a CO_2-laser fluorination system to liberate oxygen from barium sulfate.

The $^{18}O/^{16}O$ ratio of water is usually determined by equilibration of a small amount of CO_2 with a surplus of water at a constant temperature. For this technique the exact value of the fractionation for the CO_2/H_2O equilibrium at a given temperature is of crucial importance. A number of authors have experimentally determined this fractionation at 25°C with variable results. A value of 1.0412 was proposed at the 1985 IAEA Consultants Group Meeting to be the best estimate.

It is also possible to quantitatively convert all water oxygen directly to CO_2 by reaction with guanidine hydrochloride (Dugan et al. 1985) which has the advantage that it is not necessary to assume a value for the $H_2O - CO_2$ isotope fractionation in order to obtain the $^{18}O/^{16}O$ ratio. On-line pyrolysis using TC-EA systems represents another approach (de Groot 2004).

2.6.2 Standards

Two different δ–scales are in use: $\delta^{18}O(VSMOW)$ and $\delta^{18}O(VPDB)$, because of two different categories of users, who have traditionally been engaged in O-isotope studies. The VPDB scale is used in low-temperature studies of carbonate. PDB is a Cretaceous belemnite from the Pee Dee Formation and was the laboratory working standard used at the university of Chicago in the early 1950's when the paleotemperature scale was developed. The original supply of this standard has long been exhausted, therefore secondary standards have been introduced (see Table 2.5), whose isotopic compositions have been calibrated relative to PDB. All other oxygen isotope analyses (waters, silicates, phosphates, sulfates, high-temperature carbonates) are given relative to SMOW.

Table 2.5 δ^{18}O-values of commonly used O-isotope standards

Standard	Material	PDB scale	VSMOW scale
NBS-19	Marble	−2.20	(28.64)
NBS-20	Limestone	−4.14	(26.64)
NBS-18	Carbonatite	−23.00	(7.20)
NBS-28	Quartz	(−20.67)	9.60
NBS-30	Biotite	(−25.30)	5.10
GISP	Water	(−53.99)	−24.75
SLAP	Water	(−83.82)	−55.50

The conversion equations of δ^8O(PDB) versus δ^{18}O(VSMOW) and vice versa (Coplen et al. 1983) are:

$$\delta^{18}\mathrm{O}\,(\mathrm{VSMOW}) = 1.03091\delta^{18}\mathrm{O}\,(\mathrm{PDB}) + 30.91$$

and

$$\delta^{18}\mathrm{O}\,(\mathrm{PDB}) = 0.97002\delta^{18}\mathrm{O}\,(\mathrm{VSMOW}) - 29.98$$

Table 2.5 gives the δ^{18}O-values of commonly used oxygen isotope standards on both scales (parenthesis denote calculated values).

2.6.3 Fractionation Processes

Out of the numerous possibilities to fractionate oxygen isotopes in nature, the following are of special significance.

Knowledge of the oxygen isotope fractionation between liquid water and water vapor is essential for the interpretation of the isotope composition of different water types. Fractionation factors experimentally determined in the temperature range from 0 to 350°C have been summarized by Horita and Wesolowski (1994). This is shown in Fig. 2.13.

Addition of salts to water also affects isotope fractionations. The presence of ionic salts in solution changes the local structure of water around dissolved ions. Taube (1954) first demonstrated that the $^{18}O/^{16}O$ ratio of CO_2 equilibrated with pure H_2O decreased upon the addition of $MgCl_2$, $AlCl_3$ and HCl, remained more or less unchanged for NaCl, and increased upon the addition of $CaCl_2$. The changes vary roughly linearly with the molality of the solute (see Fig. 2.14).

To explain this different fractionation behavior, Taube (1954) postulated different isotope effects between the isotopic properties of water in the hydration sphere of the cation and the remaining bulk water. The hydration sphere is highly ordered, whereas the outer layer is poorly ordered. The relative sizes of the two layers are dependent upon the magnitude of the electric field around the dissolved ions. The strength of the interaction between the dissolved ion and water molecules is also dependent upon the atomic mass of the atom to which the ion is bonded.

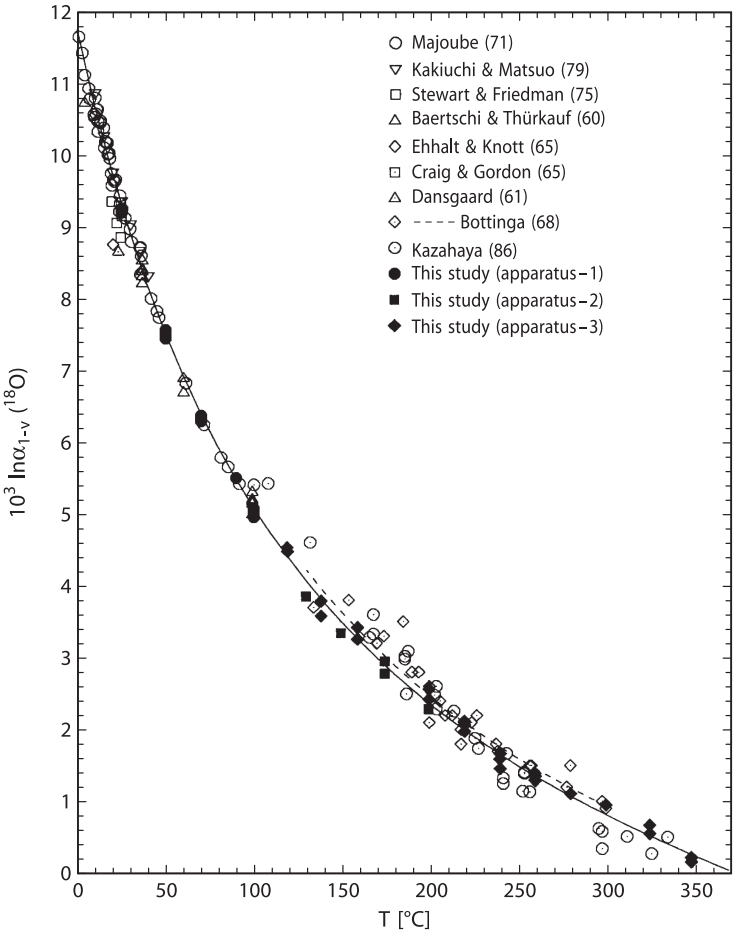

Fig. 2.13 Oxygen isotope fractionation factors between liquid water and water vapour in the temperature range 0 – 350°C (after Horita and Wesolowski 1994)

O'Neil and Truesdell (1991) have introduced the concept of "structure-making" and "structure-breaking" solutes: structure makers yield more positive isotope fractionations relative to pure water whereas structure breakers produce negative isotope fractionations. Any solute that results in a positive isotope fractionation is one that causes the solution to be more structured as is the case for ice structure, when compared to solutes that lead to less structured forms, in which cation – H_2O bonds are weaker than H_2O – H_2O bonds.

As already treated in the "hydrogen" section, isotope fractionations, the hydration of ions may play a significant role in hydrothermal solutions and volcanic vapors (Driesner and Seward 2000). Such isotope salt effects may change the oxygen isotope fractionation between water and other phases by several permil.

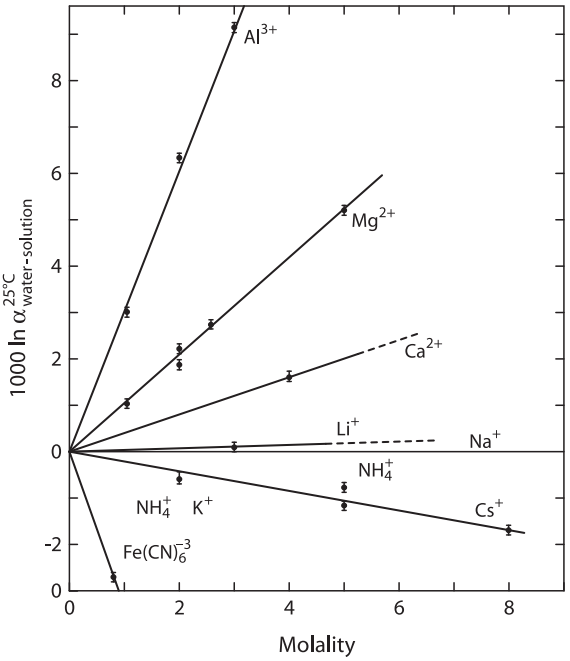

Fig. 2.14 Oxygen isotope fractionations between pure water and solutions of various ions (after O'Neil and Truesdell 1991)

Table 2.6 Experimentally determined oxygen isotope fractionation factors relative to water for the aqueous system $CO_2 - H_2O$ between 5 and 40°C according to $10^3\ \ln\alpha = A(10^6/T^{-2}) + B$ (Beck et al. 2005)

	A	B
HCO_3^-	2.59	1.89
CO_3^{2-}	2.39	−2.70
$CO_{2(aq)}$	2.52	12.12

Of equal importance is the oxygen isotope fractionation in the CO_2 – H_2O system. Early work concentrated on the oxygen isotope partitioning between gaseous CO_2 and water (Brennikmeijer et al. 1983). More recent work by Usdowski and Hoefs (1993), Beck et al. (2005) and Zeebe (2007) have determined the oxygen isotope composition of the individual carbonate species that are isotopically different at room temperature. Table 2.6 summarizes the equations for the temperature dependence between 5 and 40°C (Beck et al. 2005).

The fractionation (1,000 ln α) between dissolved CO_2 and water at 25°C is 41.6. dropping to 24.7 at high pH when CO_3^{2-} is the dominant species (see Fig. 2.15).

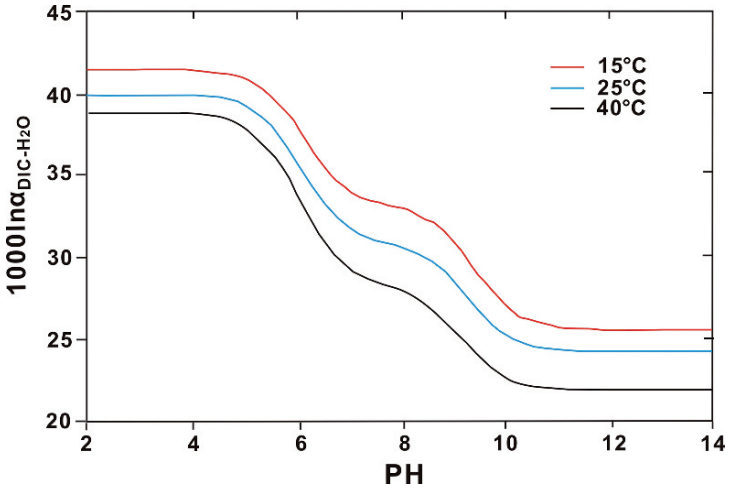

Fig. 2.15 Oxygen isotope fractionations between dissolved inorganic carbon (DIC) and water as a function of pH and temperatures (after Beck et al. 2005)

Table 2.7 Sequence of minerals in the order (bottom to top) of their increasing tendency to concentrate ^{18}O

Quartz
Dolomite
K-feldspar, albite
Calcite
Na-rich plagioclase
Ca-rich plagioclase
Muscovite, paragonite, kyanite, glaucophane
Orthopyroxene, biotite
Clinopyroxene, hornblende, garnet, zircon
Olivine
Ilmenite
Magnetite, hematite

The pH dependence of the oxygen isotope composition in the carbonate-water system has important implications in the derivation of oxygen isotope temperatures.

The oxygen isotope composition of a rock depends on the ^{18}O contents of the constituent minerals and the mineral proportions. Garlick (1966) and Taylor (1968) arranged coexisting minerals according to their relative tendencies to concentrate ^{18}O. The list given in Table 2.7 has been augmented by data from Kohn and Valley (1998a, b, c).

This order of decreasing ^{18}O-contents has been explained in terms of the bond-type and strength in the crystal structure. Semi-empirical bond-type calculations have been developed by Garlick (1966) and Savin and Lee (1988) by assuming that oxygen in a chemical bond has similar isotopic behavior regardless of the mineral in which the bond is located. This approach is useful for estimating fractionation

factors. The accuracy of this approach is limited due to the assumption that the isotope fractionation depends only upon the atoms to which oxygen is bonded and not upon the structure of the mineral, which is not strictly true. By using an electrostatic approximation to bond strength and taking into account cation mass Schütze (1980) developed an increment method for calculations of oxygen isotope fractionations in silicates, which has been modified and refined by Zheng (1991, 1993a, b). Kohn and Valley (1998a, b) determined empirically the effects of cation substitutions in complex minerals such as amphiboles and garnets spanning a large range in chemical compositions. Although isotope effects of cation exchange are generally less than 1‰ at $T > 500°C$, they increase considerably at lower temperatures. Thus use of amphiboles and garnets for thermometry requires exact knowledge of chemical compositions.

On the basis of these systematic tendencies of ^{18}O enrichment found in nature, significant temperature information can be obtained up to temperatures of 1,000°C, and even higher, if calibration curves can be worked out for the various mineral pairs. The published literature contains many calibrations of oxygen isotope geothermometers, most are determined by laboratory experiments, although some are based on theoretical calculations.

Although much effort has been directed toward the experimental determination of oxygen isotope fractionation factors in mineral- water systems, the use of water as an oxygen isotope exchange medium has several disadvantages. Some minerals become unstable in contact with water at elevated temperatures and pressures, leading to melting, breakdown and hydration reactions. Incongruent solubility and ill-defined quench products may introduce additional uncertainties. Most of the disadvantages of water can be circumvented by using calcite as an exchange medium (Clayton et al. 1989; Chiba et al. 1989). Mineral-mineral fractionations – determined by these authors (Table 2.8) – give internally consistent geothermometric information that generally is in accord with independent estimates, such as the theoretical calibrations of Kieffer (1982).

A more recent summary has been given by Chacko et al. (2001) (see Fig. 2.16).

Many isotopic fractionations between low-temperature minerals and water have been estimated by assuming that their temperature of formation and the isotopic composition of the water in which they formed (for example, ocean water) are well known. This is sometimes the only approach available in cases in which the rates of

Table 2.8 Coefficients A for silicate – pair fractionations ($1{,}000 \ln\alpha \, X - Y = A/T^2 \, 10^6$ (after Chiba et al. 1989)

	Cc	Ab	An	Di	Fo	Mt
Qtz	0.38	0.94	1.99	2.75	3.67	6.29
Cc		0.56	1.61	2.37	3.29	5.91
Ab			1.05	1.81	2.73	5.35
An				0.76	1.68	4.30
Di					0.92	3.54
Fo						2.62

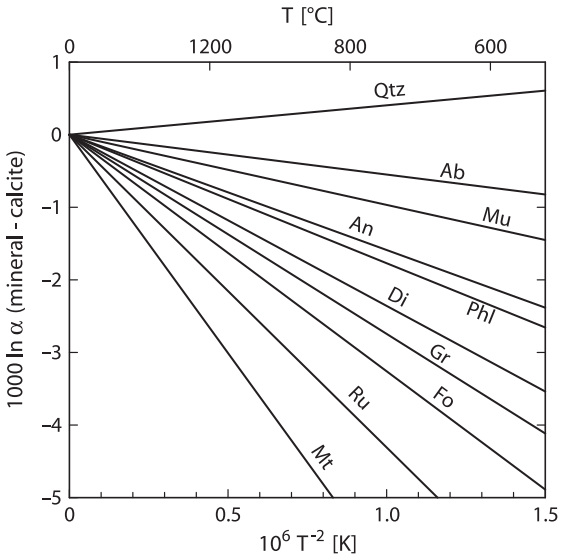

Fig. 2.16 Oxygen isotope fractionations between various minerals and calcite (after Chacko et al. 2001)

isotope exchange reactions are slow and in which minerals cannot be synthesized in the laboratory at appropriate temperatures.

2.6.4 Fluid-Rock Interactions

Oxygen isotope ratio analysis provides a powerful tool for the study of water/rock interaction. The geochemical effect of such an interaction between water and rock or mineral is a shift of the oxygen isotope ratios of the rock and/or the water away from their initial values, given that their compositions are not in equilibrium.

Detailed studies of the kinetics and mechanisms of oxygen isotope exchange between minerals and fluids show that there are three possible exchange mechanisms (Matthews et al. 1983b, c; Giletti 1985).

1. *Solution-precipitation*. During a solution-precipitation process, larger grains grow at the expense of smaller grains. Smaller grains dissolve and recrystallize on the surface of larger grains which decreases the overall surface area and lowers the total free energy of the system. Isotopic exchange with the fluid occurs while material is in solution.
2. *Chemical reaction*. The chemical activity of one component of both fluid and solid is so different in the two phases that a chemical reaction occurs. The breakdown of a finite portion of the original crystal and the formation of new crystals is implied. The new crystals would form at or near isotopic equilibrium with the fluid.

3. *Diffusion*. During a diffusion process isotopic exchange takes place at the interface between the crystal and the fluid with little or no change in morphology of the reactant grains. The driving force is the random thermal motion of the atoms within a concentration or activity gradient.

In the presence of a fluid phase, coupled dissolution – reprecipitation is known to be a much more effective process than diffusion. This has been first demonstrated experimentally by O'Neil and Taylor (1967) and later re-emphasized by Cole (2000) and Fiebig and Hoefs (2002).

The first attempts to quantify isotope exchange processes between water and rocks were made by Taylor (1974). By using a simple closed-system material balance equation these authors were able to calculate cumulative fluid/rock ratios.

$$W/R = \frac{\delta_{\mathrm{rock_f}} - \delta_{\mathrm{rock_i}}}{\delta_{\mathrm{H_2O}} - (\delta_{\mathrm{rock_f}} - \Delta)}, \tag{2.8}$$

where $\Delta = \delta_{\mathrm{rock}} f - \delta_{\mathrm{H_2O}} f$.

Their equation requires adequate knowledge of both the initial (i) and final (f) isotopic states of the system and describes the interaction of one finite volume of rock with a fluid. The utility of such "zero-dimensional" equations has been questioned by Baumgartner and Rumble (1988), Blattner and Lassey (1989), Nabelek (1991), Bowman et al. (1994) and others. Only under special conditions do one-box models yield information on the amount of fluid that actually flowed through the rocks. If the rock and the infiltrating fluid were not far out of isotopic equilibrium, then the calculated fluid/rock ratios rapidly approach infinity. Therefore, the equations are sensitive only to small fluid/rock ratios. Nevertheless, the equations can constrain fluid sources. More sophisticated one-dimensional models like the chromatographic or continuum mechanics models (i.e. Baumgartner and Rumble 1988) are physically more plausible and can describe how the isotopic composition of the rock and of the fluid change with time and space. The mathematical models are complex and are based on partial differential equations that must be solved numerically. Examples of fluid–rock interactions in contact metamorphic environments have been presented by Nabelek and Labotka 1993, Bowman et al. 1994 and application to contrasting lithologies by Bickle and Baker (1990) and Cartwright and Valley (1991).

Criss et al. (1987) and Gregory et al. (1989) developed a theoretical framework that describes the kinetics of oxygen isotope exchange between minerals and coexisting fluids. Figure 2.17 shows characteristic patterns in δ–δ plots for some hydrothermally altered granitic and gabbroic rocks. The $^{18}O/^{16}O$ arrays displayed on Fig. 2.17 cut across the 45° equilibrium lines at a steep angle as a result of the much faster oxygen isotope exchange of feldspar compared to that of quartz and pyroxene. If a low-^{18}O fluid such as meteoric or ocean water is involved in the exchange process, the slopes of the disequilibrium arrays can be regarded as "isochrons" where, with continued exchange through time the slopes become less steep and approach the 45° equilibrium line. These "times" represent the duration of a particular hydrothermal event.

Figure 2.18 summarizes the naturally observed oxygen isotope variations in important geological reservoirs.

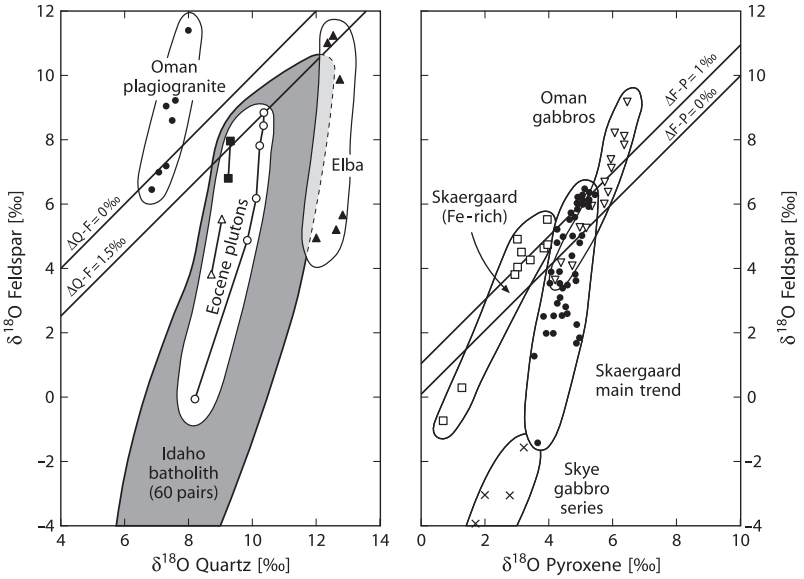

Fig. 2.17 $\delta^{18}O$ (feldspar) vs $\delta^{18}O$ (quartz) and vs $\delta^{18}O$ (pyroxene) plots of disequilibrium mineral pair arrays in granitic and gabbroic rocks. The arrays indicate open-system conditions from circulation of hydrothermal fluids (after Gregory et al. 1989)

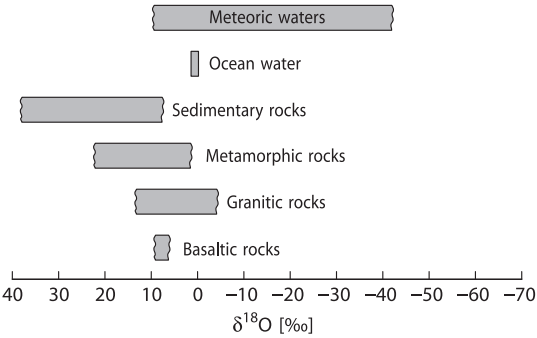

Fig. 2.18 $\delta^{18}O$ values of important geological reservoirs

2.7 Magnesium

Magnesium is composed of three isotopes (Rosman and Taylor 1998)

^{24}Mg 78.99%

^{25}Mg 10.00%

^{26}Mg 11.01%

Early investigations on Mg isotope variations have been limited by an uncertainty of 1 to 2‰. Catanzaro and Murphy (1966) for instance concluded that terrestrial Mg isotope variations are restricted to a few ‰. The introduction of multicollector-inductively coupled-plasma mass spectrometry (MC-ICP-MS) increased the precision by one order of magnitude and has initiated a new search of natural isotope variations (Galy et al. 2001, 2002). These authors obtained an overall 4‰ variation in δ^{26}Mg.

The oxidation state of magnesium always is two, thus it might be expected that the range in isotope composition is small. Mg is soluble and mobile during weathering, which, on the other hand, might initiate small fractionations during carbonate precipitation and clay formation. And indeed by investigating Mg isotope fractionation between speleothems and associated drip waters Galy et al. (2002) observed a characteristic difference in both phases, which might indicate equilibrium conditions. They further observed a 2–3‰ enrichment in dolomites relative to limestones, suggesting a mineralogical control on the isotope composition of carbonates.

Because of its relatively long mean residence time, ocean water has a constant isotope composition. Corals are about 1‰ and foraminifera are about 4.5‰ lighter than ocean water. Thus significant Mg isotope fractionations occur during biomineralization of carbonate secreting organisms which is larger than for Ca isotopes (see Section 2.11).

Tipper et al. (2006) have measured the Mg isotope composition of rivers. They observed a total variation in ^{26}Mg of 2.5‰. The lithology in the drainage area seems to be of limited significance, a major part of the variability has to be attributed to fractionations in the weathering environment.

One of the advantages of the MC-ICPMS technique compared to the SIMS technique is the ability to measure $^{25}Mg/^{24}Mg$ and $^{26}Mg/^{24}Mg$ ratios independently many times smaller than the magnitude of the natural variations. By doing this Young and Galy (2004) demonstrated that the relationship between $^{25}Mg/^{24}Mg$ and $^{26}Mg/^{24}Mg$ are diagnostic of kinetic vs equilibrium fractionations: for equilibrium processes the slope on a three-isotope diagram should be close to 0.521, for kinetic processes the slope should be 0.511. Evidence for equilibrium fractionation has been found for low-Mg calcite speleothems (Galy et al. 2002). Recently, however, Buhl et al. (2007) argued that a pure equilibrium mass fractionation cannot explain the Mg isotope data from speleothems. On the other hand biologically mediated precipitates such as foraminifera (Chang et al. 2004) and dolomites of bacterial origin (Carder et al. 2005) have a clear kinetic signature.

Galy et al. (2001) suggested that the mantle should have a homogeneous Mg isotope composition. Pearson et al. (2006), however, demonstrated that olivines from mantle xenoliths have a heterogeneous compositions with a δ^{26}Mg range of about 4‰. These authors suggested that the differences are due to diffusion-related metasomatic processes.

2.8 Silicon

Silicon has three stable isotopes with the following abundances (Rosman and Taylor 1998):

$$^{28}\text{Si } 92.23\%$$

$$^{29}\text{Si } 4.68\%$$

$$^{30}\text{Si } 3.09\%$$

Because of its high abundance on Earth, silicon is in principle a very interesting element to study for isotope variations. However, because there is no redox reaction for silicon (silicon is always bound to oxygen), only small isotope fractionations are to be expected in nature. Silicic acid, on the other hand, is an important nutrient in the ocean that is required for the growth of mainly diatoms and radiolaria. The silicon incorporation into siliceous organisms is associated with a Si isotope fractionation, because ^{28}Si is prefrentially removed as the organisms form biogenic silica. Early investigations by Douthitt (1982) and more recent ones by Ding et al. (1996) observed a total range of δ^{30}Si values in the order of 6‰. This range has extended to about 12‰ with the lowest δ^{30}Si value of -5.7‰ in siliceous cements (Basile-Doelsch et al. 2005) and the highest of $+6.1$‰ for rice grains (Ding et al. 2005).

Silicon isotope ratios have been generally measured by fluorination (Douthitt 1982; Ding et al. 1996). However, the method is time consuming and potentially hazardous, therefore, more recently MC-ICP-MS techniques have been introduced (Cardinal et al. 2003; Engstrom et al. 2006). Determinations with SIMS have been carried out by Robert and Chaussidon (2006). Very recently, Chmeleff et al. (2008) have shown that a UV-femtosecond laser ablation system coupled with MC-ICP-MS gives δ^{29}Si and δ^{30}Si-values with very high precision.

Igneous rocks have a rather uniform isotope composition with a rather constant δ^{30}Si-value of -0.3‰. In igneous rocks and minerals δ^{30}Si values exhibit small, but systematic variations with ^{30}Si enrichment increasing with the silicon contents of igneous rocks and minerals. The order of ^{30}Si enrichment is quartz, feldspar, muscovite and biotite, which is consistent with the order of ^{18}O enrichment. Thus felsic igneous rocks are slightly heavier than mafic igneous rocks.

Relative to igneous rocks rivers are isotopically enriched in ^{30}Si (De la Rocha et al. 2000a; Ding et al. 2004; Ziegler et al. 2005a, b; Basile-Doelsch et al. 2005; Reynolds et al. 2006; Georg et al. 2006). The enrichment in ^{30}Si is obviously produced during weathering which preferentially releases ^{28}Si into solution, followed by even stronger preferential incorporation of ^{28}Si during secondary mineral formation. Thus soil-clay mineral formation is responsible for high δ^{30}Si values of continental surface waters and ocean water. For the Yangtze river as an example, Ding et al. (2004) measured a δ^{30}Si range from 0.7 to 3.4‰, whereas the suspended matter has a more constant composition from 0 to -0.7‰.

In ocean water distinct ^{30}Si gradients with depth exist (Georg et al. 2006): surface waters are relatively rich in ^{30}Si whereas deep waters are more depleted in ^{30}Si, which is due to a silicon isotope fractionation during the uptake by organisms

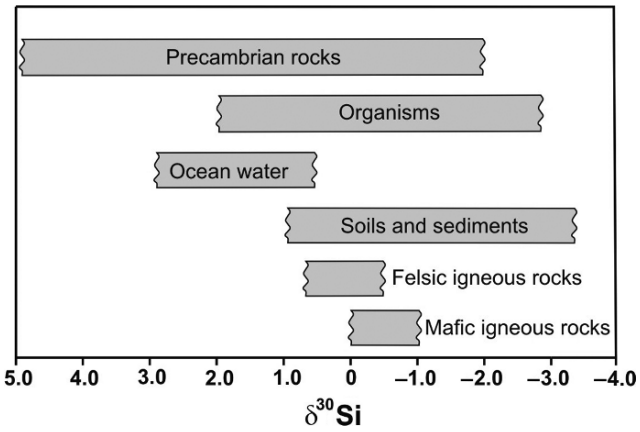

Fig. 2.19 δ^{30}Si ranges of various geologic reservoirs

in oceanic surface waters. De la Rocha et al. (1997, 1998) observed a 1‰ fractionation between dissolved and biogenic silica during opal formation by marine diatoms that does not vary with temperature nor among three species of diatoms. An increase in opal formation by diatoms results in more positive δ^{30}Si-values, whereas a decrease results in more negative δ-values. In this manner variations in ^{30}Si contents of diatoms may provide information on changes of oceanic silicon cycling (De la Rocha et al. 1998). Marine sponges fractionate silicon isotopes to a degree that is three times larger than observed by marine diatoms (De La Rocha 2003). Figure 2.19 summarizes natural silicon isotope variations.

A wide range of δ^{30}Si values from -0.8 to $+5.0$‰ have been reported for Precambrian cherts (Robert and Chaussidon 2006), much larger than for Phanerozoic cherts. These authors observed a positive correlation of δ^{18}O with δ^{30}Si values, which they interpreted as reflecting temperature changes in the ocean from about 70°C 3.5 Ga to about 20°C 0.8 Ga years ago.

2.9 Sulfur

Sulfur has four stable isotopes with the following abundances (Rosman and Taylor 1998)

^{32}S : 94.93%
^{33}S : 0.76%
^{34}S : 4.29%
^{36}S : 0.02%

Sulfur is present in nearly all natural environments. It may be a major component in ore deposits, where sulfur is the dominant nonmetal, and as sulfates in evaporites. It occurs as a minor component in igneous and metamorphic rocks, throughout

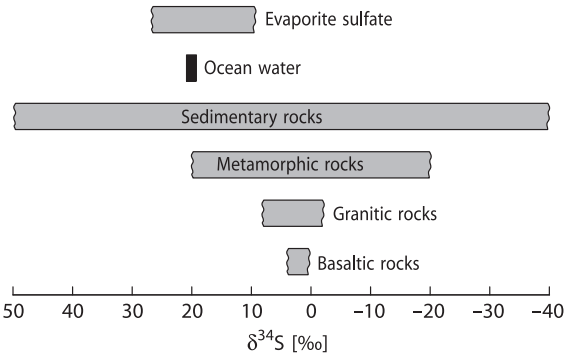

Fig. 2.20 δ^{34}S-values of some geologically important sulfur reservoirs

the biosphere in organic substances, in marine waters and sediments as both sulfide and sulfate. These occurrences cover the whole temperature range of geological interest. Thus, it is quite clear that sulfur is of special interest in stable isotope geochemistry.

Thode et al. (1949) and Trofimov (1949) were the first to observe wide variations in the abundances of sulfur isotopes. Variations on the order of 180‰ have been documented with the "heaviest" sulfates having δ^{34}S-values of greater than +120‰ (Hoefs, unpublished results), and the "lightest" sulfides having δ^{34}S-values of around −65‰. Some of the naturally occurring S-isotope variations are summarized in Fig. 2.20. Reviews of the isotope geochemistry of sulfur have been published by Nielsen (1979), Ohmoto and Rye (1979), Ohmoto (1986), Ohmoto and Goldhaber (1997), Seal et al. (2000), Canfield (2001a) and Seal (2006).

For many years the reference standard commonly referred to is sulfur from troilite of the Canyon Diablo iron meteorite (CDT). As Beaudoin et al. (1994) have pointed out, CDT is not homogeneous and may display variations in ^{34}S up to 0.4‰. Therefore a new reference scale, Vienna-CDT or V-CDT has been introduced by an advisory committee of IAEA in 1993, recommending an artificially prepared Ag_2S (IAEA-S-1) with a $\delta^{34}S_{VCDT}$ of −0.3‰ as the new international standard reference material.

2.9.1 Preparation Techniques

Chemical preparation of the various sulfur compounds for isotopic analysis have been discussed by Rafter (1957), Robinson and Kusakabe (1975) among others. The gas generally used for mass-spectrometric measurement is SO_2, although Puchelt et al. (1971) and Rees (1978) describe a method using SF_6 which has some distinct advantages: it has no mass spectrometer memory effect and because fluorine is monoisotopic, no corrections of the raw data of measured isotope ratios are necessary. Comparison of δ^{34}S-values obtained using the conventional SO_2 and the laser SF_6 technique has raised serious questions about the reliability of the SO_2

correction for oxygen isobaric interferences (Beaudoin and Taylor 1994). Therefore the SF_6 technique has been revitalized (Hu et al. 2003), demonstrating that SF_6 is an ideal gas for measuring $^{33}S/^{32}S$, $^{34}S/^{32}S$ and $^{36}S/^{32}S$ ratios.

For SO_2, pure sulfides have to be reacted with an oxidizing agent, like CuO, Cu_2O, V_2O_5 or O_2. It is important to minimize the production of sulfur trioxide since there is an isotope fractionation between SO_2 and SO_3. Special chemical treatment is necessary if pyrite is to be analyzed separately from other sulfides.

For the extraction of sulfates and total sulfur a suitable acid and reducing agent, such as tin(II)–phosphoric acid (the "Kiba" solution of Sasaki et al. 1979) is needed. The direct thermal reduction of sulfate to SO_2 has been described by Holt and Engelkemeier (1970) and Coleman and Moore (1978). Ueda and Sakai (1984) described a method in which sulfate and sulfide disseminated in rocks are converted to SO_2 and H_2S simultaneously, but analyzed separately. With the introduction of on-line combustion methods (Giesemann et al. 1994), multistep off-line preparations can be reduced to one single preparation step, namely the combustion in an elemental analyzer. Sample preparations have become less dependent on possibly fractionating wet-chemical extraction steps and less time-consuming.

Microanalytical techniques such as laser microprobe (Kelley and Fallick 1990; Crowe et al. 1990; Hu et al. 2003; Ono et al. 2006) and ion microprobe (Chaussidon et al. 1987, 1989; Eldridge et al. 1988, 1993) have become promising tools for determining sulfur isotope ratios. These techniques have several advantages over conventional techniques such as high spatial resolution and the capability for "in-situ" spot analysis. Sulfur isotopes are fractionated during ion or laser bombardment, but fractionation effects are mineral specific and reproducible.

2.9.2 Fractionation Mechanisms

Two types of fractionation mechanisms are responsible for the naturally occurring sulfur isotope variations:

1. Kinetic isotope effects during microbial processes. Micro-organisms have long been known to fractionate isotopes during their sulfur metabolism, particularly during dissimilatory sulfate reduction, which produces the largest fractionations in the sulfur cycle
2. Various chemical exchange reactions between both sulfate and sulfides and the different sulfides themselves

2.9.2.1 Dissimilatory Sulfate Reduction

Dissimilatory sulfate reduction is conducted by a large group of organisms (over 100 species are known so far, Canfield 2001a), that gain energy for their growth by reducing sulfate while oxidizing organic carbon (or H_2). Sulfate reducers are widely

distributed in anoxic environments. They can tolerate temperatures from −1.5 to over 100°C and salinities from fresh water to brines.

Since the early work with living cultures (Harrison and Thode 1957a, b; Kaplan and Rittenberg 1964) it is well known that sulfate reducing bacteria produce ^{32}S-depleted sulfide. Despite decades of intense research the factors that determine the magnitude of sulfur isotope fractionation during bacterial sulfate reduction are still under debate. The magnitude of isotope fractionation depends on the rate of sulfate reduction with the highest fractionation at low rates and the lowest fractionation at high rates. Kaplan and Rittenberg (1964) and Habicht and Canfield (1997) suggested that fractionations depend on the specific rate (cell^{-1} time^{-1}) and not so much on absolute rates (volume^{-1} time $^{-1}$). What is clear, however, is that the rates of sulfate reduction are controlled by the availabilty of dissolved organic compounds. One parameter which remains unclear is sulfate concentration. While for instance Boudreau and Westrich (1984) argued that the concentration of sulfate becomes important at rather low concentrations (less than 15% of the seawater value), Canfield (2001b) observed no influence of isotope fractionations on sulfate concentrations for natural populations. Another parameter, that has been thought to be important is temperature insofar as it regulates in natural populations the sulfate-reducing community (Brüchert et al. 2001). Furthermore differences in fractionation with temperature relate to differences in the specific temperature response to internal enzyme kinetics as well as cellular properties and corresponding exchange rates of sulfate in and out of the cell. Canfield et al. (2006) found in contrast to earlier belief high fractionations in the low and high temperature range and the lowest fractionations in the intermediate temperature range.

The reaction chain during anaerobic sulfate reduction has been described in detail by Goldhaber and Kaplan (1974). In general, the rate-limiting step is the breaking of the first S-O bond, namely the reduction of sulfate to sulfite. Pure cultures of sulfate reducing bacteria produce sulfide depleted in ^{34}S by 4–46‰ (Harrison and Thode 1957a, b; Kemp and Thode 1968; McCready et al. 1974; McCready 1975; Bolliger et al. 2001). More recently, sulfur isotope fractionations have been determined from natural populations covering a wide spectrum of environments (from rapidly metabolizing microbial mats to slowly metabolizing coastal sediments; Habicht and Canfield 1997, 2001; Canfield 2001a).

In marine coastal sediments typically 90% of the sulfide produced during sulfate reduction is reoxidized (Canfield and Teske 1996). The pathways of sulfide oxidation are poorly known but include oxidation to sulfate, elemental sulfur and other intermediate compounds. Systematic studies of sulfur isotope fractionations during sulfide oxidation are still needed, the few available data suggest that biologically mediated oxidation of sulfide to elemental sulfur and sulfate lead to only minimal isotope fractionation.

Naturally occurring sulfides in sediments and euxinic waters are commonly depleted in ^{34}S by up to 70‰ (Jørgensen et al. 2004), far beyond the apparent capabilities of sulfate reducing bacteria. As has been shown above, most of the sulfide produced by sulfate reduction in sediments is reoxidized, often via compounds in which sulfur has intermediate oxidation states that do not accumulate, but

are readily transformed and which can disproportionated by bactertia. Canfield and Thamdrup (1994) suggested that through a repeated cycle of sulfide oxidation to elemental sulfur and subsequent disproportionation, bacteria can generate the large ^{34}S depletion typical of many marine sulfides. Thus the oxidative part of the sulfur cycle may create circumstances by which sulfides become more depleted in ^{34}S than would be possible with sulfate reducing bacteria alone.

However, in contrast to microbiological experiments and near-surface studies, modelling of sulfate reduction in pore water profiles with in the ODP program has demonstrated that natural populations are able to fractionate S-isotopes by up to more than 70‰ (Wortmann et al. 2001; Rudnicki et al. 2001). Brunner et al. (2005) suggested that S isotope fractionations of around –70‰ might occur under hypersulfidic, substrate limited, but nonlimited supply of sulfate, conditions without the need of alternate pathways involving the oxidative sulfur cycle.

Another factor that is of great importance for the observed sulfur isotope variations of natural sulfides is whether sulfate reduction takes place in an open or closed system. An "open" system has an infinite reservoir of sulfate in which continuous removal from the source produces no detectable loss of material. Typical examples are the Black Sea and local oceanic deeps. In such cases, H_2S is extremely depleted in ^{34}S while consumption and change in ^{34}S remain negligible for the sulfate. In a "closed" system, the preferential loss of the lighter isotope from the reservoir has a feedback on the isotopic composition of the unreacted source material. The changes in the ^{34}S-content of residual sulfate and of the H_2S are modeled in Fig. 2.21, which shows that $\delta^{34}S$-values of the residual sulfate steadily increase with sulfate consumption (a linear relationship on the log-normal plot). The curve for the derivative H_2S is parallel to the sulfate curve at a distance which depends on the magnitude of

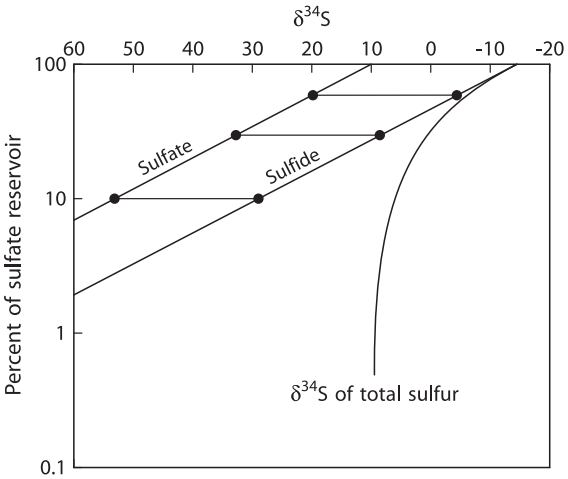

Fig. 2.21 Rayleigh plot for sulphur isotopic fractionations during the reduction of sulfate in a closed system. Assumed fractionation factor. 1.025, assumed starting composition of initial sulfate: +10‰

the fractionation factor. As shown in Fig. 2.21, H_2S may become isotopically heavier than the original sulfate when about 2/3 of the reservoir has been consumed. The $\delta^{34}S$-curve for "total" sulfide asymptotically approaches the initial value of the original sulfate. It should be noted, however, that apparent "closed-system" behavior of covarying sulfate and sulfide $\delta^{34}S$-values might be also explained by "open-system" differential diffusion of the different sulfur isotope species (Jørgensen et al. 2004).

In recent years additional informations on sulfur isotope fractionation mechanisms have been obtained from the analysis of the additional isotopes ^{33}S and ^{36}S (Farquhar et al. 2003; Johnston et al. 2005; Ono et al. 2006, 2007). For long it was thought $\delta^{33}S$ and $\delta^{36}S$ values carry no additional information, because sulfur isotope fractionations follow strictly mass-dependent fractionation laws. By studying all sulfur isotopes with very high precision these authors could demonstrate that bacterial sulfate reduction follows a mass-dependent relationship that is slightly different from that expected by equilibrium fractionations. On plots $\Delta^{33}S$ vs $\delta^{34}S$ mixing of two sulfur reservoirs is non-linear in these coordinates (Young et al. 2002). As a result samples with the same $\delta^{34}S$-value can have different $\Delta^{33}S$ and $\Delta^{36}S$ values. This opens the possibility to distinguish between different fractionation mechanisms and biosynthetic pathways (Ono et al. 2006, 2007). For instance, bacterial sulfate reduction shows slightly different fractionation relationships compared to sulfur disproportionation reactions (Johnston et al. 2005). Thus multiple sulfur isotope analyses might have great potential in identifying the presence or absence of specific metabolisms in modern environment or to have a fingerprint when a particular sulfur metabolism shows up in the geologic record.

Finally it should be mentioned that sulfate is labeled with two biogeochemical isotope systems, sulfur and oxygen. Coupled isotope fractionations of both sulfur and oxygen isotopes have been observed in experiments (Mizutani and Rafter 1973; Fritz et al. 1989; Böttcher et al. 2001) and in naturally occurring sediments (Ku et al. 1999; Aharon and Fu 2000; Wortmann et al. 2001). Brunner et al. (2005) argued that characteristic $\delta^{34}S$-$\delta^{18}O$ fractionation slopes do not exist, but depend on cell-specific reduction rates and oxygen isotope exchange rates. Despite the extremely slow oxygen isotope exchange of sulfate with ambient water, $\delta^{18}O$ in sulfate obviously depend on the $\delta^{18}O$ of water via an exchange of sulfite with water.

2.9.2.2 Thermochemical Reduction of Sulfate

In contrast to bacterial reduction thermochemical sulfate reduction is an abiotic process with sulfate being reduced to sulfide under the influence of heat rather than bacteria (Trudinger et al. 1985; Krouse et al. 1988). The crucial question, which has been the subject of a controversial debate, is whether thermochemical sulfate reduction can proceed at temperatures as low as about 100°C, just above the limit of microbiological reduction (Trudinger et al. 1985). There is increasing evidence from natural occurrences that the reduction of aqueous sulfates by organic compounds can occur at temperatures as low as 100°C, given enough time for the reduction to proceed (Krouse et al. 1988; Machel et al. 1995). S isotope fractionations during

thermochemical reduction generally should be smaller than during bacterial sulfate reduction. However, experiments by Kiyosu and Krouse (1990) have indicated S-isotope fractionations of 10 to 20‰ in the temperature range of 200 to 100°C.

To summarize, bacterial sulfate reduction is characterized by large and heterogeneous ^{34}S-depletions over very small spatial scales, whereas thermogenic sulfate reduction leads to smaller and "more homogeneous" ^{34}S-depletions.

2.9.2.3 Isotope Exchange Reactions

There have been a number of theoretical and experimental determinations of sulfur isotope fractionations between coexisting sulfide phases as a function of temperature. Theoretical studies of fractionations among sulfides have been undertaken by Sakai (1968) and Bachinski (1969), who reported the reduced partition function ratios and the bond strength of sulfide minerals and described the relationship of these parameters to isotope fractionation. In a manner similar to that for oxygen in silicates, there is a relative ordering of ^{34}S-enrichment among coexisting sulfide minerals (Table 2.9). Considering the three most common sulfides (pyrite, sphalerite and galena) under conditions of isotope equilibrium pyrite is always the most ^{34}S enriched mineral and galena the most ^{34}S depleted, sphalerite displays an intermediate enrichment in ^{34}S.

The experimental determinations of sulfur isotope fractionations between various sulfides do not exhibit good agreement. The most suitable mineral pair for temperature determination is the sphalerite–galena pair. Rye (1974) has argued that the Czamanske and Rye (1974) fractionation curve gives the best agreement with filling temperatures of fluid inclusions over the temperature range from 370 to 125°C. By contrast, pyrite – galena pairs do not appear to be suitable for a temperature determination, because pyrite tends to precipitate over larger intervals of ore deposition than galena, implying that these two minerals may frequently not be contemporaneous. The equilibrium isotope fractionations for other sulfide pairs are generally so small that they are not useful as geothermometers. Ohmoto and Rye (1979) critically examined the available experimental data and presented a

Table 2.9 Equilibrium isotope fractionation factors of sulfides with respect to H_2S. The temperature dependence is given by A/T^2 (after Ohmoto and Rye 1979)

Mineral	Chemical composition	A
Pyrite	FeS_2	0.40
Sphalerite	ZnS	0.10
Pyrrhotite	FeS	0.10
Chalcopyrite	$CuFeS_2$	−0.05
Covellite	CuS	−0.40
Galena	PbS	−0.63
Chalcosite	Cu_2S	−0.75
Argentite	Ag_2S	−0.80

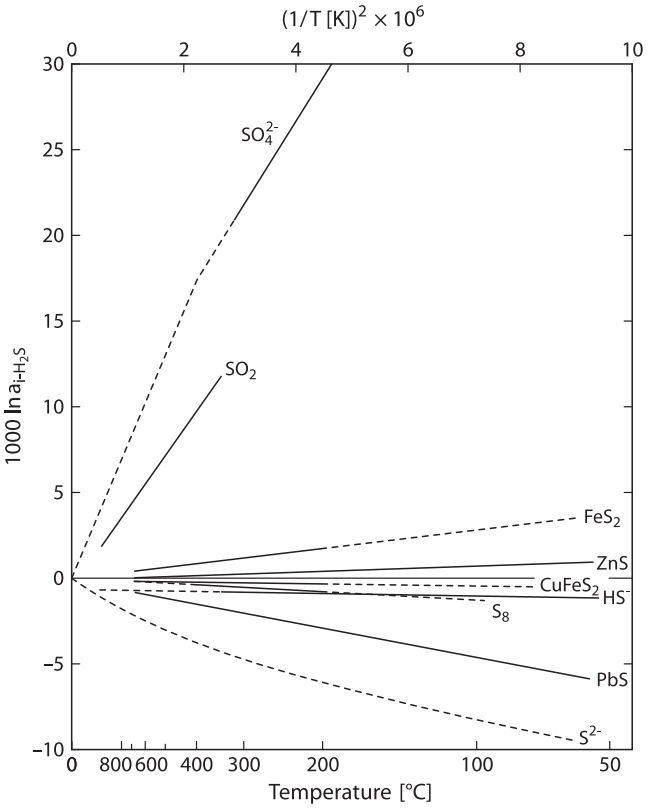

Fig. 2.22 Equilibrium fractionations among sulphur compounds relative to H_2S (*solid lines* experimentally determined, *dashed lines* extrapolated or theoretically calculated (after Ohmoto and Rye, 1979)

summary of what they believe to be the best S-isotope fractionation data. These S-isotope fractionations relative to H_2S are shown in Fig. 2.22.

Sulfur isotope temperatures from ore deposits often have been controversial; one of the reasons are strong ^{34}S zonations in sulfide minerals that have been observed by laser probe and ion probe measurements (McKibben and Riciputi 1998).

2.10 Chlorine

Chlorine has two stable isotopes with the following abundances (Coplen et al. 2002):

^{35}Cl 75.78%
^{37}Cl 24.22%

Natural isotope variations in chlorine isotope ratios might be expected due to both the mass difference between ^{35}Cl and ^{37}Cl as well as to variations in coordination of chlorine in the vapor, aqueous and solid phases. Schauble et al. (2003) calculated equilibrium fractionation factors for some geochemically important species. They showed that the magnitude of fractionations systematically varies with the oxidation state of Cl, but also depends on the oxidation state of elements to which Cl is bound with greater fractionations for 2+ cations than for 1+ cations. Silicates are predicted to be enriched compared to coexisting brines and organic molecules are enriched to dissolved Cl^-.

2.10.1 Methods

Measurements of Cl-isotope abundances have been made by different techniques. The first measurements by Hoering and Parker (1961) used gaseous chlorine in the form of HCl and the 81 samples measured exhibited no significant variations relative to the standard ocean chloride. In the early eighties a new technique has been developed by Kaufmann et al. (1984), that uses methylchloride (CH_3Cl). The chloride-containing sample is precipitated as AgCl, reacted with excess methyliodide, and separated by gas chromatography. The total analytical precision reported is near $\pm 0.1‰$ (Long et al. 1993; Eggenkamp 1994; Sharp et al. 2007). The technique requires relatively large quantities of chlorine (>1 mg), which precludes the analysis of materials with low chlorine concentrations or which are limited in supply. Magenheim et al. (1994) described a method involving the thermal ionization of Cs_2Cl^+, which, as argued by Sharp et al. (2007), is very sensitive to analytical artefacts and therefore might lead to erroneous results. δ-values are generally given relative to seawater chloride termed SMOC (Standard Mean Ocean Chloride).

2.10.2 Characteristic Features of Cl Isotope Geochemistry

Chlorine is the major anion in surface- and mantle-derived fluids. It is the most abundant anion in hydrothermal solutions and is the dominant metal complexing agent in ore forming environments (Banks et al. 2000). Despite its variable occurrence, chlorine isotope variations in natural waters commonly are small and close to the chlorine isotope composition of the ocean. This is also true for chlorine from fluid inclusions in hydrothermal minerals which indicate no significant differences between different types of ore deposits such as Mississippi-Valley and Porphyry Copper type deposits (Eastoe et al. 1989; Eastoe and Guilbert 1992).

Relatively large isotopic differences have been found in slow flowing groundwater, where Cl-isotope fractionation is attributed to a diffusion process (Kaufmann et al. 1984, 1986; Desaulniers et al. 1986). ^{37}Cl depletions detected in some pore waters have been attributed to processes such as ion filtration, alteration and dehydration

reactions and clay mineral formation (Long et al. 1993; Eggenkamp 1994; Eastoe et al. 2001; Hesse et al. 2006). A pronounced downward depletion of δ^{37}Cl-values to $-4‰$ has been reported by Hesse et al. (2006). Even lower δ^{37}Cl-values have been reported in pore waters from subduction-zone environments (Ransom et al. 1995; Spivack et al. 2002). The downward depletion trend might be explained by mixing of two fluids: shallow ocean water with a deep low ^{37}Cl fluid of unknown origin.

Controversial results have been reported for chlorine isotopes in mantle-derived rocks. According to Magenheim et al. (1995) δ^{37}Cl-values for MORB glasses show a surprisingly large range. As postulated by Magenheim et al. (1995), characteristic differences between mantle and crustal chlorine can be used as indicators of the source of volatiles in chlorine-rich mafic magmas, such as the Bushveld and Stillwater complexes (Boudreau et al. 1997; Willmore et al. 2002). For the Stillwater Complex chlorine isotopes are consistent with an influence of crustal derived fluid, whereas for the Bushveld Complex chlorine isotopes indicate a mantle-derived source. A similar approach has been taken by Markl et al. (1997) to trace the origin of chlorine in the lower crust. Since δ^{37}Cl values of granulite facies rocks cluster around ocean water composition, Markl et al. (1997) concluded that chlorine in the lower crust is derived from the upper crust and therefore does not reflect degassing of the mantle.

Recently Sharp et al. (2007) have questioned the findings of Magenheim et al. (1995). Sharp et al. (2007) found that the large differences between mantle and crustal material do not exist and that the mantle and the crust have very similar isotopic composition. A possible explanation for this apparent discrepancy might be related to analytical artifacts of the TIMS technique (Sharp et al. 2007). Bonifacie et al. (2008) also observed small Cl-isotope variations only in mantle derived rocks. They demonstrated that δ^{37}Cl values correlate with chlorine concentrations: Cl-poor basalts have low δ^{37}Cl values and represent the composition of uncontaminated mantle derived magmas, whereas Cl-rich basalts are enriched in ^{37}Cl and are contaminated by Cl-rich material such as ocean water.

Volcanic gases and associated hydrothermal waters have a large range in δ^{37}Cl-values from -2 to $+12‰$ (Barnes et al. 2006). To evaluate chlorine isotope fractionations in volcanic systems, HCl liquid-vapor experiments performed by Sharp (2006) yield large isotope fractionations of dilute HCl at 100°C. These results are in contrast to liquid–vapor experiments by Liebscher et al. (2006) observing very little fractionation at $400-450$°C. Clearly more data are needed to resolve these discrepancies.

2.10.3 Chlorine Isotopes in the Environment

Chlorine isotope studies have been applied to understand the environmental chemistry of anthropogenic organic compounds, such as chlorinated organic solvents or biphenyls. The primary goal of such studies is to identify and quantify sources and

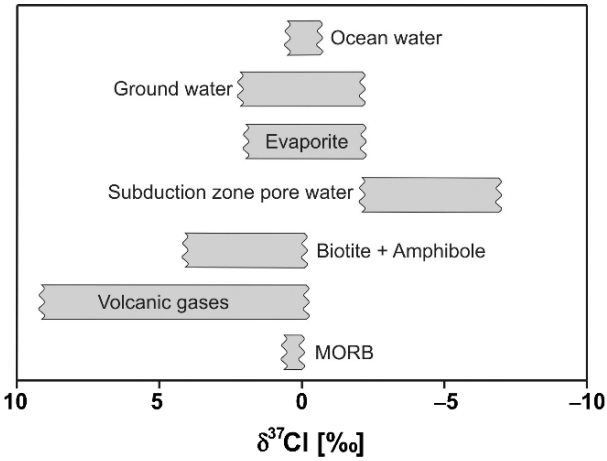

Fig. 2.23 δ^{37}Cl values in geologically important reservoirs

biodegration processes in the environment. To do this successfully chorine isotope values should differ among compounds and manufactorers. The range of reported δ^{37}Cl-values is from about -5 to $+6‰$ with distinct signatures from different suppliers (Van Warmerdam et al. 1995; Jendrzewski et al. 2001).

Perchlorate is another anthropogenic compound, which may contaminate surface and ground waters. The occurrence of natural perchlorate is limited to extremely dry environments, such as the Atacama desert. Large kinetic isotope effects during microbial reduction of perchlorate have been observed by Sturchio et al. (2003) and Ader et al. (2008), which may be used to document in-situ bioremediation.

A summary of the observed natural chlorine isotope variations is presented in Fig. 2.23. Ransom et al. (1995) gave a natural variation range in chlorine isotope composition of about 15‰ with subduction zone pore waters having δ^{37}Cl values as low as $-8‰$ whereas minerals in which Cl substitutes OH have δ^{37}Cl values as high as 7‰.

2.11 Calcium

Calcium plays an essential role in biological processes (calcification of organisms, formation of bones etc.). Calcium has six stable isotopes in the mass range of 40 to 48 with the following abundances (Rosman and Taylor 1998)

^{40}Ca : 96.94%
^{42}Ca : 0.647%
^{43}Ca : 0.135%
^{44}Ca : 2.08%
^{46}Ca : 0.004%
^{48}Ca : 0.187%

Its wide natural distribution and the large relative mass difference suggest a large isotope fractionation, which might be caused by mass-dependent fractionation processes and by radiogenic growth (radioactive decay of ^{40}K), the latter not being discussed here. Early studies on natural isotope variations found no differences or ambigous results. By using a double-spike technique and by using a mass-dependent law for correction of instrumental mass fractionation Russell et al. (1978) were the first to demonstrate that differences in the ^{44}Ca/^{40}Ca ratio are clearly resolvable to a level of 0.5‰. More recent investigations by Skulan et al. (1997) and by Zhu and MacDougall (1998) have improved the precision to about 0.1–0.15‰. These latter authors observed Ca-isotope variations – given as δ^{44}Ca-values – of about 5‰ (see also the review by DePaolo 2004). Comparing data from different laboratories, complications may arise from the use of different δ-definitions and from the use of different standards. By initiating a laboratory exchange of internal standards Eisenhauer et al. (2004) have suggested to use NIST SRM 915a as international standard.

New insights on biomineralization may be revealed by measuring Ca isotope variations in shell secreting organisms (e.g. Griffith et al. 2008). Two factors influence the Ca isotope composition of shells: (1) the chemistry of the solution, in which the organisms live and (2) the process by which Ca is precipitated.

The magnitude of Ca isotope fractionation during carbonate precipitation as well as the mechanism – either isotope equilibrium or kinetic effects – remain a matter of debate. Studies by Nägler et al. (2000), Gussone et al. (2005) and Hippler et al. (2006) reported temperature dependent Ca isotope fractionations precipitated in natural environments or under cultured laboratory conditions with a slope of about 0.02‰ per °C. The slope is identical for aragonite and calcite with an offset of about 0.6‰: aragonite being isotopically lighter (δ^{44}Ca ≈ 0.4‰) than calcite (δ^{44}Ca ≈ 1.0‰). An important question is whether the observed temperature-dependent fractionation results solely from temperature or whether it is influenced by temperature related changes in growth and calcification rates (Langer et al. 2007). And as pointed out by Gussone et al. (2006) similar temperature dependencies do not necessarily imply the same fractionation mechanism. Temperature dependent fractionations; however, have not been found in all shell secreting organisms (Lemarchand et al. 2004; Sime et al. 2005). Sime et al. (2005) analyzed 12 species of foraminifera and found negligible temperature dependence for all 12 species. Thus, no consensus on temperature controlled Ca isotope fractionations has been reached (Griffith et al. 2008).

Marine biogenic carbonates are isotopically depleted in ^{44}Ca relative to present-day seawater (Skulan et al. 1997; Zhu and MacDougall 1998). Zhu and MacDougall have made the first attempt to investigate the global Ca cycle. They found a homogeneous isotope composition of the ocean, but distinct isotope differences of the sources and sinks and suggested that the ocean is not in steady state. Since then several other studies have investigated secular changes in the Ca isotope composition of the ocean: De La Rocha and de Paolo (2000) and Fantle and de Paolo (2005) for the Neogene, Steuber and Buhl (2006) for the Cretaceous; Farkas et al. (2007). for the late Mesozoic; and Kasemann et al. (2005) for the Neoproterozoic. Model

simulations of the Ca cycle by Farkas et al. (2007) indicated that the observed Ca isotope variations can be produced by variable Ca input fluxes to the oceans. However, since the isotope effects that control the Ca isotope composition of marine carbonates are not well understood, any clear indication of secular changes in the Ca isotope composition of ocean waters must remain subject of further debate.

2.12 Chromium

Chromium has 4 stable isotopes with the following abundances (Rosman and Taylor 1998)

^{50}Cr 4.35%
^{52}Cr 83.79%
^{53}Cr 9.50%
^{54}Cr 2.36%

Chromium exists in two oxidation states, Cr(III), as a cation Cr^{3+} and Cr(VI), as an oxyanion (CrO_4^{2-} or $HCrO_4^-$) having different chemical behaviors: Cr^{3+} is the dominant form in most minerals and in water under reducing conditions, whereas Cr(VI) is stable under oxidizing conditions. These properties make Cr isotope investigations suitable to detect and quantify redox changes in different geochemical reservoirs.

Schoenberg et al. (2008) presented the first set of Cr isotope data for rocks and Cr(II) rich ores. Mantle derived rocks and chromite ores from layered intrusions have a uniform $^{53}Cr/^{52}Cr$ isotope ratio very close to the certified Cr standard NIST SRM 979. The Cr isotope composition of hydrothermal lead chromates is substantially heavier (δ^{53}Cr from 0.6 to 1.0‰) than the rocks from which the chromium was leached.

Chromium is a common anthropogenic contaminant in surface waters, therefore Cr isotope fractionations are of potential interest in tracking Cr^{6+} pollution in groundwaters. Ellis et al. (2002, 2004)) and Izbicki et al. (2008) analyzed groundwater samples from contaminated sites and observed an increase in $^{53}Cr/^{52}Cr$ ratios up to 6‰ during the reduction of chromate. Equilibrium fractionations between Cr(VI) and Cr (III) have been estimated by Schauble et al. (2002), who predicted Cr isotope fractionations >1‰ between Cr species with different oxidation states.

2.13 Iron

Iron has 4 stable isotopes with the following abundances (Beard and Johnson 1999)

^{54}Fe 5.84%
^{56}Fe 91.76%
^{57}Fe 2.12%
^{58}Fe 0.28%

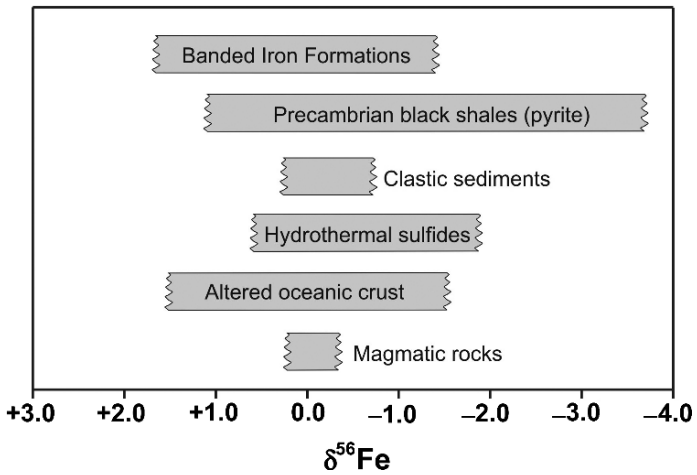

Fig. 2.24 δ^{56}Fe ranges in some important iron reservoirs

Iron is the third most abundant element that participates in a wide range of biotically and abiotically-controlled redox processes in different geochemical low- and high-temperature environments. Iron has a variety of important bonding partners and ligands, forming sulfide, oxide and silicate minerals as well as complexes with water. As is well known bacteria can use Fe during both dissimilatory and assimilatory redox processes. Because of its high abundance and its prominent role in high and low temperature processes, isotope studies of iron have received the most attention of the transition elements. Since the first investigations on Fe isotope variations by Beard and Johnson (1999), the number of studies on Fe isotope variations have increased exponentially. Recent reviews on Fe-isotope geochemistry have been given by Anbar (2004a), Beard and Johnson (2004), Johnson and Beard (2006), Dauphas and Rouxel (2006) and Anbar and Rouxel (2007). Figure 2.24 summarizes Fe-isotope variations in important geological reservoirs.

Literature data have been presented either in the form of $^{57}Fe/^{54}Fe$ or as $^{56}Fe/^{54}Fe$ ratios. In the following all data are given as $^{56}Fe/^{54}Fe$ ratios or as δ^{56}Fe values. δ^{57}Fe values would be 1.5 times greater than δ^{56}Fe values, because only mass-dependent fractionations are expected. Fe isotope aqnalysis is highly challenging because of interferences from $^{40}Ar^{14}N^+$, $^{40}Ar^{16}O^+$ and $^{40}Ar^{16}OH^+$ at masses 54, 56 and 57 respectively. Nevertheless δ-values can be measured routinely with a precision of $\pm 0.05‰$.

Theoretical studies by Polyakov (1997), Polyakov et al. (2007) and Schauble et al. (2001) predicted Fe isotope fractionations of several ‰ between various iron oxides, carbonates and sulfides from spectroscopic data, even at high temperatures. $^{56}Fe/^{54}Fe$ ratios will be usually higher in Fe^{3+} compounds than in Fe^{2+} bearing species. First experimental studies at magmatic temperatures were conducted by Schüßler et al. (2007) for equilibrium isotope fractionations between iron sulfide

(pyrrhotite) and silicate melt and by Shahar et al. (2008) for those between fayalite and magnetite, demonstrating that Fe isotope fractionations are relatively large at magmatic temperatures and can be used as a geothermometer. At low temperatures, Johnson et al. (2002) presented experimental evidence for equilibrium fractionations between Fe^{3+} and Fe^{2+} in aqueous solutions. They observed a 2.75‰ enrichment in Fe^{3+} relative to Fe^{2+} at 25°C which is about half of that predicted by Schauble et al. (2001). While it is conceivable that Fe isotope equilibrium can be reached at high temperatures, indications for equilibrium fractionations are less straightforward at much lower temperatures. Therefore kinetic fractionations might dominate Fe isotope fractionations at low temperatures.

Igneous rocks exhibit only small variations in Fe isotope compositions (Zhu et al. 2002; Beard and Johnson 2004; Poitrasson et al. 2004; Williams et al. 2005; Weyer et al. 2005). Weyer et al. (2005) found that the Fe isotope composition in mantle peridotites is slightly lower than in basalts. As suggested by Williams et al. (2005) the relative incompatibility of ferric iron during melting might incorporate heavy iron into the melt. During magmatic differentiation the Fe isotope composition remains more or less constant except in the very SiO_2-rich differentiates (Beard and Johnson 2004; Poitrasson and Freydier 2005). A possible mechanism is removal of isotopically ^{56}Fe depleted titanomagnetite (Schüßler et al. 2008).

Under low-temperature conditions the observed natural Fe isotope variations of around 4‰ have been attributed to a large number of processes, which can be divided into inorganic reactions and into processes initiated by micro-organisms. Up to 1‰ fractionation can result from precipitation of Fe-containing minerals (oxides, carbonates, sulfides) (Anbar and Rouxel 2007). Larger Fe isotope fractionations occur during biogeochemical redox processes, which include dissimilatory Fe(III) reduction (Beard et al. 1999; Icopini et al. 2004; Crosby et al. 2007), anaerobic photosynthetic Fe(II) oxidation (Croal et al. 2004), abiotic Fe (II) oxidation (Bullen et al 2001) and sorption of aqueous Fe(II) on Fe(III) hydoxides (Balci et al. 2006). Controversy still exists whether the iron isotope variations observed are controlled by kinetic/equilibrium factors or by abiological/microbiological fractionations. This complicates the ability to use iron isotopes to identify microbiological processing in the rock record (Balci et al. 2006). However, as demonstrated by Johnson et al. (2008) microbiological reduction of Fe^{3+} produces much larger quantities of iron with distinct $\delta^{56}Fe$ values than abiological processes.

The bulk continental crust has $\delta^{56}Fe$ values close to zero. Clastic sediments generally retain the zero ‰ value. Because of its very low concentration in the ocean, the Fe isotope composition of ocean water so far has not been determined, which complicates a quantification of the modern Fe isotope cycle. Hydrothermal fluids at mid-ocean ridges and river waters have $\delta^{56}Fe$ values between 0 and -1‰ (Fantle and dePaolo 2004; Bergquist and Boyle 2006; Severmann et al. 2004), whereas fluids in diagenetic systems show a significantly larger spread with a preferential depletion in ^{56}Fe (Severmann et al. 2006). Thus, most iron isotope variations are produced by diagenetic processes that reflect the interaction between Fe^{3+} and Fe^{2+} during bacterial iron and sulfate reduction. Processes dominated by sulfide formation during sulfate reduction produce high $\delta^{56}Fe$ values for porewaters, whereas the

opposite occurs when dissimilatory iron reduction is the major pathway (Severmann et al. 2006).

Especially large iron isotope fractionations have been found in Proterozoic and Archean sedimentary rocks with lithologies ranging from oxide to carbonate in banded iron formations (BIFs) and pyrite in shales (Rouxel et al. 2005; Yamaguchi et al. 2005). In particular BIFs have been investigated to reconstruct Fe cycling through Archean oceans and the rise of $O_{2(atm)}$ during the Proterozoic (see discussion under 3.8.4 and Fig. 3.28). The pattern shown in Fig. 3.28 distinguishes three stages of Fe isotope evolution, which might reflect redox changes in the Fe cycle (Rouxel et al. 2005). The oldest samples (stage 1) are characterized by depleted δ^{56}Fe values, whereas younger samples in stage 2 are characterized by enriched δ^{56}Fe values. Interplays of the Fe-cycle with the C- and S-record might reflect changing microbial metabolims during the Earth,s history (Johnson et al. 2008).

2.14 Copper

Copper has two stable isotopes

^{63}Cu 69.1%
^{65}Cu 30.9%.

Copper occurs in two oxidation states, Cu^{+} and Cu^{++} and rarely in the form of elemental copper. The major Cu-containing minerals are sulfides (chalcopyrite, bornite, chalcosite and others), and, under oxidizing conditions, secondary copper minerals in the form of oxides and carbonates. Copper is a nutrient element, although toxic for all aquatic photosynthetic microorganisms. Copper may form a great variety of complexes with very different coordinations such as square, trigonal and tetragonal complexes. These properties are ideal prerequisites for relatively large isotope fractionations.

Early work of Shields et al. (1965) has indicated a total variation of $\sim$12‰ with the largest variations in low temperature secondary minerals. Somewhat smaller differences, but still in the range of 7 to 9‰, have been observed by Maréchal et al. (1999), Maréchal and Albarede (2002), Zhu et al. (2002), Ruiz et al. (2002), which are larger than for Fe. Nevertheless most samples so far analyzed vary between δ^{65}Cu values from $+1$ to -1‰.

Experimental investigations have demonstrated that redox reactions between CuI and CuII species are the principal process that fractionates Cu isotopes in natural systems (Ehrlich et al. 2004; Zhu et al. 2002). Precipitated CuI species are 3 to 5‰ lighter than dissolved CuII species during CuII reduction. Pokrovsky et al. (2008) observed a change in sign of Cu isotope fractionations during adsorption experiments from aqueous solutions depending on the kind of surface, either organic or inorganic: on biological cell surfaces a depletion of ^{65}Cu, wheras an enrichment of ^{65}Cu on oxy(hydr)oxide surface is observed. Although little is known about the Cu isotope composition of ocean water, Zhu et al. (2002) suggested that Cu isotopes

may be a tracer of Cu biochemical cycling. The latter authors reported Cu isotope fractionations of 1.5‰ during biological uptake.

Recent studies of Cu isotope variations have concentrated on Cu isotope fractionations during ore formation (Larson et al. 2003; Rouxel et al. 2004; Mathur et al. 2005; Markl et al. 2006a). The magnitude of isotope fractionation in copper sulfides increases with secondary alteration and reworking processes. Investigations by Markl et al. (2006) on primary and secondary copper minerals from hydrothermal veins have confirmed this conclusion. They showed that hydrothermal processes do not lead to significant Cu isotope variations, but instead, low temperature redox processes are the main cause of isotope fractionations. Thus copper isotope ratios may be used to decipher details of natural redox processes, but cannot be used as reliable fingerprints for the source of copper – as suggested by Graham et al. (2004) – because the variation caused by redox processes within a single deposit is usually much larger than the inter-deposit variation.

2.15 Zinc

Zinc has 5 stable isotopes of mass 64, 66, 67, 68 and 70 with the following abundances:

^{64}Zn 48.63,
^{66}Zn 27.90,
^{67}Zn 4.10,
^{68}Zn 18.75,
^{70}Zn 0.62.

Zinc is an essential biological nutrient in the ocean where the concentration of Zn is controlled by phytoplankton uptake and remineralization. Zn is incorporated into carbonate shells and diatoms, therefore, Zn isotopes may have great potential for tracing nutrient cycling in seawater. John et al. (2007a) measured the isotope fractionation of Zn during uptake by diatoms and demonstrated that Zn isotope fractionations are related to the extent of biological Zn uptake. In a depth profile of the upper 400 m of Pacific seawater, Bermin et al. (2006) observed small isotope variations which they interpreted as being due to biological recycling. Surface waters have a lighter δ^{66}Zn signature than deeper waters suggesting that absorption of Zn on particle surfaces carries Zn out of surface waters (John et al. 2007a). Pichat et al. (2003) suggested that variations in Zn isotopes in marine carbonates over the last 175 kyr reflect changes in upwelling and nutrient availabilty. Although it has been assumed that there is negligible fractionation between Zn in seawater and precipitated minerals, biological usage and adsorption onto particles are likely to cause isotope fractionations (Gelabert et al. 2006).

Measurements of the ^{66}Zn/^{64}Zn ratio in ores, sediments and biological materials have so far yielded a small variation of about 1‰ (Maréchal et al. 1999, 2000; Maréchal and Albarede 2002 and others). One of the main reasons for this small

variability appears to be that Zn does not participate in any redox reaction, it always occurs in the divalent state. Recently Wilkinson et al. (2005) extended the range of Zn isotope variations to ~1.5‰ by analyzing sphalerites from one ore deposit. They interpreted the variations by postulating kinetic fractionations during rapid sphalerite precipitation. John et al. (2008) have found relatively large Zn isotope fractionation in hydrothermal fluids and suggested that Zn sulfide precipitation is an important factor in causing δ^{66}Zn variations. By analyzing common anthropogenic products in the environment, John et al. (2007b) showed that δ^{66}Zn values of industrial products are smaller than of Zn ores demonstrating Zn isotope homogenezation during processing and ore purification.

2.16 Germanium

Because of nearly identical ionic radii, Ge usually replaces Si in minerals, with average concentrations around 1 ppm in the earth,s crust. Thus Ge and Si have similar chemistries, which might indicate that both elements show similarities in their isotope fractionations.

Ge has five stable isotopes with the following abundances (Rosman and Taylor 1998):

^{70}Ge 20.84%
^{72}Ge 27.54%
^{73}Ge 7.73%
^{74}Ge 36.28%
^{76}Ge 7.61%

Early investigations using the TIMS method were limited to an uncertainty of several ‰. Over the past few years advances have been made with the MC-ICP-MS technique with a long term external reproducibility of 0.2–0.4‰ (Rouxel et al. 2006; Siebert et al. 2006a).

Based on a few measurements of basalts and granites Rouxel et al. (2006) concluded that the bulk silicate earth has a homogeneous isotope composition. However, chemical sediments like sponges and authigenic glauconites are enriched in δ^{74}Ge by about 2‰. This suggests that seawater – similar to silicon – is isotopically enriched in ^{74}Ge relative to the bulk earth. Ge isotopes might offer new insights into the biogeochemistry of the past and present ocean, but more data are needed.

2.17 Selenium

Because selenium to some extent is chemically similar to sulfur, one might expect to find some analogous fractionations of selenium isotopes in nature. Six stable selenium isotopes are known with the following abundances (Coplen et al. 2002)

^{74}Se 0.89%
^{76}Se 9.37%
^{77}Se 7.63%
^{78}Se 23.77%
^{80}Se 49.61%
^{82}Se 8.73%

Interest in selenium isotope studies has grown in recent years, since selenium is both a nutrient and a toxicant and may reach significant concentrations in soils and in watersheds. Starting with work by Krouse and Thode (1962) the SeF_6 gas technique used by the early workers required relatively large quantities of Se, limiting the applications of selenium isotopes. Johnson et al. (1999) developed a double-spike solid-source technique (spike ^{74}Se and ^{82}Se, measure $^{80}Se/^{76}Se$) that corrects for fractionations during sample preparation and mass spectrometry, yielding an overall reproducibility of $\pm 0.2‰$. This technique brings sample requirements down to submicrogram levels. Even lower Se amounts (10 ng) are required for measurements with the MC-ICP-MS technique (Rouxel et al. 2002).

Reduction of selenium oxyanions by bacteria is an important process in the geochemical cycle of selenium. Selenium reduction proceeds in three steps with Se(IV) and Se(0) species as stable intermediates (Johnson 2004). Se isotope fractionation experiments by Herbel et al. (2000) indicate about 5‰ fractionations ($^{80}Se/^{76}Se$) during selenate reduction to selenite and little or no fractionation for selenite sorption, oxidation of reduced Se in soils, or Se volatilization by algae. Johnson and Bullen (2003) investigated Se isotope fractionations induced by inorganic reduction of selenate by Fe(II)–Fe(III) hydroxide sulfate ("green rust"). The overall fractionation is 7.4‰, which is larger than during bacterial selenate reduction. This indicates that the magnitude of Se isotope fractionations depends on the specific reaction mechanism. More data are needed, but selenium isotopes should be useful tracers for selenate and selenite reduction processes as well as selenium sources.

2.18 Molybdenum

Mo consists of 7 stable isotopes that have the following abundances:

^{92}Mo 15.86%,
^{94}Mo 9.12%,
^{95}Mo 15.70%,
^{96}Mo 16.50%,
^{97}Mo 9.45%,
^{98}Mo 23.75%
^{100}Mo 9.62%.

Either $^{97}Mo/^{95}Mo$ or $^{98}Mo/^{95}Mo$ ratios have been reported in the literature. Therefore care has to be taken by comparing Mo isotope values. Mo isotope data are gen-

erally given relative to laboratory standards calibrated against ocean water (Barling et al. 2001; Siebert et al. 2003).

Because Mo is a redox sensitive element that becomes enriched in reducing, organic rich sediments, Mo-isotope fractionations during redox processes might be expected (Anbar 2004b; Anbar and Rouxel 2007). In oxygenated waters insoluble MoO_4^{2-} is the dominant Mo species, which is so unreactive that Mo is the most abundant transition metal in ocean water. Mo in ocean water should have a uniform isotope composition as is expected from its long residence time in the ocean. Oxic pelagic sediments and Fe-Mn crusts or nodules are depleted in ^{98}Mo by about 3‰ relative to sea water (Barling et al. 2001; Siebert et al. 2003). A comparable fractionation has been found in pore waters (McManus et al. 2002) and in an experimental study of Mo absorption on Mn oxides (Barling and Anbar 2004). The actual fractionation mechanism is unclear, but fractionations occur in solution, where Mo is in the hexavalent state. Therefore oxidizing conditions in the marine environment are a major requirement for Mo isotope fractionations (Siebert et al. 2005).

The largest isotope effect occurs during adsorption of dissolved Mo to Mn-oxide particles, so that dissolved Mo is heavier than particle bound Mo. First observed in oxic seawater and sediments by Barling et al. (2001), Barling and Anbar (2004) have verified the fractionation effect in the laboratory. Smaller isotope fractionations occur during the reduction of Mo in suboxic environments (McManus et al. 2002, 2006; Nägler et al. 2005; Poulson et al. 2006; Siebert et al. 2003, 2006b). Observed in different sedimentary settings these effects so far have not been verified in experimental studies.

Due to the preferential extraction of ^{95}Mo from ocean water, the ocean is the heaviest Mo reservoir of all sources analyzed so far Fig. 2.24, consequently the Mo isotope composition of the ocean is sensitive to redox changes and thus can be used as a paleo-redox proxy.

Black shales that are formed in an anoxic environment such as the Black Sea have a Mo isotope composition nearly identical to ocean water (Barling et al. 2001; Arnold et al. 2004; Nägler et al. 2005). Organic carbon rich sediments formed in suboxic environments have variable ^{98}Mo/^{95}Mo ratios intermediate between those of ocean water and oxic sediments (Siebert et al. 2003). Thus Mo isotope values in ancient black shales can be used as a paleo-oceanographic proxy of the oxidation state of the ocean, as for example has been discussed by Arnold et al. (2004) for the Proterozoic. Figure 2.25 summarizes natural Mo isotope variations.

2.19 Mercury

The heaviest elements with observed fractionations of about 3 to 4‰ are mercury and thallium. This is surprising because isotope variations due to mass-dependent fractionations should be much smaller. Schauble (2007) demonstrated that isotope variations for the heaviest elements are controlled by nuclear volume, a fractionation effect being negligible for the light elements. Nuclear volume fractionations may

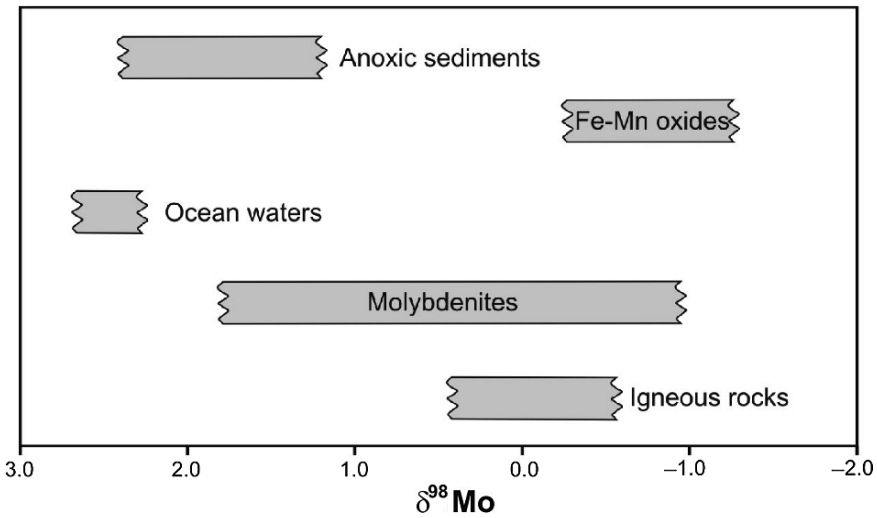

Fig. 2.25 δ^{97}Mo values in important geologic reservoirs

be about 1‰ per mass unit for Hg and Tl, declining to about 0.02‰ for sulfur. Nuclear volume fractionations also tend to enrich heavy isotopes in oxidized species (Schauble 2007).

Mercury has seven stable isotopes in the mass range from ^{196}Hg to ^{204}Hg with the following abundances (Rosman and Taylor 1998)

^{196}Hg 0.15
^{198}Hg 9.97
^{199}Hg 16.87
^{200}Hg 23.10
^{201}Hg 13.18
^{202}Hg 29.86
^{204}Hg 6.87

Due to the relative uniform isotope abundances in the mass range ^{198}Hg to ^{204}Hg, several possibilities exist for the measurement of isotope ratios, thus far δ-values are generally presented as ^{202}Hg/^{198}Hg ratios.

Mercury is very volatile and a highly toxic pollutant. Its mobility depends on its different redox states. Reduction of Hg species to Hg(0) vapor is the most important pathway for removal of Hg from aqueous systems to the atmosphere occurring by biotic and abiotic reactions. Data by Smith et al. (2005), Xie et al. (2005), Foucher and Hintelmann (2006) and Kritee et al. (2007), indicate that mercury isotopes are fractionated in hydrothermal cinnabar ores, sediments and environmental samples. The range in isotope composition (^{202}Hg/^{198}Hg) is likely to exceed 5‰, quite large considering the relatively small mass range of less than 4%. Smith et al. (2005, 2008) analyzed the Hg isotope composition of fossil hydrothermal systems and concluded that ore and spring deposits have a larger range in Hg isotope composition than

associated country rocks. They postulated that boiling of hydrothermal fluids and separation of a Hg-bearing vapor phase are the most important Hg fractionation processes.

Since Hg takes part in microbial processes, Hg fractionations should occur during methylation processes. Kritee et al. (2007) suggested that Hg isotopes might have the potential for distinguishing between different sources of mercury emissions based on the magnitude of isotope fractionations. Finally, it is important to note that abiological photochemical reduction of Hg^{2+} and CH_3Hg^+ by sunlight leads to a large mass-independent fractionation of ^{201}Hg and ^{199}Hg (Bergquist and Blum 2007).

2.20 Thallium

Thallium has two stable isotopes with masses 203 and 205.

^{204}Tl 29.54
^{205}Tl 70.48

Thallium is the heaviest element for which natural variations in isotope composition have been reported (Rehkämper and Halliday 1999). Tl exists in two valence states as Tl^+ and Tl^{3+} and forms in water a variety of complexes. Furthermore it is a highly volatile element which could induce kinetic fractionations during degassing processes. A systematic 2‰ difference between Fe–Mn crusts enriched in ^{205}Tl and seawater has been observed by Rehkämper et al. (2002), which was interpreted to be due to an fractionation effect during adsorption of Tl onto Fe–Mn particles. In a later study Rehkämper et al. (2004) found that growth layers of Fe–Mn crusts show a systematic change in Tl isotope composition with age, which they explained by time-dependent changes in Tl-isotope composition of seawater. No significant Tl isotope fractionations occur during weathering (Nielsen et al. 2005).

Tl isotope ratios might be also used as a tracer in mantle geochemistry (Nielsen et al. 2006; 2007). Since most geochemical reservoirs except Fe-Mn marine sediments and low temperature seawater altered basalts are more or less invariant in Tl isotope composition, admixing af small amounts of either of these two components into the mantle should induce small Tl isotope fractionations in mantle derived rocks. And indeed, evidence for the presence of Fe-Mn sediments in the mantle underneath Hawaii was presented by Nielsen et al. (2006).

Chapter 3
Variations of Stable Isotope Ratios in Nature

3.1 Extraterrestrial Materials

Isotope variations found in extraterrestrial materials have been classified according to different processes such as chemical mass fractionation, nuclear reactions, nucleosynthesis, and/or to different sources such as interplanetary dust, solar materials, and comet material. Various geochemical fingerprints point to the reservoir from which the planetary sample was derived and the environment in which the sample has formed. They can be attributed to a variety of processes, ranging from heterogeneities in the early solar nebula to the evolution of a planetary body. For more details the reader is referred to reviews of Thiemens (1988), Clayton (1993, 2004), and McKeegan and Leshin (2001).

Extraterrestrial materials consist of samples from the Moon, Mars, and a variety of smaller bodies such as asteroids and comets. These planetary samples have been used to deduce the evolution of our solar system. A major difference between extraterrestrial and terrestrial materials is the existence of primordial isotopic heterogeneities in the early solar system. These heterogeneities are not observed on the Earth or on the Moon, because they have become obliterated during high-temperature processes over geologic time. In primitive meteorites, however, components that acquired their isotopic compositions through interaction with constituents of the solar nebula have remained unchanged since that time.

Heterogeneities in isotope composition indicate incomplete mixing of distinct presolar materials during formation of the solar system. Such isotope anomalies in light elements have been documented on all scales, from microscopic zoning in meteoritic minerals to bulk asteroids. The most extreme examples, however, have been documented from minute presolar grains extracted from primitive meteorites and measured with the ion microprobe. These grains of silicon carbide, graphite, and diamond show isotope variations that may vary by one or more orders of magnitude. They have acquired their isotope characteristics before the solar system has been formed. The implications of these variations for models of stellar formation have been summarized by Zinner (1998) and Hoppe and Zinner (2000). The abundance

J. Hoefs, *Stable Isotope Geochemistry,*

of presolar grains in meteorites is at the level of tens of ppm, thus the bulk isotope composition of meteorites remains more or less unaffected.

Different types of primitive meteoritic materials of the so-called chondritic composition can be distinguished on the basis of their size. The term chondritic is used here to refer to undifferentiated material having approximately solar compositions of all except the most volatile elements. The smallest particles are micron-sized interplanetary dust particles that contribute about 10^4 tons per year to the Earth. They can be collected high in the Earth's stratosphere by aircraft at about 20 km altitude. Although these particles are small (typically 10 μm in diameter), they have been investigated by ion microprobe measurements (McKeegan 1987; McKeegan et al. 1985, and others).

Deuterium and nitrogen isotope compositions of interplanetary dust materials show enrichments that support an interstellar origin. These isotope enrichments are the results of ionmolecule reactions that are only efficient at very low temperatures (Rietmeijer 1998). D/H ratios of individual dust particles give δD-values ranging from −386 to +2705‰, which thus exceed by far those in terrestrial samples. The hydrogen isotopic composition is heterogeneous on a scale of a few microns demonstrating that the dust is unequilibrated. A carbonaceous phase rather than water appears to be the carrier of the D-enrichment.

In contrast to D/H and $^{15}N/^{14}N$ ratios, an anomalous carbon isotope composition has not been clearly demonstrated. However, three of the investigated particles exhibit evidence for heterogeneity in their isotopic composition. With respect to oxygen, none of the particles have large ^{16}O excesses of the type found in refractory oxide and silicate phases from carbonaceous chondrites.

These results suggest that the interplanetary dust particles are among the most primitive samples available for laboratory studies. Isotopically anomalous material constitutes only a small fraction of the investigated particles. Thus, it appears that the isotopic composition of these anomalous particles is not different from those observed in minor components of primitive meteorites.

3.1.1 Chondrites

Chondrites are the oldest and most primitive rocks in the solar system. They are hosts for interstellar grains that predate solar system formation. Most chondrites have experienced a complex history, which includes primary formation processes and secondary processes that include thermal metamorphism and aqueous alteration. It is generally very difficult to distinguish between the effects of primary and secondary processes on the basis of isotope composition. Chondrites display a wide diversity of isotopic compositions including large variations in oxygen isotopes.

The first observation, that clearly demonstrated isotopic inhomogeneities in the early solar system, was made by Clayton et al. (1973a). Earlier, it had been thought that all physical and chemical processes must produce mass-dependent O-isotope fractionations yielding a straight line with a slope of 0.52 in a plot of $^{17}O/^{16}O$ vs.

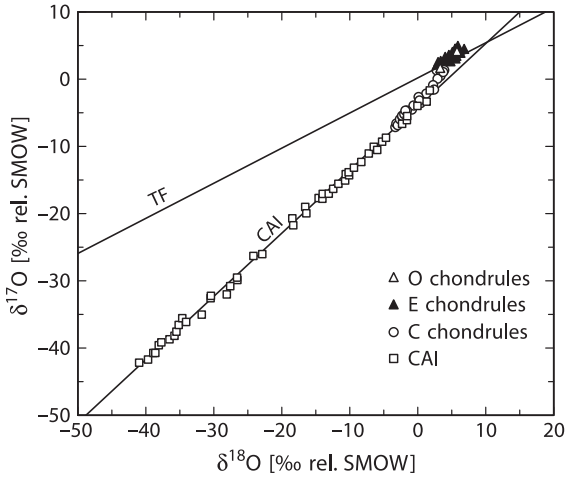

Fig. 3.1 ^{17}O- vs ^{18}O-isotope composition of Ca–Al-rich inclusions (CAI) from various chondrites (Clayton, 1993)

$^{18}O/^{16}O$. This line has been called the "Terrestrial Fractionation Line". Figure 3.1 shows that O-isotope data from miscellaneous collections of terrestrial and lunar samples fall along the predicted mass-dependent fractionation line. However, selected anhydrous high-temperature minerals in carbonaceous chondrites, notably Allende, do not fall along the chemical fractionation trend, instead define another trend with a slope of 1. Figure 3.1 shows oxygen isotope compositions for four groups of meteoritic samples. The first evidence for oxygen isotope anomalies was found in CaAl-rich refractory inclusions (CAI) in the Allende carbonaceous chondrite, which are composed predominantly of melilite, pyroxene, and spinel.

Bulk meteorites, the Moon and Mars lie within a few percentile above or below the terrestrial fractionation line on a three-oxygen isotope plot (see Fig. 3.1). Therefore, the oxygen isotope composition of the Sun has been assumed to be the same as that of the Earth. This view has changed with the suggestion of Clayton (2002) that the Sun and the initial composition of the solar system are ^{16}O-rich comparable to the most ^{16}O-rich composition of CAIs ($\delta^{17}O \approx -50; \delta^{18}O \approx -50‰$). According to this model, Solar System rocks had become poor in ^{16}O due to UV self-shielding of CO, the most abundant oxygen containing molecule in the solar system. Oxygen released by the UV dissociation of CO then form together with other components of the solar system solid minerals with mass-independent oxygen isotope compositions.

Different nebular isotopic reservoirs must have existed, since there are distinct differences in bulk meteoritic O-isotope composition. The carbonaceous chondrites display the widest range in oxygen isotope composition of any meteorite group (Clayton and Mayeda 1999). The evolution of these meteorites can be interpreted as a progression of interactions between dust and gas components in the solar nebula followed by solid/fluid interactions within parent bodies. Young et al. (1999)

have shown that reactions between rock and water inside a carbonaceous chondrite parent body could have produced groups of different carbonaceous chondrite types that explain the diversity in isotope composition.

Yurimoto et al. (2008) have summarized the oxygen isotope composition of the chondrite components (refractory inclusions, chondrules, and matrix) and concluded that O-isotope variations within a chondrite are typically larger than O-isotope variations among bulk chondrites. The question remains as to where, when, and how the isotopic anomalies were originally produced (Thiemens 1988). Even without full understanding of the causes of isotope variations in meteorites, oxygen isotopes are very useful in classifying meteorites and in relating meteorites to their precursor asteroids and planets (Clayton 2004). Oxygen isotope signatures have confirmed that eucrites, diogenites, howardites, and mesosiderites originate from one single parent body probably derived from the asteroid 4 Vesta, as shergottites, nakhlites, and chassignites come from another (Clayton and Mayeda 1996). Main group pallasites represent intermixed core-mantle material from a single disrupted asteroid with no equivalent known (Greenwood et al. 2006).

In addition to oxygen isotopes, the volatile elements H, C, N, and S also show extremely large variations in isotope composition in meteorites. In recent years, most investigations have concentrated on the analyses of individual components with more and more sophisticated analytical techniques.

3.1.1.1 Hydrogen

D/H ratios in carbonaceous chondrites may hint on the origin of water on Earth. Robert (2001) suggested that since the contribution of cometary water to terrestrial water should be less than 10%, most of the water on Earth should derive from a meteoritic source.

The D/H ratio of the sun is essentially zero: all the primordial deuterium originally present has been converted into ^{3}He during thermonuclear reactions. Analysis of primitive meteorites is the next best approach of estimating the hydrogen isotope composition of the solar system.

In carbonaceous chondrites, hydrogen is bound in hydrated minerals and in organic matter. Bulk D/H ratios give a relatively homogeneous composition with a mean δD-value of $-100‰$ (Robert et al. 2000). This relatively homogeneous composition masks the very heterogeneous distribution of individual components. Considerable efforts have been undertaken to analyze D/H ratios of the different compounds (Robert et al. 1978; Kolodny et al. 1980; Robert and Epstein 1982; Becker and Epstein 1982; Yang and Epstein 1984; Kerridge 1983; Kerridge et al. 1987; Halbout et al. 1990; Krishnamurthy et al. 1992). Hydrogen in organic matter reveals a δD-variation from -500 to $+6{,}000‰$ whereas water in silicates gives a variation from -400 to $+3{,}700‰$ (Deloule and Robert 1995; Deloule et al. 1998). Most strikingly, almost the entire range is observed on the scale of single chondrules when traverses are performed (Deloule and Robert 1995).

Two mechanisms have been proposed to account for the deuterium enrichment: (1) for organic molecules, high D/H ratios can be explained by ion molecule reactions that occur in interstellar space and (2) for the phyllosilicates the enrichment can be produced via isotope exchange between water and hydrogen (Robert et al. 2000).

Eiler and Kitchen (2004) have re-evaluated the hydrogen isotope composition of water-rich carbonaceous chondrites by stepped-heating analysis of very small amounts of separated water-rich materials. Their special aim has been to deduce the origin of the water with which the meteorites have reacted. They observed a decrease in δD with increasing extent of aqueous alteration from 0‰ (least altered, most volatile rich) to −200‰ (most altered, least volatile rich).

3.1.1.2 Carbon

Besides the bulk carbon isotopic composition, the various carbon phases occurring in carbonaceous chondrites (kerogen, carbonates, graphite, diamond, and silicon carbide) have been individually analyzed. The $\delta^{13}C$-values of the total carbon fall into a narrow range, whereas $\delta^{13}C$-values for different carbon compounds in single meteorites show extremely different ^{13}C-contents. Figure 3.2 shows one such example, the Murray meteorite after Ming et al. (1989). Of special interest are the minute grains of silicon carbide and graphite in primitive carbonaceous chondrites, which obviously carry the chemical signature of the pre-solar environment (Ott 1993). The SiC grains, present at a level of a few ppm, have a wide range in silicon and carbon isotope composition, with accompanying nitrogen also being isotopically highly variable. The $^{12}C/^{13}C$ ratio ranges from 2 to 2,500, whereas it is 89 for the bulk Earth. According to Ott (1993), the SiC grains can be regarded as "star dust", prob-

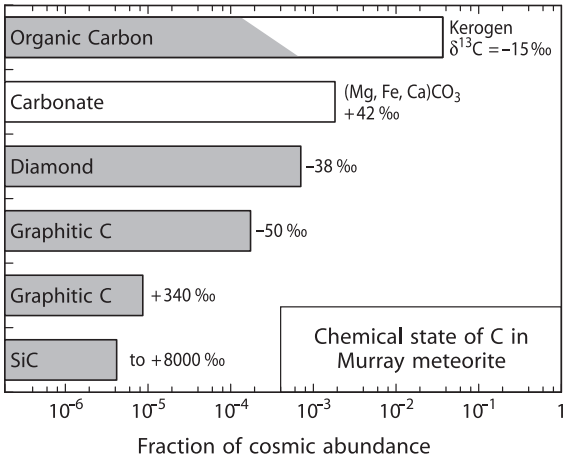

Fig. 3.2 Different carbon compounds in primitive meteorites. Species classified as interstellar on the basis of C-isotopes are *shaded*. Only a minor fraction of organic carbon is interstellar. (after Ming et al. 1989)

ably from carbon stars that existed long before our solar system. Amari et al. (1993) presented ion microprobe data of individual micrometer-sized graphite grains in the Murchison meteorite that also has large deviations from values typical for the solar system. These authors interpreted the isotope variability as indicating at least three different types of stellar sources.

Of special interest is the analysis of meteoritic organic matter, because this may provide information about the origin of prebiotic organic matter in the early solar system. Two hypotheses have dominated the debate over formation mechanisms for the organic matter (1) formation by a Fischer-Tropsch-type process (the synthesis of hydrocarbons from carbon monoxide and hydrogen) promoted by catalytic mineral grains and (2) formation by Miller-Urey-type reactions (the production of organic compounds by radiation or electric discharge) in an atmosphere in contact with an aqueous phase. However, the isotopic variability exhibited by the volatile elements in different phases in carbonaceous chondrites is not readily compatible with abiotic syntheses. Either complex variants of these reactions must be invoked, or totally different types of reactions need to be considered. $\delta^{13}C$-values reported for amino acids in the Murchison meteorite vary between $+23$ and $+44‰$ (Epstein et al. 1987). Engel et al. (1990) analyzed individual amino acids in the Murchison meteorite and also confirmed strong ^{13}C enrichment. Of particular importance is the discovery of a distinct $\delta^{13}C$ difference between D- and L-alanine, which suggests that optically active forms of material were present in the early solar system.

3.1.1.3 Nitrogen

The nitrogen isotopes ^{14}N and ^{15}N are synthesized in two different astrophysical processes: ^{14}N during hydrostatic hydrogen burning and ^{15}N during explosive hydrogen and helium burning (Prombo and Clayton 1985). Thus, it can be expected that nitrogen should be isotopically heterogeneous in interstellar matter. What was considered by Kaplan (1975) to be a wide range of $\delta^{15}N$-values in meteorites has continuously expanded over the years (Kung and Clayton 1978; Robert and Epstein 1982; Lewis et al. 1983; Prombo and Clayton 1985; Grady and Pillinger 1990, 1993). In general, chondrites have whole rock nitrogen isotope values of $0 \pm 50‰$. However, some chondrites have δ-values up to $850‰$ (Grady and Pillinger 1990). Traces of interstellar graphite grains even show larger variations (Amari et al. 1993). The large ^{15}N-enrichment in bulk meteorites relative to the protosolar gas requires the existence of especially enriched ^{15}N-compounds and cannot be explained by isotope fractionation processes in planetary environments.

3.1.1.4 Sulfur

There are many sulfur components in meteorites which may occur in all possible valence states (-2 to $+6$). Troilite is the most abundant sulfur compound of iron meteorites and has a relatively constant S-isotope composition (recall

that troilite from the Canyon Diablo iron meteorite is the international sulfur standard, i.e. δ^{34}S-value = 0‰). Carbonaceous chondrites contain sulfur of all valence states: sulfates, sulfides, elemental sulfur, and complex organic sulfur-containing molecules. Monster et al. (1965), Kaplan and Hulston (1966) and Gao and Thiemens (1993a, b) separated the various sulfur components and demonstrated that sulfides are characterized by the highest δ^{34}S-values, whereas sulfates have the lowest δ^{34}S-values, just the opposite from what is generally observed in terrestrial samples. This is strong evidence against any microbiological activity and instead favors a kinetic isotope fractionation in a sulfur-water reaction (Monster et al. 1965). The largest internal isotope fractionation (7‰) is found in the Orgueil carbonaceous chondrite (Gao and Thiemens 1993a). Orgueil and Murchison have internal isotopic variations between different specimens, which may indicate that sulfur isotope heterogeneity existed in meteorite parent bodies. Since sulfur has four stable isotopes, measurements of more than two isotopes may provide some insights on nuclear processes and may help in identifying genetic relationships between meteorites in a similar way to oxygen isotopes. Early measurements by Hulston and Thode (1965) and Kaplan and Hulston (1966), and later ones by Gao and Thiemens (1993a, b), did not indicate any nuclear isotope anomaly. However, small ^{33}S enrichment was identified for monosulfides in ureilites (Farquhar et al. 2000b).

3.1.2 Evolved Extraterrestrial Materials

Evolved extraterrestrial materials are generally igneous rocks, which according to their thermal history can be discussed analogously to terrestrial samples. To this category belong planetary bodies, differentiated asteroids, and achondritic meteorites.

3.1.2.1 The Moon

The Moon is now ubiquitously viewed as the product of a collision between the early Earth and a Mars-size protoplanet. To test whether the impactor has introduced isotopic heterogeneity as a consequence of collision, Wiechert et al. (2001) have searched for small isotope variations by measuring high-precision ^{16}O, ^{17}O, and ^{18}O abundances in lunar samples. The three oxygen isotopes, however, provide no evidence of isotopic heterogeneity and suggest that the proto-Earth and the impactor planet formed from an identical mixture of components.

Since the early days of the Apollo missions, it is well known that the oxygen isotope composition of the common lunar igneous minerals is very constant, with very little variation from one sampled locality to another (Onuma et al. 1970; Clayton et al. 1973b). This constancy implies that the lunar interior should have a δ^{18}O-value of about 5.5‰, essentially identical to terrestrial mantle rocks. The fractionations observed among coexisting minerals indicate temperatures of crystallization of about 1,000°C or higher, similar to values observed in terrestrial basalts

(Onuma et al. 1970). By comparison with other terrestrial rocks, the range of observed δ^{18}O-values is very narrow. For instance, terrestrial plagioclase exhibits an O-isotope variation which is at least ten times greater than that for all lunar rocks (Taylor 1968). This difference may be attributed to the much greater role of low-temperature processes in the evolution of the Earth's crust and to the presence of water on the Earth.

The most notable feature of the sulfur isotope geochemistry of lunar rocks is the uniformity of δ^{34}S-values and their proximity to the Canyon Diablo standard. The range of published δ^{34}S-values is between -2 to $+2.5$‰. However, as noted by Des Marais (1983), the actual range is likely to be considerably narrower than 4.5‰ due to systematic discrepancies either between laboratories or between analytical procedures. The very small variation in sulfur isotope composition supports the idea that the very low oxygen fugacities on the Moon prevent the formation of SO_2 or sulfates, thus eliminate exchange reactions between oxidized and reduced sulfur species.

As further shown by Des Marais (1983) nitrogen and carbon abundances are extremely low in lunar rocks. Des Marais presented compelling evidence that all lunar rocks are contaminated by complex carbon compounds during sample handling. This carbon, which is released at relatively low combustion temperatures, exhibits low δ^{13}C-values, whereas the carbon liberated at higher temperatures has higher $^{13}C/^{12}C$ ratios. Another complication for the determination of the indigenous isotope ratios of lunar carbon and nitrogen arises from spallation effects, which results from the interaction of cosmic ray particles with the lunar surface. These spallation effects lead to an increase in ^{13}C and ^{15}N, the extent depending upon cosmic ray exposure ages of the rocks. Enrichments of the heavy isotopes on the surfaces of the lunar fines are most probably due to the influence of the solar wind. Detailed interpretation of their isotopic variations is difficult due to both the lack of knowledge of the isotopic composition of the solar wind and uncertainties of the mechanisms for trapping. Kerridge (1983) demonstrated that nitrogen trapped in lunar surface rocks consists of at least two components differing in release characteristics during experimental heating and isotopic composition: the low-temperature component is consistent with solar wind nitrogen, whereas the high-temperature component consists of solar energetic particles.

3.1.2.2 Mars

In the late 1970s and early 1980s, it was realized that differentiated meteorites referred to as the SNC (Shergottites, Nakhlites, Chassignites) group were samples from Mars (McSween et al. 1979; Bogard and Johnson 1983, besides others). This conclusion is based on young crystallization ages compared to that of other meteorites and compositions of trapped volatiles that match those of the martian atmosphere.

SNC-meteorites have an average δ^{18}O-value of 4.3‰, which is distinctly lower than the 5.5‰ value for the Earth-Moon system (Clayton and Mayeda 1996; Franchi

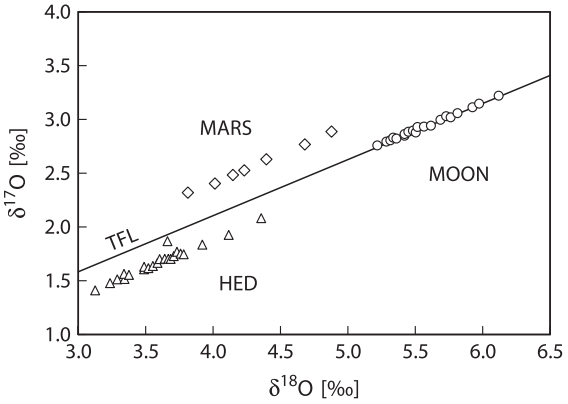

Fig. 3.3 Three oxygen isotope plot of lunar and Martian rocks and HED meteorites supposed to be fragnments of asteroid Vesta (after Wiechert et al. 2003)

et al. 1999). Small ^{18}O-variations among the different SNC-meteorites result primarily from different modal abundances of the major minerals. On a three-isotope plot the δ^{17}O offset between Mars and Earth is 0.3‰ (see Fig. 3.3). In this connection, it is interesting to note that the so-called HED (howardites, eucrites, and diogenites) meteorites, possibly reflecting material from the asteroid Vesta, have an oxygen isotope composition of 3.3‰ (Clayton and Mayeda 1996). The δ^{17}O-offset to the Earth is about -0.3‰ (Fig. 3.3). These differences in O-isotope composition among the terrestrial planets must reflect differences in the raw material from which the planets were formed.

Volatiles, especially water, on Mars are of special relevance to reveal the geological and geochemical evolution of the planet. The hydrogen isotope composition of the present day Martian atmosphere is enriched by a factor of 5 relative to terrestrial ocean water with a δD-value of $+4,000$‰. This enrichment is thought to result from preferential loss of H relative to D from the Martian atmosphere over time (Owen et al. 1988). Ion microprobe studies of amphibole, biotite, and apatite in SNC meteorites by Watson et al. (1994) and stepwise heating studies by Leshin et al. (1996) reported large variations in δD-values. These authors observed that water in the samples originated from two sources: a terrestrial contaminant released largely at low temperatures and an extraterrestrial component at high temperatures showing extreme D-enrichments. Boctor et al. (2003) observed D-rich water in all minerals analyzed – including nominally anhydrous minerals – but also found low δD-values, consistent with a more Earth-like composition and concluded no single process can explain the large range in D/H ratios. Instead they suggested that the δD-values are affected by three reservoirs and mechanisms: a magmatic water component, devolatilization by impact melting and terrestrial contamination.

As is the case for hydrogen, carbon isotope signatures in Martian meteorites present evidence for different carbon reservoirs. Wright et al. (1990) and Romanek et al. (1994) distinguished three carbon compounds: one component released

at temperatures below ≈500°C, mostly derived from terrestrial contamination, a second component, released between 400 and 700°C in heating experiments or by reaction with acid, originates mostly from breakdown of carbonates and gives δ^{13}C-values up to +40‰ and the third component, released at temperatures above 700°C, has δ^{13}C-values between −20 and −30‰ reflecting the isotope composition of magmatic carbon on Mars.

Carbonates in Martian meteorites have been especially well studied due to the hypothesis that they might indicate past life on Mars (McKay et al. 1996). Understanding the conditions of formation of the carbonates is thus crucial to the whole debate. Despite extensive chemical and mineralogical studies, the environment of carbonate formation has remained unclear. δ^{18}O-values of the carbonates are highly variable ranging from about 5‰ to 25‰ depending on different investigators and the carbonate investigated (Romanek et al. 1994; Valley et al. 1997; Leshin et al. 1998). In situ C-isotope analysis by Niles et al. (2005) gave highly zoned δ^{13}C-values from ≈+30 to +60‰ consistent with a derivation from the Martian atmosphere and suggesting abiotic formation.

McKay et al. (1996) furthermore suggested on the basis of morphology that tiny sulfide grains inside the carbonates may have formed by sulfate-reducing bacteria. δ^{34}S-values of sulfides range from 2.0 to 7.3‰ (Greenwood et al. 1997), which is similar to values from terrestrial basalts and probably not the result of bacterial reduction of sulfate.

The isotopic results are therefore not in favor of a microbiological activity on Mars, but the discussion will certainly continue on this exciting topic.

Further evidence about a nonbiogenic origin of Martian carbonates (and even less abundant sulfates) has been presented by Farquhar et al. (1998) and Farquhar and Thiemens (2000). By measuring δ^{17}O- and δ^{18}O-values Farquhar et al. (1998) observed an ^{17}O anomaly in the carbonates relative to the silicates which they interpreted as being produced by the photochemical decomposition of ozone just as in the Earth's stratosphere. The atmospheric oxygen isotope composition was subsequently transferred to carbonate minerals by CO_2–H_2O exchange. This finding suggests that carbonates (and sulfates) are derived from atmosphere/regolith interactions on Mars. Similar interactions have also been determined for sulfur isotopes in Martian meteorites (Farquhar et al. 2000a). Photolysis experiments with SO_2 and H_2S can produce the observed S-isotope compositions and provide a mechanism for abiogenic ^{34}S fractionations on Mars. Thus, large S isotope fractionations are also not necessarily indicative of biological activity on Mars.

3.1.2.3 Venus

The mass spectrometer on the Pioneer mission in 1978 measured the atmospheric composition relative to CO_2, the dominant atmospheric constituent. The $^{13}C/^{12}C$ and $^{18}O/^{16}O$ ratios were observed to be close to the Earth value, whereas the $^{15}N/^{14}N$ ratio is within 20% of that of the Earth (Hoffman et al. 1979). One of the major problems related to the origin and evolution of Venus is that of its "missing

water". There is no liquid water on the surface of Venus today and the water vapor content in the atmosphere is probably not more than 220 ppm (Hoffman et al. 1979). This means that either Venus was formed from a material very poor in water or whatever water that was originally present has disappeared, possibly as the result of escape of hydrogen into space. And indeed Donahue et al. (1982) measured a 100-fold enrichment of deuterium relative to the Earth, which is consistent with such an outgassing process. The magnitude of this process is, however, difficult to understand.

3.2 The Isotopic Composition of the Earth's Upper Mantle

Considerable geochemical and isotopic evidence has accumulated supporting the concept that many parts of the mantle have experienced a complex history of partial melting, melt emplacement, crystallization, recrystallization, deformation, and metasomatism. A result of this complex history is that the mantle is chemically and isotopically heterogeneous.

Heterogeneities in stable isotopes are difficult to detect, because stable isotope ratios are affected by the various partial melting-crystal fractionation processes that are governed by temperature-dependent fractionation factors between residual crystals and partial melt and between cumulate crystals and residual liquid. Unlike radiogenic isotopes, stable isotopes are also fractionated by low temperature surface processes. Therefore, they offer a potentially important means by which recycled crustal material can be distinguished from intra-mantle fractionation processes.

O, H, C, S, and N isotope compositions of mantle-derived rocks are substantially more variable than expected from the small fractionations at high temperatures. The most plausible process that may result in variable isotope ratios in the mantle is the input of subducted oceanic crust, and less frequent of continental crust, into some portions of the mantle. Because different parts of subducted slabs have different isotopic compositions, the released fluids may also differ in the O, H, C, and S isotope composition. In this context, the process of mantle metasomatism is of special significance. Metasomatic fluids rich in Fe^{3+}, Ti, K, LREE, P, and other large ion lithophile (LIL) elements tend to react with peridotite mantle and form secondary micas, amphiboles and other accessory minerals. The origin of metasomatic fluids is likely to be either (1) exsolved fluids from an ascending magma or (2) fluids or melts derived from subducted, hydrothermally altered crust and its overlying sediments.

With respect to the volatile behavior during partial melting, it should be noted that volatiles will be enriched in the melt and depleted in the parent material. During ascent of melts, volatiles will be degassed preferentially, and this degassing will be accompanied by isotopic fractionation (see discussion in Sect. 3.4).

Sources of information about the isotopic composition of the upper portion of the lithospheric mantle come from the direct analysis of unaltered ultramafic xenoliths brought rapidly to the surface in explosive volcanic vents. Due to rapid transport, these peridotite nodules are in many cases chemically fresh and considered by most

workers to be the best samples available from the mantle. The other primary source of information is from basalts, which represents partial melts of the mantle. The problem with basalts is that they do not necessarily represent the mantle composition because partial melting processes may have caused an isotopic fractionation relative to the precursor material. Partial melting of peridotites would result in the preferential melting of CaAl-rich minerals leaving behind refractory residues dominated by olivine and orthopyroxene which may differ slightly in the isotopic composition from the original materials. Also, basaltic melts may interact with the crustal lithosphere through which the magmas pass on their way to the Earth's surface. The following section will focus on ultramafic xenoliths, the isotopic characteristics of basalts is discussed in Sect. 3.3.

3.2.1 Oxygen

The δ^{18}O-value of the bulk Earth is constrained by the composition of lunar basalts and bulk chondritic meteorites to be close to 6‰. Insight into the detailed oxygen isotope composition of the subcontinental lithospheric mantle has mostly come from the analysis of peridotitic xenoliths entrained in alkali basalts and kimberlites. The first oxygen isotope studies of such ultramafic nodules by Kyser et al. (1981, 1982) created much debate (e.g., Gregory and Taylor 1986; Kyser et al. 1986). The Kyser et al. data showed that clinopyroxene and orthopyroxene had similar and rather constant δ^{18}O-values around 5.5‰, whereas olivine exhibited a much broader variation with δ^{18}O-values extending from 4.5 to 7.2‰. Oxygen isotope fractionations between clinopyroxene and olivine ($\Delta_{\mathrm{cpx-ol}}$) were suggested to vary from -1.4 to $+1.2$‰, implying that these phases are not in isotopic equilibrium at mantle temperatures. Gregory and Taylor (1986) suggested that the fractionations in the peridotite xenoliths analyzed by Kyser et al. (1981, 1982) arose through open-system exchange with fluids having variable oxygen isotope compositions and with olivine exchanging ^{18}O more rapidly than pyroxene.

It should be recognized, however, that olivine is a very refractory mineral and, as a result, quantitative reaction yields are generally not achieved, when analyzed by conventional fluorination techniques. Mattey et al. (1994) analyzed 76 samples of olivine in spinel-, garnet- and diamond-facies peridotites using laser fluorination techniques and observed an almost invariant O-isotope composition around 5.2‰. Assuming modal proportions of olivine, orthopyroxene, and clinopyroxene of 50:40:10, the calculated bulk mantle δ^{18}O-value would be 5.5‰. Such a mantle source could generate liquids, depending on melting temperatures and degree of partial melting, with O-isotope ratios equivalent to those observed for MORB and many ocean island basalts.

Although the results of Mattey et al. (1994) have been confirmed by Chazot et al. (1997), it should be kept in mind that most of the mantle peridotites that have been analyzed for δ^{18}O originate from the continental lithospheric mantle and not from the mantle as a whole. More recently, there have been several indications that

the O-isotope composition of mantle xenoliths from certain exotic settings can be more variable than indicated by Mattey et al. (1994) and Chazot et al. (1997). Zhang et al. (2000) and Deines and Haggerty (2000) documented complex disequilibrium features among peridotitic minerals and intra-crystalline isotope zonations, which presumably result from metasomatic fluid/rock interactions.

Eclogite xenoliths from diamondiferous kimberlites constitute an important suite of xenoliths because they may represent the deepest samples of the continental lithospheric mantle. Eclogite xenoliths have the most diverse range in δ^{18}O-values between 2.2 and 7.9‰ (McGregor and Manton 1986; Ongley et al. 1987). This large range of ^{18}O-variation indicates that the oxygen isotope composition of the continental lithosphere varies substantially, at least in any region where eclogite survives and is the most compelling evidence that some nodules represent metamorphic equivalents of hydrothermally altered oceanic crust.

3.2.2 Hydrogen

The origin of the water on Earth is a controversial topic with very different schools of thought. One view postulates that water was delivered to Earth from exogeneous sources such as comets and/or meteorites, the other holds that the Earth's water has an indigeneous origin (Drake and Righter 2002). Delivery of water from comets and meteorites can be evaluated in the light of their D/H ratios, suggesting that comets and meteorites cannot be major sources of water on Earth. The origin of water on Earth can be best explained by an indigeneous source, indicating that the Earth accreted at least in part from hydrous materials, which are not represented by known meteorite classes (Drake and Righter 2002).

In this connection, the concept of "juvenile water" has to be introduced, which has influenced thinking in various fields of igneous petrology and ore genesis. Juvenile water is defined as water that originates from degassing of the mantle and that has never been part of the surficial hydrologic cycle. The analysis of OH-bearing minerals such as micas and amphiboles of deep-seated origin has been considered to be a source of information for juvenile water (e.g. Sheppard and Epstein 1970). Because knowledge about fractionation factors is limited and temperatures of final isotope equilibration between the minerals and water not known, calculations of the H-isotope composition of water in equilibrium with the mantle is rather crude.

Figure 3.4 gives δD-data on phlogopites and amphiboles, indicating that the hydrogen isotope composition of mantle water should lie in general between −80 and −50‰, the range first proposed by Sheppard and Epstein (1970) and subsequently supported by several other authors. Also shown in Fig. 3.4 are analyses for a considerable number of phlogopites and amphiboles which have δD-values higher than −50‰. Such elevated δD-values may indicate that water from subducted oceanic crust has played a role in the genesis of these minerals. Similar conclusions have been reached as a result of the analysis of water of submarine basalts from the Mariana arc (Poreda 1985) and from estimates of the original δD-values in boninites from Bonin Island (Dobson and O'Neil 1987).

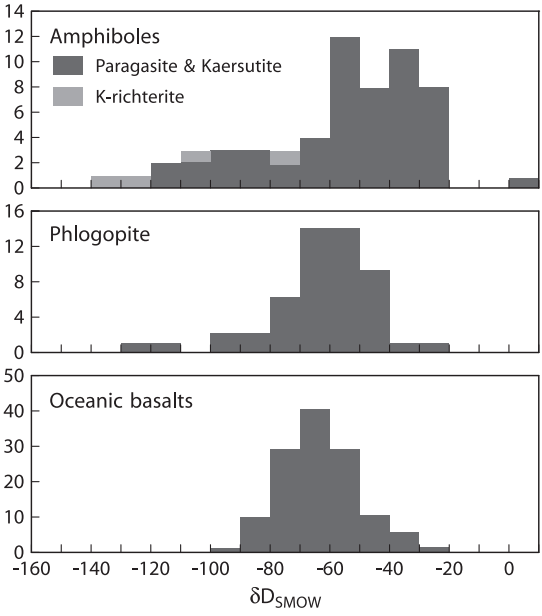

Fig. 3.4 Hydrogen isotope variations in mantle-derived materials (modified after Bell and Ihinger, 2000)

Water in the mantle is found in different states: as a fluid especially near subduction zones, as a hydrous phase and as a hydroxyl point defect in nominally anhydrous minerals. δD-values between -90 and $-110‰$ have been obtained by Bell and Ihinger (2000) analyzing nominally anhydrous mantle minerals (garnet, pyroxene) containing trace quantities of OH. Nominally anhydrous minerals from mantle xenoliths are the most D-depleted of all mantle materials with δD-values 50‰ lower than MORB (O'Leary et al. 2005). This difference may either imply that these minerals represent an isotopically distinct mantle reservoir or that the samples analyzed have exchanged hydrogen during or after their ascent from the mantle (meteoric/water interaction?).

Similarly, complex results have been obtained from ion probe measurements of amphiboles on the scale of a few tens of microns with a precision not better than $\pm 10‰$ (Deloule et al. 1991; Harford and Sparks 2001). Samples analyzed included ultramafic xenoliths and megacrysts of various localities, e.g., andesites from Soufriere volcano. Some of the investigated amphiboles show a marked internal crystal heterogeneity, a satisfactory explanation for this has still to be found. Given the rapid diffusion of hydrogen in most minerals, large D/H gradients within individual mantle amphiboles should be homogenenized on short time scales under mantle conditions. The existence of heterogeneities imposes significant time constraints on mantle metasomatism and/or on uplift rates of the sampled material.

3.2.3 Carbon

The presence of carbon in the upper mantle has been well documented through several observations: CO_2 is a significant constituent in volcanic gases associated with basaltic eruptions with the dominant flux at mid-ocean ridges. The eruption of carbonatite and kimberlite rocks further testifies to the storage of CO_2 in the upper mantle. Additionally, the presence of diamond and graphite in kimberlites, peridotite, and eclogite xenoliths reflects a wide range of mantle redox conditions, suggesting that carbon is related to a number of different processes in the mantle.

The isotopic composition of mantle carbon varies by more than 30‰ (see Fig. 3.2). To what extent this wide range is a result of mantle fractionation processes, the relict of accretional heterogeneities, or a product of recycling of crustal carbon is still unanswered. In 1953, Craig noted that diamonds exhibited a range of δ^{13}C-values which clustered around −5‰. Subsequent investigations which included carbonatites (e.g., Deines 1989) and kimberlites (e.g., Deines and Gold 1973) indicated similar δ^{13}C-values, which led to the concept that mantle carbon is relatively constant in C-isotopic composition, with δ^{13}C-values between −7 and −5‰. During the formation of a carbonatite magma, carbon is concentrated in the melt and is almost quantitatively extracted from its source reservoir. Since the carbon content of the mantle is low, the high carbon concentration of carbonatite melts requires extraction over volumes up to 10,000 times higher than the volume of a carbonatite magma (Deines 1989). Thus, the mean δ^{13}C-value of a carbonatite magma should represent the average carbon isotope composition of a relatively large volume of the mantle.

The C-isotope distribution of diamonds is in total contrast to that for carbonatites. As more and more data for diamonds became available (Deines et al. 1984; Galimov 1985b; Cartigny 2005, and others) (at present more than 4,000 C-isotope data; Cartigny 2005), the range of C-isotope variation broadened to more than 40‰. (from −38 to +5‰ (Galimov 1991; Kirkley et al. 1991; Cartigny 2005). The large ^{13}C variability is not random but restricted to certain genetic classes: Common "peridotitic diamonds" (diamonds associated with peridotitic xenoliths) have less variable carbon isotope compositions than "eclogitic diamonds", which span the entire range of $^{13}C/^{12}C$ variations (see Fig. 3.5; Cartigny 2005). Current debate centers on whether the more extreme values are characteristic of the mantle source regions or whether they have resulted from isotope fractionation processes linked to diamond formation.

While some workers have argued that the variations are the result of high-temperature isotope fractionation processes within the mantle (Deines 1980; Galimov 1991), others consider that peridotitic diamonds have formed from primitive carbon, whereas eclogitic diamonds have resulted from recycling of organic carbon (e.g., Kirkley et al. 1991). Recent ion probe measurements by Farquhar et al. (2002) on sulfide inclusions in diamonds from the Orapa kimberlite have yielded anamolous Δ^{33}S-values in 4 out of 26 investigated diamonds. This confirms the conclusion that at least the sulfur in some diamonds derives from the surface. Spatially resolved analyses of individual diamonds by SIMS measurements first described by Harte and Otter (1992) and later by others have been summarized by

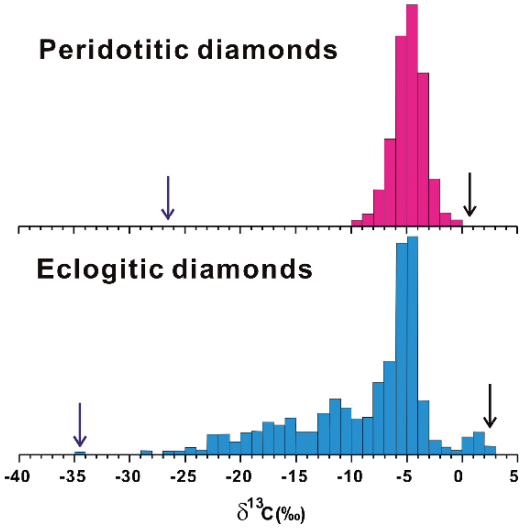

Fig. 3.5 Carbon isotope variations of diamonds (modified after Cartigny 2005)

Hauri et al. (2002). The latter authors have shown $\delta^{13}C$ variations of about 10‰ and more than 20‰ in $\delta^{15}N$ which are associated with cathodoluminescence-imaged growth zones. Although the origin of these large variations is still unclear, they point to complex growth histories of diamonds.

3.2.4 Nitrogen

Because of the inert nature of nitrogen, it might be expected that the nitrogen isotopic composition of the mantle would be similar to that of the atmosphere. This is, however, not the case. Diamonds provide the most important source of information about mantle nitrogen, because nitrogen is their main trace component. Nitrogen isotopes have been measured in over 700 diamond samples with $\delta^{15}N$-values from $+13$ to -23‰ (Hauri et al. 2002). Despite this broad distribution, the majority range beween -2 and -8‰ (Javoy et al. 1986; Boyd et al. 1992; Boyd and Pillinger 1994; Cartigny et al. 1997, 1998). A similar range in $\delta^{15}N$-values has been obtained by Marty and Humbert (1997) and Marty and Zimmermann (1999) for nitrogen trapped in MORB and OIB glasses (see Fig. 3.6). These negative δ-values clearly indicate that the mantle contains nonatmospheric nitrogen. Surprisingly, positive δ-values of about $+3$‰ have been found in deep mantle material sampled by mantle plumes which may suggest that recycling of oceanic crust may account for heavy nitrogen in the deep mantle (Dauphas and Marty 1999).

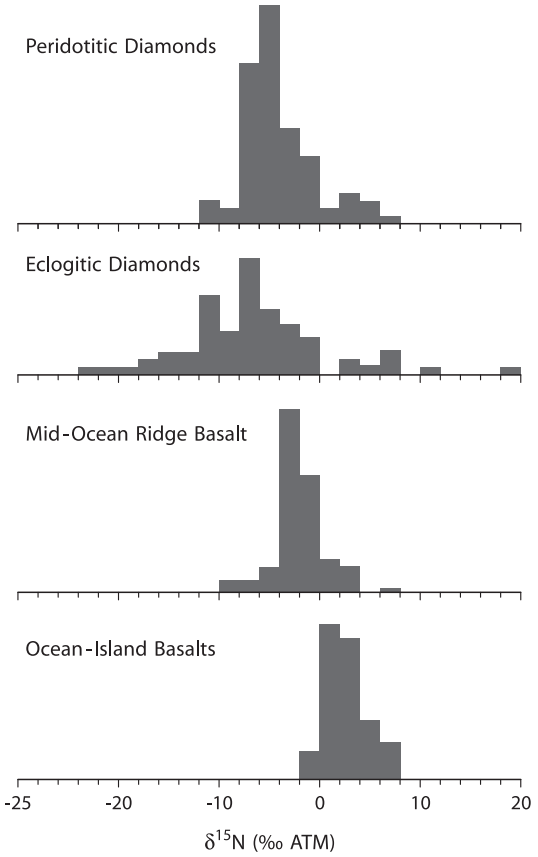

Fig. 3.6 Nitrogen isotope variations in mantle-derived materials (modified after Marty and Zimmermann, 1999)

3.2.5 Sulfur

Sulfur occurs in a variety of forms in the mantle, the major sulfur phase is monosulfide solid solution between Fe, Ni, and Cu. Recent ion microprobe measurements on sulfide inclusions from megacrysts and pyroxenite xenoliths from alkali basalts and kimberlites and in diamonds gave δ^{34}S-values from -11 to $+14$‰ (Chaussidon et al. 1987, 1989; Eldridge et al. 1991). Sulfur isotope variations within diamonds exhibit the same characteristics as previously described for carbon: i.e., eclogitic diamonds are much more variable than peridotitic diamonds.

Interesting differences in sulfur isotope compositions are observed when comparing high-S peridotitic tectonites with low-S peridotite xenoliths (Fig. 3.7). Tectonites from the Pyrenees predominantly have negative δ^{34}S-values of around -5‰, whereas low-S xenoliths from Mongolia have largely positive δ^{34}S-values of up to $+7$‰. Ionov et al. (1992) determined sulfur contents and isotopic compositions in

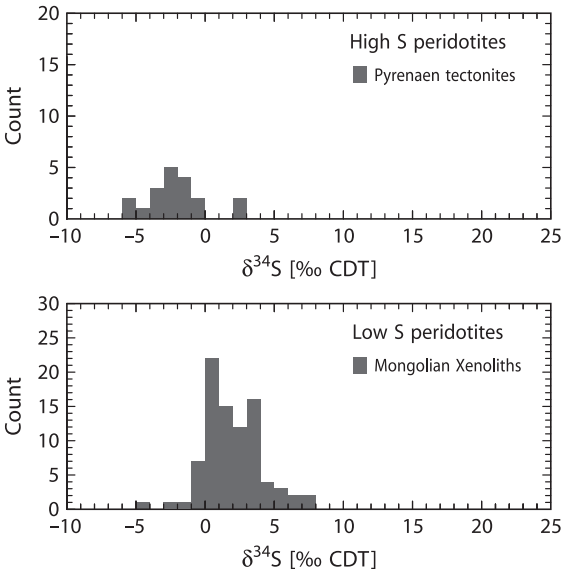

Fig. 3.7 Sulfur isotope compositions of high- and low-S peridotites

some 90 garnet and spinel lherzolites from six regions in southern Siberia and Mongolia for which the range of δ^{34}S-values is from -7 to $+7$‰. Ionov et al. (1992) concluded that low sulfur concentrations (<50 ppm) and largely positive δ^{34}S-values predominate in the lithospheric continental mantle worldwide. S-isotope compositions typical of MORB (δ^{34}S: 0–1‰) may be produced by melting of moderately depleted lherzolites. Primary melts with positive δ^{34}S-values may be generated from mantle peridotites with larger degrees of depletion and/or from rocks metasomatized by subduction-related fluids.

3.2.6 Lithium and Boron

Since lithium and boron isotope fractionations mainly occur during low temperature processes, Li and B isotopes may provide a robust tracer of surface material that is recycled to the mantle (Elliott et al. 2004). Heterogeneous distribution of subducted oceanic and continental crust in the mantle will thus result in variations in Li and B isotope ratios. Furthermore, dehydration processes active in subduction zones appear to be of crucial importance in the control of Li and B isotope composition of different parts of the mantle. For the upper mantle as a whole Jeffcoate et al. (2007) gave an estimated δ^{7}Li-value of 3.5‰.

Seitz et al. (2004), Magna et al. (2006) and Jeffcoate et al. (2007) reported significant Li isotope fractionation among mantle minerals. Olivines are about 1.5‰ lighter than coexisting orthopyroxenes, clinopyroxenes and phlogopites are in contrast highly variable, which might indicate isotope disequilibrium. In situ SIMS

analyses show Li isotope zonations in peridotite minerals. Jeffcoate et al. (2007) report a 40‰ variation in a single orthopyroxene crystal from San Carlos, which is attributed to diffusive fractionation during ascent and cooling.

Since boron concentrations in mantle minerals are exceedingly low, boron isotope analysis of mantle minerals are very restricted. On the basis of a boron budget between mantle and crust, Chaussidon and Marty (1995) concluded that the primitive mantle had a δ^{11}B-value of -10 ± 2‰. For MORB Spivack and Edmond (1987) and Chaussidon and Marty (1995) reported a δ^{11}B-value of around -4‰. Higher and lower δ^{11}B-values observed in some ocean island basalts should be due to crustal assimilation (Tanaka and Nakamura 2005).

3.3 Magmatic Rocks

On the basis of their high temperature of formation, it could be expected that magmatic rocks exhibit relatively small differences in isotopic composition. However, as a result of secondary alteration processes and the fact, that magmas can have a crustal and a mantle origin, the variation observed in isotopic composition of magmatic rocks can actually be quite large.

Provided an igneous rock has not been affected by subsolidus isotope exchange or hydrothermal alteration, its isotope composition will be determined by:

1. The isotope composition of the source region in which the magma was generated
2. The temperature of magma generation and crystallization
3. The mineralogical composition of the rock
4. The evolutionary history of the magma including processes of isotope exchange, assimilation of country rocks, magma mixing, etc

In the following sections, which concentrate on $^{18}O/^{16}O$ measurements, some of these points are discussed in more detail (see also Taylor 1968, 1986; Taylor and Sheppard 1986).

3.3.1 Fractional Crystallization

Because fractionation factors between melt and solid are small at magmatic temperatures, fractional crystallization is expected to play only a minor role in influencing the oxygen isotopic composition of magmatic rocks. Matsuhisa (1979), for example, reported that δ^{18}O-values increased by approximately 1‰ from basalt to dacite within a lava sequence from Japan. Muehlenbachs and Byerly (1982) analyzed an extremely differentiated suite of volcanic rocks at the Galapagos spreading center and showed that 90% fractionation only enriched the residual melt by about 1.2‰. On Ascension Island Sheppard and Harris (1985) measured a difference of nearly 1‰ in a volcanic suite ranging from basalt to obsidian. Furthermore,

modeling closed-system crystal fractionation, an ^{18}O-enrichment of about 0.4‰ per 10 wt% increase in SiO_2 content can be predicted.

3.3.2 Differences between Volcanic and Plutonic Rocks

Systematic differences in O-isotope composition are observed between fine-grained, rapidly quenched volcanic rocks and their coarse-grained plutonic equivalents (Taylor 1968; Anderson et al. 1971). Fractionations among minerals in plutonic mafic rocks are on average about twice as great as for the corresponding fractionations observed in equivalent extrusive mafic rocks. This difference may result from retrograde exchange between minerals or post-crystallization exchange reactions of the plutonic rocks with a fluid phase. This interpretation is supported by the fact that basaltic and gabbroic rocks from the lunar surface yield the same "isotopic temperatures" corresponding to their initial temperatures of crystallization. Due to the absence of water on the Moon, no retrograde exchange took place.

3.3.3 Low-Temperature Alteration Processes

Because of their high glass contents and very fine grain size, volcanic rocks are very susceptible to low-temperature processes such as hydration and weathering, which are characterized by large ^{18}O-enrichment effects in the altered rocks.

In general, it is probable that Tertiary and older volcanic rocks will exhibit O-isotope compositions that have been modified to higher $^{18}O/^{16}O$ ratios from their primary state to some extent (Taylor 1968; Muehlenbachs and Clayton 1972; Cerling et al. 1985; Harmon et al. 1987). Although there is no way to ascertain the magnitude of these ^{18}O-enrichments on a sample by sample basis, a crude estimate can be made by determining the water (and carbon dioxide) content and "correcting" to what are considered primary values of the suite of rocks to be analyzed (Taylor et al. 1984; Harmon et al. 1987). The primary water content of a magma is difficult to estimate, however, but it is generally accepted that primary basaltic magmas should not contain more than 1 wt % water. Thus, any water content $>1\%$ could be of secondary origin and the $\delta^{18}O$-value for such samples should be corrected before such ^{18}O-measurements are to be used for primary, magmatic interpretations.

3.3.4 Assimilation of Crustal Rocks

Because the various surface and crustal environments are characterized by different and distinctive isotope compositions, stable isotopes provide a powerful tool for discriminating between the relative role of mantle and crust in magma genesis. This

is especially true when stable isotopes are considered together with radiogenic isotopes, because variations within these independent isotopic systems may arise from unrelated geologic causes. For instance, a mantle melt that has been affected by contamination processes within the upper crust will exhibit increases in $^{18}O/^{16}O$ and $^{87}Sr/^{86}Sr$ ratios that correlate with an increase in SiO_2 and decrease in Sr content. In contrast, a mantle melt, which evolves only through differentiation unaccompanied by interaction with crustal material, will have an O-isotope composition that mainly reflects that of its source region, independent of variations in chemical composition. In this latter case, correlated stable and radiogenic isotope variations would be an indication of variable crustal contamination of the source region (i.e., crustal material that has been recycled into the mantle via subduction).

Modeling by Taylor (1980) and James (1981) has demonstrated that it is possible to distinguish between the effects of source contamination as well as crustal contamination. Magma mixing and source contamination are two-component mixing processes which obey two-component hyperbolic mixing relations, whereas crustal contamination is a three-component mixing process, involving the magma, the crustal contaminant, and the cumulates, that results in more complex mixing trajectories on an oxygen–radiogenic isotope plot.

3.3.5 Basaltic Rocks from Different Tectonic Settings

Harmon and Hoefs (1995) have assembled a database consisting of 2,855 O-isotope analyses of Neogene volcanic rocks worldwide. They observed a 5‰ variation in the $\delta^{18}O$-values of fresh basalts and glasses, which they have taken as evidence of significant oxygen isotope heterogeneities in the mantle sources of the basalts. This is documented in Fig. 3.8, which plots $\delta^{18}O$-values vs. Mg-numbers (Harmon and Hoefs 1995).

The usage of whole rock data has, however, its ambiguities. Estimates of original magmatic $\delta^{18}O$-values is best achieved through analysis of unaltered phenocrysts within rocks. Laser-based extraction methods on small amounts of separated mineral phases have documented subtle, but resolvable differences among different types of basaltic lavas (Eiler et al. 1996, 2000; Dorendorf et al. 2000; Cooper et al. 2004; Bindeman et al. 2004, 2005, and others).

MORB has a rather uniform O-isotope composition of all basalt types (5.5 ± 0.2‰) and can be used as a reference against which basalts erupted in other tectonic settings can be compared. By performing high precision laser isotope analyses on MORB glasses from the North Atlantic, Cooper et al. (2004) observed a $\delta^{18}O$-variation range of about 0.5‰, which is larger than originally thought by Harmon and Hoefs (1995). ^{18}O variations correlate with geochemical parameters of mantle enrichment such as high $^{87}Sr/^{86}Sr$ and low $^{143}Nd/^{144}Nd$ ratios. According to Cooper et al. (2004) the enriched material reflects subducted altered dehydrated oceanic crust.

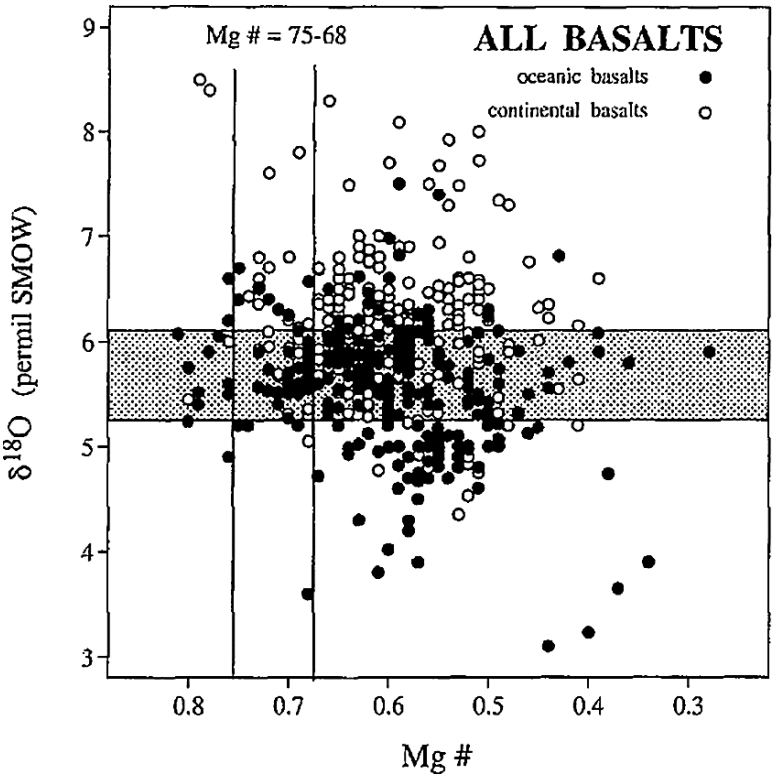

Fig. 3.8 Plot of $\delta^{18}O$ values vs Mg numbers for oceanic basalts (*filled circles*) and continental basalts (*open circles*). The *shaded field* denotes the $\pm 2\sigma$ range of a MORB mean value of +5.7‰, the *clear vertical field* denotes the range for primary basaltic partial melts in equilibrium with a peridotitic source (Harmon and Hoefs, 1995)

The largest variability in oxygen isotope composition has been found in subduction related basalts. Bindeman et al. (2005) observed a $\delta^{18}O$ range in olivine phenocrysts between 4.9 and 6.8‰. Oxygen isotope variations in arc-related lavas can constrain the contributions of subducted sediments and fluids to the sub-arc mantle assuming the $\delta^{18}O$ of the subducted component is known (Eiler et al. 2000; Dorendorf et al. 2000). These authors demonstrated that crustal assimilation or a contribution of oceanic sediments is negligible (<1–2%). Instead, the observed ^{18}O-enrichment in olivines and clinopyroxenes may result from exchange with high ^{18}O fluids derived from subducted altered oceanic crust.

Continental basalts tend to be enriched in ^{18}O relative to oceanic basalts and exhibit considerably more variability in O-isotope composition, a feature attributed to interaction with ^{18}O-enriched continental crust during magma ascent (Harmon and Hoefs 1995; Baker et al. 2000).

3.3.6 Ocean Water/Basaltic Crust Interactions

Information about the O-isotope character of the oceanic crust comes from DSDP/ODP drilling sites and from studies of ophiolite complexes, which presumably represent pieces of ancient oceanic crust. Primary, unaltered oceanic crust has δ^{18}O-values close to MORB (δ^{18}O:5.7‰). Two types of alteration can be distinguished within the oceanic lithosphere: at low temperatures weathering may markedly enrich the groundmass of basalts in ^{18}O, but does not affect phenocrysts. The extent of this low-temperature alteration correlates with the water content: the higher the water content, the higher the δ^{18}O-values (e.g., Alt et al. 1986). At temperatures in excess of about 300°C hydrothermal circulation beneath the mid-ocean ridges leads to a high-temperature water/rock interaction in which deeper parts of the oceanic crust become depleted in ^{18}O by 1–2‰. Similar findings have been reported from ophiolite complexes, the most cited example is that of Oman (Gregory and Taylor 1981). Maximum ^{18}O contents occur in the uppermost part of the pillow lava sequence and decrease through the sheeted dike complex. Below the base of the dike complex down to the Moho, δ^{18}O-values are lower than typical mantle values by about $1-2$‰.

Thus, separate levels of the oceanic crust are simultaneously enriched and depleted in ^{18}O relative to "normal" mantle values because of reaction with sea water at different temperatures. Muehlenbachs and Clayton (1976) and Gregory and Taylor (1981) concluded that the ^{18}O enrichments are balanced by the ^{18}O depletions which acts like a buffer for the oxygen isotope composition of ocean water.

Recently, Gao et al. (2006) evaluated the existing database and concluded that apparent differences in mass-weighed δ^{18}O-values exist among profiles through the recent and the fossil oceanic crust depending on differences in spreading rates. Oceanic crust formed under fast spreading ridges usually have depleted or balanced δ^{18}O-values, whereas oceanic crust formed under slow spreading ridges is characterized by enriched δ^{18}O-values. This difference might be due to different depths of sea water penetration in fast and slow spreading ridges.

3.3.7 Granitic Rocks

On the basis of $^{18}O/^{16}O$ ratios, Taylor (1977, 1978) subdivided granitic rocks into three groups: (1) normal ^{18}O-granitic rocks with δ^{18}O-values between 6 and 10‰, (2) high ^{18}O-granitic rocks with δ^{18}O-values >10‰ and (3) low ^{18}O-granitic rocks with δ^{18}O-values <6‰. Although this is a somewhat arbitrary grouping, it nevertheless turns out to be a useful geochemical classification.

Many granitic plutonic rocks throughout the world have relatively uniform ^{18}O-contents with δ^{18}O-values between 6 and 10‰. Granitoids at the low ^{18}O end of the normal group have been described from oceanic island – arc areas where continental crust is absent (e.g., Chivas et al. 1982). Such plutons are considered to be entirely mantle-derived. Granites at the high end of the normal ^{18}O-group may have

formed by partial melting of crust that contained both a sedimentary and a magmatic fraction. It is interesting to note that many of the normal ^{18}O-granites are of Precambrian age and that metasediments of this age quite often have δ^{18}O-values below 10‰ (Longstaffe and Schwarcz 1977).

Granitic rocks with δ^{18}O-values higher than 10‰ require derivation from some type of ^{18}O-enriched sedimentary or metasedimentary protolith. For instance, such high δ^{18}O-values are observed in many Hercynian granites of western Europe (Hoefs and Emmermann 1983), in Damaran granites of Africa (Haack et al. 1982) and in granites from the Himalayas of Central Asia (Blattner et al. 1983). All these granites are easily attributed to anatexis within a heterogeneous crustal source, containing a large metasedimentary component.

Granitic rocks with δ^{18}O-values lower than 6‰ cannot be derived by any known differentiation process from basaltic magmas. Excluding those low ^{18}O granites which have exchanged with ^{18}O depleted meteoric–hydrothermal fluids under subsolidus conditions, a few primary low ^{18}O granitoids have been observed (Taylor 1987). These granites obviously inherited their ^{18}O depletion while still predominantly liquid, prior to cooling and crystallization. Such low ^{18}O magmas may be formed by remelting of hydrothermally altered country rocks or by large-scale assimilation of such material in a rift-zone tectonic setting.

3.3.7.1 Oxygen Isotopes in Zircon

Recent advances in combining in situ measurements of radiogenic and stable isotopes in zircons allow a better understanding of the petrogenesis of granites and the evolution of the continental crust (Hawkesworth and Kemp 2006). Nonmetamict zircons preserve their δ^{18}O-value from the time of crystallization because of their refractory and robust nature (Valley 2003). Magmas in equilibrium with the mantle crystallize zircon that have a narrow range in δ^{18}O-values of 5.3 ± 0.3‰. ^{18}O-variations toward higher values result if the parental magma incorporates higher ^{18}O material (supracrustal rocks through melting or assimilation). Zircons with δ^{18}O-values lower than 5.3‰ have been found in A-type granites (Wei et al. 2008) indicating that the zircons originate from low ^{18}O magmas. O-isotope ratios in zircons thus can be used to discriminate between new mantle derived crust and crust that has been reworked.

Analyses of the oxygen isotope composition of zircons that have been dated may provide a record of growth and maturation of the crust. Valley et al. (2005) have analyzed 1,200 dated zircons representing the whole spectrum of geologic ages. Uniformly low δ^{18}O-values are found in the first half of Earth history, but much more varied values are observed in younger rocks. In contrast to the Archean, ^{18}O-values during the Proterozoic gradually increase possibly indicating a maturation of the crust (see Fig. 3.9). After 1.5 Ga high δ^{18}O-values above 8‰ reflect gradual changes in the composition of sediments and the rate and style of recycling of surface-derived material into magmas (Valley et al. 2005).

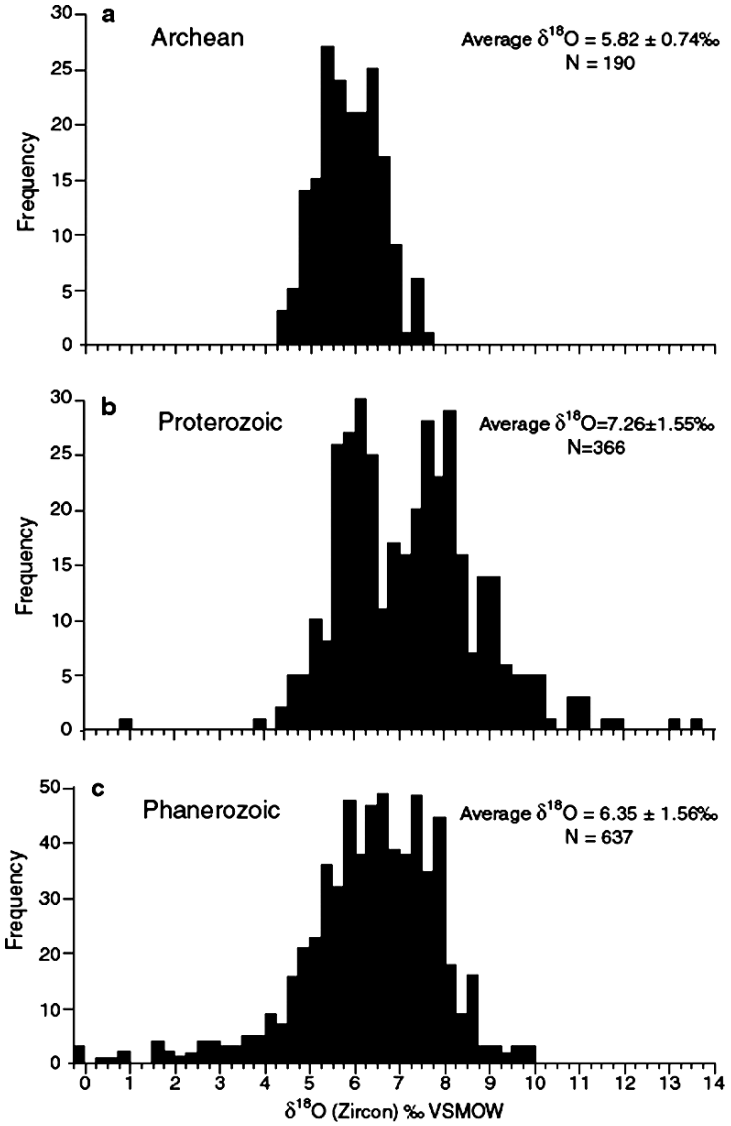

Fig. 3.9 Histograms of $\delta^{18}O$-values for igneous zircons ((**a**) Archean, (**b**) Proterozoic and (**c**) Phanerozoic) (after Valley et al. 2005)

3.4 Volatiles in Magmatic Systems

The isotope composition of magmatic volatiles and related isotope fractionation processes can be deduced by analyses of glasses, volcanic gases, and hot springs. The main process that can cause isotope fractionation of volatile compounds is degassing

and/or change in speciation (e.g. SO_2-H_2S). The other process which can alter the isotopic composition of magmatic volatiles is assimilation and contamination. The ultimate origin of volatiles in magmatic systems – whether juvenile in the sense that they originate from primary mantle degassing, or recycled by subduction processes – is difficult to assess, but may be deduced in some cases. Because large differences exist in the isotope compositions of surface rocks relative to the mantle, the analysis of volatiles is important in assessing the extent of volatile transfer from the surface reservoirs to the mantle via subduction. Volatiles from arc related volcanic and hydrothermal systems may indicate an appreciable amount of surface derived materials and provide strong evidence of volatile recycling in subduction zones (Hauri 2002; Snyder et al. 2001; Fischer et al. 2002).

3.4.1 Glasses

Hydrogen. Water dissolves in silicate melts and glasses in at least two distinct forms: water molecules and hydroxyl groups. Because the proportions of these two species change with total water content, temperature and chemical composition of the melt, the bulk partitioning of hydrogen isotopes between vapor and melt is a complex function of these variables. Dobson et al. (1989) determined the fractionation between water vapor and water dissolved in felsic glasses in the temperature range from 530 to 850°C. Under these conditions, the total dissolved water content of the glasses was below 0.2%, with all water present as hydroxyl groups. The measured hydrogen fractionation factors vary from 1.051 to 1.035 and are greater than those observed for most hydrous mineral – water systems, perhaps reflecting the strong hydrogen bonding of hydroxyl groups in glasses.

Hydrogen isotope and water content data for MORB, OIB, and BAB glasses have been determined by Kyser and O'Neil (1984), Poreda (1985), and Poreda et al. (1986). The range of δD-values for MORB glasses is from -90 to $-40‰$ and is indistinguishable from that reported for phlogopites and amphiboles from kimberlites and peridotites (see Fig. 3.4). Kyser and O'Neil (1984) demonstrated that D/H ratios and water content in fresh submarine basalt glasses can be altered by (1) degassing, (2) addition of sea water at magmatic temperature and (3) low-temperature hydration. Extrapolations to possible unaltered D/H-ratios indicate that primary δD-values for most basalts are $-80 \pm 5‰$.

The process of degassing has been documented best for rhyolitic magmas where water-rich magmas (about 2%) have a δD-value of $-50‰$. At very late eruption stages with remaining water contents of around 0.1% the δD-value is around $-120‰$ (Taylor et al. 1983; Taylor 1986). For this process, the decisive parameter is the isotopic fractionation between the vapor and the melt, which can be between 15 and 35‰ (Taylor 1986) and the amount of water lost from the system (Rayleigh fractionation). The degassing process produces an opposite trend to a meteoric water hydrothermal alteration, showing decreasing δD-values with increasing water content.

Carbon. Isotopic fractionation between CO_2 and dissolved carbon in melts has been estimated by various authors to vary between 2 and 4‰ (as summarized by Holloway and Blank 1994), the vapor being enriched in ^{13}C relative to the melt. This fractionation can be used to interpret the carbon isotope composition of glasses and CO_2 in volcanic gases and to estimate the initial carbon concentration of undegassed basaltic melts.

Reported $\delta^{13}C$-values for basaltic glass vary from -30 to about -3‰ that represent isotopically distinct carbon extracted at different temperatures by stepwise heating (Pineau et al. 1976; Pineau and Javoy 1983; Des Marais and Moore 1984; Mattey et al. 1984). A "low-temperature" component of carbon is extractable below 600°C, whereas a "high-temperature" fraction of carbon is liberated above 600°C. There are two different interpretations regarding the origins of these two different types of carbon. While Pineau et al. (1976) and Pineau and Javoy (1983) consider that the whole range of carbon isotope variation observed to represent primary dissolved carbon, which becomes increasingly ^{13}C depleted during multistage degassing of CO_2, Des Marais and Moore 1984) and Mattey et al. (1984) suggest that the "low-temperature" carbon originates from surface contamination. For MORB glasses, the "high-temperature" carbon has an isotopic composition typical for that of mantle values. Island arc glasses have lower $\delta^{13}C$-values, which might be explained by mixing two different carbon compounds in the source regions: an MORB – like carbon and an organic carbon component from subducted pelagic sediments (Mattey et al. 1984).

Nitrogen. The determination of nitrogen isotopes in basaltic glasses is severely complicated by its low concentration, which makes nitrogen sensitive to atmospheric contamination and to addition of surface-derived materials i.e., organic matter. Nitrogen in basaltic glasses has been determined by Exley et al. (1987), Marty and Humbert (1997), and Marty and Zimmermann (1999). The recent studies by Marty and coworkers indicate that nitrogen in MORB and OIB glasses has an average $\delta^{15}N$-value of around -4 ± 1‰ (see Fig. 3.6). The major factors affecting its isotopic composition appear to be magma degassing and assimilation of surface-derived matter.

Sulfur. The behavior of sulfur in magmatic systems is particularly complex: sulfur can exist as both sulfate and sulfide species in four different forms: dissolved in the melt, as an immiscible sulfide melt, in a separate gas phase, and in various sulfide and sulfate minerals. MORB glasses and submarine Hawaiian basalts have a very narrow range in sulfur isotope composition, with $\delta^{34}S$-values clustering around zero (Sakai et al. 1982, 1984). In subaerial basalts, the variation of $\delta^{34}S$-values is larger and generally shifted towards positive values. One reason for this larger variation is the loss of a sulfur-bearing phase during magmatic degassing. The effect of this process on the sulfur isotope composition depends on the ratio of sulfate to sulfide in the magma which is directly proportional to the fugacity of oxygen (Sakai et al. 1982). Arc volcanic rocks are particularly enriched in ^{34}S, with $\delta^{34}S$-values up to +20‰ (Ueda and Sakai 1984; Harmon and Hoefs 1986) which is considered to be mainly a product of recycling of marine sulfate during subduction.

3.4.2 Volcanic Gases and Hot Springs

The chemical composition of volcanic gases is naturally variable and can be modified significantly during sample collection, storage, and handling. While it is relatively simple to recognize and correct for atmospheric contamination, the effects of natural contamination processes in the near-surface environment are much more difficult to address. Thus, the identification of truly mantle-derived gases except helium remains very problematic. In addition to assimilation/contamination processes, the degassing history can significantly alter the isotopic composition of magmatic volatiles.

3.4.2.1 Water

A long-standing geochemical problem is the source of water in volcanic eruptions and geothermal systems: how much is derived from the magma itself and how much is recycled meteoric water? One of the principal and unequivocal conclusions drawn from stable isotope studies of fluids in volcanic hydrothermal systems is that most hot spring waters are meteoric waters derived from local precipitation (Craig et al. 1956; Clayton et al. 1968; Clayton and Steiner 1975; Truesdell and Hulston 1980, and others).

Most hot spring waters have deuterium contents similar to those of local precipitation, but are usually enriched in ^{18}O as a result of isotopic exchange with the country rock at elevated temperatures. The magnitude of the oxygen isotope shift depends on the O-isotope composition of both water and rock, the mineralogy of the rock, temperature, water/rock ratio, and the time of interaction.

There is increasing evidence, however, that a magmatic water component cannot be excluded in some volcanic systems. As more and more data have become available from volcanoes around the world, especially from those at very high latitudes, Giggenbach (1992) demonstrated that "horizontal" ^{18}O shifts are actually the exception rather than the rule: shifts in oxygen isotope composition are also accompanied by a change in the deuterium content (Fig. 3.10). Giggenbach (1992) argued that all these waters followed similar trends corresponding to mixing of local ground waters with a water having a rather uniform isotopic composition with a $\delta^{18}O$-value of about 10‰ and a δD-value of about -20‰. He postulated the existence of a common magmatic component in andesite volcanoes having a δD of -20‰ which is much higher than the generally assumed mantle water composition. The most likely source would be recycled sea water carried to zones of arc magma generation by the subducted slab.

What is sometimes neglected in the interpretation of isotope data in volcanic degassing products are the effects of boiling. Loss of steam from a geothermal fluid can cause isotopic fractionations. Quantitative estimates of the effects of boiling on the isotopic composition of water can be made using known temperature-dependent fractionation coefficients and estimates of the period of contact between the steam and liquid water during the boiling process (Truesdell and Hulston 1980).

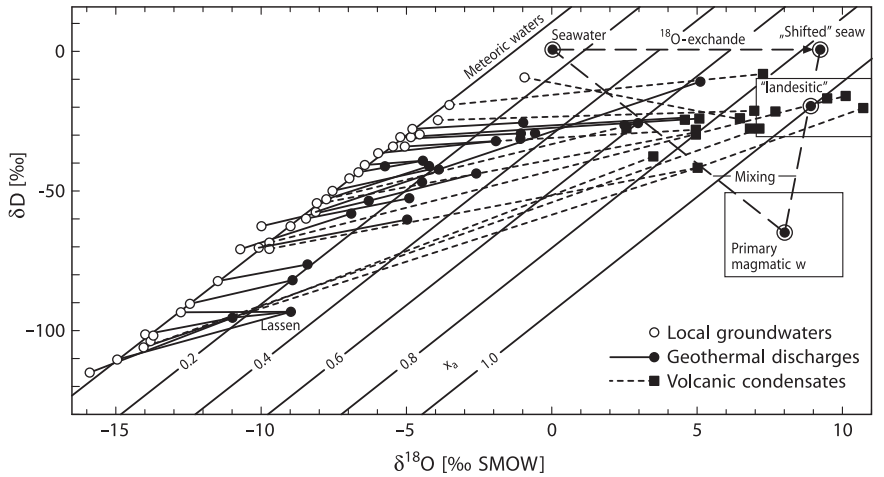

Fig. 3.10 Isotopic composition of thermal waters and associated local groundwaters. Lines connect corresponsing thermal waters to local groundwaters (Giggenbach, 1992)

3.4.2.2 Carbon

CO_2 is the second most abundant gas species in magmatic systems. In a survey of CO_2 emanations from tectonically active areas worldwide, Barnes et al. (1978) attributed δ^{13}C-values between -8 and $-4‰$ to a mantle source. This is, however, problematic, because average crustal and mantle isotope compositions are more or less identical and surficial processes that can modify the carbon isotope composition are numerous. A more promising approach may be to analyze the ^{13}C-content of CO_2 collected directly from magmas at high temperatures.

The volcano where gases have been collected and analyzed for the longest time is Kilauea in Hawaii, the database covering a period from about 1960 to 1985 (Gerlach and Thomas 1986; Gerlach and Taylor 1990). Gerlach and Taylor (1990) consider a δ^{13}C-value of $-3.4 \pm 0.05‰$ to be the best estimate of the mean for the total summit gas emission of Kilauea. A two-stage degassing model was developed to explain these values: (1) ascent and pressure equilibration in the summit magma chamber and (2) rapid, near surface decompression of summit-stored magma during ascent and eruption. The study demonstrated that the gas at the summit is a direct representation of the parental magma C-isotope ratio (δ^{13}C: $-3.4‰$), whereas gases given off during East Rift Zone eruptions have a δ^{13}C-value of $-7.8‰$, corresponding to a magma which had been affected by a degassing in a shallow magmatic system.

It is well documented that carbon dioxide in vesicles of MORB is derived from the upper mantle. In island arcs and subduction-related volcanism major portions of carbon may derive from limestones and organic carbon. Sano and Marty (1995) demonstrated that the $CO_2/^3$He ratio in combination with the δ^{13}C-value can be used to distinguish between sedimentary organic, limestone, and MORB carbon. Using this approach Nishio et al. (1998) and Fischer et al. (1998) concluded

that about two-thirds of the carbon in a subduction zone originates from carbonates, whereas up to one-third is derived from organic carbon. Even larger portions (>80%) of CO_2 derived from marine carbonates have been found by Shaw et al. (2003) in volcanoes from the Central American arc. Carbon derived from a primary mantle source thus only plays a minor role in a subduction environment.

Besides CO_2, methane has been reported in high-temperature hydrothermal vent fluids (Welhan 1988; Ishibashi et al. 1995). The origin of this methane is somewhat unclear, even in systems which are associated with ^{3}He anomalies. Whereas a non-biogenic magmatic origin of methane has been assumed for the East Pacific Rise (Welhan 1988), a thermogenic origin has been proposed for the Okinawa trough (Ishibashi et al. 1995).

In recent years there is a growing evidence that methane can be produced abiogenic during a Fischer-Tropsch type synthesis (reduction of CO or CO_2 by H_2 in the presence of a catalyst) (Sherwood-Lollar et al. 2006; McCollom and Seewald 2006 and others). Hydrocarbons (C_1–C_4) synthesized under abiogenic hydrothermal conditions are significantly depleted in ^{13}C relative to their CO_2 source. The magnitude of ^{13}C depletion may be similar to C-isotope fractionations during biological processes making it impossible to distinguish between biogenic and abiogenic sources of reduced carbon. This finding has important implications for the discussion of the Earth earliest biosphere. Sherwood-Lollar et al. (2002) observed a trend of decreasing ^{13}C contents with increasing carbon numbers C_1–C_4 just opposite to gases derived from biologic sources. Experiments by Fu et al. (2007), however, could not confirm the trend observed by Sherwood-Lollar et al. (2002).

3.4.2.3 Nitrogen

Nitrogen in particular is a potential tracer of volatile recycling between the surface and the mantle, because of the large differences in N-isotope composition of MORB (δ^{15}N: − 5‰), the atmosphere 0‰ and sediments (6–7‰). As demonstrated by Zimmer et al. (2004), Clor et al. (2005) and Elkins et al. (2006), nitrogen isotopes are very well suited for determining the fate of organic matter in subduction zones. These authors have demonstrated variable contributions of organic matter-derived nitrogen along arcs in Costa Rica, Nicaragua, and Indonesia. For instance, Elkins et al. (2006) estimated that sediment contributions to volcanic and geothermal gases in the Nicaraguan volcanic front are around 70%.

3.4.2.4 Sulfur

Elucidation of the origin of sulfur in volcanic systems is complicated by the fact that next to SO_2, significant amounts of H_2S, sulfate and elemental sulfur can also be present. The bulk sulfur isotope composition must be calculated using mass balance constraints. The principal sulfur gas in equilibrium with basaltic melts at low pressure and high temperature is SO_2. With decreasing temperature and/or increasing

water fugacity, H_2S becomes more stable. $\delta^{34}S$-values of SO_2 sampled at very high temperatures provide the best estimate of the ^{34}S-content of magmas (Taylor 1986). Sakai et al. (1982) reported $\delta^{34}S$-values of 0.7 to 1‰ in the solfataric gases of Kilauea which can be compared well with the $\delta^{34}S$-values of 0.9 to 2.6‰ for Mount Etna gases, measured by Allard (1983). SO_2 from volcanoes of andesitic and dacitic composition is more enriched in ^{34}S. This is especially pronounced in arc volcanoes from Indonesia, where Poorter et al. (1991) measured a $\delta^{34}S$-value of 5‰ for the bulk sulfur. Subducted oceanic crust may provide the ^{34}S enriched sulfur to arc volcanoes.

In summary, stable isotope analysis (H, C, S) of volcanic gases and hot springs allow for estimates of the isotopic composition of the mantle source. However, it must be kept in mind that numerous possibilities for contamination, assimilation, and gas phase isotopic fractionation, especially in the surficial environment, make such deductions problematic at best. In cases where it may possible to "see through" these secondary effects, small differences in H, C, N, and S isotope compositions of volcanic gases and hot springs might be characteristic of different geotectonic settings.

3.4.3 Isotope Thermometers in Geothermal Systems

Although there are many isotope exchange processes occurring within a geothermal fluid, many of which have the potential to provide thermometric information, only a few have generally been applied, because of suitable exchange rates for achieving isotope equilibrium (Hulston 1977; Truesdell and Hulston 1980; Giggenbach 1992). Temperatures are determined on the basis of calculated fractionation factors of Richet et al. (1977). Differences among geothermometers in the C–O–H–S system are generally ascribed to differences in exchange rates in the decreasing order CO_2–H_2O (oxygen) > H_2O–H_2 (hydrogen) > SO_2–H_2S (sulfur) > CO_2–CH_4 (carbon). Especially pronounced are the differences for the CO_2–CH_4 thermometer which are often higher than the actual measured temperatures. Recent investigations on Nisyros volcano, Greece, however, suggest that chemical and isotopic equilibrium between CO_2 and CH_4 may occur down to temperatures as low as 320°C (Fiebig et al. 2004).

3.5 Ore Deposits and Hydrothermal Systems

Stable isotopes have become an integral part of ore deposits studies. The determination of light isotopes of H, C, O, and S can provide information about the diverse origins of ore fluids, about temperatures of mineralization and about physico-chemical conditions of mineral deposition. In contrast to early views, which assumed that almost all metal deposits owed their genesis to magmas, stable isotope investigations

have convincingly demonstrated that ore formation has taken place in the Earth's near-surface environment by recycling processes of fluids, metals, sulfur, and carbon. Reviews of the application of stable isotopes to the genesis of ore deposits have been given by Ohmoto (1986), Taylor (1987) and Taylor (1997).

In as much as water is the dominant constituent of ore-forming fluids, knowledge of its origin is fundamental to any theory of ore genesis. There are two ways for determining δD- and δ^{18}O-values of ore fluids:

1. By direct measurement of fluid inclusions contained within hydrothermal minerals
2. By analysis of hydroxyl-bearing minerals and calculation of the isotopic composition of fluids from known temperature-dependent mineral-water fractionations, assuming that minerals were precipitated from solutions under conditions of isotope equilibrium.

A. There are two different methods through which fluids and gases may be extracted from rocks: (1) thermal decrepitation by heating in vacuum and (2) crushing and grinding in vacuum. Serious analytical difficulties may be associated with both techniques. The major disadvantage of the thermal decrepitation technique is that, although the amount of gas liberated is higher than by crushing, compounds present in the inclusions may exchange isotopically with each other and with the host mineral at the high temperatures necessary for decrepitation. Crushing in vacuum largely avoids isotope exchange processes. However, during crushing large new surfaces are created which easily adsorb some of the liberated gases and that, in turn, might be associated with fractionation effects. Both techniques preclude separating the different generations of inclusions in a sample and, therefore, the results obtained represent an average isotopic composition of all generations of inclusions.

Numerous studies have used the δD-value of the extracted water to deduce the origin of the hydrothermal fluid. However, without knowledge of the internal distribution of hydrogen in quartz, such a deduction can be misleading (Simon 2001). Hydrogen in quartz mainly occurs in two reservoirs: (1) in trapped fluid inclusions and (2) in small clusters of structurally bound molecular water. Because of hydrogen isotope fractionation between the hydrothermal fluid and the structurally bound water, the total hydrogen extracted from quartz does not necessarily reflect the original hydrogen isotope composition. This finding may explain why δD-values from fluid inclusions often tend to be lower than δD-values from associated minerals (Simon 2001).

B. Oxygen-bearing minerals crystallize during all stages of mineralization, whereas the occurrence of hydrogen-bearing minerals is restricted in most ore deposits. Examples of hydroxyl-bearing minerals include biotite and amphibole at high temperatures (in porphyry copper deposits), chlorite and sericite at temperatures around 300°C , and kaolinite at around 200°C.

The mineral alunite, and its iron equivalent jarosite, is a special case. Alunite $(KAl_2(SO_2)_2(OH)_2)$ contains four sites where elements containing stable isotopes are found and both the sulfate and hydroxyl anionic groups may provide information on fluid source and condition of formation.

Alunite forms under highly acidic oxidizing conditions and is characterized by the assemblage alunite + kaolinite + quartz ± pyrite. Stable isotope data of alunite in combination with associated sulfides and kaolinite permit recognition of environments and temperatures of formation (Rye et al. 1992).

The indirect method of deducing the isotope composition of ore fluids is more frequently used, because it is technically easier. Uncertainties arise from several sources: uncertainty in the temperature of deposition, and uncertainty in the equations for isotope fractionation factors. Another source of error is an imprecise knowledge of the effects of fluid chemistry ("salt effect") on mineral-water fractionation factors.

Several studies (e.g., Berndt et al. 1996; Driesner and Seward 2000; Horita et al. 1995; Shmulovich et al. 1999) have demonstrated that the approach of using mineral – pure water fractionation factors to deduce the origin of the water is incorrect. Isotope fractionations involving aqueous solutions depend not only on temperature and fluid composition, but also on the presence or absence of phase separation ("boiling"). Phase separation is an important process causing potentially isotope fractionation. Hydrogen isotope studies (Berndt et al. 1996; Shmulovich et al. 1999) indicate that high temperature phase separation produces D-enrichment in the vapor and D-depletion in the conjugate fluid. If the fractionation effect inherent in a boiling fluid system is disregarded, one may easily misinterpret the isotope composition of hydrothermal minerals, since boiling may mask the source of the parent fluids. In addition, for hydrogen isotope fractionations, pressure may have some control on mineralwater fractionations (Driesner 1997; Horita et al. 1999).

3.5.1 Origin of Ore Fluids

Ore fluids may be generated in a variety of ways. The principal types include (1) sea water, (2) meteoric waters and (3) juvenile water, all of which have a strictly defined isotopic composition. All other possible types of ore fluids such as formation, metamorphic, and magmatic waters can be considered recycled derivatives or mixtures from one or more of the three reference waters (see Fig. 3.11).

1. Sea water

The isotopic composition of present day ocean water is more or less constant with δ-values close to 0‰. The isotopic composition of ancient ocean water is less well constrained, but still should not be removed from 0 by more than 1 or 2‰. Many volcanogenic massive sulfide deposits are formed in submarine environments from heated oceanic waters. This concept gains support from the recently observed hydrothermal systems at ocean ridges, where measured isotopic compositions of fluids are only slightly modified relative to 0‰. $\delta^{18}O$ and δD-values of vent fluids are best understood in terms of sea water interaction with the ocean crust (Shanks 2001).

Bowers and Taylor (1985) have modeled the isotopic composition of an evolving sea water hydrothermal system. At low temperatures, the $\delta^{18}O$-value of the fluid decreases relative to ocean water because the alteration products in the oceanic crust are ^{18}O-rich. At around 250°C, the solution returns to its initial sea water isotopic

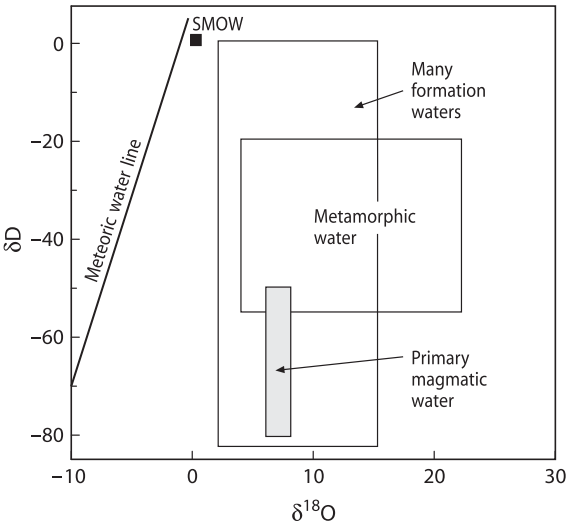

Fig. 3.11 Plot of δD vs $\delta^{18}O$ of waters of different origins

composition. Further reaction with basalt at 350°C increases the $\delta^{18}O$-value of modified sea water to ∼2‰. The δD-value of the solution increases slightly at all temperatures because mineral-water fractionations are generally less than 0. At 350°C, the δD-value of the solution is 2.5‰. The best-documented example for the role of ocean water during ore deposition is for the Kuroko-type deposits (Ohmoto et al. 1983).

2. Meteoric waters

Heated meteoric waters are a major constituent of ore-forming fluids in many ore deposits and may become dominant during the latest stages of ore deposition. The latter has been documented for many porphyry skarn-type deposits. The isotopic variations observed for several Tertiary North American deposits vary systematic with latitude and, hence, palaeo-meteoric water composition (Sheppard et al. 1971). The ore-forming fluid has commonly been shifted in O-isotope composition from its meteoric $\delta^{18}O$-value to higher ^{18}O contents through water-rock interaction. Meteoric waters may become dominant in epithermal gold deposits and other vein and replacement deposits.

3. Juvenile water

The concept of juvenile water has influenced early discussions about ore genesis tremendously. The terms "juvenile water" and "magmatic water" have been used synonymously sometimes, but they are not exactly the same. Juvenile water originates from degassing of the mantle and has never existed as surface water. Magmatic water is a non-genetic term and simply means a water that has equilibrated with a magma.

It is difficult to prove that juvenile water has ever been sampled. One way to search for juvenile water is by analyzing hydroxyl-bearing minerals of mantle origin (Sheppard and Epstein 1970). The estimated isotopic composition of juvenile water from such an approach is δD:-60 ± 20‰ and $\delta^{18}O$:$+6 \pm 1$‰ (Ohmoto 1986).

3.5.1.1 Magmatic Water

Despite the close association of intrusions with many ore deposits, there is still debate about the extent to which magmas contribute water and metals to ore-forming fluids. Many early studies of the stable isotope composition of hydrothermal minerals indicated a dominance of meteoric water (Taylor 1974), more recent studies show that magmatic fluids are commonly present, but that their isotopic compositions may be masked or erased during later events such as the influx of meteoric waters (Rye 1993; Hedenquist and Lowenstern 1994).

The δD-value of magmatic water changes progressively during degassing, resulting in a positive correlation between δD and the residual water content of an igneous body. Thus, late-formed hydroxyl-bearing minerals represent the isotopic composition of a degassed melt rather than that of the initial magmatic water. The δD-values of most of the water exsolved from many felsic melts are in the range of -60 to $-30‰$, whereas the associated magmatic rocks may be significantly depleted in D.

The calculated range of isotopic composition for magmatic waters is commonly between 6 and 10‰ for δ^{18}O-values and -50 and $-80‰$ for δD-values. Magmatic fluids may change their isotopic composition during cooling through isotope exchange with country rocks and mixing with fluids entrained within the country rocks. Thus, the participation of a magmatic water component during an ore-forming process is generally not easily detected.

3.5.1.2 Metamorphic Water

Metamorphic water is defined as water associated with metamorphic rocks during metamorphism. Thus, it is a descriptive, non-genetic term and may include waters of different ultimate origins. In a narrower sense, metamorphic water refers to the fluids generated by dehydration of minerals during metamorphism. The isotopic composition of metamorphic water may be highly variable, depending on the respective rock types and their history of fluid/rock interaction. A wide range of δ^{18}O-values (5–25‰) and δD-values (-70 to $-20‰$) is generally attributed to metamorphic waters (Taylor 1974).

3.5.1.3 Formation Waters

The changes in the D- and ^{18}O-contents of pore fluids depend on the origin of initial fluid (ocean water, meteoric water), temperature and the lithology of rocks with which the fluids are or have been associated. Generally, formation waters with the lowest temperature and salinity have the lowest δD- and δ^{18}O-values, approaching those of meteoric waters. Brines of the highest salinities are generally more restricted in isotopic composition. It is still an unanswered question though whether meteoric water was the only source of water to these brines. The final isotope

composition of brines can be produced by reactions between meteoric water and sediments, or result from mixtures of fossil ocean water trapped in the sediments and meteoric water.

3.5.2 Wall-Rock Alteration

Information about the origin and genesis of ore deposits can also be obtained by analyzing the alteration products in wall-rocks. Hydrogen and oxygen isotope zonation in wall-rocks around hydrothermal systems can be used to define the size and the conduit zones of a hydrothermal system. The fossil conduit is a zone of large water fluxes, generally causing a strong alteration in the rocks and lowering the δ^{18}O-values. Thus, fossil hydrothermal conduits can be outlined by following the zones of ^{18}O-depletion. Oxygen isotope data are especially valuable in rock types that do not show diagnostic alteration mineral assemblages as well as those in which the assemblages have been obliterated by subsequent metamorphism (e.g., Beaty and Taylor 1982; Green et al. 1983). Criss et al. (1985, 1991) found excellent spatial correlations between low δ^{18}O-values and economic mineralization in siliceous rocks. Similar zonation around ore deposits in carbonate rocks has also been observed (e.g., Vazquez et al. 1998). Thus, zones having anomalously low ^{18}O-contents may be a useful guide for exploration of hydrothermal ore deposits.

3.5.3 Fossil Hydrothermal Systems

Mainly through the work of Taylor and coworkers, it has become well established that many epizonal igneous intrusions have interacted with meteoric groundwaters on a very large scale. The interaction and transport of large amounts of meteoric water through hot igneous rocks produces a depletion in ^{18}O in the igneous rocks by up to 10–15‰ and a corresponding shift in the ^{18}O content of the water. About 60 of such systems have been observed to date (Criss and Taylor 1986). They exhibit great variations in size from relatively small intrusions ($<100\,km^2$) to large plutonic complexes ($>1{,}000\,km^2$). Amongst the best documented examples are the Skaergaard intrusion in Greenland, the Tertiary intrusions of the Scottish Hebrides, and the Tertiary epizonal intrusions of the northwestern United States and southern British Columbia, where 5% of the land surface has been altered by meteoric hydrothermal water (Criss et al. 1991).

The best-studied example of a hydrothermal system associated with a gabbro is the Skaergaard intrusion (Taylor and Forester 1979; Norton and Taylor 1979). The latter authors carried out a computer simulation of the Skaergaard hydrothermal system and found a good match between calculated and measured δ^{18}O-values. They further demonstrated that most of the subsolidus hydrothermal exchange took place at very high temperatures (400–800°C), which is compatible with the general

absence of hydrous alteration products in the mineral assemblages and with the presence of clinopyroxene.

In granitic hydrothermal systems, temperatures of alteration are significantly lower because of differences in the intrusion temperatures. The most conspicuous petrographic changes are chloritization of mafic minerals, particularly of biotite, and a major increase in the turbidity of feldspars. Large nonequilibrium quartz – feldspar oxygen isotope fractionations are typical. Steep linear trajectories on plots of $\delta^{18}O_{(feldspar)}$ vs. $\delta^{18}O_{(quartz)}$ are a characteristic feature of these hydrothermally altered rocks (see Fig. 2.17 (Chap. 2)). The trajectories result from the fact that feldspar exchanges ^{18}O with hydrothermal fluids much faster than coexisting quartz and from the fact that the fluids entering the rock system have $\delta^{18}O$-values which are out of equilibrium with the mineral assemblage. The process seldom goes to completion, so the final mineral assemblage is in isotope disequilibrium, which is the most obvious fingerprint of the hydrothermal event.

Taylor (1988) distinguished three types of fossil hydrothermal systems on the basis of varying water/rock ratios, temperatures, and the length of time that fluid/rock interaction proceeds:

Type I. Epizonal systems with a wide variation in whole rock ^{18}O-contents and extreme oxygen isotope disequilibrium among coexisting minerals. These systems typically have temperatures between 200 and 600°C and life-times $<10^6$ y.

Type II. Deeper-seated and/ or longer-lived systems, also with a wide spectrum of whole rock $^{18}O/^{16}O$ ratios, but with equilibrated $^{18}O/^{16}O$ ratios among coexisting minerals. Temperatures are between 400 and 700°C and life-times $>10^6$ y.

Type III. Equilibrated systems with a relatively uniform oxygen isotope composition in all lithologies. These systems require a large water/rock ratio, temperatures between 500 and 800°C, and life times around 5×10^6 y.

These types are not mutually exclusive, Type III systems for example may have been subjected to Type I or Type II conditions at an earlier stage of their hydrothermal history.

3.5.4 Hydrothermal Carbonates

The measured $\delta^{13}C$- and $\delta^{18}O$-values of carbonates can be used to estimate the carbon and oxygen isotope composition of the fluid in the same way as has been discussed before for oxygen and hydrogen. The isotopic composition of carbon and oxygen in any carbonate precipitated in isotopic equilibrium with a fluid depends on the isotopic composition of carbon and oxygen in the fluid, the temperature of formation, and the relative proportions of dissolved carbon species (CO_2, H_2CO_2, HCO_2^-, and/or CO_2^{2-}). To determine carbonate speciation, pH and temperature must be known; however, in most geologic fluids with temperatures above about 100°C, the content of HCO_3^- and CO_3^{2-} is negligible compared to CO_2 and H_2CO_2.

Experimental investigations have shown that the solubility of carbonate increases with decreasing temperature. Thus, carbonate cannot be precipitated from

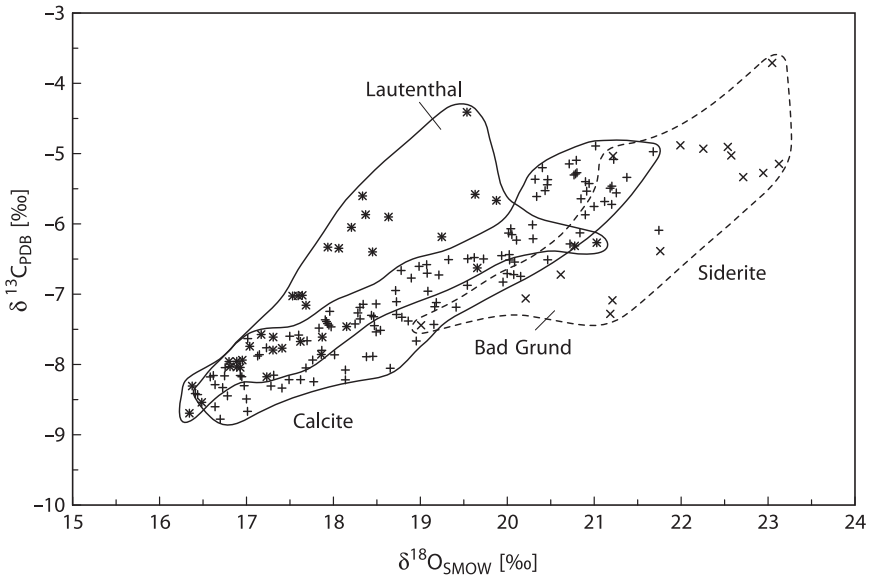

Fig. 3.12 C- and O-isotope compositions of calcites and siderites from the Bad Grund and Lautenthal deposits, Harz, Germany (after Zheng and Hoefs, 1993)

a hydrothermal fluid due to simple cooling in a closed system. Instead, an open system is required in which processes such as CO_2 degassing, fluid–rock interaction or fluid mixing can cause the precipitation of carbonate. These processes result in correlation trends in $\delta^{13}C$ vs. $\delta^{18}O$ space for hydrothermal carbonates as often observed in nature and theoretically modeled by Zheng and Hoefs (1993).

Figure 3.12 presents $\delta^{13}C$ and $\delta^{18}O$-values of hydrothermal carbonates from the Pb–Zn deposits of Bad Grund and Lautenthal, Germany. The positive correlation between $^{13}C/^{12}C$- and $^{18}O/^{16}O$-ratios can be explained either by calcite precipitation due to the mixing of two fluids with different NaCl concentrations or by calcite precipitation from a H_2CO_3-dominant fluid due to a temperature effect coupled with either CO_2 degassing or with fluid–rock interaction.

3.5.5 Sulfur Isotope Composition of Ore Deposits

A huge amount of literature exists about the sulfur isotope composition in hydrothermal ore deposits. Some of this information has been discussed in earlier editions and, therefore, is not repeated here. Out of the numerous papers on the subject, the reader is referred to comprehensive reviews by Rye and Ohmoto (1974), Ohmoto and Rye (1979), Ohmoto (1986), Taylor (1987) and Ohmoto and Goldhaber (1997). The basic principles to be followed in the interpretation of $\delta^{34}S$-values in sulfidic ores were elucidated by Sakai (1968), and subsequently, were extended by Ohmoto (1972).

The isotopic composition of a hydrothermal sulfide is determined by a number of factors such as (1) isotopic composition of the hydrothermal fluid from which the mineral is deposited, (2) temperature of deposition, (3) chemical composition of the dissolved element species including pH and fO_2 at the time of mineralization, and (4) relative amount of the mineral deposited from the fluid. The first parameter is characteristic of the source of sulfur, the three others relate to the conditions of deposition.

3.5.5.1 The Importance of fO_2 and pH

First, consider the effect of pH-increase due to the reaction of an acidic fluid with a carbonate-bearing host rocks. At pH = 5, practically all of the dissolved sulfur is undissociated H_2S, whereas at pH = 9 the dissolved sulfide is almost entirely dissociated. Since H_2S concentrates ^{34}S relative to dissolved sulfide ion, an increase in pH leads directly to an increase in the $\delta^{34}S$ of precipitated sulfides.

An increase in oxygen fugacities has a much stronger effect on the $\delta^{34}S$-values than a pH change, because of the large isotope fractionation between sulfate and sulfide. Figure 3.13 shows an example of the effect of pH and fO_2 variation on the

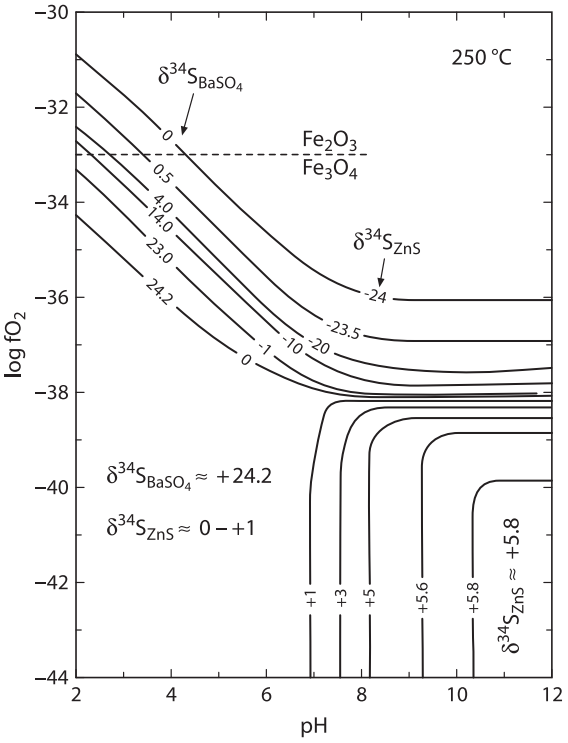

Fig. 3.13 Influence of fO_2 and pH on the sulfur isotope composition of sphalerite and barite at 250°C and $\delta^{34}S_{\Sigma S} = 0$ (modified after Ohmoto, 1972)

sulfur isotope compositions of sphalerite and barite in a closed system at 250°C with $\delta^{34}S_{\Sigma S} = O‰$. The curves are $\delta^{34}S$ contours, which indicate the sulfur isotope compositions of the minerals in equilibrium with the solution. Sphalerite $\delta^{34}S$-values can range from −24 to +5.8‰ and those for barite from about 0 to 24.2‰ within geologically reasonable limits of pH and fO_2. In the low fO_2 and pH region, sulfide ^{34}S contents can be similar to $\delta^{34}S_{\Sigma S}$ and can be rather insensitive to pH and fO_2Changes. In the region of high fO_{2-} values where the proportion of sulfate species becomes significant, mineral $\delta^{34}S$-values can be greatly different from $\delta^{34}S_{\Sigma S}$ and small changes in pH or fO_2 may result in large changes in the sulfur isotope composition of either sulfide or sulfate. Such a change must, however, be balanced by a significant change in the ratio of sulfate to sulfide.

In summary, interpretation of the distribution of $\delta^{34}S$-values relies on information about the source of sulfur and on a knowledge of the mineral parageneses that constrain the ambient temperature, EH and pH. If the oxidation state of the fluid is below the sulfate/H_2S boundary, then the $^{34}S/^{32}S$ ratios of sulfides will be insensitive to redox shifts.

In the following section different classes of ore deposits are discussed.

3.5.5.2 Magmatic Ore Deposits

Magmatic deposits are characterized by sulfides which precipitate from mafic silicate melts rather than hydrothermal fluids. They can be divided into S-poor (deposits of platinum group elements) and S-rich magmatic sulfide systems (Ni–Cu deposits) (Ripley and Li 2003). Typical examples are the deposits of Duluth, Stillwater, Bushveld, Sudbury, and Norils'k. In many of these deposits, relatively large deviations in $\delta^{34}S$-values from the presumed mantle melt value near zero are observed, which may indicate magma contamination by interactions with country rocks. The large spread in $\delta^{34}S$ is generally attributed to assimilation of sulfur from the wall rocks, provided that the sulfur isotope composition of the country rocks is significantly different from the magma.

3.5.5.3 Magmatic Hydrothermal Deposits

This group of deposits is closely associated in space and time with magmatic intrusions that were emplaced at relatively shallow depths. They have been developed in hydrothermal systems driven by the cooling of magma (e.g., porphyry-type deposits and skarns). From δD- and $\delta^{18}O$-measurements, it has been concluded that porphyry copper deposits show the clearest affinity of a magmatic water imprint (Taylor 1974) with variable involvement of meteoric water generally at late stages of ore formation.

The majority of $\delta^{34}S$-values of sulfides fall between −3 and 1‰ and of sulfates between 8 and 15‰ (Field and Gustafson 1976; Shelton and Rye 1982; Rye 2005). Sulfate–sulfide isotope date suggest a general approach to isotope equilibrium.

Calculated sulfate–sulfide temperatures, for conditions of complete isotope equilibrium, are typically between 450 and 600°C and agree well with temperatures estimated from other methods. Thus, the sulfur isotope data and temperatures support the magmatic origin of the sulfur in porphyry deposits.

3.5.5.4 Epithermal Deposits

Epithermal ore deposits are hydrothermal deposits that form at shallow crustal levels. A wide spectrum of ore deposits of a different nature occurs in this category. Typical temperatures of mineralization range from 150 to 350°C with variable salinities. Individual deposits often reveal that more than one type of fluid was involved in the formation of a single ore deposit. One of the fluids involved often appears to be of meteoric origin. In many deposits different fluids were alternatively discharged into the vein system and promoted the precipitation of a specific suite of minerals, such as one fluid precipitating sulfides and another precipitating carbonates (Ohmoto 1986).

Compared to porphyry copper deposits δ^{34}S-values in epithermal deposits are more variable due to lower temperatures of formation and significant amounts of both sulfide and sulfate in the hydrothermal fluid.

3.5.5.5 Recent and Fossil Sulfide Deposits at Mid-Ocean Ridges

Numerous sulfide deposits have been discovered in the sea floor along the East Pacific Rise, Juan de Fuca Ridge, Explorer Ridge, and Mid-Atlantic Ridge (Shanks 2001). These deposits are formed from hydrothermal solutions which result from the interaction of circulating hot sea water with oceanic crust. Sulfides are derived mainly from two sources: (1) leaching from igneous and sedimentary wall rocks and (2) thermochemical sulfate reduction due to interaction with ferrous silicates and oxides or with organic matter.

The role of sulfur in these vents is complex and often obscured by its multiple redox states and by uncertainties in the degree of equilibration. Studies by Styrt et al. (1981), Arnold and Sheppard (1981), Skirrow and Coleman (1982), Kerridge et al.(1983), Zierenberg et al. (1984), and others have shown that the sulfur in these deposits is enriched in ^{34}S relative to a mantle source (typical δ^{34}S ranges are between 1 and 5‰), implying small additions of sulfide derived from sea water.

Vent sulfides at sediment covered hydrothermal systems may carry, in addition, signatures of sulfides derived from bacterial reduction. δ^{34}S-values alone may be unable to distinguish between the different sulfur sources. High precision measurements of δ^{33}S, δ^{34}S, and δ^{36}S allow, however, the distinction of biological isotope fractionation from abiological fractionation (Ono et al. 2007; Rouxel et al. 2008). Biogenic sulfides are characterized by relatively high Δ^{33}S-values compared to hydrothermal sulfides. Sulfides from the East Pacific Rise and the Mid-Atlantic Ridge,

analyzed by Ono et al. (2007), gave low $\Delta^{33}S$-values compared to biogenic sulfides suggesting no contribution of biogenic sulfides. In altered oceanic basalts at ODP Site 801, however, Rouxel et al. (2008) provided evidence for secondary biogenic pyrite. These authors estimated that at least 17% of pyrite sulfur was derived from bacterial reduction.

For ancient seafloor sulfide deposits an alternative model has been discussed by Ohmoto et al. (1983), in which H_2S and sulfides are buffered by precipitated anhydrite and where $\delta^{34}S$-values reflect temperature dependent equilibrium fractionations between SO_4 and H_2S.

To the category of ancient hydrothermal seafloor ore deposits belong volcanic associated massive sulfide deposits. They are characterized by massive Cu–Pb–Zn–Fe sulfide ores associated with submarine volcanic rocks. They appear to have been formed near the seafloor by submarine hot springs at temperatures of 150–350°C. Massive sulfide deposits have $\delta^{34}S$-values typically between zero and the δ-value of contemporaneous oceanic sulfate, whereas the sulfate has δ-values similar to or higher than contemporaneous sea water. According to Ohmoto et al. (1983) the ore-forming fluid is evolved sea water fixed as disseminated anhydrite and then reduced by ferrous iron and organic carbon in the rocks.

Another group belonging to this category of ore deposits is sedimentary-exhalative (sedex) massive sulfide deposits. Just as volcanic massive sulfide deposits, this group has formed on the seafloor or in unconsolidated marine sediments. Its members differ from volcanogenic massive deposits in that the dominant host-rock lithologies are marine shales and carbonates, the associated igneous activity is minor or negligible, and water depths seem to be considerably less than the >2,000 m proposed for most volcanogenic deposits. The total range of sulfide $\delta^{34}S$-values is much larger than the range observed in volcanogenic massive sulfide deposits.

Sulfides are fine-grained and texturally complex containing multiple generations of minerals. Two different origins of sulfur can be envisaged: biogenic and hydrothermal. Mineral separation methods cannot insure that mineral separates contain only one type of sulfur. Therefore, conventional techniques cannot answer questions such as: is most of the sulfur produced by bacterial reduction of sea water or is it inorganically acquired and hydrothermally introduced together with the metals? In situ ion microprobe techniques allow isotope analysis on a scale as small as 20 μm. Studies by Eldridge et al. (1988, 1993) have revealed extremely large variations on distances of millimeters with gross disequilibrium between base metal sulfides and overgrown pyrites. Thus, the mean $\delta^{34}S$-values of these deposits are not particularly diagnostic of its origin, but additional measurements of $\Delta^{33}S$ might be able to distinguish between different sulfur sources.

3.5.5.6 Mississippi Valley Type Deposits

The Mississippi Valley Type (MVT) deposits are epigenetic Zn–Pb deposits which mainly occur in carbonates from continental settings (Ohmoto 1986).

Characteristics often ascribed to MVT deposits include temperatures generally $<200^{\circ}C$ and deposition from externally derived fluids, possibly basinal brines. Sulfur isotope values from MVT deposits suggest two major sulfide reservoirs, one between -5 and $+15‰$ and one greater than $+20‰$ (Seal 2006). Both sulfide reservoirs can be related, however, to a common sea water sulfate source that has undergone different sulfur fractionation processes. Reduction of sulfate occurs either bacterially or by abiotic thermochemical reduction. High $\delta^{34}S$-values should reflect minimal fractionations associated with thermochemical reduction of sea water sulfate (Jones et al. 1996).

3.5.5.7 Biogenic Deposits

The discrimination between bacterial sulfate and thermal sulfate reduction in ore deposits on the basis of $\delta^{34}S$-values is rather complex. The best criterion to distinguish between both types is the internal spread of δ-values. If individual sulfide grains at a distance of only a few millimeters exhibit large and nonsystematic differences in $\delta^{34}S$-values, then it seems reasonable to assume an origin involving bacterial sulfate reduction. Irregular variations in ^{34}S-contents are attributed to bacteria growing in reducing microenvironments around individual particles of organic matter. In contrast, thermal sulfate reduction requires higher temperatures supplied by external fluids, which is not consistent with the closed system environment of bacterial reduction.

Two types of deposits, where the internal S-isotope variations fit the expected scheme of bacterial reduction, but where the biogenic nature was already known from other geological observations, are the "sandstone-type" uranium mineralization in the Colorado Plateau (Warren 1972) and the Kupferschiefer in Central Europe (Marowsky 1969), although thermal sulfate reduction may have occurred at the base of the Kupferschiefer (Bechtel et al. 2001).

3.5.5.8 Metamorphosed Deposits

It is generally assumed that metamorphism reduces the isotopic variations in a sulfide ore deposit. Recrystallization, liberation of sulfur from fluid and vapor phases, such as the breakdown of pyrite into pyrrhotite and sulfur, and diffusion at elevated temperatures should tend to reduce initial isotopic heterogeneities.

Studies of regionally metamorphosed sulfide deposits (Seccombe et al. 1985; Skauli et al. 1992) indicate, however, little evidence of homogenisation on the deposit scale. Significant changes may take place in certain restricted parts of the deposit as a result of special local conditions, controlled by factors such as fluid flow regimes and tectonics. Thus, a very limited degree of homogenisation takes place during metamorphism (Cook and Hoefs 1997). The extent of this is obscured by primary distribution and zonation patterns.

3.5.6 Metal Isotopes

One of the most important questions in the genesis of ore deposits is the origin of the metals. Recent analytical developments have provided a new tool for the analysis of metal isotopes (Fe, Cu, Zn, Mo). Since the bulk silicate earth (crust + mantle) shows a uniform mean isotope composition of the metals, different metal reservoirs with distinct isotopic compositions are not easily recognizable. Thus, investigations by Markl et al. (2006a, b) on Cu and Fe ores have indicated that tracing of ore sources is ambiguous.

Magmatic processes do not appear to produce significant Cu and Fe isotope variations. Markl et al. (2006a, b) demonstrated that primary ores from high temperature hydrothermal ores from the Schwarzwald mining district show a restricted range despite the fact that the analyzed ores came from a large area and formed during different mineralization events.

A range of more than 5‰ in δ^{65}Cu has been interpreted by Markl et al. (2006a) as being due to redox processes among dissolved Cu-species and to fractionations during precipitation of Cu minerals. A 2.5‰ variation of iron minerals in δ^{56}Fe has been explained by mixing models either through mixing with oxygen-rich surface waters resulting in ^{56}Fe-depleted hematite or through mixing with CO_2-rich fluids leading to precipitation of isotopically depleted siderite (Markl et al. 2006b). Thus, an important new research field is the identification of low-temperature alteration processes in hydrothermal ore deposits, where biogenic and abiogenic redox processes potentially lead to significant isotope fractionations as already has been demonstrated in Sects. 2.13, 2.14, and 2.18, for Fe, Cu and Mo isotopes.

3.6 Hydrosphere

First, some definitions concerning water of different origin are given. The term *meteoric* applies to water that has been part of the meteorological cycle, and participated in processes such as evaporation, condensation, and precipitation. All continental surface waters, such as rivers, lakes, and glaciers, fall into this general category. Because meteoric water may seep into the underlying rock strata, it will also be found at various depths within the lithosphere dominating all types of continental ground waters. The *ocean*, although it continuously receives the continental run-off of meteoric waters as well as rain, is not regarded as being meteoric in nature. *Connate* water is water, which has been trapped in sediments at the time of burial. *Formation* water is present in sedimentary rocks and may be a useful nongenetic term for waters of unknown origin and age within these rocks.

3.6.1 Meteoric Water: General Considerations

When water evaporates from the surface of the ocean, the water vapor is enriched in H and ^{16}O because $H_2{}^{16}O$ has a higher vapor pressure than HDO and $H_2^{18}O$ (see Table 1.1 in Chap. 1). Under equilibrium conditions at 25°C, the fractionation factors for evaporating water are 1.0092 for ^{18}O and 1.074 for D (Craig and Gordon 1965). However, under natural conditions, the actual isotopic composition of water is more negative than the predicted equilibrium values due to kinetic effects (Craig and Gordon 1965). Vapor leaving the surface of the ocean cools as it rises and rain forms when the dew point is reached. During removal of rain from a moist air mass, the residual vapor is continuously depleted in the heavy isotopes, because the rain leaving the system is enriched in ^{18}O and D. If the air mass moves poleward and becomes cooler, additional rain formed will contain less ^{18}O than the initial rain. This relationship is schematically shown in Fig. 3.14. The isotope composition of mean world-wide precipitation is estimated to be $\delta D = -22$ and $\delta^{18}O = -4‰$ (Craig and Gordon 1965).

The theoretical approaches to explain isotope variations in meteoric waters evolved from the "isolated air mass" models, which are based on Rayleigh condensation, with immediate removal of precipitation and with a part of the condensate being kept in the cloud during the rain-out process. Isotope studies of individual rain events have revealed that successive portions of single events may vary drastically (Rindsberger et al. 1990). Quite often the pattern is "V-shaped", a sharp decrease of δ-values is usually observed at the beginning of a storm with a minimum somewhere in the middle of the event. The most depleted isotope values usually correspond to the period of most intense rain with little evaporation experienced by individual rain drops. It has also been observed that convective clouds produce precipitation with higher δ-values than stratiform clouds. Thus, the isotope composition of precipitation from a given rain event depends on meteorological history of the air mass in which the precipitation is produced and the type of cloud through

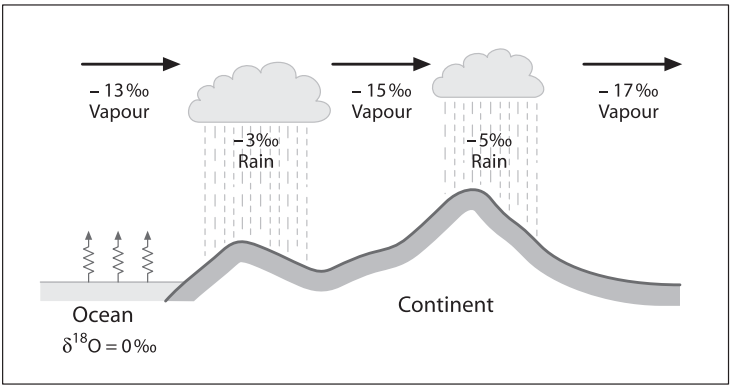

Fig. 3.14 Schematic O-isotope fractionation of water in the atmosphere (after Siegenthaler 1979)

which it falls. Liquid precipitation (rain) and solid precipitation (snow, hail) may differ in their isotope composition in so far as rain drops may undergo evaporation and isotope exchange with atmospheric vapor on their descent to the surface. By analyzing hailstones, discrete meteorological events can be studied because hailstones keep a record on the internal structure of a cloud. Jouzel et al. (1975) concluded that hailstones grow during a succession of upward and downward movements in a cloud.

The International Atomic Energy Agency (IAEA) has conducted a world-wide survey of the isotope composition of monthly precipitation for more than 35 years. The global distribution of D and ^{18}O in rain has been monitored since 1961 through a network of stations (Yurtsever 1975). From this extensive database it can be deduced how geographic and meteorological factors (rainout, temperature, humidity) influence the isotopic composition of precipitation.

The first detailed evaluation of the equilibrium and nonequilibrium factors that determine the isotopic composition of precipitation was published by Dansgaard (1964). He demonstrated that the observed geographic distribution in isotope composition is related to a number of environmental parameters that characterize a given sampling site, such as latitude, altitude, distance to the coast, amount of precipitation, and surface air temperature. Out of these, two factors are of special significance: temperature and the amount of precipitation. The best temperature correlation is observed in continental regions nearer to the poles, whereas the correlation with amount of rainfall is most pronounced in tropical regions as shown in Fig. 3.15. The apparent link between local surface air temperature and the isotope composition of precipitation is of special interest mainly because of the potential importance of stable isotopes as palaeoclimatic indicators. The amount effect is ascribed to gradual saturation of air below the cloud, which diminishes any shift to higher $\delta^{18}O$-values caused by evaporation during precipitation (Fricke and O'Neil 1999).

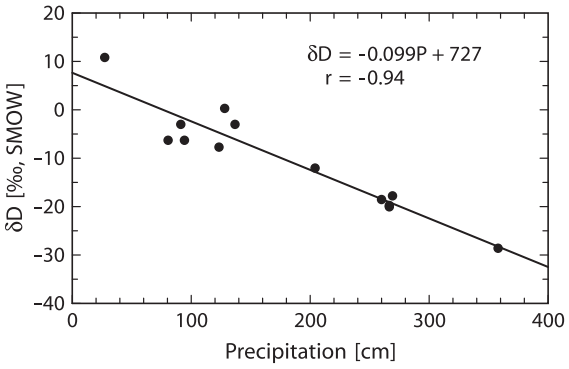

Fig. 3.15 Average δD values of the annual precipitation from oceanic islands as a function of the average amount of annual rainfall. The island stations are distant from continents, within 30° of the equator and at elevations less than 120 m (after Lawrence and White, 1991)

A compilation of studies throughout the world's mountain belts has revealed a consistent and linear relationship between change in the isotopic composition of precipitation and change in elevation (Poage and Chamberlain 2001). The isotopic composition of precipitation decreases linearly with increasing elevation by about 0.28‰/100 m in most regions of the world except in the Himalayas and at elevations above 5,000 m.

3.6.1.1 δD–$\delta^{18}O$ Relationship

In all processes concerning evaporation and condensation, hydrogen isotopes are fractionated in proportion to oxygen isotopes, because a corresponding difference in vapor pressures exists between H_2O and HDO in one case and $H_2^{16}O$ and $H_2\,^{18}O$, in the other. Therefore, hydrogen and oxygen isotope distributions are correlated in meteoric waters. Craig (1961a) first defined the following relationship:

$$\delta D = 8\,\delta^{18}O + 10$$

which is generally known as the "Global Meteoric Water Line".

Later, Dansgaard (1964) introduced the concept of "deuterium excess", d defined as $d = \delta D - 8\,\delta^{18}O$. Neither the numerical coefficient, 8, nor the deuterium excess, d, are really constant, both depend on local climatic processes. The long-term arithmetic mean for all analyzed stations of the IAEA network (Rozanski et al. 1993) is:

$$\delta D = (8.17 \pm 0.06)\,\delta 18O + (10.35 \pm 0.65)\; r^2 = 0.99,\; n = 206.$$

Relatively large deviations from the general equation are evident when monthly data for individual stations are considered (Table 3.1). In an extreme situation, represented by the St. Helena station, a very poor correlation between δD and $\delta^{18}O$ exists. At this station, it appears that all precipitation comes from nearby sources and represents the first stage of the rain-out process. Thus, the generally weaker correlations for the marine stations (Table 3.1) may reflect varying contributions of air masses with different source characteristics and a low degree of rain-out.

The imprint of local conditions can also be seen at other coastal and continental stations. The examples in Table 3.1 demonstrate that varying influences of different sources of vapor with different isotope characteristics, different air mass trajectories, or evaporation and isotope exchange processes below the cloud base, may often lead to much more complex relationships at the local level between δD and $\delta^{18}O$ than suggested for the regional or continental scale by the global "Meteoric Water Line" equation.

Knowledge about the isotopic variations in precipitation is increased when single rain events are analyzed from local stations. Especially under mid-latitude weather conditions, such short-term variations arise from varying contributions of tropical, polar, marine, and continental air masses.

Table 3.1 Variations in the numerical constant and the deuterium excess for selected stations of the IAEA global network (Rozanski et al. 1993)

Station	Numerical constant	Deuterium excess	r^2
Continental and coastal stations			
Vienna	7.07	−1.38	0.961
Ottawa	7.44	+5.01	0.973
Addis Ababa	6.95	+11.51	0.918
Bet Dagan, Israel	5.48	+6.87	0.695
Izobamba (Ecuador)	8.01	+10.09	0.984
Tokyo	6.87	+4.70	0.835
Marine Stations			
Weathership E (N.Atlantic)	5.96	+2.99	0.738
Weathership V (N.Pacific)	5.51	−1.10	0.737
St.Helena (S.Atlantic)	2.80	+6.61	0.158
Diego Garcia Isl. (Indian Oc.)	6.93	+4.66	0.880
Midway Isl. (N.Pacific)	6.80	+6.15	0.840
Truk Isl. (N.Pacific)	7.07	+5.05	0.940

3.6.1.2 $\delta^{17}O$–$\delta^{18}O$ Relationships

It has been common belief for many years that the ^{17}O abundance in meteoric waters carries no additional information to that of ^{18}O. Although mass-independent fractionations are not known to occur in water, $H_2{}^{17}O$ is a useful tracer within the hydrologic cycle (Angert et al. 2004; Luz and Barkan 2007). Improvements in analytical techniques allow to measure $\delta^{17}O$ and $\delta^{18}O$ with a precision of a few 0.01‰ which permits calculation of $\Delta^{17}O$ with similar precision and the tracing of very small $\delta^{17}O$ variations.

As is well known the isotopic composition of water is controlled by two mass-dependent processes (1) the equilibrium fractionation that is caused by the different vapor pressures of $H_2{}^{17}O$ and $H_2{}^{18}O$ and (2) the kinetic fractionation that is caused by the different diffusivities of $H_2{}^{17}O$ and $H_2{}^{18}O$ during transport in air. Angert et al. (2004) have demonstrated that for kinetic water transport in air, the slope in a $\delta^{17}O$–$\delta^{18}O$ diagram is 0.511, whereas it is 0.526 for equilibrium effects. Similar values have been given by Luz and Barkan (2007). $\Delta^{17}O$ is thus a unique tracer, which is, in contrast to the deuterium excess, temperature-independent and which may give additional information on humidity relations.

3.6.1.3 Ancient Meteoric Waters

Assuming that the H- and O-isotope compositions and temperatures of ancient ocean waters are comparable to present day values, the isotopic composition of ancient meteoric waters may have been governed by relations similar to those existing presently. However, given the local complexities, the application of this relation-

ship back through time should be treated with caution. To date, however, there is no compelling evidence that the overall systematics of ancient meteoric waters were very different from the present meteoric water relationship (Sheppard 1986). If the isotope composition of ocean water has changed with time, but global circulation patterns were like today, the "meteoric water line" at a specific time would be parallel to the modern meteoric water line, that is the slope would remain at a value of 8, but the intercept would be different.

The systematic behavior of stable isotopes in precipitation as a function of altitude can be used to provide estimates of paleoaltitude. In this approach the isotopic composition of paleoprecipitation is estimated from the analysis of in situ formed authigenic minerals (Chamberlain and Poage 2000; Blisnink and Stern 2005, and others). These authors have demonstrated that the effect of topography on the isotopic composition of precipitation is most straightforward in temperate mid-latitude regions, in topographically and in climatically simple settings.

3.6.2 Ice Cores

The isotopic composition of snow and ice deposited in the Polar Regions and at high elevations in mountains depend primarily on temperature. Snow deposited during the summer has less negative $\delta^{18}O$- and δD-values than snow deposited during the winter. A good example of the seasonal dependence has been given by Deutsch et al. (1966) on an Austrian glacier, where the mean δD-difference between winter and summer snow was observed to be $-14‰$. This seasonal cycle has been used to determine the annual stratigraphy of glaciers and to provide short-term climatic records. However, alteration of the snow and ice by seasonal melt water can result in changes of the isotopic composition of the ice, thus biasing the historical climate record. Systematic isotope studies also have been used to study the flow patterns of glaciers. Profiles through a glacier should exhibit lower isotope ratios at depth than nearer the surface, because deep ice may have originated from locations upstream of the ice-core site, where temperatures should be colder.

In the last decades, several ice cores over 1,000 m depth have been recovered from Greenland and Antarctica. In these cores, seasonal variations are generally observed only for the uppermost portions. After a certain depth, which depends on accumulation rates, seasonal variations disappear completely and isotopic changes reflect long-term climatic variations. No matter how thin a sample one cuts from the ice core, its isotope composition will represent a mean value of several years of snow deposition.

The most recent ice cores – investigated in great detail by large groups of researchers – are the Vostok core from East Antarctica (Lorius et al. 1985; Jouzel et al. 1987) and the GRIP and GISP 2 cores from Greenland (Dansgaard et al. 1993; Grootes et al. 1993). In the Vostok core, the low accumulation rate of snow in Antarctica results in very thin annual layers, which means that climate changes of a century or less are difficult to resolve. The newer Greenland ice cores GRIP and

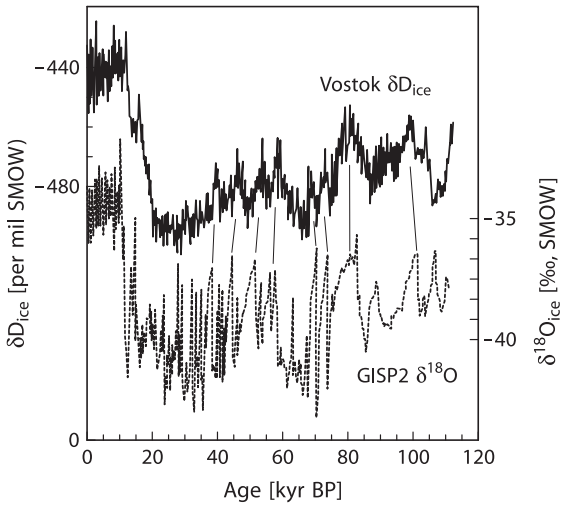

Fig. 3.16 Correlations of δD- and δ^{18}O-values of Greenland (GISP-2) and Antartic (Vostok) ice cores covering the last glacial–interglacial cycles (http://www.gisp2.sr.unh.edu/GISP2/DATA/Bender.html)

GISP 2 were drilled in regions with high snow accumulation near the centre of the Greenland ice sheet. In these cores, it is possible to resolve climate changes on the timescale of decades or less, even though they occurred a hundred thousand years ago. The GRIP and GISP 2 data indicate a dramatic difference between our present climate and the climate of the last interglacial period. Whereas the present interglacial climate seems to have been very stable over the last 10,000 years, the early and late parts of the last interglacial (c.135,000 and c.115,000 years before present, respectively) were characterized by rapid fluctuations between temperatures, both warmer and very much colder than the present. It apparently took only a decade or two to shift between these very different climatic regimes.

Figure 3.16 compares δ^{18}O profiles from Antarctica and Greenland. The dramatic δ-shifts observed in Greenland cores are less pronounced in the δ-record along the Vostok core, probably because the shifts in Greenland are connected to rapid ocean/atmosphere circulation changes in the North Atlantic (for more details, see Sect. 3.12.1).

3.6.3 Groundwater

In temperate and humid climates the isotopic composition of groundwater is similar to that of the precipitation in the area of recharge (Gat 1971). This is strong evidence for direct meteoric recharge to an aquifer. The seasonal variation of all meteoric water is strongly attenuated during transit and storage in the ground. The degree of attenuation varies with depth and with surface and bedrock geologic characteristics,

but in general deep groundwaters show no seasonal variation in δD and $\delta^{18}O$-values and have an isotopic composition close to amount-weighted mean annual precipitation values.

The characteristic isotope fingerprint of precipitation provides an effective means for identifying possible groundwater recharge areas and hence subsurface flow paths. For example, in areas close to rivers fed from high altitudes, groundwaters represent a mixture of local precipitation and high-altitude low-^{18}O waters. In suitable cases, quantitative estimates about the fraction of low-^{18}O river water in the groundwater can be carried out as a function of the distance from the river.

The main mechanisms that can cause variations between precipitation and recharged groundwater are (Gat 1971):

(1) Recharge from partially evaporated surface water bodies
(2) Recharge that occurred in past periods of different climate when the isotopic composition of precipitation was different from that at present
(3) Isotope fractionation processes resulting from differential water movement through the soil or the aquifer or due to kinetic or exchange reactions within geologic formations

In semiarid or arid regions, evaporative losses before and during recharge shift the isotopic composition of groundwater toward higher δ-values. Furthermore, transpiration of shallow groundwater through plant leaves may also be an important evaporation process. Detailed studies of soil moisture evaporation have shown that evaporation loss and isotopic enrichment are greatest in the upper part of the soil profile and are most pronounced in unvegetated soils (Welhan 1987). In some arid regions, groundwater may be classified as paleowaters, which were recharged under different meteorological conditions than present in a region today and which imply ages of water of several thousand years. Gat and Issar (1974) have demonstrated that the isotopic composition of such paleowaters can be distinguished from more recently recharged groundwaters, which have been experienced some evaporation.

In summary, the application of stable isotopes to groundwater studies is based on the fact that the isotopic composition of water behaves conservatively in low-temperature environments where water–rock contact times are short relative to the kinetics of mineral–water isotope exchange reactions.

3.6.4 Isotope Fractionations during Evaporation

In an evaporative environment, one could expect to find extreme enrichments in the heavy isotopes D and ^{18}O. However, this is generally not the case. Taking the Dead Sea as the typical example of an evaporative system, Fig. 3.17 shows only moderately enriched $\delta^{18}O$-values and even to an even lesser degree δD-values (Gat 1984). Isotope fractionations accompanying evaporation are rather complex and can be best described by subdividing the evaporation process into several steps (Craig and Gordon 1965):

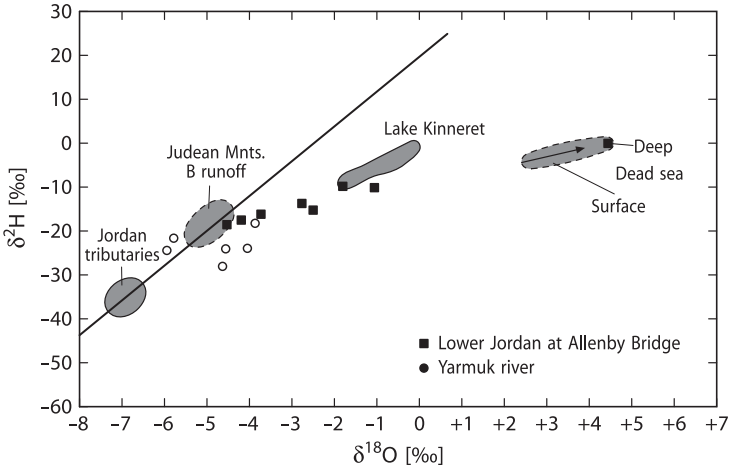

Fig. 3.17 δD vs $\delta^{18}O$ values of the Dead Sea and its water sources as an example of an evaporative environment (after Gat 1984)

(A) The presence of a saturated sublayer of water vapor at the water–atmosphere interface, which is depleted in the heavy isotopes
(B) The migration of vapor away from the boundary layer, which results in further depletion of heavy isotopes in the vapor due to different diffusion rates
(C) The vapor reaching a turbulent region where mixing with vapor from other sources occurs
(D) The vapor of the turbulent zone then condensing and back-reacting with the water surface

This model qualitatively explains the deviation of isotopic compositions away from the "Meteoric Water Line" because molecular diffusion adds a non-equilibrium fractionation term and the limited isotopic enrichment occurs as a consequence of molecular exchange with atmospheric vapor. It is mainly the humidity which controls the degree of isotope enrichment. Only under very arid conditions, and only in small water bodies, really large enrichments in D and ^{18}O are observed. For example, Gonfiantini (1986) reported a $\delta^{18}O$-value of $+31.3‰$ and a δD-value of $+129‰$ for a small, shallow lake in the western Sahara.

3.6.5 Ocean Water

The isotopic composition of ocean water has been discussed in detail by Craig and Gordon (1965), and Broecker (1974). It is governed by fractionation during evaporation and sea-ice formation and by the isotope content of precipitation and runoff entering the ocean.

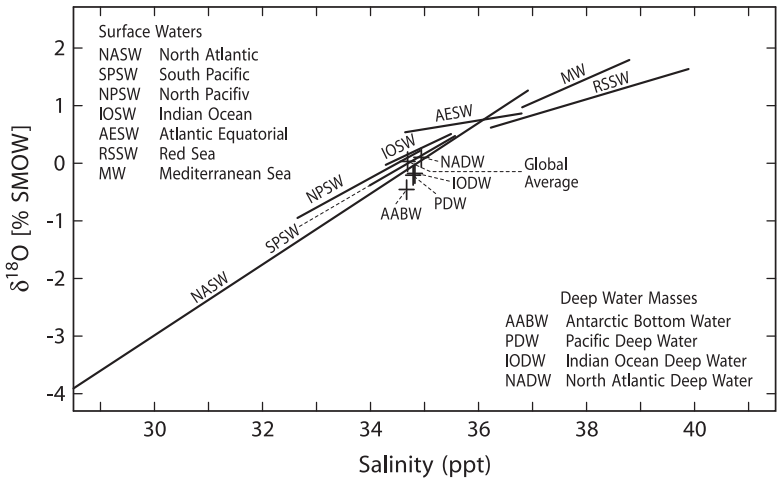

Fig. 3.18 Salinity vs $\delta^{18}O$ relationships in modern ocean surface and deep waters (after Railsback et al. 1989)

Ocean water with 3.5% salinity exhibits a very narrow range in isotopic composition. There is, however, a strong correlation with salinity because evaporation, which increases salinity, also concentrates ^{18}O and D. Low salinities, which are caused by freshwater and melt water dilution, correlate with low D and ^{18}O concentrations. As a consequence modern ocean waters plot along two trends that meet at an inflection point where salinity is 3.55% and $\delta^{18}O$ is 0.5‰ (Fig. 3.18).

The high-salinity trend represents areas where evaporation exceeds precipitation and its slope is determined by the volume and isotopic composition of the local precipitation and the evaporating water vapor. However, isotope enrichments due to evaporation are limited in extent, because of back-exchange of atmospheric moisture with the evaporating fluid. The slope of the low salinity trend (see Fig. 3.18) extrapolates to a freshwater input of about -21‰ for $\delta^{18}O$ at zero salinity, reflecting the influx of high-latitude precipitation and glacial melt water. This δ-value is, in all probability, not typical of freshwater influx in nonglacial periods. Thus, the slope of the low salinity trend may have changed through geologic time.

Delaygue et al. (2000) have modeled the present day ^{18}O distribution in the Atlantic and Pacific Ocean and its relationship with salinity (see Fig. 3.19). A good agreement is found between observed and simulated $\delta^{18}O$-values using an oceanic circulation model. As shown in Fig. 3.19 the Atlantic Ocean is enriched by more than 0.5‰ relative to the Pacific Ocean, but both ocean basins show the same general patterns with high ^{18}O-values in the subtropics and lower values at high latitudes.

Another important question concerning the isotopic composition of ocean water is how constant its isotopic composition has been throughout geological history. This remains an area of ongoing controversy in stable isotope geochemistry (see

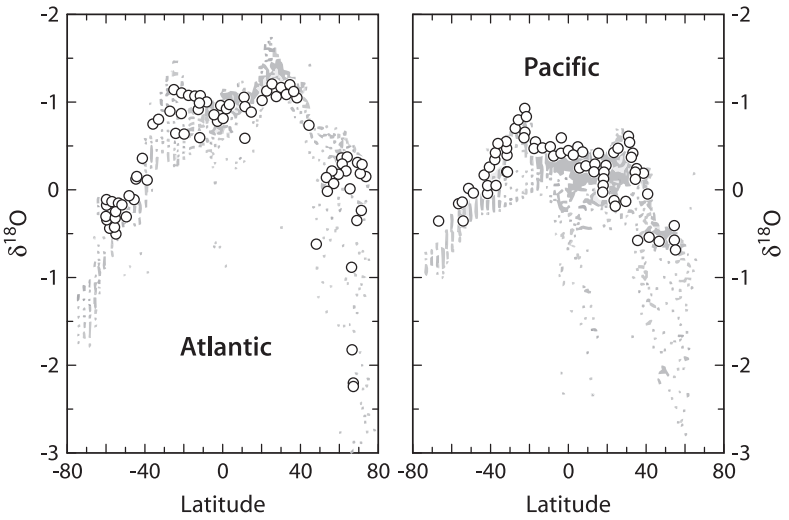

Fig. 3.19 Comparison of measured and modeled $\delta^{18}O$ values of surface ocean waters. Characteristic features are: tropical maxima, equatorial low- and high-latitude minima, enrichment of the Atlantic relative to the Pacific (after Delaygue et al. 2000)

Sect. 3.8). Short-term fluctuations in the isotope composition of sea water must arise during glacial periods. If all the present ice sheets in the world were melted, the $\delta^{18}O$-value of the ocean would be lowered by about 1‰. By contrast, Fairbanks (1989) has calculated an ^{18}O-enrichment of 1.25‰ for ocean water during the last maximum glaciation.

3.6.6 Pore Waters

In the marine environment oxygen and hydrogen isotope compositions of pore waters may be inherited from ocean water or influenced by diagenetic reactions in the sediment or underlying basement. Knowledge of the chemical composition of sedimentary pore waters has increased considerably since the beginning of the Deep-Sea-Drilling-Project. From numerous drill sites, similar depth-dependent trends in the isotopic composition have been observed.

For oxygen this means a decrease in ^{18}O from an initial δ-value very near 0‰ (ocean water) to about −2‰ at depths around 200 m (Perry et al. 1976; Lawrence and Gieskes 1981; Brumsack et al. 1992). Even lower $\delta^{18}O$-values of about −4‰ at depths of around 400 m have been observed by Matsumoto (1992). This decrease in ^{18}O is mainly due to the formation of authigenic ^{18}O-enriched clay minerals such as smectite from alteration of basaltic material and volcanic ash. Other diagenetic reactions include recrystallization of biogenic carbonates, precipitation of

authigenic carbonates and transformation of biogenic silica (opal-A) through opal-CT to quartz. The latter process, however, tends to increase $\delta^{18}O$-values of the water. Material balance calculations by Matsumoto (1992) have indicated that the ^{18}O-shift towards negative δ-values is primarily controlled by low-temperature alteration of basement basalts, which is slightly compensated by the transformation of biogenic opal to quartz.

D/H ratios may also serve as tracers of alteration reactions. Alteration of basaltic material and volcanic ash should increase δD-values of pore waters because the hydroxyl groups in clay minerals incorporate the light hydrogen isotope relative to water. However, measured δD-values of pore waters generally decrease from sea water values around 0‰ at the core tops to values that are 15–25‰ lower, with a good correlation between δD and $\delta^{18}O$. This strong covariation suggests that the same process is responsible for the D and ^{18}O depletion observed in many cores recovered during DSDP/ODP drilling. Quite a different process has been suggested by Lawrence and Taviani (1988) to explain the depth-dependent decrease in pore-water δD-values. They proposed oxidation of local organic matter or oxidation of biogenic or mantle methane. Lawrence and Taviani (1988) favored the oxidation of mantle methane, or even hydrogen, noting that oxidation of locally derived organic compounds may not be feasible because of the excessive quantity of organic material required. In conclusion, the depletion of D in porewaters is not clearly understood.

3.6.7 Formation Water

Formation waters are saline with salt contents ranging from ocean water to very dense Ca–Na–Cl brines. Their origin and evolution are still controversial, because the processes involved in the development of saline formation waters are complicated by the extensive changes that have taken place in the brines after sediment deposition.

Oxygen and hydrogen isotopes are a powerful tool in the study of the origin of subsurface waters. Prior to the use of isotopes, it was generally assumed that most of the formation waters in marine sedimentary rocks were of connate marine origin. This widely held view was challenged by Clayton et al. (1966), who demonstrated that waters from several sedimentary basins were predominantly of local meteoric origin.

Although formation waters show a wide range in isotopic composition, waters within a sedimentary basin are usually isotopically distinct. As is the case with surface meteoric waters, there is a general decrease in isotopic composition from low to high latitude settings (Fig. 3.20). Displacements of δD and $\delta^{18}O$-values from the Meteoric Water Line (MWL) are very often correlated with salinity: the most depleted waters in D and ^{18}O are usually the least saline, fluids most distant from the MWL tend to be the most saline.

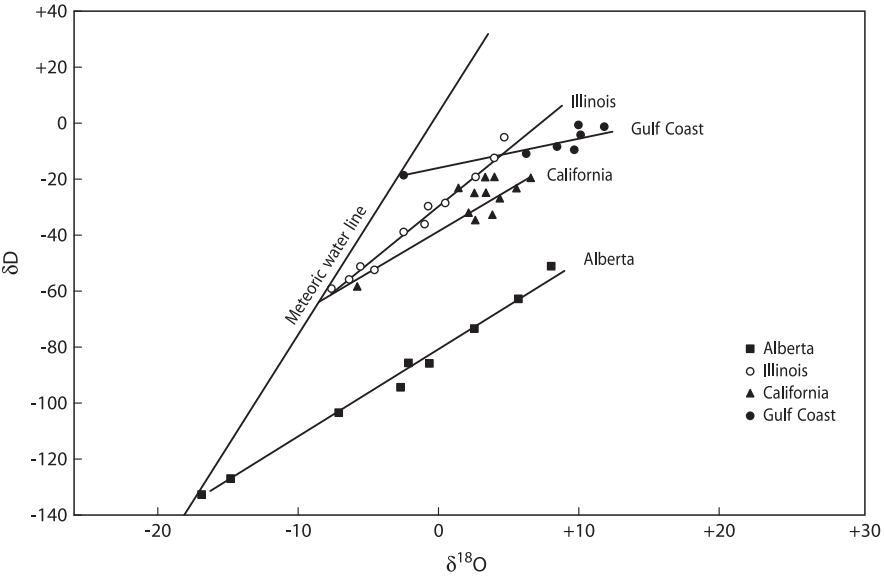

Fig. 3.20 δD vs $\delta^{18}O$ values for formation waters from the midcontinental region of the United States (after Taylor 1974)

Presently, in the view of numerous subsequent studies, (i.e., Hitchon and Friedman 1969; Kharaka et al. 1974; Banner et al. 1989; Connolly et al. 1990; Stueber and Walter 1991), it is obvious that basin subsurface waters have complicated histories and frequently are mixtures of waters with different origins. As was proposed by Knauth and Beeunas (1986) and Knauth (1988), formation waters in sedimentary basins may not require complete flushing by meteoric water, but instead can result from mixing between meteoric water and the remnants of original connate waters.

The characteristic $\delta^{18}O$ shift observed in formation waters may be due to isotopic exchange with ^{18}O-rich sedimentary minerals, particularly carbonates. The δD-shift is less well understood, possible mechanisms for D-enrichment are (1) fractionation during membrane filtration, and/or (2) exchange with H_2S, hydrocarbons and hydrous minerals. (1) It is well known that shales and compacted clays can act as semipermeable membranes which prevent passage of ions in solution while allowing passage of water (ultrafiltration). Coplen and Hanshaw (1973) have shown experimentally that ultrafiltration may be accompanied by hydrogen and oxygen isotope fractionation. However, the mechanism responsible for isotopic fractionation is poorly understood. Phillips and Bentley (1987) proposed that fractionation may result from increased activity of the heavy isotopes in the membrane solution, because high cation concentrations increase hydration sphere fractionation effects. (2) Hydrogen isotope exchange between H_2S and water will occur in nature, but probably will not be quantitatively important. Due to the large fractionation factor between H_2S and H_2O, this process might be significant on a local scale. Isotope exchange with methane or higher hydrocarbons will probably not be important, because exchange rates are extremely low at sedimentary temperatures.

Somewhat unusual isotopic compositions have been observed in highly saline deep waters from Precambrian crystalline rocks as well as in deep drill holes, which plot above or to the left of the Meteoric Water Line (Frape et al. 1984; Kelly et al. 1986; Frape and Fritz 1987). There are two major theories about the origin of these Ca-rich brines:

(A) The brines represent modified Paleozoic sea water or basinal brines (Kelly et al. 1986)
(B) The brines are produced by leaching of saline fluid inclusions in crystalline rocks or by intense water/rock interactions (Frape and Fritz 1987)

Since then quite a number of studies have indicated that the unusual composition is a wide-spread phenomenon in low-permeability fractured rocks with slow water movement and not too high temperatures. Kloppmann et al. (2002) summarized the existing data base of 1,300 oxygen and hydrogen isotope analyses from crystalline rocks and suggested that the isotope shift to the left side can be explained by sea water which has dissolved and precipitated fracture minerals and subsequently been diluted by meteoric waters. Bottomley et al. (1999) argued that the extremely high concentrations of chloride and bromide in the brines make crystalline host rocks a less likely source for the high salinities. By measuring Li-isotopes these authors postulated that the brines in crystalline rocks share a common marine origin.

3.6.8 Water in Hydrated Salt Minerals

Many salt minerals have water of crystallization in their crystal structure. Such water of hydration can provide information on the isotope compositions and/or temperatures of brines from which the minerals were deposited. To interpret such isotope data, it is necessary to know the fractionation factors between the hydration water and the solution from which they are deposited. Several experimental studies have been made to determine these fractionation factors (Matsuo et al. 1972; Matsubaya and Sakai 1973; Stewart 1974; Horita 1989). Because most saline minerals equilibrate only with highly saline solutions, the isotopic activity and isotopic concentration ratio of water in the solution are not the same (Sofer and Gat 1972). Most studies determined the isotopic concentration ratios of the source solution and as Horita (1989) demonstrated, these fractionation factors have to be corrected using the "salt effect" coefficients when applied to natural settings (Table 3.2).

3.7 The Isotopic Composition of Dissolved and Particulate Compounds in Ocean and Fresh Waters

The following section will discuss the carbon, nitrogen, oxygen, and sulfur isotope composition of dissolved and particulate compounds in ocean and fresh waters. The isotopic compositions of dissolved components in waters of different origins depend

Table 3.2 Experimentally determined fractionation factors of salt minerals and their corrections using "salt effect" coefficients (after Horita 1989)

Mineral	Chemical formula	T°C	αD	$\alpha D_{(corr)}$	$\alpha^{18}O$	$\alpha^{18}O_{(corr)}$
Borax	$Na_2B_4O_7 \times 10H_2O$	25	1.005	1.005		
Epsomite	$MgSO_4 \times 7H_2O$	25	0.999	0.982		
Gaylussite	$Na_2CO_3 \times CaCO_3 \times 5H_2O$	25	0.987	0.966		
Gypsum	$CaSO_4 \times 2H_2O$	25	0.980	0.980	1.0041	1.0041
Mirabilite	$Na_2SO_4 \times 10H_2O$	25	1.017	1.018	1.0014	1.0014
Natron	$Na_2CO_3 \times 10H_2O$	10	1.017	1.012		
Trona	$Na_2CO_3 \times NaHCO_3 \times 2H_2O$	25	0.921	0.905		

on a variety of processes such as the composition of the minerals which have been dissolved during weathering, the inorganic or organic nature of the precipitation process, and exchange with atmospheric gases. Of special importance are biological processes acting mainly in surface waters, which tend to deplete certain elements such as carbon, nitrogen, and silicon in surface waters by biological uptake, and which subsequently are returned at depth by oxidation and dissolution processes.

3.7.1 Carbon Species in Water

3.7.1.1 Bicarbonate in Ocean Water

In addition to organic carbon, four other carbon species exist in natural water: dissolved CO_2, H_2CO_3, HCO_3^- and CO_3^{2-}, all of which tend to equilibrate as a function of temperature and pH. HCO_3^- is the dominant C-bearing species in ocean water. The first global measurements of dissolved inorganic carbon (DIC) $\delta^{13}C$-values were published by Kroopnick et al. (1972) and Kroopnick (1985) within the geochemical ocean sections study (GEOSECS). These studies have yielded a global average $\delta^{13}C$-value of 1.5‰ with a variation range of ± 0.8‰ with the least variations at equatorial regions and greater variability at higher latitudes.

The distribution of $\delta^{13}C$-values with water depth is mainly controlled by biological processes: Conversion of CO_2 into organic matter removes ^{12}C resulting in a ^{13}C enrichment of the residual DIC. In turn, the oxidation of organic matter releases ^{12}C-enriched carbon back into the inorganic reservoir, which results into a depth-dependent isotope profile. A typical example is shown in Fig. 3.21.

North Atlantic Deep Water (NADW), which is formed with an initial $\delta^{13}C$-value between 1.0 and 1.5‰, becomes gradually depleted in ^{13}C as it travels southward and mixes with Antarctic bottom water, which has an average $\delta^{13}C$-value of 0.3‰ (Kroopnick 1985). As this deep water travels to the Pacific Ocean, its $^{13}C/^{12}C$ ratio is further reduced by 0.5‰ by the continuous flux and oxidation of organic matter in the water column. This is the basis for using $\delta^{13}C$-values as a tracer of paleooceanographic changes in deep water circulation (e.g., Curry et al. 1988).

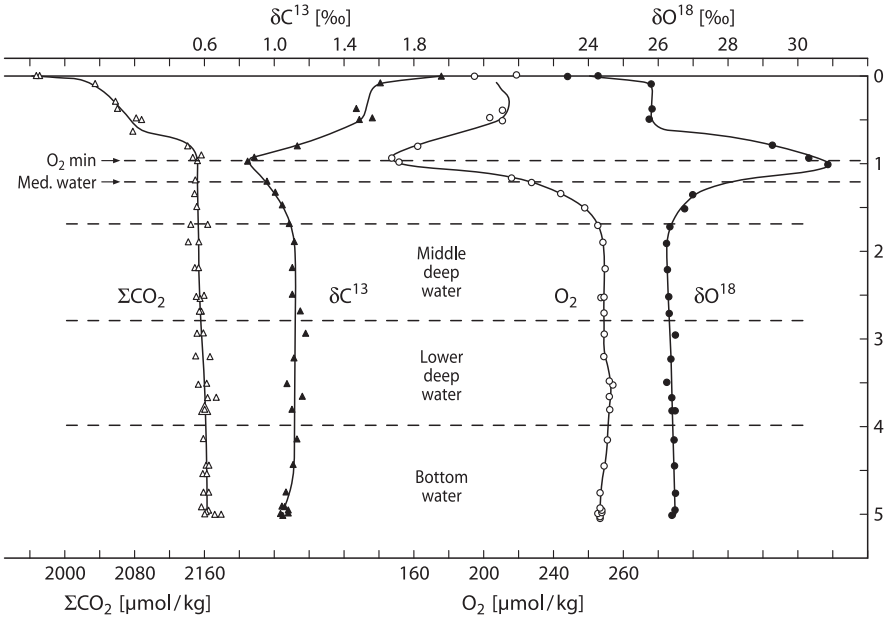

Fig. 3.21 Vertical profiles of dissolved CO_2, $\delta^{13}C$, dissolved O_2 and $\delta^{18}O$ in the North Atlantic (Kroopnick et al. 1972)

The uptake of anthropogenic CO_2 by the ocean is a crucial process for the carbon cycle, resulting in changes of the $\delta^{13}C$-value of dissolved oceanic bicarbonate (Quay et al. 1992; Bacastow et al. 1996; Gruber 1998; Gruber et al. 1999; Sonnerup et al. 1999). Quay et al. (1992) first demonstrated that the $\delta^{13}C$-value of dissolved bicarbonate in the surface waters of the Pacific has decreased by about 0.4‰ between 1970 and 1990. If this number is valid for the ocean as a whole, it would allow a quantitative estimate for the net sink of anthropogenically produced CO_2. Recent accounts estimate that the Earth's ocean has absorbed around 50% of the CO_2 emitted over the industrial period (Mikaloff-Fletcher et al. 2006).

3.7.1.2 Particulate Organic Matter (POM)

Particulate organic matter (POM) in the ocean originates largely from plankton in the euphotic zone and reflects living plankton populations. Between 40°N and 40°S $\delta^{13}C$ of POM varies between -18.5 and -22‰. In cold Arctic waters $\delta^{13}C$-values are on average -23.4‰ and in high latitude southern ocean $\delta^{13}C$ are even lower with values between -24 and -36‰ (Goericke and Fry 1994). As POM sinks, biological reworking changes its chemical composition, the extent of this reworking depends on the residence time in the water column. Most POM profiles described in the literature exhibit a general trend of surface isotopic values comparable to those for living plankton, with $\delta^{13}C$-values becoming increasingly lower with depth.

Jeffrey et al. (1983) interpreted this trend as the loss of labile, ^{13}C-enriched amino acids and sugars through biological reworking which leaves behind the more refractory, isotopically light lipid components.

C/N ratios of POM increase with depth of the water column consistent with preferential loss of amino acids. This implies that nitrogen is more rapidly lost than carbon during degradation of POM, which is the reason for the much greater variation in $\delta^{15}N$-values than in $\delta^{13}C$-values (Saino and Hattori 1980; Altabet and McCarthy 1985).

3.7.1.3 Carbon Isotope Composition of Pore Waters

Initially the pore water at the sediment/water interface has a $\delta^{13}C$-value near that of sea water. In sediments, the decomposition of organic matter consumes oxygen and releases isotopically light CO_2 to the pore water, while the dissolution of $CaCO_3$ adds CO_2 that is isotopically heavy. The carbon isotope composition of pore waters at a given locality and depth should reflect modification by the interplay of these two processes. The net result is to make porewaters isotopically lighter than the overlying bottom water (Grossman 1984). McCorkle et al. (1985) and McCorkle and Emerson (1988) have shown that steep gradients in porewater $\delta^{13}C$-values exist in the first few centimeters below the sediment–water interface. The observed $\delta^{13}C$-profiles vary systematically with the "rain" of organic matter to the sea floor, with higher carbon rain rates resulting in isotopically lower $\delta^{13}C$-values (Fig. 3.22).

One would expect that pore waters would have $^{13}C/^{12}C$ ratios no lower than organic matter. However, a more complex situation is actually observed due to bacterial methanogenesis. Bacterial methane production generally follows sulfate

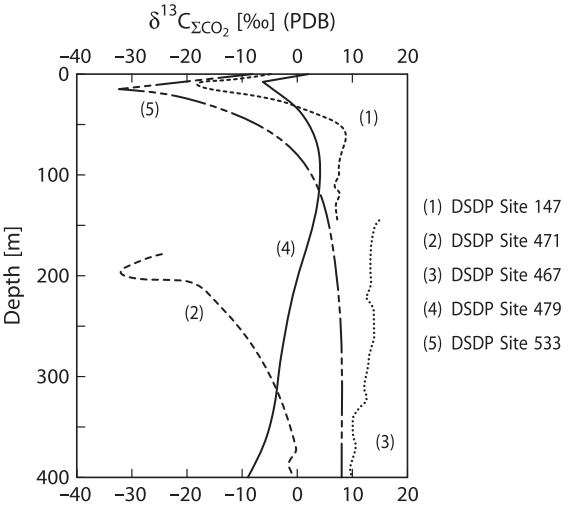

Fig. 3.22 $\delta^{13}C$ records ot total dissolved CO_2 from pore waters of anoxic sediments recovered in various DSDP sites (after Anderson and Arthur 1983)

reduction in anaerobic carbon-rich sediments, the two microbiological environments being distinct from one another, except for substrate-rich sections. Since methane-producing bacteria produce very ^{12}C-rich methane, the residual pore water can become significantly enriched in ^{13}C as shown in some profiles in Fig. 3.22.

3.7.1.4 Carbon in Fresh Waters

Dissolved carbonate in fresh waters may exhibit an extremely variable isotopic composition, because it represents varying mixtures of carbonate species derived from weathering of carbonates and that originating from biogenic sources like freshwater plankton or CO_2 from bacterial oxidation of organic matter in the water column or in soils (Hitchon and Krouse 1972; Longinelli and Edmond 1983; Pawellek and Veizer 1994; Cameron et al. 1995).

Although the CO_2 partial pressures in rivers vary widely, studies of major rivers often show that CO_2 concentrations are about 10–15 times greater than expected for equilibrium conditions with the atmosphere. Rivers thus are actively degassing CO_2 into the atmosphere, affecting the natural carbon cycle. This explains an increased interest in analyzing river systems for their carbon isotope composition. Despite the fact that the carbon isotopic compositions of carbonate minerals and of soil–CO_2 are distinctive, the observed $\delta^{13}C$-variations of dissolved inorganic carbon are often not easy to interpret, because riverine respiration and exchange processes with atmospheric CO_2 play a role. Figure 3.23 gives some examples where carbon sources can be clearly identified. In the Amazon dissolved CO_2 originates from decomposition of organic matter (Longinelli and Edmond 1983) whereas in the St. Lawrence river system CO_2 Originates from the dissolution of carbonates and equilibration with the atmosphere (Yang et al. 1996). The Rhine represents a mixture of both sources (Buhl et al. 1991).

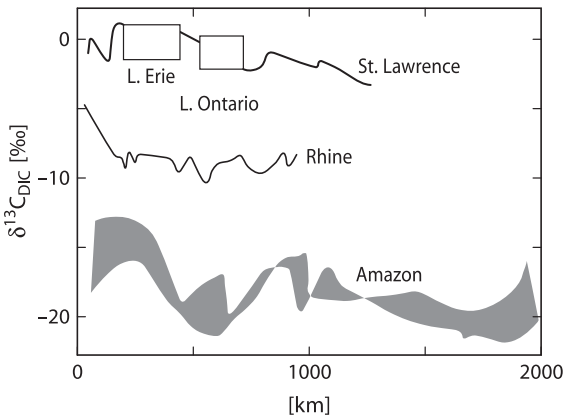

Fig. 3.23 Carbon isotopic composition of total dissolved carbon in some large river systems. Data source: Amazon: Longinelli and Edmond (1983), Rhine: Buhl et al. (1991), St Lawrence: Yang et al. (1996)

In river systems often a progressive ^{13}C enrichment is observed from upstream to downstream due to enhanced isotopic exchange with atmospheric CO_2 and/or in situ photosynthetic activity (Telmer and Veizer 1999). Variable seasonal signals can be explained by changes in the oxidation rate of ^{13}C-depleted organic matter from the soils in watersheds. Rivers that are characterized by the presence of large lakes at their head – like the Rhone and St. Lawrence – show heavy ^{13}C-values at their head (Ancour et al. 1999; Yang et al. 1996). Due to the long residence time of dissolved carbon in lakes, the bicarbonate is in near equilibrium with atmospheric CO_2.

3.7.1.5 Silicon

Silicon isotope variations in the ocean are caused by biological Si-uptake through siliceous organisms like diatoms. Insofar strong similarities exist with C-isotope variations. Diatoms preferentially incorporate ^{28}Si as they form biogenic silica. Thus, high $\delta^{30}Si$ values in surface waters go parallel with low Si-concentrations and depend on differences in silicon surface water productivity. In deeper waters dissolution of sinking silica particles causes an increase in Si concentration and a decrease of $\delta^{30}Si$-values.

3.7.2 Nitrogen

Nitrogen is one of the limiting nutrients in the ocean. Apparently, the rate of nitrate formation is so slow, and marine denitrification so rapid, that nitrate is in short supply. Dissolved nitrogen is subject to isotope fractionation during microbial processes and during biological uptake. Nitrate dissolved in oceanic deep waters has a $\delta^{15}N$-value of 6–8‰ (Cline and Kaplan 1975; Wada and Hattori 1976). Denitrification seems to be the principal mechanism that keeps marine nitrogen at higher $\delta^{15}N$-values than atmospheric nitrogen.

The $\delta^{15}N$-value of particulate material was originally thought to be determined by the relative quantities of marine and terrestrial organic matter. However, temporal variations in the ^{15}N-content of particulate matter predominate and obscure N-isotopic differences previously used to distinguish terrestrial from marine organic matter. Altabet and Deuser (1985) observed seasonal variations in particles sinking to the ocean bottom and suggested that $\delta^{15}N$-values of sinking particles represent a monitor for nitrate flux in the euphotic zone. Natural ^{15}N-variations can thus provide information about the vertical structure of nitrogen cycling in the ocean.

Saino and Hattori (1980) first observed distinct vertical changes in the ^{15}N content of suspended particulate nitrogen and related these changes to particle diagenesis. A sharp increase in ^{15}N below the base of the euphotic zone has been ubiquitously observed (Altabet and McCarthy 1985; Saino and Hattori 1987; Altabet 1988). These findings imply that the vertical transport of organic matter is

mediated primarily by rapidly sinking particles and that most of the decomposition of organic matter takes place in the shallow layer beneath the bottom of the euphotic zone.

3.7.3 Oxygen

As early as 1951, Rakestraw et al. demonstrated that dissolved O_2 in the oceans is enriched in ^{18}O relative to atmospheric oxygen. Like its concentration, the $\delta^{18}O$ of dissolved oxygen is affected by three processes: air–water gas exchange, respiration and photosynthesis. When gas exchange dominates over photosynthesis and respiration as in the surface ocean dissolved oxygen is close to saturation and the $\delta^{18}O$ is $\sim$24.2‰, because there is a 0.7‰ equilibrium fractionation during gas dissolution (Quay et al. 1993). Extreme enrichments up to 14‰ (Kroopnick and Craig 1972) occur in the oxygen minimum region of the deep ocean due to preferential consumption of ^{16}O by bacteria in abyssal ocean waters, which is evidence for a deep metabolism (see Fig. 3.21).

Quay et al. (1995) measured $^{18}O/^{16}O$ ratios of dissolved oxygen in rivers and lakes of the Amazon Basin. They observed a large $\delta^{18}O$ range from 15 to 30‰. When respiration dominates over photosynthesis in fresh waters, dissolved O_2 will be undersaturated and $\delta^{18}O$ is > 24.2‰; when photosynthesis exceeds respiration, dissolved O_2 will be supersaturated and $\delta^{18}O$ will be <24.2‰.

3.7.4 Sulfate

Modern ocean water sulfate has a fairly constant $\delta^{34}S$-value of 21‰ (Rees et al. 1978) and $\delta^{18}O$-value of 9.6‰ (Lloyd 1967, 1968; Longinelli and Craig 1967). From theoretical calculations of Urey (1947), it is quite clear that the $\delta^{18}O$-value of dissolved sulfate does not represent equilibrium with $\delta^{18}O$-value of the water. Under surface conditions oxygen isotope exchange of sulfate with ambient water is extremely slow (Chiba and Sakai 1985). Lloyd (1967, 1968) proposed a model in which the fast bacterial turnover of sulfate at the sea bottom determines the oxygen isotope composition of dissolved sulfate. Böttcher et al. (2001), Aharon and Fu (2000, 2003) and others demonstrated that the $\delta^{18}O$ of sulfate is not only influenced by microbial sulfate reduction, but also by disproportionation and reoxidation of reduced sulfur compounds. In marine pore waters ^{18}O-enrichments up to 17‰ have been observed, generally associated with a concurrent ^{34}S enrichment. By plotting $\delta^{18}O_{(SO4)}$ vs. $\delta^{34}S_{(SO4)}$ two different slopes can be distinguished, which have been modeled by Böttcher et al. (1998) and by Brunner et al. (2005): (1) a model that postulates the predominance of kinetic oxygen isotope fractionation steps linked to different sulfate reduction steps and (2) a model postulating a

predominance of oxygen isotope exchange between cell-internal sulfur compounds and ambient water (Brunner et al. 2005; Wortmann et al. 2007).

In freshwater environments, the sulfur and oxygen isotope composition of dissolved sulfate is much more variable and potentially the isotope ratios can be used to identify the sources. However, such attempts have been only partially successful because of the variable composition of the different sources. δ^{34}S-values of dissolved sulfate of different rivers and lakes show a rather large spread as is demonstrated in Fig. 3.24. The data of Hitchon and Krouse (1972) for water samples from the MacKenzie River drainage system exhibit a wide range of δ^{34}S-values reflecting contributions from marine evaporites and shales. In a recent study, Calmels et al. (2007) argue that around 85% of the sulfate in the MacKenzie river is derived from pyrite oxidation and not from sedimentary sulfate. For the Amazon River, Longinelli and Edmond (1983) found a very narrow range in δ^{34}S-values which they interpreted as representing a dominant Andean source for sulfate from the dissolution of Permian evaporites with a lesser admixture of sulfide sulfur. Rabinovich and Grinenko (1979) reported time-series measurements for the large European and Asian rivers in Russia. The sulfur in the European river systems should be dominated by anthropogenically derived sources, which in general have δ^{34}S-values between 2 and 6‰.

A special case represents acid sulfate waters released from mines where metal sulfide ores and lignite have been exploited. S- and O-isotope data may define the conditions and processes of pyrite oxidation, such as the presence or absence of dissolved oxygen and the role of sulfur-oxidizing bacteria (i.e. Taylor and Wheeler 1994).

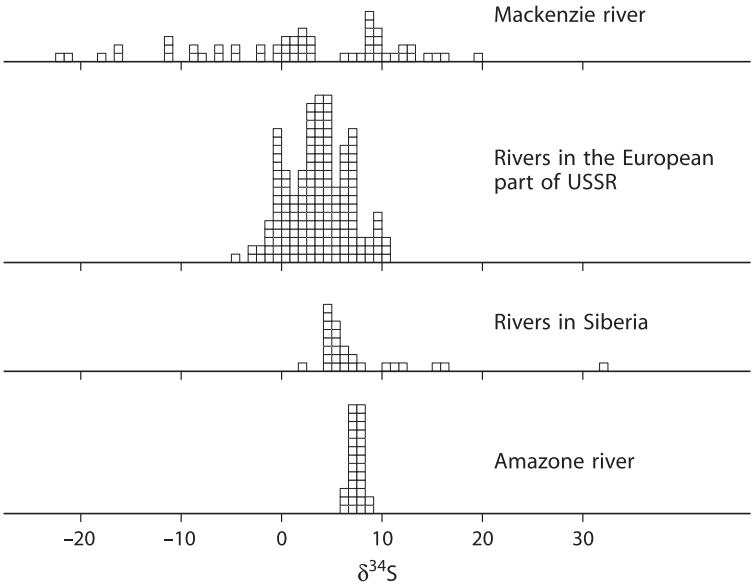

Fig. 3.24 Frequency distribution of δ^{34}S values in river sulfate

The oxygen isotope composition of freshwater sulfate can be highly variable too. Cortecci and Longinelli (1970) and Longinelli and Bartelloni (1978) observed a range in δ^{18}O-values from 5 to 19‰ in rainwater samples from Italy and postulated that most of the sulfate is not oceanic in origin, but rather produced by oxidation of sulfur during the burning of fossil fuels. The oxidation of reduced sulfur to sulfate is a complex process which involves chemical and microbiological aspects. Two general pathways of oxidation have been suggested: (1) oxidation by molecular oxygen and (2) oxidation by ferric iron plus surface water.

3.8 Isotopic Composition of the Ocean during Geologic History

The growing concern with respect to "global change" brings with it the obvious need to document and understand the geologic history of sea water. From paleoecological studies, it can be deduced that ocean water should not have changed its chemical composition very drastically, since marine organisms can only tolerate relatively small chemical changes in their marine environment. The similarity of the mineralogy and to some extent paleontology of sedimentary rocks during the Earth's history strengthens the conclusion that the chemical composition of ocean water has not varied substantially. This was the general view for many years. More recently, fluid inclusions in evaporate minerals have indicated that the concentrations of major ions in ocean water such as Ca, Mg, and SO_4 have changed significantly over the Phanerozoic (Horita et al. 2002b and others). It is, thus, likely that the input fluxes to the oceans and the output fluxes are not always equal during Earth's history. The rapidity which changes in ocean chemistry might occur is dictated by the residence time of ions in the ocean.

One of the most sensitive tracers recording the composition of ancient sea water is the isotopic composition of chemical sediments precipitated from sea water. The following discussion concentrates on the stable isotope composition of oxygen, carbon, and sulfur, but in recent years other isotope systems have been included such as Ca (De La Rocha and De Paolo 2000; Schmitt et al. 2003; Fantle and de Paolo 2005; Farkas et al. 2007) and B (Lemarchand et al. 2000, 2002; Joachimski et al. 2005) and Li (Hoefs and Sywall 1997). One of the fundamental questions in all these approaches is which kind of sample provides the necessary information, in the sense that it represents the ocean water composition at its time of formation and has not been modified subsequently by diagenetic reactions.

3.8.1 Oxygen

It is generally agreed that continental glaciation and deglaciation induce changes in the δ^{18}O-value of the ocean on short time scales. There is, however, considerable debate about long-term changes.

The present ocean is depleted in ^{18}O by at least 6‰ relative to the total reservoir of oxygen in the crust and mantle. Muehlenbachs and Clayton (1976) presented a model in which the isotopic composition of ocean water is held constant by two different processes: (1) low temperature weathering of oceanic crust which depletes ocean water in ^{18}O, because ^{18}O is preferentially bound in weathering products and (2) high-temperature hydrothermal alteration of ocean ridge basalts which enriches ocean water in ^{18}O, because ^{16}O is preferentially incorporated into the solid phase during the hydrothermal alteration of oceanic crust. If sea floor-spreading ceased, or its rate were to decline, the $\delta^{18}O$-value of the oceans would slowly change to lower values because of continued continental and submarine weathering. Gregory and Taylor (1981) presented further evidence for this rock/water buffering and argued that the $\delta^{18}O$ of sea water should be invariant within about ± 1‰, as long as sea-floor spreading was operating at a rate of at least 50% of its modern value.

The sedimentary record, however, is not in accord with this model for constant oxygen isotope compositions because in a general way carbonates, cherts, and phosphates show a decrease in $\delta^{18}O$ in progressively older samples (Veizer and Hoefs 1976; Knauth and Lowe 1978; Shemesh et al. 1983). The prime issue arising from these trends is whether they are of primary or secondary (post-depositional) origin. Veizer et al. (1997, 1999) presented a strong evidence that they are, at least partly, of primary origin. Based on well-selected Phanerozoic low-Mg calcite shells (mostly brachiopods), they observed a 5‰ decline from the Quaternary to the Cambrian. Because well-preserved textures and trace element contents are comparable to modern low-Mg calcitic shells, Veizer and coworkers argue that the shells reflect the primary oxygen isotope composition of the ocean at the time the shells have been formed. Prokoph et al. (2008) provided on updated compilation of 39,000 $\delta^{18}O$- and $\delta^{13}C$-isotope data for the entire earth history confirming earlier observation of Veizer and coworkers.

Jaffres et al. (2007) reviewed models of how the long-term trends in $\delta^{18}O$ can be influenced by varying chemical weathering and hydrothermal circulation rates. These authors argued that sea water $\delta^{18}O$-values increased from -13.3 to -0.3‰ over a period of 3.4 Ga (see Fig. 3.25) with ocean surface temperatures fluctuating between 10 and 33°C. The most likely explanation for the long-term trend in sea water $\delta^{18}O$ involves stepwise increases in the ratio of high- to low-temperature fluid/rock interactions. Presumably, global changes in spreading rate will affect $\delta^{18}O$ of the oceans, albeit by a smaller amount. Model calculations on the geological water cycle by Wallmann (2001) support the idea that sea water $\delta^{18}O$-values are not constant through time, but evolved from an ^{18}O-depleted state to the current value. Kasting et al. (2006) argue that the low $\delta^{18}O$-values during the Precambrian might be a consequence of changes in midocean ridge-crest depth associated with higher heat flow. However, the processes responsible for the ^{18}O changes during Earth's earliest history are presently not fully understood.

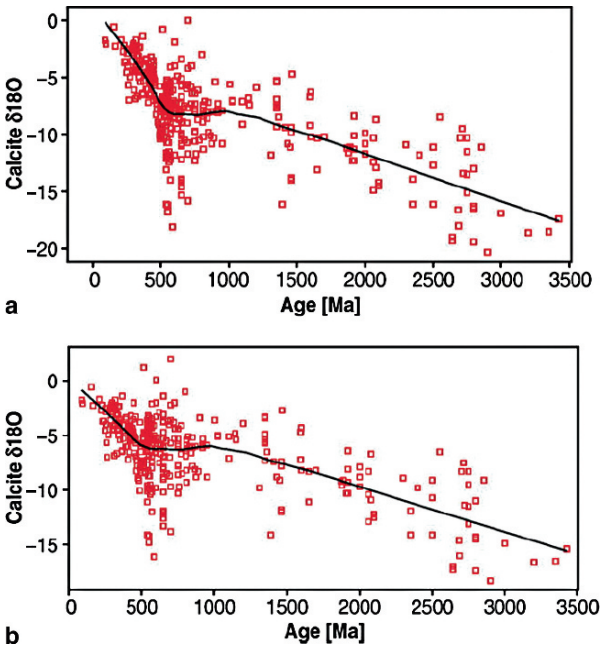

Fig. 3.25 $\delta^{18}O$ data of bulk rock calcite and brachiopods over time for (**a**) measured and (**b**) shifted values (upward shift of 2‰ for all bulk rock data) (Jaffrés et al. 2007)

3.8.2 Carbon

The ^{13}C content of a marine carbonate is closely related to that of the dissolved marine bicarbonate from which the carbonate precipitated. For a long time the $\delta^{13}C$-value of ancient oceans was regarded as essentially constant around 0‰. Only in the 1980s was it realized that the observed fluctuations represent regular secular variations. Shifts in the carbon isotopic composition of marine carbonates may be interpreted as representing shifts in the amount of organic carbon being buried. An increase in the amount of buried organic carbon means that ^{12}C would be preferentially removed from sea water, so that the ocean reservoir would become isotopically heavier. Negative $\delta^{13}C$-shifts accordingly may indicate a decrease in the rate of carbon burial and/or enhanced oxidative weathering of once buried organic matter.

$\delta^{13}C$-values of limestones vary mostly within a band of 0 ± 3‰ since at least 3.5 Ga (Veizer and Hoefs 1976). The longer term C-isotope trend for carbonates has be punctuated by sudden shifts over short time intervals named "carbon isotope events", which are considered to represent characteristic features, and have been used as time markers for stratigraphic correlations.

Especially noteworthy are very high $\delta^{13}C$-values of up to 10‰ and higher, which have been measured for 2.2–2.0 Ga old carbonates and at the end of the Proterozoic with both periods representing periods of increased burial of organic carbon (Knoll

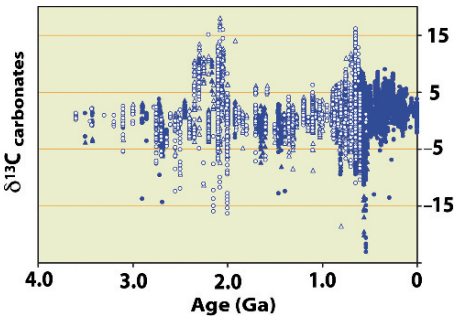

Fig. 3.26 δ^{13}C-values for marine carbonates over time. Note persistent mean values of 0–3‰ and anomaleous variability at 2.3 to 2.0 Ga and 0.8 to 0.6 Ga correlative with snowball earth episodes (Shields and Veizer, 2002)

et al. 1986; Baker and Fallick 1989; Derry et al. 1992, and others). By compiling the database for the Proterozoic, Shields and Veizer (2002) (Fig. 3.26) demonstrated ^{13}C fluctuations of at least 15‰, coincident with wide spread glaciations (see also Special Issue of Chemical Geology 237, No. 1–2, 2007). Highly ^{13}C enriched intervals are related to interglacial times, where the ^{13}C enrichment appears to be the result of unusually efficient burial of organic carbon. Hayes and Waldbauer (2006), on the other hand, interpreted the unusual ^{13}C-enrichment as indicating the importance of methanogenic bacteria in sediments.

Negative δ^{13}C intervals are generally associated with glaciations (Kaufman and Knoll 1995). The most negative ^{13}C-values have been found in massive carbonates that cap glaciogenic sequences ("cap" carbonates), which record the most profound carbon isotope variations on Earth. The change from very heavy to very light δ^{13}C-values has been interpreted by Hoffmann et al. (1998) as a collapse of biological productivity for millions of years due to global glaciations and represents one the central arguments of the "snowball Earth" hypothesis. Glaciations ended abruptly when subaerial volcanic outgassing raised atmospheric CO_2 to very high levels shifting the ^{13}C of carbonates to values around −5‰.

Because of the relationship between carbonate and organic carbon, a parallel shift in the isotope composition of both carbon reservoirs should be observed. Unfortunately, very often carbonate–carbon and organic carbon have not been investigated together. Hayes et al. (1999) have compiled the existing data base on both reservoirs. In contrast to previous assumptions, the long-term fractionation is invariant and its average close to 30‰ rather than 25‰. Variations in the fractionations between the two reservoirs can, in principle, be interpreted as reflecting variations in the pCO_2 content of the atmosphere (Kump and Arthur 1999). By employing a simple model which is subjected to different perturbations each lasting 500,000 years, Kump and Arthur (1999) demonstrated that increased burial of organic carbon leads to a fall in atmospheric pCO_2 and to positive ^{13}C-shifts in both carbonate and organic carbon. Lately, shifts in ^{13}C have been correlated to variations in the O_2/CO_2 ratio of the ambient atmosphere (Strauss and Peters-Kottig 2003).

3.8.3 Sulfur

Because isotope fractionation between dissolved sulfate in ocean water and gypsum/anhydrite is negligible (Raab and Spiro 1991), evaporite sulfates should closely reflect the sulfur isotope composition of marine sulfate through time. The first S-isotope "age curves" were published by Nielsen and Ricke (1964) and Thode and Monster (1964). Since then, this curve has been updated by many more analyses (Holser and Kaplan 1966; Holser 1977; Claypool et al. 1980). The sulfur isotope curve varies from a maximum of $\delta^{34}S = +30‰$ in early Paleozoic time, to a minimum of $+10‰$ in Permian time. These shifts are considered to reflect net fluxes of isotopically light sulfur generated during bacterial reduction of oceanic sulfate to the reservoir of reduced sulfide in sediments, thus increasing the ^{34}S-content in the remaining oceanic sulfate reservoir. Conversely, a net return flux of the light sulfide to the ocean during weathering decreases marine sulfate $\delta^{34}S$-values. Modeling by Strauss (1997, 1999) has indicated that pyrite burial was twice as large as today during most of the early Paleozoic followed by a decrease to values that are about half of today's rate during the Carboniferous and Permian and by approximately constant rates for the last 180 Ma.

Since evaporites through geologic time contain large gaps and considerable scatter in sulfur isotope composition, two alternative approaches for the reconstruction of sea water $\delta^{34}S$-values through time have been utilized: (1) structurally substituted sulfate in marine carbonates (Burdett et al. 1989; Kampschulte and Strauss 2004). This approach avoids apparent disadvantages of the evaporite record namely that evaporites are discontinuous with a poor age resolution. Hence, a much better temporal resolution has been obtained. (2) Marine barite in pelagic sediments. Paytan et al. (1998, 2004) generated a sea water sulfur curve for the Cenozoic and for the Cretaceous with a resolution of $\sim$1 million years. Barite has advantages over the other two sulfate proxies, because of its resistance to diagenesis (see Fig. 3.27).

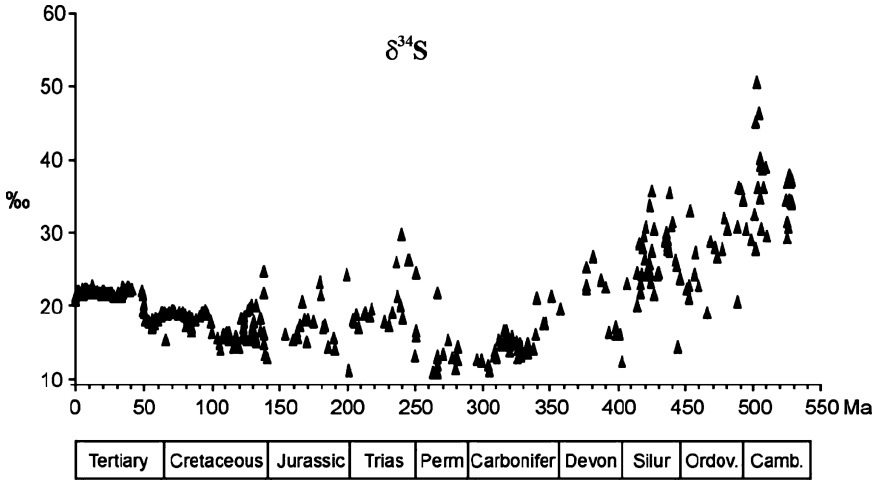

Fig. 3.27 $\delta^{34}S$ data of structurally substituted sulfur in carbonate and in barite vs time (Prokoph et al. 2008)

The oxygen isotope composition of marine barite might be also a useful tracer for the sulfate cycle in the past. Turchyn and Schrag (2004) observed a 5‰ variability in $\delta^{18}O$ over the past 10 million years. Oxygen is incorporated into sulfate through sulfide oxidation and released through sulfate reduction. Turchyn and Schrag (2004) suggested that sea level fluctuations reducing the area of continental shelves and increasing sulfide weathering may be responsible for the observed variations.

It might be expected that a parallel age curve to that for sulfates should exist for sedimentary sulfides. However, the available S-isotope data for sulfides range widely and seem to depend strongly on the degree to which the reduction system is "open" and on the sedimentation rate so that age trends are obscured (Strauß 1997, 1999). The large variability in $\delta^{34}S_{sulfide}$-values within age-equivalent strata might be best explained by time-dependent steps of pyrite formation during progressive diagnesis.

Accepting a difference in $\delta^{34}S$-values of 40–60‰ between bacteriogenic sulfide and marine sulfate in present-day sedimentary environments, similar fractionations in ancient sedimentary rocks may be interpreted as evidence for the activity of sulfate-reducing bacteria. The presence or absence of such fractionations in sedimentary rocks thus may constrain the time of emergence of sulfate-reducing bacteria. In early Archean sedimentary rocks most sulfides and the rare sulfates have $\delta^{34}S$-values near 0‰ (Monster et al. 1979; Cameron 1982). The lack of substantial isotope fractionation between sulfate and sulfide has been interpreted initially as indicating an absence of bacterial reduction in the Archean. Ohmoto et al. (1993) employed a laser microprobe approach to analyze single pyrite grains from the ca 3.4 Ga Barberton greenstone belt and observed a variation of up to 10‰ among pyrites from a single small rock specimen, which could imply that bacterial reduction has occurred since at least 3.4 Ga. Shen and Buick (2004) argued that the large spread in $\delta^{34}S$-values of microscopic pyrites aligned along growth faces of former gypsum in the 3.47 Ga North Pole barite deposit, Australia represents the oldest evidence for microbial sulfate reduction.

3.8.4 Iron

Besides carbon and sulfur, iron as a third element controls the redox chemistry of the ocean. Rouxel et al. (2005) demonstrated a progressive change in iron cycling from 3.5 to 0.5 Ga that was associated with the oxygenation of the ocean (see Fig. 3.28 after Anbar and Rouxel 2007). According to Rouxel et al. (2005) the iron isotope distribution during the Earth's history can be divided into three stages: stage I (2.8–2.3 Ga) is characterized by highly variable and negative $\delta^{56}Fe$-values of pyrite, stage II (2.3–1.6 Ga) is characterized by unusually high δ-values and stage III (from 1.6 till today) is characterized by pyrite having a small $\delta^{56}Fe$ range from about 0 to −1‰. These different stages might reflect changes in the redox state of the Earth. In stage I (older than 2.3 Ga), the atmosphere and much of the ocean was free of oxygen. During this stage iron was removed from the ocean as iron oxides and

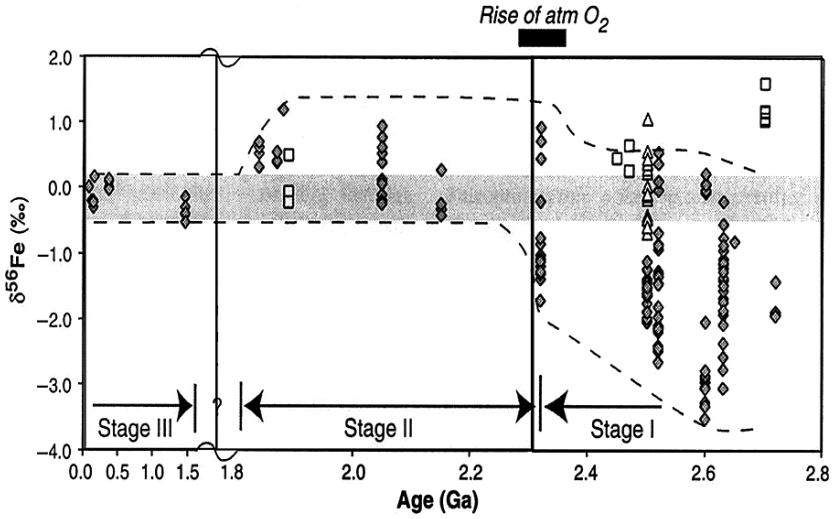

Fig. 3.28 δ^{56}Fe values of pyrite and Fe oxides vs time showing three evolutionary stages of the ocean (Anbar and Rouxel (2007))

pyrite. Iron oxides enriched in ^{56}Fe were precipitated by anaerobic oxidation, which drove the ocean toward lower δ^{56}Fe-values as recorded in pyrite (Kump 2005). In stage II from 2.3 to 1.8 Ga, the atmosphere became oxidized, but the ocean remained more or less anoxic. In stage III atmosphere and ocean were oxygenated, ensuring that iron did not accumulate in the ocean, but was removed as insoluble Fe^{3+} that retained the iron isotope composition of the iron inputs to the ocean which are close to the crustal average.

3.9 Atmosphere

The basic chemical composition of the atmosphere is quite simple, being made up almost entirely of three elements: nitrogen, oxygen, and argon. Other elements and compounds are present in amounts that although small are nevertheless significant. A mixture of gases with different molecular weights should partially segregate and fractionate in a gravity field. However, the lower atmosphere – the troposphere – is much too turbulent for gravitational fractionation to be observed. While it appears possible that certain gases in the upper atmosphere – the stratosphere – could be affected by this process, isotopic evidence for this has not been found so far (Thiemens et al. 1995). (Gravitational fractionation can, however, be observed in air trapped in ice cores and in sand dunes (Sowers et al. 1993 see p. 214). As will be shown later, very different fractionation effects and reactions can be observed in the troposphere compared to the stratosphere.

In recent years, tremendous progress has been achieved in the analysis of the isotope composition of important trace compounds in the atmosphere. The major elements – nitrogen, oxygen, carbon – continually break apart and recombine in a multitude of photochemical reactions, which have the potential to produce isotope fractionations (Kaye 1987). Isotope analysis is increasingly employed in studies of the cycles of atmospheric trace gases e.g., CH_4 and N_2O, which can give insights into sources and sinks and transport processes of these compounds. The rationale is that various sources have characteristic isotope ratios and that sink processes are accompanied by isotope fractionation.

Many of the processes responsible for isotope fractionations in the Earth's atmosphere may also occur in the atmospheres of other planetary systems, such as the atmospheric escape of atoms and molecules to outer space. Likely unique to Earth are isotope fractionations related to biological processes or to interactions with the ocean. One aspect of atmospheric research which has great potential for the application of stable isotope investigations is the study of anthropogenic pollution.

3.9.1 Atmospheric Water Vapor

While the major compounds nitrogen, oxygen and argon have a constant concentration in the lower part of the atmosphere, water vapor concentrations are highly variable: Craig and Gordon (1965) first measured the isotopic composition of atmospheric water vapor over the North Pacific. Later Rozanski and Sonntag (1982) and Johnson et al. (2001) observed in vertical profiles of tropospheric and stratospheric water vapor a gradual depletion of δD (and $\delta^{18}O$) with increasing altitude up to the tropopause with a reversal in the stratosphere. The depletion trend in the troposphere can be explained by isotope fractionation associated with cloud formation and rain-out processes leading to preferential removal of heavy isotopes from water vapor. In the stratosphere photochemical oxidation of methane might be responsible for the observed increase in δD.

3.9.2 Nitrogen

Nearly 80% of the atmosphere consists of elemental nitrogen. This nitrogen, collected from different altitudes, exhibits a constant isotopic composition (Dole et al. 1954; Sweeney et al. 1978) and represents the "zero-point" of the naturally occurring isotope variations. Besides the overwhelming predominance of elemental nitrogen, there are various other nitrogen compounds in the atmosphere, which play a key role in atmospheric pollution and determining the acidity of precipitation.

Nitrate originates from gaseous emissions of $NO_x(NO + NO_2)$. Heaton (1986) has discussed the possibility of isotopically differentiating between naturally produced and anthropogenic NO_x. Since very little isotope fractionation is expected at

the high temperatures of combustion in power plants and vehicles, the δ^{15}N-value of pollution nitrate is expected to be similar to that of the nitrogen which is oxidized. In soils, NO_x is produced by nitrification and denitrification processes which are kinetically controlled. This, in principle, should lead to more negative δ^{15}N-values in natural nitrate compared to anthropogenic nitrate. However, Heaton (1986) concluded that this distinction cannot be made on the basis of ^{15}N-contents, which has been confirmed by Durka et al. (1994). The latter authors demonstrated, however, that the oxygen isotope composition of nitrate is more indicative. Industrially produced nitrate contains oxygen from the atmosphere (δ^{18}O-values of 23.5‰) while nitrate originating from a nitrification process must have water as the main oxygen source (Amberger and Schmidt 1987).

3.9.2.1 Nitrous Oxide

Besides NO_x oxides, there is nitrous oxide (N_2O), which is of special interest in isotope geochemistry. N_2O is present in air at around 300 ppb and increases by about 0.2% per year. Nitrous oxide is an important greenhouse gas that is, on a molecular basis, a much more effective contributor to global warming than CO_2 and that is also a major chemical control on stratospheric ozone budgets.

Quantification of the atmospheric N_2O budget is difficult, because of its extensive sources and its long atmospheric lifetime of around 130 years. The first δ^{15}N-values for N_2O were determined by Yoshida et al. (1984), the first δ^{18}O-values were published by Kim and Craig (1990) and the first dual isotope determinations have been presented by Kim and Craig (1993). These authors suggested that the stable isotope composition of tropospheric N_2O results from mixing of three end members: tropical soil emissions, the return flux from the stratosphere and a near surface oceanic N_2O source. There are, however, still many uncertainties concerning the global budget of N_2O and the mechanisms of its formation and loss in the atmosphere (Stein and Yung 2003).

The δ^{15}N- and δ^{18}O-values of atmospheric N_2O today, range from 6.4 to 7.0‰ and 43 to 45.5‰ (Sowers 2001). Terrestrial emissions have generally lower δ-values than marine sources. The δ^{15}N and δ^{18}O-values of stratospheric N_2O gradually increase with altitude due to preferential photodissociation of the lighter isotopes (Rahn and Wahlen 1997). Oxygen isotope values of atmospheric nitrous oxide exhibit a mass-independent component (Cliff and Thiemens 1997; Cliff et al. 1999), which increases with altitude and distance from the source. The responsible process has not been discovered so far. First isotope measurements of N_2O from the Vostok ice core by Sowers (2001) indicate large ^{15}N and ^{18}O variations with time (δ^{15}N from 10 to 25‰ and δ^{18}O from 30 to 50‰), which have been interpreted to result from in situ N_2O production via nitrification.

There is another aspect that makes N_2O a very interesting compound for isotope geochemists. N_2O is a linear molecule in which there is one nitrogen atom at the centre and one at the end. The center site is called α-position, the end site β-position. Yoshida and Toyoda (2000) proposed that N_2O produced by microbes will be more

fractionated at the N^{α} than at the N^{β} position relative to industrial emissions. This uneven intramolecular distribution, thus, may help to identify the sources and sinks of N_2O.

3.9.3 Oxygen

Atmospheric oxygen has a rather constant isotopic composition with a $\delta^{18}O$-value of 23.5‰ (Dole et al. 1954; Kroopnick and Craig 1972; Bender et al. 1994). It is produced by photosynthesis without fractionation with respect to the substrate water (Helman et al. 2005). Urey (1947) calculated that if equilibrium was attained between atmospheric oxygen and water, then atmospheric oxygen should be enriched in ^{18}O by 6‰ at 25°C. This means atmospheric oxygen cannot be in equilibrium with the hydrosphere and thus, the ^{18}O-enrichment of atmospheric oxygen, the so-called "Dole" effect, must have another explanation. It is generally agreed that the ^{18}O-enrichment is of biological origin and results from the fact that during respiration most species preferentially use ^{16}O (Lane and Dole 1956). Oxygen consumed during respiration has an ^{18}O-content that is about 20‰ lower than the intake of O_2 (Guy et al. 1993). The Dole effect can be separated into terrestrial and oceanic contributions. Bender et al. (1994) propose a δ-value between 17 and 19‰ for the oceanic contribution and between 22 and 27‰ for the terrestrial contribution.

As has been shown by the analysis of molecular oxygen trapped in ice cores, the $\delta^{18}O$-value of atmospheric oxygen has varied with geologic time. Sowers et al. (1991) and Bender et al. (1994) have pioneered the analysis of $\delta^{18}O$ of O_2 in air bubbles trapped in ice cores. They examined the response of the terrestrial and marine biomass to climate change by measuring the difference between the $\delta^{18}O$-values of atmospheric oxygen and ocean water, and documented that the variability of the Dole effect is small between glacial and interglacial periods. Observed variations in the ^{18}O-contents during the past 130,000 years follow the $\delta^{18}O$-value of sea water because photosynthesis transmits variations in ^{18}O of sea water through the meteoric water cycle and biosphere to O_2 in air.

Further, insight into the isotopic composition of atmospheric oxygen comes from the simultaneous measurement of $\delta^{17}O$ and $\delta^{18}O$ (Luz et al. 1999; Luz and Barkan 2000, 2005). Photosynthesis and respiration fractionate ^{17}O and ^{18}O in a mass-dependent way, whereas photochemical reactions among O_3, O_2, and CO_2 in the stratosphere (Thiemens et al. 1995) give rise to a mass independent isotope fractionation of atmospheric O_2. As a result, atmospheric oxygen is depleted in ^{17}O by about 0.2‰ relative to oxygen affected by photosynthesis and respiration alone. The magnitude of the ^{17}O depletion depends on the relative proportions of biological productivity and stratospheric mixing. Thus, as proposed by Luz et al. (1999) and Luz and Barkan (2000) the magnitude of the tropospheric ^{17}O anomaly can be used as a tracer of global biosphere production rates.

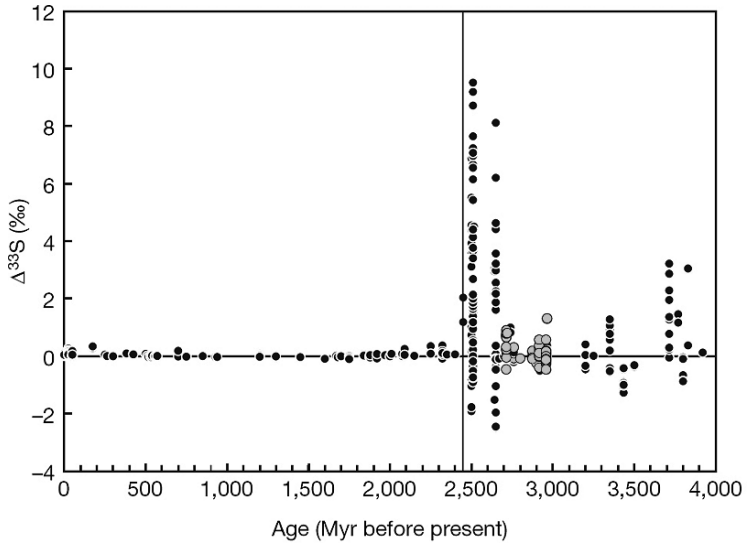

Fig. 3.29 Compilation of $\Delta^{33}S$ vs age for rock samples. Note large $\Delta^{33}S$ before 2.45 Ga, indicated by vertical line, and small but measurable $\Delta^{33}S$ after 2.45 Ga (Farquhar et al. 2007)

3.9.3.1 Evolution of Atmospheric Oxygen

Understanding the evolution of atmospheric oxygen during the Earth history is a fundamental problem in the Earth sciences. Geological, mineralogical, and geochemical indicators have been used to deduce oxygen levels of past atmospheres. Recently, a new proxy has been introduced by Farquhar and coworkers (i.e. Farquhar and Wing 2003). These authors demonstrated that the sulfur isotope record throughout much of the Archean preserves a clear mass-independent signal (see Fig. 3.29). The record of large magnitude $\Delta^{33}S$-values for sulfides terminates abruptly at approximately 2.4 Ga, the so-called "Great Oxidation Event." Before 2.4 Ga, photochemical reactions in the atmosphere had the capacity to fractionate sulfur isotopes by mass-independent mechanisms. The specific chemical reaction that produced the effect observed in Archean samples is unknown, but SO_2 is a likely candidate (Farquhar and Wing 2003). The disappearance of mass-independent fractionations after 2.4 Ga is taken as evidence for the transition from an anoxic to an oxic atmosphere.

3.9.4 Carbon Dioxide

3.9.4.1 Carbon

The increasing CO_2-content of the atmosphere is a problem of world-wide concern. By measuring both the concentration and isotope composition of CO_2 on the same

samples of air, it is possible to determine whether variations are of anthropogenic, oceanic, or biologic origin. The first extensive measurements of the carbon isotope ratio of CO_2 were made in 1955/56 by Keeling (1958, 1961). He noted daily, seasonal, secular, local, and regional variations as regular fluctuations. Daily variations exist over continents, which depend on plant respiration and reach a distinct maximum around midnight or in the early morning hours. At night there is a measurable contribution of respiratory CO_2, which shifts $\delta^{13}C$-values toward lower values (see Fig. 3.30). Seasonal variations in ^{13}C are very similar to CO_2-concentrations and result from terrestrial plant activity. As shown in Fig. 3.31, the seasonal cycle diminishes from north to south, as expected from the greater seasonality of plant activity at high latitude and the larger amount of land area in the northern hemisphere. This effect is hardly discernible in the southern hemisphere (Keeling et al. 1989).

Long-term measurements of atmospheric CO_2 are available for a few clean-air locations on an almost continuous basis since 1978 (Keeling et al. 1979, 1984, 1989, 1995; Ciais et al. 1995; Mook et al. 1983). These measurements clearly demonstrate that on average atmospheric CO_2 increases by about 1.5 ppm per year while the isotope ratio shifts toward lower $^{13}C/^{12}C$ ratios. The annual combustion of 10^{15} g of fossil fuel with an average $\delta^{13}C$-value of $-27‰$ would change the ^{13}C-content of atmospheric CO_2 by $-0.02‰$ per year. The observed change is, however, much smaller. Of the CO_2 emitted into the atmosphere, roughly half remains in the atmosphere and the other half is absorbed into the oceans and the terrestrial biosphere. The partitioning between these two sinks is a matter of debate. Whereas most oceanographers argue that the oceanic sink is not large enough to account for the entire absorption, terrestrial ecologists doubt that the terrestrial biosphere can be a large carbon sink.

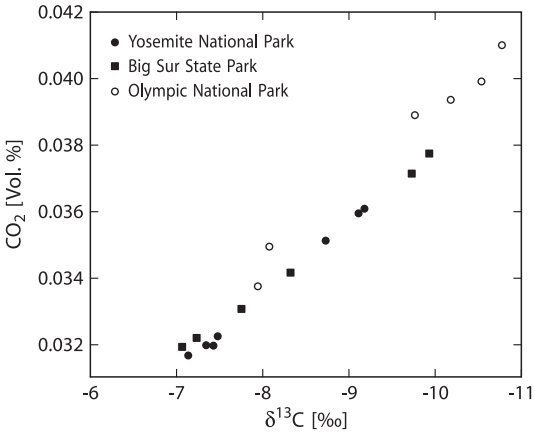

Fig. 3.30 Relationship between atmospheric CO_2 concentration and $\delta^{13}C_{CO2}$ (after Keeling, 1958)

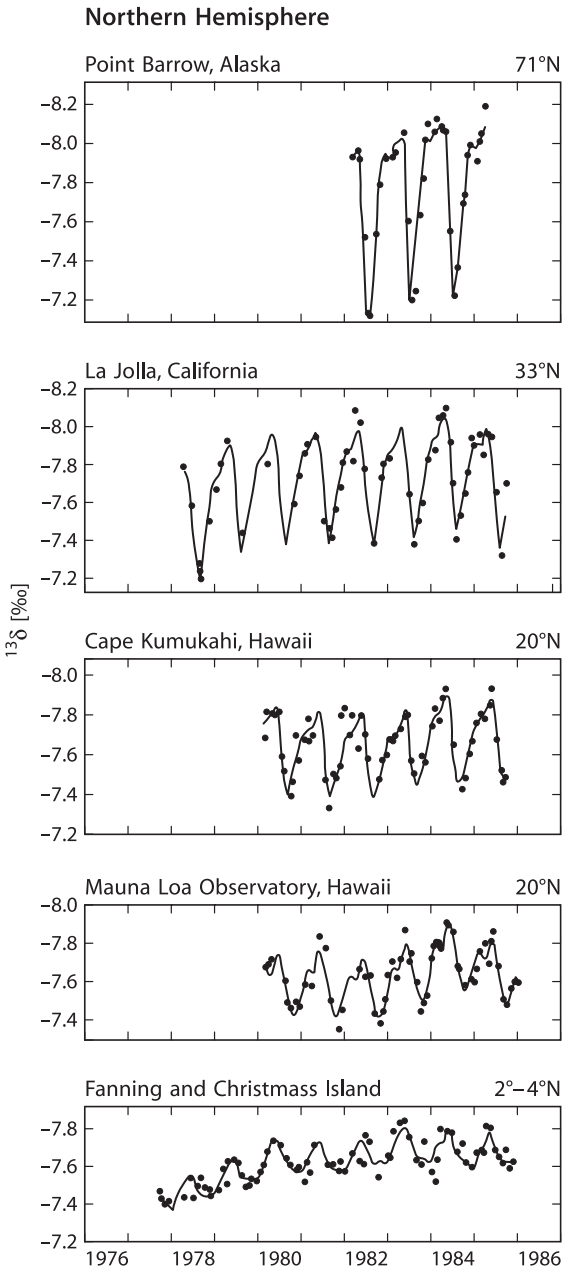

Fig. 3.31 Seasonal $\delta^{13}C$ variations of atmospheric CO_2 from five stations in the Northern Hemisphere. *Dots* denote monthly averages, *oscillating curves* are fits of daily averages (after Keeling et al. 1989)

3.9.4.2 Oxygen

Atmospheric CO_2 has a $\delta^{18}O$-value of about +41‰, which means that atmospheric CO_2 is in approximate isotope equilibrium with ocean water, but not with atmospheric oxygen (Keeling 1961; Bottinga and Craig 1969). Measurements by Mook et al. (1983) and Francey and Tans (1987) have revealed large-scale seasonal and regional variations. There is a North–South shift in the average ^{18}O-contents of almost 2‰ increasing towards the south, about ten times larger than for ^{13}C. Seasonal cycles are similar in magnitude to those of $\delta^{13}C$ (see Fig. 3.32). This North–South gradient is caused by the unequal distribution of ocean and land between the two hemispheres and by the very different oxygen isotope composition of ocean and meteoric water. Farquhar et al. (1993) demonstrated that much more CO_2 comes into contact with leaf water than is actually taken up by plants during photosynthesis. For every CO_2 molecule that is taken up by photosynthesis, two others enter the leaf through the stomata. They rapidly equilibrate with the leaf water and then diffuse back to the atmosphere without having been incorporated by the plant. This large flux therefore only influences the ^{18}O content of atmospheric CO_2 and has no influence on the $\delta^{13}C$-value.

3.9.4.3 Long-Term Variations in the CO_2 Concentration

There is increasing awareness that the CO_2 content of the Earth's atmosphere has varied considerably over the last 500 Ma. The clearest evidence comes from measurements of CO_2 from ice cores, which have yielded an impressive record of CO_2 variations over the past 420,000 years (Petit et al. 1999).

In a much broader context, Berner (1990) has modeled how long-term changes in CO_2 concentrations can result from the shifting balance of processes that deliver CO_2 to the atmosphere (such as volcanic activity) and processes that extract

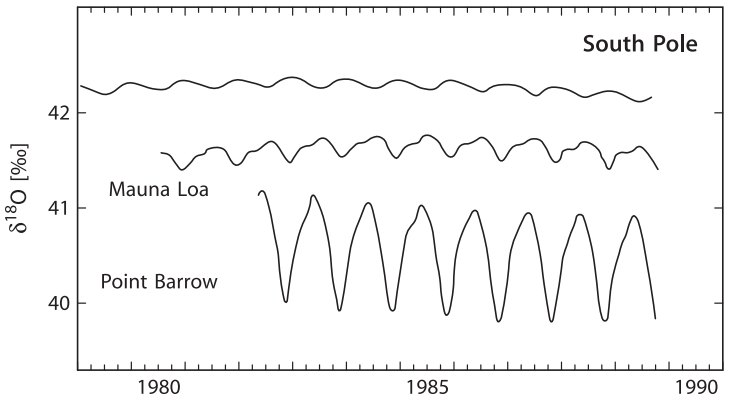

Fig. 3.32 $\delta^{18}O$ seasonal record of atmospheric CO_2 from three stations: Point Barrow 71.3°N, Mauna Loa 19.5°S, South Pole 90.0°S. (after Ciais et al., 1998)

CO_2 (such as weathering and the deposition of organic material). The theoretical carbon dioxide curve calculated for the past 500 Ma matches the climate record at several key points: it is low during the ice age of the Carboniferous and Permian and rises to a maximum in the Cretaceous. Although the exact curve is far from being known, it is clear that fluctuations in the CO_2 content of the ancient atmosphere may have played a critical role in determining global surface paleotemperatures. To elucidate these short- and long-term CO_2-fluctuations, several promising "CO_2-paleobarometers" use variations of carbon isotopes in different materials.

Short-term carbon isotope variations in tree rings have been interpreted as indicators of anthropogenic CO_2 combustion (Freyer 1979; Freyer and Belacy 1983). While different trees show wide variability in their isotope records due to climatic and physiological factors, many tree-ring records indicate a 1.5‰ decrease in $\delta^{13}C$-values from 1750 to 1980. Freyer and Belacy (1983) reported C-isotope data for the past 500 years on two sets of European oak trees: forest trees exhibit large nonsystematic ^{13}C variations over the 500 years, whereas free-standing trees show smaller ^{13}C fluctuations, which can be correlated to climatic changes. Since industrialization of these areas in 1850, the ^{13}C record for the free-standing trees has been dominated by a systematic decrease of about 2‰.

The most convincing evidence for changes in atmospheric CO_2-concentrations and $\delta^{13}C$-values comes from air trapped in ice cores in Antarctica. Figure 3.33 shows a high time-resolution record for the last 1,000 years from analysis of the Law Dome, Antarctica ice core (Trudinger et al. 1999). Changes in CO_2 concentration and in $\delta^{13}C$-values during the last 150 years are clearly related to the increase of anthropogenic fossil fuel burning. During the last ice age with low

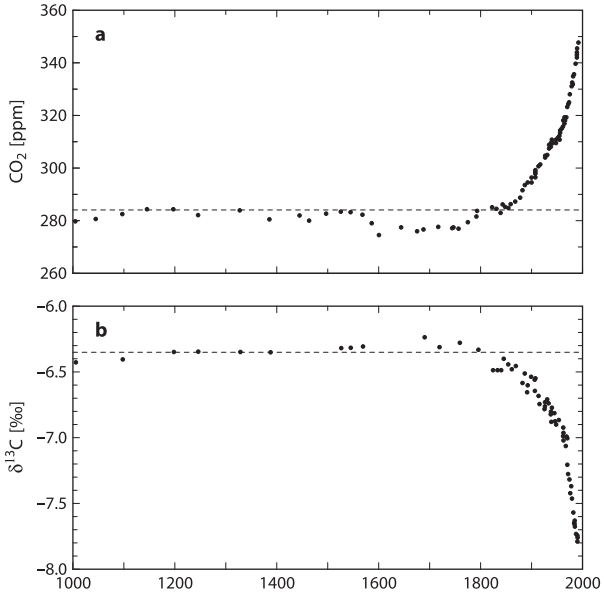

Fig. 3.33 Law Dome ice core CO_2 and $\delta^{13}C$ record for the last 1000 years (after Trudinger et al. 1999)

CO_2-concentrations, atmospheric CO_2 was isotopically lighter by about 0.3‰ relative to interglacial periods (Leuenberger et al. 1992). This somewhat surprising feature, which is opposite to the recent anthropogenic trend, is explained by either a decrease in dissolved CO_2 in surface waters because of a more efficient "biological pump" or a higher alkalinity in the glacial ocean.

Two different classes of approaches have been used in the study of long-term atmospheric CO_2 change: one utilizing deep-sea sediments, the other studying continental sediments. Cerling (1991) has been reconstructing the CO_2 content of the ancient atmosphere by analyzing fossil soil carbonate that formed from CO_2 diffusion from the atmosphere or plant roots. This method relies on certain assumptions and prerequisites. One, for instance, is the necessity of differentiating pedogenic calcretes from those formed in equilibrium with groundwater, which can not be used for pCO_2 determinations (Quast et al. 2006).

Another approach uses the relationship between the concentration of molecular CO_2 and the $\delta^{13}C$-value of marine organic plankton (Rau et al. 1992). Attempts to quantify the relationship between $CO_{2(aq)}$ and $\delta^{13}C_{org}$ have resulted in several empirically derived calibrations (Jasper and Hayes 1990; Jasper et al. 1994; Freeman and Hayes 1992, and others). Recent theoretical considerations and experimental work demonstrated that cellular growth rate (Laws et al. 1995; Bidigare et al. 1997) and cell geometry (Popp et al. 1998) also exert considerable control on $\delta^{13}C_{org}$, insofar as they influence the intracellular CO_2 concentration. Other complicating factors are potential contamination of terrestrial organic matter and marine photosynthesizers with varying carbon fixation pathways that are integrated in bulk organic matter. Therefore, it is preferable to use specific biomarkers, such as alkenones. Alkenones are long-chain (C_{36}–C_{39}) unsaturated ketones, produced by a few taxa of phytoplankton such as the common *Emiliani huxleyi*, in which the number of double bonds is correlated with the water temperature at the time of synthesis. Palaeo–CO_2 levels can be estimated from the carbon isotope composition of alkenones and coeval carbonates (Jasper and Hayes 1990; Pagani et al. 1999a, b).

The boron isotope approach to pCO_2 estimation relies on the fact that a rise in the atmospheric CO_2 concentration will increase pCO_2 of the surface ocean which in turn causes a reduction of its pH. By measuring the boron isotope composition of planktonic foraminifera Palmer et al. (1998) and Pearson and Palmer (2000) have reconstructed the pH-profile of Eocene sea water and estimated past atmospheric CO_2 concentrations. However, Lemarchand et al. (2000) argued that $\delta^{11}B$ records of planktonic foraminifera partly reflect changes in the marine boron isotope budget rather than changes in ocean pH.

3.9.5 Carbon Monoxide

Carbon monoxide is an important trace gas, which has a mean residence time of about two months and a mean concentration of the order of 0.1 ppm. The principal sources of CO are (1) oxidation of methane and other higher hydrocarbons, (2) biomass burning, (3) traffic, industry and domestic heating, (4) oceans, and (5)

vegetation. The dominant sinks are (1) in situ oxidation by OH and (2) uptake by soils. The first isotope data on CO have been presented by Stevens et al. (1972), which have later been confirmed by Brenninkmeijer (1993) and Brenninkmeijer et al. (1995). Seasonal variations in δ^{13}C-values appear to reflect a shift in the relative contributions from two major sources, biomass burning and atmospheric oxidation of methane. δ^{18}O-values are even more variable than δ^{13}C due to a kinetic isotope effect accompanying the removal of CO from the atmosphere. Oxygen in CO also exhibits a mass independent fractionation with a pronounced ^{17}O excess of up to 7.5‰, which must be related to the removal reaction with OH (Röckmann et al. 1998).

3.9.6 Methane

Methane enters the atmosphere from biological and anthropogenic sources and is destroyed by reaction with the hydroxyl radical. Thus, a mass-weighted average composition of all CH_4 sources is equal to the mean δ^{13}C-value of atmospheric methane, corrected for any isotope fractionation effects in CH_4 sink reactions. Based on the concentration measured in air contained in polar ice cores, methane concentrations have doubled over the past several 100 years (Stevens 1988). Concentrations were increasing at almost 1% per year in the late 1970s and early 1980s, the growth rate has slowed down since then for unknown reasons.

Methane is produced by bacteria under anaerobic conditions in wet environments such as wetlands, swamps and rice fields. It is also produced in the stomachs of cattle and by termites. Typical anthropogenic sources are from fossil fuels such as coal mining and as a byproduct in the burning of biomass. The latter sources are considerably heavier in ^{13}C than the former. Recently, Keppler et al. (2006) demonstrated that methane is formed in terrestrial plants under oxic conditions by an unknown mechanism. The size of this methane source is still unknown but it might play an important role for the methane cycle.

Atmospheric methane has a mean δ^{13}C-value of around -47‰ (Stevens 1988). Quay et al. (1999) presented global time series records between 1988 and 1995 on the carbon and hydrogen isotope composition of atmospheric methane. They measured spatial and temporal variation in ^{13}C and D with a slight enrichment observed for the southern hemisphere (-47.2‰) relative to the northern hemisphere (-47.4‰). The mean δD was -86 ± 3‰ with a 10‰ depletion in the northern relative to the southern hemisphere.

Methane extracted from air bubbles in polar ice up to 350 years in age has a δ^{13}C-value which is 2‰ lower than at present (Craig et al. 1988). This may indicate that anthropogenic burning of the Earth's biomass may be the principal cause of the recent ^{13}C enrichment in methane.

Stratospheric methane collected over Japan gave a δ^{13}C-value of -47.5‰ at the tropopause and increased to -38.9‰ at around 35 km (Sugawara et al. 1998). These authors suggested that reaction with Cl in the stratosphere might be responsible for the ^{13}C-enrichment.

3.9.7 Hydrogen

Molecular hydrogen (H_2) is after methane the second most abundant reduced gas in the atmosphere with an average concentration of 0.55 ppm. The isotope geochemistry of hydrogen in the atmosphere is very complex, because there are numerous hydrogen-containing compounds undergoing continuous chemical and physical transformations. Many studies of the isotope composition of H_2 have been performed in conjunction with the measurement of atmospheric tritium. The major result from these studies is that there is a large variability in deuterium content both in time and location. The best estimate for δD of H_2 is in the vicinity of $70 \pm 30‰$ (Friedman and Scholz 1974). This high δD-value can be ascribed to the presence of two hydrogen components: a "background" component with enhanced deuterium and tritium and a locally produced "industrial" component which is very depleted in deuterium. Rahn et al. (2002a) demonstrated that D/H ratios in urban air from the Los Angeles region define a mixing curve between unpolluted winter air with δD-values of ca $+100$ to $+125‰$ and that of urban sources with δD-values of $\sim -270‰$. Rahn et al. (2002b) analyzed D/H of H_2 in stratospheric air samples. δD-values vary up to $+440‰$, representing the most D-enriched natural material on Earth.

3.9.8 Sulfur

Sulfur is found in trace compounds in the atmosphere, where it occurs in aerosols as sulfate and in the gaseous state as H_2S and SO_2. Sulfur can orginate naturally (volcanic, sea spray, aeolian weathering, biogenic) or anthropogenically (combustion and refining of fossil fuels, ore smelting, gypsum processing). These different sources differ greatly in their isotopic composition as shown in Fig. 3.34.

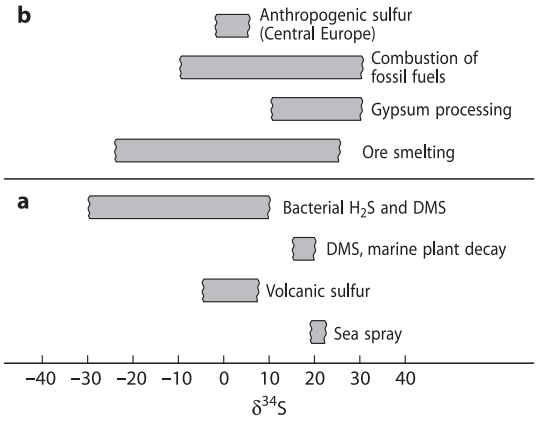

Fig. 3.34 S-isotope composition of (**a**) natural and (**b**) anthropogenic sulfur sources in the atmosphere. *DMS* Dimethyl-sulfide

The isotopic compositions of the industrial sulfur sources are generally so variable, that the assessment of anthropogenic contributions to the atmosphere is extremely difficult. Krouse and Case (1983) were able to give semiquantitative estimates for a unique situation in Alberta where the industrial SO_2 had a constant $\delta^{34}S$-value near 20‰. Generally, situations are much more complicated which limits the "fingerprint" character of the sulfur isotope composition of atmospheric sulfur to such rare cases.

Very interesting seasonal dependencies for sulfur in precipitation and in aerosol samples have been observed by Nriagu et al. (1991). $\delta^{34}S$-data for aerosol samples of the Canadian arctic show pronounced seasonal differences, with the sulfur being more ^{34}S-enriched in summer than in winter. This situation is quite different from that observed for airborne sulfur in southern Canada. In rural and remote areas of southern Canada, the $\delta^{34}S$-values of atmospheric samples are higher in winter and lower in summer. While during the winter sulfur is mainly derived from sources used for heating and industrial sources, in summer the large emission of ^{34}S-depleted biogenic sulfur from soils, vegetation, marshes, and wetlands results in the lowering of the $\delta^{34}S$-values of airborne sulfur. The opposite trend observed for aerosol sulfur in the Arctic suggests a different origin of the sulfur in these high latitude areas.

3.9.9 Mass-Independent Isotope Effects in Atmospheric Compounds

Mass independent isotope compositions have been observed in a number of atmospheric molecules such as ozone, CO_2, N_2O, and CO (Thiemens 1999, 2006) as shown in Fig. 3.35.

Ozone has become one of the most important molecules in atmospheric research. In situ mass-spectrometric measurements by Mauersberger (1981, 1987) demonstrated that an equal enrichment in ^{17}O and ^{18}O of about 40% exists in the stratosphere, with a maximum at about 32 km. The rate of formation of isotopically partially substituted ozone (mass 50) is obviously faster than that of unsubstituted ozone (mass 48). Later measurements by Krankowsky et al. (2000) did not confirm the very large enrichments originally reported by Mauersberger, but gave enrichments of 7–11%. Similar mass-independent fractionations have been observed in laboratory experiments by Thiemens and Heidenreich (1983); which are clearly temperature dependent.

Another oxygen isotope fractionation effect is documented in CO_2 samples collected between 26 and 35 km altitude, which show a mass – independent enrichment in both ^{17}O and ^{18}O of up to about 15‰ above tropospheric values (Thiemens et al. 1995). The enrichment of stratospheric CO_2 relative to tropospheric CO_2 should make it possible to study mixing processes across the tropopause.

Similar effects have also been observed in stratospheric nitrous oxide. $\delta^{17}O$ and $\delta^{18}O$ measurements by Cliff and Thiemens (1997) reveal that stratospheric

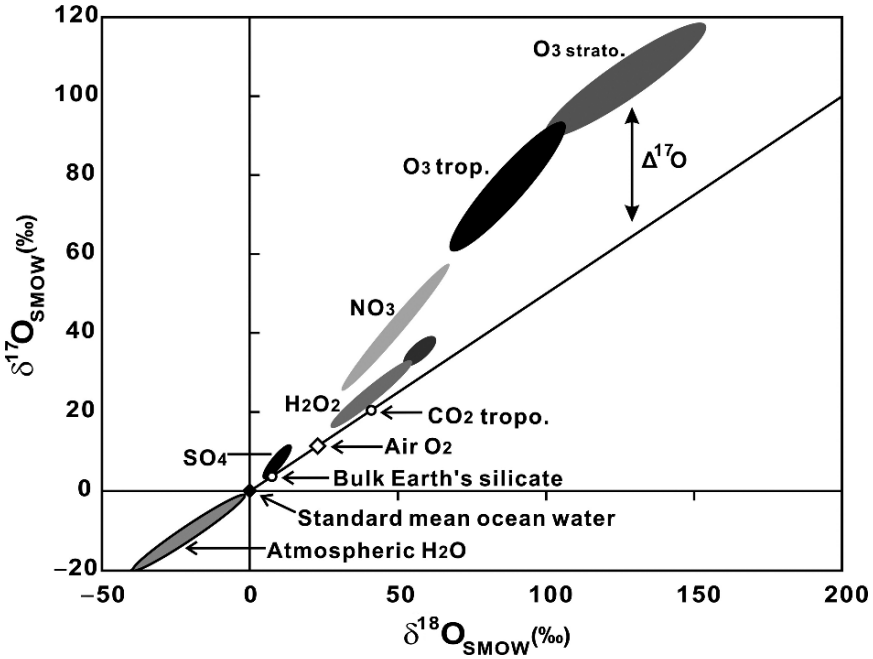

Fig. 3.35 $\delta^{17}O$ vs $\delta^{18}O$ plot of atmospheric oxygen species (Thiemens, 2006)

N_2O possesses a large variable mass-independent isotope composition, which also requires a mass-independent process – a source, sink, or exchange reaction (Thiemens 1999).

Carbon monoxide, which is predominantly produced during combustion processes, may exhibit an ^{17}O excess of up to 7.5‰ in summer at high northern latitudes (Röckmann et al. 1998). The major source of this fractionation is its atmospheric removal reaction $CO + OH = CO_2 + H_2$, in which the remaining CO gains excess ^{17}O.

3.9.9.1 Sulfate and Nitrate in Ice Cores

Upon oxidation of SO_2 and NO_2 to sulfate and nitrate, the mass-independent composition of ozone and H_2O_2 is transferred to sulfate and nitrate. Measurements of the oxygen isotope composition of ice core sulfate and nitrate can thus provide a historical record of natural variations in sulfur and nitrogen pathways (Alexander et al. 2002, 2004; Thiemens 2006). Such a record is of importance in understanding global climate change particularly through glacial and volcanic events. Alexander et al. (2002) showed that the mass independent fractionation of sulfate is significantly greater during the warmer interglacials than during the colder glacials. However, as discussed by Alexander et al. (2002) it is not a record of temperatures,

but a measure of the oxidative efficiency of the atmosphere. During colder periods the oxidation of SO_2 to sulfate in clouds is obviously suppressed. In a later study Alexander et al. (2004) demonstrated that a combined approach of sulfate and nitrate measurements in ice cores may give additional evidence for changes in the oxidative capacity of the atmosphere over different time periods.

Additional information can be gained by measurements of the different sulfur isotopes in stratospheric sulfate aerosols (Baroni et al. 2007). During large explosive eruptions that release large amounts of SO_2 (Pinatubo, Agung, Tambora), sulfur gases rise to the stratosphere where they form small sulfuric acid aerosols that can remain in the stratosphere for several years before they settle to the ground. By extracting sulfate from the Antartic ice sheet, Baroni et al. (2007) demonstrated that sulfate from the Agung and Pinatubo eruptions exhibit large mass-independent sulfur isotope fractionations. The sign of the $\Delta^{33}S$ changed over time from an initial positive component to a negative component, which indicates a fast process during photochemical oxidation of SO_2 to sulfuric acid on a time scale of months.

3.10 Biosphere

As used here, the term "biosphere" includes the total sum of living matter – plants, animals, and microbial biomass and the residues of the living matter in the geological environment such as coal and petroleum. A fairly close balance exists between photosynthesis and respiration, although over the whole of geological time respiration has been exceeded by photosynthesis, and the energy derived from this is stored mostly in disseminated organic matter, and, of course, in coal and petroleum.

Photosynthesis is responsible for isotope fractionations in the biosphere, not only for carbon, but also for hydrogen and oxygen too. Nevertheless, as will be shown, the transformation of biogenic matter to organic matter in sediments also involves isotope fractionations, occurring in two stages: a biochemical and a geochemical stage. During the biochemical stage microorganisms play the major role in reconstituting the organic matter. During the geochemical stage, increasing temperature and to a much lesser extent pressure are responsible for the further transformation of organic matter (see recent review of Galimov, 2006).

3.10.1 Living Organic Matter

3.10.1.1 Bulk Carbon

Wickman (1952) and Craig (1953) were the first to demonstrate that marine plants are about 10‰ enriched in ^{13}C relative to terrestrial plants. Since that time numerous studies have broadened this view and provided a much more detailed account of isotope variations in the biosphere. The reason for the large C-isotope differences

found in plants was only satisfactorily explained after the discovery of new photosynthetic pathways in the 1960s. The majority of land plants (80–90%) employ the C3 (or Calvin) photosynthetic pathway which results in organic carbon approximately 18‰ depleted in ^{13}C with respect to atmospheric CO_2. Around 10–20% of carbon uptake by modern land plants is via C4 (or Hatch–Slack) photosynthesis with a carbon isotope fractionation of only 6‰ on average. The C4 pathway is thought to represent an adaptation to CO_2 limited photosynthesis, which developed relatively late in the Earth's history. It is advantageous under warm, dry, and saline environmental conditions. Differences in the isotope composition of C3 and C4 plants are widely used as a palaeoenvironmental indicator to trace climatic changes or changes in the diet of animals and humans.

One of the most important groups of all living matter is marine phytoplankton. Natural oceanic phytoplankton populations vary in $\delta^{13}C$-value by about 15‰ (Sackett et al. 1973; Wong and Sackett 1978). Rau et al. (1982) demonstrated that different latitudinal trends in the carbon isotope composition of plankton exist between the northern and the southern oceans: south of the equator the correlation between latitude and plankton ^{13}C-content is significant, whereas a much weaker relationship exists in the northern oceans.

The unusual ^{13}C depletion in high latitude Southern Ocean plankton has been puzzling for years. Rau et al. (1989, 1992) found a significant inverse relationship between high-latitude ^{13}C-depletion in plankton and the concentration of molecular CO_2 in surface waters. Thus, it has been assumed that the major factor controlling the C-isotope composition of phytoplankton is the availability of aqueous dissolved CO_2. However, as has been shown in culture experiments with marine microalgae (Laws et al. 1995; Bidigare et al. 1997; Popp et al. 1998) the carbon isotope composition of phytoplankton depends on many more factors including cell wall permeability, growth rate, cell size and the ability of the cell to actively assimilate inorganic carbon. Therefore, estimates of paleo-CO_2 concentrations based on the C-isotope composition of marine organic matter need to consider the paleoenvironmental conditions at the time of phytoplankton production, which are difficult to constrain for the geologic past.

Organic material that comprises living matter consists of carbohydrates (saccharides, "Sacc") – the first product of carbon fixation – and proteins ("Prot"), nucleic acids ("NA") and lipids ("Lip") with prevailing regularities within these compound classes:

$$\delta_{NA} \sim \delta_{Prot},$$

$$\delta_{Prot} - \delta_{Sacc} \sim -1‰ \text{ and}$$

$$\delta_{Lip} - \delta_{Sacc} \sim -6‰ \text{ (Hayes 2001).}$$

What is known for a long-time lipids are depleted in ^{13}C by 5–8‰ relative to the bulk biomass. Recently, Teece and Fogel (2007) demonstrated that the carbohydrate fraction of various organisms on average is enriched in ^{13}C by 4.6‰ relative to the bulk. Even larger variations are observed for individual amino acids (Abelson

and Hoering 1961) and individual carbohydrates (Teece and Fogel 2007), where variations are probably associated with different metabolic pathways during their synthesis.

The $\delta^{13}C$-value of the total marine organic matter represents a mixed isotope signal from land plant detritus, primary production by aquatic organisms, and microbial biomass. The possibility of analyzing individual components has refined the interpretation of bulk $\delta^{13}C$-data. Compound-specific isotope analyses allow the resolution of the isotopic composition of material derived from primary sources from that of secondary inputs. These source-specific molecules have become known as biomarkers, which are complex organic compounds derived from living organisms and showing little structural difference from their parent biomolecules. Due to the specificity of their origin, biomarkers allow for an investigation of the extent to which various organisms contribute organic materials to complex mixtures. In the Messel Shale, Freeman et al. (1990) observed C-isotope variations of individual compounds from -73.4 to $-20.9‰$ (see Table 3.3). This large range can be interpreted as representing a mixture of secondary, bacterially mediated processes and primary producers. While the major portion of the analyzed hydrocarbons reflects the primary biological source material, some hydrocarbons having low concentrations are extremely ^{13}C depleted indicating their secondary microbial origin in a methane-rich environment. Later studies by Summons et al. (1994), Thiel et al. (1999), Hinrichs et al. (1999), and Peckmann and Thiel (2005) clearly suggested that fermentative and chemoautotrophic organisms must have made significant contributions to total sedimentary organic matter. For example, extremely depleted $\delta^{13}C$-values as low as $-120‰$ of specific biomarkers indicate that ^{13}C-depleted methane must be the carbon source for the respective archaea rather than the metabolic product.

Table 3.3 $\delta^{13}C$-values of separated individual hydrocarbons from the Messel shale (Freeman et al. 1990)

Peak	$\delta^{13}C$	Compound
1	−22.7	Norpristane
2	−30.2	C19 acyclic isoprenoid
3	−25.4	Pristine
4	−31.8	Phytane
5	−29.1	C23 Acyclic isoprenoid
8	−73.4	C32 Acyclic isoprenoid
9	−24.2	Isoprenoid alkane
10	−49.9	22, 29, 30-trisnorhopane
11	−60.4	Isoprenoid alkane
15	−65.3	30-norhopane
19	−20.9	Lycophane

3.10.1.2 Hydrogen

During photosynthesis plants remove hydrogen from water and transfer it to organic compounds. Because plants utilize environmental water during photosynthesis, δD-values of plants are primarily determined by the δD-value of the water available for plant growth. Hydrogen enters the plant as water from roots in the case of terrestrial plants or via diffusion in the case of aquatic plants. In both cases, the water enters the organisms without any apparent fractionation. In higher terrestrial plants, water transpires from the leaf due to evaporation, which is associated with a H-isotope fractionation of up to 40–50‰ (White 1989).

Large negative isotope fractionations occur in biochemical reactions during the synthesis of organic compounds (Schiegl and Vogel 1970). A generalized picture of the hydrogen isotope fractionations in the metabolic pathway of plants is shown in Fig. 3.36 (after White 1989). There are systematic differences in the D/H ratios among classes of compounds in plants: lipids usually contain less deuterium than the protein and the carbohydrate fractions (Estep and Hoering 1980). Lipids can be divided into two groups: straight-chain lipids are depleted in D by 150–200‰ relative to water whereas isoprenoid lipids are depleted by about 200–300‰.

The component typically analyzed in plants is cellulose, which is the major structural carbohydrate in plants (Epstein et al. 1976, 1977). Cellulose contains 70% carbon-bound hydrogen, which is isotopically non-exchangeable and 30% of exchangeable hydrogen in the form of hydroxyl groups (Epstein et al. 1976; Yapp and Epstein 1982). The hydroxyl-hydrogen readily exchanges with the environmental water and its D/H ratio is not a useful indicator of the D/H ratio of the water used by the plants.

A further step towards improved reconstruction of the primary environment is represented by the determination of the hydrogen isotope composition of individual compounds. Hydrogen and carbon in organic matter, although both of biological origin, undergo very different changes during diagenesis and maturation. Whereas carbon tends to be preserved, hydrogen is exchanged during various diagenetic re-

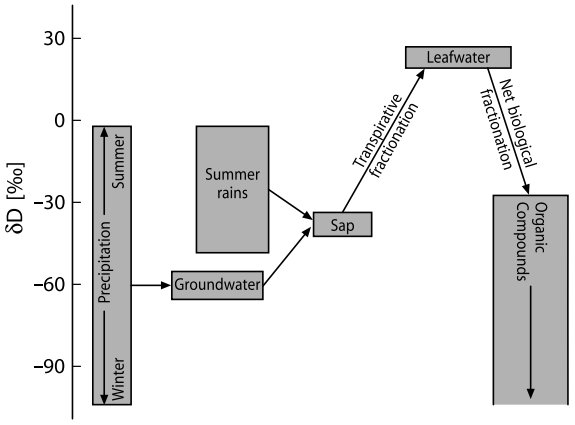

Fig. 3.36 Generalized scheme of hydrogen isotope changes in plants (White 1989)

actions with environmental water. To reconstruct the original environmental conditions, it is therefore necessary to measure individual lipid biomarkers (Sessions et al. 1999; Sauer et al. 2001). The latter authors demonstrated that D/H ratios of lipid biomarkers record the isotopic composition of the water in which these compounds formed. Certain sterols in freshwater systems can serve specifically as aquatic biomarkers and can be used to reconstruct δD-values of lakewater to within ±10‰. The compound-specific isotope technique has the advantage that it can separate compounds formed unambiguously in aquatic environments and those which are not affected by terrestrial sources.

3.10.1.3 Oxygen

The experimental difficulties in determining the oxygen isotope composition of biological materials is due to the rapid exchange between organically bound oxygen, in particular the oxygen of carbonyl and carboxyl functional groups, with water. This explains why studies on the oxygen isotope fractionation within living systems have concentrated on cellulose, the oxygen of which is only very slowly exchangeable (Epstein et al. 1977; DeNiro and Epstein 1979, 1981).

Oxygen potentially may enter organic matter from three different sources: CO_2, H_2O, and O_2. DeNiro and Epstein (1979) have shown that ^{18}O-contents of cellulose for two sets of plants grown with water having similar oxygen isotope ratios, but with CO_2 having different oxygen isotope ratios, did not differ significantly. This means that CO_2 is in oxygen isotope equilibrium with the water. Therefore, the isotopic composition of water determines the oxygen isotope composition of organically bound oxygen. Similar to hydrogen, oxygen isotope fractionation does not occur during uptake of soil water through the root, but rather in the leaf because of evapotranspiration.

3.10.1.4 Nitrogen

There are various pathways by which inorganic nitrogen can be fixed into organic matter during photosynthesis. N-autotrophs can utilize a variety of materials and thus can have a wide range of $\delta^{15}N$-values depending on environmental conditions. However, most plants have $\delta^{15}N$-values between -5 and $+2$‰. Plants fixing atmospheric nitrogen have δ-values between 0 and + 2‰. Isotope fractionation will occur when the inorganic nitrogen source is in excess (Fogel and Cifuentes 1993). Isotope fractionations during assimilation of NH_4 by algae varied extensively from -27 to 0‰ (Fogel and Cifuentes 1993). A similar range of fractionations has been observed with algae grown on nitrate as the source of nitrogen.

3.10.1.5 Sulfur

Sulfur occurs mainly in proteins that typically display a C/S ratio of about 50. The processes responsible for the direct primary production of organically bound sulfur are the direct assimilation of sulfate by living plants and microbiological assimilatory processes in which organic sulfur compounds are synthesized. Land plants use sulfate available from precipitation, marine phytoplankton use ocean water sulfate.

At present, only a limited number of sulfur isotope measurements of biological materials are available. Mekhtiyeva and Pankina (1968) and Mekhtiyeva et al. (1976) have demonstrated that $^{34}S/^{32}S$ ratios of aquatic plants from a given water are slightly lower than those for the sulfur of the dissolved sulfate. The same relationship has been obtained by Kaplan et al. (1963) for marine organisms (plants and animals).

3.10.2 Indicators of Diet and Metabolism

A similarity in $\delta^{13}C$-values between animals and plants from the same environment was first noted by Craig (1953). Later, many field and laboratory studies have documented small shifts of 1–2‰ in ^{13}C and even smaller shifts in ^{34}S between an organism and its food source (DeNiro and Epstein 1978; Peterson and Fry 1987; Fry 1988).

This technique has been widely used in tracing the origin of carbon, sulfur and nitrogen in modern and prehistoric food webs (e.g., De Niro and Epstein 1978) and culminates in the classic statement "You are what you eat plus/minus a few permil". The precise magnitude of the isotopic difference between diet and a particular tissue depends on the extent to which the heavy isotope is incorporated or lost during synthesis. In contrast to carbon and sulfur, nitrogen shows a 3–4‰ enrichment in ^{15}N in the muscle tissue, bone collagen or whole organism relative to the food source (Minigawa and Wada 1984; Schoeninger and DeNiro 1984). When this fractionation is taken into account, nitrogen isotopes are also a good indicator of dietary source. Due to the preferential excretion of ^{14}N, the 3–4‰ shift in $\delta^{15}N$-values occurs with each trophic level along the food chain and thus provides a basis for establishing trophic structure.

Archaeological studies have used the stable isotope analysis of collagen extracted from fossil bones to reconstruct the diet of prehistoric human populations (e.g. Schwarcz et al. 1985).

Carbon isotopes have been used successfully to explore changes in the vegetation on Earth. Ecosystems with abundant C4 biomass have been documented only from the late Neogene to the present (Cerling et al. 1993, 1997). In South Asia, isotopic records from soil carbonates and tooth enamel reveal a dramatic increase in the abundance of C4 plants at 7 ± 1 million years ago (Quade et al. 1992; Quade and Cerling 1995 and others).

3.10.3 Tracing Anthropogenic Organic Contaminant Sources

Of special concern for the environment are chlorinated hydrocarbons which are extensively used in many industries and which are, therefore, a potential source of environmental pollution. Coupling the study of C- with Cl-isotopes represents a powerful tool to trace sources and pathways of chlorinated hydrocarbons (Heraty et al. 1999; Huang et al. 1999; Jendrzewski et al. 2001). The use of C- and Cl-isotopes as tracers of pollution requires the isotope ratios of the polluting product to be significantly different from the natural abundance. Jendrzewski et al. (2001) demonstrated on a set of chlorinated hydrocarbons from various manufacturers that both carbon ($\delta^{13}C$ from -24 to $-51‰$) and chlorine ($\delta^{37}Cl$ from -2.7 to $+3.4‰$) had a large compositional range. The range for chlorine is especially significant, because it is much larger than that of inorganic Cl and distinctly different from values for inorganic compounds. Natural attenuation processes, however, may preclude easy application of the isotope ratios as a tracer of pollution. It is expected that the first-formed products of incomplete degradation reactions will be depleted in the heavier isotope resulting in an enrichment of the remaining material. Besides bacterial degradation, isotope fractionations during evaporation and migration of chlorinated hydrocarbons may also affect the isotope composition.

3.10.4 Fossil Organic Matter

Similar to living organisms, organic matter in the geosphere is a complex mixture of particulate organic remains and living bacterial organisms. This complexity results from the multitude of source organisms, variable biosynthetic pathways, and transformations that occur during diagenesis and catagenesis. Of special importance are different stabilities of organic compounds in biological and inorganic degradation processes during diagenesis and subsequent metamorphism.

Immediately after burial of the biological organic material into sediments, complex diagenetic changes occur. Two processes have been proposed to explain the observed changes in carbon isotope composition: (1) preferential degradation of organic compounds which have different isotope composition compared to the preserved organic compounds. Since easily degradable organic compounds like amino acids are enriched in ^{13}C compared to the more resistant compounds like lipids, this causes a shift to slightly more negative δ-values. (2) Isotope fractionations due to metabolism of microorganisms. Early diagenesis does not only encompass degradation of organic matter, but also production of new compounds that potentially have different isotopic compositions than the original source material. A classic example has been presented by Freeman et al. (1990) analyzing hydrocarbons from the Messel shale in Germany (see Table 3.2). Considered as a whole, recent marine sediments show a mean $\delta^{13}C$-value of $-25‰$. Some ^{13}C loss occurs with transformation to kerogen, leading to an average $\delta^{13}C$-value of $-27.5‰$ (Hayes et al. 1983). This ^{13}C depletion might be best explained by the large losses of CO_2 that occur during

the transformation to kerogen and which are especially pronounced during the decarboxylation of some ^{13}C-rich carboxyl groups. With further thermal maturation the opposite effect (a ^{13}C enrichment) is observed. Experimental studies of Chung and Sackett (1979), Peters et al. (1981) and Lewan (1983) indicate that thermal alteration produces a maximum ^{13}C change of about +2‰ in kerogens. Changes of more than 2‰ are most probably not due to isotope fractionation during thermal degradation of kerogen, but rather to isotope exchange reactions between kerogen and carbonates.

Whereas carbon tends to be preserved during diagenesis and maturation, hydrogen is exchanged during various diagenetic reactions with environmental water. δD-values of organic compounds, therefore, can be regarded as a continuously evolving system that can provide information about processes during burial of sedimentary rocks (Sessions et al. 2004). Radke et al. (2005) examined how maturation processes alter the δD-value of individual compounds. They demonstrated that aliphatic hydrocarbons are most favorable to record the primary composition because they resist hydrogen exchange. Pedentschouk et al. (2006) argued that *n*-alkanes and isoprenoids have the potential to preserve the original biological signal till the onset of oil generation.

The isotopic compositions of the end products of organic matter diagenesis – carbon dioxide, methane, and insoluble complex kerogen – may record the primary depositional environment. Boehme et al. (1996) determined the C-isotope budget in a well-defined coastal site. These authors demonstrated that the degradation of biogenic carbon proceeds via sulfate reduction and methanogenesis. The dominant carbon isotope effect during diagenesis is associated with methanogenesis, which shifts the carbon isotope value of the carbon being buried towards higher ^{13}C-contents.

3.10.5 Marine vs. Terrestrial Organic Matter

The commonly observed difference in δ^{13}C of about 7‰ between organic matter of marine primary producers and land plants has been successfully used to trace the origin of recent organic matter in coastal oceanic sediments (e.g. Westerhausen et al. 1993). Samples collected along riverine-offshore transects reveal very consistent and similar patterns of isotopic change from terrestrial to marine values (for instance Sackett and Thompson 1963; Kennicutt et al. 1987 and others). It is evident that the decreasing contribution of terrestrial organic matter to distal marine sediments is reflected in the C-isotope composition of the marine sedimentary organic matter. But even deep-sea sediments deposited in areas remote from continents may contain a mixture of marine and continental organic matter.

The C-isotope difference between terrestrial and marine organic matter cannot, however, be used as a facies indicator as originally thought. Carbon isotope fractionation associated with the production of marine organic matter has changed with geologic time, while that associated with the production of terrestrial organic matter has been nearly constant (Arthur et al. 1985; Hayes et al. 1989; Popp et al. 1989; Whittacker and Kyser 1990). Particularly intriguing has been the unusually

^{13}C-depleted organic matter in Cretaceous marine sediments, which has been interpreted as resulting from elevated aqueous CO_2 concentrations allowing for greater discrimination during algal photosynthesis.

Hayes et al. (1999) systematically evaluated the carbon isotope fractionation between carbonates and coeval organic matter for the past 800 Ma. They concluded that earlier assumptions of a constant fractionation between carbonate and organic matter is untenable and that fractionations may vary by about 10‰ depending on the dominant biogeochemical pathway as well on environmental conditions.

3.10.6 Oil

Questions concerning the origins of coal and petroleum center on three topics: the nature and composition of the parent organisms, the mode of accumulation of the organic material, and the reactions whereby this material was transformed into the end products.

Petroleum or crude oil is a naturally occurring complex mixture, composed mainly of hydrocarbons. Although there are, without any doubt, numerous compounds that have been formed directly from biologically produced molecules, the majority of petroleum components are of secondary origin, either decomposition products or products of condensation and polymerization reactions.

Combined stable isotope analysis (^{13}C, D, ^{15}N, ^{34}S) has been used successfully in petroleum exploration (Stahl 1977; Schoell 1984; Sofer 1984). The isotopic composition of crude oil is mainly determined by the isotopic composition of its source material, more specifically, the type of kerogen and the sedimentary environment in which it has been formed and by its degree of thermal alteration (Tang et al. 2005). Other secondary effects like biodegradation, water washing, and migration distances appear to have only minor effects on its isotopic composition.

Variations in ^{13}C have been the most widely used parameter. Generally, oils are depleted by 1–3‰ compared to the carbon in their source rocks. The various chemical compounds within crude oils show small, but characteristic $\delta^{13}C$-differences. With increasing polarity the ^{13}C-content increases from the saturated to aromatic hydrocarbons to the heterocomponents (N, S, O compounds) and to the asphaltene fraction. These characteristic differences in ^{13}C have been used for correlation purposes. Sofer (1984) plotted the ^{13}C-contents of the saturated and aromatic fractions against each other. Oils and suspected source rock extracts that are derived from similar types of source materials will plot together in such a graph whereas those derived from different types of source material will plot in other regions of the graph. The approach of Stahl (1977) and Schoell (1984) is somewhat different: the ^{13}C-contents of the different fractions are plotted as shown in Fig. 3.37. In this situation, oils derived from the same source rock will define a near linear relationship in the plot. Figure 3.38 illustrates a positive oil–oil correlation and a negative oil–source rock correlation.

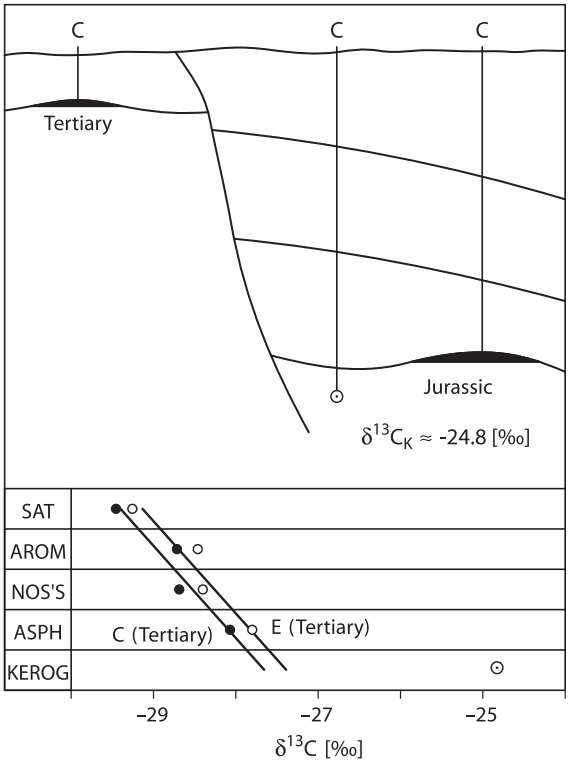

Fig. 3.37 "Petroleum-type curves" of different oil components from the North Sea showing a positive oil-oil correlation and a negative source rock – oil correlation (*SAT* saturated hydrocarbons, *AROM* aromatic hydrocarbons, *NOSS* heterocomponents, *ASPH* asphaltenes (Stahl, 1977)

More recently combined compound specific ^{13}C- and D-analyses have been applied in a number of areas of petroleum geochemistry. Tang et al. (2005) demonstrated that variation in δD-values of long chain hydrocarbons provide a sensitive measure of the extent of thermal maturation. Such studies have demonstrated that thermal maturation processes tend to alter the shape of the curves, particularly the curves for the saturate fraction, making correlations more difficult. Furthermore oil migration might affect the isotope composition. Generally, a slight ^{13}C depletion is observed with migration distance, which is caused by a relative increase in the saturate fraction and a loss in the more ^{13}C-enriched aromatic and asphaltene fraction.

Compound-specific analyses also indicate that ^{13}C differences between the isoprenoid-hydrocarbons, pristane, and phytane, for which a common origin from chlorophyll is generally assumed, point to different origins of these two components (Freeman et al. 1990). Other classes of biomarkers, such as the hopanes, are also not always derived from a common precursor. Schoell et al. (1992) have demonstrated that hopanes from an immature oil can be divided into two groups: one that is ^{13}C depleted by 2–4‰ relative to the whole oil, whereas the other is depleted by 9‰, which suggests that the latter group is derived from chemoautotrophic bacteria which utilize a ^{13}C-depleted source. These results indicate that the origin and fate of organic compounds are far more complicated than was previously assumed.

3.10.7 Coal

Carbon and hydrogen isotope compositions of coals are rather variable (Schiegl and Vogel 1970; Redding et al. 1980; Smith et al. 1982; Schimmelmann et al. 1999; Mastalerz and Schimmelmann 2002). Different plant communities and climates may account for these variations. Due to the fact that during coalification, the amount of methane and other higher hydrocarbons liberated is small compared to the total carbon reservoir, very little change in the carbon isotope composition seems to occur with increasing grade of coalification.

The D/H ratio in coals is usually measured on total hydrogen, although it consists of two portions: exchangeable and nonexchangeable hydrogen. In lignite up to 20% of hydrogen consists of isotopically labile hydrogen that exchanges fast and reversibly with ambient water. With increasing temperature (maturity) the exchangeable portion decreases to about 2% (Schimmelmann et al. 1999; Mastalerz and Schimmelmann 2002). Nonexchangeable organic hydrogen may have preserved original biochemical D/H ratios. δD-values in coals typically become isotopically heavier with increasing maturity, which suggests that exchange between organic hydrogen and formation water occurs during thermal maturation.

The origin and distribution of sulfur in coals is of special significance, because of the problems associated with the combustion of coals. Sulfur in coals usually occurs in different forms, as pyrite, organic sulfur, sulfates, and elemental sulfur. Pyrite and organic sulfur are the most abundant forms. Organic sulfur is primarily derived from two sources: the originally assimilated organically bound plant sulfur preserved during the coalification process and biogenic sulfides which reacted with organic compounds during the biochemical alteration of plant debris.

Studies by Smith and Batts (1974), Smith et al. (1982), Price and Shieh (1979) and Hackley and Anderson (1986) have shown that organic sulfur exhibits rather characteristic S-isotope variations, which correlate with sulfur contents. In low-sulfur coals δ^{34}S-values of organic sulfur are rather homogeneous and reflect the primary plant sulfur. By contrast, high-sulfur coals are isotopically more variable and typically have more negative δ^{34}S-values, suggesting a significant contribution of sulfur formed during bacterial processes.

3.10.8 Natural Gas

Natural gases are dominated by a few simple hydrocarbons, which may form in a wide variety of environments. While methane is always a major constituent of the gas, other components may be higher hydrocarbons (ethane, propane, butane), CO_2, H_2S, N_2 and rare gases. Two different types of gas occurrences can be distinguished – biogenic and thermogenic gas – the most useful parameters in distinguishing both types are their $^{13}C/^{12}C$ and D/H ratios. Complications in assessing sources of natural gases are introduced by mixing, migration, and oxidative alteration processes. For practical application an accurate assessment of the origin of a gas, the maturity

of the source rock and the timing of gas formation would be desirable. A variety of models has been published that describes the carbon and hydrogen isotope variations of natural gases (Berner et al. 1995; Galimov 1988; James 1983, 1990; Rooney et al. 1995; Schoell 1983, 1988).

Rather than using the isotopic composition of methane alone James (1983, 1990) and others have demonstrated that carbon isotope fractionations between the hydrocarbon components (particularly propane, iso-butane and normal butane) within a natural gas can be used with distinct advantages to determine maturity, gas–source rock and gas–gas correlations. With increasing molecular weight, from C_1 to C_4, a ^{13}C enrichment is observed which approaches the carbon isotope composition of the source.

Genetic models for natural gases were based in the past, primarily on field data and on empirical models. More recently, mathematical modeling based on Rayleigh distillation theory and kinetic isotopic theory (Rooney et al. 1995; Tang et al. 2000) may explain why, in a single gas $\delta^{13}C$-values increase from C_1 to C_4 and why in different gases $\delta^{13}C$-values of a given hydrocarbon increase with increasing thermal maturity. Such models may provide information on the isotope composition of each gas at any stage of generation.

Apart from gas sources and formation mechanisms, isotope effects during migration might affect the isotope composition of natural gas. Early experimental work has indicated that migrating methane could be enriched in ^{12}C or ^{13}C depending on the mechanism of migration and on the properties of the medium through which the gas is moving. Experiments by Zhang and Krooss (2001) on natural shales with different organic matter contents demonstrate variable ^{13}C depletions (1–3‰) during migration, which depend on the amount of organic matter in shales.

Of special interest in recent years has been the analysis of natural gas hydrates that form in marine sediments and polar rocks when saline pore waters are saturated with gas at high pressure and low temperature. Large $\delta^{13}C$ and δD-variations of hydrate bound methane, summarized by Kvenvolden (1995) and Milkov (2005), suggest that gas hydrates represent complex mixtures of gases of both microbial and thermogenic origin. The proportions of both gas types can vary significantly even between proximal sites.

As has been proposed by numerous studies (e.g., Röhl et al. 2000; Dickens 2003) the massive release of gas hydrates could modify climate. The best example for this hypothesis are sedimentary rocks deposited at around 55 Ma during the Paleocene–Eocene thermal maximum, where a $\delta^{13}C$ decrease of 2–3‰ in carbonate–carbon is interpreted as a consequence of an abrupt thermal release of gas–hydrate methane and its subsequent incorporation into the carbonate pool.

3.10.8.1 Biogenic Gas

According to Rice and Claypool (1981), over 20% of the world's natural gas accumulations are of biogenic origin. Biogenic methane commonly occurs in recent anoxic sediments and is well documented in both freshwater environments, such as

lakes and swamps, and in marine environments, such as estuaries and shelf regions. Two primary metabolic pathways are generally recognized for methanogenesis: fermentation of acetate and reduction of CO_2. Although both pathways may occur in marine and freshwater environments, CO_2-reduction is dominant in the sulfate-free zone of marine sediments, while acetate fermentation is dominant in freshwater sediments.

During microbial action, kinetic isotope fractionations on the organic material by methanogenic bacteria result in methane that is highly depleted in ^{13}C, typically with $\delta^{13}C$-values between -110 and $-50‰$ (Schoell 1984, 1988; Rice and Claypool 1981; Whiticar et al. 1986). In marine sediments, methane formed by CO_2 reduction is often more depleted in ^{13}C than methane formed by acetate fermentation in freshwater sediments. Thus, typical $\delta^{13}C$ ranges for marine sediments are between -110 and $-60‰$, while those for methane from freshwater sediments are from -65 to $-50‰$ (Whiticar et al. 1986; Whiticar 1999).

The difference in composition between methane of freshwater and of marine origin is even more pronounced on the basis of hydrogen isotopes. Marine bacterial methane has δD-values between -250 and $-170‰$ while biogenic methane in freshwater sediments is strongly depleted in D with δD-values between -400 and $-250‰$ (Whiticar et al. 1986; Whiticar 1999). Different hydrogen sources may account for these large differences: formation waters supply the hydrogen during CO_2 reduction, whereas during fermentation up to three quarters of the hydrogen come directly from the methyl group, which is extremely depleted in D.

3.10.8.2 Thermogenic Gas

Thermogenic gas is produced when organic matter is deeply buried and – as a consequence – temperature rises. Thereby, increasing temperatures modify the organic matter due to various chemical reactions, such as cracking and hydrogen diproportionation in the kerogen. ^{12}C–^{12}C bonds are preferentially broken during the first stages of organic matter maturation. As this results in a ^{13}C-enrichment of the residue, more ^{13}C–^{12}C bonds are broken with increasing temperatures which produces higher $\delta^{13}C$-values. Thermal cracking experiments carried out by Sackett (1978) have confirmed this process and demonstrated that the resulting methane is depleted in ^{13}C by some 4–25‰ relative to the parent material. Thus, thermogenic gas typically has $\delta^{13}C$-values between -50 and $-20‰$ (Schoell 1980, 1988). Gases generated from nonmarine (humic) source rocks are isotopically enriched relative to those generated from marine (sapropelic) source rocks at equivalent levels of maturity. In contrast to $\delta^{13}C$-values, δD-values are independent of the composition of the precursor material, but solely depend on the maturity of kerogen.

In conclusion, the combination of carbon and hydrogen isotope analysis of natural gases is a powerful tool to discriminate different origins of gases. In a plot of $\delta^{13}C$ vs. δD (see Fig. 3.38) not only is a distinction of biogenic and thermogenic gases from different environments clear, but it is also possible to delineate mixtures between the different types.

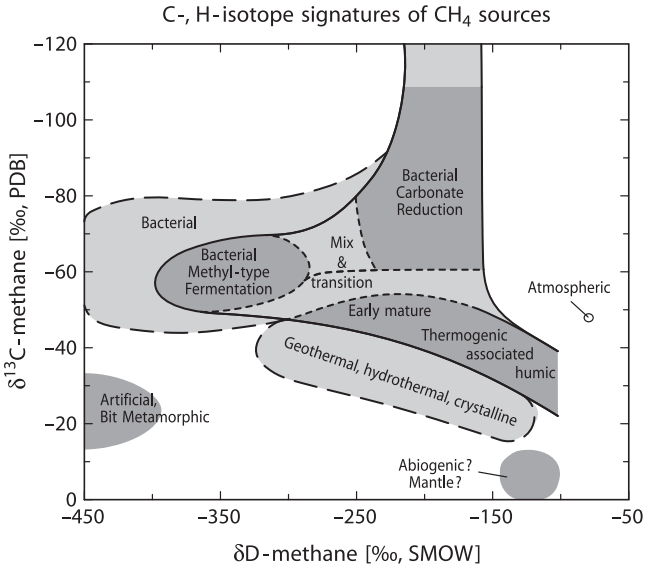

Fig. 3.38 δ^{13}C and δD variations of natural gases of different origins (after Whiticar, 1999)

Nitrogen is sometimes a major constituent of natural gases, but the origin of this nitrogen is still enigmatic. While a certain fraction is released from degrading sedimentary organic matter during burial, several nonsedimentary sources of nitrogen may also contribute to the natural gas. By analyzing nitrogen-rich natural gases from California's Great Valley, Jenden et al. (1988) demonstrated, however, that these gases had a complex origin involving mixing of multiple sources. These authors interpreted relatively constant δ^{15}N-values between 0.9 and 3.5‰ as indicating a deep-crustal metasedimentary origin. Hydrocarbon-rich and nitrogen-rich gases can thus be genetically unrelated.

3.10.8.3 Abiogenic Methane

Abiogenic methane is defined as methane that does not involve biogenic organic precursors (Welhan 1988). Methane emanating in mid-ocean ridge hydrothermal systems is one of the occurrences for which an abiogenic formation can be postulated with confidence. Considerably higher δ^{13}C-values than biogenic methanes (up to −7‰; Abrajano et al. 1988) was thought to be the characteristic feature of abiogenic methane. Recently, Horita and Berndt (1999) demonstrated that abiogenic methane can be formed under hydrothermal conditions in the presence of a nickel–iron catalyst. Isotope fractionations induced by the catalyst, however, result in very low δ^{13}C-values. Another important source of abiogenic methanogenesis has been found in crystalline rocks from the Canadian and Ferroscandian shield areas

(Sherwood-Lollar et al. 1993, 2002). In contrast to thermogenic hydrocarbons where higher hydrocarbons (ethane, propane, butane) are enriched in ^{13}C and D relative to methane, abiogenic alkanes may be depleted in ^{13}C and D relative to methane. These depletion patterns relative to methane may be produced by polymerization reactions of methane precursors (Sherwood-Lollar et al. 2002).

In recent years more and more experimental and natural evidence (Foustoukous and Seyfried 2004; McCollom and Seewald 2006; Fiebig et al. 2007; Taran et al. 2007) have been presented that Fischer–Tropsch type reactions at elevated temperatures may produce abiogenic methane and higher hydrocarbons. Thus abiogenic hydrocarbons should exist on the modern and early Earth, but it remains problematic to distinguish abiogenic from biogenic organic compounds on the basis of their $\delta^{13}C$ signatures (Taran et al. 2007).

3.11 Sedimentary Rocks

Sediments are the weathering products and residues of magmatic, metamorphic, and sedimentary rocks and reflect weathering, erosion, transport and accumulation in water, and air. As a result, sediments may be complex mixtures of material that has been derived from multiple sources. It is convenient to consider sedimentary rocks, and the components of sedimentary rocks, in two categories: clastic and chemical. Transported fragmental debris of all kinds makes up the clastic component of the rock. Inorganic and organic precipitates from water belong to the chemical constituents. According to their very different constituents and low temperatures of formation, sedimentary rocks may be extremely variable in isotopic composition. For example, the $\delta^{18}O$-values of sedimentary rocks span a large range from about +10 (certain sandstones) to about $+44‰$ (certain cherts).

3.11.1 Clay Minerals

Savin and Epstein (1970a, b) and Lawrence and Taylor (1971) established the general isotope systematics of clay minerals from continental and oceanic environments. Subsequent reviews by Savin and Lee (1988) and Sheppard and Gilg (1996) have summarized the isotope studies of clay minerals applied to a wide range of geological problems. All applications depend on the knowledge of isotope fractionation factors between clay minerals and water, the temperature, and the time when isotopic exchange with the clay ceased. Because clay minerals may be composed of a mixture of detrital and authigenic components, and because particles of different ages may have exchanged to varying degrees, the interpretation of isotopic variations of clay minerals requires a firm understanding of the clay mineralogy of a given sediment.

By comparison with many other silicate minerals, isotope studies of natural clays are complicated by a number of special problems related to their small particle size and, hence, much larger specific surface area and the presence of interlayer water in certain clays. Surfaces of clays are characterized by 1 or 2 layers of adsorbed water. Savin and Epstein (1970a) demonstrated that adsorbed and interlayer water can exchange its isotopes with atmospheric water vapor in hours. Complete removal of interlayer water for analysis with the total absence of isotopic exchange between it and the hydroxyl group, may not be possible in all instances (Lawrence and Taylor 1971).

One portion of the oxygen in clay minerals occurs as the hydroxyl ion. Hamza and Epstein (1980), Bechtel and Hoernes (1990) and Girard and Savin (1996) have attempted to separate the hydroxyl and nonhydoxyl bonded oxygen for separate isotope analysis. Techniques include thermal dehydroxylation and incomplete fluorination, both of which indicate that hydroxyl oxygen is considerably depleted in ^{18}O relative to nonhydroxyl oxygen.

Do natural clay minerals retain their initial isotopic compositions? Evidence concerning the extent of isotopic exchange for natural systems is contradictory (Sheppard and Gilg 1995). Many clay minerals such as kaolinite, smectite, and illite are often out of equilibrium with present day local waters. This is not to imply that these clay minerals never undergo any postformational or retrograde exchange. Sheppard and Gilg (1995) concluded that convincing evidence for complete O- and/or H-isotope exchange without recrystallization is usually lacking, unless the clay has been subjected to either higher temperatures or an unusual set of geological circumstances. Thus, isotopic compositions of clay minerals that formed in contact with meteoric waters should have isotopic compositions that plot on subparallel lines to the Meteoric Water Line, the offset being related to their respective fractionation factor (see Fig. 3.39). This implies that some information of past environments is usually recorded in clay minerals and in suitable cases can be used as a paleoclimate indicator (Stern et al. 1997; Chamberlain and Poage 2000; Gilg 2000).

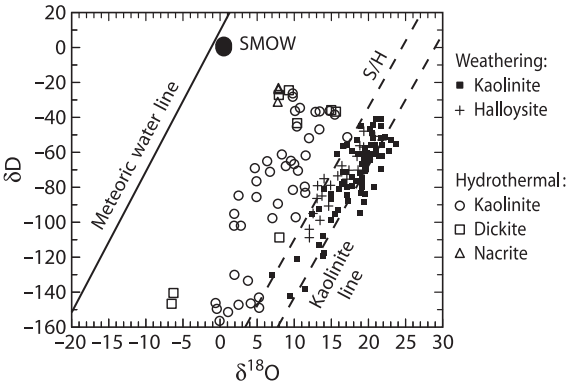

Fig. 3.39 δD and $\delta^{18}O$ values for kaolonites and related minerals from weathering and hydrothermal environments. The Meteoric Water Line, kaolinite weathering and supergene/hypogene (S/H) lines are given for reference (after Sheppard and Gilg 1995)

3.11.2 Clastic Sedimentary Rocks

Clastic sedimentary rocks are composed of detrital grains that normally retain the oxygen isotope composition of their source and of authigenic minerals formed during weathering and diagenesis, whose isotopic composition is determined by the physicochemical environment in which they formed. This means authigenic minerals formed at low temperatures will be enriched in ^{18}O compared to detrital minerals of igneous origin (Savin and Epstein 1970b). Due to the difficulty of separating authigenic overgrowths from detrital cores, few studies of this kind have been reported in the literature. However, recent improvements in the precision of ion microbe analysis with high spatial resolution (1–10 μm) both types of quartz can be clearly distinguished (see Fig. 3.40, Kelly et al. 2007). These authors suggested that the homogeneous $\delta^{18}O$-values of quartz overgrowth formed from meteoric waters at low temperatures (10–30°C).

How ^{18}O-enriched the authigenic mineral will be is determined by fluid composition, temperature, and the effective mineral/water ratio. Is the fluid a low-^{18}O meteoric water, the oxygen isotope composition of the precipitating mineral will have a low-^{18}O signature, assuming no change in temperature (Longstaffe 1989)? Thus, the changes that occur in sedimentary rocks during diagenesis are largely a function of fluid composition, fluid/rock ratio and temperature.

One way to estimate temperatures employs the oxygen isotope composition of diagenetic assemblages. For example, using quartz – illite pairs from the Precambrian Belt Supergroup, Eslinger and Savin (1973) calculated temperatures that range from 225 to 310°C, with increasing depth. In this case the $\delta^{18}O$-values were consistent with the observed mineralogy and fractionations between minerals are reasonable for the grade of burial metamorphism. This approach assumes that the diagenetic minerals used have equilibrated their O-isotopes with each other and that no retrograde re-equilibration occurred following maximum burial.

Another application of stable isotopes in clastic rocks is the analysis of weathering profiles, which can potentially provide insight into the continental climate during

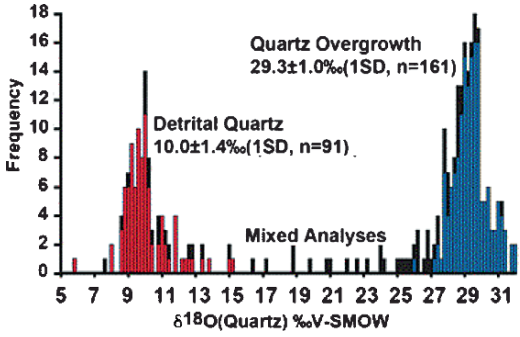

Fig. 3.40 Histogram of $\delta^{18}O$-values of quartz in sandstone from 6-10 μm spots by ion microprobe. Mixed analyses are on the boundary of detrital quartz and quartz overgrowths (Kelly et al. 2007)

their formation. Despite this potential, only few studies (Bird and Chivas 1989; Bird et al. 1992) have used this approach because of the (1) imprecise knowledge of mineral–water fractionations at surficial temperatures and (2) the difficulty of obtaining pure phases from complex, very fine grained rocks. Bird et al. (1992) developed partial dissolution techniques and used this methodology to separate nine pure minerals from a lateritic soil in Haiti (see Fig. 3.41). The measured δ^{18}O-values for some minerals agree with $^{18}O/^{16}O$ ratios predicted from available fractionation factors, whereas other do not. Discrepancies might be due to incorrect fractionation factors for the respective minerals or to processes that may have influenced the formation of particular minerals (e.g., evaporation) (Bird et al. 1992).

Lastly, the detrital minerals in clastic sediments can be used for provenance studies. If not recrystallized, many common rock-forming minerals, such as quartz, muscovite, garnets, etc. can retain their original source rock compositions up to medium-grade metamorphic conditions. Hence, they can potentially be used as tracers of provenance to the sediments. Applications of this type of approach are useful, particularly for siliciclastic sediments that may lack other indicator minerals of provenance. Examples of such applications have been given by Vennemann et al. (1992, 1996) for the provenance of Archean Au- and U-bearing conglomerates of South Africa and Canada. δ^{18}O-values of well-dated zircons may be used to document changes with time in the composition of sediments (Valley et al. 2005) (see discussion on p. 116).

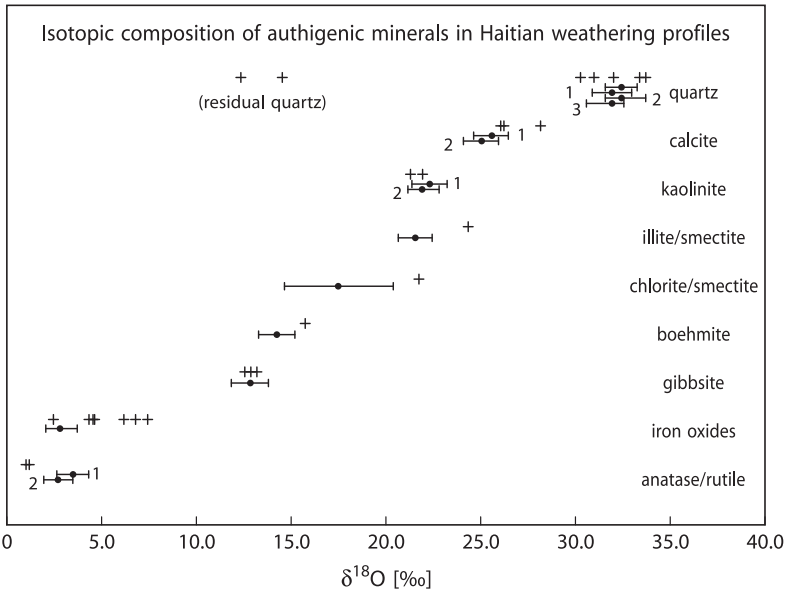

Fig. 3.41 Predicted (*bars*) and measured (*crosses*) oxygen isotope composition of separated minerals from Haitian weathering profiles. The ranges of predicted δ^{18}O values were calculated assuming a temperature of 25°C and a meteoric water δ^{18}O value of −3.1‰ (after Bird et al. 1992)

3.11.3 Biogenic Silica and Cherts

Due to the large oxygen isotope fractionation between SiO_2 and water at low temperatures, biogenic silica and cherts represent the "heaviest" oxygen isotope components in nature. Just as is the case for carbonates, the oxygen isotope composition of biogenic silica such as diatoms and radiolarians is potentially a paleoclimate indicator, which would enable the extension of climate records into oceanic regions depleted in $CaCO_3$ such as high latitude regions. Thus, a variety of techniques have been developed for the extraction of biogenic silica oxygen. The presence of loosely bound water within cherts and biogenic silica precipitates complicates measurements of the O-isotope composition of biogenic silica. At present three techniques exist:

1. *Controlled isotope exchange*. Using controlled exchange with waters of different isotope composition, Labeyrie and Juillet (1982) and Leclerc and Labeyrie (1987) were able to estimate the isotope ratio of both exchanged and unexchanged silica-bound oxygen.
2. *Stepwise fluorination.* Haimson and Knauth (1983) and Matheney and Knauth (1989) noted that the first fractions of oxygen were ^{18}O-depleted compared with oxygen recovered in later fractions, suggesting that the water-rich components of hydrous silica react preferentially in the early steps of fluorination.
3. *High temperature carbon reduction* (*Lücke et al. 2005*). The technique is based on inductive high temperature heating ($>1,500°C$) leading to carbon monoxide. It enables complete dehydration and decomposition in a single continuous process.

As investigations of Shemesh et al. (1992) have suggested, diatoms indeed can be used for reconstructions of ocean water temperatures. This conclusion was questioned by Schmidt et al. (1997), Brandriss et al. (1998), and Schmidt et al. (2001). These authors observed a 3–10‰ enrichment in fossil (sedimentary) diatoms compared to, those measured for recent laboratory cultures. Schmidt et al. (2001) demonstrated that the enrichment in sedimentary diatoms can be correlated with structural and compositional changes arising from the in situ condensation of Si–OH groups during silica maturation in surface sediments. In addition, these studies have also indicated significant variations in O-isotope fractionation between different types of biogenic silica precipitating species.

In sediments opaline skeletons are frequently dissolved and opal-CT is precipitated. As was shown from the early studies from Degens and Epstein (1962), like carbonates, cherts exhibit temporal isotopic variations: the older cherts having lower ^{18}O contents. Thus, cherts of different geological ages may contain a record of temperature, isotopic composition of ocean water, and diagenetic history. There is still debate about which of these factors is the most important. By analyzing silicon isotopes and oxygen isotopes, Robert and Chaussidon (2006) concluded that temperature changes are the dominant factor in the Precambrian.

3.11.4 Marine Carbonates

3.11.4.1 Oxygen

In 1947, Urey discussed the thermodynamics of isotopic systems and suggested that variations in the temperature of precipitation of calcium carbonate from water should lead to measurable variations in the $^{18}O/^{16}O$ ratio of the calcium carbonate. He postulated that the determination of temperatures of the ancient oceans should be possible, in principle, by measuring the ^{18}O content of fossil shell calcite. The first paleotemperature "scale" was introduced by McCrea (1950). Subsequently, this scale has been refined several times. Through experiments which compare the actual growth temperatures of foraminifera with calculated isotope temperatures Erez and Luz (1983) determined the following temperature equation:

$$T^{\circ}\mathrm{C} = 17.0 - 4.52\left(\delta^{18}O_c - \delta^{18}O_w\right) + 0.03\left(\delta^{18}O_c - \delta^{18}O_w\right)^2,$$

where $\delta^{18}O_c$ is the O-isotope composition of CO_2 derived from carbonate and $\delta^{18}O_w$ is the O-isotope composition of CO_2 in equilibrium with water at 25°C.

According to this equation an ^{18}O increase of 0.26‰ in carbonate represents a 1°C temperature decrease. Bemis et al. (1998) have re-evaluated the different temperature equations and demonstrated that they can differ as much as 2°C in the temperature range between 5 and 25°C. The reason for these differences is that in addition to temperature and water isotopic composition, the $\delta^{18}O$ of a shell may be affected by the carbonate ion concentration in sea water and by photosynthetic activity of algal symbionts.

Before a meaningful temperature calculation of a fossil organism can be carried out several assumptions have to be fulfilled. The isotopic composition of an aragonite or calcite shell will remain unchanged until the shell material dissolves and recrystallizes during diagenesis. In most shallow depositional systems, C- and O-isotope ratios of calcitic shells are fairly resistant to diagenetic changes, but many organisms have a hollow structure allowing diagenetic carbonate to be added. With increasing depths of burial and time the chances of diagenetic effects generally increase. Because fluids contain much less carbon than oxygen, $\delta^{13}C$-values are thought to be less affected by diagenesis than $\delta^{18}O$-values. Criteria of how to prove primary preservation are not always clearly resolved. Schrag (1999) argued that carbonates formed in warm tropical surface oceans are particularly sensitive to the effects of diagenesis, because pore waters – having much lower temperatures than tropical surface waters – could shift the primary composition to higher δ-values. This is not the case for high latitude carbonates, where surface and pore fluids are quite similar in their average temperature.

Shell-secreting organisms to be used for paleotemperature studies must have been precipitated in isotope equilibrium with ocean water. As was shown by studies of Weber and Raup (1966a, b), some organisms precipitate their skeletal carbonate in equilibrium with the water in which they live, but others do not. Wefer and

Berger (1991) summarized the importance of the so-called "vital effect" on a broad range of organisms (see Fig. 3.42). For oxygen isotopes, most organisms precipitate $CaCO_3$ close to equilibrium; if disequilibrium prevails, the isotopic difference from equilibrium is rather small (Fig. 3.42). For carbon, disequilibrium is the rule, with

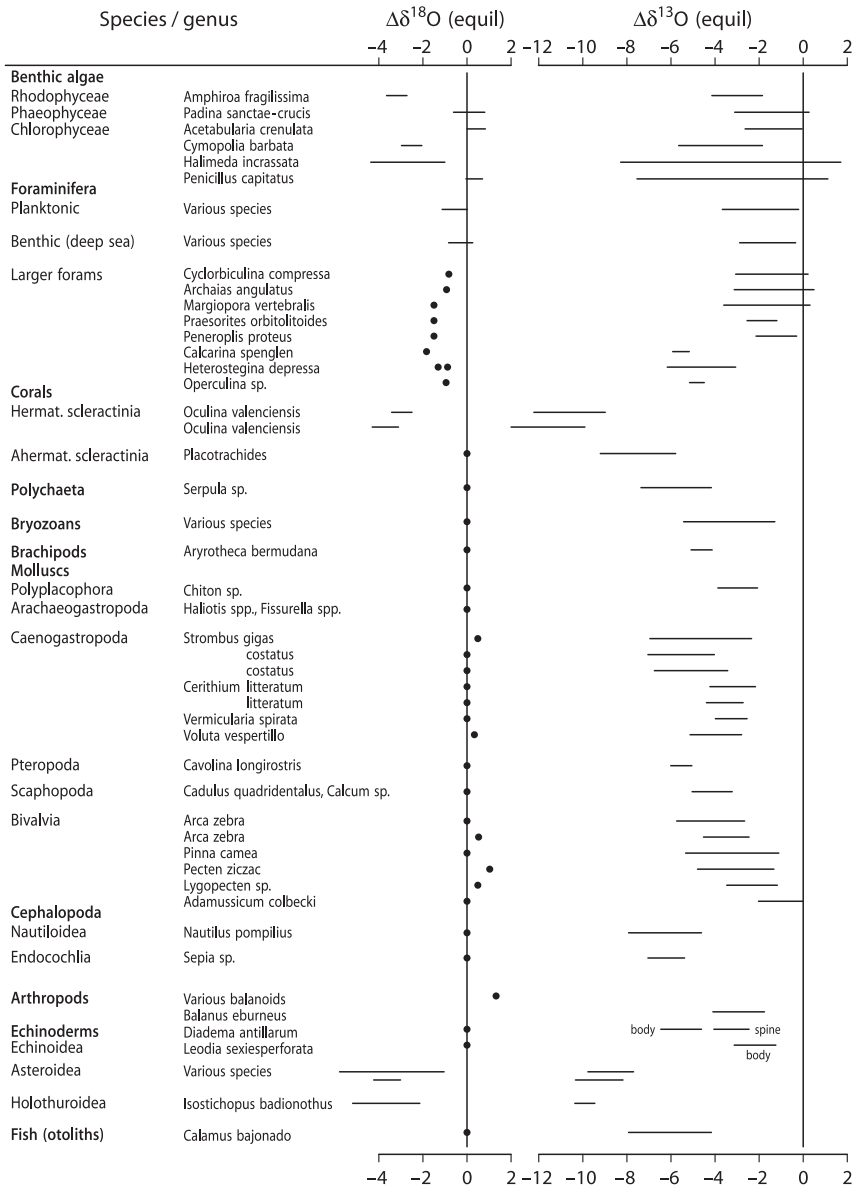

Fig. 3.42 $\Delta^{18}O$ and $\Delta^{13}C$ differences from equilibrium isotope composition of extant calcareous species (after Wefer and Berger, 1991)

δ^{13}C-values being more negative than expected at equilibrium. As discussed below, this does not preclude the reconstruction of the $^{13}C/^{12}C$ ratio of the palaeo-ocean waters.

Isotopic disequilibria effects can be classified as either metabolic or kinetic (McConnaughey 1989a, b). Metabolic isotope effects apparently result from changes in the isotopic composition of dissolved inorganic carbon in the neighborhood of the precipitating carbonate caused by photosynthesis and respiration. Kinetic isotope effects result from discrimination against ^{13}C and ^{18}O during hydration and hydroxylation of CO_2. Strong kinetic disequilibrium fractionation often is associated with high calcification rates (McConnaughey 1989).

Besides temperature, a variable isotopic composition of the ocean is another factor responsible for ^{18}O variations in foraminifera. A crucial control is salinity: ocean waters with salinities greater than 3.5% have a higher ^{18}O content, because ^{18}O is preferentially depleted in the vapor phase during evaporation, whereas waters with salinities lower than 3.5% have a lower ^{18}O content due to dilution by fresh waters, especially meltwaters. The other factor which causes variations in the isotopic composition of ocean water is the volume of low-^{18}O ice present on the continents. As water is removed from the ocean during glacial periods, and temporarily stored on the continents as ^{18}O-depleted ice, the $^{18}O/^{16}O$ ratio of the global ocean increases in direct proportion to the volume of continental and polar glaciers. The magnitude of the temperature effect vs. the ice volume effect can be largely resolved by separately analyzing planktonic and benthic foraminifera. Planktonic foraminifera live vertically dispersed in the upper water column of the ocean recording the temperature and the isotopic composition of the water. Figure 3.43 shows a latitudinal plot of annually averaged temperature distribution at the sea surface and 250 m depth together with the $\delta^{18}O$-values of different foraminifera species. The ^{18}O difference between shallow and deep-living planktonic foraminifera increases from nearly 0‰ in subpolar regions to ~3‰ in the tropics. The difference between shallow and deep-calcifying taxa can be used to calculate the vertical temperature gradient in the upper 250 m of the oceans.

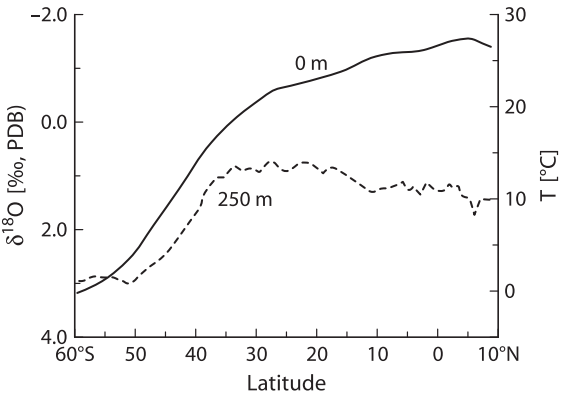

Fig. 3.43 Latitudinal distribution of O-isotope composition of planktonic foraminifera and yearly averaged temperature at sea surface and 250 m water depth (after Mulitza et al. 1997)

It is expected that the temperature of deep-water masses is more or less constant, as long as ice caps exist at the poles. Thus, the oxygen isotope composition of benthic organisms should preferentially reflect the change in the isotopic composition of the water (ice-volume effect), while the $\delta^{18}O$-values of planktonic foraminifera are affected by both temperature and isotopic water composition.

The best approach to disentangle the effect of ice volume and temperature is to study shell material from areas where constant temperatures have prevailed for long periods of time, such as the western tropical Pacific Ocean or the tropical Indian Ocean. On the other end of the temperature spectrum is the Norwegian Sea, where deep water temperatures are near the freezing point today and, therefore, cannot have been significantly lower during glacial time, particularly as the salinities are also already high in this sea. Within the framework of this set of limited assumptions, a reference record of the ^{18}O variations of a water mass which has experienced no temperature variations during the last climatic cycle can be obtained (Labeyrie et al. 1987).

It is also known from the investigations of coral reefs that during the last peak glacial period, sea level was lowered by 125 m. Fairbanks (1989) calculated that the ocean was enriched by 1.25‰ during the last glacial maximum (LGM) which indicates an ^{18}O difference of 0.1‰ for a 10 m increase of sea level. This relationship is obviously valid only for the last glacial period, because thicker ice shields might concentrate ^{16}O more than smaller ones. A direct approach to measuring the $\delta^{18}O$-value of sea water during the LGM is based on the isotopic composition of pore fluids (Schrag et al. 1996). Variations in deep water $\delta^{18}O$ caused by changes in continental ice volume diffuse down from the seafloor leaving a profile of $\delta^{18}O$ vs. depth in the pore fluid. Using this approach Schrag et al. (2002) estimated that the global $\delta^{18}O$ change of ocean water during LGM is 1.0 ± 0.1‰.

In addition to these variables, the interpretation of ^{18}O-values in carbonate shells is complicated by the sea water carbonate chemistry. In culture experiments with living foraminifera Spero et al. (1997) demonstrated that higher pH-values or increasing CO_3^{2-} concentrations result in isotopically lighter shells, which is due to changing sea water chemistry. As shown by Zeebe (1999) an increase of sea water pH by 0.2–0.3 units causes a decrease in ^{18}O of about 0.2–0.3‰ in the shell. This effect has to be considered for instance when samples from the last glacial maximum are analyzed.

3.11.4.2 Carbon

A large number of studies have investigated the use of ^{13}C-contents of foraminifera as a paleo-oceanographic tracer. As previously noted, $\delta^{13}C$-values are not in equilibrium with sea water. However, by assuming that disequilibrium $^{13}C/^{12}C$ ratios are, on average, invariant with time then systematic variations in C-isotope composition may reflect variations in ^{13}C content of ocean water. The first record of carbon isotope compositions in Cenozoic deep-sea carbonates was given by Shackleton and Kennett (1975). They clearly demonstrated that planktonic and benthic foraminifera

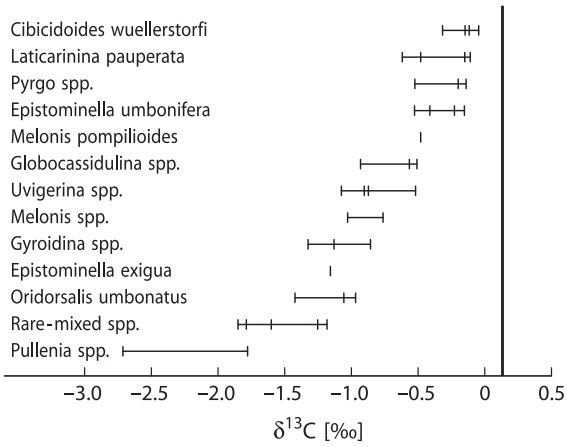

Fig. 3.44 $\delta^{13}C$ values of benthic foraminifera species. The $\delta^{13}C$ value for the dissolved bicarbonate in deep equatorial water is shown by the vertical line (after Wefer and Berger 1991)

yield consistent differences in $\delta^{13}C$-values, the former being enriched in ^{13}C by about 1‰ relative to the latter. This ^{13}C-enrichment in planktonic foraminifera is due to photosynthesis which incorporates ^{12}C preferentially in organic carbon and enriches surface waters in ^{13}C. A portion of the organic matter is transferred to deep waters, where it is reoxidized, which causes a ^{12}C-enrichment in the deeper water masses. Figure 3.44 presents $\delta^{13}C$-values of benthic foraminifera ranked according to their relative tendency to concentrate ^{13}C.

$\delta^{13}C$-values in planktonic and benthic foraminifera can be used to monitor CO_2 variations in the atmosphere by measuring the vertical carbon isotope gradient, which is a function of the biological carbon pump. This approach was pioneered by Shackleton et al. (1983), who showed that enhanced contrast between surface waters and deeper waters was correlated with intervals of reduced atmospheric CO_2 contents. Increased organic carbon production in surface waters (possibly caused by enhanced nutrient availability) leads to the removal of carbon from surface waters, which in turn draws down CO_2 from the atmospheric reservoir through re-equilibration.

Another application of carbon isotopes in foraminifera is to distinguish distinct water masses and to trace deep water circulation (Bender and Keigwin 1979; Duplessy et al. 1988). Since dissolved carbonate in the deeper waters becomes isotopically lighter with time and depths in the area of their formation due to the increasing oxidation of organic material, comparison of sites of similar paleodepth in different areas can be used to trace the circulation of deep waters as they move from their sources. Such a reconstruction can be carried out by analyzing $\delta^{13}C$-values of well-dated foraminifera.

Reconstructions of pathways of deep-water masses in the North Atlantic during the last 60,000 years have been performed by analyzing high resolution records of benthic foraminifera *Cibicides wuellerstorfi* as this species best reflects changes in the chemistry of bottom waters (Duplessy et al. 1988; Sarntheim et al. 2001). The initial $\delta^{13}C$-signature of North Atlantic Deep Water (NADW) is $\sim$1.3–1.5‰. As

NADW flows southward the ongoing oxidation of organic matter results in a progressive ^{13}C-depletion down to less than 0.4‰ in the Southern Ocean. Reductions in ^{13}C observed in many cores from the North-Atlantic (Sarntheim et al. 2001; Elliot et al. 2002) have been interpreted as meltwater input to the surface ocean (Heinrich events), which caused changes in deep water circulation.

3.11.5 Diagenesis

Diagenetic modification of carbonates may begin immediately after the formation of primary carbonates. Two processes may change the isotope composition of carbonate shells: (1) cementation and (2) dissolution and reprecipitation. Cementation means the addition of abiogenic carbonate from ambient pore waters. Cements added early after primary formation may be in equilibrium with ocean water, whereas late cements depend on the isotope composition of pore waters and temperature. Dissolution and reprecipitation occurs in the presence of a bicarbonate containing pore fluid and represents the solution of an unstable carbonate phase such as aragonite and the reprecipitation of a stable carbonate phase, mostly low Mg-calcite. Diagenetic modification may occur in two subsequent pathways, often termed as burial and meteoric diagenesis.

3.11.5.1 Burial Pathway

This type of diagenetic stabilization is best documented in deep-sea environments. Entrapped pore waters are of marine origin and in equilibrium with the assemblage of carbonate minerals. The conversion of sediment into limestone is not achieved by a chemical potential gradient, but rather through a rise in pressure and temperature due to deposition of additional sediments. In contrast to the meteoric pathway, fluid flow is confined to squeezing off pore waters upwards into the overlying sedimentary column. Theoretically, O-isotope ratios should not change appreciably with burial, because the $\delta^{18}O$ is of sea water origin. Yet, with increasing depth, the deep-sea sediments and often also the pore waters exhibit ^{18}O depletions by several permil (Lawrence 1989). The major reason for this ^{18}O depletion seems to be a low-temperature exchange with the oceanic crust in the underlying rock sequence. The ^{18}O shift in the solid phases is mostly due to an increase in temperature with increasing burial.

The other important diagenetic process is the oxidation of organic matter. With increasing burial, organic matter in sediments passes successively through different zones which are characterized by distinct redox reactions that are mediated by assemblages of specific bacteria. The usual isotopic changes of these processes will result in a shift towards lighter C-isotope values, the degree of ^{13}C-depletion being proportional to the relative contribution of carbon from the oxidation of organic

matter. Under special conditions of fermentation, the CO_2 released may be isotopically heavy, which may cause a shift in the opposite direction.

3.11.5.2 Meteoric Pathway

Carbonate sediments deposited in shallow marine environments are often exposed to the influence of meteoric waters during their diagenetic history. Meteoric diagenesis lowers $\delta^{18}O$- and $\delta^{13}C$-values, because meteoric waters have lower $\delta^{18}O$-values than sea water. For example, Hays and Grossman (1991) demonstrated that oxygen isotope compositions of carbonate cements depend on the magnitude of ^{18}O depletion of respective meteoric waters. $\delta^{13}C$-values are lowered because soil bicarbonate is ^{13}C-depleted relative to ocean water bicarbonate.

A more unusual effect of diagenesis is the formation of carbonate concretions in argillaceous sediments. Isotope studies by Hoefs (1970), Sass and Kolodny (1972), and Irwin et al. (1977) suggest that micobiological activity created localized supersaturation of calcite in which dissolved carbonate species were produced more rapidly than they could be dispersed by diffusion. Extremely variable $\delta^{13}C$-values in these concretions indicate that different microbiological processes participated in concretionary growth. Irwin et al. (1977) presented a model in which organic matter is diagenetically modified in sequence by (a) sulfate reduction, (b) fermentation, and (c) thermally induced abiotic CO_2 formation which can be distinguished on the basis of their $\delta^{13}C$-values (a) $-25‰$, (b) $+15‰$ and (c) $-20‰$.

3.11.6 Limestones

Early limestone studies utilized whole-rock samples, but later individual components, such as different generations of cements, have been analyzed (Hudson 1977; Dickson and Coleman 1980; Moldovanyi and Lohmann 1984; Given and Lohmann 1985; Dickson et al. 1990). These studies suggest that early cements exhibit higher $\delta^{18}O$ and $\delta^{13}C$-values with successive cements becoming progressively depleted in both ^{13}C and ^{18}O. The ^{18}O trend may be due to increasing temperatures and to isotopic evolution of pore waters. Employing a laser ablation technique, Dickson et al. (1990) identified a very fine-scale O-isotope zonation in calcite cements, which they interpreted as indicating changes in the isotope composition of the pore fluids.

3.11.7 Dolomites

Dolomite is found abundantly in Paleozoic and older strata, but is rare in younger rocks. There are only few locations where dolomite is forming today. In laboratory

experiments, researchers have struggled to produce dolomite at temperatures and pressures realistic to its natural formation. This is the crux of the "dolomite problem".

Since dolomitization takes place in the presence of water, oxygen isotope compositions are determined by the pore fluid composition and by the temperature of formation. Carbon isotope compositions, in contrast, are determined by the precursor carbonate composition, because pore fluids generally have low carbon contents so that the δ^{13}C-value of the precursor is generally retained. Two problems complicate the interpretation of isotope data to delineate the origin and diagenesis of dolomites: (1) extrapolations of high-temperature experimental dolomite–water fractionations to low temperatures suggest that at 25°C dolomite should be enriched in ^{18}O relative to calcite by 4–7‰ (e.g., Sheppard and Schwarcz 1970). On the other hand, the oxygen isotope fractionation observed between Holocene calcite and dolomite is somewhat lower, namely in the range between 2 and 4‰ (Land 1980; McKenzie 1984) The fractionation also may depend partly on the crystal structure, more specifically on the composition and the degree of crystalline order. (2) For many years it has not been possible to determine the equilibrium oxygen isotope fractionations between dolomite and water at sedimentary temperatures directly, because the synthesis of dolomite at these low temperatures is problematic. With the discovery, that bacteria mediate the precipitation of dolomite, Vasconcelos et al. (2005) presented however, a new paleothermometer enabling the reconstruction of temperature conditions of ancient dolomite deposits.

Figure 3.45 summarizes oxygen and carbon isotope compositions of some recent and Pleistocene dolomite occurences (after Tucker and Wright 1990). Variations in oxygen isotope composition reflect the involvement of different types of waters (from marine to fresh waters) and varying ranges of temperatures. With respect to carbon, δ^{13}C-values between 0 and 3‰ are typical of marine compositions. In the presence of abundant organic matter, negative δ^{13}C-values in excess of -20‰ indicate that carbon is derived from the decomposition of organic matter. Very positive δ^{13}C-values up to $+15$‰ result from fermentation of organic matter (Kelts and McKenzie 1982). Such isotopically heavy dolomites have been described, for example, from the Guaymas Basin, where dolomite formation has taken place in the zone of active methanogenesis.

3.11.8 Freshwater Carbonates

Carbonates deposited in freshwater lakes exhibit a wide range in isotopic composition, depending upon the isotopic composition of the rainfall in the catchment area, its amount and seasonality, the temperature, the rate of evaporation, the relative humidity, and the biological productivity. Lake carbonates typically consist of a matrix of discrete components, such as detrital components, authigenic precipitates, neritic, and benthic organisms. The separate analysis of such components has the potential to permit investigation of the entire water column. For example, the oxygen isotopic

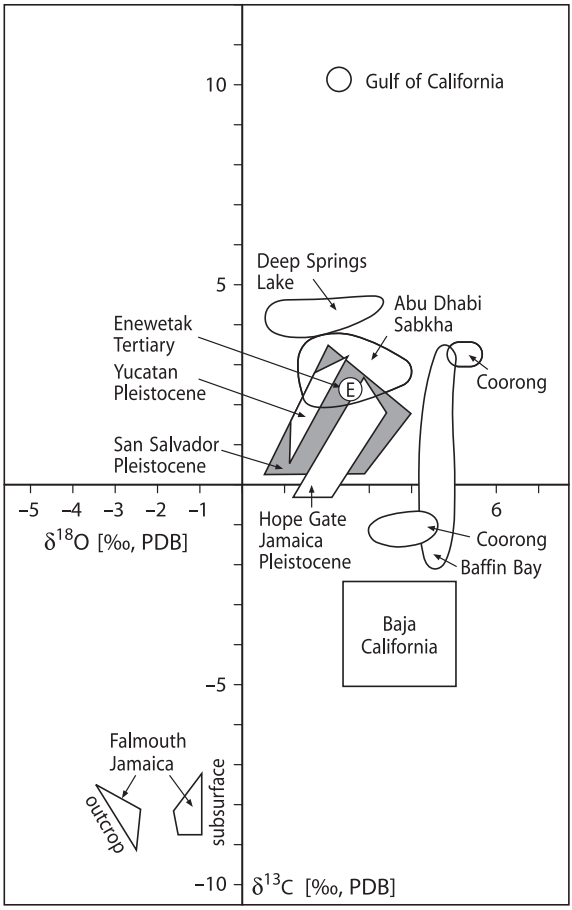

Fig. 3.45 Carbon and oxygen isotope compositions of some recent and Pleistocene dolomite occurrences (after Tucker and Wright 1990)

composition of authigenic carbonates and diatoms can be used to obtain a surface water signal of changes in temperature and meteoric conditions, while the composition of bottom dwellers can be used as a monitor of the water composition, assuming that the bottom water temperatures remained constant.

The carbon and oxygen isotope compositions of carbonate precipitated from many lakes show a strong covariance with time, typically in those lakes which represent closed systems or water bodies with long residence times (Talbot 1990). In contrast, weak or no temporal covariance is typical of lakes which represent open systems with short residence times. Figure 3.46 gives examples of such covariant trends. Each closed lake appears to have a unique isotopic identity defined by its covariant trend, which depends on the geographical and climatic setting of a basin, its hydrology and the history of the water body (Talbot 1990).

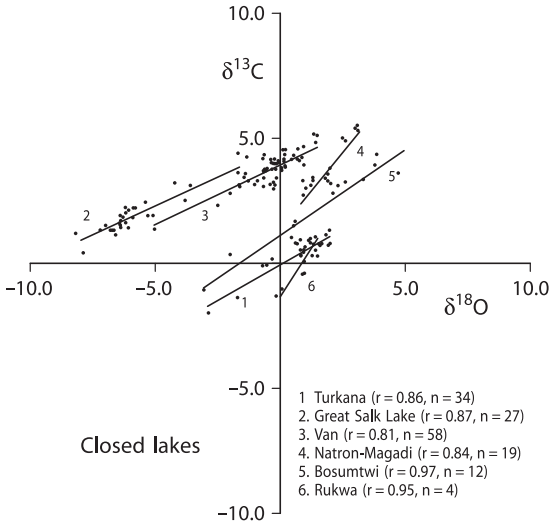

Fig. 3.46 Carbon and oxygen isotope compositions of freshwater carbonates from recently closed lakes (after Talbot, 1990)

3.11.9 Phosphates

The stable isotope composition of biogenic phosphates record a combination of environmental parameters and biological processes. Biogenic phosphate, $Ca_5(PO_4, CO_3)_3(F, OH)$, for paleoenvironmental reconstructions were first used by Longinelli (e.g., Longinelli 1966, 1984; Longinelli and Nuti 1973), and later by Kolodny and his coworkers (Kolodny et al. 1983; Luz and Kolodny 1985). However, the use was rather limited for many years, because of analytical difficulties. More recently these problems have been overcome by refinements in analytical techniques (Crowson et al. 1991; O'Neil et al. 1994; Cerling and Sharp 1996; Vennemann et al. 2002; Lecuyer et al. 2002), so the isotope analyses of phosphates for paleoenvironmental reconstruction has been used much more widely.

Under abiotic surface conditions phosphate is resistant to oxygen isotope exchange. During biological reactions, however, phosphate–water oxygen isotope exchange is rapid due to enzymatic catalysis (Kolodny et al. 1996; Blake et al. 1997, 2005; Paytan et al. 2002). O'Neil et al. (1994) have shown the importance of phosphate speciation in determining O isotope fractionation among different $PO_4(aq)$ species and between $PO_4(aq)$ species and water.

Phosphate materials that may be analyzed are bone, dentine, enamel, fish scales and invertebrate shells. In contrast to bone and dentine, enamel is extremely dense, so it is least likely to be affected diagenetically and the prime candidate for paleoevironmental reconstructions. Biogenic apatites contain besides the PO_4 group CO_3^{2-} that substitutes for PO_4^{3-} and OH^- as well as "labile" CO_3^{2-} (Kohn and Cerling 2002), the latter is removed by pretreatment with a weak acid. The

remaining CO_3^{2-} component in bioapatites is then analyzed similar to the analysis of carbonates (McCrea 1950). Early results of the carbonate–carbon seemed to imply diagenetic overprint and it was not until the 1990s that it became accepted that the carbon isotope composition of tooth enamel carbonate is a recorder of diet (Cerling et al. 1993, 1997).

Studies on mammals, invertebrates and fishes clearly indicate that the oxygen isotope composition of biogenic apatite varies systematically with the isotope composition of the body water that depends on local drinking water (Longinelli 1984; Luz et al. 1984; Luz and Kolodny 1985). For mammals, there is a constant offset between the $\delta^{18}O$ of body water and PO_4 ($\sim$18‰, Kohn and Cerling 2002) and between PO_4 and CO_3 components of bioapatite of $\sim$8‰ (Bryant et al. 1996; Iacumin et al. 1996). Studies by Luz et al. (1990), and Ayliffe and Chivas (1990) demonstrated that $\delta^{18}O$ of biogenic apatite can also depend on humidity and on diet.

Of special geological interest is the isotopic analyses of coeval carbonate–phosphate pairs (Wenzel et al. 2000), which helps to distinguish primary marine signals from secondary alteration effects and sheds light on the causes for $\delta^{18}O$ variations of fossil ocean water. Wenzel et al. (2000) compared Silurian calcitic brachiopods with phosphatic brachiopods and conodonts from identical stratigraphic horizons. They showed that primary marine oxygen isotope compositions are better preserved in conodonts than in brachiopod shell apatite and suggested that conodonts record paleotemperature and $^{18}O/^{16}O$ ratios of Silurian sea water. Joachimski et al. (2004) reached similar conclusions for Devonian sea water.

3.11.10 Iron Oxides

Hematite (α - Fe_2O_3) and goethite (α – FeOOH) are the two most common stable iron oxide phases. The determination of oxygen isotope fractionations in the iron oxide–water system has led to controversial results (Yapp 1983, 1987, 2007; Bao and Koch 1999), yet oxygen isotope fractionations are small and relatively insensitive to changes in temperatures. This seems to make iron oxides ideal recorders of the isotope composition of ambient waters. The initial precipitates in natural settings are water–rich ferric oxide gels and poorly ordered ferrihydrite, which are later slowly aged to goethite and hematite. Bao and Koch (1999) argued that the isotopic composition of original ferric oxide gels and ferrihydrite are erased by later exchange with ambient water during the ageing process. Thus, $\delta^{18}O$-values of natural crystalline iron oxides may monitor the long-term average $\delta^{18}O$-value of soil waters.

During conversion of goethite to hematite only small fractionation effects seem to occur, because most of the oxygen remains in the solid (Yapp 1987). Thus, in principle it should be possible to reconstruct the sedimentary environment of iron oxides from Precambrian banded iron formations (BIF). By analyzing the least metamorphosed BIFs, Hoefs (1992) concluded, however, that the situation is not so simple. Infiltration of external fluids during diagenesis and/or low temperature metamor-

phism appears to have erased the primary isotope record in these ancient sediments. The isotopic composition of Fe in iron oxides is discussed in Sect. 3.8.4.

3.11.11 Sedimentary Sulfur

Analysis of the sulfur isotope composition of sediments may yield important information about the origin and diagenesis of sulfur compounds. Due to the activity of anaerobic sulfate reducing bacteria, most sulfur isotope fractionation takes place in the uppermost mud layers in shallow seas and tidal flats. As a result, sedimentary sulfides are depleted in ^{34}S relative to ocean water sulfate. The depletion is usually in the order of 20–60‰ (Hartmann and Nielsen 1969; Goldhaber and Kaplan 1974), although bacteria in pure cultures have been observed to produce fractionations of only 10–30‰ with a maximum reported value of 47‰ (Kaplan and Rittenberg 1964; Bolliger et al. 2001). Sedimentary sulfides depleted in ^{34}S by more than 46‰ suggest additional fractionations that probably accompany sulfide oxidation in closed systems. To explain the discrepancy between culture experiments and natural environments the bacterial disproportionation of intermediate sulfur compounds has been proposed (Canfield and Thamdrup 1994; Cypionka et al. 1998; Böttcher et al. 2001).

Sulfur isotope variations in sediments reflect a record of primary syngenetic as well as secondary diagenetic processes (Jorgenson et al. 2004). For a given range of sulfur isotope values the most negative value should represent the least affected, most primary signal or the one that is most affected by the oxidative part of the sulfur cycle. In a few cases pyrite sulfur with higher $\delta^{34}S$-values than coexisting sea water has been found in the fossil record, which has been attributed to post-depositional diagenetic overprint by anaerobic methane oxidation (Jorgenson et al. 2004).

Bacterial sulfate reduction is accomplished by the oxidation of organic matter:

$$2CH_2O + SO_4^{2-} \rightarrow H_2S + 2HCO_3^-$$

the resulting H_2S reacting with available iron, which is in the reactive nonsilicate bound form (oxy-hydroxides). Thus, the amount of pyrite formed in sediments may be limited by (1) the amount of sulfate, (2) the amount of organic matter, and (3) the amount of reactive iron. Based upon the relationships between these three reservoirs different scenarios for pyrite formation in anoxic environments can be envisaged (Raiswell and Berner 1985). In normal marine sediments, where oxygen is present in the overlying water body, the formation of pyrite appears to be limited by the supply of organic matter. In recent years, there has been much progress to identify and measure the isotopic composition of different forms of sulfur in sediments (e.g., Mossmann et al. 1991; Zaback and Pratt 1992; Brüchert and Pratt 1996; Neretin et al. 2004). Pyrite is generally considered to be the end product of sulfur diagenesis in anoxic marine sediments. Acid–volatile sulfides (AVS), which include "amorphous" FeS, mackinawite, greigite, and pyrrhotite, are considered to be transient early species, but investigations by Mossmann et al. (1991) have demonstrated

that AVS can form before, during and after precipitation of pyrite within the upper tens of centimeters of sediment.

Up to six or even seven sulfur species have been separated and analyzed for their isotope composition by Zaback and Pratt (1992), Brüchert and Pratt (1996) and Neretin et al. (2004). Their data provides information regarding the relative timing of sulfur incorporation and the sources of the individual sulfur species. Pyrite exhibits the greatest ^{34}S depletion relative to sea water. Acid–volatile sulfur and sulfur in organic compounds are generally enriched in ^{34}S relative to pyrite. This indicates that pyrite is precipitated nearest to the sediment–water interface under mildly reducing conditions, while AVS and kerogen sulfur resulted from formation at greater depth under more reducing conditions with low concentrations of pore water sulfate. Elemental sulfur is most abundant in surface sediments and, probably, formed by oxidation of sulfide diffusing across the sediment–water interface.

By summarizing the isotope record of sedimentary sulfides throughout the Phanerozoic, Strauß (1997) and (1999) argued that the long-term trend for the entire Phanerozoic broadly parallels the sulfate curve with maximum values in the early Paleozoic, minimum values in the Permian, and a shift back to higher values in the Cenozoic. The isotopic difference between sulfate sulfur and minimum sulfide sulfur varies within $-51 \pm 8‰$.

Riciputi et al. (1996) have investigated the sulfur isotope composition of pyrites from Devonian carbonates with the ionprobe. $\delta^{34}S$-values of sulfides are very heterogeneous on a thin section scale varying by as much as 25‰ and show a bimodal distribution. The predominantly low δ-values indicate bacterial sulfate reduction, whereas the higher values reflect formation at much greater depths by thermochemical sulfate reduction. Correlations between pyrite morphology and isotope values suggest that sulfate reduction was a very localized process, which varied considerably on a small scale. Similar large ^{34}S-variations within and among individual pyrite grains have been reported by Kohn et al. (1998).

Besides bacterial sulfate reduction, thermochemical sulfate reduction in the presence of organic matter is another process which can produce large quantities of H_2S. The crucial question is whether abiological sulfate reduction can occur at temperatures as low as 100°C, which is just above the limit of microbiological reduction. Trudinger et al. (1985) concluded that abiological reduction below 200°C had not been unequivocally demonstrated, although they did not dismiss its possible significance. As shown by Krouse et al. (1988) and others, the evidence for thermochemical sulfate reduction, even at temperatures near 100°C or lower, has increased. Thus, it is likely that this process is much more prevalent than originally thought.

3.12 Palaeoclimatology

Past climates leave their imprint in the geologic record in many ways. For temperature reconstructions, the most widely used geochemical method is the measurement of stable isotope ratios. Samples for climate reconstruction have in common that their isotope composition depends in a sensitive way on the temperature at the time of their formation.

Climatic records can be divided into (1) marine and (2) continental records. Because the ocean system is very large and well -mixed, the oceanic record carries a global signal, while continental records are affected by regional factors. One restriction in reconstructing climates is the temporal resolution. This is especially true for marine sediments. Sedimentation rates in the deep-ocean generally are between $1-5\,\mathrm{cm}/10^3$ years, highly productive areas have $20\,\mathrm{cm}/10^3$ years, which limits the temporal resolution to 50 years for productive areas and to 200 years for the other areas. Furthermore, benthic organisms can mix the top 20 cm of marine sediments, which further reduces temporal resolutions.

3.12.1 Continental Records

Isotopic reconstruction of climatic conditions on the continents is difficult, because land ecosystems and climates exhibit great spatial and temporal heterogeneity. The most readily determined terrestrial climatic parameter is the isotopic composition of precipitation, which is in turn dependent largely but not exclusively on temperature. Relevant climatic information from meteoric precipitation is preserved in a variety of natural archives, such as (1) tree rings, (2) organic matter and (3) hydroxyl-bearing minerals.

1. *Tree rings.* Tree rings offer an absolute chronology with annual resolution, but the scarcity of suitable old material and uncertainties about the preservation of original isotope ratios are major restrictions in the application of tree rings. The cellulose component of plant material is generally used for isotope studies because of its stability and its well-defined composition. Numerous studies have investigated the stable isotope composition of tree rings. However, in many respects climatic applications are limited. Although there are strong correlations of δD and $\delta^{18}O$ with source water, there are variable fractionations between water and cellulose. An increasing number of studies have investigated the complex processes that transfer the climatic signal in the meteoric water to tree cellulose (for instance White et al. 1994; Tang et al. 2000). The complexities result from the interplay of various factors such as humidity, amount of precipitation, topography, biological isotope fractionation, root structure, ageing of late-wood. Tang et al. (2000) assessed both systematic (variations of temperature, humidity, precipitation, etc.) and random isotopic variations in tree rings from a well-characterized area in the northwestern United States, and demonstrated for instance that temperature only explains up to 26% of the total variance of δD-values of cellulose nitrate.
2. *Organic matter.* The utility of D/H ratios in organic matter as paleoclimatic proxies relies on the preservation of its primary biosynthetic signal. The question arises at what point paleoclimatic information is lost during diagenesis and thermal maturation. Schimmelmann et al. (2006) argued that in the earliest stages of diagenesis δD-values of most lipid biomarkers are unaffected. With the onset of catagenesis quantitative information diminishes, but qualitative information may be still preserved. At the highest levels of maturity, biomarkers become thermally

unstable and can undergo degradation leading to extensive hydrogen isotope exchange (Sessions et al. 2004) and therefore limiting paleoclimate information.

3. *Hydroxyl-bearing minerals*. Hydroxyl-bearing minerals might be regarded as another tool to reconstruct climatic changes. Again there are major difficulties that restrict a general application. Fractionation factors of clay minerals and hydroxides are not well constrained, especially at low temperatures and meaningful δD and $\delta^{18}O$ measurements require pure mineral separates, which are extremely difficult to achieve due to their small particle size and because these phases are often intergrown. Furthermore, there is a concern that some clays are detrital, whereas others are authigenic; thus, mixtures may be difficult to interpret.

3.12.1.1 Lake Sediments

The isotope composition of biogenic and authigenic mineral precipitates from lake sediments can be used to infer changes in either temperature or the isotope composition of lake water. Knowledge of the factors that may have influenced the isotope composition of the lake water is essential for the interpretation of the precipitated phases (Leng and Marshall 2004). In many lakes the combined analysis of different types of authigenic components (precipitated calcite, ostracodes, bivalves, diatoms, etc.) may offer the possibility of obtaining seasonally specific information.

One of the most useful components for estimating past climate variations are nonmarine ostracodes (small bivalved crustaceans), which can live in most types of fresh-water and can be regarded as the "foraminifera of the continent". In recent years, an increasing number of studies have demonstrated the potentials of ostracodes to reconstruct changes in temperatures of mean annual precipitation, changes in paleohydrology and evaporation histories (Lister et al. 1991; Xia et al. 1997a, b; von Grafenstein et al. 1999; Schwalb et al. 1999). A number of authors have demonstrated systematic differences in $\delta^{18}O$ of up to 2‰ between ostracodes and calcite precipitated under equilibrium conditions and even larger differences for $\delta^{13}C$. These differences have not been explained satisfactorily, because the knowledge about life cycles, habitat preferences and valve formation mechanisms of ostracodes is still limited.

3.12.1.2 Speleothems

Two features in caves facilitate the use of stable isotopes as a palaeoarchive (1) cave air temperatures remain relatively constant throughout the year and are similar to the mean annual temperature above the cave. (2) In cool temperate climate regions, cave air is characterized by very high humidity that minimizes evaporation effects. Interest in speleothems as recorders of continental palaeoenvironments has increased considerably in recent years. The potential of speleothems as climate indicators was first discussed by Hendy and Wilson (1968) followed by Thompson et al. (1974). These early investigators already recognized the complexity of cave carbonate iso-

tope compositions. An early goal was to reconstruct absolute changes in mean annual temperatures, but this appears to be rather unrealistic because various effects can influence the isotope composition of drip water, and thus the precipitated cave carbonate (see review by McDermott 2004).

Most isotope studies on speleothems have concentrated on $\delta^{18}O_{calcite}$ as the principal paleoclimatic indicator. Some studies have discussed the potential of using δD and $\delta^{18}O$ of fluid inclusions in speleothems (Dennis et al. 2001; McGarry et al. 2004; Zhang et al. 2008). With respect to oxygen, isotope exchange may occur between calcite and water, which may lead to a shift of the original drip water composition, but for hydrogen no isotope exchange can take place. With an improved crushing technique for the liberation of the fluid inclusion water, Zhang et al. (2008) were able to recover the water without isotopic fractionation. They demonstrated that it is possible to obtain accurate paleotemperatures.

3.12.1.3 Phosphates

Oxygen isotope compositions of phosphates have also been used as a paleotemperature indicator. Since the body temperature of mammals is constant at around 37°C, $\delta^{18}O$-values in either bones or teeth depend only on the $\delta^{18}O$-value of the body water, which in turn depends on drinking water (Kohn 1996). Thus, phosphates from continental environments are an indirect proxy of ancient meteoric waters.

The best proxy appears to be mammalian tooth enamel (Ayliffe et al. 1994; Fricke et al. 1998a, b), which forms incrementally from the crown to the base of the tooth. Enamel, therefore, preserves a time series of $\delta^{18}O$-values of precipitation along the direction of growth that reflect only ^{18}O-changes of ingested water. Oxygen isotope data for teeth of mammal herbivores that lived over a wide range of climatic conditions demonstrate that intra tooth $\delta^{18}O$-values mirror both seasonal and mean annual differences in the ^{18}O-content of local precipitation (Fricke et al. 1998a). Records going back to glacial-interglacial transitions have been described by Ayliffe et al. (1992). Fricke et al. (1998b) even postulated that tooth enamel may provide a temperature record as far back as the Early Cenozoic.

3.12.1.4 Ice Cores

Ice cores from polar regions represent prime recorders of past climates. They have revolutionized our understanding of Quaternary climates by providing high-resolution records of changing isotope compositions of snow or ice and of changing air compositions from air bubbles occluded in the ice. The best documented ice-core record from Greenland is a pair of 3 km long ice cores from the summit of Greenland. These cores provide a record of climate as far back as 110,000 years ago. Precise counting of individual summer and winter layers extends back to at least 45,000 years ago.

The Antarctic ice sheet also has provided numerous ice cores for paleoclimate research. Antarctica is colder and its ice sheet is larger and thicker than that on Greenland. It accumulates more slowly than at the Greeenland sites, however, such that its temporal resolution is not as good. The Vostok ice core has provided strong evidence of the nature of climate changes over the past 420 ky. More recently, a core from Dome C, Antarctica has almost doubled the age range to the past 740 ky (Epica Community Members 2004). A good agreement with the Vostok core was observed for the four most recent glacial cycles, the Dome C core extends back to eight glacial cycles.

Glaciers at very high elevations even near the equator are also of interest. High elevation ice cores, which have been drilled in Africa (Kilimanjaro), South America, and Asian Himalayas (e.g., Thompson et al. 2006) represent an important addition to the polar region ice cores. Some of these high altitude, low latitude ice cores span the last 25,000 years, representing a high resolution record of the late glacial stage and the Holocene (Thompson et al. 2000). In ice-cores from Huascaran, Peru the lowest few meters contain ice from the last glacial maximum with δ^{18}O-values of about 8‰ lower than Holocene values. This suggests that tropical temperatures were significantly reduced during the last glacial maximum and were much lower than those indicated by the reconstructions of the CLIMAP members.

Oxygen and hydrogen isotope ratios and various atmospheric constituents in ice cores have revealed a detailed climatic record for the past 700 ky. To convert isotopic changes to temperatures, temperature – δ^{18}O correlations must be known. In early work, Dansgaard et al. (1993) proposed a relationship of 0.63‰ per 1°C, whereas Johnsen et al. 1995) have used 0.33‰ per 1°C (but see the remarks of caution by Allen and Cuffey 2001). The δ - T relationship varies with climatic conditions, especially between interglacial and glacial periods, because a more extensive sea-ice cover increases the distance to moisture sources and the isotopic composition of oceans changed during glacial periods.

Figure 3.47 compares δ^{18}O ice core data from GRIP and NGRIP in Greenland for the time period 50,000–30,000 years with significantly colder temperatures during the LGM than the time period for the last 10,000 years. Characteristic features of Fig. 3.47 are fast changes in δ^{18}O-values fluctuating between -37 and -45‰. These so-called Dansgaard–Oeschger events (Dansgaard et al. 1993; Grootes et al. 1993) are characterized by rapid warming episodes within decades followed by gradual cooling over a longer period. 23 Dansgaard–Oeschger events have been identified between 110,000 and 23,000 years before present, the causes for these sawtooth patterns are still unclear.

1. Correlations of ice-core records. Ice-core isotope stratigraphy represents a major advance in paleoclimatology because it enables the correlation of climate records from the two poles with each other and with the high-resolution deep-sea marine climate records over the past 100 ka (Bender et al. 1994), allowing the study of phasing between the ocean and the atmosphere. One of the most difficult problems in correlating ice-cores is determining the age-depth relationship. If accumulation rates are high enough, accurate timescales have been achieved for the last 10,000 years. Prior to that there is increasing uncertainty, but in recent years new approaches have been

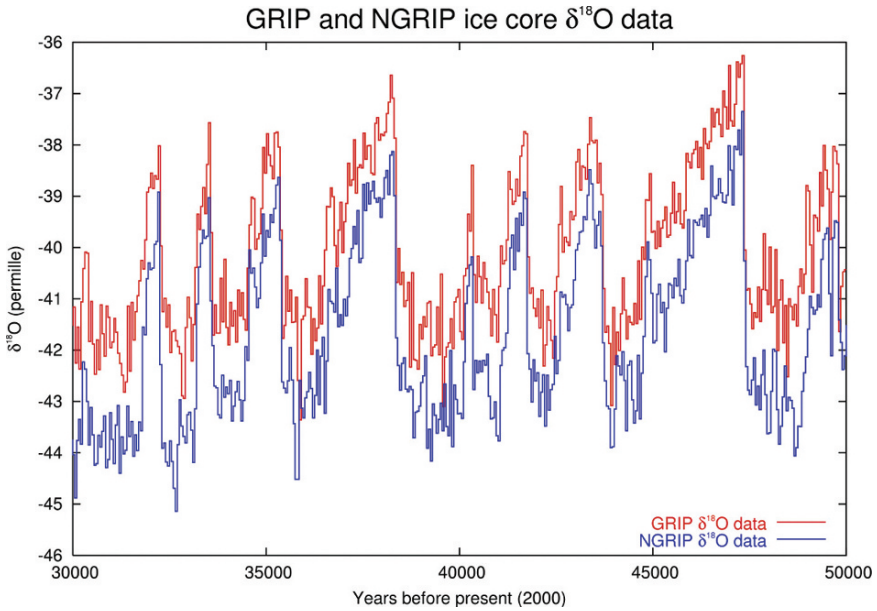

Fig. 3.47 Dansgaard-Oeschger events in the time period from 45000 to 30000 years before present from GRIP and NGRIP ice core data (http://en.wikipedia.org/wiki/Image:Grip-ngrip-do18-closeup.png)

developed, improving age determinations and allowing age correlations between different ice cores (see Fig. 3.47).

A very promising method for correlation purposes relies on changes in atmospheric gas composition. As the mixing time of the atmosphere is on the order of 1–2 years, changes in gas composition should be synchronous. Bender et al. (1994) have used variations of $\delta^{18}O$ in gas inclusions from ice-cores correlating the Vostok and GISP-2 ice cores. Similar ^{18}O-variations in both cores makes an alignment of the two records possible (Bender et al. 1985; Sowers et al. 1991, 1993), which then allows the comparison of other parameters such as CO_2 and CH_2 with temperature changes as deduced from the isotopic composition of the ice.

2. Gas-inclusions in ice cores

Atmospheric trace gas chemistry is a new rapidly growing field of paleo-atmospheric research, because the radiative properties of CO_2, CH_4, and N_2O make them potential indicators of climate change. A fundamental problem in constructing a record of trace gas concentrations from ice-cores is the fact that the air in bubbles is always younger than the age of the surrounding ice. This is because as snow is buried by later snowfalls and slowly becomes transformed to firn and ice, the air between the snow crystals remains in contact with the atmosphere until the air bubbles become sealed at the firn/ice transition, when density increases to about $0.83\,g\,cm^{-3}$. The trapped air is thus younger than the matrix, with the age difference

depending mainly on accumulation rate and temperature. In Greenland, for instance the age difference varies between 200 and 900 years.

Sowers et al. (1993) and Bender et al. (1994) showed that it is possible to construct an oxygen isotope curve similar to that derived from deep-sea foraminifera from molecular O_2 trapped in ice. These authors argued that $\delta^{18}O_{(atm)}$ can serve as a proxy for ice volume just as $\delta^{18}O$-values in foraminifera. The isotope signal of atmospheric oxygen can be converted from sea water via photosynthetic marine organisms according to the following scheme

$$\delta^{18}O_{(seawater)} \rightarrow \text{photosynthesis} \rightarrow \delta^{18}O_{(atm)} \rightarrow \text{polar ice} \rightarrow \delta^{18}O_{(ice)}$$

This conversion scheme is, however, complex and several hydrological and ecological factors have to be considered. Sowers et al. (1993) argued that these factors remained near constant over the last glacial–interglacial cycle, so that the dominant signal in the atmospheric oxygen isotope record represents an ice-volume signal.

Air composition in ice cores is slightly modified by physical processes, such as gravitational and thermal fractionation. A gas mixture in ice cores with different molecular weights will partially segregate due to thermal diffusion and gravitational fractionation. Generally, the species with greater mass will migrate towards the bottom and/or the cold end of a column of air. By slow diffusion, air trapped in ice-cores can develop slight changes in atmospheric ratios such as the Ar/N_2 ratio as well as fractionate the nitrogen and oxygen isotope composition of air molecules. This approach was pioneered by Severinghaus et al. (1996), who first showed that thermal diffusion can be observed in sand dunes. Later Severinghaus et al. (1998), Severinghaus and Brook (1999) and Grachev and Severinghaus (2003) demonstrated that thermally driven isotopic anomalies are detectable in ice core air bubbles. Since gases diffuse about 50 times faster than heat, rapid climatic temperature changes will cause an isotope anomaly. Nitrogen in bubbles in snow thus may serve as a tracer for palaeoclimatic reconstructions because the $^{29}N/^{28}N$ ratio of atmospheric N_2 has stayed constant in the atmosphere. The measurement of $^{29}N/^{28}N$ ratios can, therefore, supplement the oxygen isotope record and can be used to determine the rapidity and scale of climate change. By measuring the thickness of ice separating nitrogen and oxygen isotope anomalies at the end of Younger Dryas 11,500 years ago, Severinghaus et al. (1998) estimated the rate of temperature change to be less than 50–100 years and suggested that the Younger Dryas was about 15°C colder than today which is about twice as large as estimated from Dansgaard–Oeschger events.

3.12.2 Marine Records

Most oceanic paleoclimate studies have concentrated on foraminifera. In many cases analyses have been made both of planktonic and benthonic species. Since the first pi-

oneering paper of Emiliani (1955), numerous cores from various sites of the DSDP and ODP program have been analyzed and, when correlated accurately, have produced a well-established oxygen isotope curve for the Pleistocene and Tertiary. These core studies have demonstrated that similar $\delta^{18}O$-variations are observed in all areas. With independently dated time scales on hand, these systematic $\delta^{18}O$ variations result in synchronous isotope signals in the sedimentary record because the mixing time of the oceans is relatively short (10^3 years). These signals provide stratigraphic markers enabling correlations between cores which may be thousands of kilometers apart. Several Pleistocene biostratigraphic data have been calibrated with oxygen isotope stratigraphy, which helps to confirm their synchrony. This correlation has greatly facilitated the recognition of both short- and long-time periods of characteristic isotopic compositions, and times of rapid change from one period with characteristic composition to another, thus, making oxygen isotope stratigraphy a practical tool in modern paleoceanographic studies. Figure 3.48 shows the oxygen isotope curve for the Pleistocene. This diagram exhibits several striking features: the most obvious one is the cyclicity, furthermore, fluctuations never go beyond a certain maximum value on either side of the range. This seems to imply that very effective feedback mechanisms are at work stopping the cooling and warming trends at some maximum level. The "sawtooth"-like curve in Fig. 3.48 is characterized by very steep gradients: maximum cold periods are immediately followed by maximum warm periods.

Emiliani (1955) introduced the concept of "isotopic stages" by designating stage numbers for identifiable events in the marine foraminiferal oxygen isotope record for the Pleistocene. Odd numbers identify interglacial or interstadial (warm) stages, whereas even numbers define ^{18}O-enriched glacial (cold) stages. A second terminology used for subdividing isotope records is the concept of terminations labeled with Roman numbers I, II, III, etc. which describe rapid transitions from peak glacial to peak interglacial values. This approach was used by Martinson et al. (1987) to produce a high-resolution chronology, called the Specmap time scale which is used when plotting different isotope records on a common time scale. With these different techniques a rather detailed chronology can be worked out.

A careful examination of the curve shown in Fig. 3.49 shows a periodicity of approximately 100,000 years. Hays et al. (1976) argued that the main structure of the oxygen isotope record is caused by variations in solar insolation, promoted by

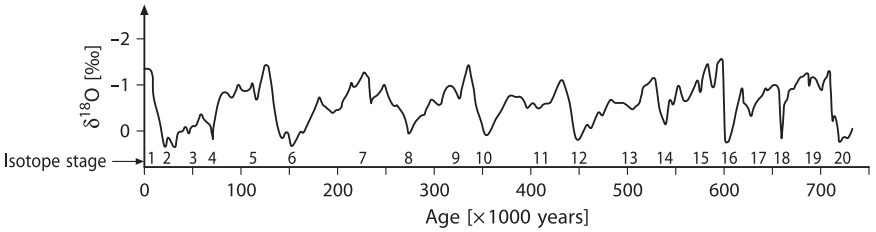

Fig. 3.48 Composite $\delta^{18}O$ fluctuations in the foraminifera species *G sacculifer* from Caribbean cores (Emiliani, 1966)

variations in the Earth's orbital parameters. Thus, isotope data have played a capital role in the confirmation of the "Milankovitch Theory" which argues that the isotope and paleoclimate record is a response to the forcing of the orbital parameters operating at specific frequencies.

3.12.2.1 Corals

Two types of coral exist: near surface dwelling photosynthesizing corals forming reefs along tropical coastlines and nonphotosynthesizing deep ocean corals. Since massive corals such as *porites* have a life span of many centuries they can be used to reconstruct the palaeoenvironment of the last centuries. Coral skeletons are well known for strong vital effects, their oxygen isotope composition is generally depleted relative to equilibrium by 1–6‰. Because of this strong nonequilibrium fractionation early workers were highly skeptical about the usefulness of δ^{18}O-values as climate indicators. Later workers, however, realized that the δ^{18}O records reveal subseasonal variations in sea water temperature and salinity. Most climate studies circumvent the problem of equilibrium offsets by assuming a time independent constant offset and interpret relative changes only. Thus δ^{18}O-values of corals generally are not interpreted as temperature records, but as records reflecting combinations of temperature and salinity changes. δ^{18}O-values in corals may record anomalies associated with El Nino (Cole et al. 1993; Dunbar et al. 1994), including the dilution effect on δ^{18}O by high amounts of precipitation (Cole and Fairbanks 1990).

Coral growth rates vary over the course of a year, which is expressed in an annual banding. Leder et al. (1996) demonstrated that a special microsampling technique (50 samples a year) is necessary to accurately reproduce annual sea surface conditions. Generally, δ^{18}O records show a long-term warming and/or decrease in salinity throughout the tropical oceans (Gagan et al. 2000; Grottoli and Eakin 2007). Fossil coral samples imply an additional problem. Since corals dominantly are composed of aragonite, subaereal exposure of fossil corals will easily change oxygen isotope values due to diagenetic recrystallization to calcite.

3.12.2.2 Characteristic Climatic Events During the Last 65 Ma

During the last decade a rapid growth of high-resolution isotope records across the Cenozoic has taken place. Zachos et al. (2001) have summarized 40 DSDP and ODP sites representing various intervals in the Cenozoic. Their compilation of benthic foraminifera shows a range of 5.4‰ over the course of the Cenozoic. This variation provides constraints on the evolution of deep-sea temperature and continental ice volume. Because deep ocean waters are derived primarily from cooling and sinking of water in polar regions, the deep-sea temperature data also reflect high-latitude sea-surface temperatures.

For the period prior to the first onset of Antarctic glaciation (around 33 Ma), oxygen isotope variations in global benthic foraminifera records reflect temperature

changes only. Oxygen isotope data suggest the deep oceans of Cretaceous and Paleocene age may have been as warm as 10–15°C, which is very different from today's conditions, when deep waters vary from about +4 to −1°C . The compilation of Zachos et al. (2001) indicates a bottom water temperature increase of about 5°C over five million years during the Paleocene to the early Eocene.

Variations in the benthic foraminifera record after 33 Ma indicate fluctuations in global ice volume in addition to temperature changes. Since then the majority of the $\delta^{18}O$ variations can be attributed to fluctuations in the global ice volume. Thus, Tiedemann et al. (1994) demonstrated the presence of at least 45 glacial-interglacial cycles over the last 2.5 Ma.

Zachos et al. (2001) discussed the Cenozoic climatic history in respect to three different time frames: (1) long-term variations driven mainly by tectonic processes on time scales of 10^5–10^7 years, (2) rhythmic and periodic cycles driven by orbital processes with characteristic frequencies of roughly 100, 40, and 23 kyr. (These orbitally driven variations in the spatial and seasonal distribution of solar radiation are thought to be the fundamental drivers of glacial and interglacial oscillations.), (3) Brief, aberrant events with durations of 10^3–10^5 years. These events are usually accompanied by a major perturbation in the global carbon cycle; the three largest occurred at 55, 34, and 23 Ma.

Figure 3.49 summarizes the oxygen isotope curve for the last 65 Ma. The most pronounced warming trend is expressed by a 1.5‰ decrease in $\delta^{18}O$ and occurred early in the Cenozoic from 59 to 52 Ma, with a peak in Early Eocene. Coinciding with this event is a brief negative carbon isotope excursion, explained as a massive release of methane into the atmosphere (Norris and Röhl 1999). These authors used high resolution analysis of sedimentary cores to show that two thirds of the carbon shift occurred just in a few thousand years, indicating a catastrophic release of carbon from methane clathrates into the ocean and atmosphere.

A 17 Ma trend toward cooler conditions followed, as expressed by a 3‰ rise in $\delta^{18}O$, which can be attributed to a 7°C decline in deep-sea temperatures. All subsequent changes reflect a combined effect of ice-volume and temperature.

To investigate the rhythmic scales, Zachos et al. (2001) looked in detail to four time intervals (0–4.0; 12.5–16.5; 20.5–24. 5; 31–35 Ma) each representing an interval of major continental ice-sheet growth or decay. These intervals demonstrate that climate varies in a quasi-periodic fashion. In terms of frequency, Zachos et al. (2001) concluded that much of the power in the climate spectrum appears to be related with changes in the obliquity (40 ky). This inference of a 40 ky periodicity contrasts with the obvious 100 ky periodicity indicated by isotope curves for the last 1–2 Ma.

3.13 Metamorphic Rocks

The isotope composition of metamorphic rocks is mainly controlled by three factors, besides the temperature of exchange (1) the composition of the pre-metamorphic protolith, (2) the effects of volatilization with increasing temperatures and (3) an

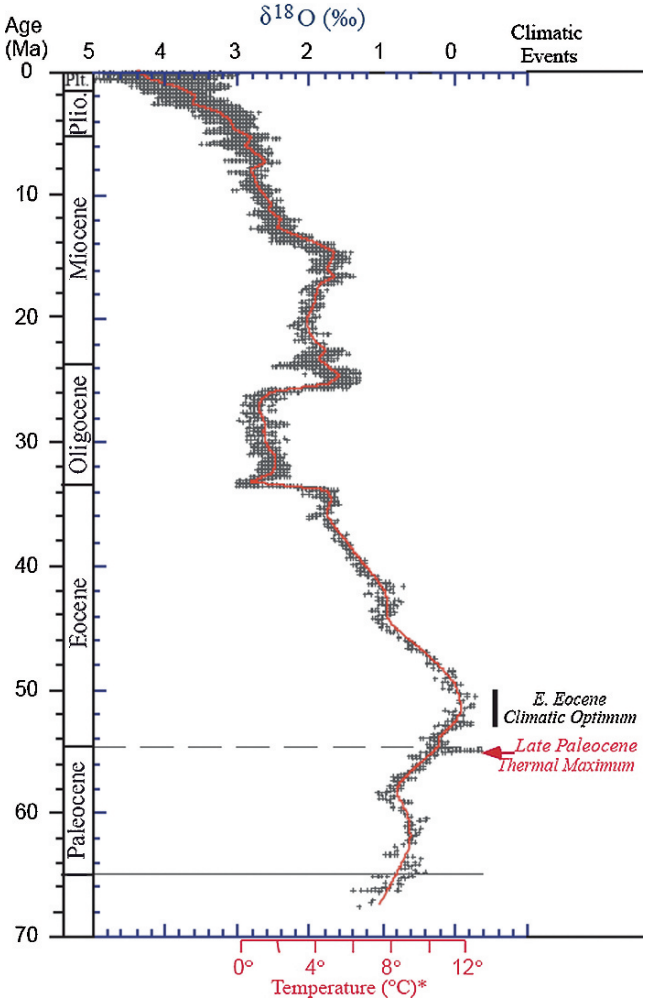

Fig. 3.49 Global deep-sea isotope record from numerous DSDP and ODP cores. *PETM* Paleocene-Eocene Thermal Maximum (Zachos et al. 2001)

exchange with infiltrating fluids or melts. The relative importance of these three factors can vary extremely from area to area and from rock type to rock type; and the accurate interpretation of the causes of isotope variations in metamorphic rocks requires knowledge of the reaction history of the respective metamorphic rocks.

(1) The isotope composition of the precursor rock – either sedimentary or magmatic – is usually difficult to estimate. Only in relatively dry nonvolatile-bearing precursor rocks do retain metamorphic rocks their original composition.
(2) Prograde metamorphism of sediments causes the liberation of volatiles, which can be described by two end-member processes (Valley 1986):
(a) Batch volatilization, where all fluid is evolved before any is permitted to escape and (b) Rayleigh volatilization, which requires that once fluid is generated

it is isolated immediately from the rock. Natural processes seem to fall between both end-member processes, nevertheless they describe useful limits. Metamorphic volatilization reactions generally reduce the $\delta^{18}O$-value of a rock because CO_2 and, in most cases, H_2O lost are enriched in ^{18}O compared to the bulk rock. The magnitude of ^{18}O depletion can be estimated by considering the relevant fractionations at the respective temperatures. In most cases, the effect on the $\delta^{18}O$-value should be small (around 1‰), because the amount of oxygen liberated is small compared to the remaining oxygen in the rock and isotope fractionations at these rather high temperatures are small and, in some cases, may even reverse sign.

(3) The infiltration of externally derived fluids is a controversial idea, but has gained much support in recent years. Many studies have convincingly demonstrated that a fluid phase plays a far more active role than was previously envisaged, although it is often not clear that the isotopic shifts observed are metamorphic rather than diagenetic (see also Kohn and Valley 1994).

A critical issue is the extent to which the isotope composition of a metamorphic rock is modified by a fluid phase. Volatilization reactions leave an isotope signature greatly different from that produced when fluid–rock interaction accompanies mineral–fluid reaction. Changes of 5–10‰ are a strong indication that fluid–rock interaction rather than volatilization reactions occurred during the metamorphic event. Coupled O–C depletions are seen in many metamorphic systems involving carbonate rocks. Figure 3.50 summarizes results from 28 studies of marble mostly

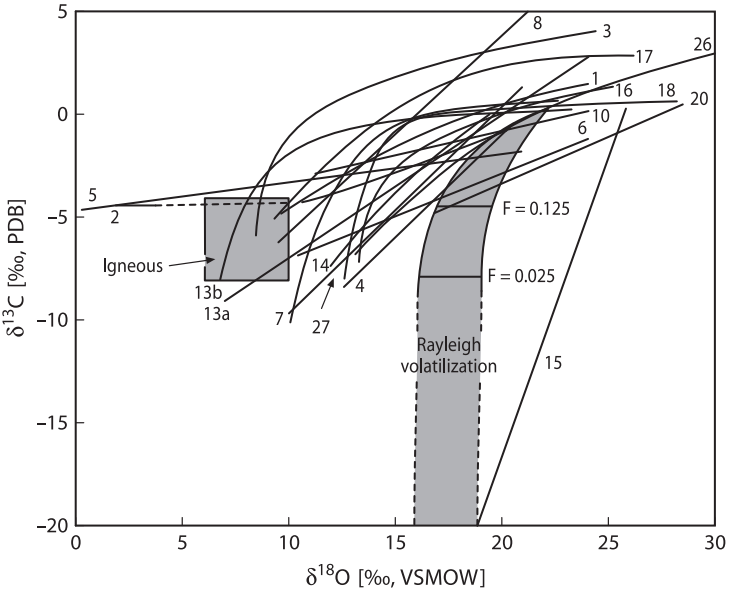

Fig. 3.50 Coupled O-C trends showing decreasing values of $\delta^{13}C$ and $\delta^{18}O$ with increasing metamorphic grade from numerous contact metamorphic localities (Baumgartner and Valley, 2001)

in contact metamorphic settings. In each of the localities shown in Fig. 3.50, the O–C trend has a negative slope, qualitatively similar to the effects of devolatilization. However, in each area the magnitude of depletions is too large to be explained by closed-system devolatilization processes, but fluid infiltration and exchange with low ^{18}O and ^{13}C fluids is indicated (Valley 1986; Baumgartner and Valley 2001).

Two end-member situations can be postulated in which coexisting minerals would change their isotopic composition during fluid–rock interaction (Kohn and Valley 1994):

(1) A pervasive fluid moves independently of structural and lithologic control through a rock and leads to a homogenization of whatever differences in isotopic composition may have existed prior to metamorphism.
(2) A channelized fluid leads to local equilibration on the scale of individual beds or units, but does not result in isotopic homogenization of all rocks or units. Channelized flow favors chemical heterogeneity, allowing some rocks to remain unaffected. Although both types of fluid flow appear to be manifest in nature, the latter type appears to be more common.

Numerical modeling of isotope exchange amongst minerals has provided a detailed view of how fluid flow occurs during metamorphism. Stable isotope fronts similar to chromatographic fronts will develop when fluids infiltrate rocks that are not in equilibrium with the infiltrating fluid composition. Isotope ratios increase or decrease abruptly at the front depending on the initial ratio in the rock and infiltrating fluid. Taylor and Bucher-Nurminen (1986), for instance, report sharp isotopic gradients of up to 17‰ in $\delta^{18}O$ and 7‰ in $\delta^{13}C$ over distances of a few millimeters in calcite around veins in the contact aureole of the Bergell granite. Similar sharp gradients have been also observed in other metasomatic zones but are often unrecognized because an unusually detailed millimeter-scale sampling is required.

Well-defined stable isotope profiles may be used to provide quantitative information on fluid fluxes such as the direction of fluid flow and the duration of infiltration events (Baumgartner and Rumble 1988; Bickle and Baker 1990; Cartwright and Valley 1991; Dipple and Ferry 1992; Baumgartner and Valley 2001). In well constrained situations, fluid flow modeling permits estimation of fluid fluxes that are far more realistic than fluid/rock ratios calculated from a zero-dimensional model.

Due to the invention of new microanalytical techniques (laser sampling and ion microprobe) it has become possible to document small-scale isotope gradients within single mineral grains. Oxygen isotope zoning in magnetite is especially pronounced. From ion microprobe analyses, Eiler et al. (1995) presented evidence that closed-system diffusion may produce internal zonation in magnetite. For garnets small (generally <1‰) zoning has been observed in several cases with increases or decreases from core to rim (Kohn et al. 1993; Young and Rumble 1993; Xiao et al. 2002). The shape of the isotopic gradient across a grain contact will allow distinction among processes controlled by open-system fluid migration or closed-system diffusion, and may also help to interpret inconsistencies in geothermometric data.

3.13.1 Contact Metamorphism

Because the isotopic composition of igneous rocks is quite different from those of sedimentary rocks, studies of the isotope variations in the vicinity of an intrusive contact offer the possibility of investigating the role of fluids interacting with rocks around cooling plutons. Two types of aureole can be distinguished (Nabelek 1991) (a) "closed" aureoles where fluids are derived from the pluton or the wall-rock and (b) "open" aureoles that for at least part of their metamorphic history have been infiltrated by fluids of external origin. Some aureoles will be dominated by magmatic or metamorphic fluids, whereas others by surface-derived fluids. The occurrence of meteoric–hydrothermal systems around many plutonic complexes has been documented by Taylor and his coworkers and has been described in more detail in p. 128. The depth to which surface-derived fluids can penetrate is still under debate, but most meteoric-hydrothermal systems appear to have developed at depths less than $\sim$6 km (Criss and Taylor 1986). However, Wickham and Taylor (1985) suggested that sea water infiltration has been observed to a depth of 12 km in the Trois Seigneur Massif, Pyrenees.

In many contact aureoles combined petrologic and isotope studies have provided evidence that fluids were primarily locally derived. Oxygen isotope compositions of calc-silicates from many contact aureoles have revealed that the ^{18}O-contents of the calc-silicate hornfelses approach those of the respective intrusions. This, together with characteristic hydrogen and carbon isotope ratios, has led many workers to conclude that magmatic fluids were dominant during contact metamorphism with meteoric fluids becoming important during subsequent cooling only (Taylor and O'Neil 1977; Nabelek et al. 1984; Bowman et al. 1985; Valley 1986). Ferry and Dipple (1992) developed different models to simulate fluid–rock interaction on the Notch Peak aureole, Utah. Their preferred model assumes fluid flow in the direction of increasing temperature, thus arguing against magmatic fluids, but instead proposing fluids derived from volatilization reactions. Nabelek (1991) calculated model δ^{18}O-profiles which should result from both "down-temperature" and "up-temperature" flow in a contact aureole. He demonstrated that the presence of complex isotopic profiles can be used to get information about fluid fluxes. Gerdes et al. (1995) have examined meter-scale ^{13}C and ^{18}O transport in a thin marble layer near a dike in the Adamello contact aureole, Southern Alps. They observed systematic stable isotope changes in the marble over $<$1 m as the dike is approached with δ^{13}C-values ranging from 0 to -7‰ and δ^{18}O-values from 22.5 to 12.5‰. These authors have compared the isotope profiles to one- and two-dimensional models of advective-dispersive isotope transport. Best agreement is obtained using a two-dimensional model that specifies (1) a high permeability zone flow and (2) a lower permeability zone in marble away from the dike.

3.13.2 Regional Metamorphism

It is a general observation that low-grade metamorphic pelites have δ^{18}O-values between 15 and 18‰ whereas high-grade gneisses have δ^{18}O-values between 6 and 10‰ (Garlick and Epstein 1967; Shieh and Schwarcz 1974; Longstaffe and Schwarcz 1977; Rye et al. 1976; Wickham and Taylor 1985; Peters and Wickham 1995). In the absence of infiltration of a fluid phase, isotopic shifts resulting from net transfer reactions in typical amphibolite or lower granulite facies metapelites and metabasites are about 1‰ or less for about 150°C of heating (Kohn et al. 1993; Young 1993). Thus, the processes responsible for this decrease in ^{18}O must be linked to large-scale fluid transport in the crust.

There are several factors which control fluid transport. One is the lithology of a metamorphic sequence. Marbles, in particular, are relatively impermeable during metamorphism (Nabelek et al. 1984) and, therefore, may act as barriers to fluid flow, limiting the scale of homogenization and preferentially channeling fluids through silicate layers. Marbles may act as local high - ^{18}O reservoirs and may even increase the ^{18}O content of adjacent lithologies (Peters and Wickham 1995). Therefore, massive marbles generally preserve their sedimentary isotope signatures, even up to the highest metamorphic grades (Valley et al. 1990).

Sedimentary sequences undergoing a low-grade metamorphism initially may contain abundant connate pore fluids which provide a substantial low-^{18}O reservoir and a medium for isotopic homogenization. An additional important fluid source is provided by metamorphic dehydration reactions at higher grades of metamorphism (e.g., Ferry 1992). In some areas, petrological and stable isotope studies suggest that metamorphic fluid compositions were predominantly internally buffered by devolatilization reactions and that large amounts of fluid did not interact with the rocks during regional metamorphism (e.g., Valley et al. 1990). In a high-grade polymetamorphic terrane, later metamorphic events are likely to be dominated by magmatic fluid sources since previous events would have caused extensive dehydration, thereby limiting potential fluid sources (Peters and Wickham 1995). A detailed study of the O-isotope composition of pelites, amphibolites, and marbles from the island of Naxos, Greece demonstrates that the isotopic pattern observed today is the result of at least three processes: two fluid flow events and a pre-existing isotopic gradient (Baker and Matthews 1995).

Shear zones are particularly good environments to investigate fluid flow at various depths within the crust (Kerrich et al. 1984; Kerrich and Rehrig 1987; McCaig et al. 1990; Fricke et al. 1992). During retrograde metamorphism aqueous fluids react with dehydrated rocks and fluid flow is concentrated within relatively narrow zones. By analyzing quartzite mylonites in Nevada, Fricke et al. (1992) demonstrated that significant amounts of meteoric waters must have infiltrated the shear zone during mylonitization to depths of at least 5–10 km. Similarly, McCaig et al. (1990) showed that formation waters were involved in shear zones in the Pyrenees and that the mylonitization process occurred at a depth of about 10 km.

Unusually low δ^{18}O-values – as light as -5 to -10‰ – have been observed in ultra-high pressure (UHP)-rocks from Dabie Shan and Sulu, China (Rumble and

Yui 1998; Zheng et al. 1998; Xiao et al. 2006 besides others). UHP-rocks are characterized by coesite and microdiamond in eclogite and other crustal rocks, which is strong evidence that a sizable segment of ancient continental crust was subducted to mantle depths. The extremely low δ^{18}O-values result from meteoric water interaction prior to UHP metamorphism. Surprisingly, these rocks have preserved their extremely low δ^{18}O-values indicating a short-residence time at mantle depth followed by a rapid uplift. Quartz–garnet oxygen isotope temperatures in the range $700-900°C$ are consistent with an approach to grain-scale oxygen isotope equilibrium under UHP conditions (Rumble and Yui 1998; Xiao et al. 2006). Figure 3.51 shows a 5,000 m oxygen isotope profile through the CCSD (Chinese Continental Scientific Drilling) UHP drill hole, which indicates meteoric water interaction till a depth of 3,300 m. Mineral δ^{18}O compositions are homogeneous on a mm to cm scale, but heterogeneous on a meter scale.

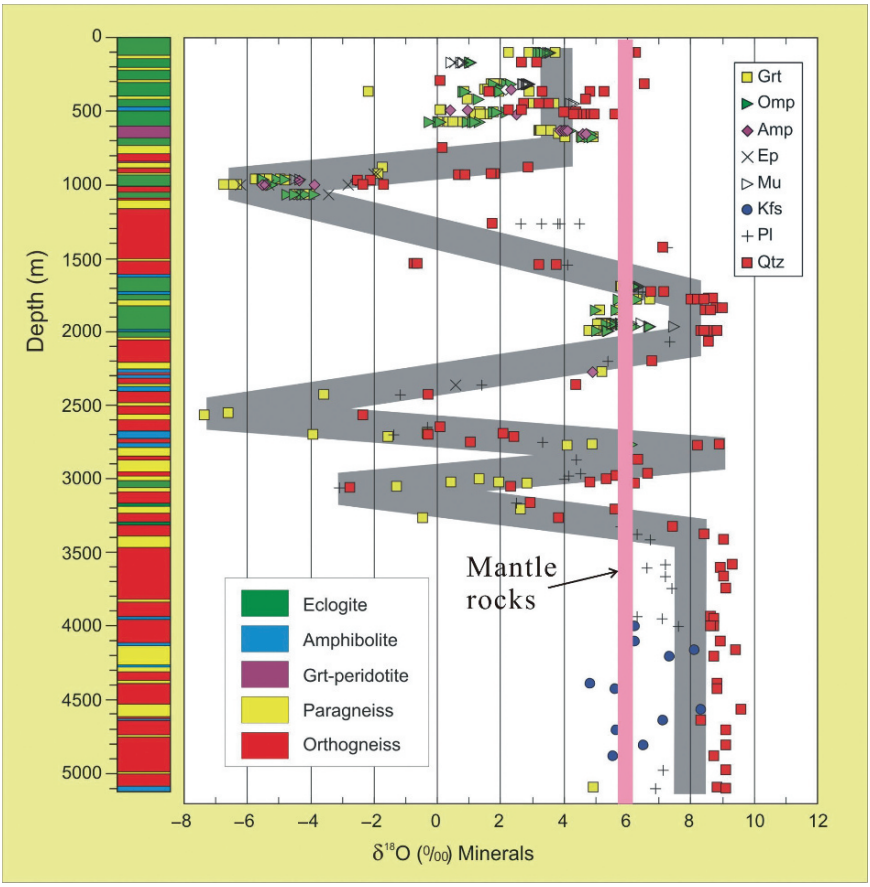

Fig. 3.51 A δ^{18}O continuous profile from the Chinese Continental Scientific Drilling (CCSD) project drilling entirely through ultrahigh pressure rocks (Xiao et al. Unpublished)

The Dabie–Sulu terrain is the largest among the UHP belts worldwide and covers an area of $5,000\,km^2$ in Dabie and $>10,000\,km^2$ in Sulu. The huge amounts of meteoric water necessary to cause the ^{18}O-depletions probably originate from the deglaciation of the Neoproterozoic snowball earth.

3.13.3 Lower Crustal Rocks

Granulites constitute the dominant rock type in the lower crust. Granulites may be found at the Earth's surface in two different settings: (1) exposed in high grade regional metamorphic belts and (2) found as small xenoliths in basaltic pipes. Both types of granulites suggest a compositionally diverse lower crust ranging in composition from mafic to felsic.

Stable isotope studies of granulite terranes (Sri Lanka – Fiorentini et al. 1990, South India – Jiang et al. 1988, Limpopo Belt – Hoernes and Van Reenen 1992; Venneman and Smith 1992, Adirondacks – Valley and coworkers) have shown that terranes are isotopically heterogeneous and are characterized by $\delta^{18}O$-values that range from "mantle-like" values to typical metasedimentary values above 10‰. Investigations of amphibolite/granulite transitions have shown little evidence for a pervasive fluid flux as a major factor in granulite facies metamorphism (Valley et al. 1990; Cartwright and Valley 1991; Todd and Evans 1993).

Similar results have been obtained from lower crustal granulite xenoliths, which also exhibit a large range in $\delta^{18}O$-values from 5.4 to 13.5‰ (Mengel and Hoefs 1990; Kempton and Harmon 1992). Mafic granulites are characterized by the lowest $\delta^{18}O$-values and range of ^{18}O-contents. By contrast, silicic meta-igneous and meta-sedimentary granulites are significantly enriched in ^{18}O with an average $\delta^{18}O$-value around 10‰. The overall variation of 8‰ emphasizes the O-isotope heterogeneity of the lower crust and demonstrates that pervasive deep crustal fluid flow and isotopic homogenization is not a major process.

3.13.4 Thermometry

Oxygen isotope thermometry is widely used to determine temperatures of metamorphic rocks. The principal concern in isotope thermometry continues to be the preservation of peak metamorphic temperatures during cooling. It has long been recognized that oxygen isotope thermometers often record discordant temperatures in slowly cooled metamorphic rocks. Figure 3.52 gives a compilation of literature data (Kohn 1999) showing $\delta^{18}O$-values and calculated temperature ranges for quartz–magnetite and muscovite–biotite. Muscovite-biotite pairs from rocks whose metamorphic conditions range from greenschist to granulite facies cluster around an apparent temperature of $\sim 300^{\circ}C$, whereas quartz–magnetite pairs have an apparent temperature of $\sim 540^{\circ}C$. These data demonstrate substantial diffusional resetting, which is consistent with relatively high water fugacities during cooling (Kohn 1999).

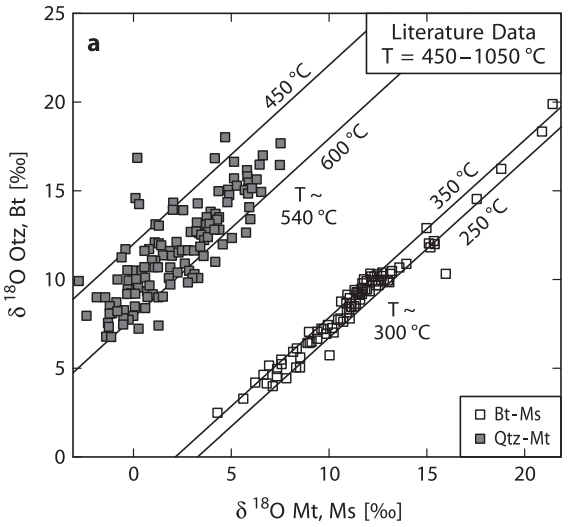

Fig. 3.52 Plot of $\delta^{18}O$ of quartz vs magnetite (*solid squares*) and of biotite vs muscovite (*open squares*) from rocks whose peak metamorphic conditions range from greenschist through granulite facies (after Kohn, 1999)

Assuming that a rock behaves as a closed system and consists of the three mineral assemblage quartz, feldspar and horblende, then hornblende will be the slowest diffusing phase and feldspar the fastest diffusing phase. Using the formulation of Dodson (1973) for closure temperature and a given set of parameters (diffusion constants, cooling rate and grain size), Giletti (1986) calculated apparent temperatures that would be obtained in rocks with different modal proportions of the three minerals once all isotope exchange had ceased in the rock. In the Giletti model, the apparent quartz – hornblende temperature is dependent only on the quartz/feldspar ratio and is independent of the amount of hornblende in the rock, since hornblende is the first phase to reach its closure temperature. Eiler et al. (1992, 1993), however, demonstrated that the abundance of the slow diffusing phase (e.g. hornblende) can affect apparent equilibrium temperatures because of continued exchange between the grain boundaries of this phase and fast diffusing phases. Thus, retrograde diffusion-related oxygen isotope exchange makes the calculation of peak metamorphic temperatures impossible, but can be used to estimate cooling rates.

Diffusion modeling, on the other hand, also predicts that accurate temperatures can be obtained from refractory accessory minerals, if they occur in a rock that is modally dominated by a readily exchangeable mineral (Valley 2001). The basis of this approach is that the accessory mineral preserves the isotope composition from crystallization because of slow diffusion while the dominant mineral preserves its isotope composition by mass balance because there are no other sufficiently abundant exchangeable phases.

Several refractory accessory mineral thermometers have been applied, including aluminosilicate, magnetite, garnet and rutile in quartz-rich rocks and magnetite,

titanite or diopside in marble. Refractory minerals are defined based on their relative diffusion rates relative to the matrix of the total rock. Thus plagioclase – magnetite or plagioclase – rutile may be good thermometers in amphibolite or eclogite-facies basic rocks, but fail in the granulite facies.

Other suitable phases for the preservation of peak metamorphic temperatures are the Al_2SiO_5 polymorphs kyanite and sillimanite, having both slow oxygen diffusion rates. By analyzing the alumosilicate polymorphs from a variety of rocks with different temperature histories, Sharp (1995) could derive empirical equilibrium fractionation factors for kyanite and sillimanite. In some rocks, oxygen-isotope temperatures are far higher than the regional metamorphic temperatures, possibly reflecting early high-temperature contact metamorphic effects that are preserved only in the most refractory phases.

Despite extensive diffusional resetting under water-buffered conditions, some rocks clearly retain oxygen isotope fractionations that are not reset by diffusion during cooling. Farquhar et al. (1996) have investigated two granulite terrains from NW Canada and Antarctica. Quartz–garnet temperatures of around $1,000°C$ are in good agreement with a variety of independent temperature estimations. Quartz–pyroxene

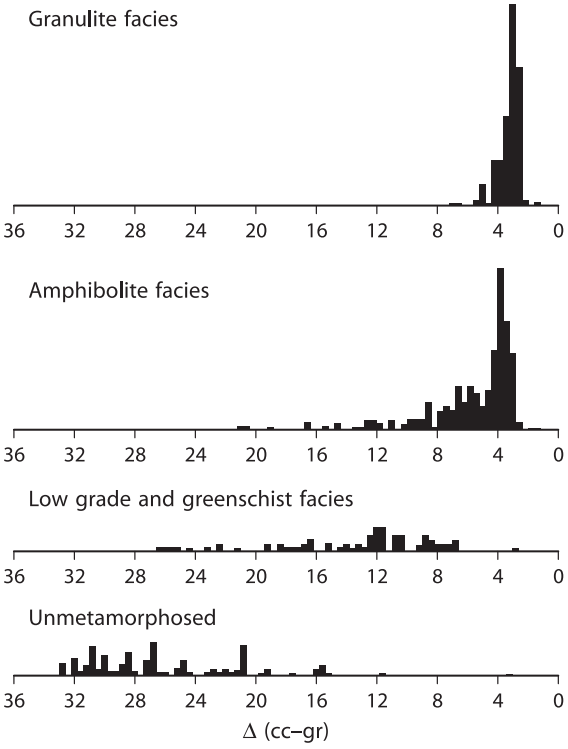

Fig. 3.53 Frequency distribution of calcite-graphite fractionations (Δ) with increasing metamorphic grade (after Des Marais 2001)

temperatures are significantly lower and still lower quartz–magnetite temperatures of around 670°C are attributed to a combination of faster oxygen diffusion in quartz and magnetite and recrystallization during late-stage deformation. The "dry" nature of granulites is obviously critical for preservation of high-temperature records. Cooler and more hydrous rocks seem to be less capable of retaining a record of peak temperatures.

Carbon isotope partitioning between calcite and graphite is another example of a favorable thermometer to record peak metamorphic temperatures in marbles because calcite is the abundant phase with relatively high carbon diffusivities whereas graphite is of minor abundance and has a very slow diffusion rate. Figure 3.53 shows the decrease of fractionation of calcite and graphite (Δ) with increasing metamorphic grade. The narrow range of graphite δ-values associated with granulite facies rocks indicates isotope equilibrium between carbonate and graphite at high temperatures. Figure 3.53 also indicates that under granulite-facies conditions the original carbon isotope composition has been obliterated due to exchange between carbonate and reduced carbon.

References

Abelson PH, Hoering TC (1961) Carbon isotope fractionation in formation of amino acids by photosynthetic organisms. Proc Natl Acad Sci U S A 47: 623

Abrajano TA, Sturchio NB, Bohlke JH, Lyon GJ, Poreda RJ, Stevens MJ (1988) Methane - hydrogen gas seeps Zambales ophiolite, Phillippines: deep or shallow origin. Chem Geol 71: 211–222

Ader M, Chaudhuri S, Coates JD, Coleman M (2008) Microbial perchlorate reduction: a precise laboratory determination of the chlorine isotope fractionation and its possible biochemical basis. Earth Planet Sci Lett 269: 604–612

Affek HP, Eiler JM (2006) Abundance of mass 47 CO_2 in urban air, car exhaust and human breath. Geochim Cosmochim Acta 70: 1–12

Aharon P, Fu B (2000) Microbial sulfate reduction rates and sulfur and oxygen isotope fractionation at oil and gas seeps in deepwater Gulf of Mexico. Geochim Cosmochim Acta 64: 233–246

Aharon P, Fu B (2003) Sulfur and oxygen isotopes of coeval sulphate-sulfide in pore fluids of cold seep sediments with sharp redox gradients. Chem Geol 195: 201–218

Alexander B, Savarino J, Barkov N, Delmas RJ, Thiemens MH (2002) Climate driven changes in the oxidation pathways of atmospheric sulfur. Geophys Res Lett 29: 30–31

Alexander B, Savarino J, Kreutz KJ, Thiemens MH (2004) Impact of preindustrial biomass-burning emissions on the oxidation pathways of troposheric sulfur and nitrogen. J Geophys Res 109: 8030–8038

Allard P (1983) The origin of hydrogen, carbon, sulphur, nitrogen and rare gases in volcanic exhalations: evidence from isotope geochemistry. In: Tazieff H, Sabroux JC (eds) Forecasting volcanic events. Elsevier, Amsterdam, pp 337–386

Allen RB, Cuffey KM (2001) Oxygen- and hydrogen-isotopic ratios of water in precipitation: beyond paleothermometry. Rev Miner Geochem 43: 527–553

Alt JC, Muehlenbachs K, Honnorez J (1986) An oxygen isotopic profile through the upper kilometer of the oceanic crust, DSDP hole 504 B. Earth Planet Sci Lett 80: 217–229

Altabet MA (1988) Variations in nitrogen isotopic compositions among particle classes: implications for particle transformation and flux in the open ocean. Deep Sea Res 35: 535–544

Altabet MA, Deuser WC (1985) Seasonal variations in natural abundance of ^{15}N in particles sinking to the deep Sargasso Sea. Nature 315: 218–219

Altabet MA, McCarthy JJ (1985) Temporal and spatial variations in the natural abundance of ^{15}N in POM from a warm-core ring. Deep Sea Res 32: 755–772

Altabet MA, Deuser WG, Honjo S, Stienen C (1991) Seasonal and depth related changes in the source of sinking particles in the North Atlantic. Nature 354: 136–139

Amari S, Hoppe P, Zinner E, Lewis RS (1993) The isotopic compositions of stellar sources of meteoritic graphite grains. Nature 365: 806–809

Amberger A, Schmidt HL (1987) Natürliche Isotopengehalte von Nitrat als Indikatoren für dessen Herkunft. Geochim Cosmochim Acta 51: 2699–2705

Anbar AD (2004a) Iron stable isotopes: beyond biosignatures. Earth Planet Sci Lett 217: 223–236

Anbar AD (2004b) Molybdenum stable isotopes: observations, interpretations and directions. Rev Miner Geochem 55: 429–454

Anbar AD, Rouxel O (2007) Metal stable isotopes in paleoceanography. Ann Rev Earth Planet Sci 35: 717–746

Ancour AM, Sheppard SMF, Guyomar O, Wattelet J (1999) Use of ^{13}C to trace origin and cycling of inorganic carbon in the Rhone river system. Chem Geol 159: 87–105

Anderson AT, Clayton RN, Mayeda TK (1971) Oxygen isotope thermometry of mafic igneous rocks. J Geol 79: 715–729

Anderson TF, Arthur MA (1983) Stable isotopes of oxygen and carbon and their application to sedimentologic and paleoenvironmental problems. In: Stable isotopes in sedimentary geology. SEPM short course no. 10, Dallas 1983, 111–151

Angert A, Cappa CD, DePaolo DJ (2004) Kinetic O-17 effects in the hydrologic cycle: indirect evidence and implications. Geochim Cosmochim Acta 68: 3487–3495

Arnold M, Sheppard SMF (1981) East Pacific Rise at 21°N: isotopic composition and origin of the hydrothermal sulfur. Earth Planet Sci Lett 56: 148–156

Arnold GL, Anbar AD, Barling J, Lyons TW (2004) Molybdenum isotope evidence for widespread anoxia in Mid-Proterozoic oceans. Science 304: 87–90

Arthur MA, Dean WE, Claypool CE (1985) Anomalous ^{13}C enrichment in modern marine organic carbon. Nature 315: 216–218

Assonov SS, Brenninkmeijer CA (2005) Reporting small $\delta^{17}O$ values: existing definitions and concepts. Rapid Commun Mass Spectrom 19: 627–636

Ayliffe LK, Chivas AR (1990) Oxyen isotope composition of the bone phosphate of Australian kangaroos: potential as a palaeoenvironmental recorder. Geochim Cosmochim Acta 54: 2603–2609

Ayliffe LK, Lister AM, Chivas AR (1992) The preservation of glacial-interglacial climatic signatures in the oxygen isotopes of elephant skeletal phosphate. Palaeogeogr Palaeoclimatol Palaeoecol 99: 179–191

Ayliffe LK, Chivas AR, Leakey MG (1994) The retention of primary oxygen isotope compositions of fossil elephant skeletal phosphate. Geochim Cosmochim Acta 58: 5291–5298

Bacastow RB, Keeling CD, Lueker TJ, Wahlen M, Mook WG (1996) The $\delta^{13}C$ Suess effect in the world surface oceans and its implications for oceanic uptake of CO_2: analysis of observations at Bermuda. Global Biochem Cycles 10: 335–346

Bachinski DJ (1969) Bond strength and sulfur isotope fractionation in coexisting sulfides. Econ Geol 64: 56–65

Baertschi P (1976) Absolute ^{18}O content of standard mean ocean water. Earth Planet Sci Lett 31: 341–344

Baker AJ, Fallick AE (1989) Heavy carbon in two-billion-year-old marbles from Lofoten-Vesteralen, Norway: implications for the Precambrian carbon cycle. Geochim Cosmochim Acta 53: 1111–1115

Baker J, Matthews A (1995) The stable isotopic composition of a metamorphic complex, Naxos, Greece. Cont Mineral Petrol 120:391–403

Baker JA, Macpherson CG, Menzies MA, Thirlwall MF, Al-Kadasi M, Mattey DP (2000) Resolving crustal and mantle contributions to continental flood volcanism, Yemen: constraints from mineral oxygen isotope data. J Petrol 41: 1805–1820

Balci N, Bullen TD, Witte-Lien K, Shanks WC, Motelica M, Mandernack KW (2006) Iron isotope fractionation during microbially simulated Fe(II) oxidation and Fe(III) precipitation. Geochim Cosmochim Acta 70: 622–639

Balistrieri L, Borrok DM, Wanty RB, Ridley WI (2008) Fractionation of Cu and Zn isotopes during adsorption onto amorphous Fe(III) oxyhydroxide: experimental mixing of acid rock drainage and ambient river water. Geochim Cosmochim Acta 72: 311–328

Banks DA, Green R, Cliff RA, Yardley BWD (2000) Chlorine isotopes in fluid inclusions: determination of the origins of salinity in magmatic fluids. Geochim Cosmochim Acta 64: 1785–1789

Banner JL, Wasserburg GJ, Dobson PF, Carpenter AB, Moore CH (1989) Isotopic and trace element constraints on the orgin and evolution of saline groundwaters from central Missouri. Geochim Cosmochim Acta 53: 383–398

Bao H, Koch PL (1999) Oxygen isotope fractionation in ferric oxide-water systems: low temperature synthesis. Geochim Cosmochim Acta 63: 599–613

Bao H, Thiemens MH (2000) Generation of O_2 from $BaSO_4$ using a CO_2-laser fluorination system for simultaneous $\delta^{18}O$ and $\delta^{17}O$ analysis. Anal Chem 72: 4029–4032

Bao H, Thiemens MH, Farquahar J, Campbell DA, Lee CC, Heine K, Loope DB (2000) Anomalous ^{17}O compositions in massive sulphate deposits on the Earth. Nature 406: 176–178

Bao H, Thiemens MH, Heine K (2001) Oxygen-17 excesses of the Central Namib gypcretes: spatial distribution. Earth Planet Sci Lett 192: 125–135

Barling J, Anbar AD (2004) Molybdenum isotope fractionation during absorption by manganese oxides. Earth Planet Sci Lett 217: 315–329

Barling J, Arnold GL, Anbar AD (2001) Natural mass-dependent variations in the isotopic composition of molybdenum. Earth Planet Sci Lett 193: 447–457

Barnes I, Irwin WP, White DE (1978) Global distribution of carbon dioxide discharges and major zones of seismicity. US Geological Survey, Water-Resources Investigation 78–39, Open File Report

Barnes JD, Sharp ZD, Fischer TP (2006) Chlorine stable isotope systematics and geochemistry along the Central American and Izu-Bonin-Mariana volcanic arc. EOS Trans AGU 87(52), Fall Meet Suppl V52B–08

Baroni M, Thiemens MH, Delmas RJ, Savarino J (2007) Mass-independent sulfur isotopic composition in stratospheric volcanic eruptions. Science 315: 84–87

Barth S (1993) Boron isotope variations in nature: a synthesis. Geologische Rundschau 82: 640–651

Basile-Doelsch I, Meunier JD, Parron C (2005) Another continental pool in the terrestrial silicon cycle. Nature 433: 399–402

Baumgartner LP, Rumble D (1988) Transport of stable isotopes. I. Development of a kinetic continuum theory for stable isotope transport. Contr Miner Petrol 98: 417–430

Baumgartner LP, Valley JW (2001) Stable isotope transport and contact metamorphic fluid flow. In: Stable Isotope Geochemistry. Rev Miner Geochem 43: 415–467

Beard BL, Johnson CM (1999) High-precision iron isotope measurements of terrestrial and lunar materials. Geochim Cosmochim Acta 63: 1653–1660

Beard BL, Johnson C (2004) Fe isotope variations in the modern and ancient Earth and other planetary bodies. Rev Miner Geochem 55: 319–357

Beard BL, Johnson CM, Cox L, Sun H, Nealson KH, Aguilar C (1999) Iron isotope biosphere. Science 285: 1889–1892

Beaty DW, Taylor HP (1982) Some petrologic and oxygen isotopic relationships in the Amulet Mine, Noranda, Quebec, and their bearing on the origin of Archaean massive sulfide deposits. Econ Geol 77: 95–108

Beaudoin G, Taylor BE (1994) High precision and spatial resolution sulfur-isotope analysis using MILES laser microprobe. Geochim Cosmochim Acta 58: 5055–5063

Beaudoin G, Taylor BE, Rumble D, Thiemens M (1994) Variations in the sulfur isotope composition of troilite from the Canyon Diablo iron meteorite. Geochim Cosmochim Acta 58: 4253–4255

Bebout GE, Fogel ML (1992) Nitrogen isotope compositions of metasedimentary rocks in the Catalina Schist, California: implications for metamorphic devolatilization history. Geochim Cosmochim Acta 56: 2839–2849

Bechtel A, Hoernes S (1990) Oxygen isotope fractionation between oxygen of different sites in illite minerals: a potential geothermometer. Contr Miner Petrol 104: 463–470

Bechtel A, Sun Y, Püttmann W, Hoernes S, Hoefs J (2001) Isotopic evidence for multi-stage base metal enrichment in the Kupferschiefer from the Sangershausen Basin, Germany. Chem Geol 176: 31–49

Beck WC, Grossman EL, Morse JW (2005) Experimental studies of oxygen isotope fractionation in the carbonic acid system at 15°, 25°, and 40°C. Geochim Cosmochim Acta 69: 3493–3503

Becker RH, Epstein S (1982) Carbon, hydrogen and nitrogen isotopes in solvent-extractable organic matter from carbonaceous chondrites. Geochim Cosmochim Acta 46: 97–103

Bell DR, Ihinger PD (2000) The isotopic composition of hydrogen in nominally anhydrous mantle minerals. Geochim Cosmochim Acta 64: 2109–2118

Bemis BE, Spero HJ, Bijma J, Lea DW (1998) Reevaluation of the oxygen isotopic composition of planktonic foraminifera: experimental results and revised paleotemperature equations. Paleoceanography 13: 150–160

Bender ML, Keigwin LD (1979) Speculations about upper Miocene changes in abyssal Pacific dissolved bicarbonate $\delta^{13}C$. Earth Planet Sci Lett 45: 383–393

Bender M, Sowers T, Labeyrie L (1994) The Dole effect and its variations during the last 130000 years as measured in the Vostok ice core. Global Biogeochem Cycles 8: 363–376

Benson BB, Parker PDM (1961) Nitrogen/argon and nitrogen isotope ratios in aerobic sea water. Deep Sea Res 7: 237–253

Bergquist BA, Blum JD (2007) Mass-dependent and mass-independent fractionation of Hg isotopes in aquatic systems. Geochim Cosmochim Acta 71: A83 (abstr)

Bergquist BA, Boyle EA (2006) Iron isotopes in the Amazon River system: weathering and transport signatures. Earth Planet Sci Lett 248: 54–68

Bermin J, Vance D, Archer C, Statham PJ (2006) The determination of the isotopic composition of Cu and Zn in seawater. Chem Geol 226: 280–297

Berndt ME, Seal RR, Shanks WC, Seyfried WE (1996) Hydrogen isotope systematics of phase separation in submarine hydrothermal systems: experimental calibration and theoretical models. Geochim Cosmochim Acta 60: 1595–1604

Berner RA (1990) Atmospheric carbon dioxide levels over Phanerozoic time. Science 249: 1382–1386

Berner U, Faber E, Scheeder G, Panten D (1995) Primary cracking of algal and landplant kerogens: kinetic models of isotope variations in methane, ethane and propane. Chem Geol 126: 233–245

Bickle MJ, Baker J (1990) Migration of reaction and isotopic fronts in infiltration zones: assessments of fluid flux in metamorphic terrains. Earth Planet Sci Lett 98: 1–13

Bidigare RR et al. (1997) Consistent fractionation of ^{13}C in nature and in the laboratory: growth-rate effects in some haptophyte algae. Global Biogeochem Cycles 11: 279–292

Bigeleisen J (1965) Chemistry of isotopes. Science 147: 463–471

Bigeleisen J, Mayer MG (1947) Calculation of equilibrium constants for isotopic exchange reactions. J Chem Phys 15: 261–267

Bigeleisen J, Wolfsberg M (1958) Theoretical and experimental aspects of isotope effects in chemical kinetics. Adv Chem Phys 1: 15–76

Bigeleisen J, Perlman ML, Prosser HC (1952) Conversion of hydrogenic materials for isotopic analysis. Anal Chem 24: 1356

Bindeman IN, Ponomareva VV, Bailey JC, Valley JW (2004) Volcanic arc of Kamchatka: a province with high-$\delta^{18}O$ magma sources and large scale $^{18}O/^{16}O$ depletion of the upper crust. Geochim Cosmochim Acta 68: 841–865

Bindeman IN, Eiler JN, et al. (2005) Oxygen isotope evidence for slab melting in modern and ancient subduction zones. Earth Planet Sci Lett 235: 480–496

Bird MI, Chivas AR (1989) Stable-isotope geochronology of the Australian regolith. Geochim Cosmochim Acta 53: 3239–3256

Bird MI, Longstaffe FJ, Fyfe WS, Bildgen P (1992) Oxygen isotope systematics in a multiphase weathering system in Haiti. Geochim Cosmochim Acta 56: 2831–2838

Blake RE, O'Neil JR, Garcia GA (1997) Oxygen isotope systematics of biologically mediated reactions of phosphate: I Microbial degradation of organophosphorus compounds. Geochim Cosmochim Acta 61: 441–4422

Blake RE, O'Neil JR, Surkov A (2005) Biogeochemical cycling of phosphorus: insights from oxygen isotope effects of phosphoenzymes. Am J Sci 305: 596–620

Blattner P, Lassey KR (1989) Stable isotope exchange fronts, Damköhler numbers and fluid to rock ratios. Chem Geol 78: 381–392

Blattner P, Dietrich V, Gansser A (1983) Contrasting ^{18}O enrichment and origins of High Himalayan and Transhimalayan intrusives. Earth Planet Sci Lett 65: 276–286

Blisnink PM, Stern LA (2005) Stable isotope altimetry: a critical review. Am J Sci 305: 1033–1074

Boctor NZ, Alexander CM, Wang J, Hauri E (2003) The sources of water in Martian meteorites: clues from hydrogen isotopes. Geochim Cosmochim Acta 67: 3971–3989

Boehme SE, Blair NE, Chanton JP, Martens CS (1996) A mass balance of ^{13}C and ^{12}C in an organic-rich methane-producing marine sediment. Geochim Cosmochim Acta 60: 3835–3848

Bogard DD, Johnson P (1983) Martian gases in an Antarctic meteorite. Science 221: 651–654

Bolliger C, Schroth MH, Bernasconi SM, Kleikemper J, Zeyer J (2001) Sulfur isotope fractionation during microbial reduction by toluene-degrading bacteria. Geochim Cosmochim Acta 65: 3289–3299

Bonifacie M, Jendrzejewski N, Agrinier P, Humler E, Coleman M, Javoy M (2008) The chlorine isotope composition of the Earth,s mantle. Science 319: 1518–1520

Borthwick J, Harmon RS (1982) A note regarding ClF_3 as an alternative to BrF_5 for oxygen isotope analysis. Geochim Cosmochim Acta 46: 1665–1668

Böttcher ME (1996) $^{18}O/^{16}O$ and $^{13}C/^{12}C$ fractionation during the reaction of carbonates with phosphoric acid: effects of cationic substitution and reaction temperature. Isotopes Environ Health Stud 32: 299–305

Böttcher ME, Brumsack HJ, Lange GJ (1998) Sulfate reduction and related stable isotope (^{34}S, ^{18}O) variations in interstitial waters from the eastern Mediterranean. Proc Ocean Drilling Program, Scientific Res 160: 365–373

Böttcher ME, Thamdrup B, Vennemann TW (2001) Oxygen and sulfur isotope fractionation during anaerobic bacterial disproportionation of elemental sulfur. Geochim Cosmochim Acta 65: 1601–1609

Bottinga Y (1969a) Calculated fractionation factors for carbon and hydrogen isotope exchange in the system calcite-carbon dioxide-graphite-methane-hydrogen-water-vapor. Geochim Cosmochim Acta 33: 49–64

Bottinga Y (1969b) Carbon isotope fractionation between graphite, diamond and carbon dioxide. Earth Planet Sci Lett 5: 301–307

Bottinga Y, Craig H (1969) Oxygen isotope fractionation between CO_2 and water and the isotopic composition of marine atmospheric CO_2. Earth Planet Sci Lett 5: 285–295

Bottinga Y, Javoy M (1973) Comments on oxygen isotope geothermometry. Earth Planet Sci Lett 20: 250–265

Bottomley DJ, Katz A, Chan LH, Starinsky A, Douglas M, Clark ID, Raven KG (1999) The origin and evolution of Canadian Shield brines: evaporation or freezing of seawater? New lithium isotope and geochemical evidence from the Slave craton. Chem Geol 155: 295–320

Boudreau BP, Westrich JT (1984) The dependence of bacterial sulfate reduction on sulfate concentration in marine sediments. Geochim Cosmochim Acta 48: 2503–2516

Boudreau AE, Stewart MA, Spivack AJ (1997) Stable Cl-isotopes and origin of high-Cl magmas of the Stillwater complex. Geology 25: 791–794

Bowman JR, O'Neil JR, Essene EJ (1985) Contact skarn formation at Elkhorn, Montana. II. Origin and evolution of C-O-H skarn fluids. Am J Sci 285: 621–660

Bowman JR, Willett SD, Cook SJ (1994) Oxygen isotope transport and exchange during fluid flow. Am J Sci 294: 1–55

Boyd SR, Pillinger CT (1994) A preliminary study of $^{15}N/^{14}N$ in octahedral growth from diamonds. Chem Geol 116: 43–59

Boyd SR, Pillinger CT, Milledge HJ, Mendelssohn MJ, Seal M (1992) C and N isotopic composition and the infrared absorption spectra of coated diamonds: evidence for the regional uniformity of CO_2-H_2O rich fluids in lithospheric mantle. Earth Planet Sci Lett 109: 633–644

Brand W (2002) Mass spectrometer hardware for analyzing stable isotope ratios. In: P de Groot (ed.) Handbook of stable isotope analytical techniques. Elsevier, Amsterdam

Brandriss ME, O'Neil JR, Edlund MB, Stoermer EF (1998) Oxygen isotope fractionation between diatomaceous silica and water. Geochim Cosmochim Acta 62: 1119–1125

Bremner JM, Keeney DR (1966) Determination and isotope ratio analysis of different forms of nitrogen in soils, III. Soil Sci Soc Am Proc 30: 577–582

Brenninkmeijer CAM (1993) Measurement of the abundance of ^{14}CO in the atmosphere and the $^{13}C/^{12}C$ and $^{18}O/^{16}O$ ratio of atmospheric CO with applications in New Zealand and Australia. J Geophys Res 98: 10595–10614

Brennikmeijer CAM, Kraft MP, Mook WG (1983) Oxygen isotope fractionation between CO_2 and H_2O. Isotope Geosci 1: 181–190

Brenninkmeijer CAM, Lowe DC, Manning MR, Sparks RJ, van Velthoven PFJ (1995) The ^{13}C, ^{14}C and ^{18}O isotopic composition of CO, CH_4 and CO_2 in the higher southern latitudes and lower stratosphere. J Geophys Res 100: 26163–26172

Broecker WS (1974) Chemical oceanography. Harcourt Brace Jovanovich, New York

Brooker R, Blundy J, James R (2004) Trace element and Li isotope systematics in zabargad peridotites: evidence of ancient subduction processes in the Red Sea mantle. Chem Geol 212: 179–204

Brüchert V, Pratt LM (1996) Contemporaneous early diagenetic formation of organic and inorganic sulfur in estuarine sediments from the St Andrew Bay, Florida, USA. Geochim Cosmochim Acta 60: 2325–2332

Brüchert V, Knoblauch C, Jörgensen BB (2001) Controls on stable sulfur isotope fractionation during bacterial sulfate reduction in Arctic sediments. Geochim Cosmochim Acta 65: 763–776

Brumsack HJ, Zuleger E, Gohn E, Murray RW (1992) Stable and radiogenic isotopes in pore waters from Leg 1217, Japan Sea. Proc Ocean Drilling Progr 127128: 635–649

Brunner B, Bernasconi SM, Kleikemper J, Schroth MH (2005) A model of oxygen and sulfur isotope fractionation in sulfate during bacterial sulfate reduction. Geochim Cosmochim Acta 69: 4773–4785

Bryant JD, Koch PL, Froelich PN, Showers WJ, Genna BJ (1996) Oxygen isotope partitioning between phosphate and carbonate in mammalian apatite. Geochim Cosmochim Acta 60: 5145–5148

Buhl D, Neuser RD, Richter DK, Riedel D, Roberts B, Strauss H, Veizer J (1991) Nature and nurture: environmental isotope story of the river Rhine. Naturwissenschaften 78: 337–346

Buhl D, Immenhauser A, Smeulders G, Kabiri L, Richter DK (2007) Time series $\delta^{26}Mg$ analysis in speleothem calcite: kinetic versus equilibrium fractionation, comparison with other proxies and implications for palaeoclimate research. Chem Geol 244: 715–729

Bullen TO, White AF, Childs CW, Vivit DV, Schulz MS (2001) Demonstration of significant abiotic iron isotope fractionation in nature. Geology 29:699–702

Burdett JW, Arthur MA, Richardson A (1989) A Neogene seawater sulfate isotope age curve from calcareous pelagic microfossils. Earth Planet Sci Lett 94: 189–198

Burgoyne TW, Hayes JM (1998) Quantitative production of H_2 by pyrolysis of gas chromatographic effluents. Anal Chem 70: 5136–5141

Calmels D, Gaillerdet J, Brenot A, France-Lanord C (2007) Sustained sulfide oxidation by physical erosion processes in the Mackenzie River basin: climatic perspectives. Geology 35: 1003–1006

Came RE, Eiler JM, Veizer J, Azmy K, Brand U, Weidman CR (2007) Coupling of surface temperatures and atmospheric CO_2 concentrations during the Paleozoic era. Nature 449: 198–201

Cameron EM (1982) Sulphate and sulphate reduction in early Precambrian oceans. Nature 296: 145–148

Cameron EM, Hall GEM, Veizer J, Krouse HR (1995) Isotopic and elemental hydrogeochemistry of a major river system: Fraser River, British Columbia, Canada. Chem Geol 122: 149–169

Canfield DE (2001a) Biogeochemistry of sulfur isotopes. Rev Miner 43: 607–636

Canfield DE (2001b) Isotope fractionation by natural populations of sulfate-reducing bacteria. Geochim Cosmochim Acta 65: 1117–1124

Canfield DE, Teske A (1996) Late Proterozoic rise in atmospheric oxygen concentration inferred from phylogenetic and sulphur-isotope studies. Nature 382: 127–132
Canfield DE, Thamdrup B (1994) The production of ^{34}S depleted sulfide during bacterial disproportion to elemental sulfur. Science 266: 1973–1975
Canfield DE, Olsen CA, Cox RP (2006) Temperature and ist control of isotope fractionation by a sulfate reducing bacterium. Geochim Cosmochim Acta 70: 548–561
Carder EA, Galy A, McKenzie JA, Vasconcelos C, Elderfield HE (2005) Magnesium isotopes in bacterial dolomites: a novel approach to the dolomite problem. Geochim Cosmochim Acta 69: A213
Cardinal D, Alleman LY, de Jong J, Ziegler K, Andre L (2003) Isotopic composition of silicon measured by multicollector plasma source mass spectrometry in dry plasma mode. J Anal At Spectrom 18: 213–218
Carothers WW, Adami LH, Rosenbauer RJ (1988) Experimental oxygen isotope fractionation between siderite-water phosphoric acid liberated CO_2-siderite. Geochim Cosmochim Acta 52: 2445–2450
Cartigny P (2005) Stable isotopes and the origin of diamond. Elements 1: 79–84
Cartigny P, Boyd SR, Harris JW, Javoy M (1997) Nitrogen isotopes in peridotitic diamonds from Fuxian, China: the mantle signature. Terra Nova 9: 175–179
Cartigny P, Harris JW, Javoy M (1998) Subduction related diamonds? The evidence for a mantle-derived origin from coupled delta ^{13}C - delta ^{15}N determinations. Chem Geol 147: 147–159
Cartwright I, Valley JW (1991) Steep oxygen isotope gradients at marble-metagranite contacts in the NW Adirondacks Mountains, N.Y. Earth Planet Sci Lett 107: 148–163
Catanzaro EJ, Murphy TJ (1966) Magnesium isotope ratios in natural samples. J Geophys Res 71: 1271
Cerling TE (1984) The stable isotopic composition of modern soil carbonate and its relationship to climate. Earth Planet Sci Lett 71: 229–240
Cerling TE (1991) Carbon dioxide in the atmosphere: evidence from Cenozoic and Mesozoic paleosols. Am J Sci 291: 377–400
Cerling TE, Harris JM (1999) Carbon isotope fractionation between diet and bioapatite in ungulate mammals and implications for ecological and paleocogical studies. Oecologia 120: 347–363
Cerling TE, Sharp ZD (1996) Stable carbon and oxygen isotope analyses of fossil tooth enamel using laser ablation. Palaeogeogr Palaeoclimatol Palaeoecol 126: 173–186
Cerling TE, Brown FH, Bowman JR (1985) Low-temperature alteration of volcanic glass: hydration, Na, K,^{18}O and Ar mobility. Chem Geol 52: 281–293
Cerling TE, Wang Y, Quade J (1993) Expansion of C4 ecosystems as an indicator of global ecological change in the late Miocene. Nature 361: 344–345
Cerling TE, Harris JM, MacFadden BJ, Leakey MG, Quade J, Eisenmann V, Ehleringer JR (1997) Global vegetation change through the Miocene/Pliocene boundary. Nature 389: 153–158
Chacko T, Riciputi LR, Cole DR, Horita J (1999) A new technique for determining equilibrium hydrogen isotope fractionation factors using the ion microprobe: application to the epidote-water system. Geochim Cosmochim Acta 63: 1–10
Chacko T, Cole DR, Horita J (2001) Equilibrium oxygen, hydrogen and carbon fractionation factors applicable to geologic systems. Rev Miner Geochem 43: 1–81
Chamberlain CP, Poage MA (2000) Reconstructing the paleotopography of mountain belts from the isotopic composition of authigenic minerals. Geology 28: 115–118
Chan L-H, Kastner M (2000) Lithium isotopic composition of pore fluids and sediments in the Costa Rica subduction zone: implications for fluid processes and sediment contribution to the arc volcanoes. Earth Planet Sci Lett 183: 275–290
Chang V, Williams R, Makishima A, Belshaw N, O'Nions RK (2004) Mg and Ca isotope fractionation during $CaCO_3$ biomineralisation. Biochem Biophys Res Commun 32: 79–85
Chaussidon M, Albarede F (1992) Secular boron isotope variations in the continental crust: an ion microprobe study. Earth Planet Sci Lett 108: 229–241
Chaussidon M, Marty B (1995) Primitive boron isotope composition of the mantle. Science 269: 383–386

Chaussidon M, Albarede F, Sheppard SMF (1987) Sulphur isotope heterogeneity in the mantle from ion microprobe measurements of sulphide inclusions in diamonds. Nature 330: 242–244
Chaussidon M, Albarede F, Sheppard SMF (1989) Sulphur isotope variations in the mantle from ion microprobe analysis of microsulphide inclusions. Earth Planet Sci Lett 92: 144–156
Chazot G, Lowry D, Menzies M, Mattey D (1997) Oxygen isotope compositions of hydrous and anhydrous mantle peridotites. Geochim Cosmochim Acta 61: 161–169
Chiba H, Sakai H (1985) Oxygen isotope exchange rate between dissolved sulphate and water at hydrothermal temperatures. Geochim Cosmochim Acta 49: 993–1000
Chiba H, Chacko T, Clayton RN, Goldsmith JR (1989) Oxygen isotope fractionations involving diopside, forsterite, magnetite and calcite: application to geothermometry. Geochim Cosmochim Acta 53: 2985–2995
Chivas AR, Andrew AS, Sinha AK, O'Neil JR (1982) Geochemistry of Pliocene-Pleistocene oceanic arc plutonic complex, Guadalcanal. Nature 300: 139–143
Chmeleff J, Horn I, Steinhöfel G, von Blanckenburg F (2008) In situ determination of precise stable Si isotope ratios by UV-femtosecond laser ablation high-resolution multi-collector ICP-MS. Chem Geol 249: 155–160
Chung HM, Sackett WM (1979) Use of stable carbon isotope compositions of pyrolytically derived methane as maturity indices for carbonaceous materials. Geochim Cosmochim Acta 43: 1979–1988
Ciais P, Tans PP, Trolier M, White JWC, Francey RJ (1995) A large northern hemisphere terrestrial CO_2 sink indicated by the $^{13}C/^{12}C$ ratio of atmospheric CO_2. Science 269: 1098–1102
Ciais P, Meijer HAJ (1998) The $^{18}O/^{16}O$ isotope ratio of atmospheric CO_2 and its role in global carbon cycle research. In: Griffiths H (ed) Stable Isotopes. Bios Sc. Publ Oxford, 409–431
Cifuentes LA, Fogel ML, Pennock JR, Sharp JR (1989) Biogeochemical factors that influence the stable nitrogen isotope ratio of dissolved ammonium in the Delaware Estuary. Geochim Cosmochim Acta 53: 2713–2721
Claypool GE, Holser WT, Kaplan IR, Sakai H, Zak I (1980) The age curves of sulfur and oxygen isotopes in marine sulfate and their mutual interpretation. Chem Geol 28: 199–260
Clayton RN (1993) Oxygen isotopes in meteorites. Ann Rev Earth Planet Sci 21: 115–149
Clayton RN (2002) Self-shielding in the solar nebula. Nature 451: 860–861
Clayton RN (2004) Oxygen isotopes in meteorites. In: Treatise on geochemistry, vol 1. Elsevier, Amsterdam, pp. 129–142
Clayton RN, Epstein S (1958) The relationship between $^{18}O/^{16}O$ ratios in coexisting quartz, carbonate and iron oxides from various geological deposits. J Geol 66: 352–373
Clayton RN, Kieffer SW (1991) Oxygen isotope thermometer calibrations. In: Taylor HP, O'Neil JR, Kaplan IR (eds.) Stable isotope geochemistry: A tribute to Sam Epstein. Geochem Soc Spec Publ 3: 3–10
Clayton RN, Mayeda TK (1963) The use of bromine pentafluoride in the extraction of oxygen from oxides and silicates for isotopic analysis. Geochim Cosmochim Acta 27: 43–52
Clayton RN, Mayeda TK (1996) Oxygen isotope studies of achondrites. Geochim Cosmochim Acta 60: 1999–2017
Clayton RN, Mayeda TK (1999) Oxygen isotope studies of carbonaceous chondrites. Geochim Cosmochim Acta 63: 2089–2104
Clayton RN, Steiner A (1975) Oxygen isotope studies of the geothermal system at Warakei, New Zealand. Geochim Cosmochim Acta 39: 1179–1186
Clayton RN, Friedman I, Graf DL, Mayeda TK, Meents WF, Shimp NF (1966) The origin of saline formation waters. 1. Isotopic composition. J Geophys Res 71: 3869–3882
Clayton RN, Muffler LJP, White (1968) Oxygen isotope study of calcite and silicates of the River Branch No. I well, Salton Sea Geothermal Field, California. Am J Sci 266: 968–979
Clayton RN, Grossman L, Mayeda TK (1973a) A component of primitive nuclear composition in carbonaceous meteorites. Science 182: 485–488
Clayton RN, Hurd JM, Mayeda TK (1973b) Oxygen isotopic compositions of Apollo 15, 16 and 17 samples and their bearing on lunar origin and petrogenesis. Proc 4th Lunar Sci Conf Geochim Cosmochim Acta Suppl 2: 1535–1542

Clayton RN, Goldsmith JR, Karel KJ, Mayeda TK, Newton RP (1975) Limits on the effect of pressure in isotopic fractionation. Geochim Cosmochim Acta 39: 1197–1201
Clayton RN, Onuma N, Grossman C, Mayeda TK (1977) Distribution of the presolar component in Allende and other carbonaceous chondrites. Earth Planet Sci Lett 34: 209–224
Clayton RN, Goldsmith JR, Mayeda TK (1989) Oxygen isotope fractionation in quartz, albite, anorthite and calcite. Geochim Cosmochim Acta 53: 725–733
Cliff SS, Thiemens MH (1997) The $^{18}O/^{16}O$ and $^{17}O/^{16}O$ ratios in atmospheric nitrous oxide: a mass independent anomaly. Science 278: 1774–1776
Cliff SS, Brenninkmeijer CAM, Thiemens MH (1999) First measurement of the $^{18}O/^{16}O$ and $^{17}O/^{16}O$ ratios in stratospheric nitrous oxide: a mass-independent anomaly. J Geophys Res 104: 16171–16175
Cline JD, Kaplan IR (1975) Isotopic fractionation of dissolved nitrate during denitrification in the eastern tropical North Pacific Ocean. Mar Chem 3: 271–299
Clor LE, Fischer TP, Hilton DR, Sharp ZD, Hartono U (2005) Volatile and N isotope chemistry of the Molucca Sea collision zone: tracing source components along the Sangihe arc, Indonesia. Geochem Geophys Geosys 6, Q03J14, doi: 10.1029/2004GC00825
Cole DR (2000) Isotopic exchange in mineral-fluid systems IV: The crystal chemical controls on oxygen isotope exchange rates in carbonate-H_2O and layer silicate-H_2O systems. Geochim Cosmochim Acta 64: 921–933
Cole DR, Chakraborty S (2001) Rates and mechanisms of isotopic exchange. Rev Mineral Geochem 43: 83–223
Cole JE, Fairbanks RG (1990) The southern oscillation recorded in the δ18O of corals from Tarawa atoll. Paleoceanography 5: 669–683
Cole JE, Fairbanks RG, Shen GT (1993) The spectrum of recent variability in the southern oscillation: results from a Tarawa atoll. Science 260: 1790–1793
Coleman ML, Moore MP (1978) Direct reduction of sulfates to sulfur dioxide for isotope analysis. Anal Chem 50: 1594–1595
Coleman ML, Sheppard TJ, Durham JJ, Rouse JE, Moore GR (1982) Reduction of water with zinc for hydrogen isotope analysis. Anal Chem 54: 993–995
Connolly CA, Walter LM, Baadsgaard H, Longstaffe F (1990) Origin and evolution of formation fluids, Alberta Basin, western Canada sedimentary basin: II. Isotope systematics and fluid mixing. Applied Geochem 5: 397–414
Cook N, Hoefs J (1997) Sulphur isotope characteristics of metamorphosed Cu-(Zn) volcanogenic massive sulphide deposits in the Norwegian Caledonides. Chem Geol 135: 307–324
Cooper KM, Eiler JM, Asimov PD, Langmuir CH (2004) Oxygen isotope evidence for the origin of enriched mantle beneath the mid-Atlantic ridge. Earth Planet Sci Lett 220: 297–316
Coplen TB (1996) New guidelines for the reporting of stable hydrogen, carbon and oxygen isotope ratio data. Geochim Cosmochim Acta 60: 3359–3360
Coplen TB, Hanshaw BB (1973) Ultrafiltration by a compacted clay membrane. I. Oxygen and hydrogen isotopic fractionation. Geochim Cosmochim Acta 37: 2295–2310
Coplen TB, Kendall C, Hopple J (1983) Comparison of stable isotope reference samples. Nature 302: 236–238
Coplen TB, et al. (2002) Isotope abundance variations of selected elements. Pure Appl Chem 74: 1987–2017
Coplen TB, Brand WA, Gehre M, Gröning M, Meijer HA, Toman B, Verkouteren RM (2006) New guidelines for $\delta^{13}C$ measurements. Anal Chem 78: 2439–2441
Cortecci G, Longinelli A (1970) Isotopic composition of sulfate in rain water, Pisa, Italy. Earth Planet Sci Lett 8: 36–40
Craig H (1953) The geochemistry of the stable carbon isotopes. Geochim Cosmochim Acta 3: 53–92
Craig H (1957) Isotopic standards for carbon and oxygen and correction factors for mass-spectrometric analysis of carbon dioxide. Geochim Cosmochim Acta 12: 133–149
Craig H (1961a) Isotopic variations in meteoric waters. Science 133: 1702–1703

Craig H (1961b) Standard for reporting concentrations of deuterium and oxygen-18 in natural waters. Science 133: 1833–1834
Craig H, Gordon L (1965) Deuterium and oxygen-18 variations in the ocean and the marine atmosphere. In: Symposium on marine geochemistry. Graduate School of Oceanography, Univ Rhode Island, OCC Publ No 3: 277
Craig H, Keeling CD (1963) The effects of atmospheric N_20 on the measured isotopic composition of atmospheric CO_2. Geochim Cosmochim Acta 27: 549–551
Craig H, Boato G, White DE (1956) Isotopic geochemistry of thermal waters. Proc 2nd Conf Nucl Process Geol Settings, p 29
Craig H, Chou CC, Welhan JA, Stevens CM, Engelkemeier A (1988) The isotopic composition of methane in polar ice cores. Science 242: 1535–1539
Criss RE (1999) Principles of stable isotope distribution. Oxford University Press, New York
Criss RE, Taylor HP (1986) Meteoric-hydrothermal systems. In: Stable isotopes in high temperature geological processes. Rev Miner 16: 373–424
Criss RE, Champion DE, McIntyre DH (1985) Oxygen isotope, aeromagnetic and gravity anomalies associated with hydrothermally altered zones in the Yankee Fork Mining District, Custer County, Idaho. Econ Geol 80: 1277–1296
Criss RE, Gregory RT, Taylor HP (1987) Kinetic theory of oxygen isotopic exchange between minerals and water. Geochim Cosmochim Acta 51: 1099–1108
Criss RE, Fleck RJ, Taylor HP (1991) Tertiary meteoric hydrothermal systems and their relation to ore deposition, Northwestern United States and Southern British Columbia. J Geophys Res 96: 13335–13356
Croal LR, Johnson CM, Beard BL, Newman DK (2004) Iron isotope fractionation by Fe(II)-oxidizing photoautotrophic bacteria. Geochim Cosmochim Acta 68: 1227–1242
Crosby HA, Roden EE, Johnson CE, Beard BL (2007) The mechanisms of iron isotope fractionation produced during dissimilatory Fe(III) reduction by *Shewanella putrefaciens* and *Geobacter sulfurreducens*. Geobiology 5: 169–189
Crowe DE, Valley JW, Baker KL (1990) Micro-analysis of sulfur isotope ratios and zonation by laser microprobe. Geochim Cosmochim Acta 54: 2075–2092
Crowson RA, Showers WJ, Wright EK, Hoering TC (1991) Preparation of phosphate samples for oxygen isotope analysis. Anal Chem 63: 2397–2400
Curry WB, Duplessy JC, Labeyrie LD, Shackleton NJ (1988) Quaternary deep-water circulation changes in the distribution of $\delta^{13}C$ of deep water ΣCO_2 between the last glaciation and the Holocene. Paleoceanography 3: 317–342
Cypionka H, Smock A, Böttcher MA (1998) A combined pathway of sulfur compound disproportionation in Desulfovibrio desulfuricans. FEMS Microbiol Lett 166: 181–186
Czamanske GK, Rye RO (1974) Experimentally determined sulfur isotope fractionations between sphalerite and galena in the temperature range 600°C to 275°C. Econ Geol 69: 17–25
Dansgaard W (1964) Stable isotope in precipitation. Tellus 16: 436–468
Dansgaard W, et al. (1993) Evidence for general instability of past climate from a 250 kyr ice-core record. Nature 364: 218–220
Das Sharma S, Patil DT, Gopalan K (2002) Temperature dependence of oxygen isotope fractionation of CO_2 from magnesite-phosphoric acid reaction. Geochim Cosmochim Acta 66: 589–593
Dauphas N, Marty B (1999) Heavy nitrogen in carbonatites of the Kola peninsula: a possible signature of the deep mantle. Science 286: 2488–2490
Dauphas N, Rouxel O (2006) Mass spectrometry and natural variations in iron isotopes. Mass Spectrom Rev 25: 515–550
Degens ET, Epstein S (1962) Relationship between $^{18}O/^{16}O$ ratios in coexisting carbonates, cherts and diatomites. Bull Am Assoc Pet Geol 46: 534–535
De Groot PA (2004) Handbook of stable isotope analytical techniques. Elsevier, Amsterdam
Deines P (1980) The isotopic composition of reduced organic carbon. In: Fritz P, Fontes JC (eds.) Handbook of environmental geochemistry, vol l. Elsevier, New York Amsterdam, pp. 239–406
Deines P (1989) Stable isotope variations in carbonatites. In: Carbonatites, genesis and evolution, K.Bell (ed) Unwin Hyman, London 619p

Deines P, Gold DP (1973) The isotopic composition of carbonatite and kimberlite carbonates and their bearing on the isotopic composition of deep-seated carbon. Geochim Cosmochim Acta 37: 1709–1733

Deines P, Haggerty SE (2000) Small-scale oxygen isotope variations and petrochemistry of ultradeep (>300 km) and transition zone xenoliths. Geochim Cosmochim Acta 64: 117–131

Deines P, Gurney JJ, Harris JW (1984) Associated chemical and carbon isotopic composition variations in diamonds from Finsch and Premier Kimberlite, South Africa. Geochim Cosmochim Acta 48: 325–342

De La Rocha C (2003) Silicon isotope fractionation by marine sponges and the reconstruction of the silicon isotope composition of ancient deep water. Geology 31: 423–426

De La Rocha CL, De Paolo DJ (2000) Isotopic evidence for variations in the marine calcium cycle over the Cenozoic. Science 289: 1176–1178

De La Rocha CL, Brzezinski MA, De Niro MJ (1997) Fractionation of silicon isotopes by marine diatoms during biogenic silica formation. Geochim Cosmochim Acta 61: 5051–5056

De La Rocha CL, Brzezinski MA, De Niro MJ, Shemesh A (1998) Silicon-isotope composition of diatoms as an indicator of past oceanic change. Nature 395: 680–683

De La Rocha CL, Brzezinski MA, De Niro MJ (2000) A first look at the distribution of the stable isotopes of silicon in natural waters. Geochim Cosmochim Acta 64: 2467–2477

Delaygue G, Jouzel J, Dutay JC (2000) Oxygen-18 - salinity relationship simulated by an oceanic general simulation model. Earth Planet Sci Lett 178: 113–123

Deloule E, Robert F (1995) Interstellar water in meteorites? Geochim Cosmochim Acta 59: 4695–4706

Deloule E, Albarede F, Sheppard SMF (1991) Hydrogen isotope heterogeneities in the mantle from ionprobe analysis of amphiboles from ultramafic rocks. Earth Planet Sci Lett 105: 543–553

Deloule E, Robert F, Doukhan JC (1998) Interstellar hydroxyl in meteoritic chondrules: implications for the origin of water in the inner solar system. Geochim Cosmochim Acta 62: 3367–3378

DeNiro MJ, Epstein S (1977) Mechanism of carbon isotope fractionation associated with lipid synthesis. Science 197: 261–263

DeNiro MJ, Epstein S (1978) Influence of diet on the distribution of carbon isotopes in animals. Geochim Cosmochim Acta 42: 495–506

DeNiro MJ, Epstein S (1979) Relationship between the oxygen isotope ratios of terrestrial plant cellulose, carbon dioxide and water. Science 204: 51–53

DeNiro MJ, Epstein S (1981) Isotopic composition of cellulose from aquatic organisms. Geochim Cosmochim Acta 45: 1885–1894

Dennis PF, Rowe PJ, Atkinson TC (2001) The recovery and isotopic measurement of water from fluid inclusions in speleothems. Geochim Cosmochim Acta 65: 871–884

DePaolo D (2004) Calcium isotope variationsproduced by biological, kinetic, radiogenic and nucleosynthetic processes. Rev Miner Geochem 55: 255–288

Derry LA, Kaufmann AJ, Jacobsen SB (1992) Sedimentary cycling and environmental change in the Late Proterozoic: evidence from stable and radiogenic isotopes. Geochim Cosmochim Acta 56: 1317–1329

Desaulniers DE, Kaufmann RS, Cherry JO, Bentley HW (1986) ^{37}Cl-^{35}Cl variations in a diffusion-controlled groundwater system. Geochim Cosmochim Acta 50: 1757–1764

Des Marais DJ (1983) Light element geochemistry and spallogenesis in lunar rocks. Geochim Cosmochim Acta 47: 1769–1781

Des Marais DJ, Moore JG (1984) Carbon and its isotopes in mid-oceanic basaltic glasses. Earth Planet Sci Lett 69: 43–57

Deutsch S, Ambach W, Eisner H (1966) Oxygen isotope study of snow and firn of an Alpine glacier. Earth Planet Sci Lett 1: 197–201

Dickens GR (2003) Rethinking the global carbon cycle with a large dynamic and micrmediated gas hydrate capacitor. Earth Planet Sci Lett 213: 169–182

Dickson JAD, Coleman ML (1980) Changes in carbon and oxygen isotope composition during limestone diagenesis. Sedimentology 27: 107–118

Dickson JAD, Smalley PC, Raheim A, Stijfhoorn DE (1990) Intracrystalline carbon and oxygen isotope variations in calcite revealed by laser micro-sampling. Geology 18: 809–811
Ding T, et al. (1996) Silicon isotope geochemistry. Geological Publishing House, Beijing, China
Ding T, Wan D, Wang C, Zhang F (2004) Silicon isotope compositions of dissolved silicon and suspended matter in the Yangtze River, China. Geochim Cosmochim Acta 68: 205–216
Ding T, Ma GR, Shui MX, Wan DF, Li RH (2005) Silicon isotope study on rice plants from the Zhejiang province, China. Chem Geol 218: 41–50
Dipple GM, Ferry JM (1992) Fluid flow and stable isotope alteration in rocks at elevated temperatures with applications to metamorphism. Geochim Cosmochim Acta 56: 3539–3550
Dobson PF, O'Neil JR (1987) Stable isotope composition and water contents of boninite series volcanic rocks from Chichi-jima, Bonin Islands, Japan. Earth Planet Sci Lett 82: 75–86
Dobson PF, Epstein S, Stolper EM (1989) Hydrogen isotope fractionation between coexisting vapor and silicate glasses and melts at low pressure. Geochim Cosmochim Acta 53: 2723–2730
Dodson MH (1973) Closure temperature in cooling geochronological and petrological systems. Contr Miner Petrol 40: 259–274
Dole M, Lange GA, Rudd DP, Zaukelies DA (1954) Isotopic composition of atmospheric oxygen and nitrogen. Geochim Cosmochim Acta 6: 65–78
Donahue TM, Hoffman JH, Hodges RD, Watson AJ (1982) Venus was wet: a measurement of the ratio of deuterium to hydrogen. Science 216: 630–633
Dorendorf F, Wiechert U, Wörner G (2000) Hydrated sub-arc mantle: a source for the Kluchevskoy volcano, Kamchatka, Russia. Earth Planet Sci. Lett 175: 69–86
Douthitt CB (1982) The geochemistry of the stable isotopes of silicon. Geochim Cosmochim Acta 46: 1449–1458
Drake MJ, Righter K (2002) Determining the composition of the Earth. Nature 416: 39–44
Driesner T (1997) The effect of pressure on deuterium-hydrogen fractionation in high-temperature water. Science 277: 791–794
Driesner T, Seward TM (2000) Experimental and simulation study of salt effects and pressure/density effects on oxygen and hydrogen stable isotope liquid-vapor fractionation for 4 - 5 molal aqueous NaCl and KCl solutions to 400°C. Geochim Cosmochim Acta 64: 1773–1784
Dugan JP, Borthwick J, Harmon RS, Gagnier MA, Glahn JE, Kinsel EP, McLeod S, Viglino JA (1985) Guadinine hydrochloride method for determination of water oxygen isotope ratios and the oxygen-18 fractionation between carbon dioxide and water at 25°C. Anal Chem 57: 1734–1736
Dunbar RB, Wellington GM, Colgan MW, Glynn PW (1994) Eastern sea surface temperature since 1600 A.D.: the $\delta^{18}O$ record of climate variability in Galapagos corals. Paleoceanography 9: 291–315
Duplessy JC, Shackleton NJ, Fairbanks RG, Labeyrie L, Oppo D, Kallel N (1988) Deepwater source variations during the last climatic cycle and their impact on the global circulation. Paleoceanography 3: 343–360
Durka W, Schulze ED, Gebauer G, Voerkelius S (1994) Effects of forest decline on uptake and leaching of deposited nitrate determined from ^{15}N and ^{18}O measurements. Nature 372: 765–767
Eastoe CJ, Guilbert JM (1992) Stable chlorine isotopes in hydrothermal processes. Geochim Cosmochim Acta 56: 4247–4255
Eastoe CJ, Gilbert JM, Kaufmann RS (1989) Preliminary evidence for fractionation of stable chlorine isotopes in ore-forming hydrothermal deposits. Geology 17: 285–288
Eastoe CJ, Long A, Land LS, Kyle JR (2001) Stable chlorine isotopes in halite and brine from the Gulf Coast Basin: brine genesis and evolution. Chem Geol 176: 343–360
Eggenkamp HGM (1994) $\delta^{37}Cl$: the geochemistry of chlorine isotopes. Thesis University of Utrecht
Ehrlich S, Butler I, Halicz L, Rickard D, Oldroyd A, Matthews A (2004) Experimental study of the copper isotope fractionation between aqueous Cu(II) and covellite, CuS. Chem Geol 209: 259–269

Eiler JM (2007) The study of naturally-occuring multiply-substituted isotopologues. Earth Planet Sci Lett 262: 309–327
Eiler JM, Kitchen N (2004) Hydrogen isotope evidence for the origin and evolution of the carbonaceous chondrites. Geochim Cosmochim Acta 68: 1395—1411
Eiler JM, Schauble E (2004) $^{18}O^{13}C^{16}O$ in earth·s atmosphere. Geochim Cosmochim Acta 68: 4767—4777
Eiler JM, Baumgartner LP, Valley JW (1992) Intercrystalline stable isotope diffusion: a fast grain boundary model. Contr Miner Petrol 112: 543–557
Eiler JM, Valley JW, Baumgartner LP (1993) A new look at stable isotope thermometry. Geochim Cosmochim Acta 57: 2571–2583
Eiler JM, Valley JW, Graham CM, Baumgartner LP (1995) Ion microprobe evidence for the mechanisms of stable isotope retrogression in high-grade metamorphic rocks. Contr Miner Petrol 118: 365–378
Eiler JM, Farley KA, Valley JW, Hofmann A, Stolper EM (1996) Oxygen isotope constraints on the sources of Hawaiian volcanism. Earth Planet Sci Lett 144: 453–468
Eiler JM, Crawford A, Elliott T, Farley KA, Valley JW, Stolper EM (2000) Oxygen isotope geochemistry of oceanic-arc lavas. J Petrol 41: 229–256
Eisenhauer A, et al. (2004) Proposal for an international agreement on Ca notation as result of the discussion from the workshops on stable isotope measurements in Davos (Goldschmidt 2002) and Nice (EUG 2003). Geostand Geoanal Res 28: 149–151
Eldridge CS, Compston W, Williams IS, Both RA, Walshe JL, Ohmoto H (1988) Sulfur isotope variability in sediment hosted massive sulfide deposits as determined using the ion microprobe SHRIMP. I. An example from the Rammelsberg ore body. Econ Geol 83: 443–449
Eldridge CS, Compston W, Williams IS, Harris JW, Bristow JW (1991) Isotopic evidence for the involvement of recycled sediments in diamond formation. Nature 353: 649–653
Eldridge CS, Williams IS, Walshe JL (1993) Sulfur isotope variability in sediment hosted massive sulfide deposits as determined using the ion microprobe SHRIMP. II. A study of the H.Y.C. deposit at McArthur River, Northern Territory, Australia. Econ Geol. 88: 1–26
Elkins LJ, Fischer TP, Hilton DR, Sharp ZD, McKnight S, Walker J (2006) Tracing nitrogen in volcanic and geothermal volatiles from the Nicaraguan volcanic front. Geochim Cosmochim Acta 70: 5215–5235
Elliot M, Labeyrie L, Duplessy JC (2002) Changes in North Atlantic deep-water formation associated with the Dansgaard-Oeschger temperature oscillations (60–10 ka). Quat Sci Rev 21: 1153–1165
Elliott T, Jeffcoate AB, Bouman C (2004) The terrestrial Li isotope cycle: light-weight constraints on mantle convection. Earth Planet Sci Lett 220: 231–245
Ellis AS, Johnson TM, Bullen TD (2002) Chromium isotopes and the fate of hexavalent chromium in the environment. Science 295: 2060–2062
Ellis AS, Johnson TM, Bullen TD (2004) Using chromium stable isotope ratios to quantify Cr(VI) reduction: lack of sorption effects. Environ Sci Techn 38: 3604–3607
Elsenheimer D, Valley JW (1992) In situ oxygen isotope analysis of feldspar and quartz by Nd-YAG laser microprobe. Chem Geol 101: 21–42
Emiliani C (1955) Pleistocene temperatures. J Geol 63: 538–578
Emiliani C (1966) Paleotemperature analysis of Caribbean core P6304-8 and P6304-9 and a generalized temperature curve for the past 425000 years. J Geol 74: 109–126
Emrich K, Ehhalt DH, Vogel JC (1970) Carbon isotope fractionation during the precipitation of calcium carbonate. Earth Planet Sci Lett 8: 363–371
Engel MH, Macko SA, Silfer JA (1990) Carbon isotope composition of individual amino acids in the Murchison meteorite. Nature 348: 47–49
Engstrom E, Rodushkin I, Baxter DC, Ohlander B (2006) Chromatographic purification for the determination of dissolved silicon isotopic compositions in natural waters by high-resolution multicollector inductively coupled mass spectrometry. Anal Chem 78: 250–257
Epica community members (2004) Eight glacial cycles from an Antarctic ice core. Nature 429: 623–628

Epstein S, Yapp CJ, Hall JH (1976) The determination of the D/H ratio of non-exchangeable hydrogen in cellulose extracted from aquatic and land plants. Earth Planet Sci Lett 30: 241–251

Epstein S, Thompson P, Yapp CJ (1977) Oxygen and hydrogen isotopic ratios in plant cellulose. Science 198: 1209–1215

Epstein S, Krishnamurthy RV, Cronin JR, Pizzarello S, Yuen GU (1987) Unusual stable isotope ratios in amino acid and carboxylic acid extracts from the Murchison meteorite. Nature 326: 477–479

Erez J, Luz B (1983) Experimental paleotemperature equation for planktonic foraminifera. Geochim Cosmochim Acta 47: 1025–1031

Eslinger EV, Savin SM (1973) Oxygen isotope geothermometry of the burial metamorphic rocks of the Precambrian Belt Supergroup, Glacier National Park, Montana. Bull Geol Soc Am 84: 2549–2560

Estep MF, Hoering TC (1980) Biogeochemistry of the stable hydrogen isotopes. Geochim Cosmochim Acta 44: 1197–1206

Exley RA, Mattey DP, Boyd SR, Pillinger CT (1987) Nitrogen isotope geochemistry of basaltic glasses: implications for mantle degassing and structure. Earth Planet Sci Lett 81: 163–174

Fairbanks RG (1989) A 17000 year glacio-eustatic sea level record: influence of glacial melting rates on the Younger Dryas event and deep ocean circulation. Nature 342: 637–642

Fantle MS, De Paolo DJ (2005) Variations in the marine Ca cycle over the past 20 million years. Earth Planet. Sci Lett 237: 102–117

Fantle MS, De Paolo DJ (2004) Iron isotope fractionation during continental weathering. Earth Planet Sci Lett 228: 547–562

Farkas J, Buhl D, Blenkinsop J, Veizer J (2007) Evolution of the oceanic calcium cycle during the late Mesozoic: evidence from $\delta^{44/40}$ Ca of marine skeletal carbonates. Earth Planet Sci Lett 253: 96–111

Farquhar GD, Ehleringer JR, Hubick KT (1989) Carbon isotope discrimination and photosynthesis. Ann Rev Plant Physiol Plant Mol Biol 40: 503–537

Farquhar GD, et al. (1993) Vegetation effects on the isotope composition of oxygen in atmospheric CO_2. Nature 363: 439–443

Farquhar J, Thiemens MH (2000) The oxygen cycle of the Martian atmosphere-regolith system: $\Delta^{17}O_m$ secondary phases in Nakhla and Lafayette. J Geophys Res 105: 11991–11998

Farquhar J, Chacko T, Ellis DJ (1996) Preservation of oxygen isotopic compositions in granulites from Northwestern Canada and Enderby Land, Antarctica: implications for high-temperature isotopic thermometry. Contr Miner Petrol 125: 213–224

Farquhar J, Thiemens MH, Jackson T (1998) Atmosphere-surface interactions on Mars: $\Delta^{17}O$ measurements of carbonate from ALH 84001. Science 280: 1580–1582

Farquhar J, Savarino J, Jackson TL, Thiemens MH (2000a) Evidence of atmospheric sulfur in the Martian regolith from sulphur isotopes in meteorites. Nature 404: 50–52

Farquhar J, Jackson TL, Thiemens MH (2000b) A ^{33}S enrichment in ureilite meteorites: evidence for a nebular sulfur component. Geochim Cosmochim Acta 64: 1819–1825

Farquhar J, Bao H, Thiemens M (2000c) Atmospheric influence of Earth's earliest sulfur cycle. Science 289: 756–759

Farquhar J, Savarino J, Airieau S, Thiemens M (2001) Observation of wavelength sensitive mass independent sulfur isotope effects during SO_2 photolysis: Applications to the early atmosphere. J Geophys Res Planets 12: 32829–32839

Farquhar J, Wing B, McKeegan KD, Harris JW (2002) Insight into crust-mantle coupling from anomalous $\Delta^{33}S$ of sulfide inclusions in diamonds. Geochim Cosmochim Acta Spec Suppl 66: A225

Farquhar J, Wing BA (2003) Multiple sulfur isotope analysis: applications in geochemistry and cosmochemistry. Earth Planet Sci. Lett 213: 1–13

Farquhar J, Johnston DT, Wing BA, Habicht KS, Canfield DE, Airieau S, Thiemens MH (2003) Multiple sulphur isotope interpretations for biosynthetic pathways: implications for biological signatures in the sulphur isotope record. Geobiology 1: 27–36

Farquhar J, Peters M, Johnston DT, Strauss H, Masterson A, Wiechert LI, Kaufman AJ (2007) Isotopic evidence for Mesoarchean anoxia and changing atmospheric sulfur chemistry. Nature 449: 706–710

Farrell JW, Pedersen TF, Calvert SE, Nielsen B (1995) Glacial-interglacial changes in nutrient utilization in the equatorial Pacific Ocean. Nature 377: 514–517

Ferry JM (1992) Regional metamorphism of the Waits River Formation: delineation of a new type of giant hydrothermal system. J Petrol 33: 45–94

Ferry JM, Dipple GM (1992) Models for coupled fluid flow, mineral reaction and isotopic alteration during contact metamorphism: the Notch Peak aureole, Utah. Am Miner 77: 577–591

Fiebig J, Hoefs J (2002) Hydrothermal alteration of biotite and plagioclase as inferred from intragranular oxygen isotope- and cation-distribution patterns. Eur J Miner 14: 49–60

Fiebig J, Wiechert U, Rumble D, Hoefs J (1999) High-precision in-situ oxygen isotope analysis of quartz using an ArF laser. Geochim Cosmochim Acta 63: 687–702

Fiebig J, Chiodini G, Caliro S, Rizzo A, Spangenberg J, Hunziker JC (2004) Chemical and isotopic equilibrium between CO_2 and CH_4 in fumarolic gas discharges: generation of CH_4 in arc magmatic-hydrothermal systems. Geochim Cosmochim Acta 68: 2321–2334

Fiebig J, Woodland AB, Spangenberg J, Oschmann W (2007) Natural evidence for rapid abiogenic hydrothermal generation of CH_4. Geochim Cosmochim Acta 71: 3028–3039

Field CW, Gustafson LB (1976) Sulfur isotopes in the porphyry copper deposit at El Salvador, Chile. Econ Geol 71: 1533–1548

Fiorentini E, Hoernes S, Hoffbauer R, Vitanage PW (1990) Nature and scale of fluid-rock exchange in granulite-grade rocks of Sri Lanka: a stable isotope study. In: D. Vielzeuf, Ph.Vidal (eds.) Granulites and crustal evolution. Kluwer, Dordrecht, p. 311–338

Fischer TP, Giggenbach WF, Sano Y, Williams SN (1998) Fluxes and sources of volatiles discharged from Kudryavy, a subduction zone volcano, Kurile Islands. Earth Planet Sci Lett 160: 81–96

Fischer TP, Hilton DR, Zimmer MM, Shaw AM, Sharp ZD, Walker JA (2002) Subduction and recycling of nitrogen along the Central American margin. Science 297: 1154–1157

Fitzsimons ICW, Harte B, Clark RM (2000) SIMS stable isotope measurement: counting statistics and analytical precision. Min Mag 64: 59–83

Fogel ML, Cifuentes LA (1993) Isotope fractionation during primary production. In: Organic Geochemistry, ed. by MH Engel, SA Macko, Plenum Press, New York, p. 73–98

Foucher D, Hintelmann H (2006) High-precision measurement of mercury isotope ratios in sediments using cold-vapor generation multi-collector inductively coupled plasma mass spectrometry. Anal Bioanal Chem 384: 1470–1478

Foustoukous D, Seyfried WE (2004) Hydrocarbons in vent fluids: the role of chromium catalysts. Science 304: 1002–1005

Francey RJ, Tans PP (1987) Latitudinal variation in oxygen-18 of atmospheric CO_2. Nature 327: 495–497

Franchi IA, Wright IP, Sexton AS, Pillinger T (1999) The oxygen isotopic composition of Earth and Mars. Meteorit Planet Sci 34: 657–661

Frape SK, Fritz P (1987) Geochemical trends from groundwaters from the Canadian Shield. In: P. Fritz, SK Frape (eds.) Saline water and gases in crystalline rocks. Geol Ass Canada Spec Paper 33: 19–38

Frape SK, Fritz P, McNutt RH (1984) Water-rock interaction and chemistry of groundwaters from the Canadian Shield. Geochim Cosmochim Acta 48: 1617–1627

Freeman KH (2001) Isotopic biogeochemistry of marine organic carbon. Rev Miner Geochem 43: 579–605

Freeman KH, Hayes JM (1992) Fractionation of carbon isotopes by phytoplankton and estimates of ancient CO_2 levels. Global Biogeochem Cycles 6: 185–198

Freeman KH, Hayes JM, Trendel JM, Albrecht P (1990) Evidence from carbon isotope measurements for diverse origins of sedimentary hydrocarbons. Nature 343: 254–256

Freyer HD (1979) On the ^{13}C-record in tree rings. I. ^{13}C variations in northern hemisphere trees during the last 150 years. Tellus 31: 124–137

Freyer HD, Belacy N (1983) $^{13}C/^{12}C$ records in northern hemispheric trees during the past 500 years - anthropogenic impact and climatic superpositions. J Geophys Res 88: 6844–6852
Fricke HC, O'Neil JR (1999) The correlation between $^{18}O/^{16}O$ ratios of meteoric water and surface temperature: its use in investigating terrestrial climate change over geologic time. Earth Planet Sci Lett 170: 181–196
Fricke HC, Wickham SM, O'Neil JR (1992) Oxygen and hydrogen isotope evidence for meteoric water infiltration during mylonitization and uplift in the Ruby Mountains - East Humboldt Range core complex, Nevada. Contr Miner Petrol 111: 203–221
Fricke HC, Clyde WC, O'Neil JR (1998a) Intra-tooth variations in $\delta^{18}O$ (PO_4) of mammalian tooth enamel as a record of seasonal variations in continental climate variables. Geochim Cosmochim Acta 62: 1839–1850
Fricke HC, Clyde WC, O'Neil JR, Gingerich PD (1998b) Evidence for rapid climate change in North America during the latest Paleocene thermal maximum: oxygen isotope compositions of biogenic phosphate from the Bighorn Basin (Wyoming). Earth Planet Sci Lett 160: 193–208
Friedman I (1953) Deuterium content of natural waters and other substances. Geochim Cosmochim Acta 4: 89–103
Friedman I, O'Neil JR (1977) Compilation of stable isotope fractionation factors of geochemical interest. In: Data Geochem, 6th ed Geol Surv Prof Pap 440KK
Friedman I, Scholz TG (1974) Isotopic composition of atmospheric hydrogen (1967–1969). J Geophys Res 79: 785–788
Fritz P, Basharmel GM, Drimmie RJ, Ibsen J, Qureshi RM (1989) Oxygen isotope exchange between sulphate and water during bacterial reduction of sulphate. Chem Geol 79: 99–105
Fry B (1988) Food web structure on Georges Bank from stable C, N and S isotopic compositions. Limnol Oceanogr 3: 1182–1190
Fu Q, Sherwood Lollar B, horita J, Lacrampe-Couloume G, Seyfried WE (2007) Abiotic formation of hydrocarbons under hydrothermal conditions: constraints from chemical and isotope data. Geochim Cosmochim Acta 71: 1982–1998
Gagan MK, Ayliffe LK, Beck JW, Cole JE, Druffel ER, Schrag DP (2000) New views of tropical paleoclimates from corals. Q Sci Rev 19: 45–64
Galimov EM (1985a) The biological fractionation of isotopes. Academic Press, London
Galimov EM (1985b) The relation between formation conditions and variations in isotope compositions of diamonds. Geochem Int 22, 1: 118–141
Galimov EM (1988) Sources and mechanisms of formation of gaseous hydrocarbons in sedimentary rocks. Chem Geol 71: 77–95
Galimov EM (1991) Isotopic fractionation related to kimberlite magmatism and diamond formation. Geochim Cosmochim Acta 55: 1697–1708
Galimov EM (2006) Isotope organic geochemistry. Org Geochem 37: 1200–1262
Galy A, Belshaw NS, Halicz L, O'Nions RK (2001) High-precision measurement of magnesium isotopes by multiple-collector inductively coupled plasma mass spectrometry. Inter J Mass Spectr 208: 89–98
Galy A, Bar-Matthews M, Halicz L, O'Nions RK (2002) Mg isotopic composition of carbonate: insight from speleothem formation. Earth Planet Sci Lett 201: 105–115
Gao YQ, Marcus RA (2001) Strange and unconventional isotope effects in ozone formation. Science 293: 259–263
Gao X, Thiemens MH (1993a) Isotopic composition and concentration of sulfur in carbonaceous chondrites. Geochim Cosmochim Acta 57: 3159–3169
Gao X, Thiemens MH (1993b) Variations of the isotopic composition of sulfur in enstatite and ordinary chondrites. Geochim Cosmochim Acta 57: 3171–3176
Gao Y, Hoefs J, Przybilla R, Snow JE (2006) A complete oxygen isotope profile through the lower oceanic crust, ODP hole 735B. Chem Geol 233: 217–234
Garlick GD (1966) Oxygen isotope fractionation in igneous rocks. Earth Planet Sci Lett 1: 361–368
Garlick GD, Epstein S (1967) Oxygen isotope ratios in coexisting minerals of regionally metamorphosed rocks. Geochim Cosmochim Acta 31: 181

Gat JR (1971) Comments on the stable isotope method in regional groundwater investigation. Water Resource Res 7: 980

Gat JR (1984) The stable isotope composition of Dead Sea waters. Earth Planet Sci Lett 71: 361–376

Gat JR, Issar A (1974) Desert isotope hydrology: water sources of the Sinai desert. Geochim Cosmochim Acta 38: 1117–11131

Gehre M, Hoefling R, Kowski P, Strauch G (1996) Sample preparation device for quantitative hydrogen isotope analysis using chromium metal. Anal Chem 68: 4414–4417

Gelabert A, Pokrovsky OS, Viers J, Schott J, Boudou A, Feurtet-Mazel A (2006) Interaction between zinc and marine diatom species: surface complexation and Zn isotope fractionation. Geochim Cosmochim Acta 70: 839–857

Georg RB, Reynolds BC, Frank M, Halliday AN (2006) Mechanisms controlling the silicon isotopic compositions of river water. Earth Planetary Sci Lett 249: 290–306

Gerdes ML, Baumgartner LP, Person M, Rumble D (1995) One- and two-dimensional models of fluid flow and stable isotope exchange at an outcrop in the Adamello contact aureole, Southern Alps, Italy. Am Miner 80: 1004–1019

Gerlach TM, Taylor BE (1990) Carbon isotope constraints on degassing of carbon dioxide from Kilauea volcano. Geochim Cosmochim Acta 54: 2051–2058

Gerlach TM, Thomas DM (1986) Carbon and sulphur isotopic composition of Kilauea parental magma. Nature 319: 480–483

Ghosh P, et al. (2006) ^{13}C-^{18}O bonds in carbonate minerals: a new kind of paleothermometer. Geochim Cosmochim Acta 70: 1439–1456

Giesemann A, Jäger HA, Norman AL, Krouse HR, Brand WA (1994) On-line sulphur isotope determination using an elemental analyzer coupled to a mass spectrometer. Anal Chem 66: 2816–2819

Giggenbach WF (1992) Isotopic shifts in waters from geothermal and volcanic systems along convergent plate boundaries and their origin. Earth Planet Sci Lett 113: 495–510

Giletti BJ (1985) The nature of oxygen transport within minerals in the presence of hydrothermal water and the role of diffusion. Chem Geol 53: 197–206

Giletti BJ (1986) Diffusion effect on oxygen isotope temperatures of slowly cooled igneous and metamorphic rocks. Earth Planet Sci Lett 77: 218–228

Gilg HA (2000) D/H evidence for the timing of kaolinization in Northeast Bavaria, Germany. Chem Geol 170: 5–18

Gilg HA, Taubald H, Struck U (2007) Phosphoric acid fractionation factors for aragonite between 25 and 72°C with implications on aragonite-calcite oxygen isotope fractionations. Geochim Cosmochim Acta 71: A323.

Girard JP, Savin S (1996) Intercrystalline fractionation of oxygen isotopes between hydroxyl and non-hydroxyl sites in kaolinite measured by thermal dehydroxylation and partial fluorination. Geochim Cosmochim Acta 60: 469–487

Given RK, Lohmann KC (1985) Derivation of the original isotopic composition of Permian marine cements. J Sediment Petrol 55: 430–439

Godfrey JD (1962) The deuterium content of hydrous minerals from the East Central Sierra Nevada and Yosemite National Park. Geochim Cosmochim Acta 26: 1215–1245

Goericke R, Fry B (1994) Variations of marine plankton $\delta^{13}C$ with latitude, temperature and dissolved CO_2 in the world ocean. Global Geochem Cycles 8: 85–90

Goldhaber MB, Kaplan IR (1974) The sedimentary sulfur cycle. In: Goldberg EB (ed) The sea, vol. 4. Wiley, New York

Gonfiantini R (1978) Standards for stable isotope measurements in natural compounds. Nature 271: 534–536

Gonfiantini R (1984) Advisory group meeting on stable isotope reference samples for geochemical and hydrological investigations. Rep Director General IAEA Vienna

Gonfiantini R (1986) Environmental isotopes in lake studies. In: P. Fritz, J. Fontes (eds.) Handbook of environmental isotope geochemistry, vol 2. Elsevier, Amsterdam, pp. 112–168

Grachev AM, Severinghaus JP (2003) Laboratory determination of thermal diffusion constants for $^{29}N/^{28}N_2$ in air at temperatures from −60 to 0°C for reconstruction of magnitudes of abrupt climate changes using the ice core fossil-air paleothermometer. Geochim Cosmochim Acta 67: 345–360

Grady MM, Pillinger CT (1990) ALH 85085: nitrogen isotope analysis of a highly unusual primitive chondrite. Earth Planet Sci Lett 97: 29–40

Grady MM, Pillinger CT (1993) Acfer 182: search for the location of ^{15}N-enriched nitrogen. Earth Planet Sci Lett 116: 165–180

Graham CM, Sheppard SMF, Heaton THE (1980) Experimental hydrogen isotope studies. I. Systematics of hydrogen isotope fractionation in the systems epidote-H_2O, zoisite-H_2O and AlO(OH)-H_2O. Geochim Cosmochim Acta 44: 353–364

Graham CM, Harmon RS, Sheppard SMF (1984) Experimental hydrogen isotope studies: hydrogen isotope exchange between amphibole and water. Am Miner 69: 128–138

Graham S, Pearson N, Jackson S, Griffin W, O'Reilly SY (2004) Tracing Cu and Fe from source to porphyry: in situ determination of Cu and Fe isotope ratios in sulfides from the Grasberg Cu-Au deposit. Chem Geol 207: 147–169

Green GR, Ohmoto D, Date J, Takahashi T (1983) Whole-rock oxygen isotope distribution in the Fukazawa-Kosaka Area, Hokuroko District, Japan and its potential application to mineral exploration. Econ Geol Monogr 5: 395–411

Greenwood JP, Riciputi LR, McSween HY (1997) Sulfide isotopic compositions in shergottites and ALH 84001, and possible implications for life on Mars. Geochim Cosmochim Acta 61: 4449–4453

Greenwood RC, Franchi IA, Jambon A, Barrat JA, Burbine TH (2006) Oxygen isotope variation in stony-iron meteorites. Science 313: 1763–1765

Gregory RT, Taylor HP (1981) An oxygen isotope profile in a section of Cretaceous oceanic crust, Samail Ophiolite, Oman: evidence for $\delta^{18}O$ buffering of the oceans by deep (>5 km) seawater-hydrothermal circulation at Mid-Ocean Ridges. J Geophys Res 86: 2737–2755

Gregory RT, Taylor HP (1986) Possible non-equilibrium oxygen isotope effects in mantle nodules, an alternative to the Kyser-O'Neil-Carmichael $^{18}O/^{16}O$ geothermometer. Contr Miner Petrol 93: 114–119

Gregory RT, Criss RE, Taylor HP (1989) Oxygen isotope exchange kinetics of mineral pairs in closed and open systems: applications to problems of hydrothermal alteration of igneous rocks and Precambrian Iron Formations. Chem Geol 75: 1–42

Griffith EM, Paytan A, Kozdon R, Eisenhauer A, Ravelo AC (2008) Influences on the fractionation of calcium isotopes in planktonic foraminifera. Earth Planet Sci Lett 268: 124–136

Grootes PM, Stuiver M, White JWC, Johnsen S, Jouzel J (1993) Comparison of oxygen isotope records from the GISP-2 and GRIP Greenland ice cores. Nature 366: 552–554

Grossman EL (1984) Carbon isotopic fractionation in live benthic foraminifera - comparison with inorganic precipitate studies. Geochim Cosmochim Acta 48: 1505–1512

Grossman EL, Ku TL (1986) Oxygen and carbon isotope fractionation in biogenic aragonite: temperature effects. Chem Geol 59: 59–74

Grottoli AG, Eakin CM (2007) A review of modern coral $\delta^{18}O$ and $\delta^{14}C$ proxy records. Earth Sci Rev 81: 67–91

Gruber N (1998) Anthropogenic CO_2in the Atlantic Ocean. Global Biogeochem Cycles 12: 165–191

Gruber N, et al. (1999) Spatiotemporal patterns of carbon-13 in the global surface oceans and the oceanic Suess effect. Global Biogeochem Cycles 13: 307–335

Gussone N, et al. (2005) Calcium isotope fractionation in calcite and aragonite. Geochim Cosmochim Acta 69: 4485–4494

Gussone N, et al. (2006) Cellular calcium pathways and isotope fractionation in *Emiliania huxleyi*. Geology 34: 625–628

Guy RD, Fogel ML, Berry JA (1993) Photosynthetic fractionation of the stable isotopes of oxygen and carbon. Plant Phys 101: 37–47

Haack U, Hoefs J, Gohn E (1982) Constraints on the origin of Damaran granites by Rb/Sr and $\delta^{18}O$ data. Contrib Miner Petrol 79: 279–289
Habicht KS, Canfield DE (1997) Sulfur isotope fractionation during bacterial sulfate reduction in organic-rich sediments. Geochim Cosmochim Acta 61: 5351–5361
Habicht KS, Canfield DE (2001) Isotope fractionation by sulfate-reducing natural populations and the isotopic composition of sulfide in marine sediments. Geology 29: 555–558
Hackley KC, Anderson TF (1986) Sulfur isotopic variations in low-sulfur coals from the Rocky Mountain region. Geochim Cosmochim Acta 50: 703–1713
Haendel D, Mühle K, Nitzsche HIM, Stiehl G, Wand U (1986) Isotopic variations of the fixed nitrogen in metamorphic rocks. Geochim Cosmochim Acta 50: 749–758
Hagemann R, Nief G, Roth E (1970) Absolute isotopic scale for deuterium analysis of natural waters. Absolute D/H ratio for SMOW. Tellus 22: 712–715
Haimson M, Knauth LP (1983) Stepwise fluorination-a useful approach for the isotopic analysis of hydrous minerals. Geochim Cosmochim Acta 47: 1589–1595
Halbout J, Robert F, Javoy M (1990) Hydrogen and oxygen isotope compositions in kerogen from the Orgueil meteorite: clues to a solar origin. Geochim Cosmochim Acta 54: 1453–1462
Hamza MS, Epstein S (1980) Oxygen isotope fractionation between oxygen of different sites in hydroxyl-bearing silicate minerals. Geochim Cosmochim Acta 44: 173–182
Harford CL, Sparks RSJ (2001) Recent remobilisation of shallow-level intrusions on Montserrat revealed by hydrogen isotope compositions of amphiboles. Earth Planet Sci Lett: 185: 285–298
Harmon RS, Hoefs J (1986) S-isotope relationships in Late Cenozoic destructive plate margin and continental intraplate volcanic rocks. Terra Cognita 6: 182
Harmon RS, Hoefs J (1995) Oxygen isotope heterogeneity of the mantle deduced from global ^{18}O systematics of basalts from different geotectonic settings. Contr Miner Petrol 120: 95–114
Harmon RS, Hoefs J, Wedepohl KH (1987) Stable isotope (O,H,S) relationships in Tertiary basalts and their mantle xenoliths from the Northern Hessian Depression, W.Germany. Contr Miner Petrol 95: 350–369
Harrison AG, Thode HG (1957a) Kinetic isotope effect in chemical reduction of sulphate. Faraday Soc Trans 53: 1648–1651
Harrison AG, Thode HG (1957b) Mechanism of the bacterial reduction of sulphate from isotope fractionation studies. Faraday Soc Trans 54: 84–92
Harte B, Otter M (1992) Carbon isotope measurements on diamonds. Chem Geol 101: 177–183
Hartmann M, Nielsen H (1969) $\delta^{34}S$-Werte in rezenten Meeressedimenten und ihre Deutung am Beispiel einiger Sedimentprofile aus der westlichen Ostsee. Geol Rundsch 58: 621–655
Hauri EH (2002) SIMS analysis of volatiles in silicate glasses: 2. Isotopes and abundances in Hawaiian melt inclusions. Chem Geol 183: 115–141
Hauri EH, Wang J, Pearson DG, Bulanova GP (2002) Microanalysis of $\delta^{13}C$, $\delta^{15}N$ and N abundances in diamonds by secondary ion mass spectrometry. Chem Geol 185: 149–163
Hawkesworth CJ, Kemp AIS (2006) Using hafnium and oxygen isotopes in zircons to unravel the record of crustal evolution. Chem Geol 226: 144–162
Hayes JM (1983) Practice and principles of isotopic measurements in organic geochemistry. In: Organic geochemistry of contemporaneous and ancient sediments, Great Lakes Section, SEPM, Bloomington, pp 51–53
Hayes JM (1993) Factors controlling 13C contents of sedimentary organic compounds: principle and evidence. Mar Geol 113: 111–125
Hayes JM (2001) Fractionation of carbon and hydrogen isotopes in biosynthetic processes. In: JW Valley, DR Cole (eds.) Stable isotope geochemistry. Rev Miner Geochem 43: 225–277
Hayes JM, Waldbauer JR (2006) The carbon cycle and associated redox processes through time. Phil Trans R.Soc B 361: 931–950
Hayes JM, Kaplan IR, Wedeking KW (1983) Precambrian organic chemistry, preservation of the record. In: JW Schopf (ed.) Earth's earliest biosphere: Its origin and evolution, Chapt 5. Princeton University Press, New Jersey, pp. 93–132

Hayes JM, Popp BN, Takigiku R, Johnson MW (1989) An isotopic study of biogeochemical relationships between carbonates and organic carbon in the Greenhorn Formation. Geochim Cosmochim Acta 53: 2961–2972

Hayes JM, Strauss H, Kaufman AJ (1999) The abundance of ^{13}C in marine organic matter and isotopic fractionation in the global biogeochemical cycle of carbon during the past 800 Ma. Chem Geol 161: 103–125

Hays JD, Imbrie J, Shackleton NJ (1976) Variations in the earth's orbit: pacemaker of the ice ages. Science 194: 943–954

Hays PD, Grossman EL (1991) Oxygen isotopes in meteoric calcite cements as indicators of continental paleoclimate. Geology 19: 441–444

Heaton THE (1986) Isotopic studies of nitrogen pollution in the hydrosphere and atmosphere: a review. Chem Geol 59: 87–102

Hedenquist JW, Lowenstern JB (1994) The role of magmas in the formation of hydrothermal ore deposits. Nature 370: 519–527

Heidenreich JE, Thiemens MH (1983) A non-mass-dependent isotope effect in the production of ozone from molecular oxygen. J Chem Phys 78: 892–895

Helman Y, Barkan E, Eisenstadt D, Luz B, Kaplan A (2005) Fractionation of the three stable oxygen isotopes by oxygen producing and consuming reactions in photosynthetic organisms. Plant Phys (2005) 2292–2298

Hemming NG, Hanson GN (1992) Boron isotopic composition in modern marine carbonates. Geochim Cosmochim Acta 56: 537–543

Hendy CH, Wilson AT (1968) Paleoclimatic data from speleothems. Nature 219: 48–51

Heraty LJ, Fuller ME, Huang L, Abrajano T, Sturchio NC (1999) Isotopic fractionation of carbon and chlorine by microbial degradation of dichlormethane. Org Geochem 30: 793–799

Herbel MJ, Johnson TM, Oremland RS, Bullen TD (2000) Fractionation of selenium isotopes during bacterial respiratory reduction of selenium oxyanions. Geochim Cosmochim Acta 64: 3701–3710

Hervig RL, Moore GM, Williams LB, Peacock SM, Holloway JR, Roggensack K (2002) Isotopic and elemental partitioning of boron between hydrous fluid and silicate melt. Am Miner 87: 769–774

Hesse R, Egeberg PK, Frape SK (2006) Chlorine stable isotope ratios as tracer for pore-water advection rates in a submarine gas-hydrate field: implication for hydrate concentration. Geofluids 6: 1–7

Hesterberg R, Siegenthaler U (1991) Production and stable isotopic composition of CO_2 in a soil near Bern, Switzerland. Tellus 43: 197–205

Hinrichs KU, Hayes JM, Sylva SP, Brewer PG, DeLong EF (1999) Methane-consuming archaebacteria in marine sediments. Nature 398: 802–805

Hippler D, Eisenhauer A, Nägler TF (2006) Tropical Atlantic SST history inferred from Ca isotope thermometry over the last 140 ka. Geochim Cosmochim Acta 70: 90–100

Hitchon B, Friedman I (1969) Geochemistry and origin of formation waters in the western Canada sedimentary basin. 1. Stable isotopes of hydrogen and oxygen. Geochim Cosmochim Acta 33: 1321–1349

Hitchon B, Krouse HR (1972) Hydrogeochemistry of the surface waters of the Mackenzie River drainage basin, Canada. III. Stable isotopes of oxygen, carbon and sulfur. Geochim Cosmochim Acta 36: 1337–1357

Hoefs J (1970) Kohlenstoff-und Sauerstoff-Isotopenuntersuchungen an Karbonatkonkretionen und umgebendem Gestein. Contrib Miner Petrol 27: 66–79

Hoefs J (1992) The stable isotope composition of sedimentary iron oxides with special reference to Banded Iron Formations. In: Isotopic signatures and sedimentary records. Lecture Notes in Earth Sci 43: 199–213, Springer Verlag, Berlin

Hoefs J, Emmermann R (1983) The oxygen isotope composition of Hercynian granites and pre-Hercynian gneisses from the Schwarzwald, SW Germany. Contrib Miner Petrol 83: 320–329

Hoefs J, Sywall M (1997) Lithium isotope composition of Quaternary and Tertiary biogene carbonates and a global lithium isotope balance. Geochim Cosmochim Acta 61: 2679–2690

Hoering TC (1955) Variations in nitrogen-15 abundance in naturally occuring substances. Science 122: 1233
Hoering T, Parker PL (1961) The geochemistry of the stable isotopes of chlorine. Geochim Cosmochim Acta 23: 186–199
Hoernes S, Van Reenen DC (1992) The oxygen isotopic composition of granulites and retrogressed granulites from the Limpopo Belt as a monitor of fluid-rock interaction. Precambrian Res 55: 353–364
Hoffman JH, Hodges RR, McElroy MB, Donahue TM, Kolpin M (1979) Composition and structure of the Venus atmosphere: results from Pioneer Venus. Science 205: 49–52
Hoffman PE, Kaufman AJ, Halverson GP, Schrag DP (1998) Neoproterozoic snowball earth. Science 281: 1342–1346
Holloway JR, Blank JG (1994) Application of experimental results to C-O-H species in natural melts. In: MR Carroll, JR Holloway (eds.) Volatiles in magmas. Rev Miner 30: 187–230
Holser WT (1977) Catastrophic chemical events in the history of the ocean. Nature 267: 403–408
Holser WT, Kaplan IR (1966) Isotope geochemistry of sedimentary sulfates. Chem Geol 1: 93–135
Holt BD, Engelkemeier AG (1970) Thermal decomposition of barium sulfate to sulfur dioxide for mass spectrometric analysis. Anal Chem 42: 1451–1453
Hoppe P, Zinner E (2000) Presolar dust grains from meteorites and their stellar sources. J Geophys Res Space Phys 105: 10371–10385
Horita J (1988) Hydrogen isotope analysis of natural waters using an H_2-water equilibration method: a special implication to brines. Chem Geol 72: 89–94
Horita J (1989) Stable isotope fractionation factors of water in hydrated salt minerals. Earth Planet Sci Lett 95: 173–179
Horita J, Berndt ME (1999) Abiogenic methane formation and isotope fractionation under hydrothermal conditions. Science 285: 1055–1057
Horita J, Wesolowski DJ (1994) Liquid-vapor fractionation of oxygen and hydrogen isotopes of water from the freezing to the critical temperature. Geochim Cosmochim Acta 58: 3425–3437
Horita J, Wesolowski DJ, Cole DR (1993) The activity-composition relationship of oxygen and hydrogen isotopes in aqueous salt solutions. I. Vapor-liquid water equilibration of single salt solutions from 50 to 100°C. Geochim Cosmochim Acta 57: 2797–2817
Horita J, Cole DR, Wesolowski DJ (1995) The activity-composition relationship of oxygen and hydrogen isotopes in aqueous salt solutions: III. Vapor-liquid water equilibration of NaCl solutions to 350°C. Geochim Cosmochim Acta 59: 1139–1151
Horita J, Driesner T, Cole DR (1999) Pressure effect on hydrogen isotope fractionation between brucite and water at elevated temperatures. Science 286: 1545–1547
Horita J, Cole DR, Polyakov VB, Driesner T (2002a) Experimental and theoretical study of pressure effects on hydrous isotope fractionation in the system brucite-water at elevated temperatures. Geochim Cosmochim Acta 66: 3769–3788
Horita J, Zimmermann H, Holland HD (2002b) Chemical evolution of seawater during the Phanerozoic: implications from the record of marine evaporates. Geochim Cosmochim Acta 66: 3733–3756
Hu G, Clayton RN (2003) Oxygen isotope salt effects at high pressure and high temperature and the calibration of oxygen isotope thermometers. Geochim Cosmochim Acta 67: 3227–3246
Hu GX, Rumble D, Wang PL (2003) An ultraviolet laser microprobe for the in-situ analysis of multisulfur isotopes and its use in measuring Archean sulphur isotope mass-independent anomalies. Geochim Cosmochim Acta 67: 3101–3118
Huang L, Strurchio NC, Abrajano T, Heraty LJ, Holt BD (1999) Carbon and chlorine isotope fractionation of chlorinated aliphatic hydrocarbons by evaporation. Org Geochem 30: 777–785
Hudson JD (1977) Stable isotopes and limestone lithification. J Geol Soc London 133: 637–660
Huh Y, Chan L-H, Zhang Edmond JM (1998) Lithium and its isotopes in major world rivers; implications for weathering and the oceanic budget. Geochim Cosmochim Acta 62: 2039–2051
Hulston JR (1977) Isotope work applied to geothermal systems at the Institute of Nuclear Sciences, New Zealand. Geothermics 5: 89–96

Hulston JR, Thode HG (1965) Variations in the ^{33}S, ^{34}S and ^{36}S contents of meteorites and their relations to chemical and nuclear effects. J Geophys Res 70: 3475–3484

Iacumin P, Bocherens H, Marriotti A, Longinelli A (1996) Oxygen isotope analysis of coexisting carbonate and phosphate in biogenic apatite; a way to monitor diagenetic alteration of bone phosphate?. Earth Planet Sci Lett 142: 1–6

Icopini GA, Anbar AD, Ruebush SS, Tien M, Brantley SL (2004) Iron isotope fractionation during microbial reduction of iron: the importance of adsorption. Geology 32: 205–208

Ingraham NL, Criss RE (1998) The effect of vapor pressure on the rate of isotopic exchange between water and vapour. Chem Geol 150: 287–292

Ionov DA, Hoefs J, Wedepohl KH, Wiechert U (1992) Contents and isotopic composition of sulfur in ultramafic xenoliths from Central Asia. Earth Planet Sci Lett 111: 269–286

Irwin H, Curtis C, Coleman M (1977) Isotopic evidence for the source of diagenetic carbonate during burial of organic-rich sediments. Nature 269: 209–213

Ishibashi J, Sano Y, Wakita H, Gamo T, Tsutsumi M, Sakai H (1995) Helium and carbon geochemistry of hydrothermal fluids from the Mid-Okinawa trough back arc basin, southwest of Japan. Chem Geol 123: 1–15

Izbicki JA, Ball JW, Bullen TD, Sutley SJ (2008) Chromium, chromium isotopes and selected trace elements, Western Mojave Desert, USA. Appl Geochemistry 23: 1325–1352

Jaffrés JB, Shields GA, Wallmann K (2007) The oxygen isotope evolution of seawater: a critical review of a long-standing controversy and an improved geological water cycle model for the past 3.4 billion years. Earth Sci Rev 83: 83–122

James DE (1981) The combined use of oxygen and radiogenic isotopes as indicators of crustal contamination. Ann Rev Earth Planet Sci 9: 311–344

James AT (1983) Correlation of natural gas by use of carbon isotopic distribution between hydrocarbon components. Am Ass Petrol Geol Bull 67: 1167–1191

James AT (1990) Correlation of reservoired gases using the carbon isotopic compositions of wet gas components. Am Ass Petrol Geol Bull 74: 1441–1458

James RH, Palmer MR (2000) The lithium isotope composition of international rock standards. Chem Geol 166: 319–326

Jasper JP, Hayes JM (1990) A carbon isotope record of CO_2 levels during the late Quaternary. Nature 347: 462–464

Jasper JP, Hayes JM, Mix AC, Prahl FG (1994) Photosynthetic fractionation of C-13 and concentrations of dissolved CO2 in the central equatorial Pacific. Paleoceanography 9: 781–798

Javoy M, Pineau F, Delorme H (1986) Carbon and nitrogen isotopes in the mantle. Chem Geol 57: 41–62

Jeffcoate AB, Elliott T, Kasemann SA, Ionov D, Cooper K, Brooker R (2007) Li isotope fractionation in peridotites and mafic melts. Geochim Cosmochim Acta 71: 202–218

Jeffrey AW, Pflaum RC, Brooks JM, Sackett WM (1983) Vertical trends in particulate organic carbon $^{13}C/^{12}C$ ratios in the upper water column. Deep Sea Res 30: 971–983

Jenden PD, Kaplan IR, Poreda RJ, Craig H (1988) Origin of nitrogen-rich natural gases in the California Great Valley: evidence from helium, carbon and nitrogen isotope ratios. Geochim Cosmochim Acta 52: 851–861

Jendrzejewski N, Eggenkamp HGM, Coleman ML (2001) Characterisation of chlorinated hydrocarbons from chlorine and carbon isotopic compositions: scope of application to environmental problems. Appl Geochem 16: 1021–1031

Jensen ML, Nakai N (1962) Sulfur isotope meteorite standards, results and recommendations. In: Jensen ML (ed) Biogeochemistry of sulfur isotopes. NSF Symp Vol, p 31

Jia Y (2006) Nitrogen isotope fractionations during progressive metamorphism: a case study from the Paleozoic Cooma metasedimentary complex, southeastern Australia. Geochim Cosmochim Acta 70: 5201–5214

Jiang SY, Palmer MR (1998) Boron isotope systematics of tourmaline from granites and tourmalines: a synthesis. Eur J Miner 10: 1253–1265

Jiang J, Clayton RN, Newton RC (1988) Fluids in granulite facies metamorphism: a comparative oxygen isotope study on the South India and Adirondack high grade terrains. J Geol 96: 517–533

Joachimski M, van Geldern R, Breisig S, Buggisch W, Day J (2004) Oxygen isotope evolution of biogenic calcite and apatite during the Middle and Late Devonian. Int J Earth Sci 93: 542–553

Joachimski M, Simon L, van Geldern R, Lecuyer C (2005) Boron isotope geochemistry of Paleozoic brachiopod calcite: implications for a secular change in the boron isotope geochemistry of seawater over the Phanerozoic. Geochim Cosmochim Acta 69: 4035–4044

John SG, Geis RW, Saito MA, 'Boyle EA (2007a) Zinc isotope fractionation during high-affinity and low-affinity ziinc transport by the marine diatom *Thalassiosira oceanica*. Limnol Oceanogr 52: 2710–2714

John SG, Park JG, Zhang Z, Boyle EA (2007b) The isotopic composition of some common forms of anthropogenic zinc. Chem Geol 245: 61–69

John SG, Rouxel OJ, Craddock PR, Engwall AM, Boyle EA (2008) Zinc stable isotopes in seafloor hydrothermal vent fluids and chimneys. Earth Planet Sci Lett 269: 17–28

Johnsen SJ, Clausen HB, Dansgaard W, Gundestrup N, Hammer CU, Tauber H (1995) The Eem stable isotope record along the GRIP ice core and ist interpretation. Quat Res 43: 117–124

Johnson TM (2004) A review of mass-dependent fractionation of selenium isotopes and implications for other heavy stable isotopes. Chem Geol 204: 201–214

Johnson CM, Beard BL (2006) Fe isotopes: an emerging technique for understanding modern and ancient biogeochemical cycles. GSA Today 16, no 11: 4–10

Johnson TM, Bullen TD (2003) Selenium isotope fractionation during reduction by Fe(II)-Fe(III) hydroxide-sulfate (green rust). Geochim Cosmochim Acta 67: 413–419

Johnson TM, Herbel MJ, Bullen TD, Zawislanski PT (1999) Selenium isotope ratios as indicators of selenium sources and oxyanion reduction. Geochim Cosmochim Acta 63: 2775–2783

Johnson DG, Jucks KW, Traub WA, Chance KV (2001) Isotopic composition of stratospheric water vapour: measurements and photochemistry. J Geophys Res 106: 12211–12217

Johnson CM, Skulan JL, Beard BL, Sun H, Nealson KH, Braterman PS (2002) Isotopic fraction between Fe(III) and Fe(II) in aqueous solutions. Earth Planet Sci Lett 195: 141–153

Johnson CM, Beard BL, Roden EE (2008) The iron isotope fingerprints of redox and biogeochemical cycling in modern and ancient Earth. Ann Rev Earth Planet Sci 36: 457–493

Johnston DT, Farquhar J, Wing BA, Kaufman AJ, Canfield DE, Habicht KS (2005) Multiple sulphur isotope fractionations in biological systems: a case study with sulphate reducers and sulphur disproportionators. Am J Sci 305: 645–660

Jones HD, Kesler SE, Furman FC, Kyle JR (1996) Sulfur isotope geochemistry of southern Appalachian Mississippi Valley-type depopsits. Econ Geol 91: 355–367

Jørgensen BB, Böttcher MA, Lüschen H, Neretin LN, Volkov II (2004) Anaerobic methane oxidation and a deep H_2S sink generate isotopically heavy sulfides in Black Sea sediments. Geochim Cosmochim Acta 68: 2095–2118

Jouzel J, Merlivat L, Roth E (1975) Isotopic study of hail. J Geophys Res 80: 5015–5030

Jouzel J, Lorius C, Petit JR, Barkov NI, Kotlyakov VM, Petrow VM (1987) Vostok ice core: a continuous isotopic temperature record over the last climatic cycle (160000 years). Nature 329: 403–408

Junk G, Svec H (1958) The absolute abundance of the nitrogen isotopes in the atmosphere and compressed gas from various sources. Geochim Cosmochim Acta 14: 234–243

Kakihana H, Kotaka M, Shohei S, Nomura M, Okamoto N (1977) Fundamental studies on the ion-exchange separation of boron isotopes. Bull Chem Soc Japan 50: 158–163

Kampschulte A, Strauss H (2004) The sulfur isotope evolution of Phanerozoic seawater based on the analyses of sructurally substituted sulfate in carbonates. Chem Geol 204: 255–280

Kaplan IR (1975) Stable isotopes as a guide to biogeochemical processes. Proc R Soc Lond Ser B 189: 183–211

Kaplan IR, Hulston JR (1966) The isotopic abundance and content of sulfur in meteorites. Geochim Cosmochim Acta 30: 479–496

Kaplan IR, Rittenberg SC (1964) Microbiological fractionation of sulphur isotopes. J Gen Microbiol 34: 195–212
Kaplan IR, Emery KO, Rittenberg SC (1963) The distribution and isotopic abundance of sulphur in recent marine sediments off Southern California. Geochim Cosmochim Acta 27: 297–332
Kasemann SA, Hawkesworth CJ, Prave AR, Fallick AE, Pearson PN (2005) Boron and calcium isotope composition in Neproterozoic carbonate rocks from Namibia: evidence for extreme environmental change. Earth Planet Sci Lett 231: 73–86
Kasting JF, Howard MT, Wallmann K, Veizer J, Shields G, Jaffrés J (2006) Paleoclimates, ocean depth and the oxygen isotopic composition of the ocean. Earth Planet Sci Lett 252: 82–93
Kaufman AJ, Knoll GM (1995) Neoproterozoic variations in the C-isotopic composition of seawater: stratigraphic and biogeochemical implications. Precambrian Res 73: 27–49
Kaufmann RS, Long A, Bentley H, Davis S (1984) Natural chlorine isotope variations. Nature 309: 338–340
Kaufmann RS, Long A, Bentley H, Campbell DJ (1986) Chlorine isotope distribution of formation water in Texas and Louisiana. Bull Am Assoc Petrol Geol 72: 839–844
Kaye J (1987) Mechanisms and observations for isotope fractionation of molecular species in planetary atmospheres. Rev Geophysics 25: 1609–1658
Keeling CD (1958) The concentration and isotopic abundance of atmospheric carbon dioxide in rural areas. Geochim Cosmochim Acta 13: 322–334
Keeling CD (1961) The concentration and isotopic abundances of carbon dioxide in rural and marine air. Geochim Cosmochim Acta 24: 277–298
Keeling CD, Mook WG, Tans P (1979) Recent trends in the $^{13}C/^{12}C$ ratio of atmospheric carbon dioxide. Nature 277: 121–123
Keeling CD, Carter AF, Mook WG (1984) Seasonal, latitudinal and secular variations in the abundance and isotopic ratio of atmospheric carbon dioxide. II. Results from oceanographic cruises in the tropical Pacific Ocean. J Geophys Res 89: 4615–4628
Keeling CD, Bacastow RB, Carter AF, Piper SC, Whorf TR, Heimann M, Mook WG, Roeloffzen H (1989) A three dimensional model of atmospheric CO_2 transport based on observed winds. 1. Analysis of observational data. Geophys Monogr 55: 165–236
Keeling CD, Whorf TP, Wahlen M, van der Plicht J (1995) Interannual extremes in the rate of rise of atmospheric carbon dioxide since 1980. Nature 375: 666–670
Kelley SP, Fallick AE (1990) High precision spatially resolved analysis of $\delta^{34}S$ in sulphides using a laser extraction technique. Geochim Cosmochim Acta 54: 883–888
Kelly WC, Rye RO, Livnat A (1986) Saline minewaters of the Keweenaw Peninsula, Northern Michigan: their nature, origin and relation to similar deep waters in Precambrian crystalline rocks of the Canadian Shield. Am J Sci 286: 281–308
Kelly J, Fu B, Kita N, Valley J (2007) Optically continuous silcrete quartz cements in the St. Peter sandstone. Geochim Cosmochim Acta 71: 3812–3832
Kelts K, McKenzie JA (1982) Diagenetic dolomite formation in Quaternary anoxic diatomaceous muds of DSDP Leg 64, Gulf of California. Initial Rep DSDP 64: 553–569
Kemp ALW, Thode HG (1968) The mechanism of the bacterial reduction of sulphate and of sulphite from isotopic fractionation studies. Geochim Cosmochim Acta 32: 71–91
Kempton PD, Harmon RS (1992) Oxygen isotope evidence for large-scale hybridization of the lower crust during magmatic underplating. Geochim Cosmochim Acta 56: 971–986
Kendall C (1998) Tracing nitrogen sources and cycling in catchments. In: Isotope Tracers in catchment hydrology. ed. by C. Kendall, JJ McDonnell, Elsevier Sci p. 519–576
Kendall C, Grim E (1990) Combustion tube method for measurement of nitrogen isotope ratios using calcium oxide for total removal of carbon dioxide and water. Anal Chem 62: 526–529
Kennicutt MC, Barker C, Brooks JM, De Freitaas DA, Zhu GH (1987) Selected organic matter indicators in the Orinoco, Nile and Changjiang deltas. Org Geochem 11: 41–51
Keppler F, Hamilton JTG, Braß M, Röckmann (2006) Methane emissions from terrestrial plants under aerobic conditions. Nature 439: 187–191

Kerrich R, Rehrig W (1987) Fluid motion associated with Tertiary mylonitization and detachment faulting: $^{18}O/^{16}O$ evidence from the Picacho metamorphic core complex, Arizona. Geology 15: 58–62

Kerrich R, Latour TE, Willmore L (1984) Fluid participation in deep fault zones: evidence from geological, geochemical and to $^{18}O/^{16}O$ relations. J Geophys Res 89: 4331–4343

Kerridge JF (1983) Isotopic composition of carbonaceous-chondrite kerogen: evidence for an interstellar origin of organic matter in meteorites. Earth Planet Sci Lett 64: 186–200

Kerridge JF, Haymon RM, Kastner M (1983) Sulfur isotope systematics at the 21°N site, East Pacific Rise. Earth Planet Sci Lett 66: 91–100

Kerridge JF, Chang S, Shipp R (1987) Isotopic characterization of kerogen-like material in the Murchison carbonaceous chondrite. Geochim Cosmochim Acta 51: 2527–2540

Kharaka YK, Berry FAF, Friedman I (1974) Isotopic composition of oil-field brines from Kettleman North Dome, California and their geologic implications. Geochim Cosmochim Acta 37: 1899–1908

Kieffer SW (1982) Thermodynamic and lattice vibrations of minerals: 5. Application to phase equilibria, isotopic fractionation and high-pressure thermodynamic properties. Rev Geophys Space Phys 20: 827–849

Kim KR, Craig H (1990) Two isotope characterization of N_2O in the Pacific Ocean and constraints on its origin in deep water. Nature 347: 58–61

Kim KR, Craig H (1993) Nitrogen-15 and oxygen-18 characteristics of nitrous oxide. Science 262: 1855–1858

Kim ST, O'Neil JR (1997) Equilibrium and nonequilibrium oxygen isotope effects in synthetic carbonates. Geochim Cosmochim Acta 61: 3461–3475

Kim S-T, Mucci A, Taylor BE (2007) Phosphoric acid fractionation factors for calcite and aragonite between 25 and 75°C. Chem Geol 246: 135–146

Kirkley MB, Gurney JJ, Otter ML, Hill SJ, Daniels LR (1991) The application of C-isotope measurements to the identification of the sources of C in diamonds. Appl Geochem 6: 477–494

Kirshenbaum I, Smith JS, Crowell T, Graff J, McKee R (1947) Separation of the nitrogen isotopes by the exchange reaction between ammonia and solutions of ammonium nitrate. J Chem Phys 15: 440–446

Kitchen NE, Valley JW (1995) Carbon isotope thermometry in marbles of the Adirondack Mountains, New York. J metamorphic Geol 13: 577–594

Kiyosu Y, Krouse HR (1990) The role of organic acid in the abiogenic reduction of sulfate and the sulfur isotope effect. Geochem J 24: 21–27

Klochko K, Kaufman AJ, Yao W, Byrne RH, Tossell JA (2006) Experimental measurement of boron isotope fractionation in seawater. Earth Planet Sci Lett 248: 276–285

Kloppmann Girard Négrel P (2002) Exotic stable isotope composition of saline waters and brines from the crystalline basement. Chem Geol 184: 49–70

Knauth LP (1988) Origin and mixing history of brines, Palo Duro Basin, Texas, USA. Applied Geochemistry 3: 455–474

Knauth LP, Beeunas MA (1986) Isotope geochemistry of fluid inclusions in Permian halite with implications for the isotopic history of ocean water and the origin of saline formation waters. Geochim Cosmochim Acta 50: 419–433

Knauth LP, Lowe DR (1978) Oxygen isotope geochemistry of cherts from the Onverwacht group (3.4 billion years), Transvaal, South Africa, with implications for secular variations in the isotopic composition of chert. Earth Planet Sci Lett 41: 209–222

Knoll AH, Hayes JM, Kaufman AJ, Swett K, Lambert IB (1986) Secular variation in carbon isotope ratios from Upper Proterozoic successions of Svalbard and East Greenland. Nature 321: 832–838

Kohn MJ (1996) Predicting animal $\delta^{18}O$: accounting for diet and physiological adaptation. Geochim Cosmochim Acta 60: 4811–4829

Kohn MJ (1999) Why most "dry" rocks should cool "wet". Am Miner 84: 570–580

Kohn MJ, Cerling TE (2002) Stable isotope compositions of biological apatite. Rev Miner Geochem 48: 455–488

Kohn MJ, Valley JW (1998a) Oxygen isotope geochemistry of amphiboles: isotope effects of cation substitutions in minerals. Geochim Cosmochim Acta 62: 1947–1958
Kohn MJ, Valley JW (1998b) Effects of cation substitutions in garnet and pyroxene on equilibrium oxygen isotope fractionations. J Metam Geol 16: 625–639
Kohn MJ, Valley JW (1998c) Obtaining equilibrium oxygen isotope fractionations from rocks: theory and examples. Contr Miner Petrol 132: 209–224
Kohn MJ, Valley JW (1994) Oxygen isotope constraints on metamorphic fluid flow, Townshend Dam, Vermont, USA. Geochim Cosmochim Acta 58: 5551–5566
Kohn MJ, Valley JW, Elsenheimer D, Spicuzza M (1993) Oxygen isotope zoning in garnet and staurolite: evidence for closed system mineral growth during regional metamorphism. Am Miner 78: 988–1001
Kohn MJ, Schoeninger MJ, Valley JW (1996) Herbivore tooth oxygen isotope compositions: effects of diet and physiology. Geochim Cosmochim Acta 60: 3889–3896
Kohn MJ, Riciputi LR, Stakes D, Orange DL (1998) Sulfur isotope variability in biogenic pyrite: reflections of heterogeneous bacterial colonzation? Am Miner 83: 1454–1486
Kolodny Y, Kerridge JF, Kaplan IR (1980) Deuterium in carbonaceous chondrites. Earth Planet Sci Lett 46: 149–153
Kolodny Y, Luz B, Navon O (1983) Oxygen isotope variations in phosphate of biogenic apatites, I. Fish bone apatite - rechecking the rules of the game. Earth Planet Sci Lett 64: 393–404
Kolodny Y, Luz B, Sander M, Clemens WA (1996) Dinosaur bones: fossils or pseudomorphs? The pitfalls of physiology reconstruction from apatitic fossils. Palaeogeogr Palaeoclimatol Palaeoecol 126: 161–171
Krankowsky D, Lämmerzahl P, Mauersberger K (2000) Isotopic measurements of stratospheric ozone. Geophys Res Lett 27: 2593–2595
Krishnamurthy RV, Epstein S, Cronin JR, Pizzarello S, Yuen GU (1992) Isotopic and molecular analyses of hydrocarbons and monocarboxylic acids of the Murchison meteorite. Geochim Cosmochim Acta 56: 4045–4058
Kritee K, Blum JD, Johnson MW, Bergquist BA, Barkay T (2007) Mercury stable isotope fractionation during reduction of Hg(II) to Hg(0) by mercury resistant microorganisms. Environ Sci Technol 41: 1889–1895
Kroopnick P (1985) The distribution of ^{13}C of ΣCO2 in the world oceans. Deep Sea Res 32: 57–84
Kroopnick P, Craig H (1972) Atmospheric oxygen: isotopic composition and solubility fractionation. Science 175: 54–55
Kroopnick P, Weiss RF, Craig H (1972) Total CO_2, ^{13}C and dissolved oxygen-^{18}O at Geosecs II in the North Atlantic. Earth Planet Sci Lett 16: 103–110
Krouse HR, Case JW (1983) Sulphur isotope abundances in the environment and their relation to long term sour gas flaring, near Valleyview, Alberta. Final Report Res.Management Division, University Alberta RMD Rep 83/18
Krouse HR, Thode HG (1962) Thermodynamicproperties and geochemistry of isotopic compounds of selenium. Can J Chem 40: 367–375
Krouse HR, Viau CA, Eliuk LS, Ueda A, Halas S (1988) Chemical and isotopic evidence of thermochemical sulfate reduction by light hydrocarbon gases in deep carbonate reservoirs. Nature 333: 415–419
Ku TCW, Walter LM, Coleman ML, Blake RE, Martini AM (1999) Coupling between sulfur recycling and syndepositional carbonate dissolution: evidence from oxygen and sulfur isotope composition of pore water sulfate, South Florida Platform, USA. Geochim Cosmochim Acta 63: 2529–2546
Kump LR (1989) Alternative modeling approaches to the geochemical cycles of carbon, sulfur and strontium isotopes. Am J. Sci 289: 390–410
Kump LR (2005) Ironing out biosphere oxidation. Science 307: 1058–1059
Kump LR, Arthur MA (1999) Interpreting carbon-isotope excursions: carbonates and organic matter. Chem Geol. 161: 181–198
Kung CC, Clayton RN (1978) Nitrogen abundances and isotopic compositions in stony meteorites. Earth Planet Sci Lett 38: 421–435

Kvenvolden KA (1995) A review of the geochemistry of methane in natural gas hydrate. Org Geochem 23: 997–1008
Kyser TK, O'Neil JR (1984) Hydrogen isotope systematics of submarine basalts. Geochim Cosmochim Acta 48: 2123–2134
Kyser TK, O'Neil JR, Carmichael ISE (1981) Oxygen isotope thermometry of basic lavas and mantle nodules. Contrib Miner Petrol 77: 11–23
Kyser TK, O'Neil JR, Carmichael ISE (1982) Genetic relations among basic lavas and mantle nodules. Contrib Miner Petrol 81: 88–102
Kyser TK, O'Neil JR, Carmichael ISE (1986) Reply to "Possible non-equilibrium oxygen isotope effects in mantle nodules, an alternative to the Kyser-O'Neil-Carmichael geothermometer. Contr Miner Petrol 93: 120–123
Labeyrie LD, Juillet A (1982) Oxygen isotope exchangeability of diatom valve silica; interpretation and consequences for paleoclimatic studies. Geochim Cosmochim Acta 46: 967–975
Labeyrie LD, Duplessy JC, Blanc PL (1987) Deep water formation and temperature variations over the last 125000 years. Nature 327: 477–482
Land LS (1980) The isotopic and trace element geochemistry of dolomite: the state of the art. In: Concepts and models of dolomitization. Soc Econ Paleontol Min Spec Publ 28: 87–110
Lane GA, Dole M (1956) Fractionation of oxygen isotopes during respiration. Science 123: 574–576
Langer G, Gussone N, Nehrke G, Riebesell U, Eisenhauer A, Thoms S (2007) Calcium isotope fractionation during coccolith formation in *Emiliania huxley*i: independence of growth and calcification. Geochem Geophys Geosys 8: Q05007, doi:10.1029/2006GC001422
Larson PB, Maher K, Ramos FC, Chang Z, Gaspar M, Meinert LD (2003) Copper isotope ratios in magmatic and hydrothermal ore-forming processes. Chem Geol 201: 337–350
Lawrence JR (1989) The stable isotope geochemistry of deep-sea pore water. In: Handbook of environmental isotope geochemistry, vol 3. Elsevier, New York, 317–356
Lawrence JR, Gieskes JM (1981) Constraints on water transport and alteration in the oceanic crust from the isotopic composition of the pore water. J Geophys Res 86: 7924–7934
Lawrence JR, Taviani M (1988) Extreme hydrogen, oxygen and carbon isotope anomalies in the pore waters and carbonates of the sediments and basalts from the Norwegian Sea: methane and hydrogen from the mantle? Geochim Cosmochim Acta 52: 2077–2083
Lawrence JR, Taylor HP (1971) Deuterium and oxygen-18 correlation: clay minerals and hydroxides in Quaternary soils compared to meteoric waters. Geochim Cosmochim Acta 35: 993–1003
Lawrence JR, White JWC (1991) The elusive climate signal in the isotopic composition of precipitation. In: Stable Isotope Geochemistry: a tribute to Samuel Epstein. Special Publication 3, 169–185 The Geochemical Society, USA
Laws EA, Popp BN, Bidigare RR, Kennicutt MC, Macko SA (1995) Dependence of phytoplankton carbon isotopic composition on growth rate and CO_{2aq}: theoretical considerations and experimental results. Geochim Cosmochim Acta 59: 1131–1138
Laws EA, Bidigare RR, Popp BN (1997) Effect of growth rate and CO_2 concentration on carbon isotope fractionation by the marine diatom *Phaeodactylum tricornutum*. Limnol Oceanogr 42: 1552–1560
Leclerc AJ, Labeyrie LC (1987) Temperature dependence of oxygen isotopic fractionation between diatom silica and water. Earth Planet Sci Lett 84: 69–74
Lécuyer C, Grandjean P, Reynard B, Albarede F, Telouk P (2002) $^{11}B/^{10}B$ analysis of geological materials by ICP-MS Plasma 54: application to bron fractionation between brachiopod calcite and seawater. Chem Geol 186: 45–55
Leder JL, Swart PK, Szmant AM, Dodge RE (1996) The origin of variations in the isotopic record of scleractinian corals: I. Oxygen. Geochim Cosmochim Acta 60: 2857–2870
Leeman WP, Tonarini S, Chan LH, Borg LE (2004) Boron and lithium isotopic variations in a hot subduction zone – the southern Washington Cascades. Chem Geol 212: 101–124
Lehmann M, Siegenthaler U (1991) Equilibrium oxygen- and hydrogen-isotope fractionation between ice and water. J Glaciology 37: 23–26

Lemarchand D, Gaillardet J, Lewin E, Allegre CJ (2000) The influence of rivers on marine boron isotopes and implications for reconstructing past ocean pH. Nature 408: 951–954
Lemarchand D, Gaillardet J, Lewin E, Allègre CJ (2002) Boron isotope systematics in large rivers: implications for the marine boron budget and paleo-pH reconstruction over the Cenozoic. Chem Geol 190: 123–140
Lemarchand D, Wasserburg GJ, Papanastassiou DA (2004) Rate-controlled calcium isotope fractionation in synthetic calcite. Geochim Cosmochim Acta 68: 4665–4678
Leng MJ, Marshall JD (2004) Palaeoclimate interpretation of stable isotope data from lake sediment archives. Q Sci Rev 23: 811–831
Leshin LA, Epstein S, Stolper EM (1996) Hydrogen isotope geochemistry of SNC meteorites. Geochim Cosmochim Acta 60: 2635–2650
Leshin LA, McKeegan KD, Carpenter PK, Harvey RP (1998) Oxygen isotopic constraints on the genesis of carbonates from Martian meteorite ALH 84001. Geochim Cosmochim Acta 62: 3–13
Letolle R (1980) Nitrogen-15 in the natural environment. In: Fritz P, Fontes JCh (eds) Handbook of environmental isotope geochemistry. Elsevier, Amsterdam, p 407–433
Leuenberger M, Siegenthaler U, Langway CC (1992) Carbon isotope composition of atmospheric CO_2 during the last ice age from an Antarctic ice core. Nature 357: 488–490
Lewan MD (1983) Effects of thermal maturation on stable carbon isotopes as determined by hydrous pyrolysis of Woodford shale. Geochim Cosmochim Acta 47: 1471–1480
Lewis RS, Anders E, Wright IP, Norris SJ, Pillinger CT (1983) Isotopically anomalous nitrogen in primitive meteorites. Nature 305: 767–771
Liebscher A, Meixner A, Romer R, Heinrich W (2005) Liquid-vapor fractionation of boron and boron isotopes: experimental calibration at 400°C/23 Mpa to 450°C/42Mpa. Geochim Cosmochim Acta 69: 5693–5704
Liebscher A, Barnes J, Sharp Z (2006) Chlorine isotope vapor-liquid fractionation during experimental fluid-phase separation at 400°C/23 Mpa to 450°C/42Mpa. Chem Geol 234: 340–345
Lister GS, Kelts K, Chen KZ, Yu JQ, Niessen F (1991) Lake Qinghai, China: closed-basin lake levels and the oxygen isotope record for ostracoda since the latest Pleistocene. Palaeogeogr Palaeoclimatol Palaeoecol 84: 141–162
Lloyd MR (1967) Oxygen-18 composition of oceanic sulfate. Science 156: 1228–1231
Lloyd MR (1968) Oxygen isotope behavior in the sulfate-water system. J Geophys Res 73: 6099–6110
Long A, Eastoe CJ, Kaufmann RS, Martin JG, Wirt L, Fincey JB (1993) High precision measurement of chlorine stable isotope ratios. Geochim Cosmochim Acta 57: 2907–2912
Longinelli A (1966) Ratios of oxygen-18: oxygen-16 in phosphate and carbonate from living and fossil marine organisms. Nature 211: 923–926
Longinelli A (1984) Oxygen isotopes in mammal bone phosphate: a new tool for paleohydrological and paleoclimatological research?. Geochim Cosmochim Acta 48: 385–390
Longinelli A, Bartelloni M (1978) Atmospheric pollution in Venice, Italy, as indicated by isotopic analyses. Water Air Soil Poll 10: 335–341
Longinelli A, Craig H (1967) Oxygen-18 variations in sulfate ions in sea-water and saline lakes. Science 156: 56–59
Longinelli A, Edmond JM (1983) Isotope geochemistry of the Amazon basin. A reconnaissance. J Geophys Res 88: 3703–3717
Longinelli A, Nuti S (1973) Revised phosphate-water isotopic temperature scale. Earth Planet Sci Lett 19: 373–376
Longstaffe FJ (1989) Stable isotopes as tracers in clastic diagenesis. In: Short course in burial diagenesis, ed. IE Hutcheon, Min Ass Canada Short Course Series 15: 201–277
Longstaffe FJ, Schwarcz HP (1977) $^{18}O/^{16}O$ of Archean clastic metasedimentary rocks: a petrogenetic indicator for Archean gneisses?. Geochim Cosmochim Acta 41: 1303–1312
Lorius C, Jouzel J, Ritz C, Merlivat L, Barkov NI, Korotkevich YS, Kotlyakov VM (1985) A 150000 year climatic record from Antarctic ice. Nature 316: 591–596
Lücke A, Moschen R, Schleser G (2005) High-temperature carbon reduction of silica: a novel approach for oxygen isotope analysis of biogenic opal. Geochim Cosmochim Acta 69: 1423–1433

Lundstrom CC, Chaussidon M, Hsui AT, Keleman P, Zimmermann M (2005) Observations of Li isotope variations in the Trinity ophiolite: evidence for isotope fractionation by diffusion during mantle melting. Geochim Cosmochim Acta 69: 735–751

Luz B, Barkan E (2000) Assessment of oceanic productivity with the triple-isotope composition of dissolved oxygen. Science 288: 2028–2031

Luz B, Barkan E (2005) The isotopic ratios $^{17}O/^{16}O$ and $^{18}O/^{16}O$ in molecular oxygen and their significance in biogeochemistry. Geochim Cosmochim Acta 69: 1099–1110

Luz B, Barkan E (2007) Excess ^{17}O – a new tracer in hydrology. Geochim Cosmochim Acta 71: A604

Luz B, Kolodny Y (1985) Oxygen isotope variations in phosphate of biogenic apatites, IV: Mammal teeth and bones. Earth Planet Sci Lett 75: 29–36

Luz B, Kolodny Y, Horowitz M (1984) Fractionation of oxygen isotopes between mammalian bone-phosphate and environmental drinking water. Geochim Cosmochim Acta 48: 1689–1693

Luz B, Cormie AB, Schwarcz HP (1990) Oxygen isotope variations in phosphate of deer bones. Geochim Cosmochim Acta 54: 1723–1728

Luz B, Barkan E, Bender ML, Thiemens MH, Boering KA (1999) Triple-isotope composition of atmospheric oxygen as a tracer of biosphere productivity. Nature 400: 547–550

Machel HG, Krouse HR, Sassen P (1995) Products and distinguishing criteria of bacterial and thermochemical sulfate reduction. Appl Geochemistry 10: 373–389

Magenheim AJ, Spivack AJ, Volpe C, Ranson B (1994) Precise determination of stable chlorine isotope ratios in low-concentration natural samples. Geochim Cosmochim Acta 58: 3117–3121

Magenheim AJ, Spivack AJ, Michael PJ, Gieskes JM (1995) Chlorine stable isotope composition of the oceanic crust: implications for earth·s distribution of chlorine. Earth Planet Sci Lett 131: 427–432

Magna T, Wiechert U, Halliday AN (2006) New constraints on the lithium isotope composition of the Moon and terrestrial planets. Earth Planet Sci Lett 243: 336–353

Maréchal CN, Albarede F (2002) Ion-exchange fractionation of copper and zinc isotopes. Geochim Cosmochim Acta 66: 1499–1509

Maréchal CN, Télouk P, Albarède F (1999) Precise analysis of copper and zinc isotopic compositions by plasma-source mass spectrometry. Chem Geol 156: 251–273

Maréchal CN, Nicolas E, Douchet C, Alabarède F (2000) Abundance of zinc isotopes as a marine biogeochemical tracer. Geochem Geophys Geosys $G^3$1 1999GC000029

Mariotti A, Germon JC, Hubert P, Kaiser P, Letolle R, Tardieux P (1981) Experimental determination of nitrogen kinetic isotope fractionation: some principles, illustration for the denitrification and nitrification processes. Plant Soil 62: 413–430

Markl G, Musashi M, Bucher K (1997) Chlorine stable isotope composition of granulites from Lofoten, Norway: implication for the Cl-isotope composition and for the source of Cl enrichment in the lower crust. Earth Planet Science Lett 150: 95–120

Markl G, Lahaye Y, Schwinn G (2006a) Copper isotopes as monitors of redox processes in hydrothermal mineralization. Geochim Cosmochim Acta 70: 4215–4228

Markl G, von Blanckenburg F, Wagner T (2006b) Iron isotope fractionation during hydrothermal ore deposition and alteration. Geochim Cosmochim Acta 70: 3011–3030

Marowsky G (1969) Schwefel-, Kohlenstoff-und Sauerstoffisotopenuntersuchungen am Kupferschiefer als Beitrag zur genetischen Deutung. Contrib Miner Petrol 22: 290–334

Marschall HR, Altherr R, Kalt A, Ludwig T (2008) Detrital, metamorphic and metasomatic tourmaline in high-pressure metasediments from Syros (Greece): intra-grain boron isotope patterns determined by secondary-ion mass spectrometry. Contr Miner Petrol 155: 703–717

Martinson DG, Pisias NG, Hays JD, Imbrie J, Moore TC, Shackleton NJ (1987) Age dating and the orbital theory of the ice ages: development of a high resolution 0 to 300000 year chronostratigraphy. Quat Res 27: 1–29

Marty B, Humbert F (1997) Nitrogen and argon isotopes in oceanic basalts. Earth Planet Sci Lett 152: 101–112

Marty B, Zimmermann L (1999) Volatiles (He, C, N, Ar) in mid-ocean ridge basalts: assesment of shallow-level fractionation and characterization of source composition. Geochim Cosmochim Acta 63: 3619–3633
Mastalerz M, Schimmelmann A (2002) Isotopically exchangeable organic hydrogen in coal relates to thermal maturity and maceral composition. Org Geochem 33: 921–931
Matheney RK, Knauth LP (1989) Oxygen isotope fractionation between marine biogenic silica and seawater. Geochim Cosmochim Acta 53: 3207–3214
Mathur R, Ruiz J, Titley S, Liermann L, Buss H, Brantley S (2005) Cu isotopic fractionation in the supergene environment with and without bacteria. Geochim Cosmochim Acta 69: 5233–5246
Matsubaya O, Sakai H (1973) Oxygen and hydrogen isotopic study on the water of crystallization of gypsum from the Kuroko-type mineralization. Geochem J 7: 153–165
Matsuhisa Y (1979) Oxygen isotopic compositions of volcanic rocks from the east Japan island arcs and their bearing on petrogenesis. J Volcanic Geotherm Res 5: 271–296
Matsuhisa Y, Goldsmith JR, Clayton RN (1978) Mechanisms of hydrothermal crystallization of quartz at 250°C and 15 kbar. Geochim Cosmochim Acta 42: 173–182
Matsuhisa Y, Goldsmith JR, Clayton RN (1979) Oxygen isotope fractionation in the systems quartz-albite-anorthite-water. Geochim Cosmochim Acta 43: 1131–1140
Matsumoto R (1992) Causes of the oxygen isotopic depletion of interstitial waters from sites 798 and 799, Japan Sea, Leg 128. Proc of the Ocean Drilling Progr, Scientific Results, Vol 127/128: 697–703
Matsuo S, Friedman I, Smith GI (1972) Studies of Quaternary saline lakes. I. Hydrogen isotope fractionation in saline minerals. Geochim Cosmochim Acta 36: 427–435
Mattey DP, Carr RH, Wright IP, Pillinger CT (1984) Carbon isotopes in submarine basalts. Earth Planet Sci Lett 70: 196–206
Mattey DP, Lowry D, MacPherson C (1994) Oxygen isotope composition of mantle peridotites. Earth Planet Sci Lett 128: 231–241
Matthews A, Goldsmith JR, Clayton RN (1983a) Oxygen isotope fractionation involving pyroxenes: the calibration of mineral-pair geothermometers. Geochim Cosmochim Acta 47: 631–644
Matthews A, Goldsmith JR, Clayton RN (1983b) Oxygen isotope fractionation between zoisite and water. Geochim Cosmochim Acta 47: 645–654
Matthews A, Goldsmith JR, Clayton RN (1983c) On the mechanics and kinetics of oxygen isotope exchange in quartz and feldspars at elevated temperatures and pressures. Geol Soc Am Bull 94: 396–412
Mauersberger K (1981) Measurement of heavy ozone in the stratosphere. Geophys Res Lett 8: 935–937
Mauersberger K (1987) Ozone isotope measurements in the stratosphere. Geophys Res Lett 14: 80–83
Mauersberger K, Erbacher B, Krankowsky D, Günther J, Nickel R (1999) Ozone isotope enrichment: isotopomer-specific rate coefficients. Science 283: 370–372
McCaig AM, Wickham SM, Taylor HP (1990) Deep fluid circulation in Alpine shear zones, Pyrenees, France: field and oxygen isotope studies. Contr Miner Petrol 106: 41–60
McCollom TM, Seewald JS (2006) Carbon isotope composition of organic compounds produced by abiotic synthesis under hydrothermal conditions. Earth Planet Sci Lett 243: 74–84
McConnaughey T (1989a) ^{13}C and ^{18}O disequilibrium in biological carbonates.I. Patterns. Geochim Cosmochim Acta 53: 151–162
McConnaughey T (1989b) ^{13}C and ^{18}O disequilibrium in biological carbonates. II. In vitro simulation of kinetic isotope effects. Geochim Cosmochim Acta 53: 163–171
McCorkle DC, Emerson SR (1988) The relationship between pore water isotopic composition and bottom water oxygen concentration. Geochim Cosmochim Acta 52: 1169–1178
McCorkle DC, Emerson SR, Quay P (1985) Carbon isotopes in marine porewaters. Earth Planet Sci Lett 74: 13–26
McCrea JM (1950) On the isotopic chemistry of carbonates and a paleotemperature scale. J Chem Phys 18: 849–857

McCready RGL (1975) Sulphur isotope fractionation by Desulfovibrio and Desulfotomaculum species. Geochim Cosmochim Acta 39: 1395–1401
McCready RGL, Kaplan IR, Din GA (1974) Fractionation of sulfur isotopes by the yeast Saccharomyces cerevisiae. Geochim Cosmochim Acta 38: 1239–1253
McDermott F (2004) Palaeo-climate reconstruction from stable isotope variations in speleothems: a review. Q Sci Rev 23: 901–918
McGarry S, Bar-Matthews M, Matthews A, Vaks A, Schilman B, Ayalon A (2004) Constraints on hydrological and paleotemperature variations in the eastern Mediterranean region in the last 140 ka given by the δD values of speleothem fluid inclusions. Quat Sci Rev 23: 919–934
McGregor ID, Manton SR (1986) Roberts Victor eclogites: ancient oceanic crust. J Geophys Res 91: 14063–14079
McKay DS, et al. (1996) Search for past life on Mars: possible relic biogenic activity in martian meteorite ALH 84001. Science 273: 924–930
McKeegan KD (1987) Ion microprobe measurements of H, C, O, Mg, and Si isotopic abundances in individual interplenary dust particles. Ph D Thesis, Washington University, St. Louis, Missouri
McKeegan KD, Leshin LA (2001) Stable isotope variations in extraterrestrial materials. Rev Miner Geochem 43: 279–318
McKeegan KD, Walker RM, Zinner E (1985) Ion microprobe isotopic measurements of individual interplanetary dust particles. Geochim Cosmochim Acta 49: 1971–1987
McKenzie J (1984) Holocene dolomitization of calcium carbonate sediments from the coastal sabkhas of Abu Dhabi, U.A.E.: a stable isotope study. J Geol 89: 185–198
McKibben MA, Riciputi LR (1998) Sulfur isotopes by ion microprobe. In: Applications of microanalytical techniques to understanding mineralizing processes. Rev Econ Geol 7: 121–140
McManus J, Nägler T, Siebert C, Wheat CG, Hammond D (2002) Oceanic molybdenum isotope fractionation: diagenesis and hydrothermal ridge flank alteration. Geochem Geophys Geosyst 3: 1078 doi: 10.1029/2002GC000356
McManus J, et al. (2006) Molybdenum and uranium geochemistry in continental margin sediments: palaeoproxy potential. Geochim Cosmochim Acta 70: 4643–4662
McMullen CC, Cragg CG, Thode HG (1961) Absolute ratio of $^{11}B/^{10}B$ in Searles Lake borax. Geochim Cosmochim Acta 23: 147
McSween HY, Taylor LA, Stolper EM (1979) Allan Hills 77005: a new meteorite type found in Antarctica. Science 204: 1201–1203
Mekhtiyeva VL, Pankina GR (1968) Isotopic composition of sulfur in aquatic plants and dissolved sulfates. Geochemistry 5: 624
Mekhtiyeva VL, Pankina GR, Gavrilov EY (1976) Distribution and isotopic composition of forms of sulfur in water animals and plants. Geochem Int 13: 82
Melander L (1960) Isotope effects on reaction rates. Ronald, New York
Melander L, Saunders WH (1980) Reaction rates of isotopic molecules. Wiley and Sons, New York
Mengel K, Hoefs J (1990) Li - $\delta^{18}O$ - SiO_2 systematics in volcanic rocks and mafic lower crustal xenoliths. Earth Planet Sci Lett 101: 42–53
Merritt DA, Hayes JM (1994) Nitrogen isotopic analyses of individual amino acids by isotope-ratio-monitoring gas chromatography/mass spectrometry. J Am Soc Mass Spectrom 5: 387–397
Meyer C, Wunder B, Meixner A, Romer R, Heinrich W (2008) The boron-isotope partitioning between tourmaline and fluid: an experimental re-investigation. Contr Miner Petr 156: 259–267
Mikaloff-Fletcher SE, et al. (2006) Inverse estimates of anthropogenic CO_2 uptake, transport and storage by the ocean. Global Biogeochem Cycles 20: GB2002; doi:10/10292005GB002532
Milkov AV (2005) Molecular and stable isotope compositions of natural gas hydrates: a revised global dataset and basic interpretations in the context of geological settings. Org Geochem 36: 681–702
Miller MF (2002) Isotopic fractionation and the quantification of ^{17}O anomalies in the oxygen three-isotope system: an appraisal and geochemical significance. Geochim Cosmochim Acta 66: 1881–1889

Ming T, Anders E, Hoppe P, Zinner E (1989) Meteoritic silicon carbide and its stellar sources, implications for galactic chemical evolution. Nature 339: 351–354

Minigawa M, Wada E (1984) Stepwise enrichments of ^{15}N along food chains: further evidence and the relation between $\delta^{15}N$ and animal age. Geochim Cosmochim Acta 48: 1135–1140

Mizutani Y, Rafter TA (1973) Isotopic behavior of sulfate oxygen in the bacterial reduction of sulfate. Geochem J 6: 183–191

Moldovanyi EP, Lohmann KC (1984) Isotopic and petrographic record of phreatic diagenesis: lower Cretaceous Sligo and Cupido Formations. J Sediment Petrol 54: 972–985

Monson KD, Hayes JM (1982) Carbon isotopic fractionation in the biosynthesis of bacterial fatty acids. Ozonolysis of unsaturated fatty acids as a means of determining the intramolecular distribution of carbon isotopes. Geochim Cosmochim Acta 46: 139–149

Monster J, Anders E, Thode HG (1965) $^{34}S/^{32}S$ ratios for the different forms of sulphur in the Orgueil meteorite and their mode of formation. Geochim Cosmochim Acta 29: 773–779

Monster J, Appel PW, Thode HG, Schidlowski M, Carmichael CW, Bridgwater D (1979) Sulphur isotope studies in early Archean sediments from Isua, West Greenland: implications for the antiquity of bacterial sulfate reduction. Geochim Cosmochim Acta 43: 405–413

Mook WG, Bommerson JC, Stavermann WH (1974) Carbon isotope fractionation between dissolved bicarbonate and gaseous carbon dioxide. Earth Planet Sci Lett 22: 169–174

Mook WG, Koopman M, Carter AF, Keeling CD (1983) Seasonal, latitudinal and secular variations in the abundance and isotopic ratios of atmospheric carbon dioxide. I. Results from land stations. J Geophys Res 88: 10915–10933

Montoya JP, Horrigan SG, McCarthy JJ (1991) Rapid, storm-induced changes in the natural abundance of ^{15}N in a planktonic ecosystem, Chesapeake Bay, USA. Geochim Cosmochim Acta 55: 3627–3638

Moriguti T, Nakamura E (1998) Across-arc variation of Li-isotopes in lavas and implications for crust /mantle recycling at subduction zones. Earth Planet Sci Lett 163: 167–174

Mossmann JR, Aplin AC, Curtis CD, Coleman ML (1991) Geochemistry of inorganic and organic sulfur in organic-rich sediments from the Peru Margin. Geochim Cosmochim Acta 55: 3581–3595

Muehlenbachs K, Byerly G (1982) ^{18}O enrichment of silicic magmas caused by crystal fractionation at the Galapagos Spreading Center. Contr Miner Petrol 79: 76–79

Muehlenbachs K, Clayton RN (1972) Oxygen isotope studies of fresh and weathered submarine basalts. Can J Earth Sci 9: 471–479

Muehlenbachs K, Clayton RN (1976) Oxygen isotope composition of the oceanic crust and its bearing on seawater. J Geophys Res 81: 4365–4369

Mulitza S, Duerkoop A, Hale W, Wefer S, Niebler HS (1997) Planktonic foraminifera as recorders of past surface-water stratification. Geology 25: 335–338

Nabelek PI (1991) Stable isotope monitors. In: Contact metamorphism. Rev Miner 26: 395–435

Nabelek PI, Labotka TC (1993) Implications of geochemical fronts in the Notch Peak contact-metamorphic aureole, Utah, USA. Earth Placet Sci Lett 119: 539–559

Nabelek PI, Labotka TC, O'Neil JR, Papike JJ (1984) Contrasting fluid/rock interaction between the Notch Peak granitic intrusion and argillites and limestones in western Utah: evidence from stable isotopes and phase assemblages. Contr Miner Petrol 86: 25–43

Nägler TF, Eisenhauer A, Müller A, Hemleben C, Kramers J (2000) The $\delta^{44}Ca$-temperature calibration on fossil and cultured *Globigerinoides sacculifer*: new tool for reconstruction of past sea surface temperatures. Geochem Geophys Geosystems G^3 1 (2000GC000091)

Nägler TF, Siebert C, Lüschen H, Böttcher ME (2005) Sedimentary Mo isotope records across the Holocene fresh-brackish water transition of the Black Sea. Chem Geol 219: 283–295

Nakano T, Nakamura E (2001) Boron isotope geochemistry of metasedimentary rocks and tourmalines in a subduction zone metamorphic suite. Phys Earth Planet Inter 127: 233–252

Neretin LN, Böttcher ME, Jørgensen BB, Volkov II, Lüschen H, Hilgenfeldt K (2004) Pyritization processes and greigite formation in the advancing sulfidization front in the Upper Pleistone sediments of the Black Sea. Geochim Cosmochim Acta 68: 2081–2094

Nielsen H (1979) Sulfur isotopes. In: Jager E, Hunziker J (eds.) Lectures in isotope geology. Springer, Berlin Heidelberg New York, p. 283–312
Nielsen H, Ricke W (1964) S-Isotopenverhaltnisse von Evaporiten aus Deutschland. Ein Beitrag zur Kenntnis von $\delta^{34}S$ im Meerwasser Sulfat. Geochim Cosmochim Acta 28: 577–591
Nielsen SG, et al. (2005) Thallium isotope composition of the upper continental crust and rivers – an investigation of the continental sources of dissolved marine thallium. Geochim Cosmochim Acta 69: 2007–2019
Nielsen SG, Rehkämper M, Norman MD, Halliday AN, Harrison D (2006) Thallium isotopic evidence for ferromanganese sediments in the mantle source of Hawaiian basalts. Nature 439: 314–317
Nielsen SG, Rehkämper M, Brandon AD, Norman MD, Turner S, O'Reilly SY (2007) Thallium isotopes in Iceland and Azores lavas – Implications for the role of altered crust and mantle geochemistry. Earth Planet Sci Lett 264: 332–345
Nier AO (1950) A redetermination of the relative abundances of the isotopes of carbon, nitrogen, oxygen, argon and potassium. Phys Rev 77: 789
Nier AO, Ney EP, Inghram MG (1947) A null method for the comparison of two ion currents in a mass spectrometer. Rev Sci Instrum 18: 294
Niles PB, Leshin LA, Guan Y (2005) Microscale carbon isotope variability in ALH84001 carbonates and a discussion of possible formation environments. Geochim Cosmochim Acta 69: 2931–2944
Nishio Y, Sasaki S, Gamo T, Hiyagon H, Sano Y (1998) Carbon and helium isotope systematics of North Fiji basin basalt glasses: carbon geochemical cycle in the subduction zone. Earth Planet Sci Lett 154: 127–138
Nishio Y, Nakai S, Yamamoto J, Sumino H, Matsumoto T, Prikhod'ko VS, Arai S (2004) Lithium isotope systematics of the mantle derived ultramafic xenoliths: implications for EM1 origin. Earth Planet Sci Letters 217: 245–261
Nitzsche HM, Stiehl G (1984) Untersuchungen zur Isotopenfraktionierung des Stickstoffs in den Systemen Ammonium/Ammoniak und Nitrid/Stickstoff. ZFI Mitt 84: 283–291
Norris RD, Röhl U (1999) Carbon cycling and chronology of climate warming during the Paleocene/Eocene transition. Nature 401: 775–778
Northrop DA, Clayton RN (1966) Oxygen isotope fractionations in systems containing dolomite. J Geol 74: 174–196
Norton D, Taylor HP (1979) Quantitative simulation of the hydrothermal systems of crystallizing magmas on the basis of transport theory and oxygen isotope data: an analysis of the Skaergaard intrusion. J Petrol 20: 421–486
Nriagu JO, Coker RD, Barrie LA (1991) Origin of sulphur in Canadian Arctic haze from isotope measurements. Nature 349: 142–145
Ohmoto H (1972) Systematics of sulfur and carbon isotopes in hydrothermal ore deposits. Econ Geol 67: 551–578
Ohmoto H (1986) Stable isotope geochemistry of ore deposits. Rev Miner 16: 491–559
Ohmoto H, Goldhaber MB (1997) Sulfur and carbon isotopes. In: Barnes HL (ed.) Geochemistry of hydrothermal ore deposits, 3rd edn. New York, Wiley, p. 435–486
Ohmoto H, Rye RO (1979) Isotopes of sulfur and carbon. In: Geochemistry of hydrothermal ore deposits, 2nd edn. Holt Rinehart and Winston, New York
Ohmoto H, Mizukani M, Drummond SE, Eldridge CS, Pisutha-Arnond V, Lenagh TC (1983) Chemical processes of Kuroko formation. Econ Geol Monogr 5: 570–604
Ohmoto H, Kakegawa T, Lowe DR (1993) 3.4 billion year old biogenic pyrites from Barberton, South Africa: sulfur isotope evidence. Science 262: 555
O'Leary MH (1981) Carbon isotope fractionation in plants. Phytochemistry 20: 553–567
O'Leary JA, Eiler JM, Rossman GR (2005) Hydrogen isotope geochemistry of nominally anhydrous minerals. Geochim Cosmochim Acta 69: A745
O'Neil JR (1986) Theoretical and experimental aspects of isotopic fractionation. In: Stable isotopes in high temperature geological Processes. Rev Miner 16: 1–40

O'Neil JR, Taylor HP (1967) The oxygen isotope and cation exchange chemistry of feldspars. Am Miner 52: 1414–1437

O'Neil JR, Truesdell AH (1991) Oxygen isotope fractionation studies of solute-water interactions. In: Stable Isotope Geochemistry: A tribute to Samuel Epstein. The Geochemical Soc Spec Publ 3: 17–25

O'Neil JR, Roe J, Reinhard E, Blake RE (1994) A rapid and precise method of oxygen isotope analysis of biogenic phosphate. Israel J Earth Sci 43: 203–212

Ongley JS, Basu AR, Kyser TK (1987) Oxygen isotopes in coexisting garnets, clinopyroxenes and phlogopites of Roberts Victor eclogites: implications for petrogenesis and mantle metasomatism. Earth Planet Sci Lett 83: 80–84

Ono S, Wing BA, Johnston D, Farquhar J, Rumble D (2006) Mass-dependent fractionation of quadruple sulphur isotope system as a new tracer of sulphur biogeochemical cycles. Geochim Cosmochim Acta 70: 2238–2252

Ono S, Shanks WC, Rouxel OJ, Rumble D (2007) S-33 constraints on the seawater sulphate contribution in modern seafloor hydrothermal vent sulfides. Geochim Cosmochim Acta 71: 1170–1182

Onuma N, Clayton RN, Mayeda TK (1970) Oxygen isotope fractionation between minerals and an estimate of the temperature of formation. Science 167: 536–538

Ott U (1993) Interstellar grains in meteorites. Nature 364: 25–33

Owen T, Maillard JP, DeBergh C, Lutz BL (1988) Deuterium on Mars: the abundance of HDO and the value of D/H. Science 240: 1767–1770

Owens NJP (1987) Natural variations in ^{15}N in the marine environment. Adv Mar Biol 24: 390–451

Pagani M, Arthur MA, Freeman KH (1999a) Miocene evolution of atmospheric carbon dioxide. Paleoceanography 14: 273–292

Pagani M, Freeman KH, Arthur MA (1999b) Late Miocene atmospheric CO_2concentrations and the expansion of C_4 grasses. Science 285: 876–879

Pagani M, Lemarchand D, Spivack A, Gaillardet J (2005) A critical evaluation of the boron isotope-p_H proxy: the accuracy of ancient ocean p_H estimates. Geochim Cosmochim Acta 69: 953–961

Page FZ, Ushikubo T, Kita NY, Riciputi LR, Valley JW (2007) High precision oxygen isotope analysis of picogram samples reveals 2-μm gradients and slow diffusion in zircon. Am Miner 92: 1772–1775

Palmer MR, Slack JF (1989) Boron isotopic composition of tourmaline from massive sulfide deposits and tourmalinites. Contr Miner Petrol 103: 434–451

Palmer MR, Swihart GH (1996) Boron isotope geochemistry: an overview. Rev Miner 33: 709–744

Palmer MR, Spivack AJ, Edmond JM (1987) Temperature and pH controls over isotopic fractionation during the absorption of boron on marine clays. Geochim Cosmochim Acta 51: 2319–2323

Palmer MR, London D, Morgan GB, Babb HA (1992) Experimental determination of fractionation of $^{11}B/^{10}B$ between tourmaline and aqueous vapor: a temperature- and pressure-dependent isotopic system. Chem Geol 101: 123–129

Palmer MR, Pearson PN, Conbb SJ (1998) Reconstructing past ocean pH-depth profiles. Science 282: 1468–1471

Park R, Epstein S (1960) Carbon isotope fractionation during photosynthesis. Geochim Cosmochim Acta 21: 110–126

Parkinson IJ, Hammond SJ, James RH, Rogers NW (2007) High-temperature lithium isotope fractionation: insights from lithium isotope diffusion in magmatic systems. Earth Planet Sci Lett 257: 609–621

Pawellek F, Veizer J (1994) Carbon cycle in the upper Danube and its tributaries: $\delta^{13}C_{DIC}$ constraints. Israel J Earth Sci 43: 187–194

Paytan A, Kastner M, Campbell D, Thiemens MH (1998) Sulfur isotope composition of Cenozoic seawater sulfate. Science 282: 1459–1462

Paytan A, Luz B, Kolodny Y, Neori A (2002) Biologically mediated oxygen isotope exchange between water and phosphorus. Global Biogeochem Cycles 16–13: 1–7

Paytan A, Kastner M, Campbell D, Thiemens M (2004) Seawater sulfur isotope fluctuations in the Cretaceous. Science 304: 1663–1665

Pearson PN, Palmer MR (1999) Middle Eocene seawater pH and atmospheric carbon dioxide. Science 284: 1824–1826
Pearson PN, Palmer MR (2000) Atmospheric carbon dioxide concentrations over the past 60 million years. Nature 406: 695–699
Pearson NJ, Griffin WL, Alard O, O'Reilly SY (2006) The isotopic composition of magnesium in mantle olivine: records of depletion and metasomatism. Chem Geol 226: 115–133
Peckmann J, Thiel V (2005) Carbon cycling at ancient methane-seeps. Chem Geol 205: 443–467
Pedentchouk N, Freeman KH, Harris NB (2006) Different response of δD-values of n-alkanes, isoprenoids and kerogen during thermal maturation. Geochim Cosmochim Acta 70: 2063–2072
Perry EA, Gieskes JM, Lawrence JR (1976) Mg, Ca and $^{18}O/^{16}O$ exchange in the sediment-pore water system, Hole 149, DSDP. Geochim Cosmochim Acta 40: 413–423
Peters MT, Wickham SM (1995) On the causes of ^{18}O depletion and ^{18}O ^{16}O homogenization during regional metamorphism, the east Humboldt Range core complex, Nevada. Contr Miner Petrol 119: 68–82
Peters KE, Rohrbach BG, Kaplan IR (1981) Carbon and hydrogen stable isotope variations in kerogen during laboratory-simulated thermal maturation. Am Assoc Petrol Geol Bull 65: 501–508
Peterson BJ, Fry B (1987) Stable isotopes in ecosystem studies. Ann Rev Ecol Syst 18: 293–320
Petit JR, et al. (1999) Climate and atmospheric history of the past 420000 years from the Vostok ice core, Antarctica. Nature 399: 429–436
Phillips FM, Bentley HW (1987) Isotopic fractionation during ion filtration: I. Theory. Geochim Cosmochim Acta 51: 683–695
Pichat S, Douchet C, Albarede F (2003) Zinc isotope variations in deep-sea carbonates from the eastern equatorial Pacific over the last 175 ka. Earth Planet Sci Lett 210: 167–178
Pineau F, Javoy M (1983) Carbon isotopes and concentrations in mid-ocean ridge basalts. Earth Planet Sci Lett 62: 239–257
Pineau F, Javoy M, Bottinga Y (1976) $^{13}C/^{12}C$ ratios of rocks and inclusions in popping rocks of the Mid-Atlantic Ridge and their bearing on the problem of isotopic composition of deep-seated carbon. Earth Planet Sci Lett 29: 413–421
Poage MA, Chamberlain CP (2001) Empirical relationships between elevation and the stable isotope composition of precipitation and surface waters: considerations for studies of paleoelevation change. Am J Sci 301: 1–15
Poitrasson F, Freydier R (2005) Heavy iron isotope composition of granites determined by high resolution MC-ICP-MS. Chem Geol 222: 132–147
Poitrasson F, Halliday AN, Lee DC, Levasseur S, Teutsch N (2004) Iron isotope differences between Earth, Moon, Mars and Vesta as possible records of contrasted accretion mechanisms. Earth Planet Sci Lett 223: 253–266
Pokrovsky OS, Viers J, Emnova EE, Kompantseva EI, Freydier R (2008) Copper isotope fractionation during its interaction with soil and aquatic microorganisms and metal oxy(hydr)oxides: possible structural control. Geochim Cosmochim Acta 72: 1742–1757
Polyakov VB (1997) Equilibrium fractionation of the iron isotopes: estimation from Mössbauer spectroscopy data. Geochim Cosmochim Acta 61: 4213–4217
Polyakov VB, Kharlashina NN (1994) Effect of pressure on equilibrium isotope fractionation. Geochim Cosmochim Acta 58: 4739–4750
Polyakov VB, Horita J, Cole DR (2006) Pressure effects on the reduced partition function ratio for hydrogen isotopes in water. Geochim Cosmochim Acta 70: 1904–1913
Polyakov VB, Clayton RN, Horita J, Mineev SD (2007) Equilibrium iron isotope fractionation factors of minerals: reevaluation from the data of nuclear inelastic resonant X-ray scattering and Mossbauer spectroscopy. Geochim Cosmochim Acta 71: 3833–3846
Poorter RPE, Varekamp JC, Poreda RJ, Van Bergen MJ, Kreulen R (1991) Chemical and isotopic compositions of volcanic gases from the east Sunda and Banda arcs, Indonesia. Geochim Cosmochim Acta 55: 3795–3807
Popp BN, Takigiku R, Hayes JM, Louda JW, Baker EW (1989) The post Paleozoic chronology and mechanism of ^{13}C depletion in primary organic matter. Am J Sci 289: 436–454

Popp BN, Laws EA, Bidigare RR, Dore JE, Hanson KL, Wakeham SG (1998) Effect of phytoplankton cell geometry on carbon isotope fractionation. Geochim Cosmochim Acta 62: 69–77
Poreda R (1985) Helium-3 and deuterium in back arc basalts: Lau Basin and the Mariana trough. Earth Planet Sci Lett 73: 244–254
Poreda R, Schilling JG, Craig H (1986) Helium and hydrogen isotopes in ocean-ridge basalts north and south of Iceland. Earth Planet Sci Lett 78: 1–17
Poulson RL, Siebert C, McManus J, Berelson WM (2006) Authigenic molybdenum isotope signatures in marine sediments. Geology 34: 617–620
Price FT, Shieh YN (1979) The distribution and isotopic composition of sulfur in coals from the Illinois Basin. Econ Geol 74: 1445–1461
Prokoph A, Shields GA, Veizer J (2008) Compilation and time-series analysis of a marine carbonate $\delta^{18}O$, $\delta^{13}C$, $^{87}Sr/^{86}Sr$ and $\delta^{34}S$ database through Earth history. Earth Sci Rev 87: 113–133
Prombo CA, Clayton RN (1985) A striking nitrogen isotope anomaly in the Bencubbin and Weatherford meteorites. Science 230: 935–937
Puchelt H, Sabels BR, Hoering TC (1971) Preparation of sulfur hexafluoride for isotope geochemical analysis. Geochim Cosmochim Acta 35: 625–628
Quade J, Cerling TE (1995) Expansion of C4 grasses in the late Miocene of northern Pakistan: evidence from stable isotopes in paleosols. Palaeogeogr Palaeoclimatol Palaeoecol 115: 91–116
Quade J, et al. (1992) A 16-Ma record of paleodiet using carbon and oxygen isotopes in fossil teeth from Pakistan. Chem Geol 94: 183–192
Quast A, Hoefs J, Paul J (2006) Pedogenic carbonates as a proxy for palaeo-CO_2 in the Paleozoic atmosphere. Palaeogeogr Palaeoclimatol Palaeoecol 242: 110–125
Quay PD, Tilbrook B, Wong CS (1992) Oceanic uptake of fossil fuel CO_2: carbon-13 evidence. Science 256: 74–79
Quay PD, Emerson S, Wilbur DO, Stump S (1993) The $\delta^{18}O$ of dissolved O_2 in the surface waters of the subarctic Pacific: a tracer of biological productivity. J Geophys Res 98: 8447–8458
Quay PD, Wilbur DO, Richey JE, Devol AH, Benner R, Forsberg BR (1995) The $^{18}O/^{16}O$ of dissolved oxygen in rivers and lakes in the Amazon Basin: determining the ratio of respiration to photosynthesis in freshwaters. Limnol Oceanogr 40: 718–729
Quay PD, Stutsman J, Wibur D, Snover A, Dlugokencky E, Brown T (1999) The isotopic composition of atmospheric methane. Global Geochemical Cycles 13: 445–461
Raab M, Spiro B (1991) Sulfur isotopic variations during seawater evaporation with fractional crystallization. Chem Geol 86: 323–333
Rabinovich AL, Grinenko VA (1979) Sulfate sulfur isotope ratios for USSR river water. Geochemistry 16: No 2: 68–79
Radke J, Bechtel A, Gaupp R, Püttmann W, Schwark L, Sachse D, Gleixner D (2005) Correlation between hydrogen isotope ratios of lipid biomarkers and sediment maturity. Geochim Cosmochim Acta 69: 5517–5530
Rafter TA (1957) Sulphur isotopic variations in nature, P 1: the preparation of sulphur dioxide for mass spectrometer examination. N Z J Sci Tech B38: 849
Rahn T, Wahlen M (1997) Stable isotope enrichment in stratospheric nitrous oxide. Science 278: 1776–1778
Rahn T, Kitchen N, Eiler J (2002a) D/H ratios of atmospheric H_2 in urban air: results using new methods for analysis of nano-molar H_2 samples. Geochim Cosmochim Acta 66: 2475–2481
Rahn T, et al. (2002b) The deuterium anomaly in stratospheric molecular hydrogen. Geochim Cosmochim Acta 66(spec. suppl): A622
Railsback LB, Anderson TF, Ackerly SC, Cisne JL (1989) Paleoceanic modeling of temperature-salinity profiles from stable isotope data. Paleoceanography 4: 585–591
Raiswell R, Berner RA (1985) Pyrite formation in euxinic and semi-euxinic sediments. Am J Sci 285: 710–724
Rakestraw NM, Rudd DP, Dole M (1951) Isotopic composition of oxygen in air dissolved in Pacific Ocean water as a function of depth. J Am Chem Soc 73: 2976

Ransom B, Spivack AJ, Kastner M (1995) Stable Cl isotopes in subduction-zone pore waters: implications for fluid-rock reactions and the cycling of chlorine. Geology 23: 715–718
Rau GH, Sweeney RE, Kaplan IR (1982) Plankton $^{13}C/^{12}C$ ratio changes with latitude: differences between northern and southern oceans. Deep Sea Res 29: 1035–1039
Rau GH, Takahashi T, DesMarais DJ (1989) Latitudinal variations in plankton ^{13}C: implications for CO_2 and productivity in past ocean. Nature 341: 516–518
Rau GH, Takahashi T, DesMarais DJ, Repeta DJ, Martin JH (1992) The relationship between $\delta^{13}C$ of organic matter and $\Sigma CO_{2(aq)}$ in ocean surface water: data from a JGOFS site in the northeast Atlantic Ocean and a model. Geochim Cosmochim Acta 56: 1413–1419
Rayleigh JWS (1896) Theoretical considerations respecting the separation of gases by diffusion and similar processes. Philos Mag 42: 493
Redding CE, Schoell M, Monin JC, Durand B (1980) Hydrogen and carbon isotopic composition of coals and kerogen. In: Douglas AG, Maxwell JR (eds.) Phys Chem Earth 12: 711–723
Rees CE (1978) Sulphur isotope measurements using $SO_2$and SF_6. Geochim Cosmochim Acta 42: 383–389
Rees CE, Jenkins WJ, Monster J (1978) The sulphur isotopic composition of ocean water sulphate. Geochim Cosmochim Acta 42: 377–381
Rehkämper M, Halliday A (1999) The precise measurement of Tl isotopic compositions by MC-ICPMS: application to the analysis of geological materials and meteorites. Geochim Cosmochim Acta 63: 935–944
Rehkämper M, Frank M, Hein JR, Porcelli D, Halliday A, Ingri J, Libetrau V (2002) Thallium isotope variations in seawater and hydrogenetic, diagenetic and hydrothermal ferromanganese deposits. Earth Planet Sci Lett 197: 65–81
Rehkämper M, Frank M, Hein JR, Halliday A (2004) Cenozoic marine geochemistry of thallium deduced from isotopic studies of feromanganese crusts and pelagic sediments. Earth Planet Sci Letters 219: 77–91
Reynolds BC, Frank M, Halliday AN (2006) Silicon isotope fractionation during nutrient utilization in the North Pacific. Earth Planetary Sci Letters 244: 431–443
Rice DD, Claypool GE (1981) Generation, accumulation and resource potential of biogenic gas. Am Assoc Petrol Geol Bull 65: 5–25
Richet P, Bottinga Y, Javoy M (1977) A review of H, C, N, O, S, and Cl stable isotope fractionation among gaseous molecules. Ann Rev Earth Planet Sci 5: 65–110
Richter FM (2007) Isotopic fingerprints of mass transport processes. Geochim Cosmochim Acta 71: A839
Richter R, Hoernes S (1988) The application of the increment method in comparison with experimentally derived and calculated O-isotope fractionations. Chemie der Erde 48: 1–18
Richter FM, Liang Y, Davis AM (1999) Isotope fractionation by diffusion in molten oxides. Geochim Cosmochim Acta 63: 2853–2861
Richter FM, Davis AM, DePaolo D, Watson BE (2003) Isotope fractionation by chemical diffusion between molten basalt and rhyolite. Geochim Cosmochim Acta 67: 3905–3923
Riciputi LR, Cole DR, Machel HG (1996) Sulfide formation in reservoir carbonates of the Devonian Nishu Formation, Alberta, Canada: an ion microprobe study. Geochim Cosmochim Acta 60: 325–336
Rietmeijer FJM (1998) Interplanetary dust particles. In: Planetary materials. Rev Miner 36: Chapter 2
Rindsberger MS, Jaffe S, Rahamin S, Gat JR (1990) Patterns of the isotopic composition of precipitation in time and space; data from the Israeli storm water collection program. Tellus 42: 263–271
Ripley EM, Li C (2003) Sulfur isotope exchange and metal enrichment in the formation of magmatic Cu-Ni-(PGE)-deposits. Econ Geol 98: 635–641
Robert F (2001) The origin of water on Earth. Science 293: 1056–1058
Robert F, Chaussidon M (2006) A paleotemperature curve for the Precambrian oceans based on silicon isotopes in cherts. Nature 443: 969–972

Robert F, Epstein S (1982) The concentration and isotopic composition of hydrogen, carbon and nitrogen carbonaceous meteorites. Geochim Cosmochim Acta 46: 81–95
Robert F, Merlivat L, Javoy M (1978) Water and deuterium content in ordinary chondrites. Meteoritics 12: 349–354
Robert F, Gautier D, Dubrulle B (2000) The solar system D/H ratio: observations and theories. Space Sci Rev 92: 201–224
Robinson BW, Kusakabe M (1975) Quantitative preparation of sulphur dioxide for $^{34}S/^{32}S$ analyses from sulphides by combustion with cuprous oxide. Anal Chem 47: 1179
Röckmann T, et al. (1998) Mass independent oxygen isotope fractionation in atmospheric CO as a result of the reaction CO + OH. Science 281: 544–546
Röhl U, Bralower TJ, Norris RD, Wefer G (2000) New chronology for the late Paleocene thermal maximum and its environmental implications. Geology 28: 927–930
Romanek CS, Grossman EL, Morse JW (1992) Carbon isotope fractionation in synthetic aragonite and calcite: effects of temperature and precipitation rate. Geochim Cosmochim Acta 56: 419–430
Romanek CS, et al. (1994) Record of fluid-rock interaction on Mars from the meteorite ALH 84001. Nature 372:655–657
Rooney MA, Claypool GE, Chung HM (1995) Modeling thermogenic gas generation using carbon isotope ratios of natural gas hydrocarbons. Chem Geol 126: 219–232
Rose EF, Chaussidon M, France-Lanord C (2000) Fractionation of boron isotopes during erosion processes: the example of Himalayan rivers. Geochim Cosmochim Acta 64: 397–408
Rosenbaum J, Sheppard SMF (1986) An isotopic study of siderites, dolomites and ankerites at high temperatures. Geochim Cosmochim Acta 50: 1147–1150
Rosman JR, Taylor PD (1998) Isotopic compositions of the elements (technical report): commission on atomic weights and isotopic abundances. Pure Appl Chem 70: 217–235
Rouxel O, Ludden J, Carignan J, Marin L, Fouquet Y (2002) Natural variations in Se isotopic composition detemined by hydride generation multiple collector inductively coupled plasma mass spectrometry. Geochim Cosmochim Acta 66: 3191–3199
Rouxel O, Fouquet Y, Ludden JN (2004) Copper isotope systematics of the Lucky Strike, Rainbow and Logatschev seafloor hydrothermal fields on the Mi-Atlantic Ridge. Econ Geol 99: 585–600
Rouxel O, Bekker A, Edwards KJ (2005) Iron isotope constraints on the Archean and Proterozoic ocean redox state. Science 307: 1088–1091
Rouxel O, Galy A, Elderfield H (2006) Germanium isotope variations in igneous rocks and marine sediments. Geochim Cosmochim Acta 70: 3387–3400
Rouxel O, Ono S, Alt J, Rumble D, Ludden J (2008) Sulfur isotope evidence for microbial sulfate reduction in altered oceanic basalts at ODP Site 801. Earth Planet Sci Lett 268: 110–123
Rozanski K, Sonntag C (1982) Vertical distribution of deuterium in atmospheric water vapour. Tellus 34: 135–141
Rozanski K, Araguas-Araguas L, Gonfiantini R (1993) Isotopic patterns in modern global precipitation. In: Climate change in continental isotopic records. Geophys Monogr 78: 1–36
Rubinson M, Clayton RN (1969) Carbon-13 fractionation between aragonite and calcite. Geochim Cosmochim Acta 33: 997–1002
Rudnick RL, Ionov DA (2007) Lithium elemental and isotopic disequilibrium in minerals from peridotite xenoliths from far-east Russia: product of recent melt/fluid-rock interaction. Earth Planet Sci Lett 256: 278–293
Rudnick RL, Tomascak PB, Njo HB, Gardner LR (2004) Extreme lithium isotopic fractionation during continental weathering revealed in saprolites from South Carolina. Chem Geol 212: 45–57
Rudnicki MD, Elderfield H, Spiro B (2001) Fractionation of sulfur isotopes during bacterial sulfate reduction in deep ocean sediments at elevated temperatures. Geochim Cosmochim Acta 65: 777–789
Ruiz J, Mathur R, Young S, Brantley S (2002) Controls of copper isotope fractionation. Geochim Cosmochim Acta Spec Suppl 66: A654

Rumble D, Yui TF (1998) The Qinglongshan oxygen and hydrogen isotope anomaly near Donghai in Jiangsu Province, China. Geochim Cosmochim Acta 62: 3307–3321

Russell WA, Papanastassiou DA, Tombrello TA (1978) Ca isotope fractionation on the Earth and other solar system materials. Geochim Cosmochim Acta 42: 1075–1090

Rye RO (1974) A comparison of sphalerite-galena sulfur isotope temperatures with filling-temperatures of fluid inclusions. Econ Geol 69: 26–32

Rye RO (1993) The evolution of magmatic fluids in the epithermal environment: the stable isotope perspective. Econ Geol 88: 733–753

Rye RO (2005) A review of stable isotope geochemistry of sulfate minerals in selected igneous environments and related hydrothermal systems. Chem Geol 215: 5–36

Rye RO, Schuiling RD, Rye DM, Jansen JBH (1976) Carbon, hydrogen and oxygen isotope studies of the regional metamorphic complex at Naxos, Greece. Geochim Cosmochim Acta 40: 1031–1049

Rye RO, Bethke PM, Wasserman MD (1992) The stable isotope geochemistry of acid sulfate. Econ Geol 87: 227–262

Sackett WM (1978) Carbon and hydrogen isotope effects during the thermocatalytic production of hydrocarbons in laboratory simulation experiments. Geochim Cosmochim Acta 42: 571–580

Sackett WM, Thompson RR (1963) Isotopic organic carbon composition of recent continental derived clastic sediments of Eastern Gulf Coast, Gulf of Mexico. Bull Am Ass Petrol Geol 47: 525

Sackett WM, Eadie BJ, Exner ME (1973) Stable isotope composition of organic carbon in recent Antarctic sediments. Adv Org Geochem 1973: 661

Sadofsky SJ, Bebout GE (2000) Ammonium partitioning and nitrogen isotope fractionation among coexisting micas during high-temperature fluid-rock interaction. Examples from the New England Appalachians. Geochim Cosmochim Acta 64: 2835–2849

Saino T, Hattori A (1980) ^{15}N natural abundance in oceanic suspended particulate organic matter. Nature 283: 752–754

Saino T, Hattori A (1987) Geophysical variation of the water column distribution of suspended particulate organic nitrogen and its ^{15}N natural abundance in the Pacific and its marginal seas. Deep Sea Res 34: 807–827

Sakai H (1968) Isotopic properties of sulfur compounds in hydrothermal processes. Geochem J 2: 29–49

Sakai H, Casadevall TJ, Moore JG (1982) Chemistry and isotope ratios of sulfur in basalts and volcanic gases at Kilauea volcano, Hawaii. Geochim Cosmochim Acta 46: 729–738

Sakai H, DesMarais DJ, Ueda A, Moore JG (1984) Concentrations and isotope ratios of carbon, nitrogen and sulfur in ocean-floor basalts. Geochim Cosmochim Acta 48: 2433–2441

Sano Y, Marty B (1995) Origin of carbon in fumarolic gas from island arcs. Chem Geol 119: 265–274

Sanyal A, Nugent M, Reeder RJ, Bijma J (2000) Seawater pH control on the boron isotopic composition of calcite: evidence from inorganic calcite precipitation experiments. Geochim Cosmochim Acta 64: 1551–1555

Sarntheim M, et al. (2001) Fundamental modes and abrupt changes in North Atlantic circulation and climate over the last 60 ky - concepts, reconstruction and numerical modeling. In: P Schäfer, W Ritzau, M Schlüter, J Thiede (eds.) The northern North Atlantic. Springer Verlag, Heidelberg, p.365–410

Sasaki A, Arikawa Y, Folinsbee RE (1979) Kiba reagent method of sulfur extraction applied to isotopic work. Bull Geol Surv Jpn 30: 241

Sass E, Kolodny Y (1972) Stable isotopes, chemistry and petrology of carbonate concretions (Mishash formation, Israel). Chem Geol 10: 261–286

Sauer PE, Eglinton TI, Hayes JM, Schimmelmann A, Sessions AL (2001) Compound-specific D/H ratios of lipid biomarkers from sediments as a proxy for environmental and climatic conditions. Geochim Cosmochim Acta 65: 213–222

Savarino J, Lee CCW, Thiemens MH (2000) Laboratory oxygen isotope study of sulfur IV oxidation: origin of the mass-independent oxygen isotope anomaly in atmospheric sulfates and sulfate mineral deposits on Earth. J Geophys Res (Atm) 105: 29079–29088

Savin SM, Epstein S (1970a) The oxygen and hydrogen isotope geochemistry of clay minerals. Geochim Cosmochim Acta 34: 25–42

Savin SM, Epstein S (1970b) The oxygen and hydrogen isotope geochemistry of ocean sediments and shales. Geochim Cosmochim Acta 34: 43–63

Savin SM, Lee M (1988) Isotopic studies of phyllosilicates. Rev Miner 19: 189–223

Schauble EA (2004) Applying stable isotope fractionation theory to new systems. Rev Miner Geochem 55: 65–111

Schauble EA (2007) Role of nuclear volume in driving equilibrium stable isotope fractionation of mercury, thallium and other very heavy elements. Geochim Cosmochim Acta 71: 2170–2189

Schauble EA, Rossman GR, Taylor HP (2001) Theoretical estimates of equilibrium Fe isotope fractionations from vibrational spectroscopy. Geochim Cosmochim Acta 65: 2487–2498

Schauble EA, Rossman GR, Taylor HP (2002) Theoretical estimates of equilibrium chromium isotope fractionations. Geochim Cosmochim Acta 66 Spec Suppl A675

Schauble ES, Rossman GR, Taylor HP (2003) Theoretical estimates of equilibrium chlorine-isotope fractionations. Geochim Cosmochim Acta 67: 3267–3281

Schauble EA, Ghosh P, Eiler JM (2006) Preferential formation of ^{13}C-^{18}O bonds in carbonate minerals, estimated using first-principles lattice dynamics. Geochim Cosmochim Acta 70: 2510–2519

Scheele N, Hoefs J (1992) Carbon isotope fractionation between calcite, graphite and CO_2. Contr Miner Petrol 112: 35–45

Schiegl WE, Vogel JV (1970) Deuterium content of organic matter. Earth Planet Sci Lett 7: 307–313

Schimmelmann A, Lewan MD, Wintsch RP (1999) D/H ratios of kerogen, bitumen, oil and water in hydrous pyrolysis of source rocks containing kerogen types I, II, IIS and III. Geochim Cosmochim Acta 63: 3751–3766

Schimmelmann A, Sessions AL, Mastalerz M (2006) Hydrogen isotopic (D/H) composition of organic matter during diagenesis and thermal maturation. Ann.Rev Earth Planet Sci 34: 501–533

Schmidt M, Botz R, Stoffers P, Anders T, Bohrmann G (1997) Oxygen isotopes in marine diatoms: a comparative study of analytical techniques and new results on the isotope composition of recent marine diatoms. Geochim Cosmochim Acta 61: 2275–2280

Schmidt M, Botz R, Rickert D, Bohrmann G, Hall SR, Mann S (2001) Oxygen isotopes of marine diatoms and relations to opal-A maturation. Geochim Cosmochim Acta 65: 201–211

Schmitt AD, Stille P, Vennemann T (2003) Variations of the $^{44}Ca/^{40}Ca$ ratio in seawater during the past 24 million years: evidence from $\delta^{44}Ca$ and $\delta^{18}O$ values of Miocene phosphates. Geochim Cosmochim Acta 67: 2607–2614

Schoell M (1980) The hydrogen and carbon isotopic composition of methane from natural gases of various origins. Geochim Cosmochim Acta 44: 649–661

Schoell M (1983) Genetic characterization of natural gases. Bull Am Ass Petrol Geol 67: 2225–2238

Schoell M (1984) Recent advances in petroleum isotope geochemistry. Org Geochem 6: 645–663

Schoell M (1988) Multiple origins of methane in the Earth. Chem Geol 71: 1–10

Schoell M, McCaffrey MA, Fago FJ, Moldovan JM (1992) Carbon isotope compositions of 28,30-bisnorhopanes and other biological markers in a Monterey crude oil. Geochim Cosmochim Acta 56: 1391–1399

Schoenberg R, Zink S, Staubwasser M, von Blanckenburg F (2008) The stable Cr isotope inventory of solid Earth reservoirs determined by double-spike MC-ICP-MS. Chem Geol 249: 294–306

Schoenheimer R, Rittenberg D (1939) Studies in protein metabolism: I. General considerations in the application of isotopes to the study of protein metabolism. The normal abundance of nitrogen isotopes in amino acids. J Biol Chem 127: 285–290

Schoeninger MJ, DeNiro MJ (1984) Nitrogen and carbon isotopic composition of bone collagen from marine and terrestrial animals. Geochim Cosmochim Acta 48: 625–639
Scholten SO (1991) The distribution of nitrogen isotopes in sediments. PhD Thesis University of Utrecht
Schrag DP (1999) Effects of diagenesis on the isotopic record of late Paleogene tropical sea surface temperature. Chem Geol 161: 2265–2278
Schrag DP, Hampt G, Murry DW (1996) Pore fluid constraints on the temperature and oxygen isotopic composition of the Glacial ocean. Science 272: 1930–1932
Schrag DP, Adkins JF, McIntyre K et al (2002) The oxygen isotope composition of sea water during the Glacial ocean. Quat Sci Rev 21: 331–342
Schüßler JA, Schoenberg R, Behrens H, von Blanckenburg F (2007) The experimental calibration of iron isotope fractionation factor between pyrrhotite and peralkaline rhyolitic melt. Geochim Cosmochim Acta 71: 417–433
Schüßler JA, Schoenberg R, Sigmarsson O (2008) Iron and lithium isotope systematics of the Hekla volcano, Iceland: evidence for stable Fe isotope fractionation during magma differentiation. Chem Geol (in press)
Schütze H (1980) Der Isotopenindex - eine Inkrementmethode zur näherungsweisen Berechnung von Isotopenaustauschgleichgewichten zwischen kristallinen Substanzen. Chemie Erde 39: 321–334
Schwalb A, Burns SJ, Kelts K (1999) Holocene environments from stable isotope stratigraphy of ostracods and authigenic carbonate in Chilean Altiplano lakes. Palaeogeogr Palaeoclimatol Palaeoecol 148: 153–168
Schwarcz HP, Melbye J, Katzenberg MA, Knyf M (1985) Stable isotopes in human skeletons of southern Ontario: reconstruction of palaeodiet. J Archaeol Sci 12: 187–206
Seal RR (2006) Sulfur isotope geochemistry of sulfide minerals. Rev Miner Geochem 61: 633–677
Seal RR, Alpers CN, Rye RO (2000) Stable isotope systematics of sulfate minerals. Rev Miner 40: 541–602
Seccombe PK, Spry PG, Both RA, Jones MT, Schiller JC (1985) Base metal mineralization in the Kaumantoo Group, South Australia: a regional sulfur isotope study. Econ Geol 80: 1824–1841
Seitz HM, Brey GP, Lahaye Y, Durali S, Weyer S (2004) Lithium isotope signatures of peridotite xenoliths and isotope fractionation at high temperature between olivine and pyroxene. Chem Geol 212: 163–177
Seitz HM, Brey GP, Zipfel J, Ott U, Weyer S, Durali S, Weinbruch S (2007) Lithium isotope composition of ordinary and carbonaceous chondrites and differentiated planetary bodies: bulk solar system and solar reservoirs. Earth Planet Sci Lett 260: 582–596
Sessions AL, Burgoyne TW, Schimmelmann A, Hayes JM (1999) Fractionation of hydrogen isotopes in lipid biosynthesis. Org Geochem 30: 1193–1200
Sessions AL, Sylva SP, Summons RE, Hayes JM (2004) Isotopic exchange of carbon-bound hydrogen over geologic time scales. Geochim Cosmochim Acta 68: 1545–1559
Severinghaus JP, Brook EJ (1999) Abrupt climate change at the end of the last glacial period inferred from trapped air in polar ice. Science 286: 930–934
Severinghaus JP, Bender ML, Keeling RF, Broecker WS (1996) Fractionation of soil gases by diffusion of water vapor, gravitational settling and thermal diffusion. Geochim Cosmochim Acta 60: 1005–1018
Severinghaus JP, Sowers T, Brook EJ, Alley RB, Bender ML (1998) Timing of abrupt climate change at the end of the Younger Dryas interval from thermally fractionated gases in polar ice. Nature 391: 141–146
Severmann S, Johnson CM, Beard BL, German CR, Edmonds HN, Chiba H, Green DRH (2004) The effect of plume processes on the Fe isotope composition of hydrothermally derived Fe in the deep ocean as inferred from the Rainbow vent site, Mid-Atlantic Ridge, 36°!4 N. Earth Planet Sci Lett 225: 63–76
Severmann S, Johnson CM, Beard BL, McManus J (2006) The effect of early diagenesis on the Fe isotope composition of porewaters and authigenic minerals in continental margin sediments. Geochim Cosmochim Acta 70: 2006–2022

Shackleton NJ, Kennett JP (1975) Paleotemperature history of the Cenozoic and initiation of Antarctic glaciation: oxygen and carbon isotope analyses in DSDP sites 277, 279 and 281. Initial Rep DSDP 29: 743–755

Shackleton NJ, Hall MA, Line J, Cang S (1983) Carbon isotope data in core V19–30 confirm reduced carbon dioxide concentration in the ice age atmosphere. Nature 306: 319–322

Shahar A, Young ED, Manning CE (2008) Equilibrium high-temperature Fe isotope fractionation between fayalite and magnetite: an experimental calibration. Earth Planet Sci Lett 268: 330–338

Shanks WC (2001) Stable isotopes in seafloor hydrothermal systems: vent fluids, hydrothermal deposits, hydrothermal alteration, and microbial processes. Rev Miner Geochem 43: 469–525

Sharma T, Clayton RN (1965) Measurement of 18O/16O ratios of total oxygen of carbonates. Geochim Cosmochim Acta 29: 1347–1353

Sharp ZD (1990) A laser-based microanalytical method for the in situ determination of oxygen isotope ratios of silicates and oxides. Geochim Cosmochim Acta 54: 1353–1357

Sharp ZD (1995) Oxygen isotope geochemistry of the Al_2SiO_5 polymorphs. Am J Sci 295: 1058–1076

Sharp Z (2006) Stable chlorine isotope fractionation. EOS Trans AGU 87(52), Fall Meet Suppl V14C–03

Sharp ZD, Barnes JD, Brearley AJ, Chaussidon M, Fischer TP, Kamenetsky VS (2007) Chlorine isotope homogeneity of the mantle, crust and carbonaceous chondrites. Nature 446: 1062–1065

Shaw AM, Hilton DR, Fischer TP, Walker JA, Alvarado GE (2003) Contrasting He-C relationshipsin Nicaragua and Costa Rica: insights into C cycling through subduction zones. Earth Planet Sci Lett 214: 499–513

Shelton KL, Rye DM (1982) Sulfur isotopic compositions of ores from Mines Gaspe, Quebec: an example of sulfate-sulfide isotopic disequilibria in ore forming fluids with applications to other porphyry type deposits. Econ Geol 77: 1688–1709

Shemesh A, Kolodny Y, Luz B (1983) Oxygen isotope variations in phosphate of biogenic apatites, II. Phosphorite rocks. Earth Planet Sci Lett 64: 405–441

Shemesh A, Charles CD, Fairbanks RG (1992): Oxygen isotopes in biogenic silica: global changes in ocean temperature and isotopic composition. Science 256: 1434–1436.

Shen Y, Buick R (2004) The antiquity of microbial sulfate reduction. Earth Sci Rev 64: 243–272

Sheppard SMF (1986) Characterization and isotopic variations in natural waters. In: stable isotopes in high temperature geological processes. Rev Miner 16: 165–183

Sheppard SMF, Epstein S (1970) D/H and O^{18}/O^{16}ratios of minerals of possible mantle or lower crustal origin. Earth Planet Sci Lett 9: 232–239

Sheppard SMF, Gilg HA (1996) Stable isotope geochemistry of clay minerals. Clay Miner 31: 1–24

Sheppard SMF, Harris C (1985) Hydrogen and oxygen isotope geochemistry of Ascension Island lavas and granites: variation with crystal fractionation and interaction with sea water. Contrib Miner Petrol 91: 74–81

Sheppard SMF, Schwarcz HP (1970) Fractionation of carbon and oxygen isotopes and magnesium between coexisting metamorphic calcite and dolomite. Contr Miner Petrol 26: 161–198

Sheppard SMF, Nielsen RL, Taylor HP (1971) Hydrogen and oxygen isotope ratios in minerals from Porphyry Copper Deposits. Econ Geol 66: 515–542

Sherwood Lollar B, Frape SK, Weise SM, Fritz P, Macko SA, Welhan JA (1993) Abiogenic methanogenesis in crystalline rocks. Geochim Cosmochim Acta 57: 5087–5097

Sherwood Lollar B, Westgate TD, Ward JA, Slater GF, Lacrampe-Couloume G (2002) Abiogenic formation of alkanes in the Earth,s crust as a minor source for global hydrocarbons reservoirs. Nature 416: 522–524

Sherwood Lollar B, et al. (2006) Unravelling abiogenic and biogenic sources of methane in the earth,s deep subsurface. Chem Geol 226: 328–339

Shieh YN, Schwarcz HP (1974) Oxygen isotope studies of granite and migmatite, Grenville province of Ontario, Canada. Geochim Cosmochim Acta 38: 21–45

Shields G, Veizer J (2002) Precambrian marine carbonate isotope database: version 1.1. Geochem Geophys Geosyst 300: doi: 10.1029/2001GC000266
Shields WR, Goldich SS, Garner EI, Murphy TJ (1965) Natural variations in the abundance ratio and the atomic weight of copper. J Geophys Res 70: 479–491
Shmulovich KI, Landwehr D, Simon K, Heinrich W (1999) Stable isotope fractionation between liquid and vapour in water-salt systems up to 600°C. Chem Geol 157: 343–354
Siebert C, Nägler TF, von Blanckenburg F, Kramers JD (2003) Molybdenum isotope records as potential proxy for paleoceanography. Earth Planet Sci Lett 211: 159–171
Siebert C, Kramers JD, Meisel T, Morel P, Nägler TF (2005) PGE, Re-Os and Mo isotope systematics in Archean and early Proterozoic sedimentary systems as proxies for redox conditions of the early Earth. Geochim Cosmochim Acta 69: 1787–1801
Siebert C, Ross A, McManus J (2006a) Germanium isotope measurements of high-temperature geothermal fluids using double-spike hydride generation MC-ICP-MS. Geochim Cosmochim Acta 70: 3986–3995
Siebert C, McManus J, Bice A, Poulson R, Berelson WM (2006b) Molybdenum isotope signatures in continental margin sediments. Earth Planet Sci Lett 241: 723–733
Sime NG, De la Rocha C, Galy A (2005) Negligible temperature dependence of calcium isotope fractionation in 12 species of planktonic foraminifera. Earth Planet Sci Lett 232: 51–66
Simon K (2001) Does δD from fluid inclusions in quartz reflect the original hydrothermal fluid? Chem Geol 177: 483–495
Skauli H, Boyce AJ, Fallick AE (1992) A sulphur isotope study of the Bleikvassli Zn-Pb-Cu deposit, Nordland, northern Norway. Miner Deposita 27: 284–292
Skirrow R, Coleman ML (1982) Origin of sulfur and geothermometry of hydrothermal sulfides from the Galapagos Rift, 86°W. Nature 249: 142–144
Skulan JL, DePaolo DJ, Owens TL (1997) Biological control of calcium isotopic abundances in the global calcium cycle. Geochim Cosmochim Acta 61: 2505–2510
Slack JF, Palmer MR, Stevens BPJ, Barnes RG (1993) Origin and significance of tourmaline-rich rocks in the Broken Hill district, Australia. Econ Geol 88: 505–541
Smith JW, Batts BD (1974) The distribution and isotopic composition of sulfur in coal. Geochim Cosmochim Acta 38: 121–123
Smith MP, Yardley BWD (1996) The boron isotopic composition of tourmaline as a guide to fluid processes in the southwestern England orefield: an ion microprobe study. Geochim Cosmochim Acta 60: 1415–1427
Smith JW, Gould KW, Rigby D (1982) The stable isotope geochemistry of Australian coals. Org Geochem 3: 111–131
Smith CN, Kesler SE, Klaue B, Blum J (2005) Mercury isotope fractionation in fossil hydrothermal systems. Geology 33: 825–828
Smith CN, Kesler SE, Blum JD, Rytuba JR (2008) Isotope geochemistry of mercury in source rocks, mineral deposits and spring deposits of the California Coast Ranges, USA. Earth Planet Sci Lett 269: 398–406
Snyder G, Poreda R, Hunt A, Fehn U (2001) Regional variations in volatile composition: isotopic evidence for carbonate recycling in the Central American volcanic arc. Geochem Geophys Geosystems 2: U1-U32
Sofer Z (1984) Stable carbon isotope compositions of crude oils: application to source depositional environments and petroleum alteration. Am Assoc Petrol Geol Bull 68: 31–49
Sofer Z, Gat JR (1972) Activities and concentrations of oxygen-18 in concentrated aqueous salt solutions: analytical and geophysical implications. Earth Planet Sci Lett 15: 232–238
Sonnerup RE, Quay PD, McNichol AP, Bullister JL, Westby TA, Anderson HL (1999) Reconstructing the oceanic ^{13}C Suess effect. Global Biogeochem Cycles 13: 857–872
Sowers T (2001) The N_2O record spanning the penultimate deglaciation from the Vostok ice core. J Geophy Res 106: 31903–31914
Sowers T, Bender M, Raynaud D, Korotkevich YS, Orchardo J (1991) The $\delta^{18}O$ of atmospheric O_2 from air inclusions in the Vostok ice core: timing of CO_2 and ice volume changes during the Penultimate deglaciation. Paleoceanography 6: 679–696

Sowers T, Bender M, Raynaud D, Korotkevich YS (1992) $\delta^{15}N$ of N_2 in air trapped in polar ice: a tracer of gas transport in the firn and a possible constraint on ice age-gas age differences. J Geophys Res 97: 15683–15697

Sowers T, et al. (1993) A 135000 year Vostock-SPECMAP common temporal framework. Paleoceanography 8: 737–766

Spero HJ, Bijma J, Lea DW, Bemis BE (1997) Effect of seawater carbonate concentration on foraminiferal carbon and oxygen isotopes. Nature 390: 497–500

Spivack AJ, Edmond JM (1986) Determination of boron isotope ratios by thermal ionization mass spectrometry of the dicesium metaborate cation. Anal Chem 58: 31–35

Spivack AJ, Edmond JM (1987) Boron isotope exchange between seawater and the oceanic crust. Geochim Cosmochim Acta 51: 1033–1043

Spivack AJ, Kastner M, Ransom B (2002) Elemental and isotopic chloride geochemistry in the Nankai trough. Geophysical Res Lett 29: 1661, doi:10.1029/2001GL014122

Stahl W (1977) Carbon and nitrogen isotopes in hydrocarbon research and exploration. Chem Geol 20: 121–149

Stein LY, Yung YL (2003) Production, isotopic composition, and atmospheric fate of biologically produced nitrous oxide. Ann Rev Earth Planet Sci 31: 329–356

Stern LA, Chamberlain CP, Reynolds RC, Johnson GD (1997) Oxygen isotope evidence of climate change from pedogenic clay minerals in the Himalayan molasse. Geochim Cosmochim Acta 61: 731–744

Stern MJ, Spindel W, Monse EU (1968) Temperature dependence of isotope effects. J Chem Phys 48: 2908

Steuber T, Buhl D (2006) Calcium-isotope fractionation in selected modern and ancient marine carbonates. Geochim Cosmochim Acta 70: 5507–5521

Stevens CM (1988) Atmospheric methane. Chem Geol 71: 11–21

Stevens CM, Krout L, Walling D, Venters A, Engelkemeier A, Ross LE (1972) The isotopic composition of atmospheric carbon monoxide. Earth Planet Sci Lett 16: 147–165

Stewart MK (1974) Hydrogen and oxygen isotope fractionation during crystallization of mirabilite and ice. Geochim Cosmochim Acta 38: 167–172

Strauß H (1997) The isotopic composition of sedimentary sulfur through time. Palaeogeogr Palaeoclimatol Palaeoecol 132: 97–118

Strauß H (1999) Geological evolution from isotope proxy signals - sulfur. Chem Geol 161: 89–101

Strauß H, Peters-Kottig W (2003) The Phanerozoic carbon cycle revisited: the carbon isotope composition of terrestrial organic matter. G^3 Geochem Geophys Geosys 4: 1083 doic: 10.1029/2003GC000555

Stueber AM, Walter LM (1991) Origin and chemical evolution of formation waters from Silurian - Devonian strata in the Illinois basin. Geochim Cosmochim Acta 55: 309–325

Sturchio NC, Hatzinger PB, Atkins MD, Suh C, Heraty LJ (2003) Chlorine isotope fractionation during microbial reduction of perchlorate. Environ Sci Technol 37: 3859–3863

Styrt MM, Brackmann AJ, Holland HD, Clark BC, Pisutha-Arnold U, Eldridge CS, Ohmoto H (1981) The mineralogy and the isotopic composition of sulfur in hydrothermal sulfide/sulfate deposits on the East Pacific Rise, 21°N latitude. Earth Planet Sci Lett 53: 382–390

Summons RE, Jahnke LL, Roksandic Z (1994) Carbon isotopic fractionation in lipids from methanotrophic bacteria: relevance for interpretation of the geochemical record of biomarkers. Geochim Cosmochim Acta 58: 2853–2863

Sugawara S, Nakazawa T, Shirakawa Y, Kawamura K, Aoki S, Machida T, Honda H (1998) Vertical profile of the carbon isotope ratio of stratospheric methane over Japan. Geophysic Res Lett 24: 2989–2992

Suzuoki T, Epstein S (1976) Hydrogen isotope fractionation between OH-bearing minerals and water. Geochim Cosmochim Acta 40: 1229–1240

Swart PK, Burns SJ, Leder JJ (1991) Fractionation of the stable isotopes of oxygen and carbon in carbon dioxide during the reaction of calcite with phosphoric acid as a function of temperature and technique. Chem Geol 86: 89–96

Sweeney RE, Kaplan IR (1980) Natural abundance of ^{15}N as a source indicator for near-shore marine sedimentary and dissolved nitrogen. Mar Chem 9: 81–94
Sweeney RE, Liu KK, Kaplan IR (1978) Oceanic nitrogen isotopes and their use in determining the source of sedimentary nitrogen. In: Robinson BW (ed.) DSIR Bull 220: 9–26
Swihart GH (1996) Instrumental techniques for boron isotope analysis. Rev Miner 33: 845–862
Swihart GH, Moore PB (1989) A reconnaissance of the boron isotopic composition of tourmaline. Geochim Cosmochim Acta 53: 911–916
Swihart GH, Moore PB, Callis EL (1986) Boron isotopic composition of marine and non-marine evaporite borates. Geochim Cosmochim Acta 50: 1297–1301
Talbot MR (1990) A review of the palaeohydrological interpretation of carbon and oxygen isotopic ratios in primary lacustrine carbonates. Chem Geol 80: 261–279
Tanaka R, Nakamura E (2005) Boron isotopic constraints on the source of Hawaiian shield lavas. Geochim Cosmochim Acta 69: 3385–3399
Tang Y, Perry JK, Jenden PD, Schoell M (2000) Mathematical modeling of stable carbon isotope ratios in natural gases. Geochim Cosmochim Acta 64: 2673–2687
Tang Y, Huang Y, Ellis GS, Wang Y, Kralert PG, Gillaizeau B, Ma Q, Hwang R (2005) A kinetic model for thermally induced hydrogen and carbon isotope fractionation of individual n-alkanes in crude oil. Geochim Cosmochim Acta 69: 4505–4520
Taran YA, Kliger GA, Sevastianov VS (2007) Carbon isotope effect in the open system Fischer Trosch synthesis. Geochim Cosmochim Acta 71: 4474–4487
Tarutani T, Clayton RN, Mayeda TK (1969) The effect of polymorphism and magnesium substitution on oxygen isotope fractionation between calcium carbonate and water. Geochim Cosmochim Acta 33: 987–996
Taube H (1954) Use of oxygen isotope effects in the study of hydration ions. J Phys Chem 58: 523
Taylor HP (1968) The oxygen isotope geochemistry of igneous rocks. Contr Miner Petrol 19: 1–71
Taylor HP (1974) The application of oxygen and hydrogen isotope studies to problems of hydrothermal alteration and ore deposition. Econ Geol 69: 843–883
Taylor HP (1977) Water/rock interactions and the origin of H_2O in granite batholiths. J Geol Soc 133: 509
Taylor HP (1978) Oxygen and hydrogen isotope studies of plutonic granitic rocks. Earth Planet Sci Lett 38: 177–210
Taylor HP (1980) The effects of assimilation of country rocks by magmas on $^{18}O/^{16}O$ and $^{87}Sr/^{86}Sr$ systematics in igneous rocks. Earth Planet Sci Lett 47: 243–254
Taylor BE (1986) Magmatic volatiles: isotopic variation of C, H and S. Rev Miner 16: 185–225
Taylor BE (1987) Stable isotope geochemistry of ore-forming fluids. In: stable isotope geochemistry of low-temperature fluids. Short Course Min Ass Canada Vol 13: 337–445
Taylor HP (1986) Igneous rocks: II. Isotopic case studies of circumpacific magmatism. In: stable isotopes in high temperature geological processes. Rev Miner 16: 273–317
Taylor HP (1987) Comparison of hydrothermal systems in layered gabbros and granites, and the origin of low-$\delta^{18}O$ magmas. In: Magmatic processes: physicochemical principles. Geochem Soc Spec Publ 1: 337–357
Taylor HP (1988) Oxygen, hydrogen and strontium isotope constraints on the origin of granites. Trans R Soc Edinburgh: Earth Sci 79: 317–338
Taylor HP (1997) Oxygen and hydrogen isotope relationships in hydrothermal mineral deposits. In Barnes HL (ed) Geochemistry of hydrothermal ore deposits, 3rd ed. New York, Wiley-Interscience p. 229–302
Taylor BE, Bucher-Nurminen K (1986) Oxygen and carbon isotope and cation geochemistry of metasomatic carbonates and fluids - Bergell aureole, Northern Italy. Geochim Cosmochim Acta 50: 1267–1279
Taylor HP, Epstein S (1962) Relation between $^{18}O/^{16}O$ ratios in coexisting minerals of igneous and metamorphic rocks. I Principles and experimental results. Geol Soc Am Bull 73: 461–480
Taylor HP, Forester RW (1979) An oxygen and hydrogen isotope study of the Skaergaard intrusion and its country rocks: a description of a 55 M.Y. old fossil hydrothermal system. J Petrol 20: 355–419

Taylor BE, O'Neil JR (1977) Stable isotope studies of metasomatic Ca-Fe-Al-Si skarns and associated metamorphic and igneous rocks, Osgood Mountains, Nevada. Contr Miner Petrol 63: 1–49

Taylor HP, Sheppard SMF (1986) Igneous rocks: I.Processes of isotopic fractionation and isotope systematics. In: Stable isotopes in high temperature geological processes. Rev Miner 16: 227–271

Taylor TI, Urey HC (1938) Fractionation of the lithium and potassium isotopes by chemical exchange with zeolites. J Chem Phys 6: 429–438

Taylor BE, Wheeler MC (1994) Sulfur- and oxygen isotope geochemistry of acid mine drainage in the Western United States. In: Environmental geochemistry of sulphide oxidation. Am Chem Soc. Symp ser 550: 481–514, American Chemical Society Washington, DC

Taylor BE, Eichelberger JC, Westrich HR (1983) Hydrogen isotopic evidence of rhyolitic magma degassing during shallow intrusion and eruption. Nature 306: 541–545

Taylor HP, Turi B, Cundari A (1984) $^{18}O/^{16}O$ and chemical relationships in K-rich volcanic rocks from Australia, East Africa, Antarctica and San Venanzo Cupaello, Italy. Earth Planet Sci Lett 69: 263–276

Teece MA, Fogel ML (2007) Stable carbon isotope biogeochemistry of monosaccharides in aquatic organisms and terrestrial plants. Org Geochem 38: 458–473

Telmer KH, Veizer J (1999) Carbon fluxes, pCO2 and substrate weathering in a large northern river basin, Canada: carbon isotope perspective. Chem Geol 159: 61–86

Teng FZ, et al. (2004) Lithium isotope composition and concentration of the upper continental crust. Geochim Cosmochim Acta 68: 4167–4178

Teng FZ, McDonough WF, Rudnick RL, Walker RJ (2006) Diffusion-driven extreme lithium isotopic fractionation in country rocks of the Tin Mountain pegmatite. Earth Planet Sci Lett 243: 701–710

Teng FZ, McDonough WF, Rudnick RL, Wing BA (2007) Limited lithium isotopic fractionation during progressive metamorphic dehydration in metapelites: a case study from the Onawa contact aureole, Maine. Chem Geol 239: 1–12

Thiel V, Peckmann J, Seifert R, Wehrung P, Reitner J, Michaelis W (1999) Highly isotopically depleted isoprenoids: molecular markers for ancient methane venting. Geochim Cosmochim Acta 63: 3959–3966

Thiemens MH (1988) Heterogeneity in the nebula: Evidence from stable isotopes. In: JF Kerridge, MS Matthews (eds.) Meteorites and the early solar system. University of Arizona Press, Arizona, p. 899–923

Thiemens MH (1999) Mass-independent isotope effects in planetary atmospheres and the early solar system. Science 283: 341–345

Thiemens MH (2006) History and applications of mass-independent isotope effects. Annu Rev Earth Planet Sci 34: 217–262

Thiemens MH, Heidenreich JE (1983) The mass independent fractionation of oxygen - A novel isotope effect and its cosmochemical implications. Science 219: 1073–1075

Thiemens MH, Jackson T, Zipf EC, Erdman PW, van Egmond C (1995) Carbon dioxide and oxygen isotope anomalies in the mesophere and stratosphere. Science 270: 969–972

Thode HG, Monster J (1964) The sulfur isotope abundances in evaporites and in ancient oceans. In: Vinogradov AP (ed) Proc Geochem Conf Commemorating the Centenary of V I Vernadskii's Birth, vol 2, 630 p

Thode HG, Macnamara J, Collins CB (1949) Natural variations in the isotopic content of sulphur and their significance. Can J Res 27: 361

Thompson P, Schwarcz HP, Ford DE (1974) Continental Pleistocene climatic variationa from speleothem age and isotopic data. Science 184: 893–895

Thompson LG, Mosley-Thompson E, Henderson KA (2000) Ice-core palaeoclimate records in tropical South America since the last glacial maximum. J Quaternary Sci 15: 377–394

Thompson LG, et al. (2006) Abrupt tropical climate change: past and present. Proc Nat Acad Sci 103: 10536–10543

Tiedemann R, Sarntheim M, Shackleton NJ (1994) Astronomic timescale for the Pliocene Atlantic $\delta^{18}O$ and dust flux records of Ocean Drilling Program site 659: Paleoceanography 9: 619–638
Tipper ET, Galy A, Gaillardet J, Bickle MJ, Elderfield H, Carder EA (2006) The magnesium isotope budget of the modern ocean: constraints from riverine magnesium isotope ratios. Earth Planet Sci Lett (in press)
Todd CS, Evans BW (1993) Limited fluid-rock interaction at marble-gneiss contacts during Cretaceous granulite-facies metamorphism, Seward Peninsula, Alaska. Contr Miner Petrol 114: 27–41
Tomascak PB, Tera F, Helz RT, Walker RJ (1999) The absence of lithium isotope fractionation during basalt differentiation: new measurements by multicollector sector ICP-MS. Geochim Cosmochim Acta 63: 907–910
Tomascak PB, Ryan JG, Defant MJ (2000) Lithium isotope evidence for light element decoupling in the Panama subarc mantle. Geology 28: 507–510
Tomascak PB, Widom E, Benton LD, Goldstein SL, Ryan JG (2002) The control of lithium budgets in island arcs. Earth Planet Sci Lett 196: 227–238
Tomaszak PB (2004). Lithium isotopes in earth and planetary sciences. Rev Miner Geochem
Trofimov A (1949) Isotopic constitution of sulfur in meteorites and in terrestrial objects. Dokl Akad Nauk SSSR 66: 181
Trudinger PA, Chambers LA, Smith JW (1985) Low temperature sulphate reduction: biological versus abiological. Can J Earth Sci 22: 1910–1918
Trudinger CM, Enting IG, Francey RJ, Etheridge DM, Rayner PJ (1999) Long-term variability in the global carbon cycle inferred from a high-precision CO_2 and $\delta^{13}C$ ice-core record. Tellus 51: 233–248
Truesdell AH (1974) Oxygen isotope activities and concentrations in aqueous salt solution at elevated temperatures: consequences for isotope geochemistry. Earth Planet Sci Lett 23: 387–396
Truesdell AH, Hulston JR (1980) Isotopic evidence on environments of geothermal systems. In: Fritz P, Fontes J (eds) Handbook of environmental isotope geochemistry, vol I. Elsevier, New York, Amsterdam, pp 179–226
Tucker ME, Wright PV (1990) Carbonate sedimentology. Blackwell, Oxford, p. 365–400
Turchyn AV, Schrag DP (2004) Oxygen isotope constraints on the sulfur cycle over the past 10 million years. Science 303: 2004–2007
Turner JV (1982) Kinetic fractionation of carbon-13 during calcium carbonate precipitation. Geochim Cosmochim Acta 46: 1183–1192
Ueda A, Sakai S (1984) Sulfur isotope study of Quaternary volcanic rocks from the Japanese Island Arc. Geochim Cosmochim Acta 48: 1837–1848
Urey HC (1947) The thermodynamic properties of isotopic substances. J Chem Soc 1947: 562
Urey HC, Brickwedde FG, Murphy GM (1932) A hydrogen isotope of mass 2 and its concentration. Phys Rev 40: 1
Usdowski E, Hoefs J (1993) Oxygen isotope exchange between carbonic acid, bicarbonate, carbonate, and water: a re-examination of the data of McCrea and an expression for the overall partitioning of oxygen isotopes between the carbonate species and water. Geochim Cosmochim Acta 57: 3815–3818
Valley JW (1986) Stable isotope geochemistry of metamorphic rocks. Rev Miner 16: 445–489
Valley JW (2001) Stable isotope thermometry at high temperatures. Rev Miner Geochem 43: 365–413
Valley JW (2003) Oxygen isotopes in zircon. Rev Miner Geochem 53: 343–385
Valley JW, Graham C (1993) Cryptic grain-scale heterogeneity of oxygen isotope ratios in metamorphic magnetite. Science 259: 1729–1733
Valley JW, O'Neil JR (1981) $^{13}C/^{12}C$ exchange between calcite and graphite: a possible thermometer in Greville marbles. Geochim Cosmochim Acta 45: 411–419
Valley JW, Bohlen SR, Essene EJ, Lamb W (1990) Metamorphism in the Adirondacks. II. J Petrol 31: 555–596

Valley JW, Eiler JM, Graham CM, Gibson EK, Romanek CS, Stolper EM (1997) Low temperature carbonate concretions in the martian meteorite ALH 84001: evidence from stable isotopes and mineralogy. Science 275: 1633–1637

Valley J, Graham CM, Harte B, Eiler JM, Kinney PD (1998) Ion microprobe analysis of oxygen, carbon and hydrogen isotope ratios. In: Applications of microanalytical techniques to understanding mineralizing processes. Rev Econ Geol 7: 73–98

Valley JW, et al. (2005) 4.4 billion years of crustal maturation: oxygen isotope ratios in magmatic zircon. Contr Miner Petrol 150: 561–580

Van Warmerdam EM, Frape SK, Aravena R, Drimmie RJ, Flatt H, Cherry JA (1995) Stable chlorine and carbon isotope measurements of selected chlorinated organic solvents. Appl Geochem 10: 547–552

Vasconcelos C, Mackenzie JA, Warthmann R, Bernasconi S (2005) Calibration of the $\delta^{18}O$ paleothermometer for dolomite precipitated in microbial cultures and natural environments. Geology 33: 317–320

Vazquez R, Vennemann TW, Kesler SE, Russell N (1998) Carbon and oxygen isotope halos in the host limestone, El Mochito Zn, Pb (Ag) skarn massive sulfide/oxide deposit, Honduras. Econ Geol 93: 15–31

Veizer J, Hoefs J (1976) The nature of $^{18}O/^{16}O$ and $^{13}C/^{12}C$ secular trends in sedimentary carbonate rocks. Geochim Cosmochim Acta 40: 1387–1395

Veizer J, et al. (1997) Oxygen isotope evolution of Phanerozoic seawater. Palaeogeogr Palaeoclimatol Palaeoecol 132: 159–172

Veizer J, et al. (1999) $^{87}Sr/^{86}Sr$, $\delta^{13}C$ and $\delta^{18}O$ evolution of Phanerozoic seawater. Chem Geol 161: 37–57

Vengosh A, Chivas AR, McCulloch M, Starinsly A, Kolodny Y (1991a) Boron isotope geochemistry of Australian salt lakes. Geochim Cosmochim Acta 55: 2591–2606

Vengosh A, Starinsky A, Kolodny Y, Chivas AR (1991b) Boron isotope geochemistry as a tracer for the evolution of brines and associated hot springs from the Dead Sea, Israel. Geochim Cosmochim Acta 55: 1689–1695

Vennemann T, O'Neil JR (1996) Hydrogen isotope exchange reactions between hydrous minerals and hydrogen: I. A new approach for the determination of hydrogen isotope fractionation at moderate temperatures. Geochim Cosmochim Acta 60: 2437–2451

Vennemann TW, Smith HS (1992) Stable isotope profile across the orthoamphibole isograd in the Southern Marginal Zone of the Limpopo Belt, S Africa. Precambrian Res 55: 365–397

Vennemann TW, Kesler SE, O'Neil JR (1992) Stable isotope composition of quartz pebbles and their fluid inclusions as tracers of sediment provenance: implications for gold- and uranium-bearing quartz pebble conglomerates. Geology 20: 837–840

Vennemann TW, Kesler SE, Frederickson GC, Minter WEL, Heine RR (1996) Oxygen isotope sedimentology of gold and uranium-bearing Witwatersrand and HuronianSupergroup quartz pebble conglomerates. Econ Geol 91: 322–342

Vennemann TW, Fricke HC, Blake RE, O'Neil JR, Colman A (2002) Oxygen isotope analysis of phosphates: a comparison of techniques for analysis of Ag_3PO_4. Chem Geol 185: 321–336

Vogel JC, Grootes PM, Mook WG (1970) Isotopic fractionation between gaseous and dissolved carbon dioxide. Z Physik 230: 225–238

von Grafenstein U, Erlenkeuser H, Trimborn P (1999) Oxygen and carbon isotopes in fresh-water ostracod valves: assessing vital offsets and autoecological effects of interest for paleoclimate studies. Palaeogeogr Palaeoclimatol Palaeoecol 148: 133–152

Wachter EA, Hayes JM (1985) Exchange of oxygen isotopes in carbon dioxide-phosphoric acid systems. Chem Geol 52: 365–374

Wada E, Hattori A (1976) Natural abundance of ^{15}N in particulate organic matter in North Pacific Ocean. Geochim Cosmochim Acta 40: 249–251

Wallmann K (2001) The geological water cycle and the evolution of marine $\delta^{18}O$ values. Geochim. Cosmochim Acta 65: 2469–2485

Wang Z, Schauble EA, Eiler JM (2004) Equilibrium thermodynamics of multiply substituted isotopologues of molecular gas. Geochim Cosmochim Acta 68: 4779–4797

Warren CG (1972) Sulfur isotopes as a clue to the genetic geochemistry of a roll-type uranium deposit. Econ Geol 67: 759–767
Watson LL, Hutcheon ID, Epstein S, Stolper EM (1994) Water on Mars: clues from deuterium/hydrogen and water contents of hydrous phases in SNC meteorites. Science 265: 86–90
Weber JN, Raup DM (1966a) Fractionation of the stable isotopes of carbon and oxygen in marine calcareous organisms-the Echinoidea. I. Variation of ^{13}C and ^{18}O content within individuals. Geochim Cosmochim Acta 30: 681–703
Weber JN, Raup DM (1966b) Fractionation of the stable isotopes of carbon and oxygen in marine calcareous organisms-the Echinoidea. II. Environmental and genetic factors. Geochim Cosmochim Acta 30: 705–736
Wefer G, Berger WH (1991) Isotope paleontology: growth and composition of extant calcareous species. Mar Geol 100: 207–248
Wei CS, Zhao ZF, Spicuzza MJ (2008) Zircon oxygen isotopic constraint on the sources of late Mesozoic A-type granites in eastern China. Chem Geol 250: 1–15
Welhan JA (1987) Stable isotope hydrology. In: Short course in stable isotope geochemistry of low-temperature fluids. Miner Ass Canada Vol 13: 129–161
Welhan JA (1988) Origins of methane in hydrothermal systems. Chem Geol 71: 183–198
Wenzel B, Lecuyer C, Joachimski MM (2000) Comparing oxygen isotope records of Silurian calcite and phosphate - $\delta^{18}O$ composition of brachiopods and conodonts. Geochim Cosmochim Acta 69: 1859–1872
Westerhausen L, Poynter J, Eglinton G, Erlenkeuser H, Sarntheim M (1993) Marine and terrigenous origin of organic matter in modern sediments of the equatorial East Atlantic: the $\delta^{13}C$ and molecular record. Deep Sea Res 40: 1087–1121
Weyer S, Anbar AD, Brey GP, Münker C, Mezger K (2005) Iron isotope fractionation during planetary differentiation. Earth Planet Sci Lett 240: 251–264
White JWC (1989) Stable hydrogen isotope ratios in plants: a review of current theory and some potential applications. In: Stable isotopes in ecological research. Ecological Studies 68. Springer Verlag, New York, p.142–162
White JWC, Lawrence JR, Broecker WS (1994) Modeling and interpreting D/H ratios in tree rings: a test case of white pine in the northeastern United States. Geochim Cosmochim Acta 58: 851–862
Whiticar MJ (1999) Carbon and hydrogen isotope systematics of bacterial formation and oxidation of methane. Chem Geol 161: 291–314
Whiticar MJ, Faber E, Schoell M (1986) Biogenic methane formation in marine and freshwater environments: CO_2 reduction vs. acetate fermentation-Isotopic evidence. Geochim Cosmochim Acta 50: 693–709
Whittacker SG, Kyser TK (1990) Effects of sources and diagenesis on the isotopic and chemical composition of carbon and sulfur in Cretaceous shales. Geochim Cosmochim Acta 54: 2799–2810
Wickham SM, Taylor HR (1985) Stable isotope evidence for large-scale seawater infiltration in a regional metamorphic terrane; the Trois Seigneurs Massif, Pyrenees, France. Contrib Miner Petrol 91: 122–137
Wickman FE (1952) Variation in the relative abundance of carbon isotopes in plants. Geochim Cosmochim Acta 2: 243–254
Wiechert U, Hoefs J (1995) An excimer laser-based microanalytical preparation technique for in-situ oxygen isotope analysis of silicate and oxide minerals. Geochim Cosmochim Acta 59: 4093–4101
Wiechert U, Halliday AN, Lee DC, Snyder GA, Taylor LA, Rumble D (2001) Oxygen isotopes and the moon forming giant impact. Science 294: 345–348
Wiechert U, Fiebig J, Przybilla R, Xiao Y, Hoefs J (2002) Excimer laser isotope-ratio-monitoring mass spectrometry for in situ oxygen isotope analysis. Chem Geol 182: 179–194
Wilkinson JJ, Weiss DJ, Mason TF, Coles BJ (2005) Zinc isotope variation in hydrothermal systems: preliminary evidence from the Irish Midlands ore field. Econ Geol 100: 583–590

Williams LB, Ferrell RE, Hutcheon I, Bakel AJ, Walsh MM, Krouse HR (1995) Nitrogen isotope geochemistry of organic matter and minerals during diagenesis and hydrocarbon migration. Geochim Cosmochim Acta 59: 765–779

Williams LB, Hervig RL, Holloway JR, Hutcheon I (2001) Boron isotope geochemistry during diagenesis. Part I. Experimental determination of fractionationduring illitization of smectite. Geochim Cosmochim Acta 65: 1769–1782

Williams H, Peslier A, McCammon C, Halliday A, Levasseur S, Teutsch N, Burg JP (2005) Systematic iron isotope variations in mantle rocks and minerals: the effects of partial melting and oxygen fugacity. Earth Planet Sci Lett 235: 435–452

Willmore CC, Boudreau AE, Spivack A, Kruger FJ (2002) Halogens of Bushveld Complex, South Africa: δ^{37}Cl and Cl/F evidence for hydration melting of the source region in a back-arc setting. Chem Geol 182: 503–511

Wong WW, Sackett WM (1978) Fractionation of stable carbon isotopes by marine phytoplankton. Geochim Cosmochim Acta 42: 1809–1815

Wortmann UG, Bernasconi SM, Böttcher ME (2001) Hypersulfidic deep biosphere indicates extreme sulfur isotope fractionation during single-step microbial sulfate reduction. Geology 29: 647–650

Wortmann UG, Chernyavsky B, Bernasconi SM, Brunner B, Böttcher ME, Swart PK (2007) Oxygen isotope biogeochemistry of pore water sulfate in the deep biosphere: dominance of isotope exchange reactions with ambient water during microbial sulfate reduction (ODP Site 1130). Geochim Cosmochim Acta 71: 4221–4232

Wright I, Grady MM, Pillinger CT (1990) The evolution of atmospheric CO2 on Mars: the perspective from carbon isotope measurements. J Geophys Res 95: 14789–14794

Wunder B Meixner A, Romer R, Wirth R, Heinrich W (2005) The geochemical cycle of boron: constraints from boron isotope partitioning experiments between mica and fluid. Lithos 84: 206–216

Wunder B, Meixner A, Romer R, Heinrich W (2006) Tempearature-dependent isotopic fractionation of lithium between clinopyroxene and high-pressure hydrous fluids. Contr Miner Petrol 151: 112–120

Wunder B, Meixner A, Romer RL, Feenstra A, Schettler G, Heinrich W (2007) Lithium isotope fractionation between Li-bearing staurolite, Li-mica and aqueous fluids: an experimental study. Chem Geol 238: 277–290

Xia J, Ito E, Engstrom DE (1997a) Geochemistry of ostracode calcite: Part I. An experimental determination of oxygen isotope fractionation. Geochim Cosmochim Acta 61: 377–382

Xia J, Engstrom DE, Ito E (1997b) Geochemistry of ostracode calcite: Part 2. The effects of water chemistry and seasonal temperature variation on *Candona rawsoni*. Geochim Cosmochim Acta 61: 383–391

Xiao Y, Hoefs J, van den Kerkhof AM, Simon K, Fiebig J, Zheng YF (2002) Fluid evolution during HP and UHP metamorphism in Dabie Shan, China: constraints from mineral chemistry, fluid inclusions and stable isotopes. J Petrol 43: 1505–1527

Xiao Y, Zhang Z, Hoefs J, van den Kerkhof A (2006) Ultrahigh pressure rocks from the Chinese Continental Scientific Drilling Project: II Oxygen isotope and fluid inclusion distributions through vertical sections. Contr Miner Petrol 152: 443–458

Xie Q, Liu S, Evans D, Dillon P, Hintelmann H (2005) High precision Hg isotope analysis of environmental samples using gold trap-MC-ICP-MS. J Anal At Spectrom 20: 515–522

Yamaguchi KE, Johnson CM, Beard BL, Ohmoto H (2005) Biogeochemical cycling of iron in the Archean-Paleoproterozoic Earth: constraints from iron isotope variations in sedimentary rocks from the Kapvaal and Pilbara cratons. Chem Geol 218: 135–169

Yang J, Epstein S (1984) Relic interstellar grains in Murchison meteorite. Nature 311: 544–547

Yang C, Telmer K, Veizer J (1996) Chemical dynamics of the "St Lawrence" riverine system: δD_{H2O}, $\delta^{18}O_{H2O}$, $\delta^{13}C_{DIC}$, $\delta^{34}S_{SO4}$ and dissolved $^{87}Sr/^{86}Sr$. Geochim Cosmochim Acta 60: 851–866

Yapp CJ (1983) Stable hydrogen isotopes in iron oxides - isotope effects associated with the dehydration of a natural goethite. Geochim Cosmochim Acta 47: 1277–1287

Yapp CJ (1987) Oxygen and hydrogen isotope variations among goethites (α-FeOOH) and the determination of paleotemperatures. Geochim Cosmochim Acta 51: 355–364
Yapp CJ (2007) Oxygen isotopes in synthetic goethite and a model for the apparent pH dependence of goethite-water $^{18}O/^{16}O$ fractionation. Geochim Cosmochim Acta 71: 1115–1129
Yapp CJ, Epstein S (1982) Reexamination of cellulose carbon-bound hydrogen δD measurements and some factors affecting plant-water D/H relationships. Geochim Cosmochim Acta 46: 955–965
Yoshida N, Toyoda S (2000) Constraining the atmospheric N_2O budget from intramolecular site preference in N_2O isotopomers. Nature 405: 330–334
Yoshida N, Hattori A, Saino T, Matsuo S, Wada E (1984) $^{15}N/^{14}N$ ratio of dissolved N_2O in the eastern tropical Pacific Ocean. Nature 307: 442–444
Young ED (1993) On the 18O/16O record of reaction progress in open and closed metamorphic systems. Earth Planet Sci Lett 117: 147–167
Young ED, Galy A (2004) The isotope geochemistry and cosmochemistry of magnesium. Rev Miner Geochem 55: 197–230
Young ED, Rumble D (1993) The origin of correlated variations in in-situ $^{18}O/^{16}O$ and elemental concentrations in metamorphic garnet from southeastern Vermont, USA. Geochim Cosmochim Acta 57: 2585–2597
Young ED, Ash RD, England P, Rumble D (1999) Fluid flow in chondritic parent bodies: deciphering the compositions of planetesimals. Science 286: 1331–1335
Young ED, Galy A, Nagahara H (2002) Kinetic and equilibrium mass-dependent isotope fractionation laws in nature and their geochemical and cosmochemical significance. Geochim Cosmochim Acta 66: 1095–1104
Yung YL, Miller CE (1997) Isotopic fractionation of stratospheric nitrous oxide. Science 278: 1778–1780
Yurimoto A, Krot A, Choi BG, Aléon J, Kunihiro T, Brearly AJ (2008) Oxygen isotopes in chondritic components. Rev Miner Geochem 68: 141–186
Yurtsever Y (1975) Worldwide survey of stable isotopes in precipitation. Rep Sect Isotope Hydrol IAEA, November 1975, 40 pp
Zaback DA, Pratt LM (1992) Isotopic composition and speciation of sulfur in the Miocene Monterey Formation: reevaluation of sulfur reactions during early diagenesis in marine environments. Geochim Cosmochim Acta 56: 763–774
Zachos J, Pagani M, Sloan L, Thomas E, Billups K (2001) Trends, rhythms and aberrations in global climate 65 Ma to present. Science 292: 686–693
Zeebe RE (1999) An explanation of the effect of seawater carbonate concentration on foraminiferal oxygen isotopes. Geochim Cosmochim Acta 63: 2001–2007
Zeebe RE (2005) Stable boron isotope fractionation between dissolved $B(OH)_3$ and $B(OH)_4^-$. Geochim Cosmochim Acta 69: 2753–2766
Zeebe RE (2007) An expression for the overall oxygen isotope fractionation between the sum of dissolved inorganic carbon and water. Geochem Geophys Geosys 8: 10.1029/2007GC001663
Zhang T, Krooss BM (2001) Experimental investigation on the carbon isotope fractionation of methane during gas migration by diffusion through sedimentary rocks at elevated temperature and pressure. Geochim Cosmochim Acta 65: 2723–2742
Zhang J, Quay PD, Wilbur DO (1995) Carbon isotope fractionation during gas-water exchange and dissoltion of CO2. Geochim Cosmochim Acta 59: 107–114
Zhang HF, et al. (2000) Recent fluid processes in the Kapvaal craton, South Africa: coupled oxygen isotope and trace element disequilibrium in polymict peridotites. Earth Planet Sci Lett 176: 57–72
Zhang R, Schwarcz HP, Ford DC, Schroeder FS, Beddows PA (2008) An absolute paleotemperature record from 10 to 6 ka inferred from fluid inclusion D/H ratios of a stalagmite from Vancouver Island, British Columbia, Canada. Geochim Cosmochim Acta 72: 1014–1026
Zheng YF (1991) Calculation of oxygen isotope fractionation in metal oxides. Geochim Cosmochim Acta 55: 2299–2307

Zheng YF (1993a) Oxygen isotope fractionation in SiO_2 and Al_2SiO_5 polymorphs: effect of crystal structure. Eur J Miner 5: 651–658

Zheng YF (1993b) Calculation of oxygen isotope fractionation in anhydrous silicate minerals. Geochim Cosmochim Acta 57: 1079–1091

Zheng YF (1993c) Calculation of oxygen isotope fractionation in hydroxyl-bearing minerals. Earth Planet Sci Lett 120: 247–263

Zheng YF, Hoefs J (1993) Carbon and oxygen isotopic vovariations in hydrothermal calcites. Theoretical modeling on mixing processes and application to Pb-Zn deposits in the Harz Mountains, Germany. Miner Deposita 28: 79–89

Zheng YF, Fu B, Li Y, Xiao Y, Li S (1998) Oxygen and hydrogen isotope geochemistry of ultrahigh pressure eclogites from the Dabie mountains and the Sulu terrane. Earth Planet Sci Lett 155: 113–129

Zhu P, MacDougall JD (1998) Calcium isotopes in the marine environment and the oceanic calcium cycle. Geochim Cosmochim Acta 62: 1691–1698

Zhu XK, O'Nions RK, Guo Y, Belshaw NS, Rickard D (2000a) Determination of natural Cu-isotope variations by plasma-source mass spectrometry: implications for use as geochemical tracers. Chem Geol 163: 139–149

Zhu XK, O'Nions K, Guo Y, Reynolds BC (2000b) Secular variations of iron isotopes in North Atlantic Deep Water. Science 287: 2000–2002

Zhu XK, et al. (2002) Mass fractionation processes of transition metal isotopes. Earth Planet Sci Letters 200: 47–62

Ziegler K, Chadwick OA, Brzezinski MA, Kelly EF (2005a) Natural variations of $\delta^{30}Si$ ratios during progressive basalt weathering. Geochim Cosmochim Acta 69: 4597–4610

Ziegler K, Chadwick OA, White AF, Brzezinski MA (2005b) $\delta^{30}Si$ systematics in a granitic saprolite, Puerto Rico. Geology 33: 817–820

Zierenberg RA, Shanks WC, Bischoff JL (1984) Massive sulfide deposit at 21°N, East Pacific Rise: chemical composition, stable isotopes, and phase equilibria. Bull Geol Soc Am 95: 922–929

Zimmer MM, Fischer TP, Hilton DR, Alvaredo GE, Sharp ZD, Walker JA (2004) Nitrogen systematics and gas fluxes of subduction zones: insights from Costa Rica arc volatiles. Geochem Geophys Geosys 5: Q05J11, doi:10.1029/2003GC000651

Zinner E (1998) Stellar nucleosynthesis and the isotopic composition of presolar grains from primitive meteorites. Ann Rev Earth Planet Sci 26: 147–188

Index